Isolation and characterization of African marine natural products and repositioning of the natural product antibiotic fusidic acid and privileged benzimidazole scaffold for tuberculosis and malaria

Thesis submitted for the award of Doctor of Philosophy degree in the department of Chemistry, University of Cape Town,

Godwin Akpeko Dziwornu

Supervisor: Prof. Kelly Chibale

Department of Chemistry, University of Cape Town (UCT)

Co-supervisor: Prof. Denzil R. Beukes

School of Pharmacy, University of the Western Cape (UWC)

December 2018

Declaration

I hereby declare that this thesis is my original work produced from research undertaken under supervision and has not been presented for a degree in this university or another university elsewhere for the award of any other degree.

Signed by candidate

.....

Godwin Akpeko Dziwornu

Dedication

To Beatrice Buanya

Acknowledgements

This work would not have been successfully completed without the enormous contributions and outstanding mentorship of my supervisors, Prof. Kelly Chibale and Prof. Denzil R. Beukes. I acknowledge the contributions of Dr. Sunny Sunassee and the constructive criticisms and helpful suggestions of Prof. Edith Antunes, Dr. Richard Amewu and Dr. (Mrs.) Dorcas Osei-Safo.

Special appreciation goes to Elaine Rutherfoord-Jones and Deidre Brooks for their administrative support and helpful advice and encouragement.

Special thanks to Peter Roberts for acquiring some of my NMR data and Daniel Watson for his help with acquiring and analyzing some of my HR-ESI-MS data. I appreciate the support received from Prof. Adrienne L. Edkins, Prof. Lyn-Marie Birkholtz, Dr. Jo-Anne de la Mare, Ms. Ronnet Seldon, Dr. Dale Taylor and Dr. Sergio Wittlin for conducting the biological assays.

I appreciate the efforts of the Head of Department and both teaching and non-teaching staff of the Chemistry Department, University of Cape Town.

I extend my thanks to the South African Medical Research Council, South African National Research Foundation (NRF), the Faculty of Science and Department of Chemistry for their generous financial assistance, without which this work would not have been possible.

I am grateful to my colleagues.

Finally, I thank God for the lives of Miss Beatrice Buanya and her family, my family, my church, my goddaughter, Bernice Nana Yaa Nhyiraba Amoah, Kojo Sekyi Acquah, Henrietta Attram and Constance Korkor for every support they provided me, in love, care, encouragement, prayers, etc. God richly bless you all.

Abstract

Many bioactive compounds isolated from nature (microbes, plants and animals) are successfully being used as drugs to prevent and/or cure diseases. A greater number of these natural products have not progressed to the latter stages of development as drugs largely due to the drawbacks of toxicity, limited supply, growing concerns to conserve terrestrial and marine ecosystems and their biodiversity, which impedes sample collections in adequate quantities for research, among others. However, in spite of these drawbacks, the medicinal chemistry explorations of bioactive natural products, which hitherto may have been abandoned in the repositories of research laboratories, have afforded an even greater number of drugs in clinical use. The collaboration of natural products chemistry and medicinal chemistry to discover, optimize and develop bioactive compounds as drugs remains an important endeavor today.

A chemistry-guided natural products investigation of the newly identified marine red alga *Laurencia alfredensis*, which is an endemic species of South Africa, afforded ten (10) newly reported compounds from the genus. Isolation and purification of the compounds from the DCM/MeOH 1:1 v/v crude extract was achieved through a combination of normal phase bench-top column chromatography, preparative TLC, and semi-preparative HPLC. Elucidation of the chemical structures was accomplished by 1D- and 2D-NMR, HR-ESI-MS, UV and IR spectroscopic techniques, and X-ray diffraction analysis. The isolated compounds belong to the *Laurencia* secondary metabolite classes of labdane diterpenoids, polyether triterpenoids and sterols, and a glycolipid, which is reported herein for the first time from the genus. The compounds displayed low micromolar to poor *in vitro* antiproliferative activity towards the human breast (MDA-MB-231) and cervical (HeLa) cancer cell lines with IC_{50} values in the 8.8 – 133.8 µM range.

A further natural products research effort involving the chemical investigation of two marine sponge species, *Halichondria* sp. and *Hymeniacidon* sp., is also reported herein. The specimens were collected from the Prince Edwards Islands in the Southern Ocean in the vicinity of Antarctica. With the aim to investigate the chemical and biological properties of the secondary metabolites from the cold continent, the organic crude extracts (DCM/MeOH 1:1 v/v) of the specimens were purified by DIOL flash chromatography and reverse phase semi-preparative HPLC. Two previously

unreported compounds were isolated from the *Halichondria* sp., comprising of a bis-zooanemonin betaine metabolite and a trimer of proline betaine. The two compounds were inactive (IC_{50} >10 µg/mL) towards the drug-sensitive strain of *Plasmodium falciparum* (NF54), *in vitro*. Meanwhile, the *Hymeniacidon* sp. afforded the known nucleoside, thymidine, the amino acids, tyrosine, leucine, isoleucine and valine, and the small alkaloids, choline and agmatine.

The natural product antibiotic, fusidic acid, has been in clinical use as, largely, a bacteriostatic agent against staphylococcal pathogens since 1962. Having exhibited a similar mode of action *via* inhibition of *Mycobacteria tuberculosis* and *P. falciparum* elongation factor G (EF-G), the current work expanded the structure-activity relationship (SAR) explorations in the medicinal chemistry approach of repositioning for tuberculosis and malaria. Twenty-nine (29) fusidic acid C-21 ethanamides, anilides and benzyl amides were synthesized and evaluated *in vitro* against the *M. tuberculosis* strain H_{37}Rv and asexual blood stage and gametocytes parasites of the human malaria parasite *Plasmodium falciparum*. Good antimycobacterial activity (MIC_{90} <10 µM) was observed in the analogues, which possessed bulky and/or polar substituents in close proximity to the amide bond. Moreover, hydrophilic electron-withdrawing substituents seem to enhance antimycobacterial activity. A fusidic acid anilide formed from the Mannich base, 3-((*N*,*N*-diethylamino)methyl)-4-hydroxy aniline recorded the most potent antimycobacterial activity with MIC_{90} values of 0.40 µM and 10.35 µM in the 7H9/CAS and 7H9/ADC media, respectively. Meanwhile, multi-stage antiplasmodium activity was more favored in the fusidic acid ethanamides. While the activity was not affected by diastereoisomerism, potency was enhanced by *para*-substituted lipophilic electron-withdrawing/donating groups. The (*R*)-4-fluoro ethanamide analogue of fusidic acid displayed the most potent asexual erythrocytic blood stage antiplasmodium activity with IC_{50} values of 0.57 and 0.47 µM against the NF54 and K1 strains of *P. falciparum*, respectively. The synthesized compounds, however, exhibited moderate to no inhibition of gametocyte growth at the highest concentration tested of 5 µM.

The privileged benzimidazole scaffold has afforded antiviral, antiulcer, antimicrobial, antitumor, antihypertensive, anti-inflammatory and antihistaminic clinical chemotherapeutic agents. A limited number of studies describing the utility of benzimidazoles as potential antimalarial and antimycobacterial agents have been reported. In this context, novel benzimidazole analogues

were rationally designed by incorporation of phenolic Mannich bases and synthesized in this thesis work. The synthesized compounds exhibited good *in vitro* potency towards *Mtb* in the 7H9/CAS media and sub-micromolar activity against the asexual blood stage *P. falciparum* parasites. All the compounds were relatively non-cytotoxic (IC_{50} >10 µM) to the Chinese hamster ovarian (CHO) cell line, recording acceptable selectivity indices, S1>10. No correlation was observed between the antiplasmodium activity of the synthesized analogues and their likely mode of action as inhibitors of hemozoin formation. The 1-((4-trifluoromethyl)benzyl) benzimidazole analogue based on the 3-((*N*,*N*-diethylamino)methyl)-2-hydroxy-5-methyl aniline Mannich base was the most potent analogue in both assays. It recorded a MIC_{90} value of 2.00 µM in the 7H9/CAS media. Moreover, IC_{50} values of 0.19 µM and 0.06 µM were observed against the asexual blood stage NF54 and K1 strains of *P. falciparum*, respectively, while it inhibited 91% of growth of early stage gametocytes at 1 µM. Although it showed poor aqueous kinetic solubility as a free base at pH 7.4, it conformed to Lipinski and Veber rules for oral absorption and bioavailability, while it shared a similar chemical space with the clinically used 4-aminoquinoline drug naphthoquine.

The results presented herein substantiates the fact that the complimentary efforts of natural products research and medicinal chemistry exploration of natural products and privileged scaffolds continue to remain a viable approach to discovering potent bioactive drug candidates.

Abbreviations

$(Ac)_2O$	Acetic anhydride
AR	Analytical reagent
ATP	Adenosine triphosphate
βHIA	Beta-hematin inhibition assay
^{13}C	Carbon
$CDCl_3$	Deuterated chloroform
CHO	Chinese Hamster Ovarian
CLR	Clarithromycin
CO_2	Carbon dioxide
COSY	Homonuclear correlation spectroscopy
CQ	Chloroquine
d	Density
2D	Two dimensional
3D	Three dimensional
DAD	Diode Array Detector
DCM	Dichloromethane
DIPEA	Diisopropylethylamine
DMAP	4-Dimethylaminopyridine
DMF	*N*,*N*-Dimethylformamide
DMSO-d_6	Deuterated dimethyl sulfoxide
DNA	Deoxyribonucleic acid
EDCI	1-Ethyl-3-(3-dimethylaminopropyl)carbodiimide
EF-G	Elongation factor G
EMB	Ethambutol
ERY	Erythromycin
ESI	Electrospray ionisation

Et_3N	Triethylamine
EtOAc	Ethyl acetate
EtOH	Ethanol
FICI	Fractional inhibitory concentration index
GDP	Guanosine 5′-diphosphate
GTP	Guanosine triphosphate
^1H	Proton
HATU	Hexafluorophosphate azabenztriazole tetramethyl uronium
HCl	Hydrogen chloride
HEPES	4-(2-hydroxyethyl)-1-piperazineethanesulfonic acid
HIV	Human immunodeficiency virus
HPLC	High performance liquid chromatography
HTS	High-throughput screening
HMBC	Heteronuclear multiple-bond correlation
HR-ESI-MS	High resolution electrospray ionization mass spectrometry
HSQC	Heteronuclear single quantum correlation
IC	Inhibitory concentration
IR	Infrared spectroscopy
IDM	Institute of Infectious Diseases and Molecular Medicine
INH	Isoniazid
J	Coupling constant
KH_2PO_4	Potassium dihydrogen phosphate
K_2CO_3	Potassium carbonate
LCMS	Liquid chromatography–mass spectrometry

LDH	Lactate dehydrogenase
pLDH	Plasmodium lactate dehydrogenase
M	Molar
MeOH-d_4	Deuterated methanol
mg/mL	Microgram per liter
µM	Micro molar
MHz	Mega hertz
MIC	Minimum inhibitory concentration
mL	milliliter
MoA	Mechanism of action
MoR	Mechanism of resistance
Mp	Melting point
MS	Mass spectroscopy
Mtb	Mycobacterium tuberculosis
MTT	3-(4,5-dimethylthiazol-2-yl)-2,5-diphenyltetrazoliumbromide
MW	Microwave
m/z	Mass over charge ratio
^{15}N	Nitrogen
$NaBH_4$	Sodium borohydride
$NaHCO_3$	Sodium bicarbonate
NaOAc	Sodium acetate
NaOH	Sodium hydroxide
n-BuOH	1-butanol
NH_4Cl	Ammonium chloride
NH_4OAc	Ammonium acetate
nM	Nano molar
NMR	Nuclear magnetic resonance
NOESY	Nuclear overhauser effect spectroscopy

NP-40	Nonidet P-40
O_2	Oxygen
OAc	Acetoxy
PDA	Photodiode array
Pd/C	Palladium on carbon
P. falciparum	Plasmodium falciparum
PK	Pharmacokinetics
pH	Potential of hydrogen
QSAR	Quantitative structure–activity relationship
Rf	Retardation factor
RIF	Rifampin
RMSD	Root mean square deviation
RNA	Ribonucleic acid
ROESY	Rotating-frame nuclear overhauser effect correlation spectroscopy
ROX	Roxythromycin
SAR	Structure-activity relationship
SI	Selectivity Index
SM	Streptomycin
sp.	Species
SPC	Spectinomycin
STR	Streptomycin
TAACF	Tuberculosis Antimicrobial Acquisition Coordinating Facility
TB	Tuberculosis
THF	Tetrahydrofuran
TLC	Thin layer chromatography
T3P	n-Propanephosphonic acid anhydride

UK	United Kingdom
USA	United states of America
UV	Ultra violet
v/v	Volume by volume ratio
w/v	Weight by volume ratio

Table of contents

List of Figures

List of Tables

List of Schemes

Chapter One: Introduction

1.1 Natural Products

The term 'natural product' has been used to describe any substance obtained from nature,[1] such as the biological part of an organism, extracts, formulations, and isolated chemical compounds, including those obtained by total synthesis. In their narrower definition of being chemical compounds from nature, natural products are classified as either primary or secondary metabolites.[2,3]

Primary metabolites refer to those chemical compounds that are essentially encountered in all living organisms. In effect, they are necessary for the life, growth and reproduction of the organism. These include carbohydrates, fatty acids, amino acids and nucleic acids.[2,3] Carbohydrates are integral components of membranes of cells and cell organelles, the polysaccharide forms serve as cell walls of plants, fungi, and microorganisms. Triglycerides and phospholipids of cell membranes are formed from fatty acids. The polar and non-polar components of fatty acids provide cell membranes with such architecture that ensures coordination and regulation of cellular processes. Enzymes, which regulate basic cellular functions, are proteins formed from amino acids. Nucleic acids (DNA and RNA), formed from nitrogenous bases (adenine, guanine, thymine, uracil and cytosine), monosaccharides and a phosphate group, give rise to chromosomes, the genetic 'storehouse' of every organism.

Primary metabolites undergo chemical processes, which may generally comprise synthesis of new ones from already existing compounds, degradation of old compounds to small or simpler molecules, and interconversion of one compound to another. These chemical processes, called primary metabolism, proceed by almost the same pathway per the type of primary metabolite in all living organisms. For example, metabolism of carbohydrates occurs by glycolysis and the Krebs cycle, fatty acids by β-oxidation, protein syntheses from amino acids, and so on.[4]

Secondary metabolites, unlike primary metabolites, are less abundant in nature. They comprise chemical compounds that are not directly concerned with the life, growth and reproduction of an organism. These compounds play very important evolutionary roles that ensure the continued

survival of a given organism. For example, pheromones are responsible for many and diverse social communications among specific groups of organisms, toxins are produced for protection from a predator, venoms are produced to catch a prey, repellants deter other organisms, which may compete for the same nutrients, siderophores facilitate efficient transportation of scarce nutrients from the environment, etc. Secondary metabolites are therefore unique to a group of organisms, a peculiar trait of a given taxonomic classification.[5]

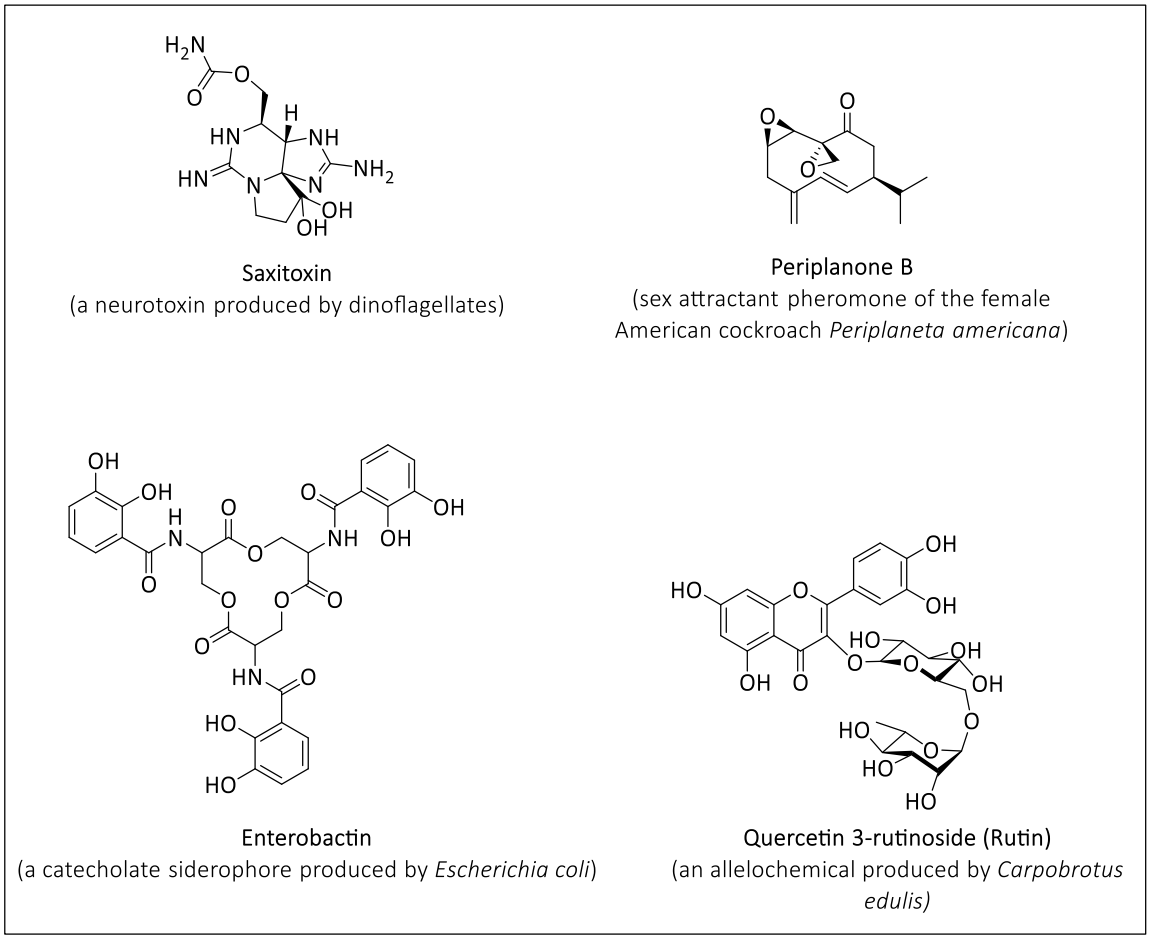

Figure 1.1: Examples of secondary metabolites

The products of the primary metabolic processes photosynthesis, glycolysis and the Krebs cycle serve as intermediates/precursors of secondary metabolic pathways leading to secondary metabolites. The metabolites obtained from principal primary metabolism, including their intermediate/precursor, which serve as building blocks from which secondary metabolites are synthesized are summarized in Table 1.1.[4]

Table 1.1: Secondary metabolites from primary metabolism		
Intermediate from primary metabolism	Precursor of secondary metabolism	Secondary metabolite
Acetyl-CoA	Acetate	Phenols Prostaglandins Macrolide antibiotics Fatty acids
Shikimic acid	Shikimate	Phenols Cinnamic acid derivatives Lignans Alkaloids
Acetyl-CoA	Mevalonate	Terpenoids Steroids
Pyruvic acid and glyceraldehyde 3-phosphate	Methylerythritol phosphate	Terpenoids Steroids
Krebs cycle intermediates Shikimate intermediates	Amino acids	Peptides Proteins Alkaloid antibiotics

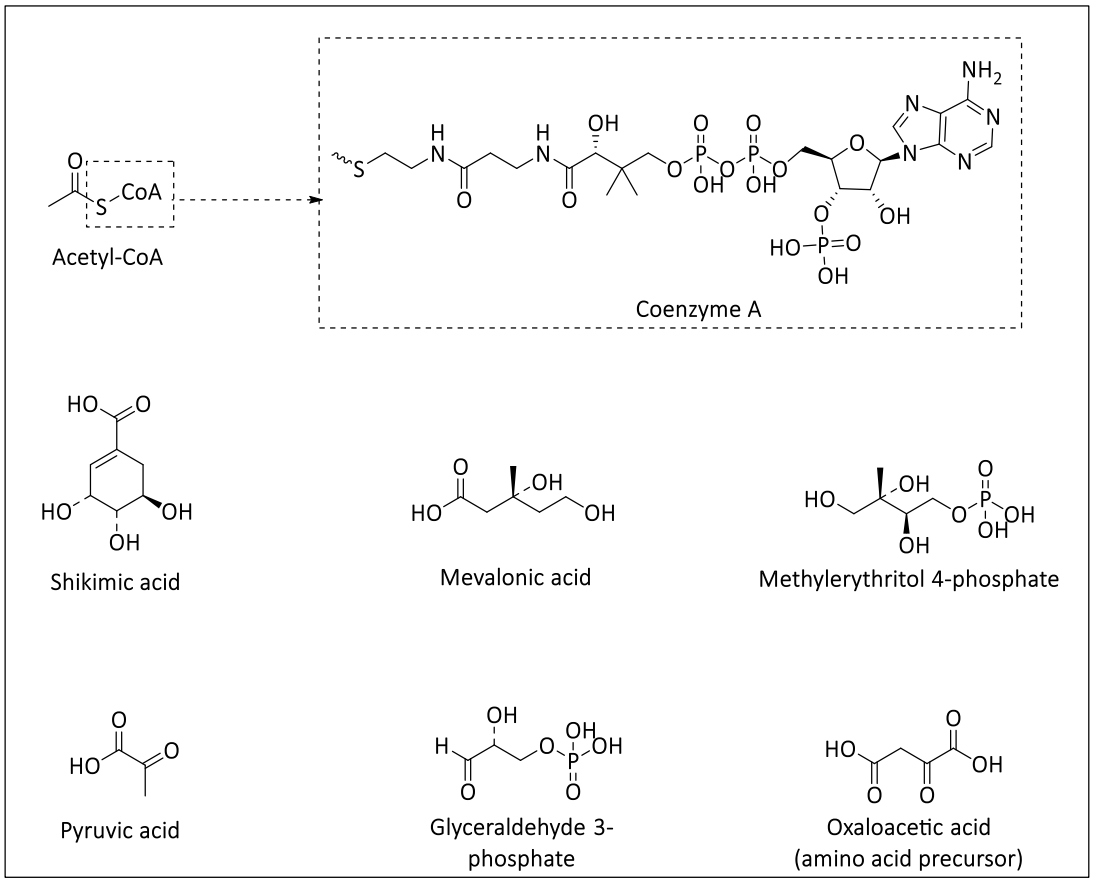

Figure 1.2: Major precursors of secondary metabolism

A natural product may comprise similar or a mixture of different building blocks. For example, papaverine, an opium alkaloid, is used as a drug for relaxation of cardiac and smooth muscles. From a biosynthesis perspective, the structure of papaverine is elucidated as arising from two L-tyrosine amino acids possessing the C_6C_2 and C_6C_2N building blocks (Figure 1.2). The C_6C_2 unit is formed from loss of the amino group from one of the molecules to give the C_6C_3 unit followed by a one carbon degradation, while decarboxylation of the other molecule leads to the C_6C_2N scaffold. The four methoxy (C_1) groups are the result of four L-methionine amino acids.[4]

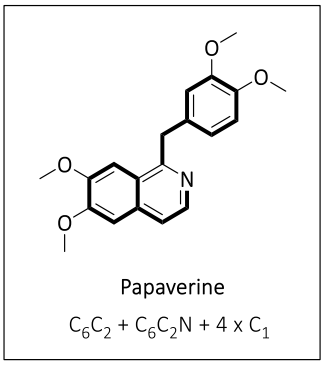

Figure 1.3: Building blocks of papaverine[4]

The anticancer drug vinblastine (Figure 1.4) offers another example of elucidating the structure of a natural product based on the building blocks from which it was made. In this example, the building blocks are not all easily discernible as some have undergone transformations. Vinblastine is a terpenoid indole alkaloid produced by *Catharanthus roseus*. It is biosynthesized from precursors from the methylerythritol phosphate (MEP) and shikimate pathways (Figure 1.5). Although the indole.C_2N scaffold is obvious, the two isoprenyl (C5) units from geraniol are lost through molecular transformations leading to secologanin and both vindoline and catharanthine.[6]

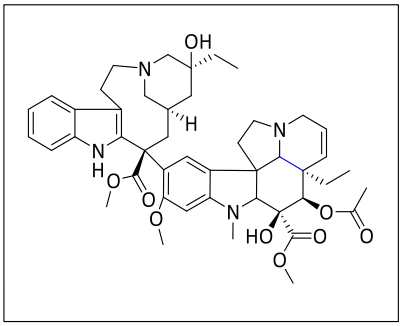

Figure 1.4: Chemical structure of vinblastine

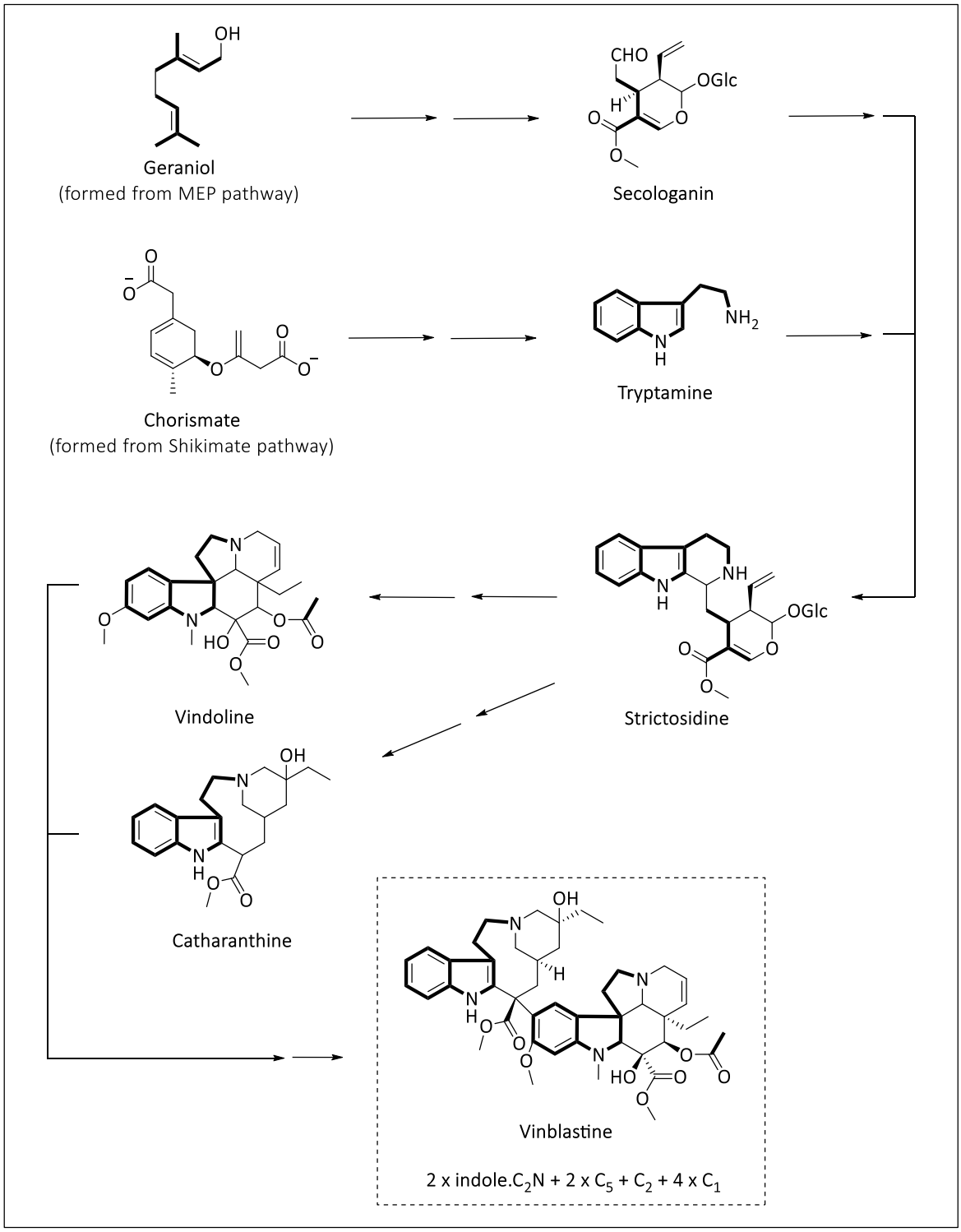

Figure 1.5: Biosynthetic pathway of vinblastine[6]

1.2 Pharmaceutical prospects of natural products

The use of extracts, concoctions, potions, and unrefined substances derived from biological sources to address the problem of diseases dates back several thousands of years. Indeed, several pharmacopoeia record the use of parts or whole plants for disease remedies, for example. Natural sources of 'drugs' or agents for treatment of diseases include plant, animals, and microbes. Although the use of whole organisms or parts of whole organisms for disease treatment is still common in indigenous/traditional medicine all over the world, many pure chemical compounds isolated from natural sources have made it as marketable drugs (Figure 1.6).

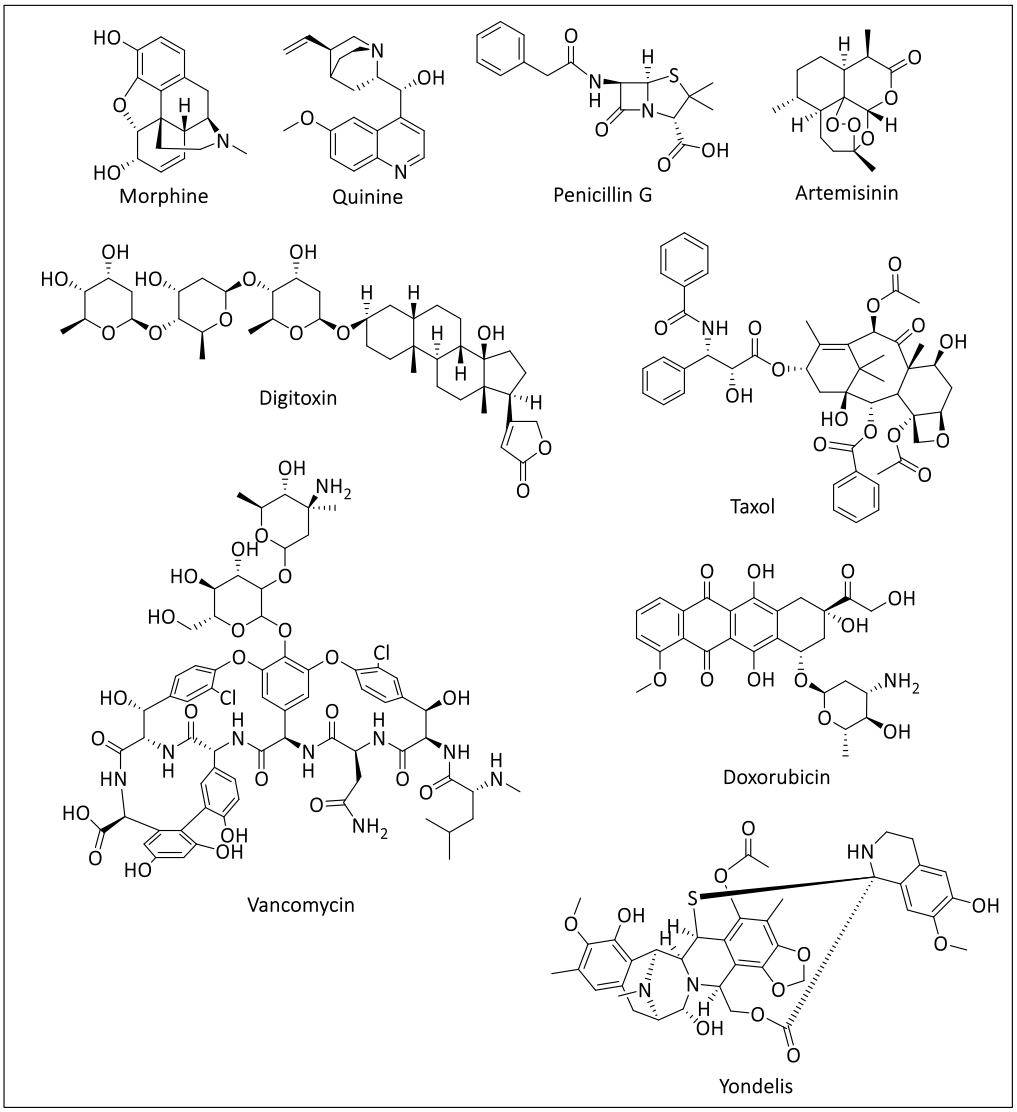

Figure 1.6: Some unaltered natural products on the market as drugs

Many other drug candidates of natural origin or related to natural products are in different stages of pharmaceutical development. In their recent review on "*Natural products as Sources of New Drugs from 1981 to 2014*",[7] Newman and Cragg report the continual significance of natural products in drug discovery. Natural products and natural product-related compounds contribute to about 51% of all new drugs approved in the period under study. However, this has increased to 65% of all approved small molecule drugs (Figure 1.7 and 1.8).

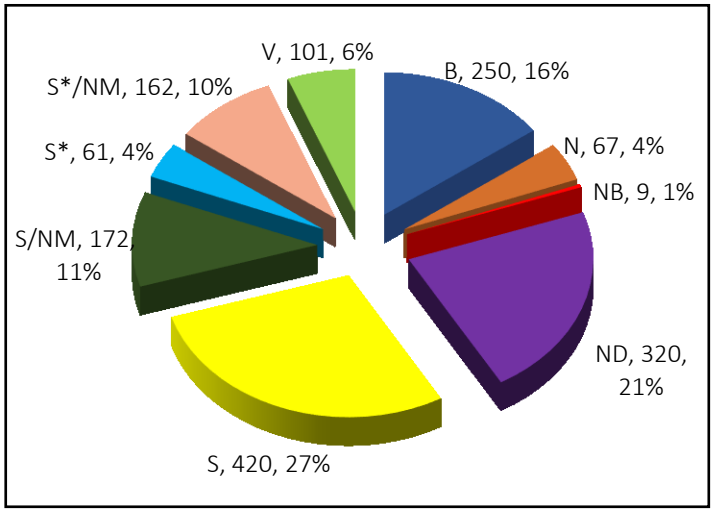

Figure 1.7: All new approved drugs 1981 – 2014; *n* = 1562[7]
(N = Unaltered natural product; NB = Botanical drug (defined mixture); ND = Natural product derivative; S = Synthetic drug; S* = Synthetic drug (natural product pharmacophore); NM = Natural product mimic; V = Vaccine; B = Biological macromolecule)

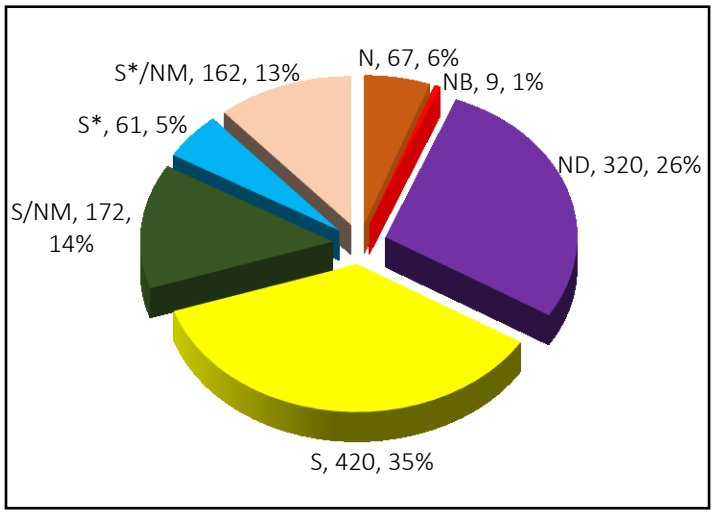

Figure 1.8: All small molecule approved drugs 1981 – 2014; *n* = 1211[7]

The success of natural products over 'purely' synthetic compounds as drugs can be attributed to a number of factors[8]: firstly, natural products are made by proteins (enzymes) in specific binding/active site in the structure of the protein and hence have inherent binding scaffold(s) in their chemical structure complementary to the enzyme active site. Since all organisms originated from a common ancestor and evolved to their current complex forms from less complex ones, very different organisms may share very similar genes or gene clusters. Furthermore, because a given gene cluster(s) may be involved in the synthesis of several proteins/enzymes, a natural product, made by a given enzyme, is able to bind to similar enzyme classes or very diverse ones arising from that gene cluster(s). A natural product formed from a peptide substructure in the enzyme of one organism may well bind in another organism which bears a similar peptide substructure in a similar enzyme or a completely different one. While the binding of a natural product to a given enzyme may result in no significant pharmacological effect, a similar binding to a different enzyme can cause very significant perturbation in the enzyme's macromolecular structure and lead to 'good or adverse' pharmacological effect. Based on the molecular complementarity of a natural product to the enzyme that made it, and the similarity in peptide substructures amongst similar or different enzymes, natural products can have different medicinal effects in different organisms.[8]

Secondly, synthesized by enzymes, there is no doubt natural products possess such intriguing structural qualities well suited for biological moieties. They are usually three-dimensional in conformation while having configurations that are well designed to fit biological targets and bypass complex cellular membranes. Natural products have therefore been a good starting point in medicinal chemistry and drug discovery explorations. Structural variabilities encountered in natural products range from a few daltons in size to very complex and huge peptides (>1000 Da). Most have stereocenters and are overall chiral molecules. Sometimes, only one stereoisomer is sensitive to the target while the other isomer may be totally inactive or toxic to the organism. With many heteroatoms, natural product molecules possess several many hydrogen bond donors and acceptors. The molecules could possess scaffolds that ensure non-polar interactions and ionic moieties, which encourage interaction with polar scaffolds in biological targets. Natural products,

therefore, occupy a wide chemical space that gives them the advantage over synthetic compounds to have medicinal properties.[8,9]

Thirdly, the physiological/pharmacological significance of a natural product can be understood from the standpoint of its importance to the producing organism, both to its continual livelihood and ecological importance in ensuring continuous thriving of the organism over its competitors. Evolution in organisms has not only been witnessed in their morphological and physiological makeup but also in the natural products they produce. In fact, the natural products produced by an organism is a consequence of many years of evolving secondary metabolic processes, and hence it can be argued to be the reason for the morphological and physiological evolution observed in the organism. Evolution therefore provides a basis for observed biomedical importance of natural products.[8]

The penicillins and other competitive secondary metabolites offer an example of the evolutionary and ecological significance of natural products.[8] Penicillin, a β-lactam antibiotic, was discovered in 1928 in a serendipitous event to inhibit bacterial growth. Alexander Fleming writes, "*It was noticed that around a large colony of a contaminating mould the staphylococcus colonies became transparent and were obviously undergoing lysis*".[10] It was his hypothesis that a "*bacteriolytic substance*" produced by the mould (*Penicillium chrysogenum*) inhibited the growth of *Staphylococci* that inspired scientific research leading to the natural product penicillin. In another example, capsaicin is a natural product produced by plant species of the genus *Capsicum*. It is an irritant for mammals, producing a burning sensation when it comes into contact with any tissue. The ecological importance of capsaicin is well understood as it promotes dispersion of seeds by birds rather than humans, for example, thereby ensuring species proliferation, which is an evolutionary advantage. Whereas humans crush the seeds as they feed on the fruits thereby preventing species propagation, the seeds are unharmed in the digestive tract of birds. Birds provide a greater evolutionary advantage to the chili peppers than humans. The vanilloid receptor TRPV1 is common to both mammals and birds, although birds have a mutated form. From an evolutionary point of view, the chili peppers have adapted to producing capsaicin which is sensitive to the TRPV1 in mammals resulting in the burning sensation and discouraging feeding on the fruits,

while the mutated form of TRPV1 in birds is not sensitive to capsaicin. Thus, birds are attracted to the fleshy and brightly coloured fruits of chilies, becoming efficient dispersers of the seeds.[8,11–13]

In view of the foregoing reasons, most drug discovery campaigns have focused on developing therapeutic agents inspired by natural products, although this trend has declined in recent times. Evidently, this approach has yielded more clinical drugs than purely synthetic/combinatorial chemistry drug discovery campaigns (Figures 1.7 and 1.8) as one would note that of the 65% of approved small drugs related to natural products, only 6% (67 drugs in 34 years) are unaltered natural products (Figure 1.8) while 58% are drugs inspired by natural products.[7] This data emphasizes the important contribution of organic synthesis in drug discovery despite the approval of only three drugs from *de novo* combinatorial chemistry; specifically, organic syntheses aimed at derivatization and mimicking of a natural product [26% (ND) and 27% (NM), respectively] are the major contributors of approved drugs on the market. Such an approach requires identifying the pharmacophore in the natural product, followed by synthetic derivatization to explore the structure-activity relationship (SAR) profiles of analogues to understand the biological target while searching for a more potent analogue than the natural product. Many successful drugs developed from this approach include the 4-aminoquinolines, penicillins, artemisinins, etc (Figure 1.9).

Drug discovery from purely natural product sources did experience a down turn in popularity in the 1990s and early 2000s due to its drawbacks of re-isolation of already existing compounds, paucity of isolated pure and active compounds, ecological and ethical concerns of collection of large amounts of the producing organism, structural complexities, which discourage synthesis to increase yield, the labour intensive nature of isolation of minute quantities of active compounds and accurate characterization of their complex structures thereof, and the 'incompatibility' of natural product extracts and semi-purified fractions for high throughput screening (HTS) technology .[14] Indeed, these challenges in natural product-based drug discovery are not cost and time efficient for pharmaceutical companies, which resorted to combinatorial chemistry in the 1990s, hence abandoning their natural products drug discovery campaigns and repositories. However, after several years of very low productivity of *de novo* combinatorial chemistry, in terms of approved drugs on the market, novel synthetic strategies/approaches (discussed in Section 1.3

below) based on natural product pharmacophores or their mimetics are proving to be useful. It has become evident, therefore, that sustainability of drug discovery campaigns in industries and academic research groups would have to integrate these two sectors of research namely, the continual search for new chemical entities through 'classical' natural products research and the medicinal chemistry explorations of synthetic derivatizations of existing natural products, natural product pharmacophores and structural mimetics of natural products. This approach promises to deliver safe and more efficacious drugs towards meeting the world's demand for sustainable health.

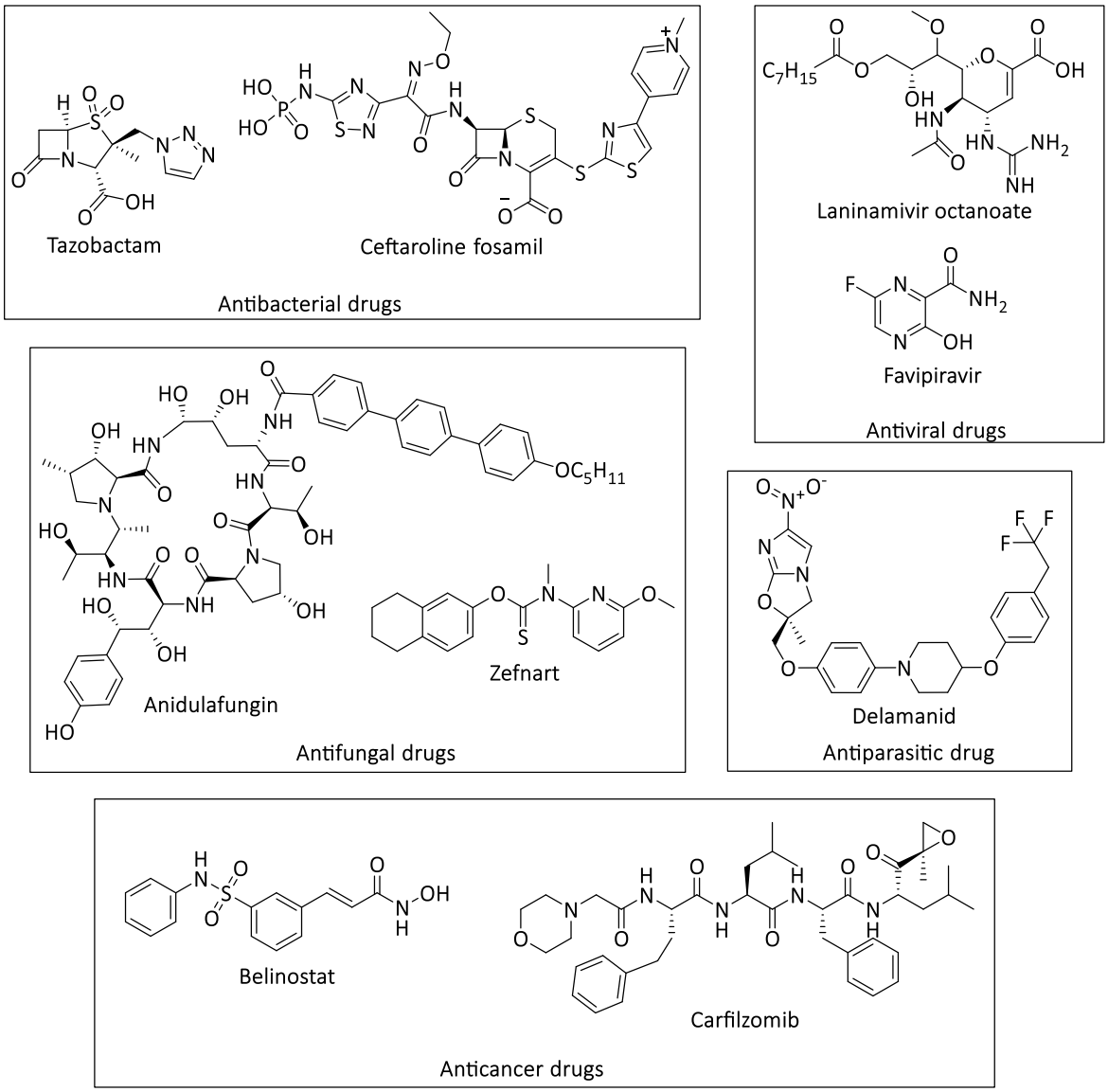

Figure 1.9: Some ND and NM approved drugs from 2010 – 2014[7]

1.3 Privileged scaffolds in natural products and medicinal chemistry

As already indicated in Table 1.1, the products from primary metabolism, acetates, shikimates, mevalonates, methylerythritol phosphate and amino acids, are the precursors of secondary metabolism leading to secondary metabolites. For example, L-methionine is the source of a single carbon atom (C_1) in natural products, for example OCH_3, NCH_3, SCH_3, and OCH_2O (methylene dioxy), etc. A two-carbon unit (C_2) is obtained from acetyl-CoA. Mevalonic acid and methylerythritol phosphate are the sources of the isoprenyl (C_5) unit of terpenoids and steroids. Shikimic acid, from which L-phenylalanine, L-tyrosine and L-tryptophan are obtained, is the source of aromatic building blocks in natural products. Loss of the alpha amino group from L-phenylalanine and L-tyrosine will both give the phenylpropyl (C_6C_3) unit, which can further degrade by loss of a carbon or two to give the C_6C_2 or C_6C_1 units, respectively. However, the phenylethylamine (C_6C_2N) unit is formed from these amino acids by loss of the carboxyl group. L-tryptophan is the source of 'indole.C_2N' scaffold arising from loss of the carboxyl group. Pyrrolidine (C_4N) and piperidine (C_5N) building blocks are obtained from L-ornithine and L-lysine, respectively.[4] Their presence in natural products confers the advantage of effective binding interactions with several protein active sites and the ability to possess a wide variety of biological activities.

Indeed, natural products are 'privileged' chemical structures in medicinal chemistry and drug discovery explorations. "Privileged scaffolds" are molecular frameworks (or substructures) that are seemingly capable of serving as ligands for a diverse array of receptors[15] and with judicious modification of such structures could provide a viable alternative in the search for new receptor agonists and antagonists[16] (Figure 1.10 – 1.12). The concept of privileged scaffolds has become useful in the advent of all the seemingly unsurmountable challenges encountered in discovering novel drugs directly from natural products[14] and the 'limitations' of *de novo* combinatorial chemistry, which has demonstrated the ease and proficiency in generating large compound libraries in a short time but poor success in producing a drug on the market.[17-18] Privileged scaffolds offer the medicinal chemist the opportunity to explore diverse biological targets with a single scaffold; selectivity for a given biological target depends on accessary structural units on the scaffold. Once selectivity has been achieved from a small compound library, some researchers

have employed combinatorial synthesis to generate large compound libraries to further explore the target [19,20] This approach has yielded several active compounds.

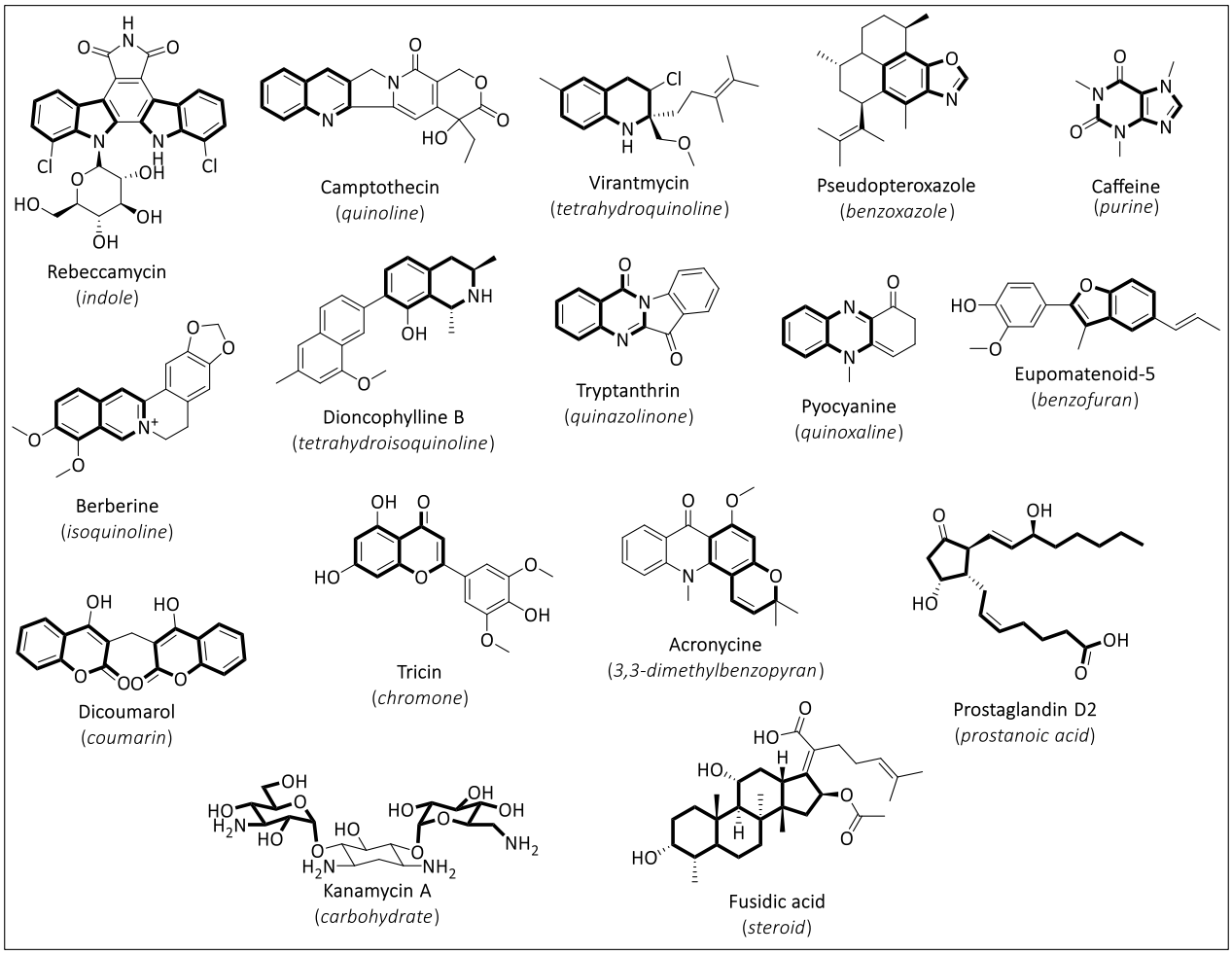

Figure 1.10: Examples of some privileged scaffolds (highlighted in bold bonds) common in natural products [21]

Exploration of privileged scaffolds for active leads has provided the medicinal chemist better and more efficient opportunities to discovering a drug than natural product-based drug discovery alone. Scaffolds identified in natural products have served as inspirations, providing the building blocks upon which analogs can be synthesized. This approach, which adopts a pharmacophore of a natural product has led to several drugs on the market (Figure 1.11). It has provided a solution to the challenges of classical natural products research. Since exploration of the chemical space around the core scaffold can afford lead compounds for various targets, the boundaries of

medicinal chemistry research seem limitless. Moreover, continued investigations into the chemical space can afford second generation drug candidates of already existing drugs, notable drug families include the penicillins and 4-aminoquinolines.

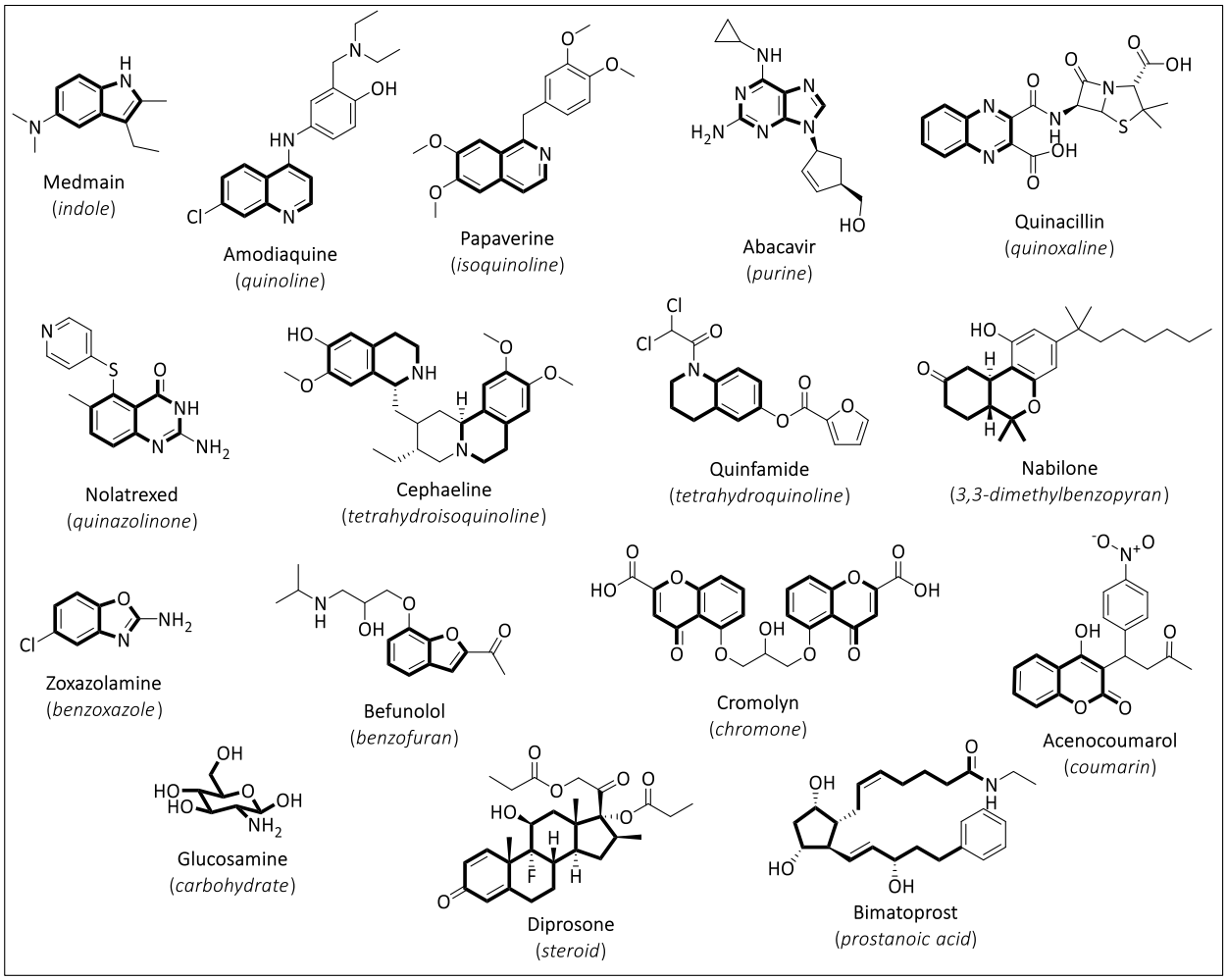

Figure 1.11: Examples of some therapeutic drugs with privileged scaffolds (highlighted in bold bonds) inspired by natural products – *example of natural product pharmacophore based drug discovery*[21]

Privileged scaffold-based drug discovery has served to synergize natural product-based drug discovery and *de novo* combinatorial chemistry and promises a solution to the limitations of its predecessors. It drives on the strength of combinatorial chemistry in being able to generate large compound libraries with increased confidence of discovering a few active drug-like leads for

potential further development into marketable drugs. The drawbacks of *de novo* combinatorial chemistry namely, the lack of diversity in the chemical space of compounds belonging to the same library and the prevalence of structural simplicity in terms of the lack of chiral centers, rigidity (less sp^3 character) of the molecular structure, low numbers of hydrophilic groups, and so on, resulted in very small numbers of druggable compounds, which fail in drug development stages. This drawback could, however, be potentially resolved by incorporation of privileged scaffolds as molecular backbones upon which compound libraries are generated.

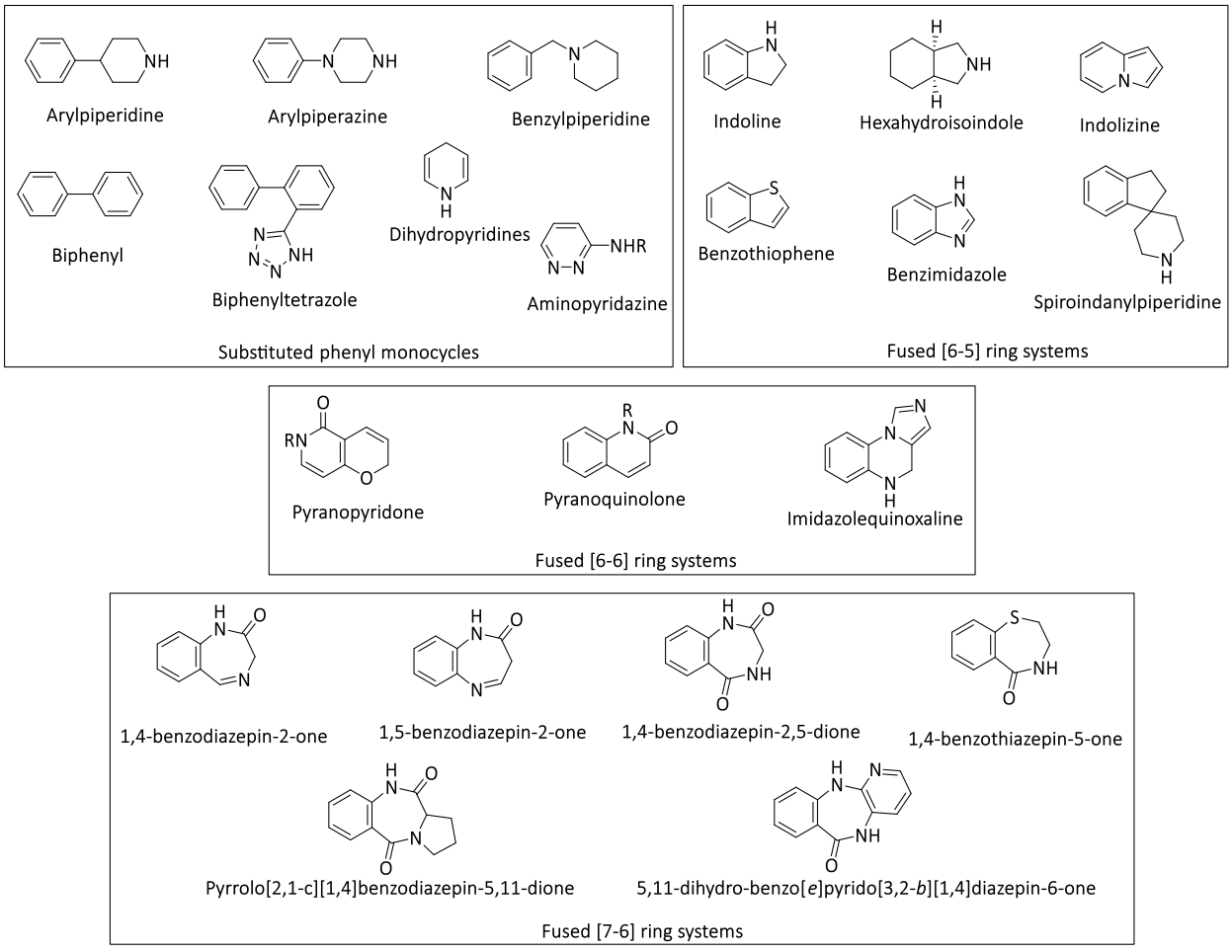

Figure 1.12: Examples of novel privileged scaffolds; discovered from medicinal chemistry explorations - *example of natural product 'mimic' based drug discovery*

In search of therapeutic agents, medicinal chemists have not been limited to privileged scaffolds clearly discerned from natural products. In fact, they have been inspired to discover and develop novel scaffolds from older ones. Moreover, some researchers have explored computational

techniques to discover such viable molecular scaffolds, which can be described as privileged.[22–28] These new scaffolds may be described as isosteres or bioisosteres of natural product pharmacophores, or molecular mimics of privileged scaffolds in natural products, or bicyclic or tricyclic frameworks with close resemblance to general natural product structural characteristics (Figure 1.12).[21,29] For example, substituted phenyl-based monocycles such as the biphenyls have been observed in many drugs with protein binding properties for several biological activities including antitumour, antihypertensive and antiatherosclerotic. The diverse biological properties observed for this group of privileged scaffolds is not surprising as one takes into account the ability of the phenyl ring to provide aromatic and hydrophobic binding interactions with proteins. The fused [6-5] ring systems of indoline, indolizine, and hexahydroisoindole and benzothiophene are based on the indole scaffold, while benzothiophene is an isostere of benzofuran. Scarcely found in natural products, the benzimidazole scaffold has resemblance to benzoxazole and purine pharmacophores and hence has such unique structural abilities to serve as mimics with diverse biological activities. The fused bicyclic [7-6] ring systems of benzodiazepines have been shown to mimic β-turns of peptides and proteins.[30,31] They have therefore been explored against diverse enzyme targets. Asperlicin, isolated from the fungus *Aspergillus alliaceus*, is a benzodiazepine containing natural product.[32–34] It occurs as the 1, 4-benzodiazepin-5-one scaffold. A well-known selective cholecystokinin receptor CCK_A antagonist, Asperlicin has inspired the development of other antagonists of CCK_A.[35] In fact, the phrase 'privileged scaffold' proposed by Evans and co-workers in 1988 was inspired by their work on benzodiazepines.[15]

It is worth mentioning at this point some new synthetic approaches/strategies developed by some researchers aimed at discovering biologically and chemically relevant compounds with druggable properties for development into marketable drugs. These strategies, namely diversity-oriented synthesis (DOS),[36–38] biology-oriented synthesis (BIOS),[39,40] complexity to diversity (CtD) strategy,[41,42] and privileged-substructure-based DOS (pDOS),[43–46] try to resolve the lack of molecular diversity in current compound libraries to achieve more biologically active hits against diverse targets for drug discovery. Diversity-oriented synthesis (DOS) is an approach that introduces and generates, in an efficient manner, multiple molecular scaffolds within a single compound library from simple starting materials (Figure 1.13). Defined as the deliberate,

simultaneous and efficient synthesis of more than one target compound in a diversity-driven approach, DOS achieves both structural complexity and functional diversity within a library thereby increasing the chances of hits against a range of druggable biological targets and 'undruggable' ones. Molecular diversity is achieved by two synthetic pathways, firstly, the reagent-based approach in which a common starting material is reacted with different reagents to obtain distinct molecular scaffolds, and the other, the substrate-based approach where different starting materials are put through common reaction conditions to obtain distinct scaffolds.[36,47–49] Unlike traditional combinatorial synthesis, DOS libraries occupy a much wider chemical space with structural diversities observed in moieties around a common molecular framework, functional groups present, stereochemistry, and molecular skeletons.[47,48,50–52] Consequently, the DOS strategy has led to the discovery of bioactive small molecules and therapeutic agents for diverse biological targets.

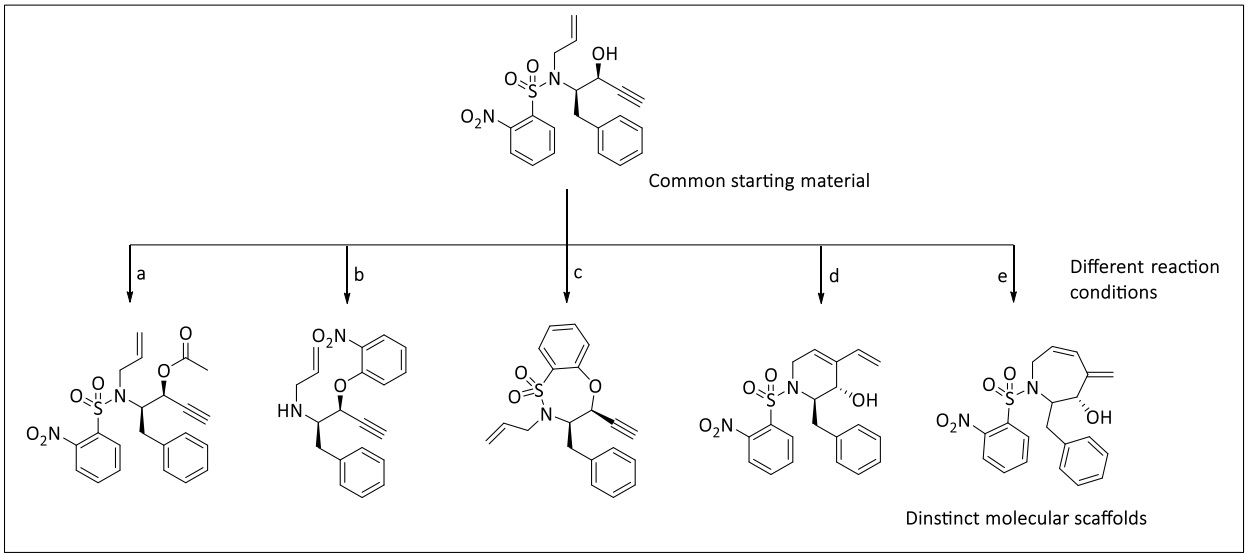

Figure 1.13: An example of reagent-based approach in DOS strategy[49,53]

Biology-oriented synthesis (BIOS) was first proposed by Waldmann and coworkers to describe an application of DOS strategy based on known biologically relevant small scaffolds derived from natural products or known drugs.[39,40] The approach focuses on generating a library of natural product-like or 'drug-like' molecules with complementarity to their protein target, while providing the added advantage of enabling bio-and cheminformatic exploration of other possible active sites

on the target or identification of new targets. BIOS was developed from the two concepts "structural classification of natural products" (SCONP) and "protein structure similarity clustering" (PSSC). In the SCONP concept, Waldman and his colleagues generated a hierarchical classification of the underlying scaffolds found in natural products that is based on cyclic frameworks and linkers.[54] Starting from complex natural products scaffolds, and applying a set of defined rules derived from organic and medicinal chemistry, the hierarchical classification is a stepwise deconstruction from complex scaffolds into smaller parent structures to arrive at a unique scaffold tree (Figure 1.14). The scaffolds represented in the hierarchy represents a well-defined chemical entity and substructure of the original natural product and provides starting points to construct new small molecules through the DOS approach to obtain a compound library of focused and biologically meaningful chemical compounds.

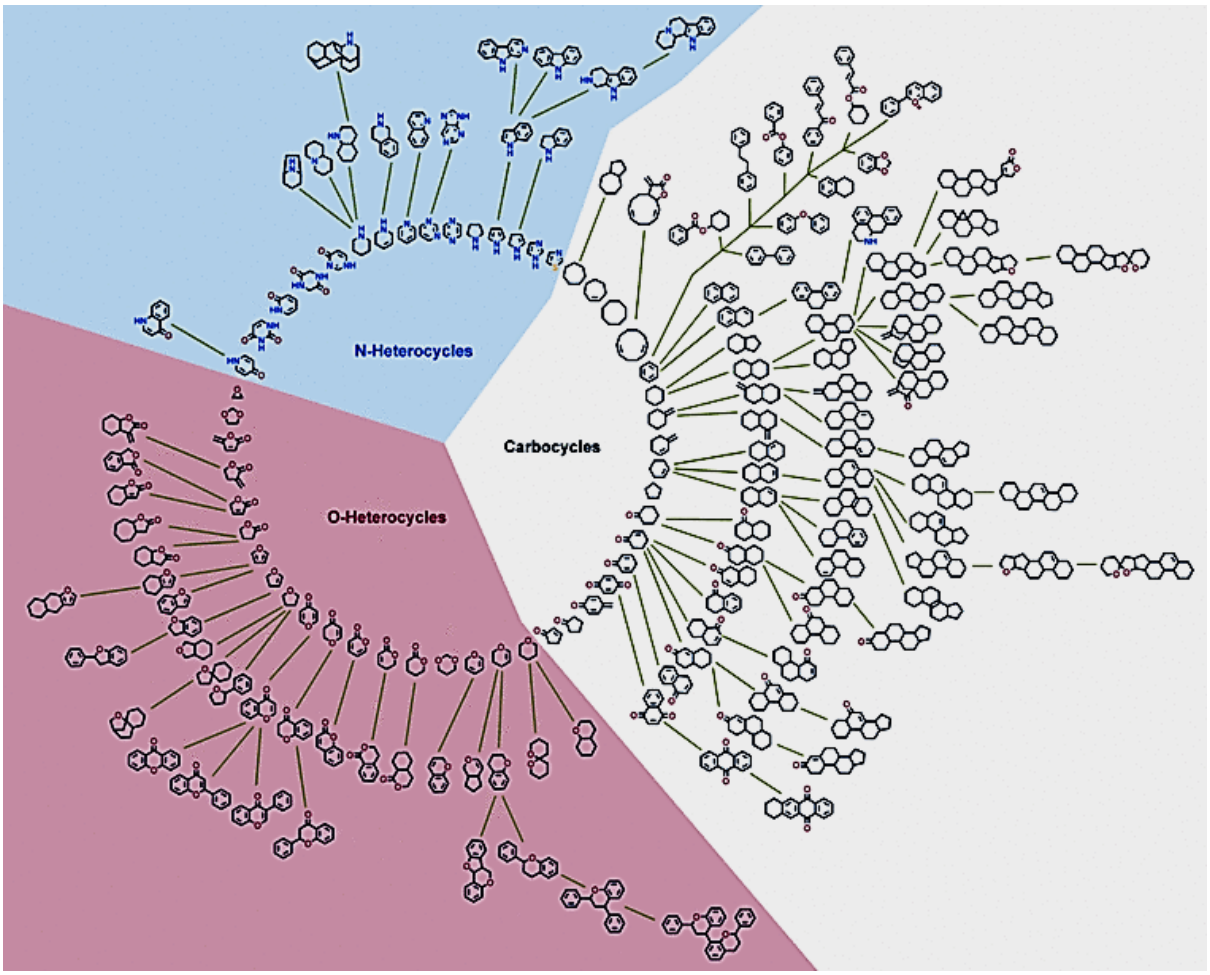

Figure 1.14: A scaffold tree generated in the SCONP[53]

In the PSSC concept, Waldmann and co-workers classified proteins, which are the major biological targets of small molecules, into clusters based on structural similarities in the ligand binding sites.[55] They explain that "*PSSC relies on bio- and cheminformatic algorithms and analysis of existing data, e.g., from the Protein Data Bank (PDB) to identify proteins in which the subfold around the ligand-binding site, the so-called "ligand-sensing core", is similar. Structures that show structural similarity of the ligand-sensing cores are assigned to one protein structure similarity cluster. If a ligand for one member of the cluster is known, the scaffold of this ligand can then be expected to be a prevalidated starting point for the synthesis of ligands for the other members of the protein cluster. Consequently, members of a library of synthesized derivatives based on the scaffold should target several members of the protein cluster*".[39] The BIOS approach merges the SCONP and PSSC concepts and generates a compound library of structurally diverse small molecules from a bioactive scaffold with prevalidated biological relevance to target proteins belonging to the same cluster.

The complexity to diversity (CtD) approach generates a collection of complex and structurally diverse small molecules from structurally complex natural products through chemical transformations which target the ring system, such as ring cleavage, ring expansion, ring fusion, ring rearrangements and combinations. Such a library contains small molecules with core scaffolds distinct from each other and from the parent natural product (Figure 1.15). The library contains molecules with 'increased' chemical space and promises to cover a larger spectrum of biological activities comparable to the parent natural product.[41,42,56]

Unlike DOS, privileged-substructure-based DOS (pDOS) employs privileged scaffolds as starting points to explore new biologically relevant chemical space. The DOS approach leads to compound collections, which occupy a wide range of chemical space but the pDOS approach, apart from having such wide range of chemical space coverage, produces libraries with high biological relevancy. Introduced by Kim and co-workers, the pDOS libraries were generated through two approaches namely, design of diverse core skeletons containing common privileged substructures, and synthesis of diverse privileged polyheterocycles using a common key intermediate.[46] Libraries generated based on pDOS have yielded some good active compounds compared to combinatorial

synthesis libraries because of the increase in chemical space coverage in the former. The biology-oriented synthesis (BIOS) libraries have high biological relevance because they are built on natural products and known therapeutic agents yet cover a much narrower biological space because it is developed with a particular cluster in mind.

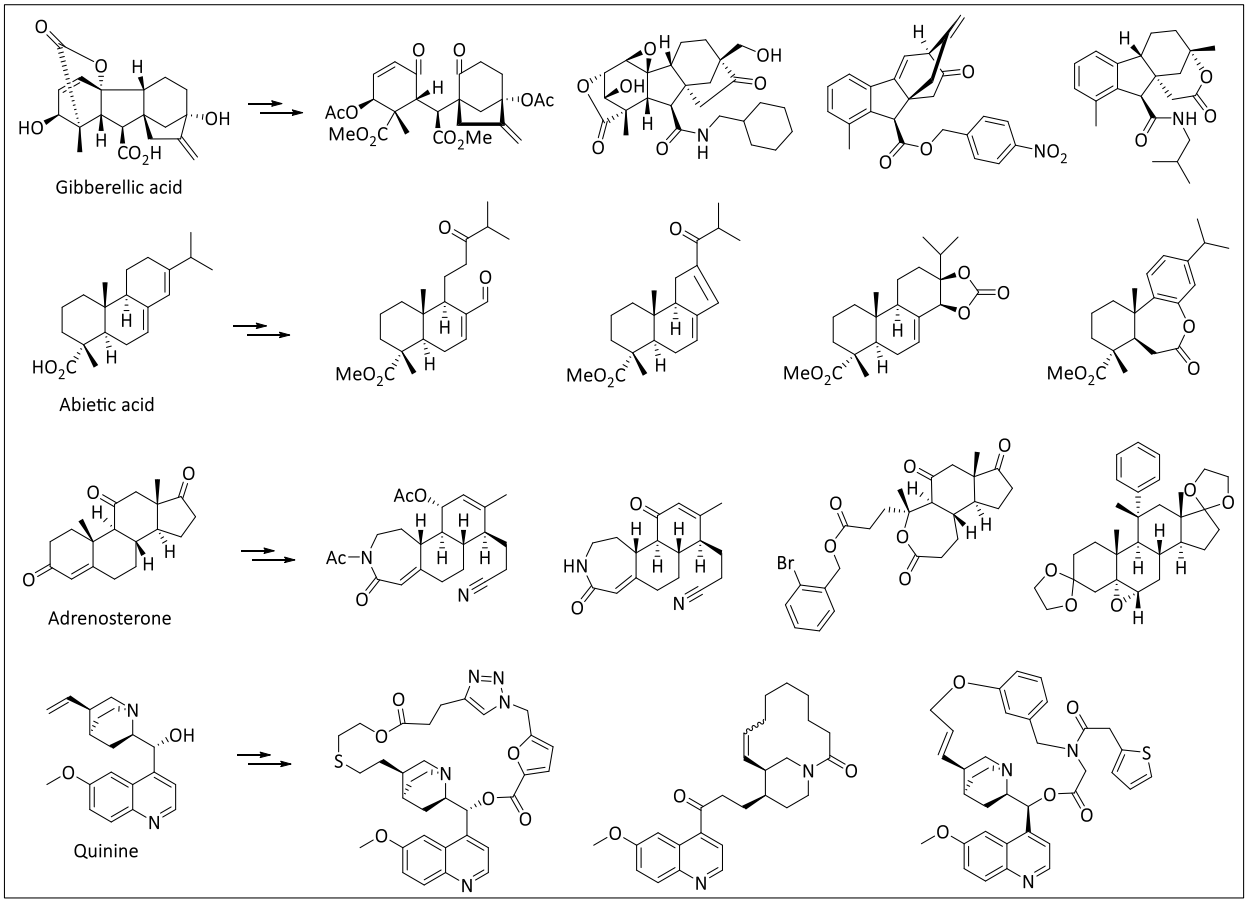

Figure 1.15: Some examples of new natural product-like molecules derived from the CtD approach[41,42,57]

The CtD approach has produced more structurally complex and chemically diverse libraries compared to the parent natural products from which they originate. However, the biological relevance of the new compounds has to be validated as they may show biological activity toward a similar target as reported for the parent natural product or a completely new one. Compared to the strategies above, developed from privileged scaffolds, pDOS libraries have both large chemical and biological space coverage together with biological relevancy. The application of DOS synthetic

methodologies on privileged scaffolds has made pDOS a powerful concept to discovering novel therapeutic agents contrary to combinatorial synthesis libraries developed from a privileged scaffold.

In conclusion, natural products and privileged scaffolds are indispensable chemical entities in medicinal chemistry and drug discovery. They serve as good starting points for discovering hit compounds for potential development into therapeutic agents. Judicious exploration of their inherent biological relevance through novel design of small molecules holds the key to discovering potent therapeutic agents for the market. For the pharmaceutical industry, it means applying novel synthetic methodologies to generate structurally complex and molecularly diverse, yet biologically relevant small molecule libraries, which hold the potential to produce more hit compounds in high throughput screening (HTS).

1.4 Scope of the present work

In view of the discussions presented in the sections above, as part of the continual search for bioactive new chemical entities, globally, the present work is a report on a 'classical' natural products research conducted on two classes of marine organisms, a red alga (belonging to the genus *Laurencia*) and two marine invertebrates (belonging to the genera *Halichondria* and *Hymeniacidon*), and a medicinal chemistry exploration of the antiplasmodium and antimycobacterial (against *Mycobacterium tuberculosis*) activities of semisynthetic derivatives of the natural product fusidic acid and the benzimidazole natural product structural mimetic.

The marine environment has been a source of novel and bioactive chemical entities. With the seas and oceans occupying close to 70% of the earth's surface, the marine ecosystem is home to rich flora and fauna biodiversity not found on land. Barely 50 years ago since their chemical diversity gained intense exploration, marine organisms have afforded some very important and useful therapeutic agents, currently in different stages of drug development (Figure 1.16). Marine algae and marine invertebrates are the most researched marine organisms.[58]

Marine algae are a prolific source of new bioactive chemical entities. They have produced such novel molecular backbones with intriguing structural characteristics including polyhalogenation.

Chapter two of this thesis is a report on the chemical investigation of a newly identified species of the red algal genus *Laurencia*. In the family Rhodomelaceae, *Laurencia* is the most researched because it is a prolific source of halogenated terpenoids, C-15 acetogenins and indoles. Notable biological activities reported for *Laurencia* secondary metabolites include cytotoxicity, antibacterial, antiviral, antifouling and anti-insecticidal activities. The results from the chemical investigation of the new red algal species *Laurencia alfredensis* is presented herein as our published article in the journal '*Molecules*' (belonging to Molecular Diversity Preservation International (MDPI)) titled, "*Isolation, Characterization and Antiproliferative activity of new metabolites from the South African endemic red algal species Laurencia alfredensis*".[59]

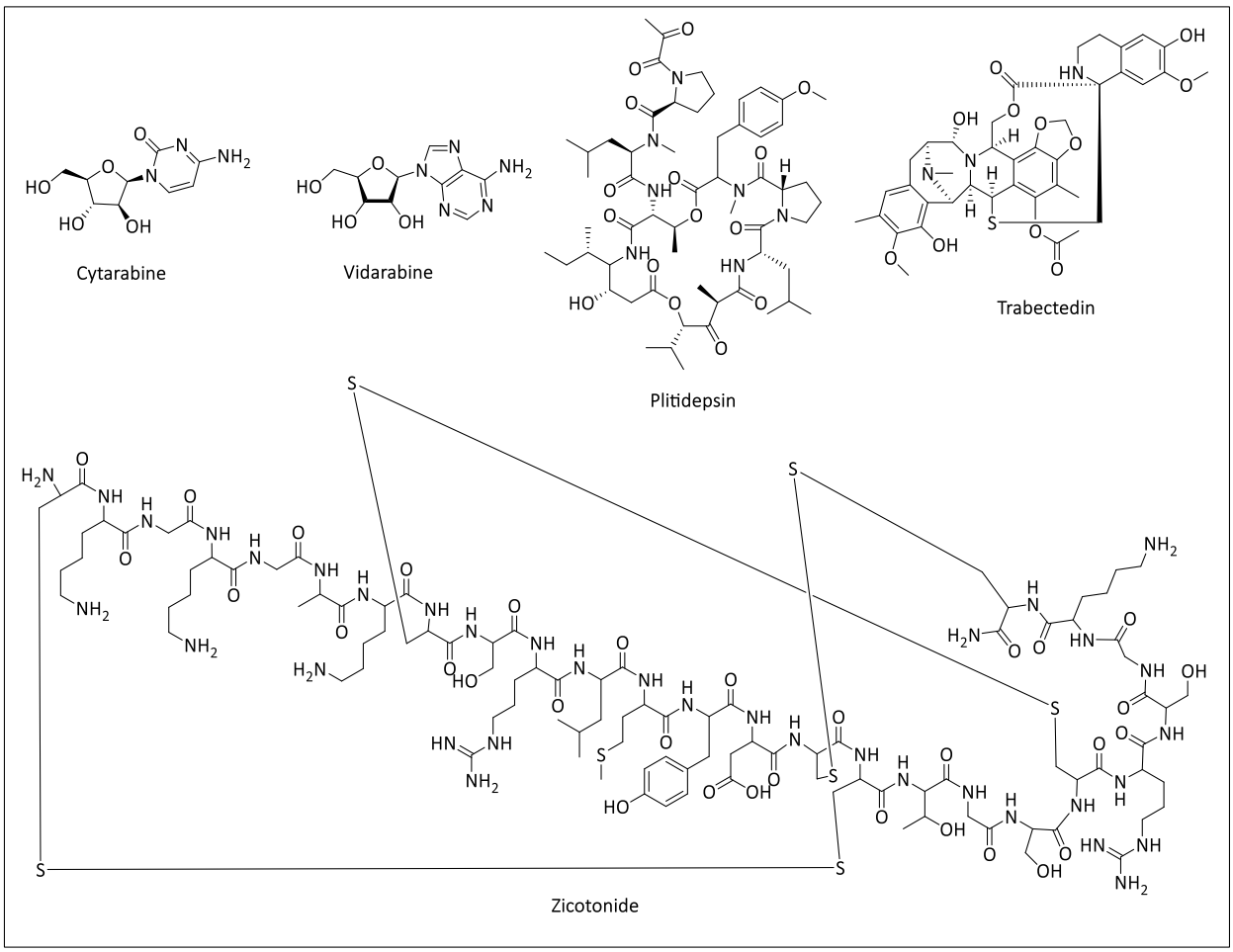

Figure 1.16: Some marine secondary metabolites as drugs

Marine invertebrates of the phylum Porifera (sponges) are sessile water filters, which feed on small floating organisms in sea water. Their rich chemical diversity and biologically active

secondary metabolites have been attributed to their life forms, being sessile and serving as home to numerous microbial symbionts. Chapter three is an account on the chemical investigations conducted on two sponges identified as *Halichondria* and *Hymeniacidon* species. Although members of these two genera have been well researched, our interest in them stems from the fact that firstly, they were collected from unexplored (from a natural products perspective) Prince Edwards Islands and Marion Islands in the southern oceans of South Africa in the vicinity of the ice-cold continent of Antarctica and, secondly, not much literature is reported on the chemical diversity of sponges from the continent. It was hypothesized that, as reported for species from the genera from other parts of the world, the two sponges collected from the extreme cold environment of Antarctica will afford new and intriguing biologically active chemical entities.

Many discoveries of therapeutic agents, as emphasized already, have come about by medicinal chemistry explorations of bioactive natural products and privileged scaffolds. The aim of these explorations has been to discover more potent, safe and efficacious agents for use as medicines. In the many cases when they are unsuccessful as drugs, due to unsatisfactory pharmacokinetic properties, for example, such agents have mostly exhibited better biological activity to serve as leads for future explorations against the intended target or a completely different one. The latter is exemplified in Chapter four in the natural product fusidic acid which is a commercially available natural product used as a topical drug against a number of gram positive bacterial infections. With unique structural properties that makes it the most potent of fusidane class of antibiotics, our research group has conducted structure-activity relationship (SAR) studies through semisynthetic derivatizations to reposition fusidic acid as an antimycobacterial agent against *Mycobacterium tuberculosis*. On the other hand, a three dimensional quantitative structure-activity relationship (3D-QSAR) studies on fusidic acid, followed by synthesis of the proposed analogs, led to fusidic acid analogs with superior antiplasmodial activity in the sub-micromolar range compared to fusidic acid. Chapter four is an account of further SAR investigations conducted on the most active analogue.

The antiplasmodial properties of the benzimidazole privileged scaffold is well reported in the literature, having been explored by various groups. Notable therapeutic agents containing the

benzimidazole core scaffold include Albendazole, Fenbendazole, Oxfenbendazole, Thiabendazole, Mebendazole, Omeprazole, lansoprasole, and Pantoprasoleetc. In Chapter five, the antiplasmodial and antimycobacterial properties of benzimidazole derived small molecules by incorporation of phenolic Mannich side chain amines, as observed in amodiaquine, was explored. The results obtained are intended to be the beginning of future SAR investigations towards antiplasmodial leads based on the privileged benzimidazole scaffold.

1.5 References

(1) All Natural. Nat. Chem. Biol. 2007, 3, 351–351.

(2) Kliebenstein, D. J. Secondary Metabolites and Plant/Environment Interactions: A View through Arabidopsis Thaliana Tinged Glasses. Plant, Cell Environ. 2004, 27 (6), 675–684.

(3) Karlovsky, P. Secondary Metabolites in Soil Ecology; 2008; pp 1–19.

(4) Dewick, P. M. Medicinal Natural Products: A Biosynthentic Approach; 2002.

(5) Pichersky, E.; Gang, D. R. Genetics and Biochemistry of Secondary Metabolites in Plants: An Evolutionary Perspective. Trends in Plant Science. 2000, pp 439–445.

(6) Yu, R.; Zhu, J.; Wang, M.; Wen, W. Biosynthesis and Regulation of Terpenoid Indole Alkaloids in Catharanthus Roseus. Pharmacogn. Rev. 2015, 9 (17), 24.

(7) Newman, D. J.; Cragg, G. M. Natural Products as Sources of New Drugs from 1981-2014. Journal of Natural Products. 2016, pp 629–661.

(8) Mander, L.; Liu, H.-W. Comprehensive Natural Products II Chemistry and Biology; 2010.

(9) Stratton, C. F.; Newman, D. J.; Tan, D. S. Cheminformatic Comparison of Approved Drugs from Natural Product versus Synthetic Origins. Bioorg. Med. Chem. Lett. 2015, 25 (21), 4802–4807.

(10) Fleming, A. On the Antibacterial Action of Cultures of a Penicillium, with Special Reference

to Their Use in the Isolation of B.Influenzae. Br. J. Exp. Pathol. 1929, 10 (1923), 226–236.

(11) Tewksbury, J. J.; Nabhan, G. P. Seed Dispersal. Directed Deterrence by Capsaicin in Chilies. Nature 2001, 412 (6845), 403–404.

(12) Appendino, G. Capsaicin and Capsaicinoids. In Modern Alkaloids: Structure, Isolation, Synthesis and Biology; 2007; pp 73–109.

(13) Appendino, G.; Minassi, a; Pagani, a; Ech-Chahad, a. The Role of Natural Products in the Ligand Deorphanization of TRP Channels. Curr. Pharm. Des. 2008, 14 (1), 2–17.

(14) Kingston, D. G. I. Modern Natural Products Drug Discovery and Its Relevance to Biodiversity Conservation. J. Nat. Prod. 2011, 74 (3), 496–511.

(15) Evans, B. E.; Rittle, K. E.; Bock, M. G.; DiPardo, R. M.; Freidinger, R. M.; Whitter, W. L.; Lundell, G. F.; Veber, D. F.; Anderson, P. S.; Chang, R. S. L.; et al. Methods for Drug Discovery: Development of Potent, Selective, Orally Effective Cholecystokinin Antagonists. J. Med. Chem. 1988, 31 (12), 2235–2246.

(16) Duarte, C.; Barreiro, E.; Fraga, C. Privileged Structures: A Useful Concept for the Rational Design of New Lead Drug Candidates. Mini-Reviews Med. Chem. 2007, 7 (11), 1108–1119.

(17) Dean, P. M.; Zanders, E. D.; Bailey, D. S. Industrial-Scale, Genomics-Based Drug Design and Discovery. Trends Biotechnol. 2001, 19 (8), 288–292.

(18) Bailey, D.; Brown, D. High-Throughput Chemistry and Structure-Based Design: Survival of the Smartest. Drug Discov. Today 2001, 6 (2), 57–59.

(19) Ding, S.; Gray, N. S.; Wu, X.; Ding, Q.; Schultz, P. G. A Combinatorial Scaffold Approach toward Kinase-Directed Heterocycle Libraries. J. Am. Chem. Soc. 2002, 124 (8), 1594–1596.

(20) Howard, A. D.; McAllister, G.; Feighner, S. D.; Liu, Q.; Nargund, R. P.; Van der Ploeg, L. H.; Patchett, A. A. Orphan G-Protein-Coupled Receptors and Natural Ligand Discovery. Trends Pharmacol. Sci. 2001, 22 (3), 132–140.

(21) Welsch, M. E.; Snyder, S. A.; Stockwell, B. R. Privileged Scaffolds for Library Design and Drug Discovery. Curr. Opin. Chem. Biol. 2010, 14 (3), 347–361.

(22) Abrous, L.; Hynes, J.; Friedrich, S. R.; Smith, A. B.; Hirschmann, R. Design and Synthesis of Novel Scaffolds for Drug Discovery: Hybrids of Beta-D-Glucose with 1,2,3,4-Tetrahydrobenzo[e][1,4]Diazepin-5-One, the Corresponding 1-Oxazepine, and 2- and 4-Pyridyldiazepines. Org. Lett. 2001, 3 (7), 1089–1092.

(23) Kombarov, R.; Altieri, A.; Genis, D.; Kirpichenok, M.; Kochubey, V.; Rakitina, N.; Titarenko, Z. BioCores: Identification of a Drug/Natural Product-Based Privileged Structural Motif for Small-Molecule Lead Discovery. Mol. Divers. 2010, 14 (1), 193–200.

(24) Smith, A. B.; Charnley, A. K.; Hirschmann, R. Pyrrolinone-Based Peptidomimetics. " Let the Enzyme or Receptor Be the Judge ." Acc. Chem. Res. 2011, 44 (3), 180–193.

(25) Araújo, A. C.; Nicotra, F.; Airoldi, C.; Costa, B.; Giagnoni, G.; Fumagalli, P.; Cipolla, L. Synthesis and Biological Evaluation of Novel Rigid 1,4-Benzodiazepine-2,5-Dione Chimeric Scaffolds. European J. Org. Chem. 2008, 2008 (4), 635–639.

(26) Lewell, X. Q.; Judd, D. B.; Watson, S. P.; Hann, M. M. RECAPRetrosynthetic Combinatorial Analysis Procedure: A Powerful New Technique for Identifying Privileged Molecular Fragments with Useful Applications in Combinatorial Chemistry. J. Chem. Inf. Comput. Sci. 1998, 38 (3), 511–522.

(27) Smith, A. B.; Favor, D. A.; Sprengeler, P. A.; Guzman, M. C.; Carroll, P. J.; Furst, G. T.; Hirschmann, R. Molecular Modeling, Synthesis, and Structures of N-Methylated 3,5-Linked Pyrrolin-4-Ones toward the Creation of a Privileged Nonpeptide Scaffold. Bioorg. Med. Chem. 1999, 7 (1), 9–22.

(28) Mason, J. S.; Morize, I.; Menard, P. R.; Cheney, D. L.; Hulme, C.; Labaudiniere, R. F. New 4-Point Pharmacophore Method for Molecular Similarity and Diversity Applications: Overview of the Method and Applications, Including a Novel Approach to the Design of Combinatorial Libraries Containing Privileged Substructures. J. Med. Chem. 1999, 42 (17), 3251–3264.

(29) Horton, D. A.; Bourne, G. T.; Smythe, M. L. The Combinatorial Synthesis of Bicyclic Privileged Structures or Privileged Substructures The Combinatorial Synthesis of Bicyclic Privileged Structures or Privileged Substructures. Chem. Rev. 2003, 103 (3), 893–930.

(30) Ripka, W. C.; De Lucca, G. V.; Bach, A. C.; Pottorf, R. S.; Blaney, J. M. Protein β-Turn Mimetics II: Design, Synthesis, and Evaluation in the Cyclic Peptide Gramicidin S. Tetrahedron 1993, 49 (17), 3609–3628.

(31) Fecik, R. A.; Frank, K. E.; Gentry, E. J.; Menon, S. R.; Mitscher, L. A.; Telikepalli, H. The Search for Orally Active Medications through Combinatorial Chemistry. Med. Res. Rev. 1998, 18 (3), 149–185.

(32) Chang, R. S.; Lotti, V. J.; Monaghan, R. L.; Birnbaum, J.; Stapley, E. O.; Goetz, M. A.; Albers-Schönberg, G.; Patchett, A. A.; Liesch, J. M.; Hensens, O. D. A Potent Nonpeptide Cholecystokinin Antagonist Selective for Peripheral Tissues Isolated from Aspergillus Alliaceus. Science 1985, 230 (4722), 177–179.

(33) Goetz, M. A.; Lopez, M.; Monaghan, R. L.; Chang, R. S.; Lotti, V. J.; Chen, T. B. Asperlicin, a Novel Non-Peptidal Cholecystokinin Antagonist from Aspergillus Alliaceus. Fermentation, Isolation and Biological Properties. J. Antibiot. (Tokyo). 1985, 38 (12), 1633–1637.

(34) Liesch, J. M.; Hensens, O. D.; Springer, J. P.; Chang, R. S.; Lotti, V. J. Asperlicin, a Novel Non-Peptidal Cholecystokinin Antagonist from Aspergillus Alliaceus. Structure Elucidation. J. Antibiot. (Tokyo). 1985, 38 (12), 1638–1641.

(35) Lattmann, E.; Billington, D. C.; Poyner, D. R.; Howitt, S. B.; Offel, M. Synthesis and Evaluation of Asperlicin Analogues as Non-Peptidal Cholecystokinin-Antagonists. Drug Des. Discov. 2001, 17 (3), 219–230.

(36) Burke, M. D.; Schreiber, S. L. A Planning Strategy for Diversity-Oriented Synthesis. Angew. Chem. Int. Ed. Engl. 2004, 43 (1), 46–58.

(37) Tan, D. S. Diversity-Oriented Synthesis: Exploring the Intersections between Chemistry and

Biology. Nat. Chem. Biol. 2005, 1 (2), 74–84.

(38) Schreiber, S. L. Organic Chemistry: Molecular Diversity by Design. Nature 2009, 457 (7226), 153–154.

(39) Kaiser, M.; Wetzel, S.; Kumar, K.; Waldmann, H. Biology-Inspired Synthesis of Compound Libraries. Cell. Mol. Life Sci. 2008, 65 (7–8), 1186–1201.

(40) Wetzel, S.; Bon, R. S.; Kumar, K.; Waldmann, H. Biology-Oriented Synthesis. Angew. Chem. Int. Ed. Engl. 2011, 50 (46), 10800–10826.

(41) Huigens, R. W.; Morrison, K. C.; Hicklin, R. W.; Flood, T. A.; Richter, M. F.; Hergenrother, P. J. A Ring-Distortion Strategy to Construct Stereochemically Complex and Structurally Diverse Compounds from Natural Products. Nat. Chem. 2013, 5 (3), 195–202.

(42) Rafferty, R. J.; Hicklin, R. W.; Maloof, K. A.; Hergenrother, P. J. Synthesis of Complex and Diverse Compounds through Ring Distortion of Abietic Acid. Angew. Chem. Int. Ed. Engl. 2014, 53 (1), 220–224.

(43) Ko, S. K.; Jang, H. J.; Kim, E.; Park, S. B. Concise and Diversity-Oriented Synthesis of Novel Scaffolds Embedded with Privileged Benzopyran Motif. Chem. Commun. 2006, No. 28, 2962.

(44) An, H.; Eum, S.-J.; Koh, M.; Lee, S. K.; Park, S. B. Diversity-Oriented Synthesis of Privileged Benzopyranyl Heterocycles from s - Cis -Enones. J. Org. Chem. 2008, 73 (5), 1752–1761.

(45) Kim, H.; Tung, T. T.; Park, S. B. Privileged Substructure-Based Diversity-Oriented Synthesis Pathway for Diverse Pyrimidine-Embedded Polyheterocycles. Org. Lett. 2013, 15 (22), 5814–5817.

(46) Kim, J.; Kim, H.; Park, S. B. Privileged Structures: Efficient Chemical “Navigators” toward Unexplored Biologically Relevant Chemical Spaces. J. Am. Chem. Soc. 2014, 136 (42), 14629–14638.

(47) Galloway, W. R. J. D.; Bender, A.; Welch, M.; Spring, D. R. The Discovery of Antibacterial Agents Using Diversity-Oriented Synthesis. Chem. Commun. 2009, No. 18, 2446.

(48) Galloway, W. R.; Spring, D. R. Is Synthesis the Main Hurdle for the Generation of Diversity in Compound Libraries for Screening? Expert Opin. Drug Discov. 2009, 4 (5), 467–472.

(49) Galloway, W. R. J. D.; Isidro-Llobet, A.; Spring, D. R. Diversity-Oriented Synthesis as a Tool for the Discovery of Novel Biologically Active Small Molecules. Nat. Commun. 2010, 1 (6), 1–13.

(50) Spring, D. R. Diversity-Oriented Synthesis; a Challenge for Synthetic ChemistsElectronic Supplementary Information (ESI) Available: Excel File of All the FDA New Molecular Entities between the Years 1998 and July 2003, and New Drug Approvals between the Years 1990 And. Org. Biomol. Chem. 2003, 1 (22), 3867.

(51) Thomas, G. L.; Wyatt, E. E.; Spring, D. R. Enriching Chemical Space with Diversity-Oriented Synthesis. Curr. Opin. Drug Discov. Devel. 2006, 9 (6), 700–712.

(52) Spandl, R. J.; Bender, A.; Spring, D. R. Diversity-Oriented Synthesis; a Spectrum of Approaches and Results. Org. Biomol. Chem. 2008, 6 (7), 1149.

(53) Pizzirani, D.; Kaya, T.; Clemons, P. A.; Schreiber, S. L. Stereochemical and Skeletal Diversity Arising from Amino Propargylic Alcohols. Org. Lett. 2010, 12 (12), 2822–2825.

(54) Koch, M. A.; Schuffenhauer, A.; Scheck, M.; Wetzel, S.; Casaulta, M.; Odermatt, A.; Ertl, P.; Waldmann, H. Charting Biologically Relevant Chemical Space: A Structural Classification of Natural Products (SCONP). Proc. Natl. Acad. Sci. U. S. A. 2005, 102 (48), 17272–17277.

(55) Koch, M. A.; Wittenberg, L.-O.; Basu, S.; Jeyaraj, D. A.; Gourzoulidou, E.; Reinecke, K.; Odermatt, A.; Waldmann, H. Compound Library Development Guided by Protein Structure Similarity Clustering and Natural Product Structure. Proc. Natl. Acad. Sci. U. S. A. 2004, 101 (48), 16721–16726.

(56) Morrison, K. C.; Hergenrother, P. J. Natural Products as Starting Points for the Synthesis of Complex and Diverse Compounds. Nat. Prod. Rep. 2014, 31 (1), 6–14.

(57) Ciardiello, J. J.; Stewart, H. L.; Sore, H. F.; Galloway, W. R. J. D.; Spring, D. R. A Novel Complexity-to-Diversity Strategy for the Diversity-Oriented Synthesis of Structurally Diverse and Complex Macrocycles from Quinine. Bioorg. Med. Chem. 2017, 25 (11), 2825–2843.

(58) Fattorusso, E.; Gerwick, W. H.; Taglialatela-Scafati, O. Handbook of Marine Natural Products; 2012.

(59) Dziwornu, G. A.; Caira, M. R.; Mare, J.-A. de la; Edkins, A. L.; Bolton, J. J.; Beukes, D. R.; Sunassee, S. N. Isolation, Characterization and Antiproliferative Activity of New Metabolites from the South African Endemic Red Algal Species Laurencia Alfredensis. Molecules 2017, 22 (4).

Chapter Two: Chemical investigation of the red algal species *Laurencia alfredensis*

2.1 General Introduction

The family of red algae (Rhodomelaceae) comprises over 1000 recognized species globally. The genus *Laurencia* (Order Ceramiales) in this family has about 285 identified species.[1] Species distribution is largely in the tropics and temperate regions, although they are widespread in the southern hemisphere (Figure 2.1).

Figure 2.1: Global distribution of the genus *Laurencia*

Species of *Laurencia* play very significant ecological roles including serving as a source of food and a habitat for microorganisms and some parasitic algae.[2–4] Although they deter profound grazing from other organisms due to their 'toxic' secondary metabolites, some grazing organisms have taken advantage, having developed appropriate mechanisms for the detoxification of the toxic principles to foster their own survival. For example, the queen conch *Strombus gigas* makes use of *Laurencia* metabolites to provide chemicals necessary for the development of its larvae, while sea hares of the genus *Aplysia* obtain their chemical defenses from ingested *Laurencia* species.[5–8]

Laurencia species have been a source of both halogenated and non-halogenated secondary metabolites. Bromine is the most common halogen in these metabolites, followed by chlorine and

then iodine. No fluorinated compounds have yet been isolated. Haloperoxidases have been identified as responsible for the biosynthesis of the halogenated metabolites in the chloroplasts.[9] They are mainly stored in cellular organelles called *corps en cerise*;[10] their absence have been attributed to the un-detection of halogenated compounds.[11–13] In a chemical defence, the metabolites are transported in intracellular vesicles from the *corps en cerise* to the cell surface where they are expelled. According to Reis and coworkers, actin microfilaments and microtubules play an underlying role in the chemical defence of red algae.[14]

2.2 Chemistry and biology of the genus *Laurencia*

2.2.1 Chemical constituents of *Laurencia*

The secondary metabolites of *Laurencia* have either carbocylic molecular backbones or aromatic backbones (indole and phenols), with or without halogen atom (s). The carbocyclics occur as terpenoids (sesquiterpenes, diterpenes and polyether triterpenes) and steroids; monoterpenes are yet to be isolated. Apart from the aromatic metabolites, another class of intriguing secondary metabolites common to the genus is the non-terpenoid C_{15} acetogenins.[15–17]

The sesquiterpenes comprise about seven different major carbon backbones. The chamigrane and related compounds are the most abundant metabolites in this class. Structurally, they are characterized by a spiro[5.5]undecane carbon skeleton (Figure 2.2).[15] There are four subclasses of the chamigranes, α-chamigrenes, β-chamigrenes, C-7-oxy chamigrenes, and the last subclass possess either a 5,10-epoxide ring system or another epoxide or a lactone ring connecting the two six-membered rings.[17]

The sesquiterpenoid class of lauranes and related compounds possess a characteristic substituted aromatic/phenyl group attached to a 1,2,3-trisubstituted cyclopentane or a 1,2-dimethylbicyclo[3.1.0]hexane system (Figure 2.2). Bromine is the most occurring halogen in lauranes, while three iodinated compounds have been isolated so far.[15,17–19] Eudesmanes, also called selinanes, have rarely been encountered in *Laurencia* species. Halogenated members of this group possess a bromine substituent at C-1, while cyclisation between between C-6 and C-8 has produced the 6,8-cycloeudesmane subclass of sesquiterpenes.

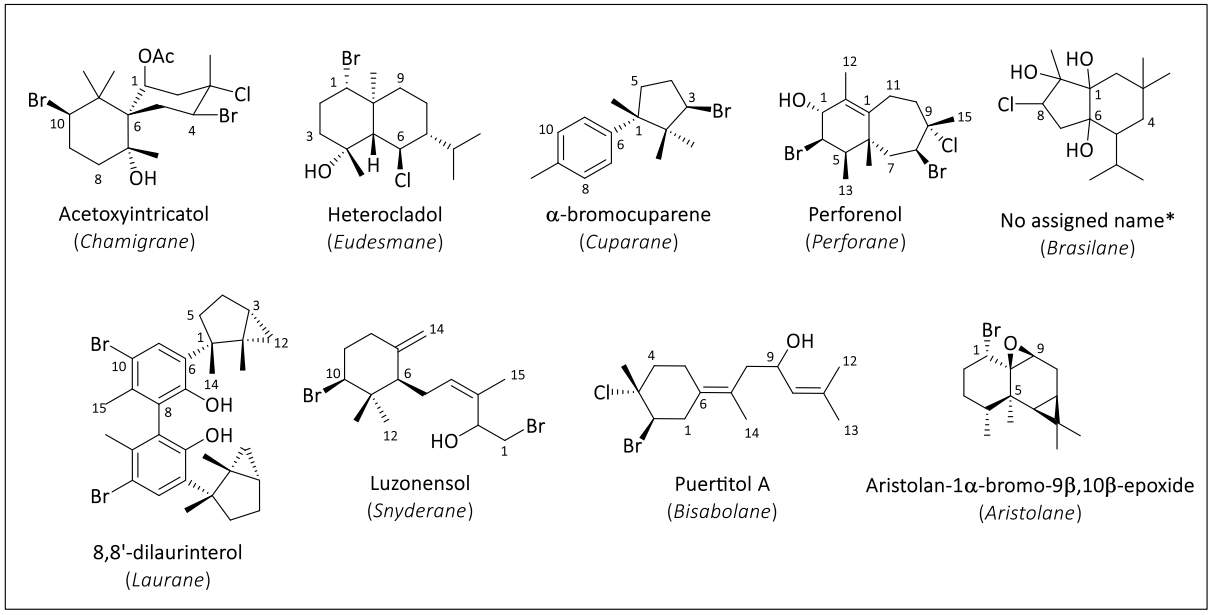

Figure 2.2: Representative sesquiterpenoid metabolites from the genus *Laurencia*[20–28]

To date, only four halogenated brasilanes have been reported.[21,29] These sesquiterpenes are characterized by a rearranged bicyclo[4.3.0]nonane carbon skeleton with a *gem*-dimethyl group at C-3, an isopropyl moiety at C-5, and another methyl substituent at C-9. A common feature of brasilanes is the presence of a tetrasubstituted double bond. Synderanes and bisabolanes, unlike brasilanes, are monocyclic compounds believed to arise from farnesane. Synderanes and related compounds are formed from C-6 to C-11 cyclisation of farnesane to give the six-membered carbocycle. Characteristic features of synderanes include C-10 bromo-substitution and Δ^6, Δ^7, $\Delta^{7,14}$, or Δ^9 unsaturated cyclohexane ring. Bisabolanes, like synderanes, possess a cyclohexane ring bearing an acyclic side chain. However, the cyclohexane is formed from a C-1 to C-6 cyclisation of farnesane. Bisabolanes and related compounds often bear bromine and chlorine atoms in a 2,3-*trans*-halide arrangement.[15,17]

Cuparanes arise from C-7 to C-11 cyclisation of the bisabolane skeleton to form a five-membered ring. The six-membered ring of some members of this class occur as phenyl rings. Cuparanes have seldom been encountered in *Laurencia*, both halogenated and non-halogenated compounds have been isolated. The most recent addition to cuparanes is the trihalogenated compound 8-deoxyalgoane isolated from *Laurencia natalensis* Kylin collected from the southern coast of South

Africa.[30] Like cuparanes, aristolanes and perforanes and related compounds represent a small group of *Laurencia* sesquiterpenes. The aristolanes arise from C-6 to C-11 cyclisation of eremophilanes, which are derived from eudesmanes. To date, only one halogenated aristolane has been isolated.[22] The perforanes, on the other hand, are believed to arise from chamigranes.[31] Members of this class are characterized by either a bicyclo[5.4.0]undecane carbon skeleton or a 4,5,6-fused tricyclic skeleton after further cyclisation of C-1 and C-9 of the seven-membered ring. Only a few halogenated compounds of perforanes have so far been isolated.

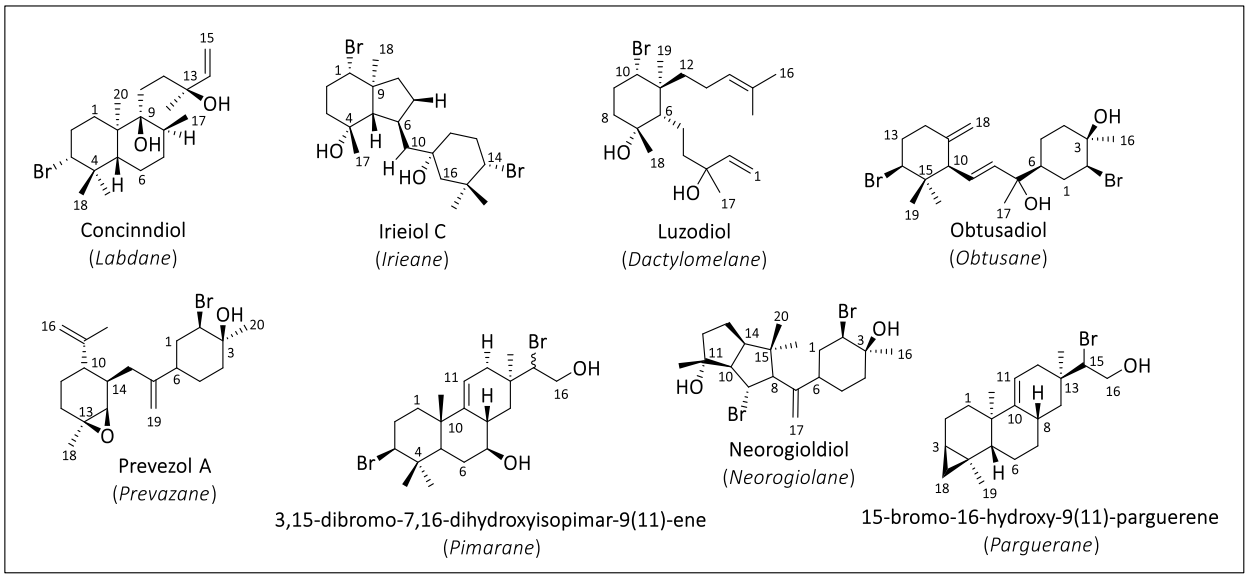

Figure 2.3: Representative diterpenoid metabolites from the genus *Laurencia*[32–39]

Diterpenoids are less abundant in *Laurencia* species compared to sesquiterpenoids. They are however a diverse group of compounds with mono- to tricarbocyclic skeletons. The labdanes, for example, are a group of bicyclic diterpenes comprising two fused cyclohexane rings with an acyclic chain at C-9 (Figure 2.3). The halogenated members of this group possess a C-3 bromine substituent. Some common structural features include C-8 or C-9 and C-13 hydroxyl substituents, and a vinyl group at C-14.[15,17]

Closely related to the labdanes are pimaranes. Only two members of this class have so far been isolated.[39] The pimaranes are characterized by a C-3-Br, C-7-OH, $\Delta^{9,11}$ and bromohydrin between C-14 and C-15. The pimaranes are, structurally, tricyclic compounds obtained after further cyclisation of C-13 and C-17 of labdanes. Even further cyclisation of C-3 and C-18 of pimaranes

gives the parguerane class of *Laurencia* diterpenes (Figure 2.3). While an isoparguerane diterpene arises from a C-3-C-18-C-19-C-4 cyclobutane moiety, rearrangement of ring A of the pimarane skeleton into a seven or eight-membered ring affords the neoparguerane diterpene.

Irieane diterpenes are another class of tricyclic diterpenes encountered in *Laurencia*. First isolated from *L. irieii*, irieanes consist of a cyclohexylmethyl unit coupled with an octahydroindene system. Members of this class of diterpenes possess bromine substitutions at C-1 and C-14, an α-C-4 oxy group and very often a C-11 oxygenation.[15,17]

Dactylomelanes are a monocyclic group of diterpenes arising from C-6 to C-11 cyclisation of a phytane carbo-skeleton. All but one member of this group bear the same side chain at C-6. Bromination in these diterpenes commonly occurs at C-10. Dactylomelanes have not been frequently encountered in *Laurencia*. Other examples of less frequently encountered diterponids of the *Laurencia* genus include the prevazanes, neorogiolanes and the obtusanes and related compounds.[17]

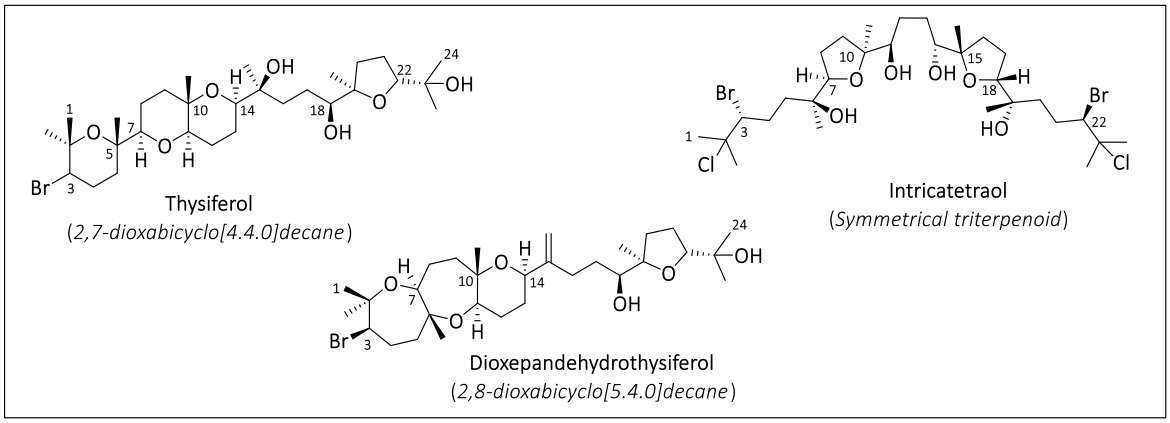

Figure 2.4: Representative triterpenoid metabolites from the genus *Laurencia*[40–42]

Triterpenoids isolated so far from *Laurencia* species are a group of noncarbocylic polyethers biosynthesized from squalene. The members of this class of *Laurencia* secondary metabolites can be divided into three subclasses namely: those possessing a 2,7-dioxabicyclo[4.4.0]decane skeleton, those with a 2,8-dioxabicyclo[5.4.0]decane ring system, and those possessing a distinctive C_2 symmetry element (Figure 2.4). Isolated non-terpenoid C_{15} acetogenins, which arise from fatty acid metabolism,[43] are grouped into 12 different classes as either linear molecules or

cyclic ethers with varying sizes. Apart from a few members, a characteristic feature of C_{15} acetogenins is the presence of conjugated (*E*) or (*Z*) enynes or bromoallene terminus. These compounds are mostly mono- or polyhalogenated with at least one bromine or chlorine atom or both (Figure 2.5).[15]

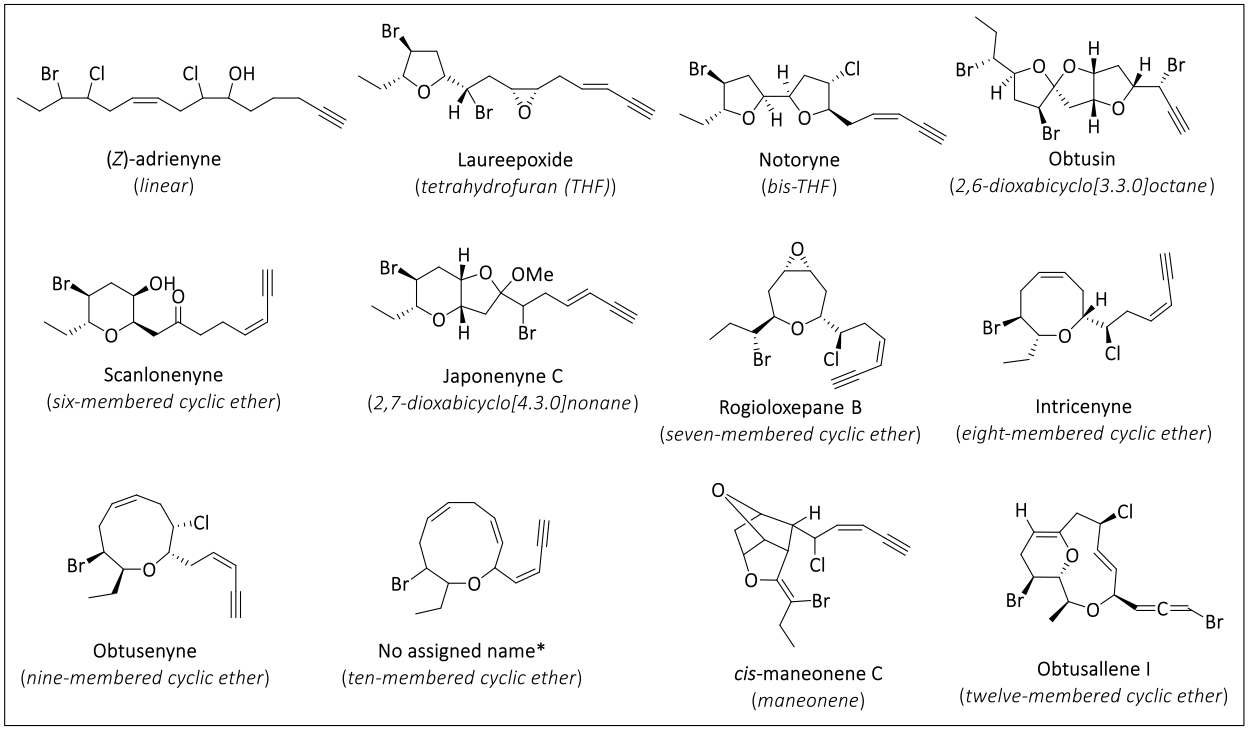

Figure 2.5: Representative C_{15} acetogenin metabolites from the genus *Laurencia*[44–55]

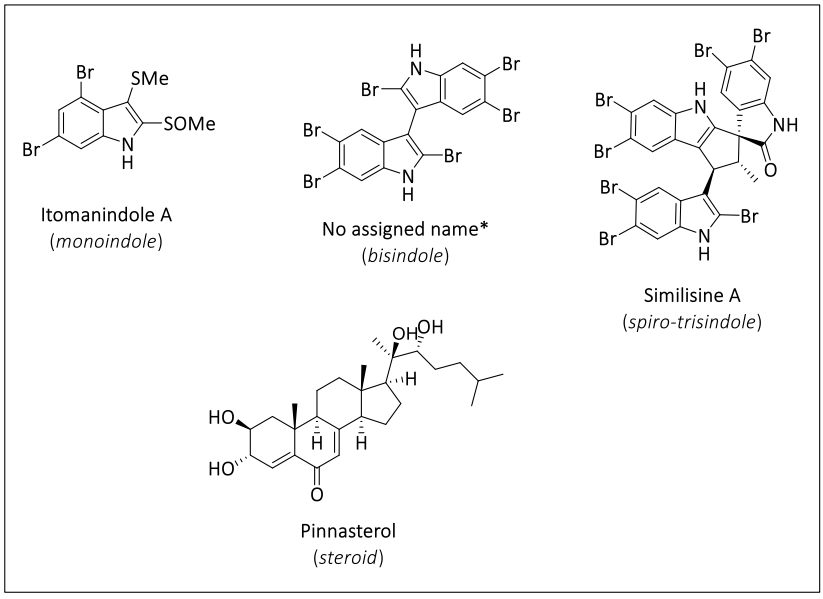

Figure 2.6: Representative indole and steroid metabolites from the genus *Laurencia*[56–59]

An even smaller group of secondary metabolites of *Laurencia* origin is the aromatic, largely indole, natural products. Brominated indoles have been reported from *L. brongniartii*, *L. decumbens* and *L. similis* species only. They have been isolated as mono-, bis-, and until recently, spiro-trisindoles[58]. Like higher plants, some *Laurencia* species have yielded steroid-type compounds such as cholesterol analogs, stigmasterol analogs and the ecdysteroid-type steroid pinnasterol from *L. pinnata*[59] (Figure 2.6).

To conclude, a cursory search through the literature reveals that *L. obtusa* has produced the most abundant of *Laurencia* natural products comprising the terpenoids and non-terpenoid C_{15} acetogenins. With such diversity, however, indole metabolites are yet to be reported. *L. viridis* have yielded more triterpenoids than the other species, while *L. brongniartii* has afforded most of the indoles so far isolated.[15–17,60]

2.2.2 Biological activities and ecological significance of *Laurencia* secondary metabolites

Laurencia natural products have been evaluated for their cytotoxic, antibacterial, antiviral, antiparasitic and anti-inflammatory activities. Moreover, their ecological roles with respect to antifeedant, insecticidal, antifouling and allelopathic activities have also been reported[15,17]. The chamigrane sesquiterpene elatol (Figure 2.7) has exhibited good to moderate cytotoxic activities (IC_{50} = 0.3 – 25 μM) against a range of cancer cell lines;[61–63] some elatol congeners exhibited cytotoxic activity at IC_{50} = 0.07 – 33 μM.[61] Elatol has displayed antibacterial activity against some human pathogenic bacteria at inhibitory concentrations comparable to augmentin, latamoxef, ceflaclor, ceftriaxone, kanamycin, and netilmicin. It's mode of action was found to be by bacteriostatic rather than bacteriocidal effects.[64] Elatol showed nematicidal activity towards *Caenorrhabditis elegans*, exhibited antitrypanosomal activity against *Trypanosoma cruzi* (IC_{50} = 0.92 μg/mL, displayed activity against the promastigote and intracellular amastigote forms of *Leishmania amazonensis* (IC_{50} = 4.0 μM and 0.45 μM, respectively, after 72 h), but no antiplasmodium activity against the human malaria parasite *Plasmodium falciparum* and no inhibition of HIV-1 reverse transcriptase.[62,65] The ecological role of elatol and some halochamigrane congeners in protecting the algal species from pathogenic marine bacteria has also been demonstrated. The biological activity and/or ecological importance of some bioactive

Laurencia secondary metabolites against some representative assays are summarized in Table 2.1. Indeed, the data presented is not exhaustive as the over 700 halogenated and non-halogenated metabolites so far isolated from *Laurencia* species have been investigated in a wide range of assays.[15,17]

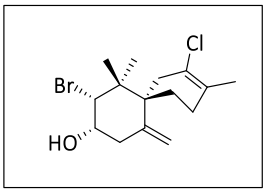

Figure 2.7: Chemical structure of elatol

Table 2.1: Biological activities of representative metabolites from *Laurencia*

Secondary metabolite	Activity
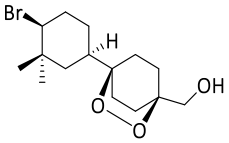 Majopolene A	Cytotoxicity[66] NCI/60 cancer cell lines: av.GI_{50} = 0.4 µM av.TGI = 0.9 µM av.LC_{50} = 2.8 µM
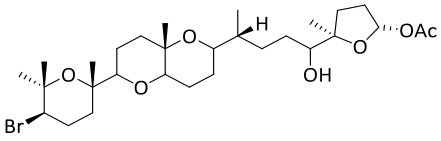 Thyrsiferyl-23-acetate	Cytotoxicity[67] P-388: ED_{50} = 0.5 nM Enzyme inhibitory activity[68] Serine/Threonine protein phosphatase 2A (PP2A): IC_{50} = 4 -16 µM
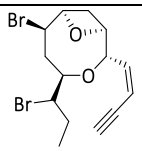 Laureatin	Anti-insecticidal[69] *Culex pipiens pallens* (mosquito): LC_{50} = 7.5 – 18.0 µM
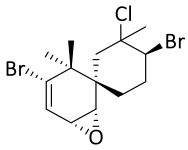 Deoxyprepacifenol	Anti-insecticidal[69] *Culex pipiens pallens* (mosquito): LC_{50} = 0.15 – 1.25 µM
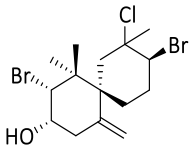 Nidificene	Antiviral[70] Herpes 1 – type (HSV-1): IC_{50} = 3.6 µM

2.3 "Isolation, Characterization and Antiproliferative activity of new metabolites from the South African endemic red algal species Laurencia alfredensis"[71⊥]

Laurencia alfredensis Francis, Bolton, Mattio & Anderson is a newly described species of the genus and is endemic to South Africa. The material investigated here was collected on a rocky intertidal seashore at Three Sisters, north of Port Alfred in the Eastern Cape Province of the Republic of South Africa in 2011.[72]

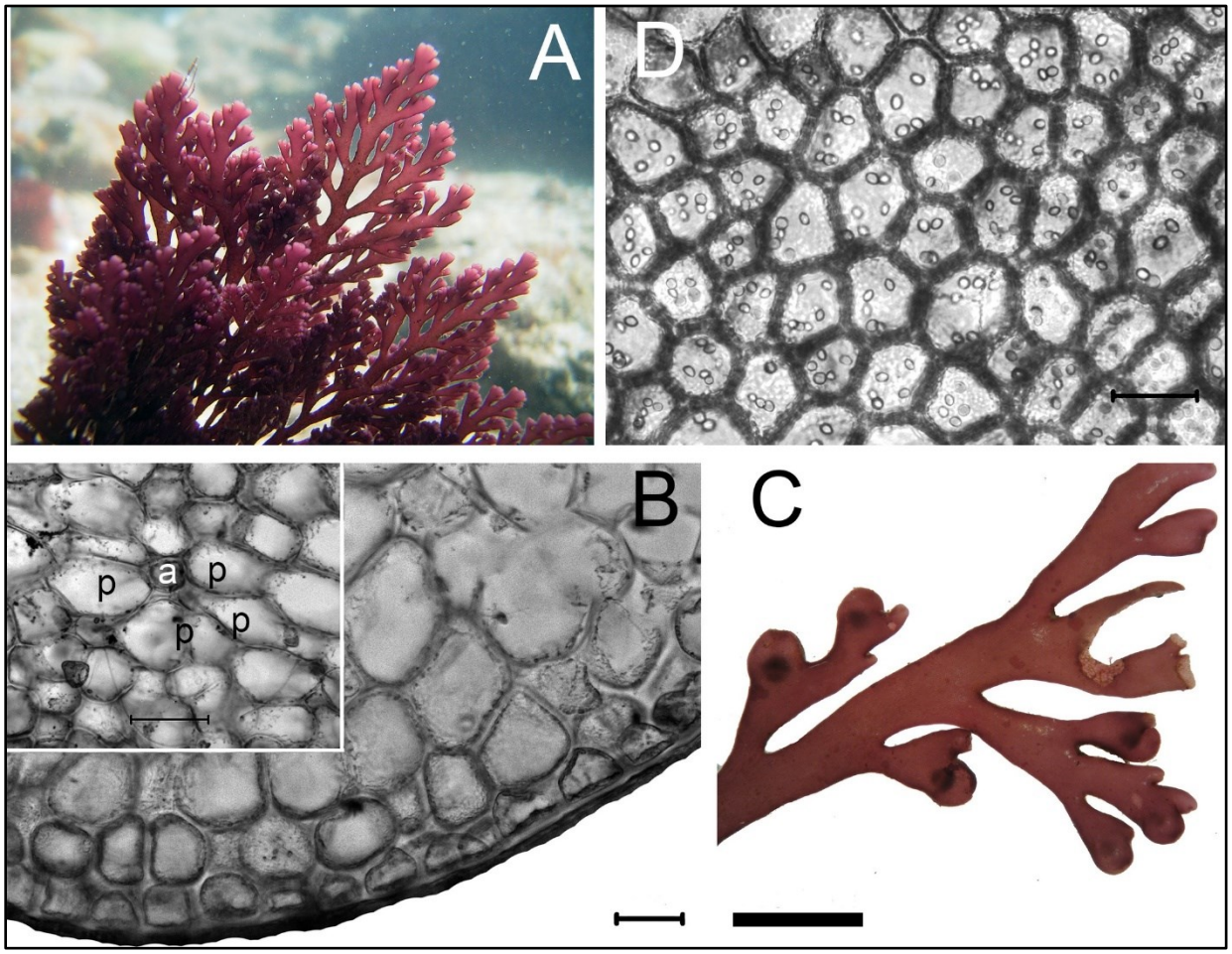

Figure 2.8: *Laurencia alfredensis* sp. nov.

[(A) Habit. (B) Outermost cortical and innermost cortical cells (scale bar = 40 lm); Inlet showing pericentral (p) and axial (a) cells (scale bar = 100lm). (C) Alternate branching pattern. Note cystocarps on the branchlets (scale bar = 0.6 mm). (D) 4–6 *corps en cerise* per cell (scale bar = 50 lm)].[72]

⊥ Results have already been published: Dziwornu *et al*. **2017**. *Molecules*, *22* (4).

A sequence of column chromatography, preparative TLC and normal phase HPLC resulted in the isolation of 11 compounds, comprising eight newly reported compounds along with the known polyether triterpene saiyacenol B (**4**),[73] the synthetic compound (**9**),[74] and the glycolipid, 1,2-di-*O*-palmitoyl-3-*O*-(6-sulfo-α-d-quinovopyranosyl)-glycerol (**11**) (Figure 2.9).[75] Except for compound **4**, none of the compounds isolated have previously been reported from the genus *Laurencia*. The structural elucidation and the relative configuration assignments of the compounds were accomplished by extensive use of 1D- and 2D-NMR, HR-ESI-MS, UV and IR spectroscopic techniques, while the absolute configuration of compound **1** was determined by single-crystal X-ray diffraction analysis. All compounds were evaluated against the MDA-MB-231 breast and HeLa cervical cancer cell lines. Compound **2** exhibited low micromolar antiproliferative activity (IC_{50} = 9.3 µM) against the triple negative breast carcinoma and compound **7** was similarly active (IC_{50} = 8.8 µM) against the cervical cancer cell line.

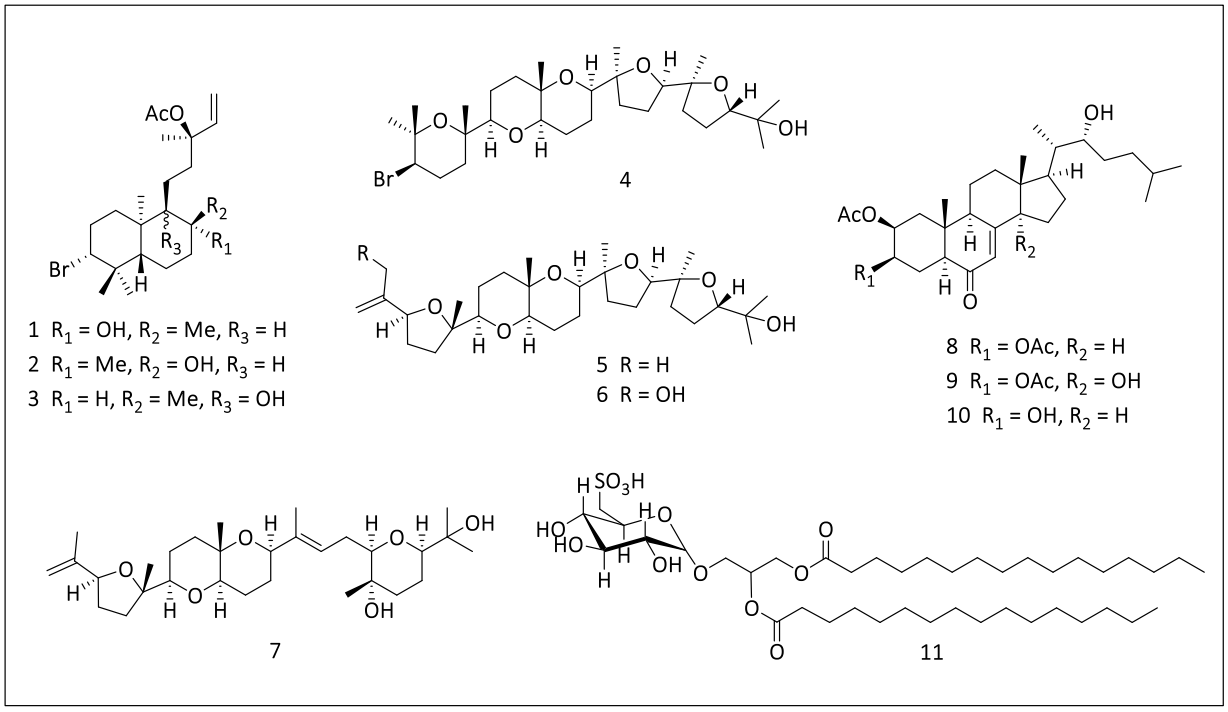

Figure 2.9: The secondary metabolites (**1**–**11**) isolated from *Laurencia alfredensis*

2.3.1 Results and Discussion

2.3.1.1. Structural Elucidation of Labdane-Type Diterpenes (1–3)

Table 2.2: ^{1}H (600 MHz, $CDCl_3$) and ^{13}C NMR (151 MHz, $CDCl_3$) data for compounds **1-3**

	1		2		3	
No.	δ_C	δ_H (*J*, Hz)	δ_C	δ_H (*J*, Hz)	δ_C	δ_H (*J*, Hz)
1a		1.14, dt (3.5, 13.4)		1.15, m		1.42, m
1b	37.4, CH_2	1.62, td (3.9, 12.9, 13.2)	37.3, CH_2	1.71, m	33.5, CH_2	1.71, m
2a		2.06, dq (3.9, 13.2)		2.09, m		2.12, m
2b	30.7, CH_2	2.30, qd (3.9, 13.2)	30.9, CH_2	2.25, qd (3.8, 13.1)	30.7, CH_2	2.15, m
3	69.7, CH	3.92, dd (4.1, 12.8)	69.2, CH	3.93, dd (4.1, 12.7)	69.6, CH	4.00, dd (4.3, 12.4)
4	39.5, C		39.4, C		39.6, C	
5	47.6, CH	1.08, dd (2.5, 10.9)	47.1, CH	1.16, m	47.0, CH	1.64, dd (2.7, 12.3)
6a		1.50, m		1.40, m		1.39, m
6b	20.2, CH_2	1.72, m	22.0, CH_2	1.64, m	23.1, CH_2	1.60, m
7a		1.46, m		1.46, m		1.29, m
7b	36.7, CH_2	1.53, m	37.2, CH_2	1.58, m	31.3, CH	1.46, m
8	74.7, C		73.1, C		35.9, CH	1.73, m
9	59.1, CH	0.84, m	60.9, CH	0.95, m	76.8, C	
10	39.0, C		38.7, C		43.3, C	
11a		1.00, m		1.28, m		1.40, m
11b	23.0, CH_2	1.38, m	20.8, CH_2	1.71, m	28.0, CH_2	1.55, m
12a		1.74, m		1.79, m		1.74, m
12b	43.0, CH_2	1.80, m	42.9, CH_2	1.82, m	35.8, CH_2	1.95, ddd, (5.1, 12.4, 13.7)
13	82.9, C		83.2, C		83.3, C	
14	141.6, CH	5.94, dd (11.0, 17.5)	141.8, CH	6.00, dd (11.0, 17.5)	141.6, CH	5.90, dd (11.0, 17.5)
15a		5.13, dd (0.9, 17.5)		5.13, dd (0.9, 17.5)		5.12, dd (0.7, 6.6)
15b	113.4, CH_2	5.15, dd (0.9, 11.0)	113.2, CH_2	5.15, dd (0.9, 11.0)	113.4, CH_2	5.14, dd (0.7, 13.1)
16	23.5, CH_3	1.52, s	23.7, CH_3	1.52, s	23.7, CH_3	1.52, s
17	30.9, CH_3	1.20, s	31.8, CH_3	1.43, s	16.0, CH_3	0.82, d (6.6)
18	17.7, CH_3	0.95, s	17.6, CH_3	0.91, s	18.4, CH_3	0.96, s
19	30.6, CH_3	1.06, s	30.5, CH_3	1.07, s	30.9, CH_3	1.05, s
20	24.7, CH_3	1.28, s	24.7, CH_3	1.09, s	16.2, CH_3	0.95, s
21	169.8, C		169.9, C		169.8, C	
22	22.1, CH_3	2.00, s	22.2, CH_3	2.00, s	22.1, CH_3	2.00, s

Compound **1** (Figure 2.9) was obtained as a white crystalline solid after recrystallization from methanol. HR-ESI-MS (*m/z* 451.1824, 453.1792 $[M + Na]^+$, calcd. 451.1824 for $C_{22}H_{37}{}^{79}BrO_3Na$) data established a molecular formula of $C_{22}H_{37}BrO_3$, signifying the presence of four degrees of unsaturation. The ^{1}H-NMR spectrum (Figure 2.10) exhibited signals of six sharp methyl groups (δ_H 0.95, s; 1.06, s; 1.20, s; 1.26, s; 1.52, s) including a characteristic acetate methyl singlet at

δ_H 2.00 (H_3-22), several overlapping multiplets at δ_H 1.00 – 2.35 characteristic of a terpenoid backbone, three methine signals with a coupling pattern indicative of the presence of a vinyl group (δ_H 5.13, dd, *J* = 0.9, 17.5 Hz, H-15a; 5.15, dd, *J* = 0.9, 11.0 Hz, H-15b; 5.94, dd, *J* = 11.0, 17.5 Hz, H-14) and a methine proton (δ_H 3.92, dd, *J* = 4.1, 12.8 Hz, H-3) (Table 2.2).

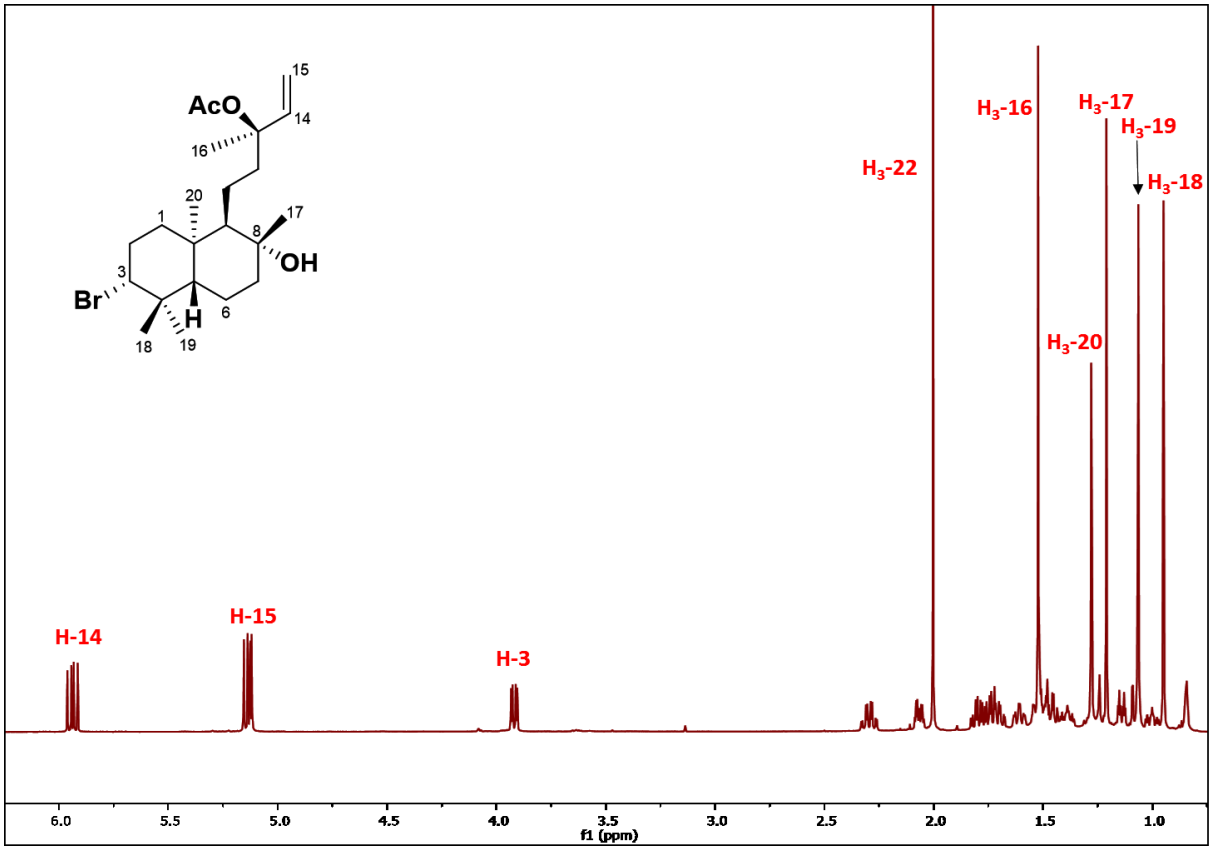

Figure 2.10: ^{1}H-NMR (600 MHz, $CDCl_3$) spectrum of compound **1**

The ^{13}C-NMR spectrum for compound **1** indicated the presence of 22 non-equivalent carbons including characteristic signals, which supported the presence of an ester group (δ_C 169.8) and two olefinic carbons (δ_C 113.4 and 141.6). The coupling constants recorded for the vicinal coupling between H-3 (δ_H 3.92, dd, *J* = 4.1, 12.8 Hz) and H_2-2, and H-5 (δ_H 1.08, dd, *J* = 2.5, 10.9 Hz) and H_2-6 were consistent with the ^3J diaxial coupling (*J* = 9 – 12 Hz) and ^3J axial-equatorial coupling (*J* = 2 – 4 Hz) observed in substituted cyclohexane rings. The four degrees of unsaturation were therefore accounted for by one carbonyl group, one olefinic double bond and two substituted cyclohexane rings. Compound **1** was therefore deduced to be a bicyclic diterpenoid molecule.

The HSQC-DEPT spectrum showed cross-peaks attributed to six methyl, seven diastereotopic methylene, four methine and five quaternary carbons. Four ^{1}H-^{1}H COSY spin systems (Figure 2.11) were observed, comprising three similar methine proton→methylene protons→methylene protons coupling patterns and the ABX coupling pattern of the vinyl protons. Key HMBC correlations included the long range coupling of H-3 to C-4 (δ_C 39.5), C-18 (δ_C 17.7) and C-19 (δ_C 30.6), and H-14 to C-13 (δ_C 82.9) and C-16 (δ_C 23.5) (Figure 2.11). The chemical shifts of the methine carbon signals at δ_C 69.7 and δ_C 82.9 suggested the presence of the bromine atom and the acetate group at C-3 and C-13, respectively. Hence, the backbone structure of compound **1** was found to be consistent with that of a brominated labdane-type diterpene, similar to the known compounds Isoconncindiol and Pinnatol A that have both been previously isolated from the *Laurencia* genus.[76–78]

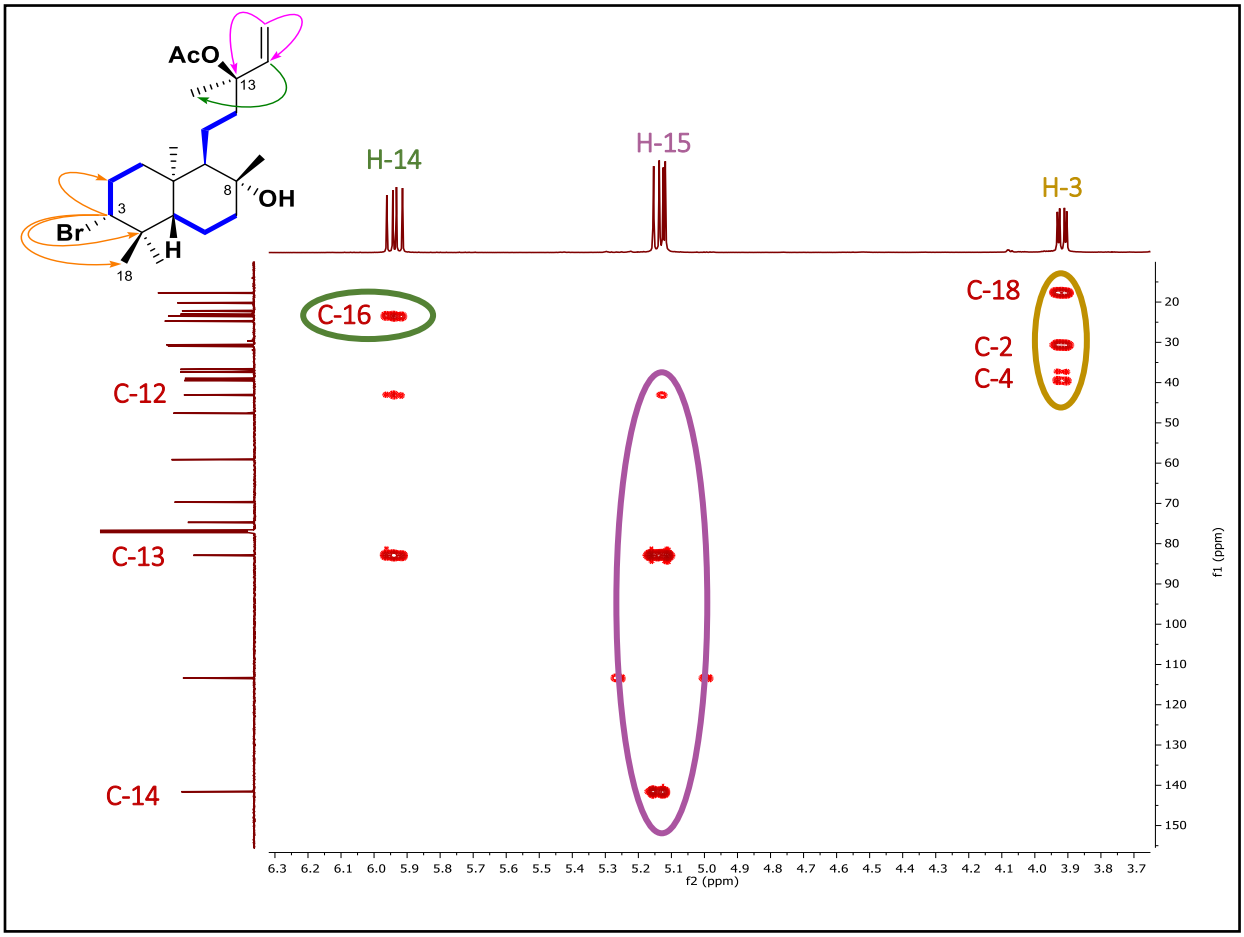

Figure 2.11: Key COSY (blue **bold** bonds) and HMBC (curved arrows) correlations of compound **1**

The presence of ROE enhancements between H_2-1b, H-3 and H_3-18 signified they occupied the same face of the cyclohexane ring, as did H_3-19 and H_3-20 (Figure 2.12). Moreover, a ROESY correlation present between H_3-20 and H-9 but not H-5 and H_3-17 was indicative of the *syn-ent* configuration about the cyclohexane ring junction and the equatorial orientation of H_3-17 in ring B. The structure of **1** was successfully assigned as the 13-acetyl derivative of the known C-3 brominated labdane diterpene Pinnatol A.[78]

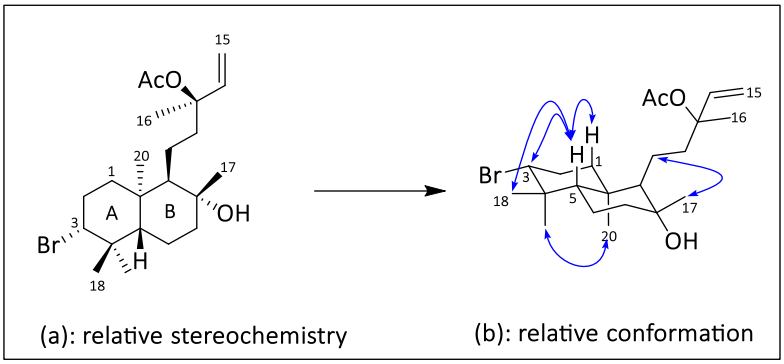

Figure 2.12: ROESY of compound **1**: (a) Relative stereochemistry and (b) relative conformation.

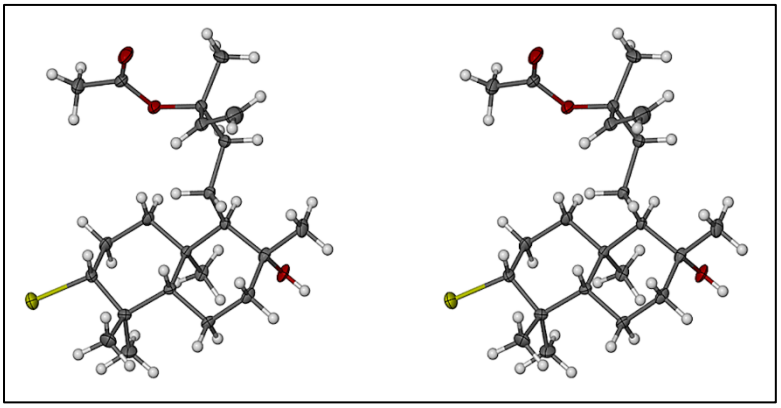

Figure 2.13: Stereoscopic view of 1 (absolute configuration). Non-H atoms are drawn as thermal ellipsoids at the 40% probability level and H atoms as spheres of arbitrary size. (Color code: C gray, H white, O red, Br yellow.)

X-ray diffraction analysis of **1** confirmed the relative stereochemistry predicted from the ROESY data. Furthermore, the absolute configuration of **1** (Figure 2.13) was unequivocally determined via the anomalous X-ray scattering of the bromine atom. Both cyclohexane rings assume the more stable chair conformation with a *syn-ent* configuration at the ring junction. Protons H-1b, H-3, H-

5 and H_3-18 occupy the same face of ring A whilst H_3-19 and H_3-20 occupy the opposite face. The equatorial orientation of H_3-17 compared to H_3-20 supports the lack of ROESY enhancement between the two methyl groups.

Compounds **2** and **3** gave similar HR-ESI-MS ion peaks (*m/z* 451.1821, 453.1809 $[M + Na]^+$, calcd. 451.1824 for $C_{22}H_{37}{}^{79}BrO_3Na$) to **1**, suggesting they were isomeric and this was indeed supported by the high degree of similarity in their NMR data. In fact, both 1D- and 2D-NMR data acquired for compound **2**, except for the ROESY data, were congruent with the NMR spectra for **1**. However, subtle differences in the proton chemical shifts of H-9 (δ_H 0.95, m), H-20 (δ_H 1.09, s), H-17 (δ_H 1.43, s) and H_2-11 (δ_H 1.28, m; 1.71, m) (Table 2.2) were observed in the ^{1}H-NMR spectrum of **2** compared to **1**. The presence of ROESY cross-peaks from H_3-20 to H-9 and H_3-17 confirmed a similar spatial orientation of these protons and the absence of such a correlation between H_3-20 and H-5, implied a similar configuration about the ring junction as observed in **1** (Figure 2.14a). The exact same chemical shift observed for H_3-16 (δ_H 1.52, s) in compounds **1**–**3** indicated that all three labdane diterpenes have the same 13*S* configuration, consistent with the absolute configuration reported for the structurally related marine natural product, isoconncindiol.[76,77] The structure of **2** was therefore elucidated as the 8*S*-diastereomer of **1**, that is with the only difference observed at the stereogenic center C-8, thus confirming the structure of **2** as the 13-acetyl derivative of isoconcinndiol.

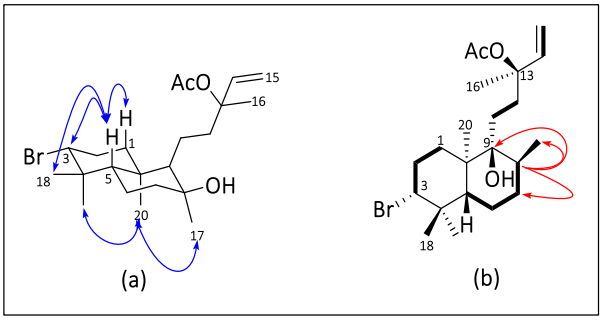

Figure 2.14: (a) Key ROESY (blue curved arrows) of compound **2**; and (b) COSY (**bold** bonds) and key HMBC (red curved arrows) of compound **3**.

Compound **3** showed signals for five methyl singlets (δ_H 0.95; 0.96; 1.05; 1.52; 2.00), a methyl doublet (δ_H 0.86, d, *J* = 6.6 Hz, H_3-17), several overlapping multiplets at δ_H 1.00 – 2.15, the vinyl

protons double doublets (δ_H 5.12, dd, *J* = 0.7, 6.6 Hz, H-15a; 5.14, dd, *J* = 0.7, 13.1 Hz, H-15b; 5.90, dd, *J* = 11.0, 17.5 Hz, H-14) and the "halo-methine" proton H-3 at δ_H 4.00 (dd, *J* = 4.3, 12.4 Hz) in its ^{1}H-NMR spectrum (Table 2.2). Four different ^{1}H-^{1}H COSY spin systems were observed (Figure 2.14b), with two of them (H_2-1→H-3 and H-14→H_2-15) similar to those also observed in compounds **1** and **2**. However, the presence of the significant H-5→H_3-17 (Figure 2.14b), concomitant with the absence of the H-9→H_2-12 COSY spin system and the splitting of H_3-17 into a doublet, suggested that **3** was a positional isomer of **1** and **2**, with its hydroxyl group present at C-9 (δ_C 76.8) rather than C-8 (δ_C 35.8). The relative configuration of the groups on the cyclohexane ring A was retained whilst no ROE cross-peak was observed between H_3-17 and H_3-20. The structure of **3** was therefore elucidated as the 13-acetyl derivative of concinndiol.[79]

2.3.1.2. *Structural Elucidation of Polyether Triterpenes* (**4**–**7**)

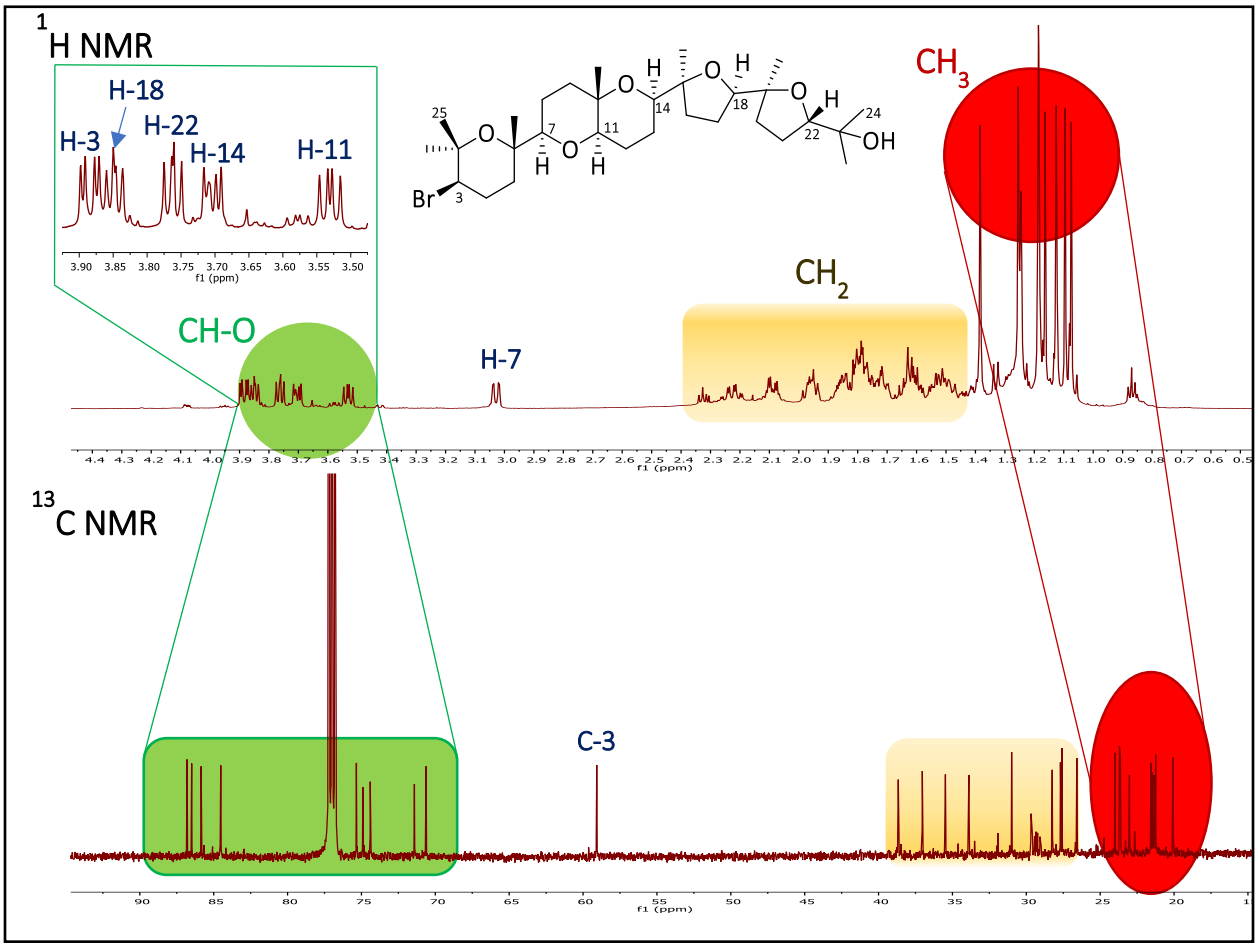

Figure 2.15: 1D NMR spectra of compound **4**

Compound **4** was isolated as a white amorphous solid. The ^{1}H-NMR spectrum (Figure 2.15) showed signals of eight methyl groups (δ_H 1.07, s; 1.10, s; 1.13, s; 1.16, s; 1.18, s; 1.19, s; 1.26, s; 1.38, s), several overlapping multiplicities at δ_H 1.3 – 2.3, and six methine proton groups (Figure 2.15 and Table 2.3). The ^{13}C-NMR spectrum showed 30 carbon signals and a high degree of oxygenation was inferred from 10 carbon resonances present in the downfield range δ_C 70 – 87 ppm. A signal observed at δ_C 59.0 suggested the presence of a bromo-methine C-3, characteristic in similar polyether triterpenes reported from the genus *Laurencia* .[80,81] This was confirmed by the presence of the mono-isotopic bromine peaks at *m/z* 611/609 $[M + Na]^+$, 571/569 $[M - OH]^+$ recorded in the LR-ESI-MS and consistent with the reported values by Cen-Pacheco and coworkers.[73] Compound **4** was deduced to be a congener of this group of secondary metabolites and the structure was found be that of the known compound saiyacenol B, previously isolated from *L. viridis.*[73]

After careful examination of the 1D NMR spectra of a fraction obtained from the same HPLC run that yielded compound **2**, we identified the presence of a mixture of the two very closely related compounds **5** and **6**. However, due to the paucity of the HPLC fraction obtained (0.5 mg), we were unable to separate these two compounds any further. The HR-ESI-MS spectrum obtained for compound **5** established a molecular formula of $C_{30}H_{50}O_6$, requiring six degrees of unsaturation. Its ^{1}H-NMR spectrum exhibited signals of seven methyls (δ_H 1.08, s; 1.10, s; 1.13, s; 1.15, s; 1.19, s; 1.20, s; 1.68, s), several overlapping multiplicities at δ_H 1.2 – 2.2, six oxygenated methine protons double doublets and two olefinic geminal protons at δ_H 4.77 (m, H-1a) and 4.98 (m, H-1b) (Table 2.3).

The ^{13}C-NMR spectrum showed the presence of 30 non-equivalent carbons and the HSQC-DEPT confirmed the presence of seven methyl, 11 diastereotopic methylene, six methine and six quaternary carbons. Thorough analysis of the 1D and 2D NMR data identified compound **5** as another polyether triterpene, which lacked a C-3 bromine atom and one methyl group (δ_H 1.26, s, H_3-1) compared to **4**. With evidence of only one double bond (C-1, δ_H 4.77/4.98, δ_C 110.2; C-2, δ_C 146.2), compound **5** was deduced to be pentacyclic.

Table 2.3: ^{1}H (600 MHz, $CDCl_3$) and ^{13}C NMR (151 MHz, $CDCl_3$) data for compounds **4**-**7**

	4[73]		**5**		**6**		**7**	
No.	δ_C	δ_H (*J*, Hz)	δ_C	δ_H (*J*, Hz)	δ_C	δ_H (*J*, Hz)	δ_C	δ_H (*J*, Hz)
1a				4.77, m		5.23, m		4.76, m
1b	31.0	1.26, s	110.2	4.98, m	114.7	5.30, m	110.2	4.97, m
2	74.9		146.2		146.0		145.9	
3	59.0	3.88, dd (4.0, 12.3)	83.4	4.35, dd (6.1, 8.9)	80.7	4.53, dd (5.2, 9.5)	83.3	4.34, dd (6.1, 8.7)
4a		2.09, dt (4.0, 13.5)		1.71, m		1.83, m		1.71, m
4b	28.2	2.23, qd (3.7, 13.1)	31.4	2.02, m	32.3	2.15, m	31.3	2.01, m
5a		1.53, m		1.64, m		1.68, m		1.62, m
5b	37.4	1.80, m	34.3	2.12, m	34.1	1.81, m	34.2	2.10, m
6	74.4		84.5		84.5		84.4	
7	86.5	3.03, dd (2.3, 11.4)	83.6	3.32, dd (2.6, 11.6)	83.6	3.31, dd (2.6, 11.6)	83.6	3.34, dd (2.7, 11.6)
8a		1.40, m		1.44, m		1.44, m		1.45, m
8b	23.0	1.70, m	25.0	1.64, m	25.0	1.64, m	24.8	1.65, m
9a		1.52, m		1.57, m		1.57, m		1.56, m
9b	38.7	1.73, m	38.8	1.76, m	38.7	1.76, m	38.8	1.78, m
10	71.4		71.3		71.2		72.1	
11	76.7	3.53, dd (7.3, 11.0)	76.6	3.58, dd (7.3, 11.0)	76.6	3.58, dd (7.3, 11.0)	77.8	3.51, dd (6.5, 11.2)
12a		1.48, m		1.52, m		1.52, m		1.57, m
12b	21.3	1.86, m	21.4	1.93, m	21.4	1.93, m	21.7	1.88, m
13a								1.70, m
13b	21.4	1.77	21.5	1.78, m	21.5	1.78, m	25.8	2.02, m
14	75.3	3.71, dd (4.3, 11.0)	75.4	3.71, dd (4.8, 11.2)	75.5	3.72, dd (4.8, 11.2)	75.1	4.19, dd (4.0, 9.5)
15	84.5		84.4		84.4		138.5	
16a		1.61, m		1.64, m		1.64, m		
16b	35.5	1.95, m	35.4	1.96, m	35.4	1.96, m	122.3	5.52, dd (2.7, 13.8)
17a		1.63, m		1.66, m		1.66, m		2.06, m
17b	27.6	1.84, m	27.7	1.86, m	27.7	1.86, m	27.6	2.40, ddd (3.1, 7.6, 15.1)
18	85.8	3.85, dd (6.1, 8.4)	85.8	3.86, dd (5.8, 8.2)	85.8	3.86, dd (5.8, 8.2)	84.0	3.16, dd (3.2, 6.7)
19	84.5		84.6		84.6		69.9	
20a		1.59, m						1.56, m
20b	33.9	1.96, m	34.0	1.96, m	34.0	1.96, m	39.7	1.84, m
21a								1.49, m
21b	26.5	1.79, m	26.6	1.80, m	26.6	1.80, m	24.5	1.60, m
22	86.8	3.76, dd (6.8, 8.6)	86.8	3.77, dd (6.7, 8.7)	86.8	3.77, dd (6.7, 8.7)	84.1	3.14, m
23	70.6		70.6		70.6		71.6	
24	24.0	1.10, s	24.0	1.10, s	24.0	1.10, s	23.9	1.12, s
25	23.7	1.38, s	17.7	1.68, s	44.7	4.09, d (0.9)	17.7	1.68, s
26	20.0	1.19, s	23.2	1.15, s	23.3	1.17, s	23.1	1.16, s
27	21.2	1.16, s	21.3	1.20, s	21.3	1.20, s	20.1	1.21, s
28	21.5	1.07, s	21.6	1.08, s	21.6	1.08, s	13.0	1.65, s
29	23.6	1.13, s	23.6	1.13, s	23.6	1.13, s	20.2	1.18, s
30	27.5	1.18, s	27.6	1.19, s	27.6	1.19, s	26.1	1.16, s

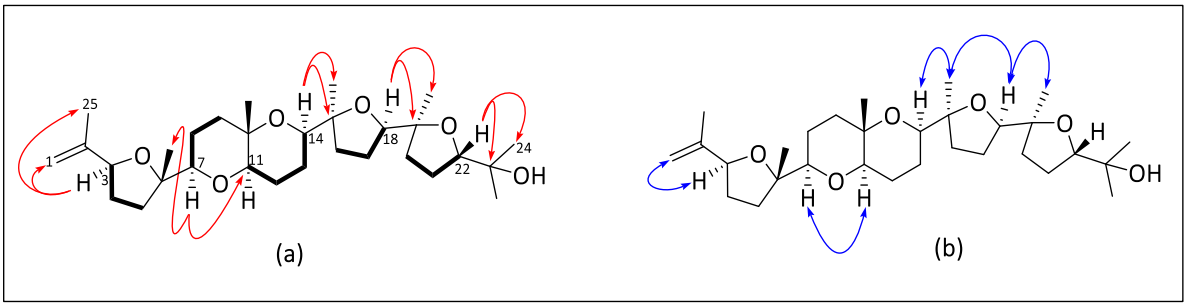

Figure 2.16: (a) COSY (**bold** bonds) and key HMBC (red curved arrows); and (b) key ROESY (blue curved arrows) of compound **5**.

Six ^{1}H-^{1}H COSY spin systems were observed, of which four exhibited the concomitant vicinal AA'BB' coupling pattern involving two methylene groups, with one of the groups further involved in an ABX vicinal coupling with a methine proton (Figure 2.16a). The coupling constants recorded, especially for the methine protons supported the presence of both substituted oxolane and oxane moieties. After careful analysis of the long range ^{1}H–^{13}C correlations, the rest of the molecule was found to be similar to **4**, apart from the change in chemical shifts observed from C-1 through C-7 and C-25. An HMBC cross-peak between H-3 and C-1 and the downfield shift of C-3 to δ_C 83.4 suggested the absence of a bromine atom to give the exocyclic 2-methyl ethylenyl group on the oxolane ring in compound **5**, which is consistent with similar isolated compounds.[82] ROESY enhancements of H-14 and H-18 by H_3-28 and H_3-29, respectively, led to a similar relative configuration for **5** as reported for **4**[73] (Figure 2.16b). Compound **5** is reported for the first time here as Alfredensinol A.

The NMR data obtained for compound **6** were superimposable with that of **5**, signifying their structures were closely related (Figure 2.17), with the exception of the olefinic geminal protons of C-1 resonating downfield at δ_H 5.23 (m, H-1a) and δ_H 5.30 (m, H-1b) due to the presence of the hydroxyl group on the methylene carbon C-25 (δ_C 44.7). Moreover, C-1 occurred downfield at δ_C 114.7, while C-3 moved upfield to δ_C 80.7 (Table 2.3). The HR-ESI-MS ion peak at *m/z* 545.3457 $[M + Na]^+$ (calcd. 545.3454) obtained for **6** established a molecular formula of $C_{30}H_{50}O_7$, implying an additional O-atom compared to **5**. Therefore, compound **6** is reported here as the new C-25 hydroxyl derivative of compound **5**, Alfredensinol B.

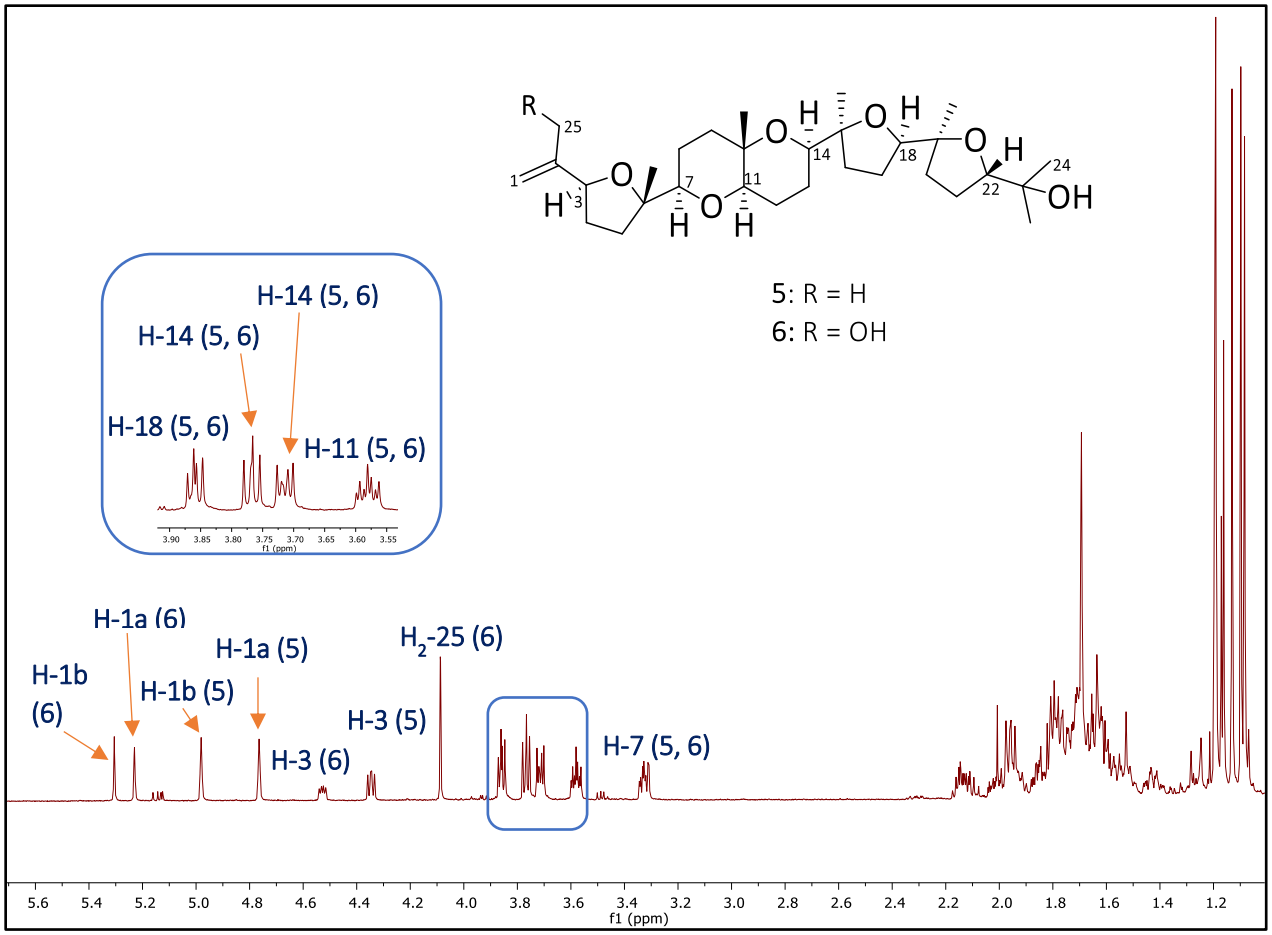

Figure 2.17: ^{1}H NMR spectrum of alfredensinol A (**5**) and B (**6**)

Compound **7** was isolated as a white amorphous solid. It recorded a HR-ESI-MS ion peak of *m/z* 507.3693 $[M + H]^+$ (calcd. 507.3686) for the molecular formula $C_{30}H_{50}O_6$ and was identified as another polyether triterpene from its ^{1}H- and ^{13}C-NMR data. Six oxygenated methine doublet of doublets including an olefinic proton (δ_H 5.52, dd, *J* = 2.7, 13.8 Hz, H-16) and similar olefinic geminal protons (δ_H 4.77, m, H-1a; 4.98, m, H-1b) to compound **5** (Table 2.3) were evident in the ^{1}H-NMR spectrum. With six degrees of unsaturation inferred from the molecular formula, compound **7** was deduced to be a tetracyclic molecule with the presence of two double bonds. Six ^{1}H-^{1}H COSY spin systems were observed, including the key correlations involving the olefinic proton H-16, the diastereotopic methylene protons H_2-17 and the oxymethine H-18 (Figure 2.18a). Key HMBC cross-peaks observed from H-16 to C-14, C-15, C-18, and C-28 established the $\Delta^{15,16}$ olefinic functionality. HMBC correlations from H-22 ($^{3}J_{C,H}$) and H_3-29 ($^{3}J_{C,H}$) to C-18, along

with key COSY correlations between H_2-20, H_2-21 and H-22, confirmed the presence of an oxane ring in the right hand side chain of **7**.

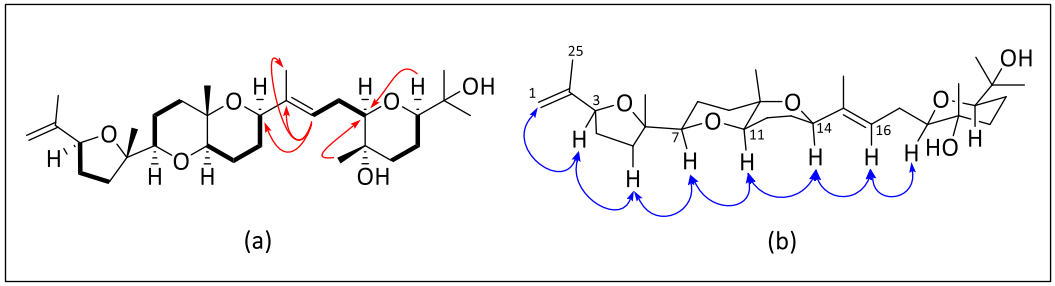

Figure 2.18: (**a**) COSY (**bold** bonds) and key HMBC (red curved arrows); and (**b**) some ROESY (blue curved arrows) correlations for compound **7**

The absence of ROE enhancement of H-16 by H_3-28 was indicative of the *trans* configuration about the double bond between C-15 and C-16, which was further supported by the ROESY correlation between H-14 and H-16 (Figure 2.18b). The relative configuration at C-18 was established as a result of the observed ROESY cross-peak from H-18 to H-16 and the absence of one to H_3-29. The absence of an ROE correlation between H-22 and H_3-29, implied axial orientations for both these groups on the oxane ring. Thus, the structure of **7** was elucidated and identified as a new compound which is named here as Alfredensinol C.

2.3.1.3. Structural Elucidation of Cholestane-Type Ecdysteroids (**8**–**10**)

Compound **8** was isolated as a white amorphous solid and HR-ESI-MS data obtained established the molecular formula as $C_{31}H_{48}O_6$. The ^{1}H-NMR spectrum (Figure 2.19) showed the presence of seven methyl singlets of which two were acetate methyls at δ_H 2.03 (s, H_3-30) and δ_H 2.04 (s, H_3-31), and five oxymethine protons. Several overlapping multiplets were observed in the methylene envelope between δ_H 1.11 – 2.15 (Figure 2.19 and Table 2.4).

The ^{13}C-NMR data showed 31 signals including three carbonyl peaks characteristic of a ketone at δ_C 199.6 (C-6) and two esters (δ_C 169.3, C-28; 169.5, C-29), two aromatic/olefinic carbons (δ_C 123.3, C-7; 162.5, C-8), and three signals at δ_C 68.5 (C-2), 68.3 (C-3), and 73.7 (C-22) suggesting the presence of C-O chemical environments (Table 2.4). The HSQC-DEPT data indicated the

presence of seven methyl, eight diastereotopic methylene, 10 methine, and six quarternary carbons.

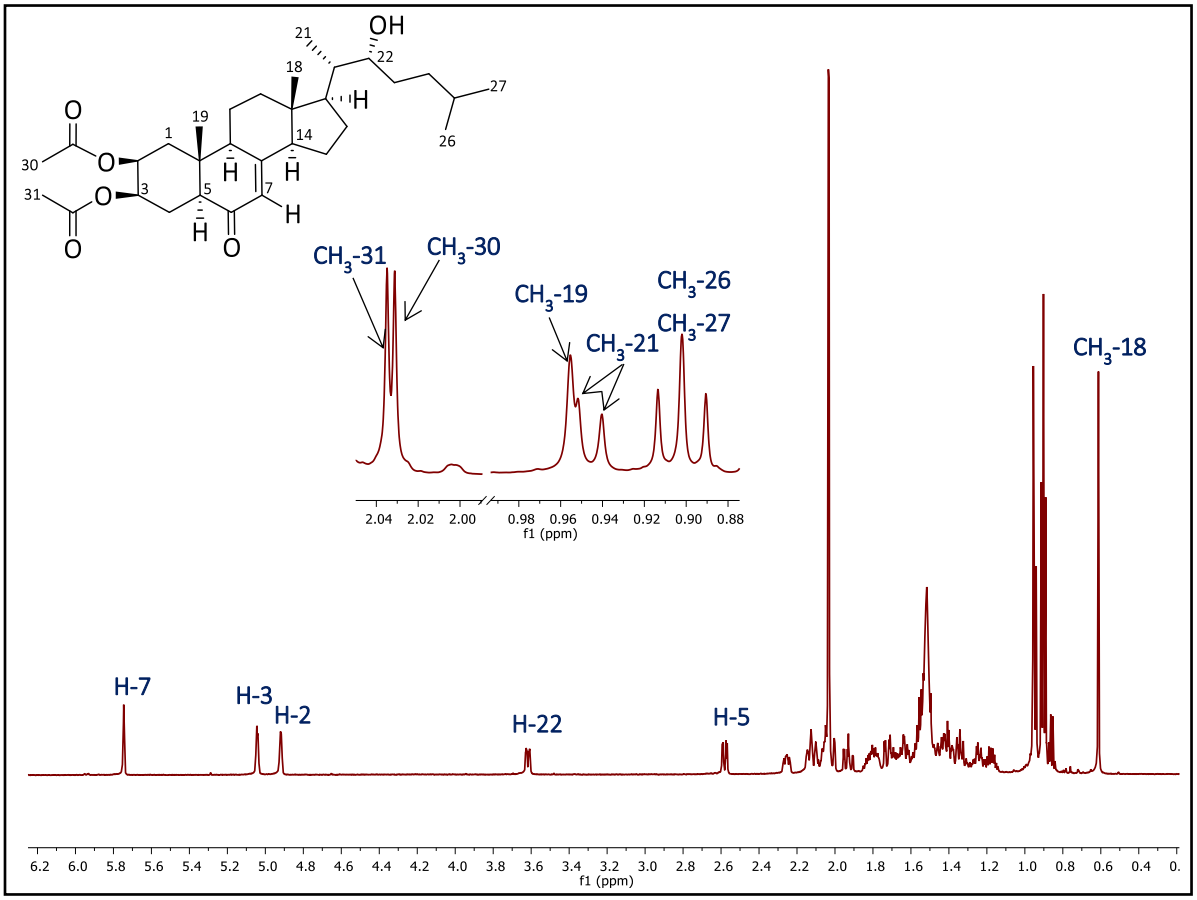

Figure 2.19: ^{1}H NMR spectrum (600 MHz, $CDCl_3$) of compound **8**

Two ^{1}H-^{1}H COSY spin systems were observed for **8**, from H_2-1 to H-5 and H-7 to H_3-27 (Figure 2.20). Some characteristic aspects of a steroidal skeleton became evident from the ^{1}H, ^{13}C and COSY NMR data; for example, the ^{1}H chemical shifts for H_3-18 and H_3-19, and the splitting of H_3-21, H_3-26 and H_3-27 into doublets (Figure 2.19) were characteristic of the side chain to C-17 for cholesterol. The chemical shifts of C-7 and C-8, together with the chemical shift of H-7 (δ_H 5.75, m) and its COSY correlation to H-9 (δ_H 2.25, ddd, J = 2.5, 6.9, 9.9) and H-14 (δ_H 2.05, m) suggested the ketone carbonyl was adjacent to the C-7-C-8 double bond at C-6 to give the endocyclic α, β-unsaturated ketone, a structural feature of ecdysteroids. HMBC cross-peaks from H_2-1 to C-2, C-5, C-9, C-10 and C-19; H_2-4 to C-2 and C-3; and H-5 to C-4, C-6, C-9, C-10 and C-19 confirmed the structure of ring A, and that the ketone was at C-6 (Figure 2.20).

Table 2.4: ^{1}H (600 MHz, $CDCl_3$) and ^{13}C NMR (151 MHz, $CDCl_3$) data for compounds **8**-**10**

	8		**9**		**10**	
No.	**δ_C**	**δ_H (*J*, Hz)**	**δ_C**	**δ_H (*J*, Hz)**	**δ_C**	**δ_H (*J*, Hz)**
1a		1.72, m				1.80, dd (3.4, 15.0)
1b	36.7, CH_2	2.00, m	36.1, CH_2	1.88, m	36.6, CH	2.01, m
2	68.5, CH	4.93, m	71.3, CH	4.88, m	68.5, CH	4.93, m
3	68.3, CH	5.04, m	66.4, CH	4.01, m	68.3, CH	5.05, m
4a		1.93, ddd (2.8, 12.6, 15.4)		1.87, m		1.94, m
4b	21.2, CH_2	2.10, m	23.6, CH_2	2.03, m	21.1, CH_2	2.10, m
5	48.7, CH	2.58, dd (3.5, 12.5)	47.8, CH	2.74, dd (3.5, 12.4)	49.0, CH	2.63, dd (3.23, 12.2)
6	199.6, C		200.6, C		199.4, C	
7	123.3, CH	5.75, m	123.3, CH	5.73, m	127.0, CH	5.93, d, (2.2)
8	162.5, C		162.6, C		157.6, C	
9	50.6, CH	2.25, ddd (2.5, 6.9, 9.9)	50.7, CH	2.25, ddd (2.5, 6.7, 11.7)	46.8, CH	2.68, m
10	37.7, C		37.9, C		38.0, C	
11a		1.62, m		1.61, m		1.58, m
11b	21.5, CH_2	1.78, m	21.5, CH_2	1.79, m	20.3, CH_2	1.76, m
12a		1.40, m		1.41, m		1.69, m
12b	38.7, CH_2	2.14, m	38.7, CH_2	2.12, dd (1.9, 13.0)	29.9, CH_2	1.94, m
13	44.8, C		44.8, C		48.2, C	
14	55.2, CH	2.05, m	55.1, CH	2.05, m	96.1, C	
15a		1.53, m		1.53, m		1.72, m
15b	22.6, CH_2	1.64, m	22.6, CH_2	1.65, m	24.7, CH_2	2.15, m
16a		1.44, m		1.44, m		1.52, m
16b	26.9, CH_2	1.80, m	26.9, CH_2	1.82, m	25.7, CH_2	1.89, m
17	53.3, CH	1.33, m	53.2, CH	1.34, m	47.9, CH	1.89, m
18	12.3, CH_3	0.61, s	12.3, CH_3	0.60, s	16.4, CH_3	0.76, s
19	14.9, CH_3	0.96, s	14.8, CH_3	0.96, s	14.7, CH_3	0.97, s
20	42.4, CH	1.68, m	42.4, CH	1.69, m	41.8, CH	1.74, m
21	12.6, CH_3	0.94, d (6.8)	12.6, CH_3	0.94, d (6.4)	12.8, CH_3	0.89, d (5.1)
22	73.7, CH	3.62, dd (1.6, 10.1)	73.8, CH	3.61, m	74.1, CH	3.63, m
23a		1.24, m		1.25, m		1.23, m
23b	27.8, CH_2	1.36, m	27.7, CH_2	1.36, m	27.2, CH_2	1.39, m
24a		1.17, m		1.16, m		1.17, m
24b	36.0, CH_2	1.39, m	36.0, CH_2	1.42, m	36.0, CH_2	1.39, m
25	28.1, CH	1.55, m	28.1, CH	1.55, m	28.2, CH	1.56, m
26	22.4, CH_3	0.89, d (6.8)	22.4, CH_3	0.89, d (6.9)	22.4, CH_3	0.90, d (6.4)
27	22.9, CH_3	0.90, d (6.8)	22.9, CH_3	0.90, d (6.9)	23.0, CH_3	0.92, d (6.4)
28	169.3, C		170.0, C		169.6, C	
29	169.5, C		21.2, CH_3	2.02, s	169.4, C	
30	21.1, CH_3	2.03, s			21.2, CH_3	2.04, s
31	21.2, CH_3	2.04, s			21.2, CH_3	2.05, s

Similarly, correlations from H-7 to C-9 and C-14; H-9 to C-7, C-8, C-11 and C-19; and from H-14 to C-7, C-8, C-12, C-13, C-15 and C-18 confirmed the structures of rings B, C and D, respectively. The single ^{1}H-^{1}H COSY spin system from H-17 to H-27 was supported by the HMBC cross-peaks to arrive at the 2-hydroxy-1, 5-dimethylhexyl side chain at C-17, and hence the position of the hydroxyl group at C-22. Finally, COSY correlation between H-2 and H-3 and HMBC correlation of H-2 and H-3 to C-28 and C-29, respectively, signified the acetates were attached to the cholestane ecdysteroid backbone at C-2 and C-3.

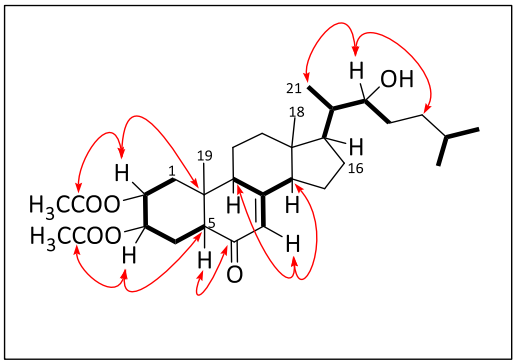

Figure 2.20: Key COSY (**bold** bonds) and HMBC (red curved arrows) of compound **8**

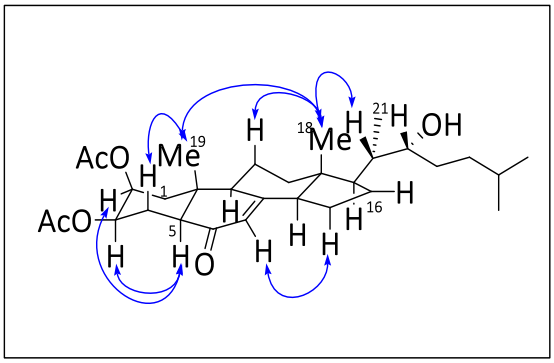

Figure 2.21: Key NOESY (blue curved arrows) of **8**

Key NOESY enhancements together with ^{13}C comparisons enabled the assignment of the relative configuration of **8** (Figure 2.21). The chair conformation and trans-fused A/B ring junction were established from two 1,3-diaxial NOESY correlations from H_3-19β to H_3-30β (OAc) and H-4β (δ_H 1.93), respectively, and a further two 1,3-diaxial NOESY correlations from H-5 to H-3 and H-9, where the latter three protons are all in the same α-orientation. The trans-ring-fusion between rings A and B was further corroborated by the absence of a NOESY cross peak between the methine proton H-5 and H_3-19. The presence of correlation between H_3-18 and H_3-19 but not H_3-21 established the β-configuration of H_3-18 and H_3-19 to the steroid backbone suggesting a chair-chair-chair conformation of rings A, B and C. The relative configurations at C-17, C-20, C-21 and C-22 were assigned, by comparison of the ^{13}C-NMR data with that of the structurally related 22*R* hydroxyl cholesterol.[83] The structure of **8** was determined as a new compound and named Alfredensterol.

Compound **9** (Figure 2.22) was isolated as a white amorphous solid and its molecular formula was found to be $C_{31}H_{48}O_7$ from the HR-ESI-MS ion peak at *m/z* 533.3488 (calcd. 533.3478). The ^{1}H- and ^{13}C-NMR spectroscopic data recorded for compound **9** were virtually identical to compound **8** and suggested a closely related cholestane-type ecdysteroid (Table 2.4). The two acetate methyl singlets (δ_H 2.04, s, H_3-30; δ_H 2.05, s, H_3-31), together with the signals for H_3-19, H_3-26 and H_3-27 for **9** were in close correspondence (±0.02 ppm) with the chemical shifts for **8**, while a downfield shift to δ_H 0.76 was observed for H_3-18. The HSQC-DEPT spectrum revealed one less methine proton and one additional quaternary carbon at δ_C 96.1, indicating the likely presence of a tertiary alcohol functionality at C-14 and therefore accounting for the extra O-atom in the molecular formula of **9**. Moreover, the ^{1}H-^{1}H COSY spectrum exhibited three spin systems from H_2-1 to H-5, H-7 to H_2-12 and H_2-15 to H_3-27, thus revealing the absence of H-14. The relative configuration of compound **9** was assigned primarily using ^{13}C and ROESY NMR data, and were found to be similar to those observed in **8**. To the best of our knowledge, there is only one report of **9** in the literature as a by-product in the synthesis of ecdysone related compounds, in which no extensive NMR assignments could be found, including ^{13}C-NMR data.[74] Therefore, this is the first report of **9** from a natural source, which we have named 14α-hydroxy Alfredensterol (Figure 2.22).

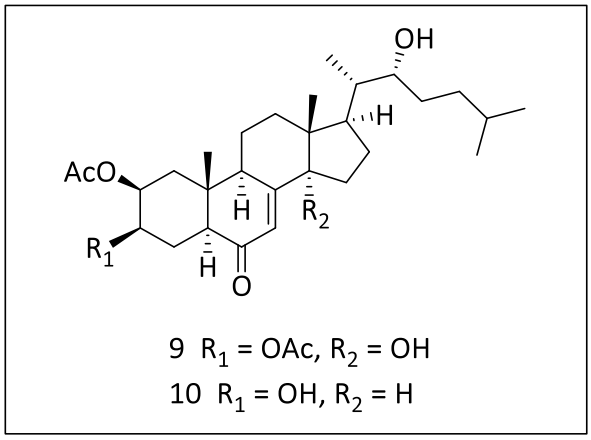

Figure 2.22: Chemical structures of compounds **9** and **10**

Compound **10** (Figure 2.22) was isolated as a white amorphous solid. It recorded a HR-ESI-MS ion peak of *m/z* 475.3432 $[M + H]^+$ (calcd. 475.3423) for the molecular formula $C_{29}H_{46}O_5$. The ^{1}H- and ^{13}C-NMR data for **10** were very similar to both compounds **8** and **9** described above. However,

key noticeable differences in the ^{1}H-NMR data of **10** were observed, including the absence of an acetate methyl singlet and the upfield chemical shifts of H-2 (δ_H 4.88, m) and H-3 (δ_H 4.01, m) compared to **8**. The ^{13}C-NMR data of **10** showed corresponding changes (δ_C 71.3, C-2; 66.4, C-3) consistent with its ^{1}H-NMR. The ^{1}H-^{1}H COSY spin systems were similarly consistent with those observed in compound **8**. The position of the single acetate group on ring A was assigned to C-2, on the basis of the chemical shifts of C-2 and C-3 (Table 2.4), and HMBC cross-peaks from H-2 to C-3, C-4, C-10 and C-28, and from H-3 to C-1, C-2 and C-5. Analysis of the ROESY data revealed the same relative configuration of **10** as observed in **8** and **9**. Compound **10** has not previously been reported and is named here as 3-deacetoxy Alfredensterol (Figure 2.22).

2.3.1.4. Characterization of Isolated Glycolipid (**11**)

Compound **11** (Figure 2.23) was isolated as a white amorphous solid. The HR-ESI-MS data of **11** suggested a molecular formula of $C_{41}H_{78}O_{12}S$ for *m/z* 793.5143 $[M - H]^-$(calcd. 793.5136). The structure was elucidated upon analyses of its NMR data as 1, 2-di-*O*-palmitoyl-3-*O*-(6-sulfo-α-d-quinovopyranosyl)-glycerol and confirmed by comparison with published data.[75] Compound **11** was previously reported from the brown alga *Lobophora variegata*, however, this is the first report of **11** from the genus *Laurencia*.

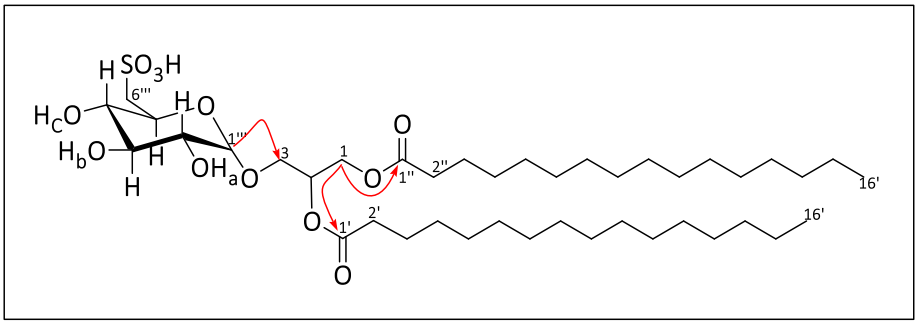

Figure 2.23: Key HMBC (red curved arrows) of **11**

2.3.1.5. Antiproliferative Activity Results

Compounds **1**–**11** were evaluated for their antiproliferative activity against MDA-MB-231 triple negative human breast carcinoma and HeLa human cervical carcinoma (Figure 2.24). Generally, all the compounds displayed antiproliferative activity in the mid-to-low micromolar range against the two cells lines tested.

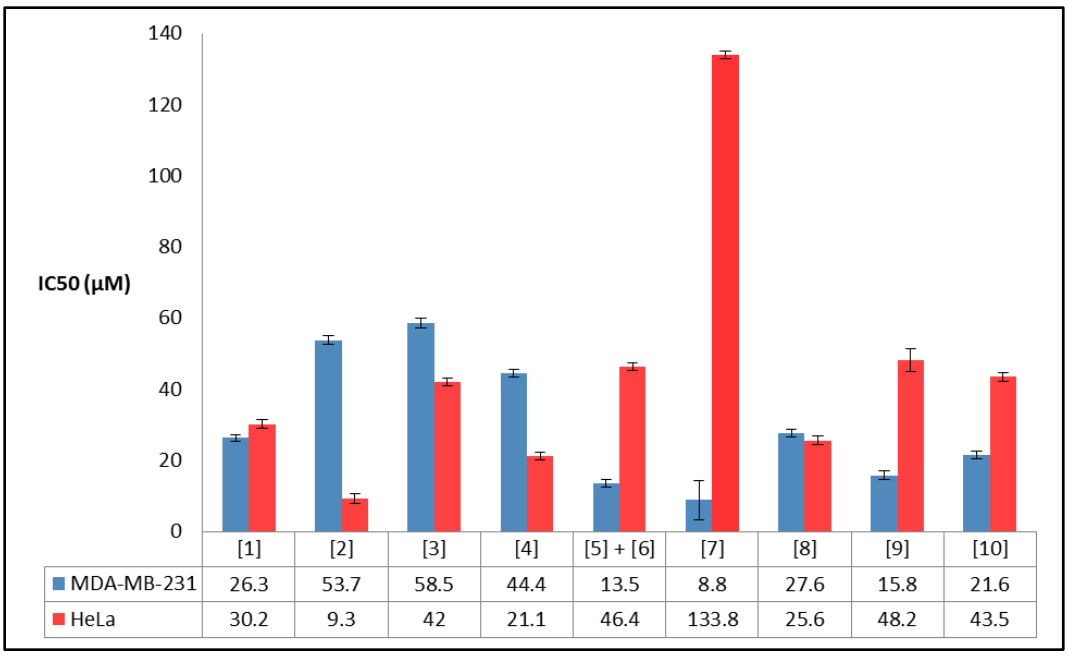

	[1]	[2]	[3]	[4]	[5] + [6]	[7]	[8]	[9]	[10]
MDA-MB-231	26.3	53.7	58.5	44.4	13.5	8.8	27.6	15.8	21.6
HeLa	30.2	9.3	42	21.1	46.4	133.8	25.6	48.2	43.5

Figure 2.24: *In vitro* antiproliferative activity of compounds **1**–**10**

To the best of our knowledge, brominated labdane diterpenes previously isolated from the genus *Laurencia* have not been investigated for their antiproliferative activity. However, non-halogenated labdanes have been reported to exhibit moderate to weak cytotoxic activity against various cancer cell lines.[84–86] In this study, the brominated labdane-type diterpenes **1**–**3** were all found to be moderately active against both cancer cell lines tested, with the exception of Isoconcinndiol 13-acetate **2**, the 8*S*-diastereomer of **1**, which showed the highest antiproliferative activity against the HeLa cancer cell line (IC_{50} = 9.3 ± 1.3 µM), not only in this class of compounds but amongst all ten compounds tested in this study (Figure 2.24), indicating that the stereochemistry at C-8 in **2** could be playing a role in the observed biological activity.

Brominated polyether triterpenes of the [4.4.0] class have been reported to have good to moderate cytotoxic activity.[87] The antiproliferative activity against the HeLa cell line recorded for the known compound **4**, saiyacenol B, in our study was found to be within the previously reported values.[73] To the best of our knowledge, this current work is the first report of the antiproliferative effects of this class of polyether triterpenes against the MDA-MB-231 breast cancer cell line, with the new compound **7**, alfredensinol C, exhibiting the highest activity (IC_{50} = 8.8 ± 5.6 µM) in this particular class of compounds and also amongst all compounds tested (Figure 2.24).

The antiproliferative activity recorded for the ecdysteroids **8**–**10** was consistent with biological activity data previously reported for both natural and semi-synthetic congeners, which have been shown to exhibit moderate antiproliferative or cytotoxic activity.[88] In this particular class of compounds, the new alfredensterol **8** was found to be the most active against the HeLa cervical cancer cell line (IC_{50} = 25.6 ± 1.2 µM), whilst its 14α-hydroxyl derivative **9** exhibited the best antiproliferative effect (IC_{50} = 15.8 ± 1.1 µM) against the MDA-MB-231 breast cancer cell line (Figure 2.24).

In summary, the new compounds **2** and **7** exhibited the best antiproliferative activity against the HeLa and MDA-MB-231 cancer cell lines, respectively, while **11** was found to be non-toxic to both cell lines.

2.3.2. Materials and Methods

2.3.2.1. General Experimental Procedures

Melting points (uncorrected) were recorded on a Reichert-Jung Thermovar hot-stage microscope (Reichert Optische Werke, Vienna, Austria). Optical rotations were measured on a PerkinElmer141 polarimeter by using Na lamp (PerkinElmer Ltd., Beaconsfield, Buckinghamshire, UK. UV spectra were obtained on a CARY 60 UV-VIS 2.00 with software version 5.0.0.999 by Agilent Technologies (Santa Clara, CA, USA). PerkinElmer Spectrum Version 10.03.02 (PerkinElmer Ltd., Llantrisant, Wales, UK) was used to record the IR spectra. NMR spectra were obtained on a BRUKER Ascend 600 ((Bruker, Billeria, MA, USA) cryoprobe prodigy at 600 MHz and 151 MHz for ^{1}H and ^{13}C nuclei, respectively. $CDCl_3$ (δ_H 7.25, δ_C 77.00) was used for **1**–**10** while DMSO-d_6 (δ_H 2.50, δ_C 49.00) was used for **11**. HR-ESI-MS data were obtained via LC-TOF-MS on a Waters Synapt G2 (Waters Corp, Boston, MA, USA), ESI probe injected into a stream of acetonitrile, Cone voltage 15 V. Normal phase HPLC was carried out on Agilent 1220LC system/1260 Infinity (Santa Clara, CA, USA) equipped with a photodiode array and refractive index detectors. Column chromatography was carried out on silica gel 60 (Fluka 70–230 mesh, 63–200 µm, (Sigma-Aldrich, Buchs, Switzerland), and preparative TLC on silica gel 60 Analtech GF_{254} (20 × 20 cm, 2000 µm, Analtech Inc., Newark, DE, USA). Analytical TLC were performed on Merck silica gel 60 F_{254} (Merck KGaA, Darmstadt,

Germany) and silica gel 60 RP-18 F_{254} plates and bands were visualized by heating after staining with ceric ammonium sulfate reagent.

2.3.2.2. Plant Material

The species studied here has only recently been described.[72] It was previously known in South Africa as *Laurencia elata* (C. Agardh) Hooker & Harvey. The latter is an Australian species, which has recently been placed in a new genus as *Coronaphycus elatus* (C. Agardh) Metti.[89] The South African material has been described as a new endemic species *Laurencia alfredensis*.[72] It is the same material previously described as "*Laurencia* cf. *elata*", and used in ^{1}H-NMR profiling of crude organic extracts as an identification tool for nine species of South African *Laurencia*.[72]

2.3.2.3. Extraction, Isolation, and Characterization

The fresh alga (239.2 g) was extracted sequentially with MeOH (15 min) and then CH_2Cl_2/MeOH (2:1 v/v) (24 h) by cold maceration at room temperature. The solvents were evaporated *in vacuo* giving 5.1 g and 1.1 g of dark green MeOH and CH_2Cl_2/MeOH (2:1 v/v) crude extracts, respectively. The two extracts were combined based on close similarity of their ^{1}H-NMR data. The resultant extract was triturated with CH_2Cl_2/MeOH (1:1 v/v) to obtain 1.5 g of organic fraction and 4.7 g of aqueous fraction. Fractionation by flash chromatography was carried out on 1 g of the organic fraction with n-hexane and EtOAc mixtures of increasing polarity and finally with EtOAc/MeOH (1:1 v/v). The fractions obtained with 80%, 70% and 40% *n*-hexane in EtOAc gave similar TLC profiles and were combined and further chromatographed on a silica column with *n*-hexane/EtOAc (9:1 v/v) with increasing polarity to *n*-hexane/EtOAc (4:6 v/v) to afford 12 sub-fractions **A**–**L**. Preparative TLC (*n*-hexane/EtOAc 8.5:1.5 v/v) of **B** gave **3** (1.1 mg) while **1** (3.7 mg) and **4** (4.8 mg) were obtained with *n*-hexane/EtOAc (3:1 v/v) from **E** and **D**, respectively. Compounds **8** (3.1 mg) and **9** (3.5 mg) were obtained from **I** with *n*-hexane/EtOAc (1:1 v/v) and **10** (1.9 mg) from **J** with the same mobile phase. Further purification on Phenomenex Luna 10 µm Prep Silica (2) 250 mm × 10 mm (Phenomenex, Torrance, CA, USA) of **F** with *n*-hexane/EtOAc (4:1 v/v) at a flow rate of 4 mL/min gave **2** (0.5 mg) and 0.5 mg of a mixture of **5** and **6**. Compound **7** (2.5 mg) was obtained on a Whatman Partisil column 10 µm, 500 mm × 10 mm (Hichrom Ltd., Reading, Berkshire, UK) from **K** and **L** with *n*-hexane/EtOAc (3:2 v/v) eluting at 4

mL/min, followed by reversed phase preparative TLC with MeOH/H_2O (1:4 v/v). Meanwhile, the EtOAc/MeOH (1:1 v/v) fraction precipitated out a solid which on trituration with CH_2Cl_2 afforded **11** (49.6 mg).

13-Acetyl Pinnatol A (**1**): Clear crystals; Mp.: 115–117 °C; +26.6 (*c* 0.15, $CHCl_3$); IR (cm^{-1}): 3450, 2950, 2850, 1700, 1350, 1250, 1100; ^{1}H- and ^{13}C-NMR data ($CDCl_3$), Table 2.2; HR-ESI-MS *m/z* 451.1824 $[M + Na]^+$ (calcd. for $C_{22}H_{37}O_3{}^{79}BrNa$, 451.1824).

Isoconcinndiol 13-acetate (**2**): White amorphous solid; +14.4 (*c* 0.09, $CHCl_3$); IR (cm^{-1}): 3455, 2943, 1732, 1367, 1251, 1095; ^{1}H- and ^{13}C-NMR data ($CDCl_3$), Table 2.2; HR-ESI-MS *m/z* 451.1821 $[M + Na]^+$ (calcd. for $C_{22}H_{37}O_3{}^{79}BrNa$, 451.1824).

Concinndiol 13-acetate (**3**): White amorphous solid; +16.7 (*c* 0.06, $CHCl_3$); IR (cm^{-1}): 3467, 2923, 1732, 1462, 1367, 1241; ^{1}H- and ^{13}C-NMR data ($CDCl_3$), Table 2.2; HR-ESI-MS *m/z* 451.1821 $[M + Na]^+$ (calcd. for $C_{22}H_{37}O_3{}^{79}BrNa$, 451.1824).

Saiyacenol B (**4**)[73]: White amorphous solid; ^{1}H- and ^{13}C-NMR data ($CDCl_3$), Table 2.3; ESI-MS *m/z* 611, 609, 606, 604, 571, 569 and 507.

Alfredensinol A (**5**): Clear oil; ^{1}H- and ^{13}C-NMR data ($CDCl_3$), Table 2.3; HR-ESI-MS *m/z* 505.3527 $[M - H]^+$ (calcd. for $C_{30}H_{49}O_6$, 505.3529).

Alfredensinol B (**6**): Clear oil; ^{1}H- and ^{13}C-NMR data ($CDCl_3$), Table 2.3; HR-ESI-MS *m/z* 545.3457 $[M + Na]^+$ (calcd. for $C_{30}H_{51}O_7Na$, 545.3454).

Alfredensinol C (**7**): White amorphous solid; +15.0 (*c* 0.25, $CHCl_3$); IR (cm^{-1}): 3409, 2940, 1374, 1092; ^{1}H- and ^{13}C-NMR data ($CDCl_3$), Table 2.3; HR-ESI-MS *m/z* 507.3693 $[M + H]^+$ (calcd. for $C_{30}H_{51}O_6$, 507.3686).

Alfredensterol (**8**): White amorphous solid; +22.0 (*c* 0.13, $CHCl_3$); UV (MeOH) λ_{max}(log ε), nm: 239 (3.43); IR (cm^{-1}): 3425, 2925, 1737, 1643, 1350, 1234, 1035; ^{1}H- and ^{13}C-NMR data ($CDCl_3$), Table 2.4; HR-ESI-MS *m/z* 517.3527 $[M + H]^+$ (calcd. for $C_{31}H_{49}O_6$, 517.3529).

14α-Hydroxy Alfredensterol (**9**): White amorphous solid; +25.8 (*c* 0.26, $CHCl_3$); UV (MeOH) λ_{max}(log ε), nm: 222 (3.76); IR (cm^{-1}): 3240, 2925, 1738, 1645, 1375, 1234, 1036; ^{1}H- and ^{13}C-NMR data ($CDCl_3$), Table 2.4; HR-ESI-MS *m/z* 533.3488 $[M + H]^+$ (calcd. for $C_{31}H_{49}O_7$, 533.3478).

3-Deacetoxy Alfredensterol (**10**): White amorphous solid; +24.0 (*c* 0.30, $CHCl_3$); UV (MeOH) λ_{max}(log ε), nm: 231 (3.27); IR (cm^{-1}): 3397, 2948, 1715, 1660, 1325, 1240, 1030; ^{1}H- and ^{13}C-NMR data ($CDCl_3$), Table 2.4; HR-ESI-MS *m/z* 475.3432 $[M + H]^+$ (calcd. for $C_{29}H_{47}O_5$, 475.3423).

1,2-di-O-Palmitoyl-3-O-(6-sulfo-α-d-quinovopyranosyl)-glycerol (**11**)[75]: White amorphous solid; ^{1}H-NMR (600 MHz, DMSO-d_6): δ 4.13 (dd, *J* = 7.3, 12.0 Hz, 1H, H-1a), 4.33 (dd, *J* = 2.8, 11.9 Hz, 1H, H-1b), 5.12 (m, 1H, H-2), 3.40 (m, 1H, H-3a), 3.88 (dd, *J* = 5.9, 10.4 Hz, 1H, H-3b), 2.28 (m, 4H, H-2′ and 2″), 1.45–1.57 (m, 4H, H-3′ and 3″), 1.19–1.31 (m, 48H, H-4′–15′ and 4″–15″), 0.85 (t, *J* = 6.8 Hz, 6H, H-16′ and 16″), 4.57 (d, *J* = 2.4 Hz, 1H, H-1‴), 3.19 (m, 1H, H-2‴), 3.35 (m, 1H, H-3‴), 2.94 (dt, *J* = 4.5, 9.1 Hz, 1H, H-4‴), 3.77 (dt, *J* = 6.2, 10.3 Hz, 1H, H-5‴), 2.56 (dd, *J* = 6.2, 13.9 Hz, 1H, H-6‴a), 2.88 (dd, *J* = 4.8, 13.9 Hz, 1H, H-6‴b), 4.58 (d, *J* = 5.1 Hz, 1H, OH-2‴), 4.65 (d, *J* = 4.6 Hz, 1H, OH-3‴), 5.39 (d, *J* = 3.6 Hz, 1H, OH-4‴); ^{13}C-NMR (151 MHz, DMSO-d_6): δ 62.5 (C-1), 69.6 (C-2), 64.6 (C-3), 172.2 (C-1′), 172.4 (C-1″), 33.3 (C-2′), 33.5 (C-2″), 24.3 (C-3′ and 3″), 28.3–28.9 (C-4′–15′ and 4″–15″), 13.8 (C-16′ and 16″), 98.3 (C-1‴), 71.5 (C-2‴), 72.8 (C-3‴), 74.3 (C-4‴), 68.4 (C-5‴), 54.5 (C-6‴); HR-ESI-MS *m/z* 793.5143 $[M - H]^-$ (calcd. for $C_{41}H_{77}O_{12}S$, 793.5136).

2.3.2.4. X-ray Crystallographic Data

The crystal for compound **1** was obtained by recrystallization from methanol and its structure was solved by direct methods from intensity data collected from the crystal specimen at 173(2) K on a Bruker Apex II Duo diffractometer and refined by full-matrix least-squares. The Flack x parameter value of −0.013(6), indicating that the correct absolute configuration had been assigned, was determined using 1652 quotients [(I+) − (I−)]/[(I+) + (I−)]. Salient crystallographic data for **1** are as follows:

Crystal Data for $C_{22}H_{37}O_3Br$ (M = 429.42 g/mol): monoclinic, space group $P2_1$ (no. 4), a = 11.1926(11) Å, *b* = 7.2138(7) Å, *c* = 14.8442(13) Å, β = 111.571(2)°, V = 1114.60(18) $Å^3$, Z = 2, T = 173(2) K, μ(MoKα) = 1.861 mm^{-1}, D_{calc} = 1.280 g cm^{-3}, 20,619 reflections measured (2.95° ≤ 2θ ≤

56.02°), 5386 unique (R_{int} = 0.0549, Rsigma = 0.0537) which were used in all calculations. The final R_1 was 0.0378 ($I > 2\sigma(I)$) and wR_2 was 0.0760 (all data).

2.3.2.5. Cell Culture and Antiproliferative Activity Assay

MDA-MB-231 breast cancer cells (ATCC HTB-26) were maintained in culture in phenol-red free L-15 medium supplemented with 10% (v/v) heat-inactivated fetal bovine serum (FBS), 1 mM l-glutamine, 100 U/mL penicillin, 100 µg/mL streptomycin and 12.5 µg/mL amphotericin (PSA) at 37 °C in a humidified incubator. HeLa cervical cancer cells (ATCC CCL-2) were cultured in Dulbecco's Modified Eagle Medium (DMEM) supplemented as above at 37 °C and 9% CO_2 in a humidified incubator.

The antiproliferative effects of the compounds were assessed using the WST-1 assay (Sigma-Aldrich, Johannesburg, South Africa) as previously described.[90,91] Briefly, cells were seeded at a density of 6000 cells per well into 96-well plates and incubated overnight, followed by treatment with a range of concentrations (0.32, 1.6, 8, 40, 200 and 1000 µM) of the compounds or dimethyl sulfoxide (DMSO) vehicle control (0.02% v/v DMSO) for 96 h. Thereafter 2.5 µL of WST-1 Cell Proliferation Reagent was added per well and the absorbance at 450 nm after 8 h recorded using a Synergy Mx spectrophotometer (BioTek). The half maximal inhibitory concentration (IC_{50}) for each compound was calculated relative to the vehicle-treated control from a dose response curve (log concentration vs absorbance at 595 nm) using non-linear regression with GraphPad Prism 4 (GraphPad Inc., San Diego, CA, USA).

2.4 References

(1) M.D. Guiry in Guiry, M.D. & Guiry, G. M. AlgaeBase. World-wide electronic publication, National University of Ireland, Galway. http://www.algaebase.org.

(2) Nonomura, A. M.; West, J. A. Ultrastructure of the parasite *Janczewskia morimotoi* and its host *Laurencia nipponica* (Ceramiales, Rhodophyta). *J. Ultrastruct. Res.* 1980, *73* (2), 183–198.

(3) Kilar, J. A.; Lou, R. M. Ecological and behavioral studies of the decorator crab, *Microphrys*

bicornutus Latreille (Decapoda: Brachyura): A test of optimum foraging theory. *J. Exp. Mar. Biol. Ecol.* 1984, *74*, 157–167.

(4) Kilar, J. A.; Lou, R. M. The subtleties of camouflage and dietary preference of the decorator crab, *Microphrys bicornutus* Latreille (Decapoda: Brachyura). *J. Exp. Mar. Biol. Ecol.* 1986, *101*, 143–160.

(5) Stoner, A. W.; Waite, J. M. Trophic biology of *Strombus gigas* in nursery habitats: Diets and food sources in seagrass meadows. *J. Mollusc. Stud.* 1991, *57*, 451.

(6) Boettcher, A. A.; Targett, N. M. Induction of metamorphosis in queen conch, *Strombus gigas* Linnaeus, larvae by cues associated with red algae from their nursery grounds. *J. Exp. Mar. Biol. Ecol.* 1996, *196*, 29–52.

(7) Suenaga, K. Bioorganic studies on marine natural products with bioactivity, such as antitumor activity and feeding attractance. *Bull. Chem. Soc. Jpn.* 2004, *77*, 443–451.

(8) Yamamura, S.; Hirata, Y. Structures of aplysin and aplysinol, naturally occurring bromo compounds. *Tetrahedron* 1963, *19*, 1485–1496.

(9) Butler, A.; Carter-Franklin, J. N. The role of vanadium bromoperoxidase in the biosynthesis of halogenated marine natural products. *Nat. Prod. Rep.* 2004, *21* (1), 180–188.

(10) Salgado, L. T.; Viana, N. B.; Andrade, L. R.; Leal, R. N.; da Gama, B. A. P.; Attias, M.; Pereira, R. C.; Amado Filho, G. M. Intra-cellular storage, transport and exocytosis of halogenated compounds in marine red alga *Laurencia obtusa*. *J. Struct. Biol.* 2008, *162* (2), 345–355.

(11) Suzuki, M.; Kurosawa, E. Halogenated and non-halogenated aromatic sesquiterpenes from the red algae *Laurencia okamurai* Yamada. *Bull. Chem. Soc. Jpn.* 1979, *52*, 3352.

(12) Suzuki, M.; Kurosawa, E.; Kurata, K. (E)-2-tridecyl-2-heptadecenal, an unusual metabolite from the red alga *Laurencia* species. *Bull. Chem. Soc. Jpn.* 1987, *60*, 3793.

(13) Vairappan, C. S.; Suzuki, M.; Abe, T.; Masuda, M. Halogenated metabolites with antibacterial

activity from the Okinawan *Laurencia* species. *Phytochemistry* 2001, *58* (3), 517–523.

(14) Reis, V. M.; Oliveira, L. S.; Passos, R. M. F.; Viana, N. B.; Mermelstein, C.; Sant'Anna, C.; Pereira, R. C.; Paradas, W. C.; Thompson, F. L.; Amado-Filho, G. M.; et al. Traffic of secondary metabolites to cell surface in the red alga *Laurencia dendroidea* depends on a two-step transport by the cytoskeleton. *PLoS One* 2013, *8* (5), e63929.

(15) Wang, B.-G.; Gloer, J. B.; Ji, N.-Y.; Zhao, J.-C. Halogenated organic molecules of Rhodomelaceae origin: Chemistry and Biology. *Chem. Rev.* 2013, *113* (5), 3632–3685.

(16) Ji, N. Y.; Wang, B. G. Nonhalogenated organic molecules from *Laurencia* algae. *Phytochemistry Reviews*. 2014, pp 653–670.

(17) Harizani, M.; Ioannou, E.; Roussis, V. The laurencia paradox: An endless source of chemodiversity; 2016; pp 91–252.

(18) Izac, R. R.; Sims, J. J. Marine natural products. 18. Iodinated sesquiterpenes from the red algal genus *Laurencia*. *J. Am. Chem. Soc.* 1979, *101*, 6136–6137.

(19) Kladi, M.; Vagias, C.; Papazafiri, P.; Furnari, G.; Serio, D.; Roussis, V. New sesquiterpenes from the red alga *Laurencia microcladia*. *Tetrahedron* 2007, *63*, 7606–7611.

(20) Vazquez, J. T.; Chang, M.; Nakanishi, K.; Martin, J. D.; Martin, V. S.; Perez, R. Puertitols: Novel sesquiterpenes from *Laurencia obtusa*. Structure elucidation and absolute configuration and conformation based on circular dichroism. *J. Nat. Prod.* 1988, *51*, 1257–1260.

(21) Aydoğmuş, Z.; Imre, S.; Ersoy, L.; Wray, V. Halogenated secondary metabolites from *Laurencia obtusa*. *Nat. Prod. Res.* 2004, *18* (1), 43–49.

(22) Li, C.-S.; Li, X.-M.; Cui, C.-M.; Wang, B.-G. Brominated metabolites from the marine red alga *Laurencia similis*. *Z. Naturforsch.* 2010, *65b*, 87–89.

(23) McMillan, J. A.; Paul, I. C.; White, R. H.; Hager, L. P. Molecular structure of acetoxyintricatol: A new bromo compound from *Laurencia intricata*. *Tetrahedron Lett* 1974, *15*, 2039–2042.

(24) Suzuki, T.; Suzuki, M.; Kurosawa, E. α-bromocuparene and α-isobromocuparene, new bromo compounds from *Laurencia* species. *Tetrahedron Lett* 1975, *16 (35)*, 3057–3058.

(25) Kazlauskas, R.; Murphy, P. T.; Wells, R. J.; Daly, J. J.; Oberhansli, W. E. Heterocladol, a halogenated selinane sesquiterpene of biosynthetic significance from *Laurencia filiformis*: Its isolation, crystal structure and absolute configuration. *Aust. J. Chem.* 1977, *30*, 2679.

(26) Kladi, M.; Xenaki, H.; Vagias, C.; Papazafiri, P.; Roussis, V. New cytotoxic sesquiterpenes from the red algae *Laurencia obtusa* and *Laurencia microcladia*. *Tetrahedron* 2006, *62*, 182–189.

(27) Kuniyoshi, M.; Marma, M. S.; Higa, T.; Bernardinelli, G.; Jefford, C. W. New bromoterpenes from the red alga *Laurencia luzonensis*. *J. Nat. Prod.* 2001, *64* (6), 696–700.

(28) Gonzalez, A. G.; Aguiar, J. M.; Darias, J.; Gonza´ lez, E.; Martín, J. D.; Martín, V. S.; Perez, C.; Fayos, J.; Martínez-Ripoll, M. Perforenol, a new polyhalogenated sesquiterpene from *Laurencia perforata*. *Tetrahedron Lett* 1978, *19*, 3931.

(29) Iliopoulou, D.; Vagias, C.; Galanakis, D.; Argyropoulos, D.; Roussis, V. Brasilane-type sesquiterpenoids from *Laurencia obtusa*. *Org. Lett.* 2002, *4* (19), 3263–3266.

(30) Rengasamy, K. R. R.; Slavětínská, L. P.; Kulkarni, M. G.; Stirk, W. A.; Van Staden, J. Cuparane sesquiterpenes from *Laurencia natalensis* Kylin as inhibitors of alpha-glucosidase, dipeptidyl peptidase IV and xanthine oxidase. *Algal Res.* 2017, *25*, 178–183.

(31) Gonzalez, A. G.; Darias, J.; Martın, J. D.; Martın, V. S.; Norte, M.; Perez, C.; Perales, A.; Fayos, J. Laurencia sesquiterpene biogenetic-type interconversions. *Tetrahedron Lett* 1980, *21*, 1151.

(32) Howard, B. M.; Fenical, W. Structures of the Irieols, new dibromoditerpenoids of a unique skeletal class from *Laurencia irieii*. *J. Org. Chem.* 1978, *43*, 4401–4408.

(33) Sims, J. J.; Lin, G. H. Y.; Wing, R. M.; Fenical, W. Marine natural products. Concinndiol, a bromo-diterpene alcohol from the red alga *Laurencia concinna*. *J. Chem. Soc. Chem.*

Commun. 1973, *14*, 470–471.

(34) Rochfort, S. J.; Capon, R. J. Parguerenes revisited: New brominated diterpenes from the southern Australian marine red alga *Laurencia filiformis*. *Aust. J. Chem.* 1996, *49*, 19–26.

(35) Kuniyoshi, M.; Wahome, P. G.; Miono, T.; Hashimoto, T.; Yokoyama, M.; Shrestha, K. L.; Higa, T. Terpenoids from *Laurencia luzonensis*. *J. Nat. Prod.* 2005, *68* (9), 1314–1317.

(36) Howard, B. M.; Fenical, W. Obtusadiol, a unique bromoditerpenoid from the marine red alga *Laurencia obtusa*. *Tetrahedron Lett* 1978, *18*, 2453.

(37) Mihopoulos, N.; Vagias, C.; Mikros, E.; Scoullos, M.; Roussis, V. Prevezols A and B: New brominated diterpenes from the red alga *Laurencia obtusa*. *Tetrahedron Lett* 2001, *42*, 3749–3752.

(38) Guella, G.; Pietra, F. A new-skeleton diterpenoid, new prenyl bisabolanes, and their putative biogenetic precursor, from the red seaweed *Laurencia microcladia* from Il rogiolo: Assigning the absolute configuration when two chiral halves are connected by single bonds. *Helv. Chim. Acta.* 2000, *83 (11)*, 2946–2952.

(39) Gonzalez, A. G.; Ciccio, J. F.; Rivera, A. P.; Martın, J. D. New halogenated diterpenes from the red alga *Laurencia perforata*. *J. Org. Chem.* 1985, *50*, 1261.

(40) Blunt, J. W.; Hartshorn, M. P.; McLennan, T. J.; Munro, M. H. G.; Robinson, W. T.; Yorke, S. C. Thyrsiferol, a squalene-derived metabolite of *Laurencia thyrsifera*. *Tetrahedron Lett* 1978, *19*, 69–72.

(41) Manrıquez, C. P.; Souto, M. L.; Gavın, J. A.; Norte, M.; Fernandez, J. J. Several new squalene-derived triterpenes from *Laurencia*. *Tetrahedron* 2001, *57*, 3117.

(42) Suzuki, M.; Matsuo, Y.; Takeda, S.; Suzuki, T. Intricatetraol, a halogenated triterpene alcohol from the red alga *Laurencia intricata*. *Phytochemistry* 1993, *33*, 651–656.

(43) Blunt, J. W.; Copp, B. R.; Keyzers, R. A.; Munro, M. H. G.; Prinsep, M. R. Marine Natural

Products. *Nat. Prod. Rep.* 2015, *32* (2), 116–211.

(44) Cox, P. J.; Imre, S.; Islimyeli, S.; Thomson, R. H. Obtusallene I, a new halogenated allene from *Laurencia obtusa*. *Tetrahedron Lett.* 1982, *23* (5), 579–580.

(45) Waraszkiewicz, S. M.; Sun, H. H.; Erickson, K. L. C15-halogenated compounds from the Hawaiian marine alga *Laurencia nidifica*. V. The maneonenes. *Tetrahedron Lett.* 1976, *17* (35), 3021–3024.

(46) Fukuzawa, A.; Kurosawa, E.; Tobetsu, I. Laureepoxide, new bromo ether from the marine red alga *Laurencia nipponica* Yamada. *Tetrahedron Lett* 1980, *21*, 1471.

(47) Gutierrez-Cepeda, A.; Fernandez, J. J.; Gil, L. V.; Lopez-Rodrıguez, M.; Norte, M.; Souto, M. L. Nonterpenoid C15 acetogenins from *Laurencia marilzae*. *J. Nat. Prod.* 2011, *74*, 441–448.

(48) Coll, J. C.; Wright, A. D. Tropical Marine Algae IV. Novel metabolites from the red alga *Laurencia implicata* (Rhodophyta, Rhodophyceae, Ceramiales, Rhodomelaceae). *Aust. J. Chem.* 1989, *42*, 1685–1693.

(49) Howard, B. M.; Schulte, G. R.; Fenical, W.; Solheim, B.; Clardy, J. Three new vinyl acetylenes from the marine red alga *Laurencia*. *Tetrahedron* 1980, *36* (12), 1747–1751.

(50) White, R. H.; Hager, L. P. Intricenyne and related halogenated compounds from *Laurencia intricata*. *Phytochemistry* 1978, *17* (5), 939–941.

(51) Guella, G.; Mancini, I.; Chiasera, G.; Pietra, F. On the unusual propensity by the red seaweed *Laurencia microcladia* of II rogiolo to form C15 oxepanes: Isolation of rogioloxepane A, B, C, and their likely biogenetic acyclic precursor, prerogioloxepane. *Helv. Chim. Acta.* 1992, *75* (1), 310–322.

(52) Takahashi, Y.; Suzuki, M.; Abe, T.; Masuda, M. Japonenynes, halogenated C15 acetogenins from *Laurencia japonensis*. *Phytochemistry* 1999, *50* (5), 799–803.

(53) Suzuki, M.; Takahashi, Y.; Matsuo, Y.; Guiry, M. D.; Masuda, M. Scanlonenyne, a novel

halogenated C15 acetogenin from the red alga *Laurencia obtusa* in Irish Waters. *Tetrahedron* 1997, *53*, 4271–4278.

(54) Howard, B. M.; Fenical, W.; Arnold, E. V.; Clardy, J. Obtusin, a unique bromine-containing polycyclic ketal from the red marine alga *Laurencia obtusa*. *Tetrahedron Lett* 1979, *20*, 2841–2844.

(55) Kikuchi, H.; Suzuki, T.; Kurosawa, E.; Suzuki, M. The structure of notoryne, a halogenated C15 nonterpenoid with a novel carbon skeleton from the red alga *Laurencia nipponica* Yamada. *Bull. Chem. Soc. Jpn.* 1991, *64*, 1763–1775.

(56) Tanaka, J.; Higa, T.; Bernardinelli, G.; Jefford, C. W. Itomanindoles A and B, methylsulfinylindoles from *Laurencia brongniartii*. *Tetrahedron Lett* 1988, *29*, 6091–6094.

(57) Su, H.; Yuan, Z. H.; Li, J.; Guo, S. J.; Deng, L. P.; Han, L. J.; Zhu, X. B.; Shi, D. Y. Two new bromoindoles from red alga *Laurencia similis*. *Chin. Chem. Lett.* 2009, *20*, 456–458.

(58) Sun, W. S.; Su, S.; Zhu, R. X.; Tu, G. Z.; Cheng, W.; Liang, H.; Guo, X. Y.; Zhao, Y. Y.; Zhang, Q. Y. A pair of unprecedented spiro-trisindole enantiomers fused through a five-member ring from *Laurencia similis*. *Tetrahedron Lett* 2013, *54*, 3617.

(59) Fukuzawa, A.; Kumagai, Y.; Masamune, T.; Furusaki, A.; Katayama, C.; Matsumoto, T. Acetylpinnasterol and pinnasterol, ecdysone-like metabolites from the marine red alga *Laurencia pinnata* Yamada. *Tetrahedron Lett* 1981, *22*, 4085–4086.

(60) Wanke, T.; Philippus, A. C.; Zatelli, G. A.; Vieira, L. F. O.; Lhullier, C.; Falkenberg, M. C15 acetogenins from the *Laurencia* complex: 50 years of research – an Overview. *Rev. Bras. Farmacogn.* 2015, *25* (6), 569–587.

(61) Juagdan, E. G.; Kalidindi, R.; Scheuer, P. Two new chamigranes from an Hawaiian red alga,. *Laurencia cartilaginea*. *Tetrahedron* 1997, *53*, 521–528.

(62) Wessels, M.; König, G. M.; Wright, A. D. New natural product isolation and comparison of

the secondary metabolite content of three distinct samples of the sea hare *Aplysia dactylomela* from Tenerife. *J. Nat. Prod.* 2000, *63* (7), 920–928.

(63) Dias, T.; Brito, I.; Moujir, L.; Paiz, N.; Darias, J.; Cueto, M. Cytotoxic sesquiterpenes from *Aplysia dactylomela*. *J. Nat. Prod.* 2005, *68* (11), 1677–1679.

(64) Vairappan, C. S. Potent Antibacterial activity of halogenated metabolites from Malaysian red algae, *Laurencia majuscula* (Rhodomelaceae, Ceramiales). *Biomol. Eng.* 2003, *20* (4–6), 255–259.

(65) Wright, A. D.; Goclik, E.; König, G. M. Three new sesquiterpenes from the red alga *Laurencia Perforata*. *J. Nat. Prod.* 2003, *66* (3), 435–437.

(66) Erickson, K. L.; Beutler, J. A.; Gray, G. N.; Cardellina, J. H. I.; Boyd, M. R. Majapolene A, a cytotoxic peroxide, and related sesquiterpenes from the red alga *Laurencia majuscula*. *J. Nat. Prod.* 1995, *58*, 1848.

(67) Suzuki, T.; Suzuki, M.; Furusaki, A.; Matsumoto, T.; Kato, A.; Imanaka, Y.; Kurosawa, E. Teurilene and thyrsiferyl 23-acetate, meso and remarkably cytotoxic compounds from the marine red alga *Laurencia obtusa* (Hudson) Lamouroux. *Tetrahedron Lett* 1985, *26*, 1329.

(68) Matsuzawa, S.; Suzuki, T.; Suzuki, M.; Matsuda, A.; Kawamura, T.; Mizuno, Y.; Kikuchi, K. Thyrsiferyl 23-acetate is a novel specific inhibitor of protein phosphatase PP2A. *FEBS Lett.* 1994, *356* (2–3), 272–274.

(69) Watanabe, K.; Umeda, K.; Miyakado, M. Isolation and identification of three insecticidal principles from the red alga *Laurencia nipponica* Yamada. *Agric. Biol. Chem.* 1989, *53*, 2513.

(70) Kimura, J.; Kamada, N.; Tsujimoto, Y. Fourteen chamigrane derivatives from a red alga *Laurencia nidifica*. *Bull. Chem. Soc. Jpn.* 1999, *72*, 289.

(71) Dziwornu, G. A.; Caira, M. R.; Mare, J.-A. de la; Edkins, A. L.; Bolton, J. J.; Beukes, D. R.; Sunassee, S. N. Isolation, characterization and antiproliferative activity of new metabolites

from the South African endemic red algal species *Laurencia alfredensis*. *Molecules* 2017, *22* (4).

(72) Francis, C.; Bolton, J. J.; Mattio, L.; Mandiwana-Neudani, T. G.; Anderson, R. J. Molecular systematics reveals increased diversity within the South African *Laurencia* complex (Rhodomelaceae, Rhodophyta). *J. Phycol.* 2017, *53* (4), 804–819.

(73) Cen-Pacheco, F.; Mollinedo, F.; Villa-Pulgarín, J. A.; Norte, M.; Fernández, J. J.; Hernández Daranas, A. Saiyacenols A and B: The key to solve the controversy about the configuration of aplysiols. *Tetrahedron* 2012, *68* (36), 7275–7279.

(74) Barton, D. H. R.; Feakins, P. G.; Poyser, J. P.; Sammes, P. G. A synthesis of the insect moulting hormone, ecdysone, and related compounds. *J. Chem. Soc. C Org.* 1970, No. 11, 1584.

(75) Cantillo-Ciau, Z.; Moo-Puc, R.; Quijano, L.; Freile-Pelegrín, Y. The tropical brown alga *Lobophora variegata*: A source of antiprotozoal compounds. *Mar. Drugs* 2010, *8* (4), 1292–1304.

(76) Howard, B. M.; Fenical, W. Isoconcinndiol, a brominated diterpenoid from *Laurencia snyderae* var. *Guadalupensis*. *Phytochemistry* 1980, *19* (12), 2774–2776.

(77) Rodríguez, M. L.; Martín, J. D.; Estrada, D. The absolute configuration of (+)-isoconcinndiol. *Acta Crystallogr. Sect. C Cryst. Struct. Commun.* 1989, *45* (2), 306–308.

(78) Fukuzawa, A.; Miyamoto, M.; Kumagai, Y.; Abiko, A.; Takaya, Y.; Masamune, T. Structure of new bromoditerpenes, pinnatols, from the marine red alga *Laurencia pinnata* Yamada. *Chem. Lett.* 1985, *14* (8), 1259–1262.

(79) Sims, J. J.; Lin, G. H. Y.; Wing, R. M.; Fenical, W. Marine natural products. Concinndiol, a bromo-diterpene alcohol from the red alga, *Laurencia concinna*. *J. Chem. Soc. Chem. Commun.* 1973, No. 14, 470.

(80) Blunt, J. W.; Hartshorn, M. P.; McLennan, T. J.; Munro, M. H. G.; Robinson, W. T.; Yorke, S.

C. Thyrsiferol: A squalene-derived metabolite of *Laurencia thyrsifera*. *Tetrahedron Lett.* 1978, *19* (1), 69–72.

(81) Gonzalez, A. G.; Arteaga, J. M.; Fernandez, J. J.; Martin, J. D.; Norte, M.; Ruano, J. Z. Terpenoids of the red alga *Laurencia pinnatifida*. *Tetrahedron* 1984, *40* (14), 2751–2755.

(82) Pacheco, F. C.; Villa-Pulgarin, J. A.; Mollinedo, F.; Martín, M. N.; Fernández, J. J.; Daranas, A. H. New polyether triterpenoids from *Laurencia viridis* and their biological evaluation. *Mar. Drugs* 2011, *9* (11), 2220–2235.

(83) Ayciriex, S.; Regazzetti, A.; Gaudin, M.; Prost, E.; Dargère, D.; Massicot, F.; Auzeil, N.; Laprévote, O. Development of a novel method for quantification of sterols and oxysterols by UPLC-ESI-HRMS: Application to a neuroinflammation rat model. *Anal. Bioanal. Chem.* 2012, *404* (10), 3049–3059.

(84) Roengsumran, S.; Petsom, A.; Kuptiyanuwat, N.; Vilaivan, T.; Ngamrojnavanich, N.; Chaichantipyuth, C.; Phuthong, S. Cytotoxic labdane diterpenoids from *Croton oblongifolius*. *Phytochemistry* 2001, *56* (1), 103–107.

(85) Lee, S. O.; Choi, S. Z.; Choi, S. U.; Lee, K. C.; Chin, Y. W.; Kim, J.; Kim, Y. C.; Lee, K. R. Labdane diterpenes from *Aster spathulifolius* and their cytotoxic effects on human cancer cell lines. *J. Nat. Prod.* 2005, *68* (10), 1471–1474.

(86) Zhang, J.; Li, Y.; Zhu, R.; Li, L.; Wang, Y.; Zhou, J.; Qiao, Y.; Zhang, Z.; Lou, H. Scapairrins A–Q, labdane-type diterpenoids from the Chinese liverwort *Scapania irrigua* and their cytotoxic activity. *J. Nat. Prod.* 2015, *78* (8), 2087–2094.

(87) Fernández, J. J.; Souto, M. L.; Norte, M. Marine Polyether Triterpenes (up to May 1999). *Nat. Prod. Rep.* 2000, *17* (3), 235–246.

(88) Martins, A.; Tóth, N.; Ványolós, A.; Béni, Z.; Zupkó, I.; Molnár, J.; Báthori, M.; Hunyadi, A. Significant activity of ecdysteroids on the resistance to doxorubicin in mammalian cancer cells expressing the human ABCB1 transporter. *J. Med. Chem.* 2012, *55* (11), 5034–5043.

(89) Metti, Y.; Millar, A. J. K.; Steinberg, P. A New molecular phylogeny of the *Laurencia* Complex (Rhodophyta, Rhodomelaceae) and a review of key morphological characters result in a new genus, *Coronaphycus*, and a description of *C. novus*. *J. Phycol.* 2015, *51* (5), 929–942.

(90) de la Mare, J.-A.; Lawson, J. C.; Chiwakata, M. T.; Beukes, D. R.; Edkins, A. L.; Blatch, G. L. Quinones and halogenated monoterpenes of algal origin show anti-proliferative effects against breast cancer cells *in vitro*. *Invest. New Drugs* 2012, *30* (6), 2187–2200.

(91) de la Mare, J.-A.; Sterrenberg, J. N.; Sukhthankar, M. G.; Chiwakata, M. T.; Beukes, D. R.; Blatch, G. L.; Edkins, A. L. Assessment of potential anti-cancer stem cell activity of marine algal compounds using an *in vitro* mammosphere assay. *Cancer Cell Int.* 2013, *13* (1), 39.

3.1 General Introduction

Marine organisms belonging to the phylum Porifera, mostly sponges, have been the most abundant source of new compounds from the marine environment.[1–3] This is due in part to their wide distribution in the world and their sedentary life form which makes them easy to collect.[4] Chemical compounds produced by sponges belong to the structural classes of terpenes, alkaloids, lipids, peptides, and steroids. Compared to their terrestrial partners, these natural products have novel molecular frameworks as well as intriguing stereochemistry and numbers of heteroatoms.

Secondary metabolites of sponge origin are not only structurally intriguing but biologically active too.[5] In fact, sponges have yielded drug candidates in clinical development, while some developed compounds based on sponge metabolites, for example cytabarine (Ara-C) and vidarabine (Ara-A), are approved drugs.[6] The rich chemical diversity of these sedentary and soft-bodied organisms is as a result of the need for effective chemical defense against the environmental threats of predation, fouling and microbial infections.[7] It is believed that some of the natural products isolated from sponges are biosynthesized by either microbial symbionts or microbes inhaled by filter feeding.[3]

3.2 Background to current work

The sponge specimens studied herein were obtained in 2015 as part of a collaboration between researchers from the University of Cape Town, Rhodes University, the Council for Scientific and Industrial Research, the South African Environmental Observation Network and the Department of Environmental Affairs who participated in the annual relief expedition to the Prince Edward Islands on board the research vessel *SA Agulhas II*. The specimens were collected as part of the inter-island biodiversity survey between Prince Edward and Marion Islands. The collection strategy involved benthic trawling using a steel dredge towed behind the vessel (for 15-20 min.) at varying depths (60-254 m) along four pre-determined stations (Figure 3.1). Nine sponge specimens were

collected in all. They were processed, frozen for storage, and later transported to the laboratory for analysis.[8]

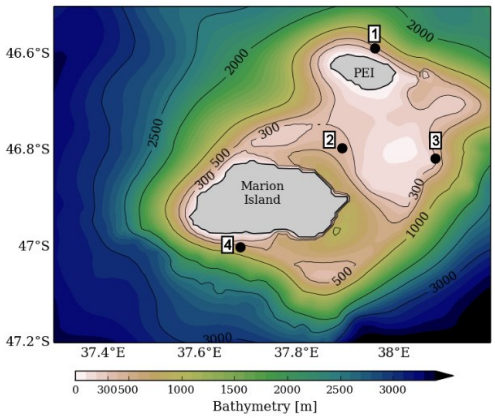

Figure 3.1: Survey area around the Prince Edward Islands, indicating the position of the four benthic dredge stations: (1) Prince Edward Island (PEI); (2 and 3) between the islands; and (4) south of Marion Island. Station depths are: 130 m (1), 65 m (2), 230 m (3) and 254 m (4).[8]

The animals were identified by Dr. Toufiek Samaai (Department of Environmental Affairs, South Africa). The sponge specimens were lyophilized, followed by preparation of aqueous (100% deionized water) and organic extracts (DCM:MeOH 1:1 v/v) using standard procedures.[9] The cytotoxic activities of the crude extracts against the HeLa, MCF7 and A549 cancer cell lines have already been published. In general, the extracts displayed poor to no activity.[8] However, based on reported work on the new and/or bioactive secondary metabolites isolated from sponges of the genera *Halichondria* and *Hymeniacidon* (Figure 3.2), we undertook a chemical investigation of the organic extracts, which is reported herein.

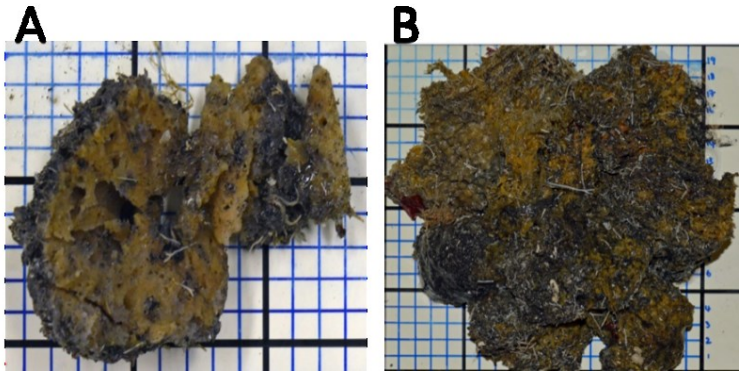

Figure 3.2: (A) *Halichondria* sp. and (B) *Hymeniacidon* sp. investigated in the current work

3.3 Chemistry and biology of the genus *Halichondria*

Secondary metabolites reported from *Halichondria* species include lipids, alkaloids, peptides, terpenes and steroid-based compounds. The rich chemical diversity and biological activities reported for *Halichondria* are discussed below. The information was retrieved from MarinLit database "compound" search of genus *Halichondria* and considers secondary metabolites from *Halichondria* species,[10] but the following discussion excludes those metabolites isolated from microorganisms (bacteria and fungi) associated with *Halichondria* species.

The 'lipid' class of *Halichondria* metabolites comprise long chain hydrocarbons,[11–15] cerebrosides, and polyketides, including macrolides and macrocycles (Figure 3.3). The long chain hydrocarbon compounds reported so far include fatty acids,[11] glycerides,[15] and polyacetylenic alcohol.[13,14] Apart from the new straight chain fatty acid metabolites isolated from the Caribbean *H. magniconulosa* and *H. lutea*,[11] halicholactone[16] and neohalicholactone[17], are unusual fatty acids having both cyclopropane and nine-membered lactone rings. Isopetrosynol, a new polyacetylenic alcohol isolated from *H*. cf. *panicea* and related congeners have been reported to inhibit protein tyrosine phosphate 1B (PTP1B) (IC_{50} = 7.8 – 21.6 µM).[13] However, in another study, the pellynols demonstrated submicromolar anti-inflammatory activity towards HeLa and K562 cancer cell lines. Isopellynol A was the least active of the compounds tested with IC_{50} values of 4.13 µM and 1.95 µM against HeLa and K562 cell lines, respectively. According to Miyamoto and coworkers, the "hexa-2,4-diyn-1,6-diol" and "pent-1-en-4-yn-3-ol" on the termini of the pellynols are essential for activity.[14] Hardardottir and coworkers found the lipophilic fractions from *H. sitiens* to decrease secretion of the proinflammatory cytokines IL-12p40 and IL-6 by dendritic cells at 10 µg/mL with maximum inhibition at 64% and 25%, respectively. However, after isolation, the new glyceride 2,3-dihydroxypropyl 2-methylhexacanoate and its known congeners showed no immunomodulatory activity.[15]

Halicylindrosides are a class of cerebrosides first isolated from the Japanese marine sponge *H. cylindrata*. The first ten members of the halicylindrosides (A1-A4 and B1-B6) were discovered based on the high antifungal activity of the ethanol crude extract against *Mortierella remanniana*. These *N*-acetylglucosaminyl ceramides were also found to be cytotoxic to P-388 cancer cell lines.[18]

The Oregon sponge *H. panacea* has also afforded two new galactosyl-ceramides.[19] This report is the second regarding the presence of galactosyl-ceramides from *Halichondria*.[20]

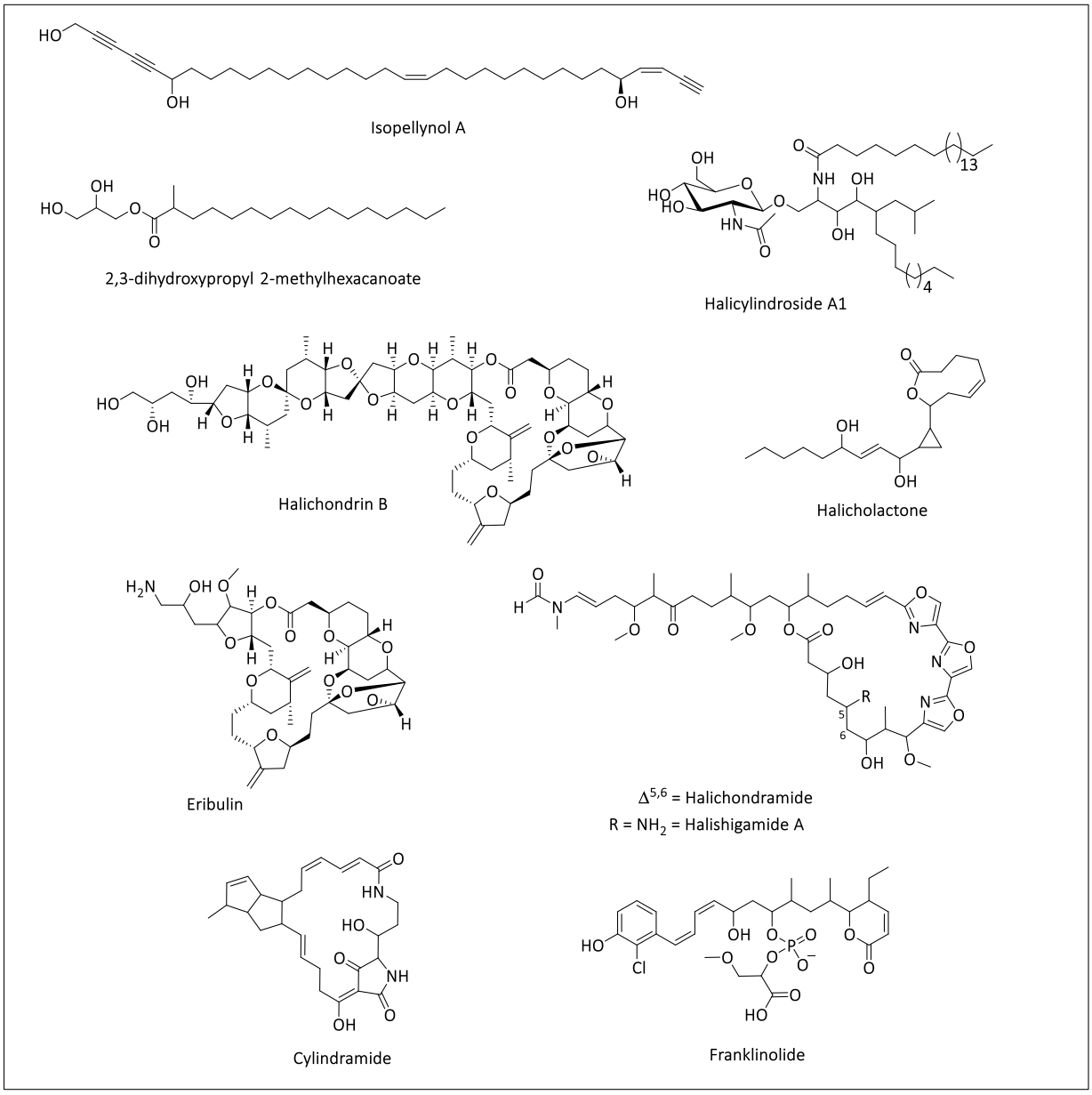

Figure 3.3: Examples of 'lipid' metabolites from *Halichondria* species

The halichondrins, halichondramides and halishigamides are macrolide-based natural products from *Halichondria*. The halichondrins were first reported from the Japanese *H. okadai*. These compounds are characterized by a long acyclic chain, a polyether macrolide and a novel 2,6,9-trioxatricyclo[3.3.2.03,7]decane system. Halichondrin B exhibited the most potent *in vitro*

cytotoxic activity against B-16 melanoma with an IC_{50} value of 0.083 nM. It also demonstrated good *in vivo* activity in mice against B-16 melanoma, P-388 and L-1210 leukemia.[21] Eribulin (Halaven®) is a synthetic analog of halichondrin B and is an anticancer drug marketed by Eisai Co.

The halichondramides and halishigamides both share similar structural features, for example the presence of oxazole rings and a straight carbon chain (Figure 3.3). Faulkner and coworkers have reported the antifungal activity and inhibition of cell division in fertilized sea urchin egg assay by the halichondramides.[22,23] Moreover, in a recent study, the parent compound halichondramide has been suggested as a potential inhibitor of tumor cell metastasis with modulation of phosphatase of regenerating liver-3 (PRL-3) in metastatic PC3 human prostate cancer cells having exhibited inhibitory activity with an IC_{50} value of 0.81 µM.[24] Lee and coworkers have also demonstrated that (19*Z*)-halichondramide, isolated from *Chondrosia corticata* causes cell cycle arrest and modulates mTOR/AMPK signaling pathways in human lung cancer cells.[25] Halishigamide A, on the other hand, has exhibited potent cytotoxic activity against murine lymphoma L-1210 and human KB cancer cells with IC_{50} values of 4 and 14 nM, respectively. It displayed antifungal activity against *Trichophyton mentagrophytes* with a MIC of 0.1 µM. Halishigamides B-D, however, displayed weak cytotoxic activity and moderate antifungal activity.[26]

Cylindramide is a macrocylic lactam bearing an acyltetramic acid and a trisubstituted bicyclo[3.3.0]octane (Figure 3.3). It exhibited cytotoxic activity against B-16 melanoma with an IC_{50} value of 1.7 µM. The franklinolides are polyketide phosphodiesters isolated from a *Geodia* sp. and a *Halichondria* sp. sponge association.[27] Franklinolide A exhibited GI_{50} values of 0.1 and 0.3 µM against HT-29 and AGS cancer cell lines, respectively, and an IC_{50} range of 1.1 - 1.8 µM against the cancer cell lines tested, including SH-SY5Y neuroblastoma cells.[28]

The alkaloid class is a rather small group of *Halichondria* secondary metabolites. The compounds so far isolated can be subclassified into indole and piperidine-based alkaloids (Figure 3.4). Halichrome A is a bisindole alkaloid isolated from *H. okadai*. It was cytotoxic against B-16 melanoma cells. It is noteworthy that the yellow pigment halichrome A is the first report of the isolation of a novel compound from a metagenomics library derived from a marine sponge.[29] *H. melanodocia* has also afforded a new indole-lactam metabolite.[30] Halichondramine is an example

of the piperidine-based alkaloids.[31] This compound is a member of a group of tetracyclic bipiperidine alkaloids. The other members of *Halichondria* origin are the three new 3-alkylpiperidine alkaloids, the tetradehydrohaliclonacyclamines,[32] which were reported for the first time from *Haliclona* sp.,[33,34] and later from *Arenosclera brazilensis*[35] and *Pachychalina alcaloidifera*[36].

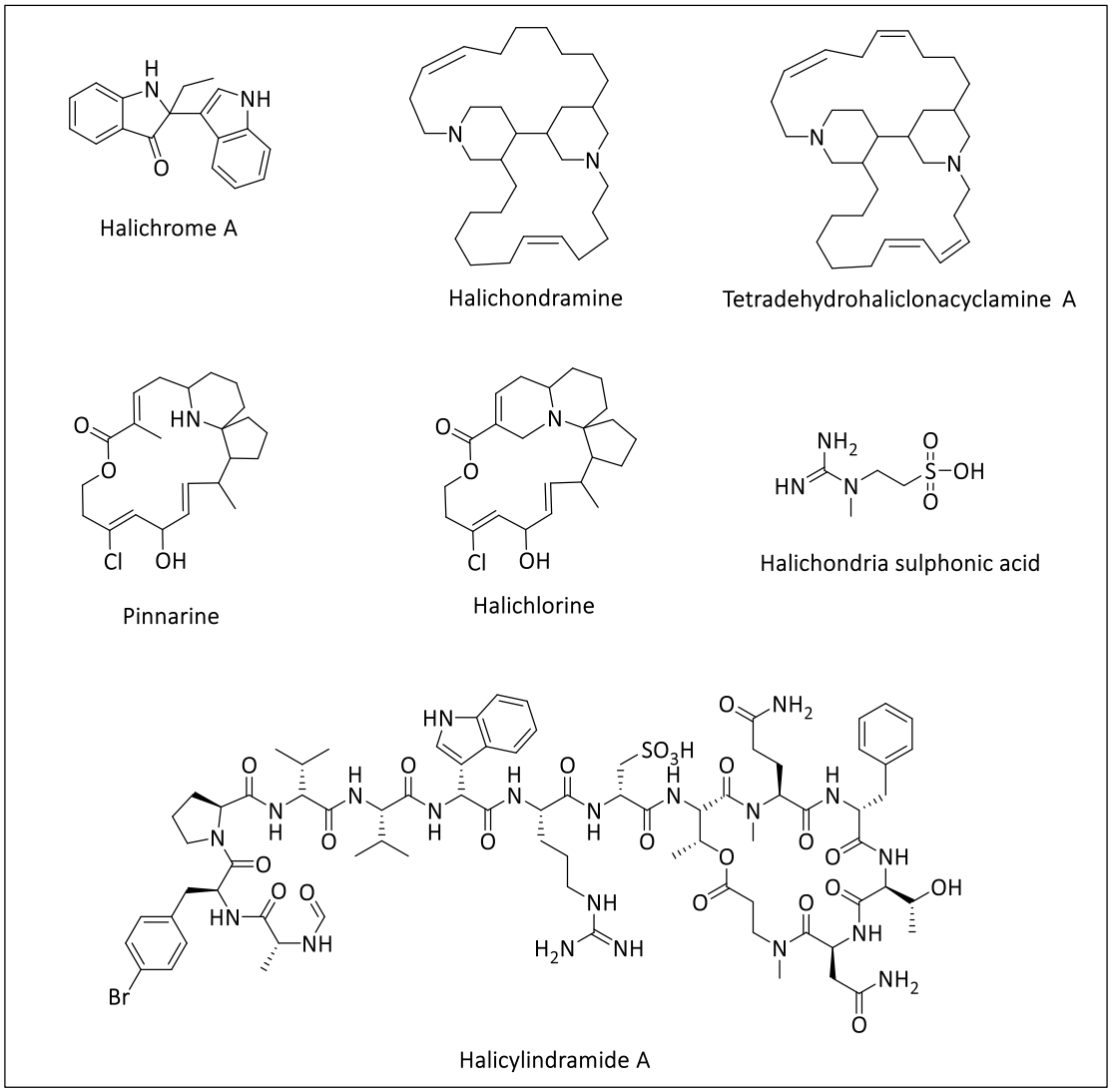

Figure 3.4: Examples of alkaloids and peptide from *Halichondria* species

Other examples of piperidine alkaloids are pinnarine[37] and halichlorine.[38] These are macrocylic alkaloids isolated from *H. okadai* in two different studies. These compounds possess an intriguing 6-aza-spiro[4.5]decane bicyclic ring system. In fact, halichlorine was described to be an

azabicyclo[4.4.0] with the nitrogen atom in the piperidine in a [5.6]-spiro ring with the cyclopentane. Proposed to be biosynthesized from pinnaic acid, a metabolite of the bivalve *Pinna muricata*, halichlorine has demonstrated significant inhibition of vascular cell adhesion molecule-1 (VCAM-1) induction in cultured human umbilical vein endothelial (HUVE) cells with an IC_{50} value of 17 µM.[38]

Halichondria sulphonic acid is a new sulphur-containing guanidine alkaloid isolated from *H. rugose*. The structure of this compound was elucidated through a combination of NMR and crystal structure analysis. Halichondria sulphonic acid exhibited anti-HIV-1 activity with an EC_{50} value of 143 µM, and IC_{50} >1.1 mM.[39]

Halicylindramides A-E are depsipeptides isolated from the Japanese sponge *H. cylindrata*.[40,41] The first three members comprise fourteen amino acid residues with a formyl group at the N-terminus and a lactonized threonine at the C-terminus. Halicylindramide D has similar termini to halicylindramides A-C but it is a thirteen-amino acid-membered peptide.[41] Halicylindramide E, unlike its congeners, is a linear peptide with eleven amino acid residues. Halicylindramides A-C exhibited antifungal activity against *Mortierella ramanniana* at 7.5 µg/disk, while halicylindramides D and E were antifungal at 5 and 160 µg/disk, respectively. The five depsipeptides have also demonstrated cytotoxicity towards P-388 murine leukemia cells in the IC_{50} range of 0.1 to 3 µM.[40,41]

Halichondria species have so far been a prolific source of terpenoid secondary metabolites. Only a few diterpenes and sesterterpenes have been isolated.[42–44] The majority of terpenoids so far reported are sesquiterpenes. They occur as aromatic sesquiterpenes (paniceins), halichonines, halichonadins, halichondriamines, halichons, and other novel scaffolds such as halipanicine,[45] amorphene isocyanide-formamide compounds,[46] and bisabolane-based sesquiterpenoids (Figure 3.5).[47] The paniceins are aromatic sesquiterpenes isolated from *H. panicea*. A characteristic feature of the paniceins is that the sesquiterpene is linked to a quinol or quinone moiety.[48] The halichonines are sesquiterpene alkaloids isolated from *H. okadai*. These natural products are characterized by a 6,6-bicyclic ring system and two prenylated amine moieties. Three members of this group, halichonines A-C, have so far been isolated and shown to be cytotoxic to L1210 mouse

leukemia cells with IC_{50} values of 7.2, 10.5, and 5.2 µM, respectively, and 11.5, 12.6, and 7.7 µM, respectively, against PC13 human lung cancer cells. Halichonine B was cytotoxic to HL60 human leukemia cells with an IC_{50} value of 1.4 µM and induced apoptosis in HL60 cells.[49]

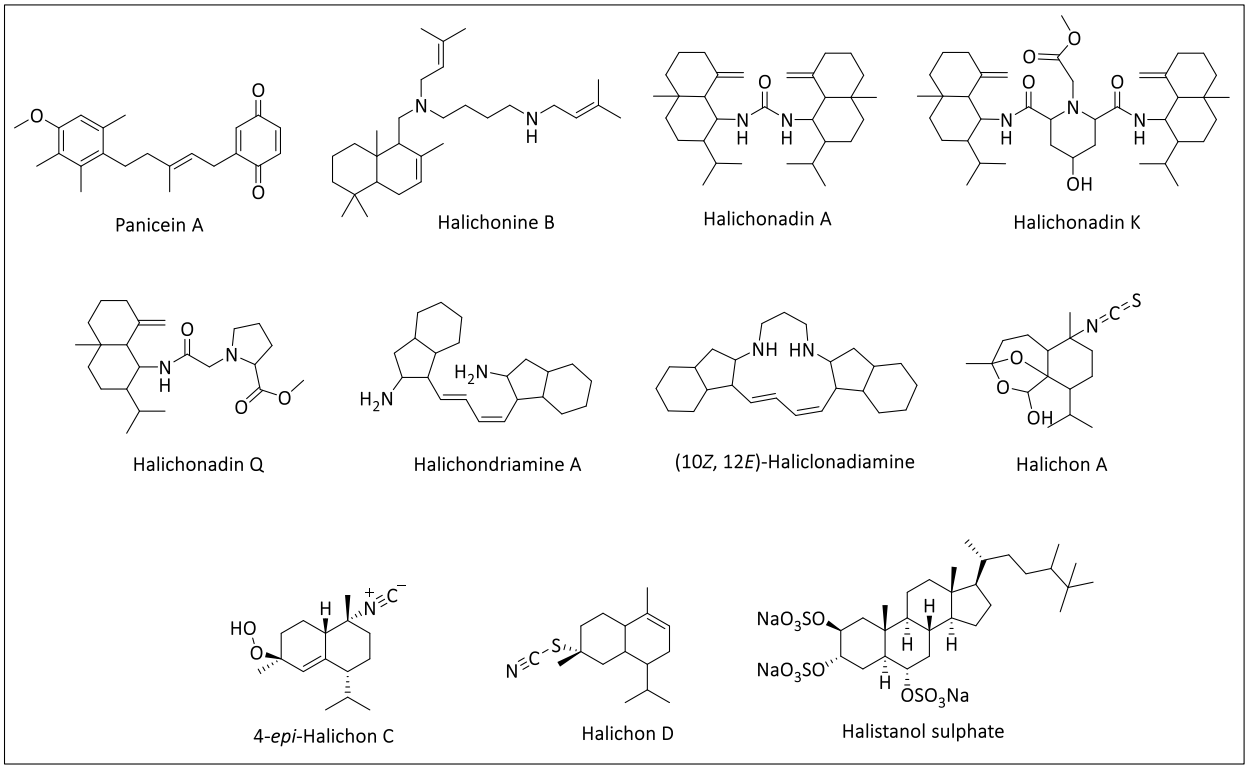

Figure 3.5: Examples of sesquiterpene and steroid-based compounds from *Halichondria* species

The halichonadins are eudesmane sesquiterpenoids (Figure 3.5). Seventeen members have so far been isolated. Halichonadin A and I possess two eudesmane scaffolds linked by a urea moiety. Halichonadin E, unlike halichonadins A and I, has eudesmane and aromadendrane sesquiterpenes linked by the urea moiety. Halichonadin G possesses a much longer linker comprising the urea moiety and two *N*-aminoacyl groups between the eudesmane sesquiterpenes. In halichonadin H, the linker is a 2-hydroxymalonamide. Halichonadins M and N have nitrotriacetic acid and pyrrolidine linkers, respectively, between the two eudesmane fragments, while halichonadin O and P have piperidine units as the linkers. The other members of this group, halichonadins B, C, D, F, J and Q, are all mono eudesmane sesquiterpene molecules. Halichonadin K was cytotoxic to human epidermoid carcinoma KB cells with an IC_{50} value of 14.9 µM. Meanwhile, halichonadin O

was reported to have demonstrated antimicrobial activity against *Staphylococcus aureus*, *Micrococcus luteus*, and *Trichophyton mentagrophytes*.[50–55]

A *Halichondria* species collected from Thailand afforded sesquiterpene isocyanides, isothiocyanates, thiocyanates and formamides (Figure 3.5). Of the 20 compounds that were isolated, 11 had been previously reported, while 9 were new. These were named the halichons. Halichons A, B, and H are isothiocyantes, halichon C and 4-epi-halichon C are isocyanides, while two thiocyanates (halichon D and E) were isolated along with the formamides, halichons F and G. Halichon C and its 4-epi isomer both showed moderate cytotoxicity, IC_{50} values of 20.9 and 29.0 µM, respectively, against the MOLT-3 cell line. Moreover, halichon C demonstrated similar activity towards HepG2 and MDA-MB-231 cell lines with IC_{50} values of 24.0 and 19.3 µM, respectively. All the compounds were not cytotoxic to HuCCA-1, A549 and HeLa cancer cell lines.[56]

3.4 Chemistry and biology of the genus *Hymeniacidon*

Hymeniacidon species have predominantly yielded alkaloidal secondary metabolites.[10] The furan fatty acid, (8*Z*,11*Z*,14*Z*,17*Z*)-3,6-epoxyeicos-3,5,8,11,14,17-hexenoic acid isolated from *H. hauraki* appears to be the only member of the 'lipid' class reported so far, exhibiting cytotoxic activity against P-388 with IC_{50} value of 13.4 µg/mL, whereas the methyl and stearyl esters of the acid showed anti-inflammatory activity (Figure 3.6).[57] Congeners of this compound, plakorsin A-C, have also been reported from *Plakortis simplex*.[58]

Alkaloidal natural products of *Hymeniacidon* origin are dominated by pyrrole-guanidine containing compounds. Apart from the characteristic presence of the pyrrole ring in all reported metabolites, which may be brominated, the guanidine functionality could cyclize into a 2-aminoimidazoyl group. The pyrrole and guanidine moieties are connected by a linker, usually a 5-unit chain, which has an amide group next to the pyrrole. This molecular framework is true for *Hymeniacidon* secondary metabolites such as hymenidin,[59] manzacidins A-C,[60] and tauroacidin A and B (Figure 3.6).[61] In other reported metabolites, however, C-4 to C-10 cyclization between the pyrrole and the linker has resulted in a seven-membered lactam ring. Examples of such compounds include hymenialdesine,[62] aldisins,[63] spongiacidins A-D,[64] and hymenin (Figure 3.6).[65] It has been

suggested that these congeners are possibly biosynthesized from oroidin through isomerization, oxidation and reduction, dimerization, and/or cyclization reactions.[66]

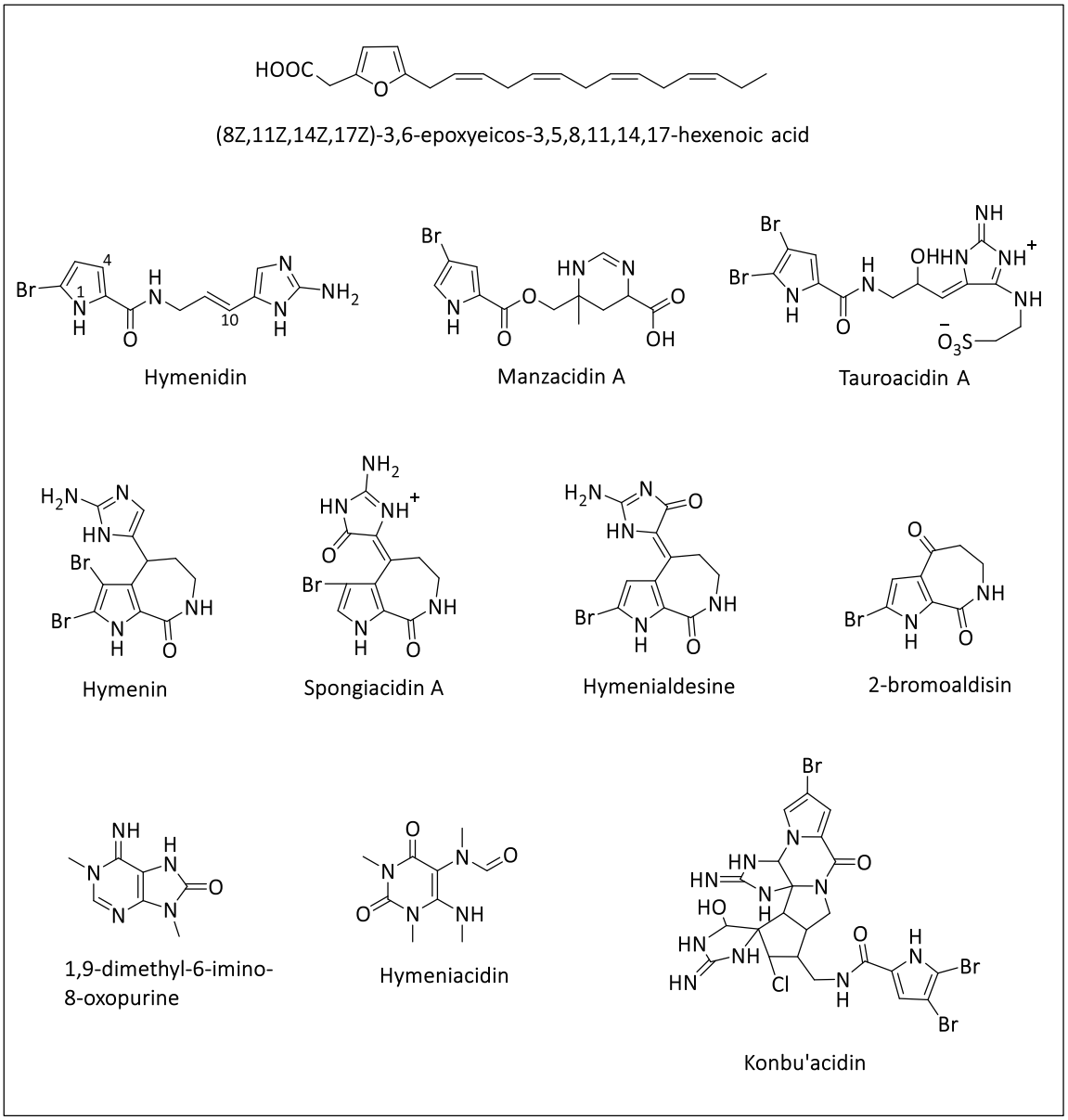

Figure 3.6: Some representative fatty acid and alkaloids from *Hymeniacidon* species.

Hymenin potently blocked α-adrenoceptor receptors. According to Miyazawa and coworkers, in the isolated rabbit aorta, the contractile response to norepinephrine (10^{-7} M) was abolished by hymenin (10^{-6} M), whereas the responses to potassium chloride (4 x 10^{-2} M) and serotonin (10^{-6} M) were not affected by hymenin (10^{-6} M).[65] Spongiacidins A and B exhibited inhibitory activity

against *c-erbB*-2 kinase with IC_{50} values of 21.2 µM and 18.5 µM, respectively, and cyclin-dependent kinase 4 (IC_{50}, 80 and 37 µM, respectively). Meanwhile, spongiacidins C and D were inactive at 50% inhibitory concentration up to 50 µg/mL.[64] Other alkaloidal natural products isolated from the genus include 1,9-dimethyl-6-imino-8-oxopurine,[67] the structurally intriguing konbu'acidin,[68]and hymeniacidin and four bromoindole ethyl esters (Figure 3.6).[69] Konbu'acidin was not cytotoxic to L1210 and KB cancer cells but inhibited cyclin dependent kinase 4 with an IC_{50} value of 26.7 µM.[68]

Hymenidin, isolated from an Okinawan marine sponge *Hymeniacidon* sp., has a potent antiserotonergic activity equal to that of keramadin, a known antagonist of serotonergic receptors.[59] Manzacidins A-C are characterized by a tetrahydropyrimidine ring in place of the 2-aminoimidazoyl moiety.[60] Like manzacidins, another Okinawan marine sponge *Hymeniacidon* sp. afforded the tauroacidins A and B. These metabolites possess a taurine group at C-15 of the 2-aminoimidazoyl moiety, hence the name *tauro*acidin. The two new compounds inhibited EFG receptor kinase and *c-erbB*-2 kinase, each with an IC_{50} value of 20 µg/mL.[61]

The first reported peptide secondary metabolite from the genus *Hymeniacidon* was hymenistatin 1 from a Western Pacific Ocean sponge. Hymenistatin 1 is a cyclo-octapeptide comprising valine, leucine, tyrosine, two isoleucine and three proline amino acid units (Figure 3.7). It was active against the P-388 leukemia cell line with an IC_{50} of 3.9 µM.[70] Moreover, an Okinawan marine sponge *Hymeniacidon* sp. afforded the hymenamides A-K. The first six members, hymenamides A-F,[71–73] are cyclic heptapeptides, while the four hymenamides G-K are cyclic octapeptides (Figure 3.7).[74] Hymenamide B and J were cytotoxic towards L1210 and KB cancer cell lines with IC_{50} values of 3.8 and 7.2 µM, respectively, and 2.4 and 0.7 µM, respectively.[71,74] Hymenamide H was only cytotoxic towards L1210 cancer cells with an IC_{50} of 7.0 µM.[74]

A cursory glance through the literature suggests that the diterpenoid isocyanides, the amphilectenes, are the only terpenoids from *Hymeniacidon*. Two amphilectene compounds were isolated from *H. amphilecta* by Cardy and his colleagues.[75] Meanwhile, a Puerto Rican marine sponge *Hymeniacidon* sp. afforded a new amphilectene-type natural product, monamphilectine, which possesses a β-lactam side chain (Figure 3.7). It showed an IC_{50} value of 0.6 µM against the

chloroquine-resistant *Plasmodium falciparum* W2 strain. When tested against the *Mycobacterium tuberculosis* H_{37}Rv strain, it displayed a MIC value of 36 µM. Furthermore, according to Rodriguéz and Avilés, preliminary KB assays against *Escherichia coli* revealed that at 150 nM, monamphilectine possessed bactericidal strength at 43% and 38% that of the β-lactam antibiotics carbenicillin and ampicillin, respectively. In fact, 8,15-diisocyano-11(20)-amphilectene, which was previously isolated by Cardy and coworkers, demonstrated better antiplasmodium and antitubercular activities than monamphilectine with an IC_{50} of 0.04 µM and a MIC of 9.8 µM, respectively.[76]

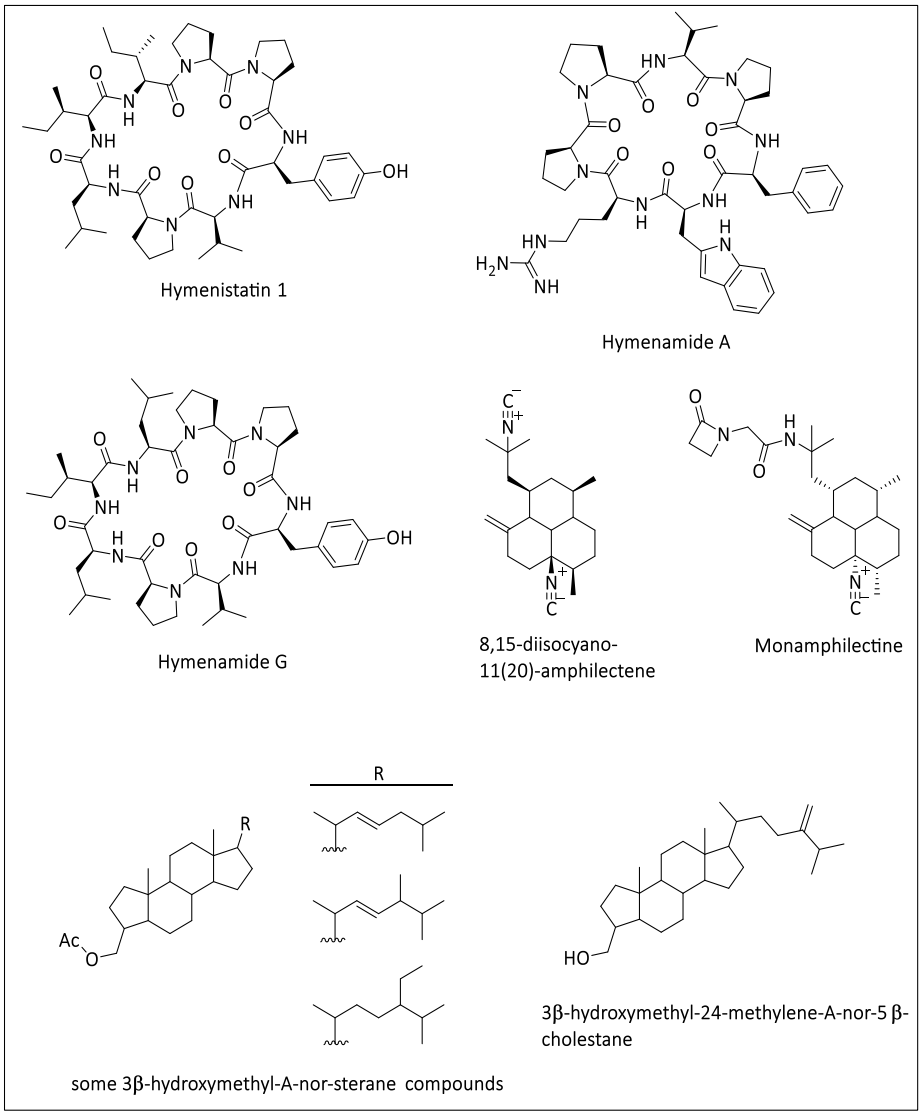

Figure 3.7: Examples of peptides, terpenes, and steroids isolated from *Hymeniacidon* species

The steroid class of *Hymeniacidon* secondary metabolites has been dominated by the metabolites isolated from the Okinawan marine sponge *H. aldis*. Six 3β-hydroxymethyl-A-nor-sterane compounds were isolated. These secondary metabolites were obtained as their acetates. The acetate group was located on the five-membered ring A for all these steroids. The structural difference was in the side chain at C-17 of the tetracyclic steroid backbone.[62] Moreover, *H. perlevis* afforded a similar steroid, 3β-hydroxymethyl-24-methylene-A-nor-5α-cholestane. This congener lacked the acetate moiety (Figure 3.7).[77]

3.5 Results and Discussion

3.5.1 Secondary metabolites from *Halichondria* sp.

A chemical investigation of the MeOH fraction of the organic extract of the *Halichondria* specimen led to the isolation and identification of betaine-type secondary metabolites comprising the previously unreported bisimidazoyl betaine (**1**) and a trimer of the proline betaine stachydrine (**2**) (Figure 3.8). The DCM/MeOH 1/1 v/v crude extract of the sponge material was initially fractionated according to the NCI protocol.[9] Two rounds of C_{18} HPLC of the MeOH fraction afforded the two compounds **1** and **2**.

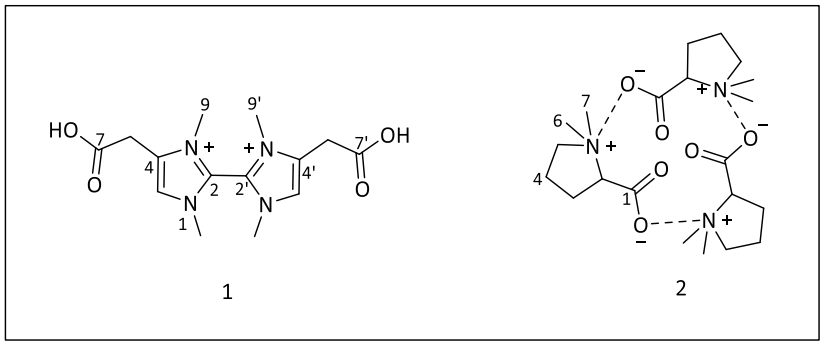

Figure 3.8: Compounds 1 and 2 isolated from *Halichondria* sp.

HR-ESI-MS analysis of compound **1** revealed a pseudomolecular ion mass peak at m/z 155.0813 (1/2M + H; calcd. for $C_7H_{11}N_2O_2$, 155.0815,) consistent with a molecular formula of the dimer $C_{14}H_{20}N_4O_4^{2+}$. The ^{1}H NMR spectrum exhibited four singlets resonating at δ_H (ppm) 3.43 (H_2-6, 6'), 3.56 (H_3-9, 9'), 3.66 (H_3-8, 8') and 7.08 (H-5, 5'). Examination of the ^{13}C NMR and the 2D

heteronuclear HSQC data suggested the presence of two NMe groups (δ_C 34.4, δ_H 3.56 ppm; δ_C 36.9, δ_H 3.66 ppm), a characteristic carboxylic acid or amide carbonyl (δ_C 176.1), and two sp^2 hybridized quaternary carbons at δ_C 133.0 and δ_C 136.0 ppm (Table 3.1).

Table 3.1: ^1H, ^{13}C and HMBC NMR data for compound **1**

No.	δ_C, type	δ_H (*J*, Hz)	HMBC
2, 2'	136.0, C		
4, 4'	133.0, C		
5, 5'	122.7, CH	7.08, s	C-2, 2', 4, 4'
6, 6'	33.4, CH_2	3.43, s	C-4, 4', 5, 5', 7, 7'
7, 7'	176.1, C		
8, 8'	36.9, CH_3	3.66, s	C-2, 2', 5, 5'
9, 9'	34.4, CH_3	3.56, s	C-2, 2', 4, 4'

Analyses of the HMBC spectrum revealed correlations from the methylene protons H_2-6 to the carboxylic acid moiety and C-4 and C-5. Moreover, the methine proton H-5 showed HMBC correlations to the two quaternary carbons C-2 and C-4. Similar correlations from the N-CH_3's to C-2, C-4 and C-5 suggested the presence of the imidazoyl scaffold. This was corroborated by ^1H-^{15}N HMBC correlations between the methine and methyl groups and the two nitrogen atoms of the imidazoyl scaffold (Figure 3.9). Finally, the presence of quaternary carbon C-2 and evidence from the HR-ESI-MS data suggested compound **1** was symmetrical about the C-2 to C-2' bond. Long range COSY cross peaks between H-5 and H_2-6 supported the assignment of the structure of **1**.

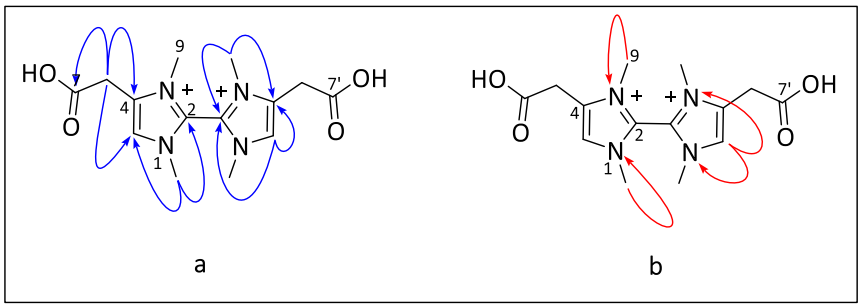

Figure 3.9: (a) ^1H – ^{13}C HMBC and (b) ^1H – ^{15}N HMBC correlations of compound **1**

Compound **2** was confirmed to be the proline betaine stachydrine by comparison of its HR-ESI-MS and NMR data to reported data.[78] Examination of the ^{13}C NMR spectrum, however, revealed that the signals due to C-2, C-5, C-6 and C-7 were tripled (Figure 3.10). The intensities of the methylene carbons (C-3 and C-4) and the carboxyl carbon C-1 were also unusually higher than expected. That compound **2** occurred as a trimer was corroborated by the presence of LR-ESI-MS m/z values responsible for 2M and 3M mass units. The structure of **2** is therefore as proposed and suggested that the betaine monomers served as counter ions of each other. It is also likely that **2** could be involved in complexation with a cation (a metal ion perhaps) although no such ion was observed.

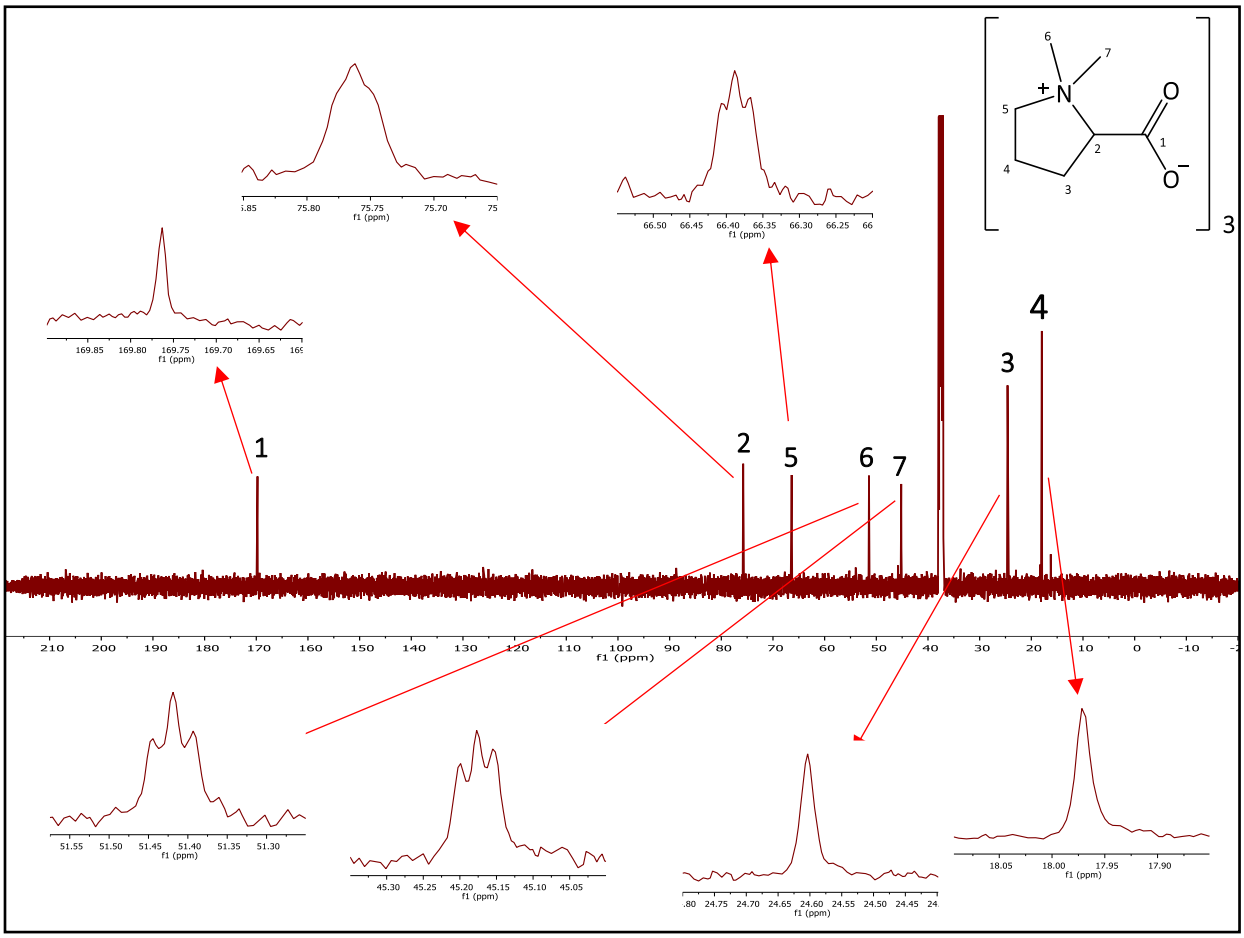

Figure 3.10: Expanded sections of the ^{13}C NMR spectrum of compound **2**

3.5.2 Secondary metabolites from *Hymeniacidon* sp.

A combination of DIOL solid phase extraction flash chromatography and C_{18} HPLC of the organic extract of the *Hymeniacidon* species led to the isolation and identification of the nucleoside thymidine, four amino acid residues tyrosine, leucine, isoleucine and valine, along with the small molecular weight ionic metabolites choline, and agmatine (Figure 3.11). The structures of these metabolites were confirmed by comparison of their NMR and mass data to authentic and/or literature information.

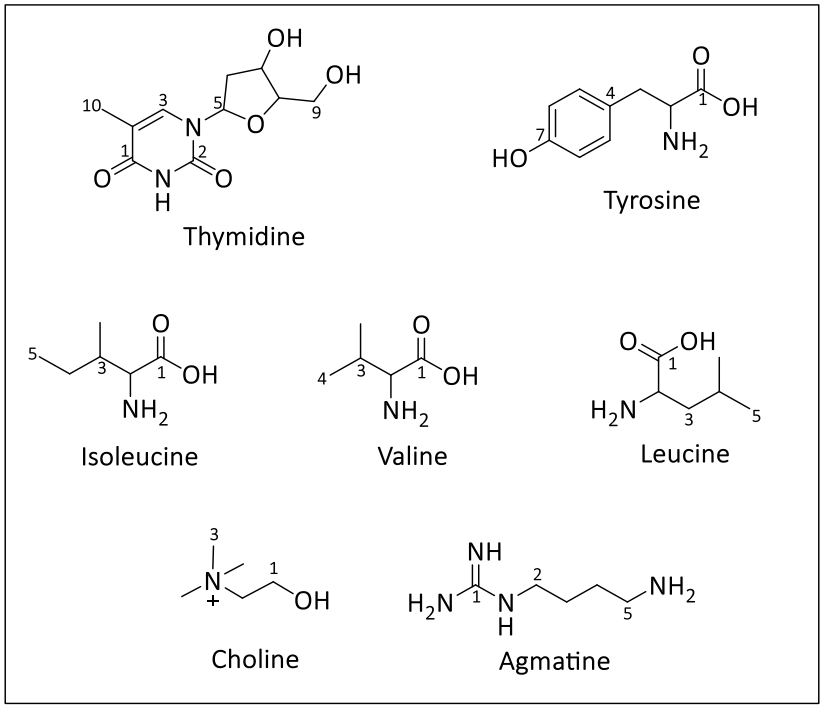

Figure 3.11: Secondary metabolites isolated from *Hymeniacidon* sp.

3.5.3 Antiplasmodium activity results

Compounds **1** and **2** were evaluated for their *in vitro* antiplasmodium activity against the drug sensitive strain of *Plasmodium falciparum*, NF54 (Table 3.2). Generally, **1** and **2** displayed no activity at the highest concentration (10 µg/mL) of test compounds. Chloroquine and artesunate were used as positive controls.

Table 3.2: *In vitro* antiplasmodium activity against *P. falciparum* (NF54) strain	
Compound	*Pf*(NF54)
	IC_{50} (µg/mL)
1	>10
2	>10
Artesunate	15 nM
Chloroquine	33 nM

Imidazoyl betaine natural products have been reported from marine organisms. Examples include zooanemonin,[79–82] norzooanemonin,[81,83,84] norzooanemonin methyl ester,[81] aminozooanemonin,[82] and echinobetaine B (Figure 3.12).[81,85] The (+)-echinobetaine B isomer exhibited nematocidal activity against *Haemonchus contortus* (LD_{99} = 8.3 µg/mL) comparable to the commercial anthelminthics closantel and levamisole (LD_{99} = 5 - 10 µg/mL). Compared to zooanemonin, norzooanemonin and its methyl ester congener, the OMe group in (+)-echinobetaine B was suggested to be necessary for the anthelminthic activity. Meanwhile, zooanemonin has exhibited antifouling activity towards the barnacle *Balanus amphitrite* comparable to that of $CuSO_4$ (4.0 – 5.2 ppm).[80] Aminozooanemonin displayed antibacterial activity against the Gram positive bacteria *Bacillus subtilis* and *Staphylococcus aureus* with MIC values of 14 µM and 50 µM, respectively.[82]

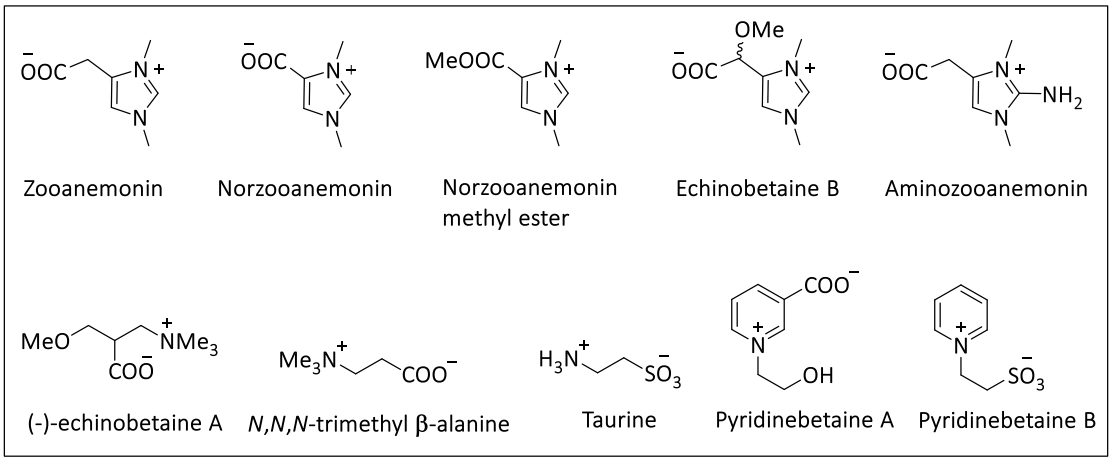

Figure 3.12: Zooanemonin-type compounds and examples of betaines from marine organisms

Glycine and proline betaine are two major organic osmolytes reported to play osmoregulatory roles in various plant species in response to environmental stress such as drought, salinity, extreme temperature, UV radiation and heavy metals.[86] Proline betaine, also known as stachydrine or cadabine, has not only been described in many plant species but in the bacteria *Klebsiella pneumoniae*, *Escherichia coli*, *Rhizobium meliloti* and *Staphylococcus aureus*, it has also been reported to play similar osmoprotective roles.[87] Moreover, Chambers and Kunin demonstrated that glycine and proline betaines are present in human urine playing osmoprotective roles against hypertonic NaCl for *E. coli*.[78] Stachydrine has been reported in marine organisms, for example the red algae *Griffithsia flosculosa* and the extremely euryhaline mollusk *Elysia chlorotica*. According to Warren and coworkers, *E. chlorotica* does not utilize intracellular free amino acids for cell volume regulation during osmotic stress but rather proline betaine.[88]

It is evident, therefore, that the metabolites isolated from the two sponge specimens investigated in the current work are necessary for the organisms' survival in the harsh environmental conditions of Antarctica. The data presented herein therefore complements reports from other researchers in the field.

3.5.4 Materials and Methods

3.5.4.1 General Experimental Procedures

UV spectra were obtained on a CARY 60 UV-VIS 2.00 with software version 5.0.0.999 by Agilent Technologies (Santa Clara, CA, USA). PerkinElmer Spectrum Version 10.03.02 (PerkinElmer Ltd., Llantrisant, Wales, UK) was used to acquire the IR data. NMR spectra were obtained on a BRUKER Ascend 600 (Bruker, Billeria, MA, USA) cryoprobe prodigy at 600 MHz and 151 MHz for ^{1}H and ^{13}C nuclei, respectively. D_2O-DMSO-d_6 (used as internal standard for calibration at δ_H 2.50 and δ_C 49.00) was used as solvent for acquiring all NMR data throughout the investigation. HR-ESI-MS data were obtained via an HRMS LC-MS/MS on a SCIEX X500R QTOF instrument. Reverse phase (C_{18}) HPLC was carried out on Agilent 1200LC system (Santa Clara, CA, USA) equipped with a G1322A degasser, G1311A quaternary pump, G1329A autosampler (maximum injection 100 µL),

and a G1316A DAD and multiple wavelength detector. Low Resolution-ESI-MS was acquired on an Agilent 1260 Infinity HPLC coupled to Agilent 6120 Quardrupole MS systems. Normal phase DIOL solid phase extraction flash column chromatography was carried out with Spe-ed Catridge DIO 2gr/6ml prepacked (Applied Separations, Allentown, PA, USA). Solvents used were of HPLC grade.

3.5.4.2 Collection and Extraction, Isolation, and Characterization

The sponge specimens were processed and extracted as previously reported.[8]

Sequential fractionation by flash chromatography on DIOL SPE was carried out on 567.2 mg of CH_2Cl_2/MeOH (1:1 v/v) organic extract of the *Halichondria* sp. with n-hexane/ CH_2Cl_2 (1:1 v/v), CH_2Cl_2/EtOAc (20:1 v/v), EtOAc, EtOAC/MeOH (5:1 v/v) and MeOH to obtain five fractions A - E. After preliminary analysis of the fractions by ^{1}H NMR, the MeOH fraction (150 mg) was proceeded on further purification by semi-preparative C18 HPLC on a Phenomenex Luna 10 µm C18 (2) 100Å 250 mm x 10 mm (Phenomenex, Torrance, CA, USA) with H_2O and acetonitrile as mobile phase (2 – 100% acetonitrile, total run time 30 min) at a flow rate of 3 mL/min and wavelength detection at 254 and 330 nm. Twenty fractions (A – U) were collected. All fractions were analyzed by ^{1}H NMR spectroscopy. Fractions F and G were further chromatographed on semi-preparative C18 HPLC on a Phenomenex Onyx monolithic C18 100 mm x 10 mm (Phenomenex, Torrance, CA, USA) isocratic at 1% acetonitrile in H_2O for 5 mins at flow rate 2 mL/min and wavelengths 254 and 330 nm to afford compounds **1** (1.3 mg) and **2** (1.8 mg), respectively.

The *Hymeniacidon* sp. was investigated in a similar manner as described above. The organic extract (7.01 g) was fractionated on DIOL SPE and the fractions analyzed by ^{1}H NMR. Fraction C (29 mg) was further purified by semi-preparative C18 HPLC on a Phenomenex Luna 10 µm C18 (2) 100Å 250 mm x 10 mm (Phenomenex, Torrance, CA, USA) with H_2O and acetonitrile as mobile phase (5 – 100% acetonitrile, total run time 26 min) at a flow rate of 3 mL/min and wavelength detection at 254 and 330 nm. Twenty-one fractions were collected, fraction J (1.5 mg) was analyzed by spectroscopic methods (NMR and MS) and identified to be the nucleoside thymidine. Meanwhile, the MeOH fraction (500 mg) was purified by semi-preparative C18 HPLC to obtain 15 fractions (HPLC conditions were same as described for the first round HPLC purification described for *Halichondria* sp. above). Four fractions, C, E, G2, and G4, were further purified by semi-preparative

C18 HPLC on a Phenomenex Onyx monolithic C18 100 mm x 10 mm (Phenomenex, Torrance, CA, USA) isocratic at 1% acetonitrile in H_2O for 5 mins at flow rate 2 mL/min and wavelengths 254 and 330 nm. A mixture of choline and agmatine (1.9 mg) was obtained from fraction C, fraction E and G2 afforded 1.4 mg of isoleucine and 3.5 mg of valine, respectively, while tyrosine and leucine (0.8 mg) were obtained as a mixture from fraction G4.

Compound **1**: Clear oil; ^{1}H- and ^{13}C-NMR data (600 MHz, D_2O, DMSO-d_6), Table 3.1; HR-ESI-MS *m/z* 155.0813 [1/2M + H] (calcd. for $C_7H_{11}N_2O_2$, 155.0815, *molecular formula* $C_{14}H_{20}N_4O_4^{2+}$).

Compound **2**:[78] Clear oil; ^{1}H-NMR (600 MHz, DMSO-d_6): δ 1.92 – 2.04 (m, 2H, H-4), 2.04 – 2.14 (m, 1H, H-3a), 2.31 (m, 1H, H-3b), 2.92 (s, 3H, H-6), 3.11 (s, H-7), 3.30 – 3.38 (m, 1H, H-5a), 3.52 (m, 1H, H-5b), 3.84 (td, *J* = 2.1, 8.7, 9.5 Hz, 1H, H-2); ^{13}C-NMR (151 MHz, D_2O, DMSO-d_6): δ 169.7 (C-1), 75.7 (C-2), 66.4 (C-5), 51.4 (C-7), 45.2 (C-6), 24.6 (C-3), 18.0 (C-4); HR-ESI-MS *m/z* 144.1018 [M + H] (calcd. for $C_7H_{14}NO_2$, 144.1019), 287.1964 [2M + H] (calcd. for $C_{14}H_{27}N_2O_4$, 287.1965).

Thymidine:[89] Clear oil; ^{1}H NMR (600 MHz, MeOH-d_4): δ 1.87 (d, *J* = 1.2 Hz, 3H, H-10), 2.17 – 2.27 (m, 2H, H-6), 3.72 (dd, *J* = 3.7, 12.0 Hz, 1H, H-9a), 3.79 (dd, *J* = 3.2, 12.0 Hz, 1H, H-9b), 3.90 (m, 1H, H-8), 4.31 – 4.44 (m, 1H, H-7), 6.22 – 6.30 (m, 1H, H-5), 7.80 (q, *J* = 1.2 Hz, 1H, H-3); ^{13}C NMR (151 MHz, MeOH-d_4): δ 166.4 (C-1), 152.4 (C-2), 138.1 (C-3), 111.5 (C-4), 88.8 (C-8), 86.3 (C-5), 72.2 (C-7), 62.8 (C-9), 41.2 (C-6), 12.4 (C-10); HR-ESI-MS *m/z* 243.0980 $[M + H]^+$ (calcd. for $C_{10}H_{15}N_2O_5$, 243.0903).

Tyrosine:[90] Clear oil; ^{1}H NMR (600 MHz, D_2O, DMSO-d_6): δ 3.18 (dd, *J* = 7.8, 14.6 Hz, 1H, H-3a), 3.34 (dd, *J* = 5.2, 14.6 Hz, 1H, H-3b), 4.04 (dd, *J* = 5.2, 7.8 Hz, 1H, H-2), 7.01 – 7.13 (m, 2H, H-6), 7.32 – 7.41 (m, 2H, H-5); ^{13}C-NMR (151 MHz, D_2O, DMSO-d_6): 175.3 (C-1), 155.0 (C-7), 130.6 (C-5), 127 (C-4), 116.1 (C-6), 56.5 (C-2), 36.4 (C-3); ESI-MS *m/z* 182.1 $[M + H]^+$.

Leucine:[91] Clear oil; ^{1}H NMR (600 MHz, D_2O, DMSO-d_6): δ 1.12 (d, *J* = 4.4 Hz, 3H, H-5), 1.14 (d, *J* = 6.5 Hz, 3H, H-6), 1.80 – 1.86 (m, 1H, H-3a), 1.86 – 1.94 (m, 2H, H-3b, 4), 3.87 (dd, *J* = 5.2, 8.4 Hz, 1H, H-2); ^{13}C NMR (151 MHz, D_2O, DMSO-d_6): δ 176.1 (C-1), 53.9 (C-2), 40.5 (C-3), 24.6 (C-4), 22.5 (C-6), 21.5 (C-5); ESI-MS *m/z* 132.2 $[M + H]^+$.

Isoleucine:[92] Clear oil; ^{1}H NMR (600 MHz, D_2O, DMSO-d_6): δ 0.77 (t, *J* = 7.4 Hz, 3H, H-5), 0.83 (d, *J* = 7.0 Hz, 3H, H-6), 1.03 – 1.12 (m, 1H, H-4a), 1.31 (dqd, *J* = 4.6, 7.4, 14.8 Hz, 1H, H-4b), 1.78 (m, 1H, H-3), 3.40 (d, *J* = 4.1 Hz, 1H, H-2); ^{13}C NMR (151 MHz, D_2O, DMSO-d_6): δ 174.9 (C-1), 60.1 (C-2), 36.6 (C-3), 24.7 (C-4), 15.4 (C-6), 11.7 (C-5); ESI-MS *m/z* 132.2 $[M + H]^+$.

Valine:[93] Clear oil; ^{1}H NMR (600 MHz, D_2O, DMSO-d_6): δ 0.82 (d, *J* = 7.0 Hz, 3H, H-4), 0.87 (d, *J* = 7.0 Hz, 3H, H-5), 2.09 (m, 1H, H-3), 3.37 (d, *J* = 4.3 Hz, 1H, H-2); ^{13}C NMR (151 MHz, D_2O, DMSO-d_6): δ 175.3 (C-1), 60.7 (C-2), 29.3 (C-3), 18.5 (C-5), 17.2 (C-4); ESI-MS *m/z* 118.1 $[M + H]^+$.

Choline:[94] Clear oil; ^{1}H NMR (600 MHz, D_2O, DMSO-d_6) δ 3.01 (s, 9H, H-3), 3.30 – 3.35 (m, 2H, H-1), 3.86 (m, 2H, H-2); ^{13}C NMR (151 MHz, D_2O, DMSO-d_6): δ 68.8 (C-1), 56.8 (C-2), 55.2 (C-3); HR-ESI-MS *m/z* 104.1069 $[M]^+$ (calcd. for $C_5H_{14}NO$, 104.1070).

Agmatine:[95] Clear oil; ^{1}H NMR (600 MHz, D_2O, DMSO-d_6) δ 1.37 (quin., *J* = 6.4Hz, 2H, H-3), 1.41 – 1.49 (quin., *J* = 7.4 Hz, 2H, H-4), 2.74 (t, *J* = 7.4 Hz, 2H, H-5), 2.94 (t, *J* = 6.9 Hz, 2H, H-2); ^{13}C NMR (151 MHz, D_2O, DMSO-d_6): δ 162.5 (C-1), 40.7 (C-2, 5), 27.6 (C-3), 25.7 (C-4); HR-ESI-MS *m/z* 131.1294 $[M + H]^+$ (calcd. for $C_5H_{15}N_4$, 131.1291).

3.5.4.3 Antiplasmodium assay

The malaria strain used for testing was the drug sensitive strain of *Plasmodium falciparum*, NF54 obtained from the Malaria Research and Reference Reagent Resource Center (MR4). The plasmodium parasites were cultured continuously *in vitro* according to a modified method described by Trager and Jensen.[96,97] The samples were tested against the NF54 strain using the parasite lactate dehydrogenase (pLDH) assay to determine *in vitro* efficacy.[98] The samples were tested at a starting concentration of 10 000 ng/ml. Chloroquine and artesunate were used as positive controls.

Plasmodium falciparum were maintained in human erythrocytes (2% hematocrit) incubated at 37°C in RPMI 1640 medium containing 25 mM HEPES buffer, 20 µg/mL of gentamicin, 27 mM bicarbonate, and 10% normal type A human serum maintained below 2% parasitemia for 48 hr under an atmosphere of a gas mixture containing in 3% 0_2, 6% CO_2, and 91% N_2.[98]

Fifteen microliters from each well of re-suspended culture was transferred into another 96-well, flat-bottomed microtiter plate that contained 100 µL of the proprietary Malstav@ reagent (Flow Inc., Portland, OR). The sample was left to lyse for thirty minutes to ensure an accurate reading. At the end of this period, each well received 25 µL of a 20:1 mixture of nitro blue tetrazolium and phenazine ethosulfate (1 mg and 0.05 mg/ml, respectively). The reduction of the tetrazolium to the blue formazan salt is followed for 10 min at 650 nm (K650 nm) [98]

3.6 References

(1) Blunt, J. W.; Copp, B. R.; Keyzers, R. A.; Munro, M. H. G.; Prinsep, M. R. Marine Natural Products. *Nat. Prod. Rep.* 2012, *29* (2), 144–222.

(2) Laport, M. S.; Santos, O. C. S.; Muricy, G. Marine sponges: Potential sources of new antimicrobial drugs. *Curr. Pharm. Biotechnol.* 2009, *10* (1), 86–105.

(3) Ebada, S. S.; Proksch, P. The Chemistry of Marine Sponges∗. In *Handbook of Marine Natural Products*; Springer Netherlands: Dordrecht, 2012; pp 191–293.

(4) Hu, G.-P.; Yuan, J.; Sun, L.; She, Z.-G.; Wu, J.-H.; Lan, X.-J.; Zhu, X.; Lin, Y.-C.; Chen, S.-P. Statistical research on marine natural products based on data obtained between 1985 and 2008. *Mar. Drugs* 2011, *9* (4), 514–525.

(5) Hu, Y.; Chen, J.; Hu, G.; Yu, J.; Zhu, X.; Lin, Y.; Chen, S.; Yuan, J. Statistical research on the bioactivity of new marine natural products discovered during the 28 Years from 1985 to 2012. *Mar. Drugs* 2015, *13* (1), 202–221.

(6) Mayer, A. M. S.; Glaser, K. B.; Cuevas, C.; Jacobs, R. S.; Kem, W.; Little, R. D.; McIntosh, J. M.; Newman, D. J.; Potts, B. C.; Shuster, D. E. The odyssey of marine pharmaceuticals: A current pipeline perspective. *Trends Pharmacol. Sci.* 2010, *31* (6), 255–265.

(7) Paul, V. J.; Ritson-Williams, R. Marine Chemical Ecology. *Nat. Prod. Rep.* 2008, *25*, 662–695.

(8) Olsen, E. K.; de Cerf, C. K.; Dziwornu, G. A.; Puccinelli, E.; Ansorge, I. J.; Samaai, T.; Dingle, L. M. K.; Edkins, A. L.; Sunassee, S. N. Cytotoxic activity of marine sponge extracts from the Sub-Antarctic Islands and the Southern Ocean. *S. Afr. J. Sci.* 2016, *Volume 112* (Number

11/12).

(9) McCloud, T. G. High throughput extraction of plant, marine and fungal specimens for preservation of biologically active molecules. *Molecules* 2010, *15* (7), 4526–4563.

(10) MarinLit. (2017) http://pubs.rsc.org/marinlit. Royal Society of Chemistry, London (accessed Dec 27, 2017).

(11) Rodríguez, W.; Osorno, O.; Ramos, F. A.; Duque, C.; Zea, S. New fatty Acids from Colombian Caribbean sea sponges. *Biochem. Syst. Ecol.* 2010, *38* (4), 774–783.

(12) Carballeira, N. M. Isolation of (Z)-17-tetracosenal from the marine sponge *Halichondria panicea*. *Chem. Phys. Lipids* 1986, *39* (4), 365–368.

(13) Abdjul, D. B.; Yamazaki, H.; Takahashi, O.; Kirikoshi, R.; Ukai, K.; Namikoshi, M. Isopetrosynol, a new protein tyrosine phosphatase 1B Inhibitor, from the marine sponge *Halichondria* cf. *panicea* collected at Iriomote Island. *Chem. Pharm. Bull. (Tokyo).* 2016, *64* (7), 733–736.

(14) Gabriel, A. F.; Li, Z.; Kusuda, R.; Tanaka, C.; Miyamoto, T. Six new polyacetylenic alcohols from the marine sponges *Petrosia* sp. and *Halichondria* sp. *Chem. Pharm. Bull. (Tokyo).* 2015, *63* (6), 469–475.

(15) Di, X.; Oskarsson, J. T.; Omarsdottir, S.; Freysdottir, J.; Hardardottir, I. Lipophilic fractions from the marine sponge *Halichondria sitiens* decrease secretion of pro-inflammatory cytokines by dendritic cells and decrease their ability to induce a Th1 type response by allogeneic CD4 + T Cells. *Pharm. Biol.* 2017, *55* (1), 2116–2122.

(16) Niwa, H.; Wakamatsu, K.; Yamada, K. Halicholactone and neohalicholactone, two novel fatty acid metabolites from the marine sponge *Halichondria okadai* Kadota. *Tetrahedron Lett.* 1989, *30* (34), 4543–4546.

(17) Kigoshi, H.; Niwa, H.; Yamada, K.; Stout, T. J.; Clardy, J. The three-dimensional structure of neohalicholactone, an unusual fatty acid metabolite from the marine sponge *Halichondria okadai* Kadota. *Tetrahedron Lett.* 1991, *32* (22), 2427–2428.

(18) Li, H.; Matsunaga, S.; Fusetani, N. Halicylindrosides, antifungal and cytotoxic cerebrosides

from the marine sponge *Halichondria cylindrata*. *Tetrahedron* 1995, *51* (8), 2273–2280.

(19) Nagle, D. G.; McClatchey, W. C.; Gerwick, W. H. New glycosphingolipids from the marine sponge *Halichondria panicea*. *J. Nat. Prod.* 1992, *55* (7), 1013–1017.

(20) Hayashi, A.; Nishimura, Y.; Matsubara, T. Occurrence of ceramide digalactoside as the main glycosphingolipid in the marine sponge *Halichondria japonica*. *Biochim. Biophys. Acta* 1991, *1083* (2), 179–186.

(21) Hirata, Y.; Uemura, D. Halichondrins - antitumor polyether macrolides from a marine sponge. *Pure Appl. Chem.* 1986, *58* (5), 701–710.

(22) Kernan, M. R.; Faulkner, D. J. Halichondramide, an antifungal macrolide from the sponge *Halichondria* sp. *Tetrahedron Lett.* 1987, *28* (25), 2809–2812.

(23) Kernan, M. R.; Molinski, T. F.; Faulkner, D. J. Macrocyclic antifungal metabolites from the Spanish dancer nudibranch *Hexabranchus sanguineus* and sponges of the genus *Halichondria*. *J. Org. Chem.* 1988, *53* (21), 5014–5020.

(24) Shin, Y.; Kim, G. D.; Jeon, J.; Shin, J.; Lee, S. K. Antimetastatic effect of halichondramide, a trisoxazole macrolide from the marine sponge *Chondrosia corticata*, on human prostate cancer cells *via* modulation of epithelial-to-mesenchymal transition. *Mar. Drugs* 2013, *11* (7), 2472–2485.

(25) Bae, S. Y.; Kim, G. D.; Jeon, J.; Shin, J.; Lee, S. K. Anti-proliferative effect of (19Z)-halichondramide, a novel marine macrolide isolated from the sponge *Chondrosia corticata*, is associated with G2/M cell cycle arrest and suppression of MTOR signaling in human lung cancer cells. *Toxicol. Vitr.* 2013, *27* (2), 694–699.

(26) Kobayashi, J.; Tsuda, M.; Fuse, H.; Sasaki, T.; Mikami, Y. Halishigamides A–D, new cytotoxic oxazole-containing metabolites from Okinawan sponge *Halichondria* sp. *J. Nat. Prod.* 1997, *60* (2), 150–154.

(27) Kanazawa, S.; Fusetani, N.; Matsunaga, S. Cylindramide: Cytotoxic tetramic acid lactam from the marine sponge *Halichondria cylindrata* Tanita & Hoshino. *Tetrahedron Lett.* 1993, *34*

(6), 1065–1068.

(28) Zhang, H.; Conte, M. M.; Capon, R. J. Franklinolides A-C from an Australian marine sponge complex: Phosphodiesters strongly enhance polyketide cytotoxicity. *Angew. Chemie Int. Ed.* 2010, *49* (51), 9904–9906.

(29) Abe, T.; Kukita, A.; Akiyama, K.; Naito, T.; Uemura, D. Isolation and structure of a novel biindole pigment substituted with an ethyl group from a metagenomic library derived from the marine sponge *Halichondria okadai*. *Chem. Lett.* 2012, *41* (7), 728–729.

(30) Gopichand, Y.; Schmitz, F. J. Two novel lactams from the marine sponge *Halichondria melanodocia*. *J. Org. Chem.* 1979, *44* (26), 4995–4997.

(31) Chill, L.; Yosief, T.; Kashman, Y. Halichondramine, a new tetracyclic bipiperidine alkaloid from the marine sponge *Halichondria* sp. *J. Nat. Prod.* 2002, *65* (11), 1738–1741.

(32) Mudianta, I. W.; Katavic, P. L.; Lambert, L. K.; Hayes, P. Y.; Banwell, M. G.; Munro, M. H. G.; Bernhardt, P. V.; Garson, M. J. Structure and absolute configuration of 3-alkylpiperidine alkaloids from an Indonesian sponge of the genus *Halichondria*. *Tetrahedron* 2010, *66* (14), 2752–2760.

(33) Clark, R. J.; Field, K. L.; Charan, R. D.; Garson, M. J.; Brereton, M.; Willis, A. C. The haliclonacyclamines, cytotoxic tertiary alkaloids from the tropical marine sponge *Haliclona* sp. *Tetrahedron* 1998, *54* (30), 8811–8826.

(34) Mudianta, I. W.; Garson, M. J.; Bernhardt, P. V. The absolute configurations of haliclonacyclamines A and B determined by X-Ray crystallographic analysis. *Aust. J. Chem.* 2009, *62* (7), 667.

(35) Torres, Y. R.; Berlinck, R. G. S.; Magalhães, A.; Schefer, A. B.; Ferreira, A. G.; Hajdu, E.; Muricy, G. Arenosclerins A–C and haliclonacyclamine E, new tetracyclic alkaloids from a Brazilian endemic haplosclerid sponge *Arenosclera brasiliensis*. *J. Nat. Prod.* 2000, *63* (8), 1098–1105.

(36) de Oliveira, J. H. H. L.; Nascimento, A. M.; Kossuga, M. H.; Cavalcanti, B. C.; Pessoa, C. O.; Moraes, M. O.; Macedo, M. L.; Ferreira, A. G.; Hajdu, E.; Pinheiro, U. S.; et al. Cytotoxic

alkylpiperidine alkaloids from the Brazilian marine sponge *Pachychalina alcaloidifera*. *J. Nat. Prod.* 2007, *70* (4), 538–543.

(37) Xu, S.; Yoshimura, H.; Maru, N.; Ohno, O.; Arimoto, H.; Uemura, D. Pinnarine, another member of the halichlorine family. Isolation and preparation from pinnaic acid. *J. Nat. Prod.* 2011, *74* (5), 1323–1326.

(38) Kuramoto, M.; Tong, C.; Yamada, K.; Chiba, T.; Hayashi, Y.; Uemura, D. Halichlorine, an Inhibitor of VCAM-1 induction from the marine sponge *Halichondria okadai* Kadata. *Tetrahedron Lett.* 1996, *37* (22), 3867–3870.

(39) Jin, Y.; Fotso, S.; Yongtang, Z.; Sevvana, M.; Laatsch, H.; Zhang, W. Halichondria sulfonic Acid, a new HIV-1 inhibitory guanidino-sulfonic acid, and halistanol sulfate isolated from the marine sponge *Halichondria rugosa* Ridley & Dendy. *Nat. Prod. Res.* 2006, *20* (12), 1129–1135.

(40) Li, H.; Matsunaga, S.; Fusetani, N. Halicylindramides A-C, antifungal and cytotoxic depsipeptides from the marine sponge *Halichondria cylindrata*. *J. Med. Chem.* 1995, *38* (2), 338–343.

(41) Li, H.; Matsunaga, S.; Fusetani, N. Halicylindramides D and E, antifungal peptides from the marine sponge *Halichondria cylindrata*. *J. Nat. Prod.* 1996, *59* (2), 163–166.

(42) Burreson, B. J.; Scheuer, P. J. Isolation of a diterpenoid isonitrile from a marine sponge. *J. Chem. Soc. Chem. Commun.* 1974, No. 24, 1035.

(43) Molinski, T. F.; Faulkner, D. J.; Van Duyne, G. D.; Clardy, J. Three new diterpene isonitriles from a Palauan sponge of the genus *Halichondria*. *J. Org. Chem.* 1987, *52* (15), 3334–3337.

(44) Nakagawa, M.; Hamamoto, Y.; Ishihama, M.; Hamasaki, S.; Endo, M. Pharmacologically active homosesterterpenes from Palauan sponges. *Tetrahedron Lett.* 1987, *28* (4), 431–434.

(45) Nakamura, H.; Deng, S.; Takamatsu, M.; Kobayashi, J.; Ohizumi, Y.; Hirata, Y. Structure of halipanicine, a new sesquiterpene isothiocyanate from the Okinawan marine sponge *Halichondria panicea* (Pallas). *Agric. Biol. Chem.* 1991, *55* (2), 581–583.

(46) Burreson, B. J.; Christophersen, C.; Scheuer, P. J. Co-occurrence of a terpenoid isocyanide-formamide pair in the marine sponge *Halichondria* species. *J. Am. Chem. Soc.* 1975, *97* (1), 201–202.

(47) Sullivan, B. W.; Faulkner, D. J.; Okamoto, K. T.; Chen, M. H. M.; Clardy, J. (6R,7S)-7-amino-7,8-dihydro-alpha-bisabolene, an antimicrobial metabolite from the marine sponge *Halichondria* sp. *J. Org. Chem.* 1986, *51* (26), 5134–5136.

(48) Cimino, G.; De Stefano, S.; Minale, L. Paniceins, unusual aromatic sesquiterpenoids linked to a quinol or quinone system from the marine sponge *Halichondria panicea*. *Tetrahedron* 1973, *29* (17), 2565–2570.

(49) Ohno, O.; Chiba, T.; Todoroki, S.; Yoshimura, H.; Maru, N.; Maekawa, K.; Imagawa, H.; Yamada, K.; Wakamiya, A.; Suenaga, K.; et al. Halichonines A, B, and C, novel sesquiterpene alkaloids from the marine sponge *Halichondria okadai* Kadota. *Chem. Commun.* 2011, *47* (46), 12453.

(50) Ishiyama, H.; Hashimoto, A.; Fromont, J.; Hoshino, Y.; Mikami, Y.; Kobayashi, J. Halichonadins A–D, new sesquiterpenoids from a sponge *Halichondria* sp. *Tetrahedron* 2005, *61* (5), 1101–1105.

(51) Kozawa, S.; Ishiyama, H.; Fromont, J.; Kobayashi, J. Halichonadin E, a dimeric sesquiterpenoid from the sponge *Halichondria* sp. *J. Nat. Prod.* 2008, *71* (3), 445–447.

(52) Ishiyama, H.; Kozawa, S.; Aoyama, K.; Mikami, Y.; Fromont, J.; Kobayashi, J. Halichonadin F and the Cu(I) complex of halichonadin C from the sponge *Halichondria* sp. *J. Nat. Prod.* 2008, *71* (7), 1301–1303.

(53) Suto, S.; Tanaka, N.; Fromont, J.; Kobayashi, J. Halichonadins G–J, New sesquiterpenoids from a sponge *Halichondria* sp. *Tetrahedron Lett.* 2011, *52* (27), 3470–3473.

(54) Tanaka, N.; Suto, S.; Ishiyama, H.; Kubota, T.; Yamano, A.; Shiro, M.; Fromont, J.; Kobayashi, J. Halichonadins K and L, new dimeric sesquiterpenoids from a sponge *Halichondria* sp. *Org. Lett.* 2012, *14* (13), 3498–3501.

(55) Kobayashi, J.; Tanaka, N.; Suto, S.; Asai, M.; Kusama, T.; Takahashi-Nakaguchi, A.; Gonoi, T.; Fromont, J. Halichonadins M-Q, sesquiterpenes from an Okinawan marine sponge *Halichondria* sp. *Heterocycles* 2015, *90* (1), 173.

(56) Prawat, H.; Mahidol, C.; Kaweetripob, W.; Prachyawarakorn, V.; Tuntiwachwuttikul, P.; Ruchirawat, S. Sesquiterpene isocyanides, isothiocyanates, thiocyanates, and formamides from the Thai sponge *Halichondria* sp. *Tetrahedron* 2016, *72* (29), 4222–4229.

(57) Prinsep, M. R.; Blunt, J. W.; Munro, M. H. G. Isolation of the furan fatty acid, (8z, 11z, 14z, 17z)-3,6-epoxyeicos-3,5,8,11,14,17-hexenoic acid from the new zealand sponge *Hymeniacidon hauraki*. *J. Nat. Prod.* 1994, *57 (11)*, 1557–1559.

(58) Shen, Y.-C.; Prakash, C. V. S.; Kuo, Y.-H. Three new furan derivatives and a new fatty acid from a Taiwanese marine sponge *Plakortis simplex*. *J. Nat. Prod.* 2001, *64* (3), 324–327.

(59) Kobayashi, J.; Ohizumi, Y.; Nakamura, H.; Hirata, Y. A novel antagonist of serotonergic receptors, Hymenidin, isolated from the Okinawan marine sponge *Hymeniacidon* sp. *Experientia* 1986, *42* (10), 1176–1177.

(60) Kobayashi, J.; Kanda, F.; Ishibashi, M.; Shigemori, H. Manzacidins A-C, novel tetrahydropyrimidine alkaloids from the Okinawan marine sponge *Hymeniacidon* sp. *J. Org. Chem.* 1991, *56* (14), 4574–4576.

(61) Kobayashi, J.; Inaba, K.; Tsuda, M. Tauroacidins A and B, new bromopyrrole alkaloids possessing a taurine residue from *Hymeniacidon* sponge. *Tetrahedron* 1997, *53* (49), 16679–16682.

(62) Kitagawa, I.; Kobayashi, M.; Kitanaka, K.; Kido, M.; Kyogoku, Y. Marine natural products. XII. On the chemical constituents of the Okinawan marine sponge *Hymeniacidon aldis*. *Chem. Pharm. Bull. (Tokyo).* 1983, *31* (7), 2321–2328.

(63) Schmitz, F. J.; Gunasekera, S. P.; Lakshmi, V.; Tillekeratne, L. M. V. Marine natural products: Pyrrololactams from several sponges. *J. Nat. Prod.* 1985, *48* (1), 47–53.

(64) Inaba, K.; Sato, H.; Tsuda, M.; Kobayashi, J. Spongiacidins A–D, new bromopyrrole alkaloids

from *Hymeniacidon* sponge. *J. Nat. Prod.* 1998, *61* (5), 693–695.

(65) Kobayashi, J.; Ohizumi, Y.; Nakamura, H.; Hirata, Y.; Wakamatsu, K.; Miyazawa, T. Hymenin, a novel α-adrenoceptor blocking agent from the Okinawan marine sponge *Hymeniacidon* sp. *Experientia* 1986, *42* (9), 1064–1065.

(66) Fattorusso, E.; Taglialatela-Scafati, O. Two novel pyrrole-imidazole alkaloids from the Mediterranean sponge *Agelas oroides*. *Tetrahedron Lett.* 2000, *41* (50), 9917–9922.

(67) Cimino, G.; de Giulio, A.; de Rosa, S.; de Stefano, S.; Puliti, R.; Mattia, C. A.; Mazzarella, L. Isolation and X-Ray crystal structure of a novel 8-oxopurine compound from a marine sponge. *J. Nat. Prod.* 1985, *48* (4), 523–528.

(68) Kobayashi, J.; Suzuki, M.; Tsuda, M. Konbu'acidin A, a new bromopyrrole alkaloid with Cdk4 inhibitory activity from *Hymeniacidon* sponge. *Tetrahedron* 1997, *53* (46), 15681–15684.

(69) Capon, R. J.; Skene, C.; Vuong, D.; Lacey, E.; Heiland, K.; Friedel, T. Equilibrating isomers: bromoindoles and a seco-xanthine encountered during a study of nematocides from the Southern Australian marine sponge *Hymeniacidon* sp. *J. Nat. Prod.* 2002, *65* (3), 368–370.

(70) Pettit, G. R.; Clewlow, P. J.; Dufresne, C.; Doubek, D. L.; Cerny, R. L.; Rützler, K. Antineoplastic Agents. 193. Isolation and structure of the cyclic peptide *Hymenistatin*. *Can. J. Chem.* 1990, *68* (5), 708–711.

(71) Kobayashi, J.; Tsuda, M.; Nakamura, T.; Mikami, Y.; Shigemori, H. Hymenamides A and B, New proline-rich cyclic heptapeptides from the Okinawan marine sponge *Hymeniacidon* sp. *Tetrahedron* 1993, *49* (12), 2391–2402.

(72) Tsuda, M.; Shigemori, H.; Mikami, Y.; Kobayashi, J. Hymenamides C ~ E, New cyclic heptapeptides with two proline residues from the Okinawan marine sponge *Hymeniacidon* sp. *Tetrahedron* 1993, *49* (31), 6785–6796.

(73) Kobayashi, J.; Nakamura, T.; Tsuda, M. Hymenamide F, new cyclic heptapeptide from marine sponge *Hymeniacidon* sp. *Tetrahedron* 1996, *52* (18), 6355–6360.

(74) Tsuda, M.; Sasaki, T.; Kobayashi, J. Hymenamides G, H, J, and K, four new cyclic octapeptides

from the Okinawan marine sponge *Hymeniacidon* sp. *Tetrahedron* 1994, *50* (16), 4667–4680.

(75) Wratten, S. J.; Faulkner, D. J.; Hirotsu, K.; Clardy, J. Diterpenoid isocyanides from the marine sponge *Hymeniacidon amphilecta*. *Tetrahedron Lett.* 1978, *19* (45), 4345–4348.

(76) Avilés, E.; Rodríguez, A. D. Monamphilectine A, a potent antimalarial β-lactam from marine sponge *Hymeniacidon* sp: Isolation, structure, semisynthesis, and bioactivity. *Org. Lett.* 2010, *12* (22), 5290–5293.

(77) Teshima, S.; Kanazawa, A.; Hyodo, S. 3-beta-hydroxymethyl-24-methylene-A-nor-5-alpha-cholestane from the sponge [Spongia, Hippospongia]. *Nippon SUISAN GAKKAISHI* 1980, *46* (12), 1517–1520.

(78) Chambers, S. T.; Kunin, C. M. Isolation of glycine betaine and proline betaine from human urine. Assessment of their role as osmoprotective agents for bacteria and the kidney. *J. Clin. Invest.* 1987, *79* (3), 731–737.

(79) Ackermann, D.; List, P. H. On the composition of zooanemonine and herbipoline. *Hoppe Seyler's Z. Physiol. Chem.* 1960, *318(3/6)*, 281.

(80) Hattori, T.; Matsuo, S.; Adachi, K.; Shizuri, Y. Isolation of antifouling substances from the Palauan pponge *Protophlitaspongia aga*. *Fish. Sci.* 2001, *67* (4), 690–693.

(81) Sauleau, P.; Moriou, C.; Al Mourabit, A. Metabolomics approach to chemical diversity of the Mediterranean marine sponge *Agelas oroides*. *Nat. Prod. Res.* 2017, *31* (14), 1625–1632.

(82) Cafieri, F.; Fattorusso, E.; Taglialatela-Scafati, O. Novel betaines from the marine sponge *Agelas dispar*. *J. Nat. Prod.* 1998, *61* (9), 1171–1173.

(83) Weinheimer, A. J.; Metzner, E. K.; Mole, M. L. A new marine betaine, norzooanemonin, in the Gorgonian *Pseudopterogorgia americana*. *Tetrahedron* 1973, *29* (20), 3135–3136.

(84) Gupta, K. C.; Miller, R. L.; Williams, J. R.; Blount, J. F. Norzooanemonin in the hydroid *Tubularia larynx*. *Experientia* 1977, *33* (12), 1556.

(85) Capon, R. J.; Vuong, D.; McNally, M.; Peterle, T.; Trotter, N.; Lacey, E.; Gill, J. H. (+)-Echinobetaine B: Isolation, structure elucidation, synthesis and preliminary SAR studies on a new nematocidal betaine from a southern Australian marine sponge, *Echinodictyum* sp. *Org. Biomol. Chem.* 2005, *3* (1), 118–122.

(86) Ashraf, M.; Foolad, M. R. Roles of glycine betaine and proline in improving plant abiotic stress resistance. *Environ. Exp. Bot.* 2007, *59* (2), 206–216.

(87) Amin, U. S.; Lash, T. D.; Wilkinson, B. J. Proline betaine is a highly effective osmoprotectant for *Staphylococcus aureus*. *Arch. Microbiol.* 1995, *163* (2), 138–142.

(88) Pierce, S. K.; Edwards, S. C.; Mazzocchi, P. H.; Klingler, L. J.; Warren, M. K. Proline betaine: a unique osmolyte in an extremely euryhaline osmoconformer. *Biol. Bull.* 1984, *167* (2), 495–500.

(89) Thymidine. (2018) http://bmrb.wisc.edu/metabolomics/mol_summary/show_data.php?molName=thymidine&id=bmse000244 (accessed Sep 28, 2018).

(90) Tyrosine. (2018) http://www.bmrb.wisc.edu/metabolomics/mol_summary/show_data.php?id=bmse000051 (accessed Sep 28, 2018).

(91) Leucine. (2018) http://www.bmrb.wisc.edu/metabolomics/mol_summary/show_data.php?id=bmse000042 (accessed Sep 28, 2018).

(92) Isoleucine. (2018) http://www.bmrb.wisc.edu/metabolomics/mol_summary/show_data.php?id=bmse000041&whichTab=1 (accessed Sep 28, 2018).

(93) Valine. (2018) http://www.bmrb.wisc.edu/metabolomics/mol_summary/show_data.php?id=bmse000052 (accessed Sep 28, 2018).

(94) Choline. (2018) http://www.bmrb.wisc.edu/metabolomics/mol_summary/show_data.php?id=bmse000285&whichTab=1 (accessed Sep 28, 2018).

(95) Agmatine. (2018) http://www.bmrb.wisc.edu/metabolomics/mol_summary/show_data.php?id=bmse000063&whichTab=1 (accessed Sep 28, 2018).

(96) Trager, W.; Jensen, J. B. Human malaria parasites in continuous culture. *Science* 1976, *193* (4254), 673–675.

(97) Trager, W.; Jensen, J. B. Human malaria parasites in continuous culture. 1976. *J. Parasitol.* 2005, *91* (3), 484–486.

(98) Makler, M. T.; Ries, J. M.; Williams, J. A.; Bancroft, J. E.; Piper, R. C.; Gibbins, B. L.; Hinrichs, D. J. Parasite lactate dehydrogenase as an assay for *Plasmodium falciparum* drug sensitivity. *Am. J. Trop. Med. Hyg.* 1993, *48* (6), 739–741.

Chapter Four: Semi-synthetic derivatization, antimycobacterial and antiplasmodium evaluations of analogues of the natural product fusidic acid

4.1 General Introduction

4.1.1 Fusidic acid and fusidane triterpenes: Chemistry

Fusidane triterpenes are a small group of fungal 29-*nor* protostane triterpenes. Only 20 congeners have so far been reported.[1,2] They are tetracyclic compounds with a similar side chain at C-17 as observed in dammarane triterpenoids (Figure 4.1).

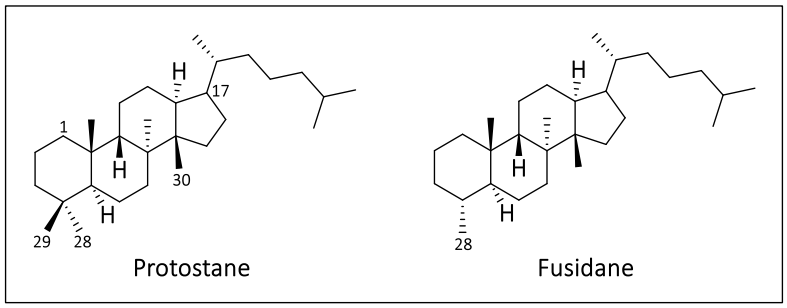

Figure 4.1: Carbon backbone of dammarane, protostane and fusidane triterpenoids

Fusidane triterpenes share similar structural conformations of the tetracycles to protostanes. A common protostane precursor, 3*β*-hydroxy-protosta-17(20)*Z*, 24-diene, has been proposed to be involved in the biosynthesis of the fusidanes. Further demethylation of C-29 produces the fusidane triterpenoid skeleton (Figure 4.2).[1]

Structural characteristics of the fusidanes include the presence of a C-O functionality at position C-3, $\Delta^{17,20}$, $\Delta^{24,25}$, a carboxylic acid group at C-21, and an acetoxy group at C-16 (except 16-deacetoxy-7-β-hydroxy fusidic acid)[3]. Oxygen substituents can be present at positions C-6, C-7, C-11 and C-12. Fusilactidic acid is the only fusidane with a seven-membered lactone functionalized ring C.[4]

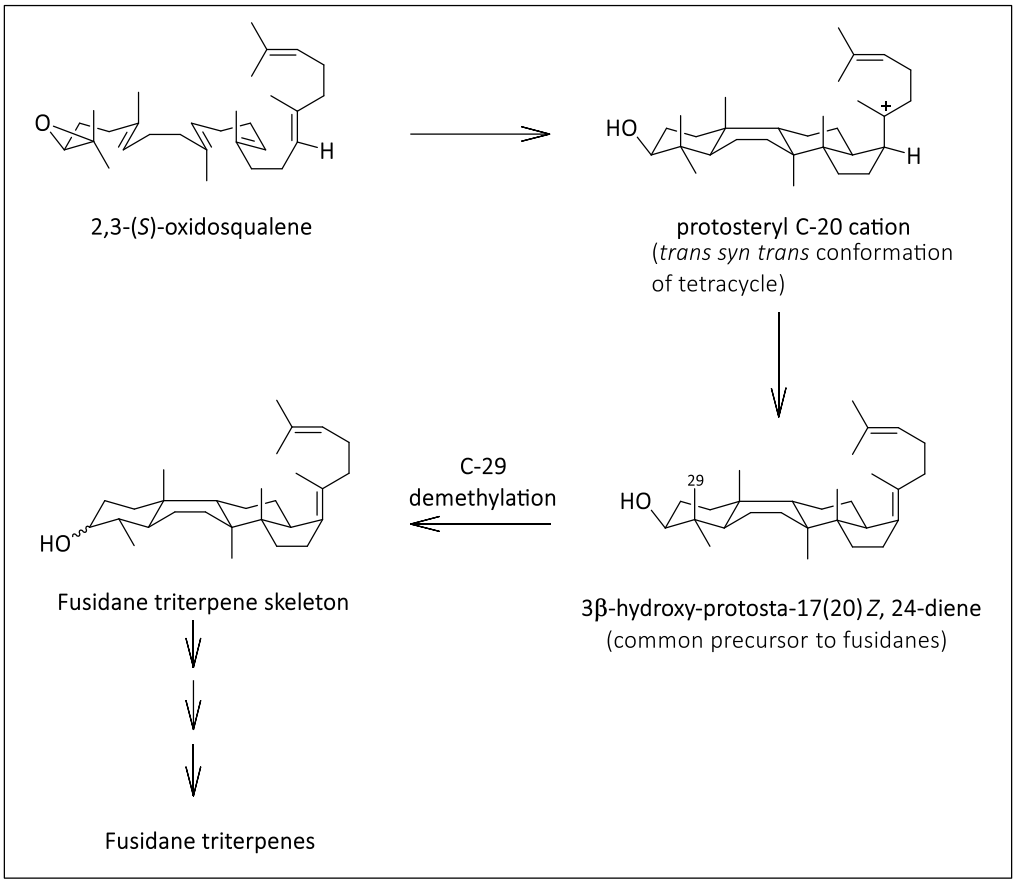

Figure 4.2: Biosynthesis of fusidane triterpenoid skeleton[1]

Naturally occurring fusidanes can be classified into four general subclasses: helvolic acid, viridominic acids A-C, cephalosporin P1 and its congeners, as well as fusidic acid and related compounds. Helvolic acid was the first reported fusidane and was isolated from the soil fungus *Aspergillus fumigatus* in 1942. It is a C-3 and C-7 di-*oxo* compound and possesses a $\Delta^{1,2}$ double bond and an extra acetoxy group at C-6.[5,6] Helvolic acid demonstrated bacteriostatic activity against gram-positive bacteria but not gram-negatives. It exhibited comparable activity to that of penicillin and exerted superior activity over the sulfonamides.[6] Its anti-tubercular activity has also been reported.[7] Helvolic acid demonstrated higher antibacterial (IC_{50} values between 0.98 - 33.19 µg/mL) and antifungal (IC_{50} value of 7.20 µg/mL) activities than all other steroids isolated from the plant endophyte fungus *Pichia guilliermondii* Ppf9[8] and similar activity against phytopathogenic fungi with a MIC value of >6.25 µg/mL, which is comparable to those of commercial fungicides such as carbendazim and hymexazol.[9,10]

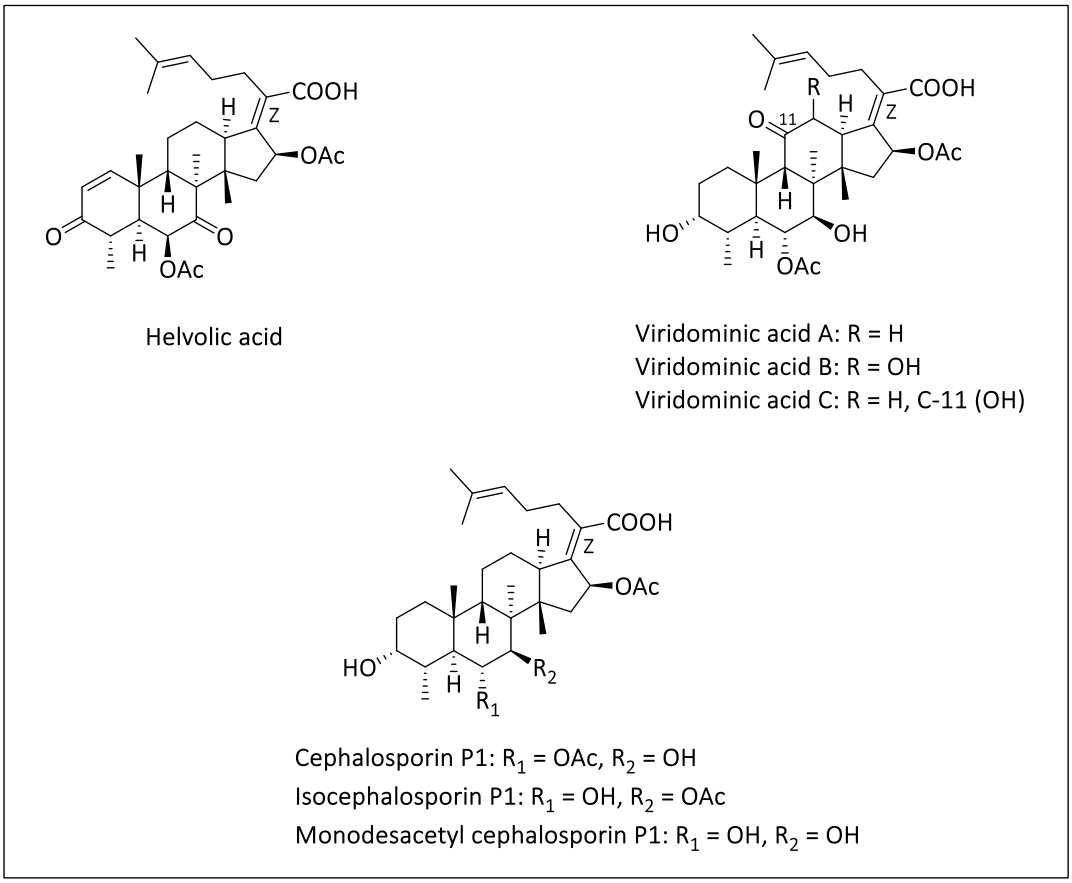

Figure 4.3: Chemical structures of helvolic acid, viridominic acids and cephalosporin P1 metabolites

The viridominic acids A-C were isolated from the culture filtrate of *Cladosporium* sp. These fusidanes are characterized by the presence of an acetoxy group at C-6 and a C-7 hydroxyl group. Viridominic acids A and B possess a C-11-*oxo*- functionality while this is reduced to the hydroxyl group in viridominic acid C. Moreover, viridominic acid B bears an extra hydroxyl group at C-12 (Figure 4.3). Viridominic acids A-C have exhibited chlorosis-inducing activity against higher plants.[11,12] Cephalosporin P1, isocephalosporin P1, and monodesacetyl cephalosporin P1 were isolated from *Cephalosporium acremonium*.[13,14] The cephalosporin P1 congeners are not related to the beta lactam cephalosporins. Cephalosporin P1 possesses an acetoxy and a hydroxyl substituent at positions 6 and 7, respectively. Isocephalosporin P1 possesses a hydroxyl and an acetoxy group at positions 6 and 7, respectively, and hence a positional isomer of cephalosporin P1. Meanwhile, C-6 deacetylation of cephalosporin P1 produces monodesacetyl cephalosporin P1

(Figure 4.3). Cephalosporin P1 has demonstrated potent antibacterial activity against methicillin-sensitive, methicillin-resistant and vancomycin-intermediate *Staphylococcus aureus*.[15,16]

Fusidane triterpenes represent a class of antibiotics and fusidic acid is the most potent congener. It was first reported from the fungus *Fusidium coccineum* by Godtfredsen and coworkers.[4,17] Since then, it has been reported from other fungal species including *Epidermophyton floccosum,*[18] *Acremonium fusidioides*, *Calcarisporium arbuscula*, *C. lamellaecula*, *C. acremonium, Gabarnaudia tholispora, Mucor ramannianus*, and *Paecilomyces fusidioides*.[19] Industrial fermentation of *F. coccineum* yielded fusidic acid and eight metabolites including 3-epifusidic acid, 11-epifusidic acid, 3-ketofusidic acid, 11-ketofusidic acid, 9,11-anhydrofusidic acid, 9,11-anhydro-9α-11α-epoxyfusidic acid, 9,11-anhydro-12-hydroxyfusidic acid, and fusilactidic acid (Figure 4.4).[4]

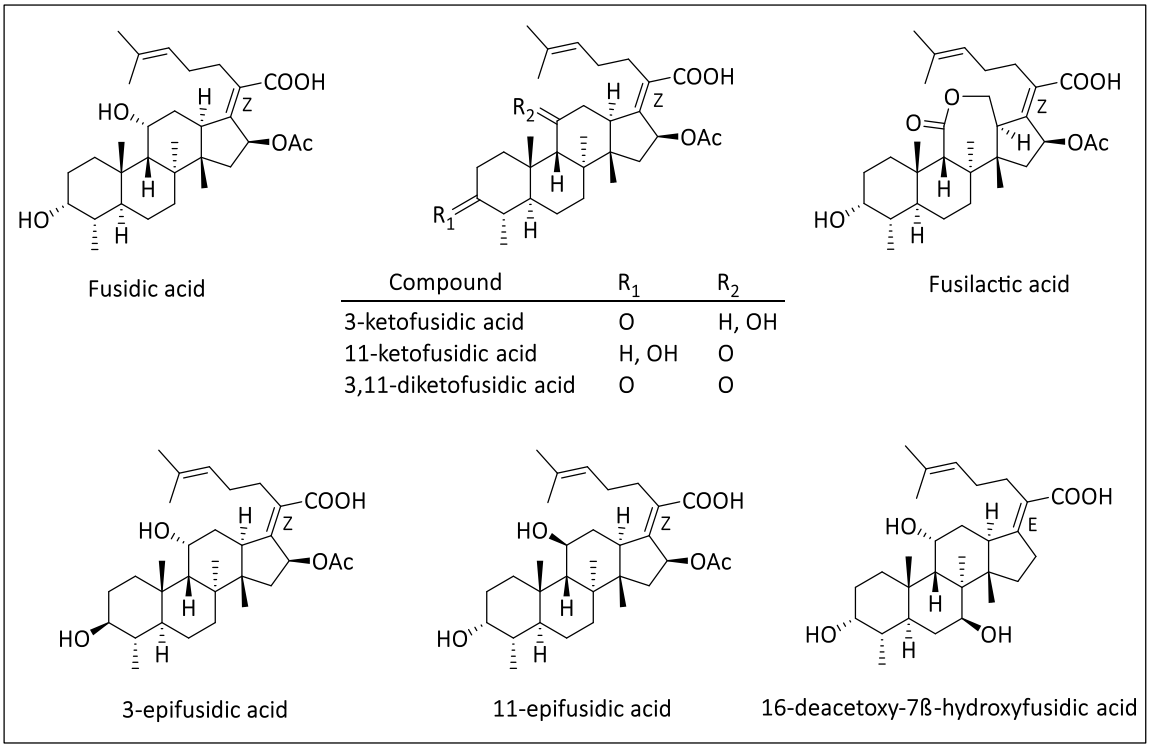

Figure 4.4: Representative structures of fusidic acid and related compounds

The dermatophyte *E. floccosum* also afforded the new 3,11-diketofusidic acid, together with fusidic acid and 3-epifusidic acid. According to Noble and coworkers, the antibacterial activity of *E. floccosum* was attributable to these three metabolites.[18] *Acremonium crotocinigenum* has yielded 16-deacetoxy-7-β-hydroxy fusidic acid,[3] while recently, two new members have been

identified after *Cunninghamella elagans* NRRL 1392 mediated hydroxylation of ring B to produce 6-β-hydroxy fusidic acid and 7-β-hydroxy fusidic acid.[2]

4.1.2 Antibacterial activity of fusidic acid

Fusidic acid has been clinically used as an antibiotic since 1962. It has displayed consistent activity against staphylococcal pathogens including methicillin-resistant *Staphylococcus aureus* (MRSA). Its major clinical indications include systemic treatment for severe staphylococcal infections, systemic treatment for colonization and infection with MRSA, topical treatment of skin infections and topical treatment of atopic dermatitis.[20] It is reported that "*at a proposed susceptible breakpoint (≤ 1 µg/mL), fusidic acid inhibited 99.7% of MRSA strains and 99.3% to 99.9% of multi-drug phenotypes of S. aureus*", and that "*S. aureus strains unsusceptible to fusidic acid (0.35%) generally had detectable resistance mechanisms (fusA, B, C, and E)*".[21]

Fusidic acid is largely bacteriostatic but exhibits bactericidal activity at high concentrations. It acts by inhibiting protein synthesis in the bacteria. It interferes with the function of the protein elongation factor G (EF-G). EF-G is necessary for the hydrolysis of guanosine triphosphate (GTP) to guanosine diphosphate (GDP) to provide energy for the translocation of the peptidyl-tRNA from the A site to the P site on the 50S unit of the ribosome. Fusidic acid binds to EF-G and the ribosome after hydrolysis of GTP, thereby sterically blocking the next stage of protein synthesis. Unlike eukaryotes, prokaryotes possess only one type of elongation factor, which when inhibited affects the process of protein synthesis.[20]

Although almost exclusively used as an anti-staphylococcol agent, fusidic acid has displayed antibacterial activity against a wide range of pathogens (Table 4.1). Gram-negative bacilli are resistant to fusidic acid with MIC values of ≥32 µg/mL.[21] Extensive studies on the antibacterial structure-activity relationship (SAR) of fusidic acid has been reported. The findings made so far on the structural features necessary for activity are depicted in Figure 4.5. Essentially, the *trans-syn-trans* conformation of the tetracylic triterpene backbone and the carboxylic acid and acetoxy groups are required for activity.[22–25]

Table 4.1: Antimicrobial spectrum of fusidic acid[26]

Microorganisms	*In vitro* MIC_{90} (μg/mL)
Gram-positive	
Staphylococcus aureus (methicillin-susceptible)	0.06
Staphylococcus aureus (methicillin-resistant)	0.12
Staphylococcus epidermidis (methicillin-susceptible)	0.25
Staphylococcus epidermidis (methicillin-resistant)	0.50
Corynebacterium diptheriae	0.0044
Clostridium tetani	0.05
Clostridium perfringens	0.5
Propionibacterium acnes	1.0
Other *Corynebacterium* spp.	2.0
Clostridium difficile	2.0
Other *Clostridium* spp.	≤1.0
Staphylococcus saprophyticus	3.12
Streptococcus faecalis	6.25
Streptococcus pyogenes	12.5
Streptococcus pneumoniae	25.0
Gram-negative	
Neisseria meningitidis	0.12
Legionella pneumophila	≤0.25
Neisseria gonorrhoeae	1.0
Bacteroides fragilis	2.0
Other *Bacteroides* spp.	≤2.0

A recent study has demonstrated the importance of the orientation of the side chain of fusidic acid to activity. Amongst the four stereoisomers synthesized based on saturation of the 17(20) double bond, only one analogue, 17*S*,20*S*-dihydrofusidic acid, exhibited activity comparable to fusidic acid while the other three showed less or no activity. The findings of this work highlighted the importance of the spatial arrangement of substituents around the Δ17(20) bond which contradicted earlier assumptions that the Δ17(20) bond was an essential feature in the molecule.[24] Further exploration *via* cyclopropanation of the Δ17(20) bond led to the analogue 17*S*,20*S*-methanofusidic acid which possessed a 17(20) spiro-cyclopropane system. The spiro-cyclopropane system orients the side chain into a bioactive conformational space. The new 17*S*,20*S*-

methanofusidic acid was found to exert antibacterial activity against several Gram-positive species with potency essentially equal to natural fusidic acid.[25]

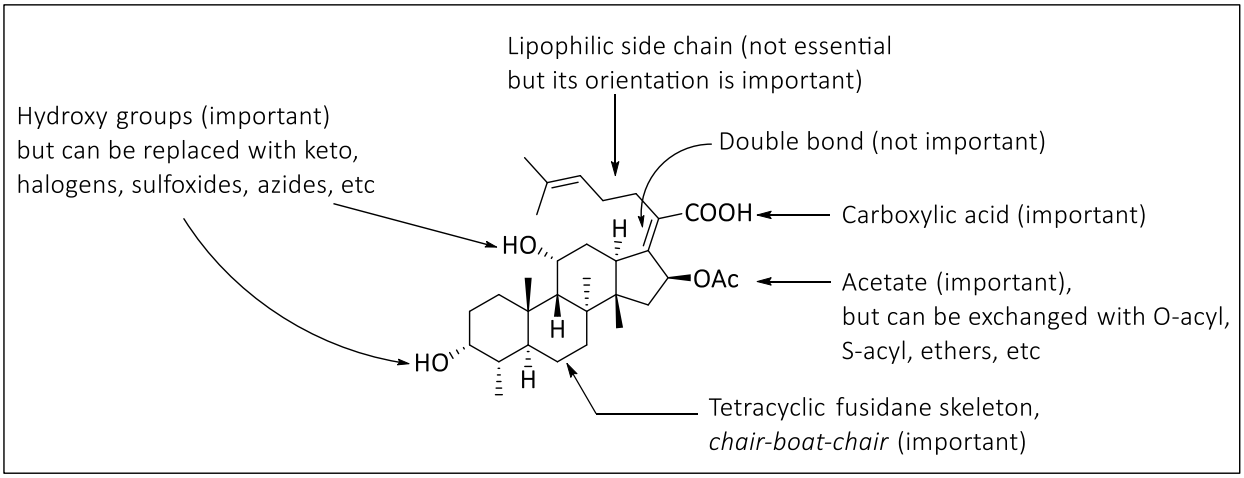

Figure 4.5: Antimicrobial structure-activity relationship of fusidic acid[22–25]

4.1.3 Repositioning of fusidic acid for tuberculosis and malaria

Drug repositioning is the medicinal chemistry approach of finding new therapeutic uses of old and existing drugs through appropriate synthetic modifications. In contrast, drug repurposing refers to using an old or existing drug in its original form for a new disease indication with modification in the dosage amounts. Examples of successful repositioned/repurposed drugs include Viagra® (repurposed from a treatment of hypertension to its current use for treatment of erectile dysfunction),[27] Thalidomide® (repositioned from a sedative, analgesic and antiemetic but currently used for erythema nodosum leprosum and multiple myeloma),[28] and Minoxidil® (repurposed from a treatment of hypertension but currently used for the treatment of hair loss).[29] Drug repositioning/repurposing is a time and cost effective approach to drug development.[30]

Examples of drugs repositioned for the treatment of tuberculosis and malaria are shown in Figure 4.6 and 4.7, respectively. Most of these drugs have been previously used for the treatment of microbial infections, including bacterial and protozoan diseases.[31]

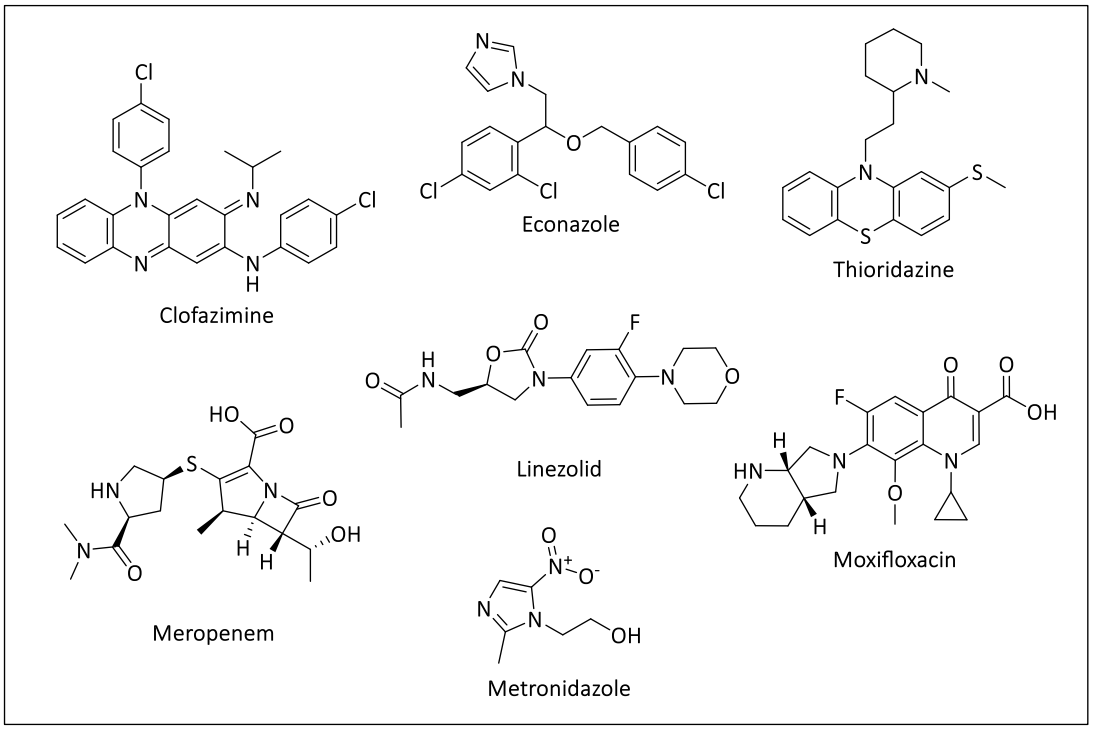

Figure 4.6: Examples of repositioned drugs for the treatment of TB[31]

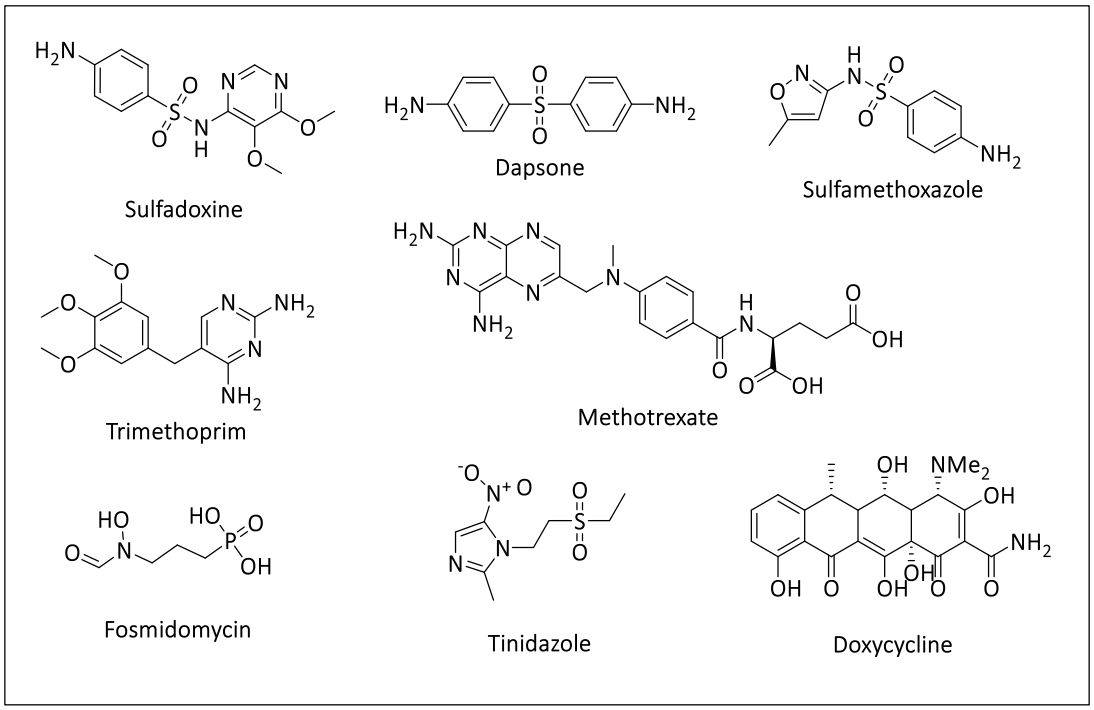

Figure 4.7: Examples of repositioned drugs for the treatment of malaria[31]

4.1.3.1 Antimycobacterial activity of fusidic acid

Fusidic acid has exhibited activity against some *Mycobacterium* species including *M. tuberculosis* (*Mtb*), *M. avium*, *M. chelonei*, *M. fortuitum* and *M. kansasii*. It exhibited *in vitro* activity against *Mtb* with MIC_{90} value of 31 µM[32–34] and displayed antimycobacterial activity against the $H_{37}Rv$ strain of *Mtb* with an IC_{90} value of 1.2 µM.[35] An *in vitro* susceptibility study of 170 clinical isolates of *Mtb* to fusidic acid was conducted. Of the 170 isolates, 19 were resistant to one or more first-line anti-tuberculosis drugs (INH, RIF, STR and ETB) while the rest were susceptible. It was found that only 3 of the 151 susceptible clinical isolates were resistant to fusidic acid with an MIC_{90} value >128 mg/L. All the 19 resistant isolates were susceptible to fusidic acid with MIC_{90} value of ≤16 mg/L. Meanwhile, no cross resistance was observed between fusidic acid and the first-line drugs.[32]

Inspired by the good antibacterial and antimycobacterial activities of fusidic acid, coupled with the need for new drugs to curb the global burden of the disease tuberculosis in terms of high mortality and increased emergence of resistance to current chemotherapy, our laboratory has adopted a multi-disciplinary approach to the repurposing and repositioning of fusidic acid as an anti-tubercular drug. This approach has involved collaborative efforts of medicinal chemists, pharmacologists and biologists.

With the goal to identify the mechanism of action (MoA) and plausible mechanisms of resistance (MoR) of fusidic acid in *M. smegmatis* and *Mtb*, resistant mutant selection and whole genome sequencing studies were conducted. The studies revealed EF-G as the target of fusidic acid in *Mtb*. This was further confirmed through target-based whole cell screening conducted using an anhydrotetracycline responsive knockdown strain of fusidic acid underexpressing EF-G, in which hypersensitivity was observed for fusidic acid and three analogues.[36]

The *in vitro* metabolism of fusidic acid has been demonstrated to be species specific. A key metabolite of fusidic acid in mouse and rat liver microsomes was found to be its inactive 3-epimer. It was observed in all analogues possessing a free hydroxyl group at C-3 and in 3-ketofusidic acid. The formation of this metabolite is hypothesized to result from C-3 oxidation, followed by non-stereoselective reduction to give fusidic acid and 3-epifusidic acid. Apart from metabolism at the

C-3 position, metabolites arising from hydroxylation reactions have also been observed.[37] Some C-3 esters were found to act as prodrugs of fusidic acid in rodent liver microsomes and plasma, following hydrolysis of the acyl group.[38] However, this was not observed in C-21 esters and amides.[36] In the cell lysate of *M. smegmatis*, a metabolite arising from first, hydrolysis of the C-16 acetyl group, followed by lactonization with C-21 was observed. However, the fusidic acid lactone was absent in either *Mtb* supernatant or in the buffer control.[37] Meanwhile, the main metabolites of fusidic acid in humans include 3-ketofusidic acid, C-21 glucoronide, C-27 carboxylic acid, and hydroxylates (Figure 4.8).[39] These compounds are less active than the parent drug. 3-epifusidic acid is not a metabolite in humans. The metabolism of fusidic acid to its inactive 3-epimer in mice has made the mouse model inappropriate for *in vivo* studies of fusidic acid and its analogues.

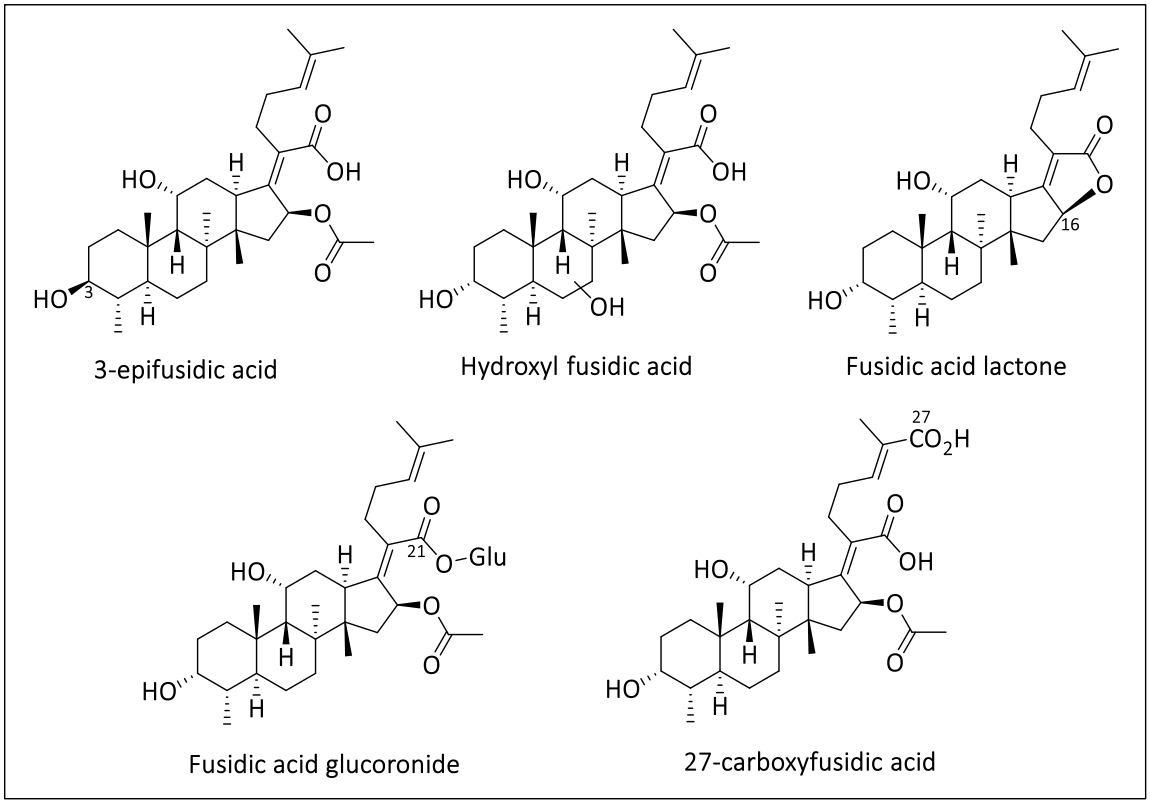

Figure 4.8: Key metabolites of fusidic acid in rodents and man

Seven current *Mtb* drugs have been shown to synergize with fusidic acid in inhibiting the growth of *Mtb*. These include rifampicin (RIF), erythromycin (ERY), clarithromycin (CLR), roxythromycin (ROX), linezolid (LZD), streptomycin (STR), and spectinomycin (SPC). The strongest synergies were

observed for the two drugs, ERY and SPC, with a fractional inhibitory concentration index (FICI) value of 0.25 observed for each drug. It is noteworthy that "*synergy with fusidic acid was achieved in vitro at concentrations lower than the reported peak plasma concentrations achievable for all the drugs, with the exception of ERY*".[40]

The biological findings presented above were possible due, in part, to the judicious efforts of medicinal chemists who synthesized fusidic acid analogues leading to fusidic acid prodrugs, bioisosteres and hybrid analogues. Some of these analogues are shown in Figure 4.9.

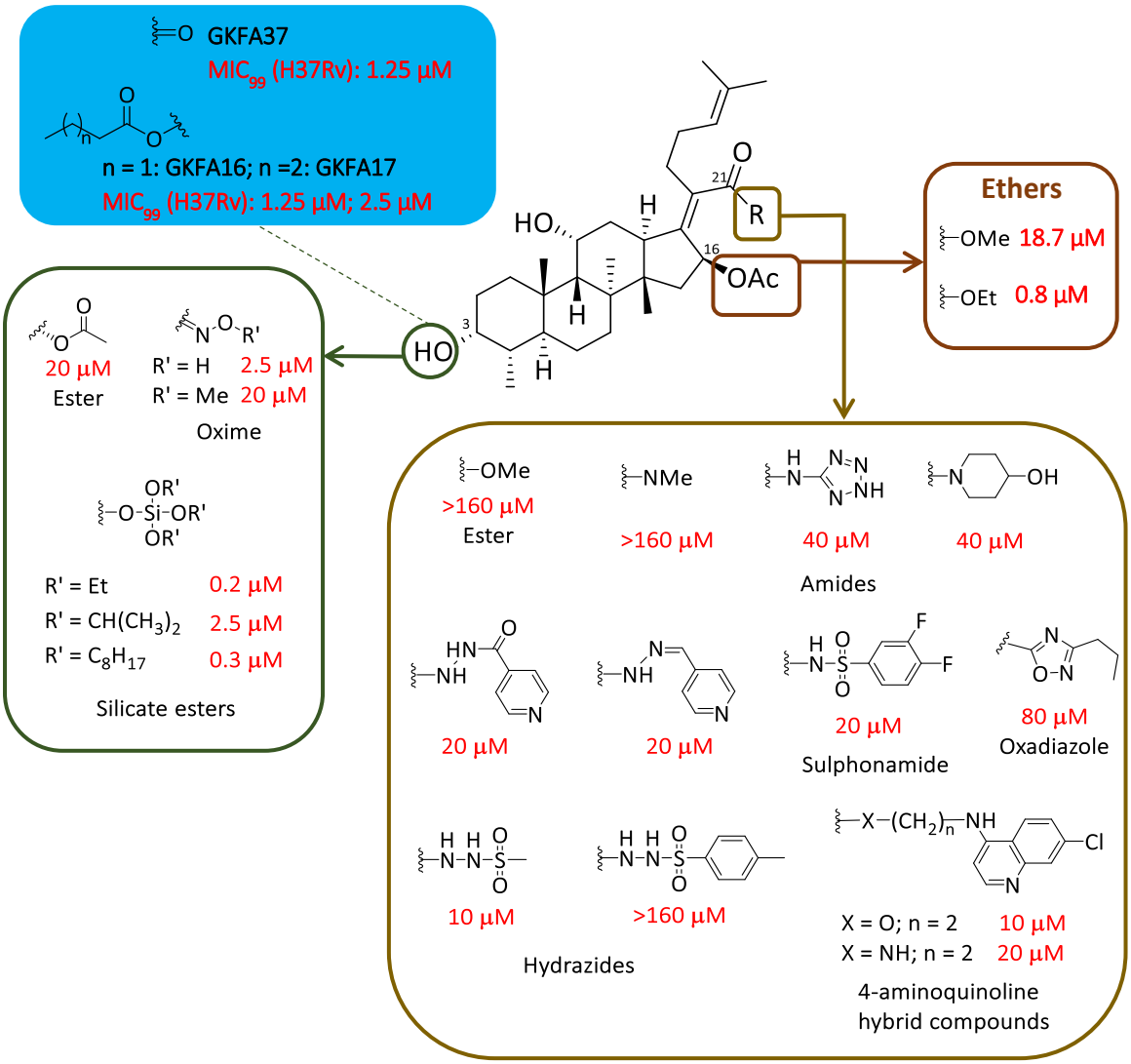

Figure 4.9: Representative fusidic acid analogues synthesized from antimycobacterial structure-activity relationship explorations.[36,38,41]

In this context, the SAR explorations have focused on synthesizing C-3, C-16, and C-21 fusidic acid analogues as antimycobacterial agents.[36,38,41] The *in vitro* antimycobacterial activity of the analogues was evaluated against the $H_{37}Rv$ strain of *Mtb*, determined at the minimum concentration required to inhibit the growth of 99% of the bacterial population (MIC_{99}).

In general, the C-3 analogues of fusidic acid have exhibited the most potent (<5 µM) antimycobacterial activity so far.[38,41] These analogues explored so far include esters, amides, silicates, oximes, and amines (Figure 4.9). 3-ketofusidic acid (**GKFA37**) exhibited good activity with a MIC_{99} value of 1.25 µM, while 3-epifusidic acid lost significant activity with a MIC_{99} value of 11.4 µM as compared to fusidic acid (MIC_{99}, 0.6 µM). The C-3 butyrate derivative (**GKFA16**, MIC_{99}, 1.25 µM) of fusidic acid was found to be the optimum chain length for the C-3 long chain ester analogues. The acetate derivative exhibited moderate activity (MIC_{99}, 20 µM) while chain lengths exceeding seven carbons resulted in poor activity. The unsubsitituted C-3 oxime (MIC_{99} = 2.5 µM) was the most active of that class of C-3 analogues of fusidic acid. The C-3 trialkoxysilicate analogues demonstrated good antimycobacterial activity (MIC_{99} 0.2 – 2.5 µM). Generally, the *n*-alkyl silicates were more active than branched ones.[38]

Hydrolysis of the C-16 acetyl group, followed by alkylation has afforded two C-16 ether analogues of fusidic acid (Figure 4.9). The C-16 ethyl ether analogue exhibited comparable activity (MIC_{99} 0.8 µM) to fusidic acid while the methyl ether analogue showed moderate activity (MIC_{99} = 18.7 µM).[38]

C-21 fusidic acid analogues were synthesized largely based on a bioisostere approach. The synthesized analogues included esters, amides, hydrazides, sulfonamides and oxadiazoles (Figure 4.9).[38,41] Moreover, fusidic acid amide and ester aminoquinoline hybrid compounds have also been explored.[36] The available antimycobacterial activity data have provided evidence for the importance of the COOH group to antimycobacterial activity. Briefly, conversion of fusidic acid to the C-21 methyl ester and amide derivatives led to loss of activity (MIC_{99} >160 µM). However, cyclic amides regained activity (MIC_{99} = 40 µM). The hydrazide analogues of fusidic acid demonstrated moderate activity (MIC_{99} 10 - 40 µM), with the exception of long chain *n*-alkyl or aromatic sulfonylhydrazides (MIC_{99} >160 µM). The methyl sulfonylhydrazide analogue and a hydrazide synthesized from fusidic acid and isoniazid both exhibited MIC_{99} value of 10 µM.

Meanwhile, substituted aryl sulfonamides displayed moderate activity (MIC_{99} 20 µM). Five 1,2,4-oxadiazole derivatives, together with 5-oxo-1,3,4-oxadiazole and 5-thioxo-1,3,4-oxadiazole derivatives, have been synthesized as C-21 bioisosteres. However, all of these derivatives were found to be either poorly active or inactive (MIC_{99} 80 - 160 µM).[38,41]

The C-3 triisopropoxy silicate analogue was found to be stable *in vivo*. It displayed a better pharmacokinetic profile than that of fusidic acid in mice. It achieved higher concentrations in blood, a longer half-life (5 h versus 1 h after oral administration), with a lower clearance rate. In contrast to the other congeners (GKFA16 and GKFA17), this analogue did not act as a prodrug of fusidic acid.[38] This could perhaps explain its *in vivo* stability in mice since it was not hydrolyzed to fusidic acid, which has been found to be rapidly converted to its inactive 3-epimer in mice. In fact, pharmacokinetic studies conducted on GKFA16 and GKFA17 revealed that the latter was rapidly cleared compared to the former. The concentrations of fusidic acid were sustained longer in GKFA16. GKFA16 and GKFA17 were evaluated for their organ distribution in the lungs and spleen, liver and kidneys, and heart and brain. The compounds showed improved organ distribution compared to fusidic acid. Thus, tissue concentrations of fusidic acid were higher than in the blood.[42]

4.1.3.2 Antiplasmodium activity of fusidic acid

Fusidic acid has displayed antiplasmodium activity against the D10, NF54, and K1 strains of *Plasmodium falciparum* with IC_{50} values of 52.8 µM, 59.0 µM, and 19.0 µM, respectively.[43,44] It has been suggested that fusidic acid exhibits antiplasmodium activity by inhibiting plasmodial EF-Gs in the apicoplast and mitochondria.[43]

A series of antiplasmodium fusidic acid derivatives were synthesized by replacing the carboxylic acid group with various bioisosteres. A 2 - 35 fold increase in antiplasmodium activity was reported for most of the derivatives. Moreover, docking studies on the most active analogue revealed similar binding orientation to fusidic acid within the active site of plasmodial EF-G.[44] Subsequent explorations around the carboxylic acid group by its replacement with amide and ester groups led

to more potent derivatives with 4 - 49 and 5 - 17 fold increase in activity against *P. falciparum* NF54 and K1 strains, respectively.[45]

In a ligand-based 3D-QSAR (Three-Dimensional Quantitative Structure–Activity Relationship) modeling approach to design fusidic acid derivatives toward the identification of derivatives with improved antiplasmodium activity, compounds I-III were shown to possess significant activity against *P. falciparum* NF54 and K1 strains (Figure 4.10).[46]

Kaur and coworkers developed the 3D-QSAR models based on the antiplasmodium activities of 61 previously synthesized fusidic acid derivatives in our laboratory. After validation of the selected model Hypo 2, a 3D query for virtual screening was conducted to search for potential hits from a fusidic acid-based combinatorial library. Eight virtual hit compounds were synthesized and evaluated for their antiplasmodium activity against *P. falciparum*. All synthesized compounds displayed superior activity than the parent compound fusidic acid (Figures 4.11 and 4.12).[46]

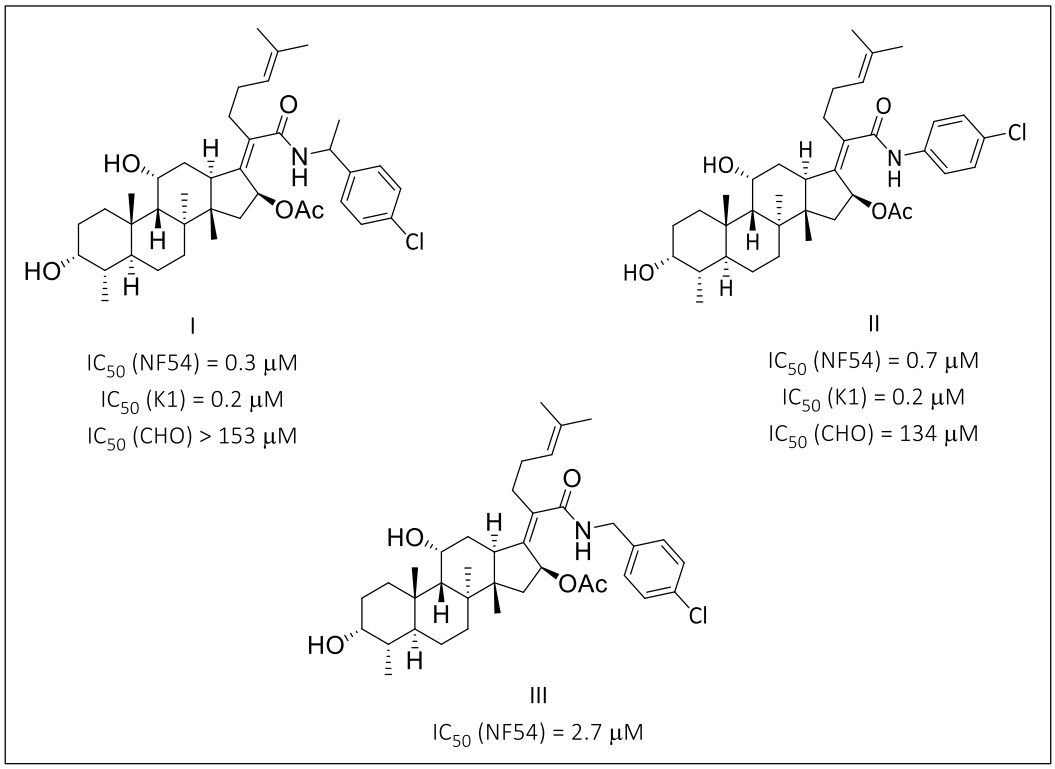

Figure 4.10: Chemical structures of lead compounds I-III

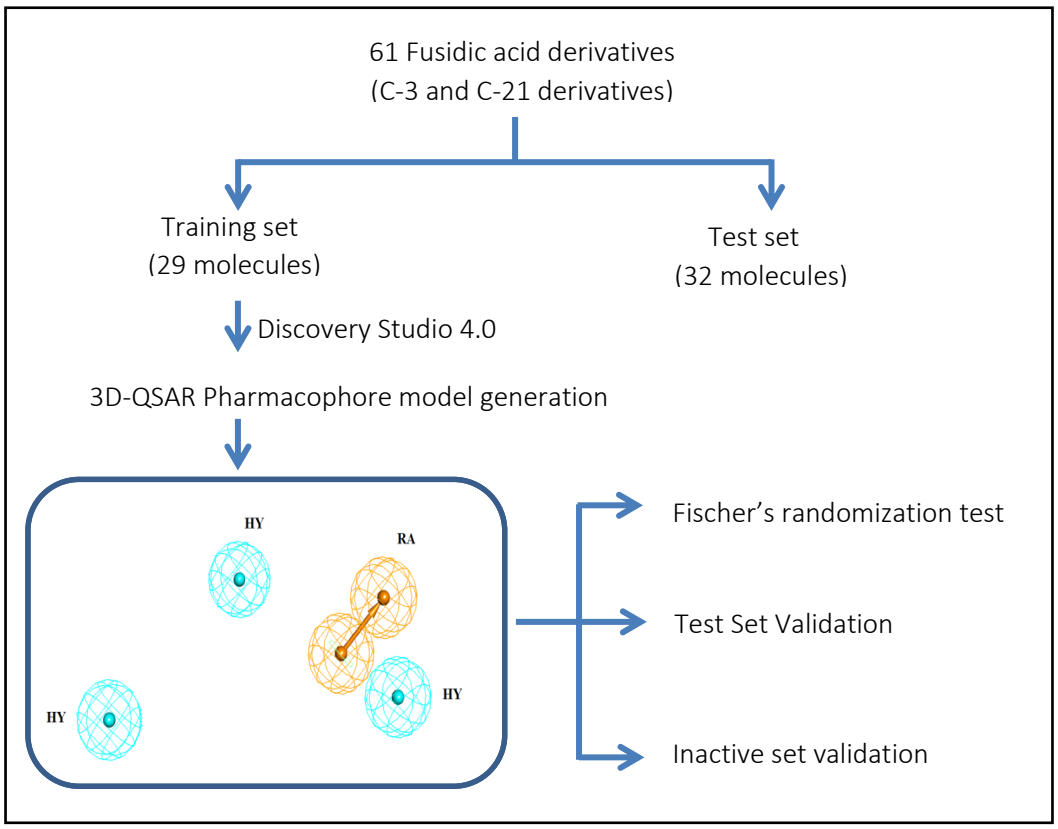

Figure 4.11: Flow chart summarizing 3D-QSAR studies[38]

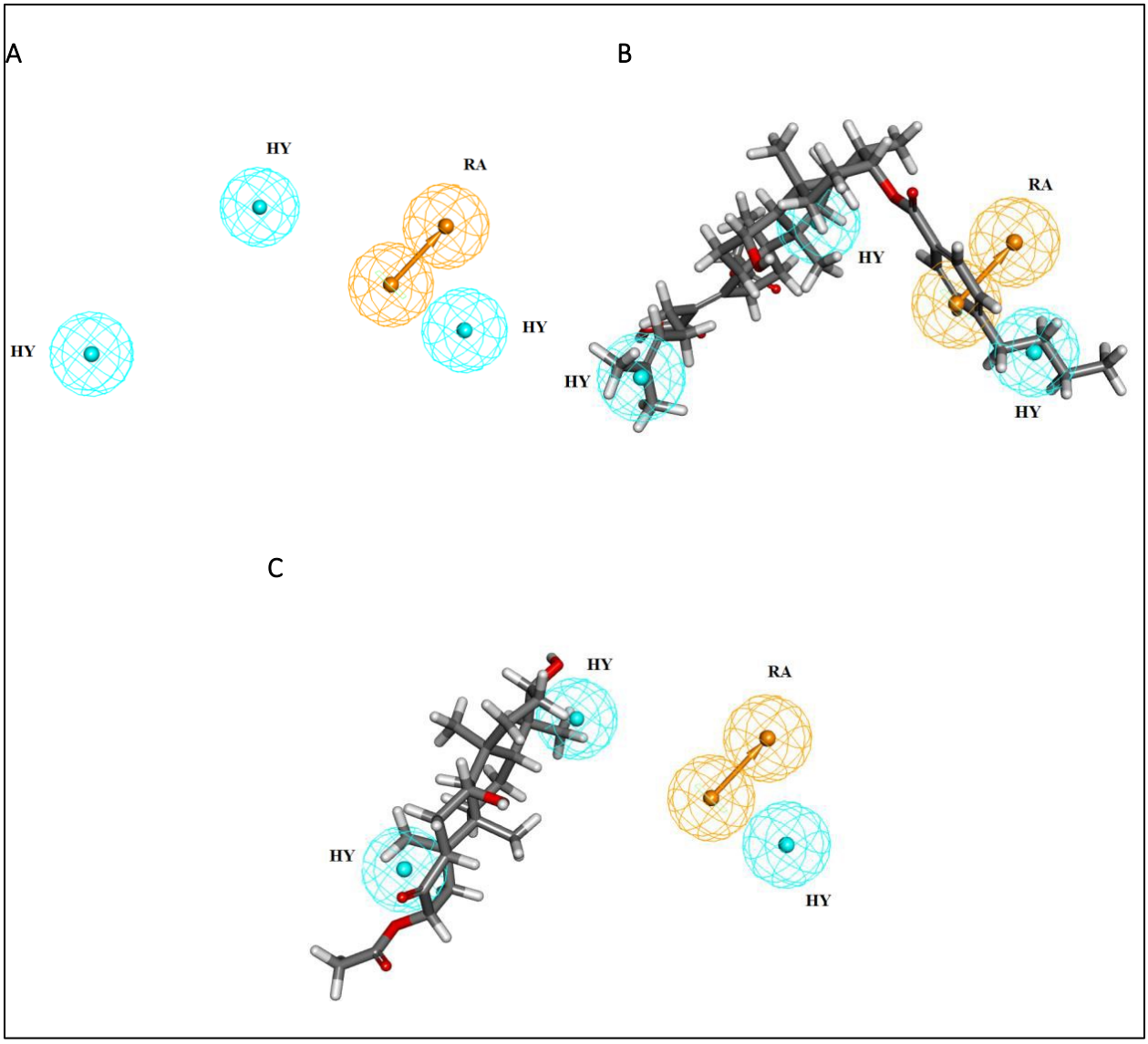

Figure 4.12: Pharmacophore models based on fusidic acid derivatives generated by HypoGen

A. The best HypoGen model, Hypo 2; **B.** Mapping of Hypo 2 with one of the most active compounds (IC_{50} = 390 nM) from the training set; **C.** Mapping of Hypo 2 with one of the least active compounds (IC_{50} = 91000 nM) from the training set; Pharmacophore features are color-coded: orange for ring aromatic (RA) and cyan for hydrophobic (HY).[38]

4.2 Research Program

4.2.1 Hypothesis

It is possible to identify new C-21 analogues of fusidic acid with superior antimycobacterial and multi-stage antiplasmodium activities through semi-synthesis towards expanding the structure-activity relationship (SAR) profile.

4.2.2 Main objective

To conduct SAR studies of fusidic acid amide derivatives **I–III** identified from 3-dimensional quantitative SAR (3D-QSAR) modeling studies.

4.2.3 Specific aims

- To synthesize anilide, *N*-benzyl amide, and 1-aryl and 1-alkyl ethanamide derivatives of fusidic acid as potential antimycobacterial and antiplasmodium agents.
- To evaluate the synthesized target compounds for *in vitro* antimycobacterial, antiplasmodium and cytotoxic activities

4.3 Design, Synthesis and characterization of fusidic acid derivatives

4.3.1 Design and Synthesis of C-21 derivatives

SAR studies based on the most active compound **I** were explored. Enantiomerically pure (*R* or *S*) and racemic *N*-aryl/alkyl ethanamines were employed. The aryl groups comprised phenyl, pyridyl, and pyrazinyl groups. The alkyl amines included both (*R*)- and (*S*)-*N*-cyclohexyl ethanamines. Anilide analogues of fusidic acid based on compound **II** were also explored. This included a 4-aminophenol analogue incorporating a Mannich base side chain. Lastly, derivatives based on the least active compound **III** were synthesized, the choice of benzyl amines used enabled exploration of which quadrant (in terms of substituents on the phenyl ring) of the Craig plot contributed the most to antiplasmodium activity.

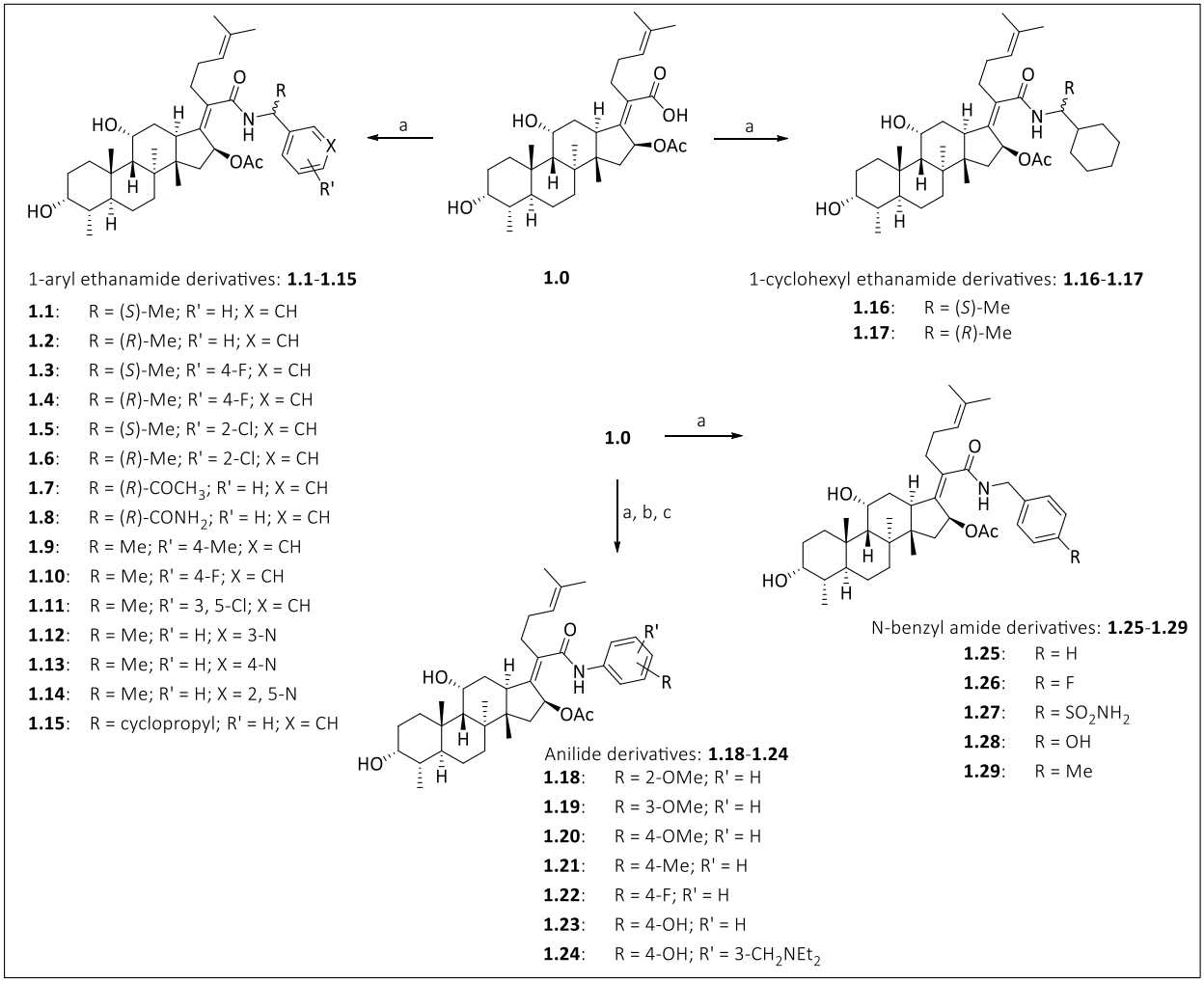

Scheme 4.1: Summary of fusidic acid derivatives. *Reagents and conditions*: (a) RNH_2, T3P (50% w/v solution in EtOAc), NEt_3, DCM, 35 ^oC, 5-24 h; (b) HATU, DCM, 30 ^oC, 2 h (for **1.23** and **1.24**); (c) RNH_2, KH_2PO_4, *n*-BuOH, 100 ^oC, 16-24 h (for **1.23** and **1.24**)

The synthetic route to arrive at the 1-aryl/alkyl ethanamides (**1.1**-**1.17**), anilides (**1.18**-**1.24**) and *N*-benzyl amides (**1.25**-**1.29**) of fusidic acid is outlined in Scheme 4.1. Synthesis of the 4-hydroxyaniline Mannich base is described in Scheme 4.2.

In Scheme 4.1 (a), the C-21 amide derivatives were obtained by heating commercially sourced fusidic acid (**1.0**) and the respective amines in DCM in the presence of triethylamine (NEt_3) as base and propylphosphonic anhydride (T3P®) as a coupling reagent. The amide coupling reactions proceeded to completion in a time range of 5-24 hours depending on the amine used. Aqueous work-up to get rid of the reaction by-products afforded the crude organic residue, which upon

further purification by normal phase silica preparative TLC gave the compounds in low to high yield (10-70%). Pure (*R*)- and (*S*)-fusidic acid ethanamide derivatives were obtained from the corresponding amines. The racemic ethanamines afforded fusidic acid diastereomers (**1.9**-**1.14**) in a 1:1 to 3:2 ratio, except **1.5** and **1.6** which were well separated and hence were isolated in their pure forms.

The fusidic acid derivative incorporating a phenolic Mannich base moiety (**1.24**) was obtained in two steps (Scheme 4.1 (b and c) and 4.2). The first step was the reaction between fusidic acid and the coupling agent HATU to obtain intermediate **6.0** (Scheme 4.2). After purification, **6.0** was then subjected to a nucleophilic substitution reaction by heating with **5.0** in the presence of KH_2PO_4 as base and *n*-BuOH as solvent. The derivative **1.23** was also obtained in a similar manner. It is noteworthy that all attempts to obtain **1.23** and **1.24** in a one-pot reaction involving fusidic acid, the amine and the coupling reagent (EDCI, T3P or HATU), exploring different reaction conditions, neither afforded the desired product nor any product at all.

Synthesis of the 4-aminophenolic Mannich base was accomplished in three steps (Section 4.2). The first step involved protection of the amine group as the acetamide (**3.0**) in the presence of acetic anhydride in THF at 60 ^{o}C. The 4-hydroxy acetamide intermediate then underwent a Mannich condensation reaction by heating in EtOH in the presence of formaldehyde and diethylamine to afford compound **4.0**. The last step was the deacetylation of **4.0** under acidic conditions to obtain the desired phenolic Mannich base amine (**5.0**).

Progress of the reactions was monitored by normal phase silica TLC and reversed phase C18 LCMS. The synthesized compounds were fully characterized by their TLC retardation factor (*R*f) values in appropriate solvents, reversed phase C18 LC retention time (t_R), mass spectrometry and 1D NMR spectroscopic data. Where necessary, 2D NMR spectroscopic data was acquired to enable correct assignment of NMR signals.

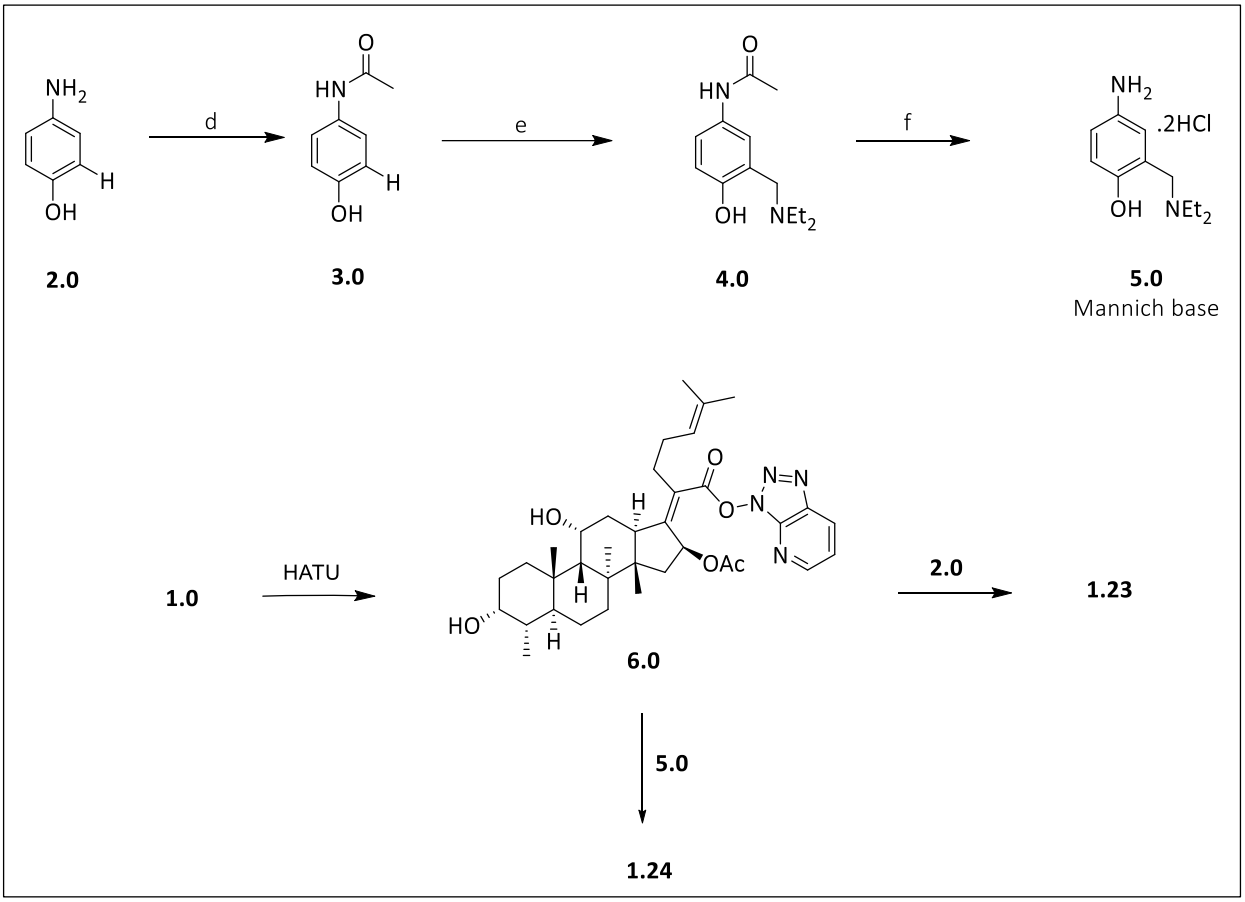

Scheme 4.2: Synthesis of 1.23 and 1.24. *Reagents and conditions*: (d) $(CH_3CO)_2O$, THF, 60 ^oC, 1 h; (e) HCHO, $NHEt_2$, EtOH, 85 ^oC, 2 h; (f) 6N HCl, 100 ^oC, 2 h

4.3.1.1 Mechanism of T3P-mediated amide coupling

Propylphosphonic anhydride (T3P®) is a highly reactive *n*-propyl phosphonic acid cyclic anhydride. It is generally employed as a coupling agent and also for scavenging water in reactions. With low toxicity and low allergenic effects, T3P tolerates a broad range of functional groups and reduces the possibility of epimerization in reactions such as peptide synthesis. The by-products of T3P are water-soluble, thus offering an easy means of reaction work-up. T3P reactions proceed under mild reaction conditions. Apart from its common use in amide coupling, other T3P-mediated reactions have been reported including formation of nitriles from carboxylic acids and amides, formation of Weinreb amides, synthesis of esters, dehydration reactions, oxidation of alcohols, synthesis of isonitriles, conversion of alcohols to alkenes, C-C coupling reactions, and so on.[47]

The T3P-mediated amide coupling reaction proceeds in the presence of a base. The base abstracts a proton from the carboxylic acid group to form the carboxylate ion (Figure 4.13). The anion attacks T3P at one of the phosphorus atoms leading to ring opening and conjugation to the carboxylic acid scaffold. The amine attacks the now activated carboxylic acid-derived intermediate. Subsequent deprotonation of the amide cation by a second equivalence of the base affords the neutral amide desired compound.

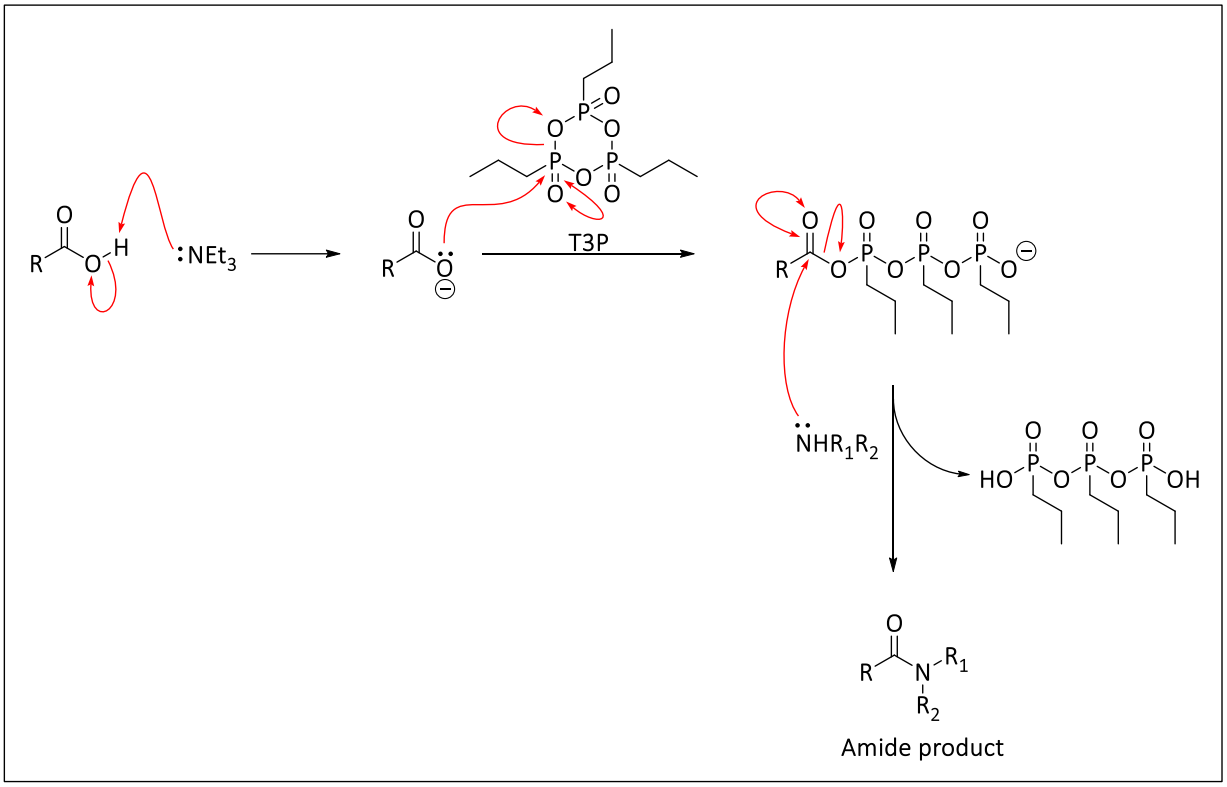

Figure 4.13: Mechanism of T3P-mediated amide coupling[48]

4.3.1.2 Mechanism of HATU-mediated amide coupling

Hexafluorophosphate Azabenzotriazole Tetramethyl Uronium (HATU) is a reagent used to generate an active ester form of a carboxylic acid. The reagent has been employed in peptide coupling reactions. HATU can exist as either the uranium salt (*O* form) or the less reactive iminium salt (*N* form) (Figure 4.14a).[49] Typical HATU reactions proceed in two steps: firstly, formation of the carboxylic acid-HATU intermediate, and secondly, addition of the hydroxyl or amino nucleophile to afford the desired acylated product.

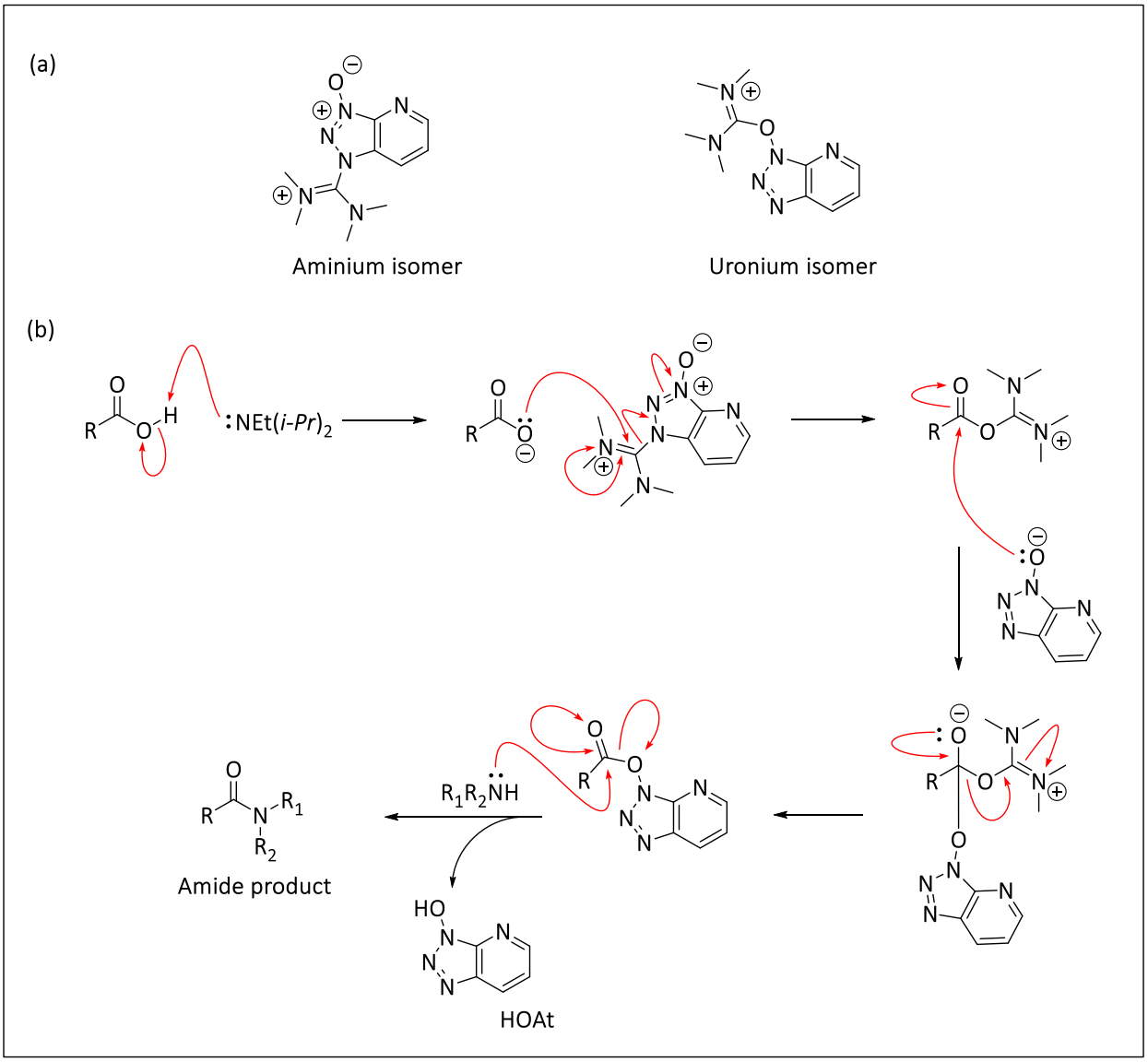

Figure 4.14: HATU-assisted formation of amide[49,50]

The mechanism of HATU assisted coupling reactions begins with deprotonation of the carboxylic acid by a base (usually diisopropyl ethylamine, DIPEA). The carboxylate ion then attacks HATU to form the *O*-acyl(tetramethyl)isouronium salt (Figure 4.14b).[50] The isouronium salt is rapidly attacked by the 1-hydroxy-7-azabenzotriazole anion ($^{-}$OAt) to form a more stable intermediate. The activated acyl-OAt ester is finally converted to the desired ester or amide product in the presence of the alcohol or amine, thereby releasing HOAt as a by-product.

4.3.1.3 Mechanism of phenolic Mannich reaction

The Mannich reaction is a multi-component condensation of a nonenolizable aldehyde, a primary or secondary amine and an enolizalible carbonyl compound to afford an aminomethylated/β-amino carbonyl compound known as a Mannich base.[51] Nucleophilic addition of the amine to the nonenolizable carbonyl group is followed by dehydration to form a Schiff base (Figure 4.15). Electrophilic addition of the Schiff base to the enol affords the desired condensation product.

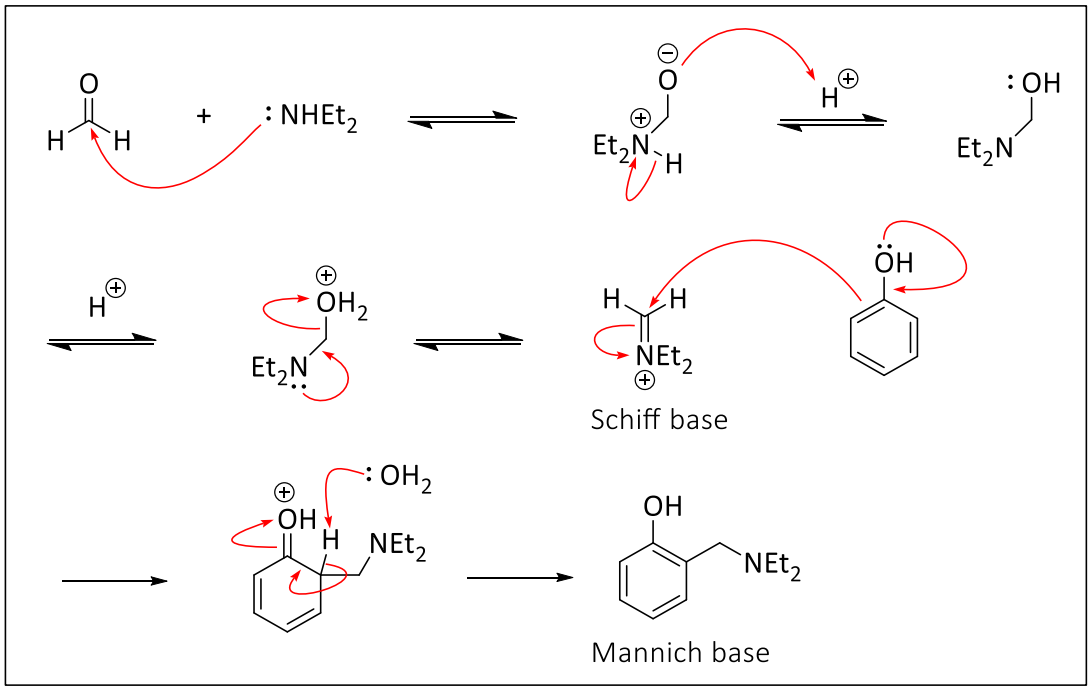

Figure 4.15: Mechanism of Mannich reaction[52]

4.3.2 Characterization of C-21 derivatives

Twenty-nine C-21 fusidic acid derivatives were synthesized in total comprising 17 1-aryl and alkyl ethanamides, 7 anilides and 5 *N*-benzyl amides (Scheme 4.1). The synthesized fusidic acid derivatives were characterized using their 1D NMR spectroscopic and mass spectrometric data. The 1D NMR signals were assigned by comparison with those of fusidic acid. The target compounds were confirmed by assignment of the new signals due to the amine moiety incorporated.

The ^{1}H and ^{13}C NMR data acquired for fusidic acid was in agreement with previously reported data.[53] Evidence of the tetracyclic triterpenoid backbone was observed by the presence of several overlapping multiplets in the methylene envelope (δ_H 1.0 - 2.6 ppm) of the ^{1}H NMR spectrum. The methyl groups resonated at δ_H 0.91 – 0.93 (m, H_3-18 and H_3-28), 0.98 (s, H_3-19), 1.38 (s, H_3-30), 1.60 (s, H_3-26), 1.67 (s, H_3-27) and 1.97 (s, OAc). The oxymethine protons, H-3, H-11 and H-16, occurred at δ_H 3.76, 4.35 and 5.89 ppm, respectively, while the signals at δ_H 3.06 and 5.10 ppm were assigned to H-13 and H-24 methine protons, respectively (Figure 4.16).

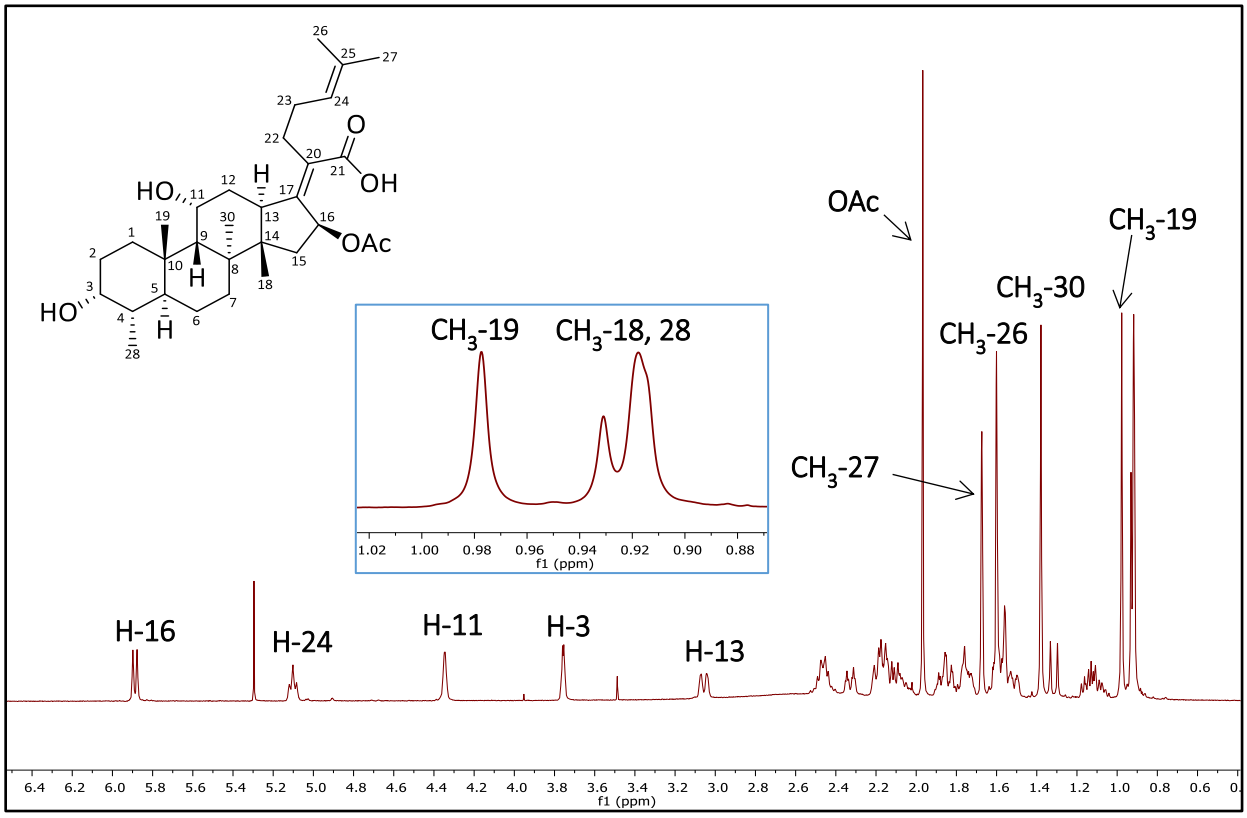

Figure 4.16: ^{1}H NMR ($CDCl_3$, 400 MHz) spectrum of fusidic acid

The ^{13}C NMR spectrum showed 31 signals including two carbonyl peaks for the acetate group (δ_C 170.5) and the carboxylic acid carbonyl carbon (δ_C 173.2). The four olefinic carbons, C-17, C-20, C-24 and C-25, resonated at δ_C 150.9, 129.4, 123.0 and 132.6 ppm, respectively. Signals due to the three C-O chemical environments of C-3, C-11 and C-16 occurred at δ_C 71.4, 68.2 and 74.4, respectively. Moreover, all other signals due to the un-functionalized carbon atoms were observed upfield between δ_C 10.0 – 50.0 ppm (Figure 4.17).

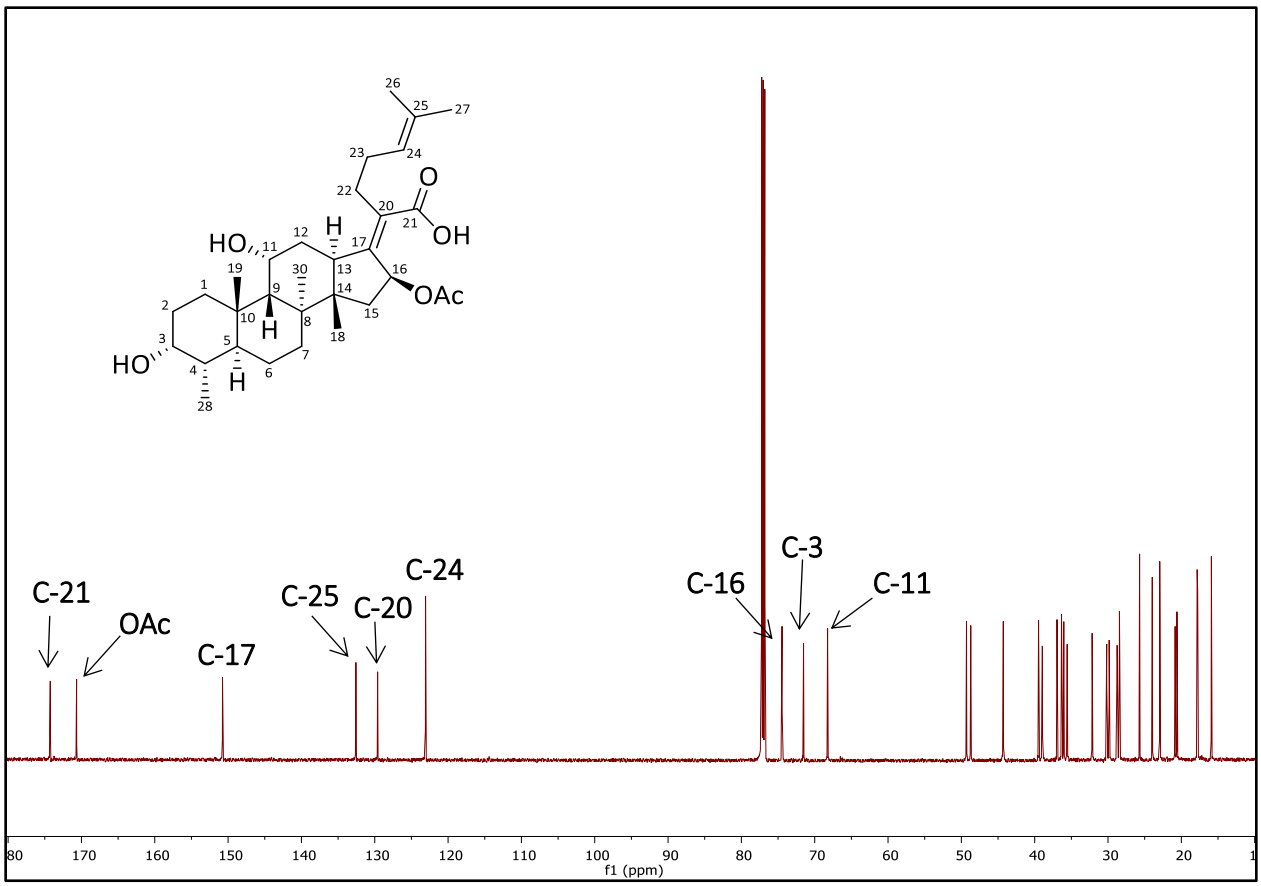

Figure 4.17: ^{13}C NMR ($CDCl_3$, 101 MHz) spectrum of fusidic acid

4.3.2.1 Characterization of 1-aryl and 1-alkyl ethanamides

Apart from **1.16** and **1.17**, all the ethanamide derivatives showed new olefinic proton and carbon signals in their NMR spectra due to the aromatic amine moiety incorporated. The structures of the synthesized compounds were also confirmed by the presence of a new methine proton (δ_H ≈5.0 for the aryl derivatives and δ_H ≈3.7 for the alkyl derivatives). Furthermore, a new methyl doublet was observed at δ_H ≈1.4 ppm for the aryl derivatives and δ_H ≈1.0 ppm for the alkyl derivatives **1.16** and **1.17**. Characterization of the 1D NMR data of **1.1** is described below (Figure 4.18 and 4.19).

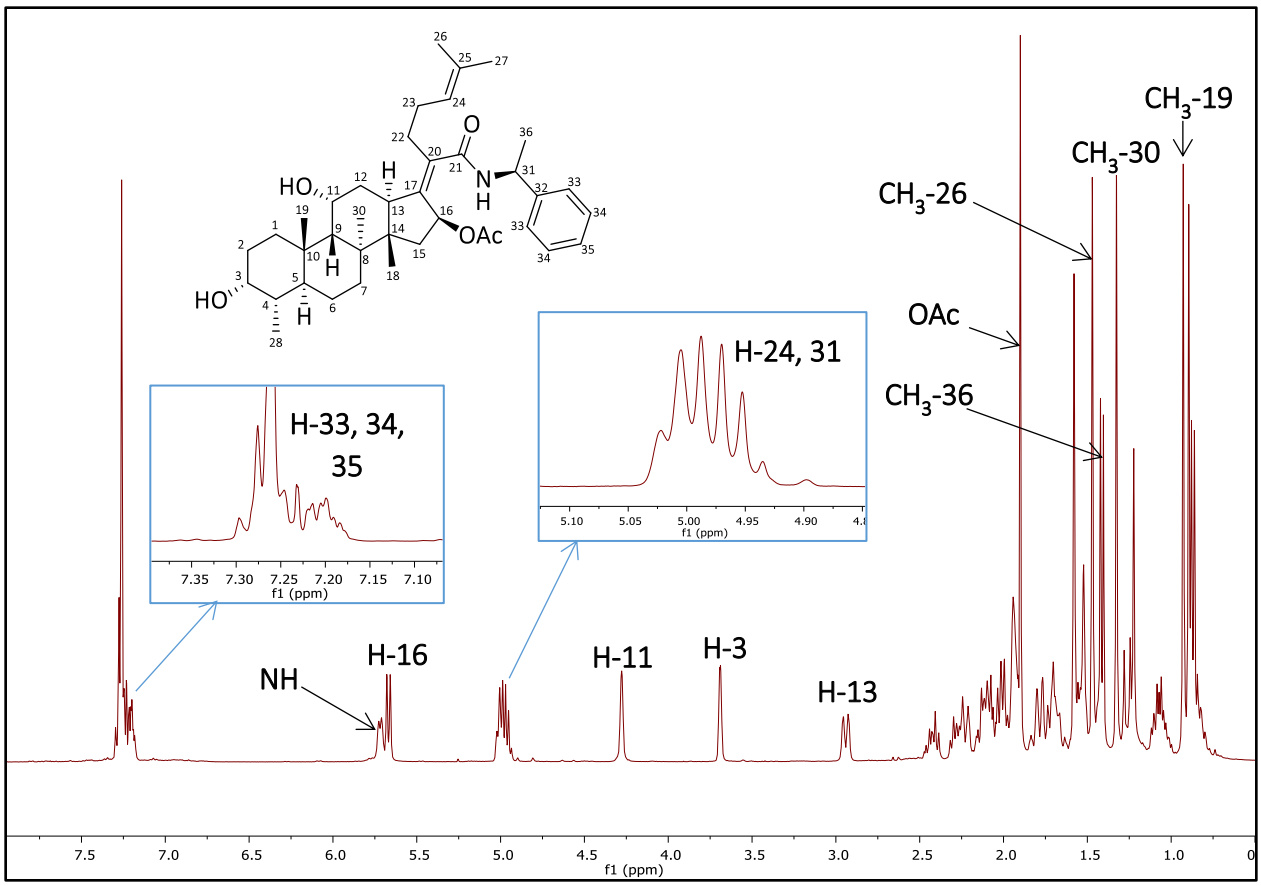

Figure 4.18: ^{1}H NMR ($CDCl_3$, 400 MHz) spectrum of **1.1**

The 1D NMR data of **1.1** were in congruence with fusidic acid (Figure 4.18 and 4.19). Its formation was confirmed by the presence of the doublet at δ_H 1.41 (d, *J* = 6.9 Hz, H_3-36), 5.00 - 4.93 (m, H-31), 5.72 (d, *J* = 7.5 Hz, NH), and overlapping multiplets in the chemical shift range δ_H 7.16 – 7.30 ppm for the five aromatic protons (H-33 – H-35). Formation of the amide bond was corroborated by the shift of C-21 more upfield to δ_C 170.9 (Figure 4.19). Similarly, C-17 shifted to δ_C 143.3 and C-20 occurred more downfield at δ_C 135.9 ppm. Four additional olefinic signals attributable to the phenyl ring at δ_C 126.2 (X2), 127.4, 128.70 (X2) and 141.2 ppm were observed. An extra signal at δ_C 77.3 due to the aminomethine carbon C-31 was also observed. All 39 carbon signals for **1.1** were therefore fully accounted for.

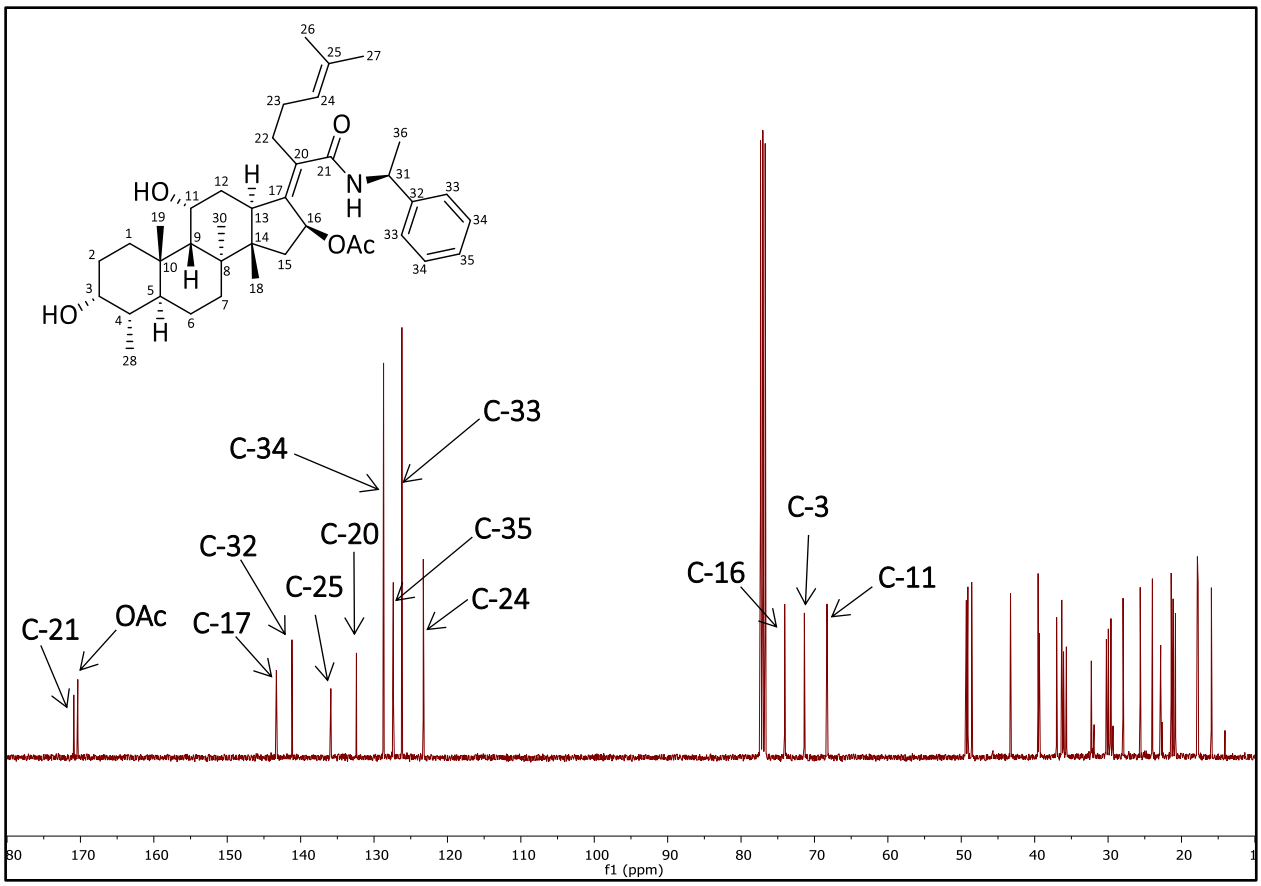

Figure 4.19: ^{13}C NMR ($CDCl_3$, 101 MHz) spectrum of **1.1**

It is noteworthy that all fluorinated analogues exhibited characteristic coupling patterns in their ^{1}H NMR and ^{13}C NMR spectra, specifically within the aromatic moiety, due to the fluorine atom. This is exemplified in the 1D NMR spectra of the fusidic acid ethanamide **1.3** (Figure 4.20 and 4.21). Contrary to the ^{1}H NMR spectrum of the other *para* substituted congeners, wherein the aromatic protons were split into doublets as a result of *ortho* coupling, the aromatic protons of compound **1.3** exhibited splitting patterns as a result of firstly, *ortho* coupling between H-33 and H-34 and, secondly, further *meta* and *ortho* couplings between the fluorine atom and H-33 and H-34, respectively (Figure 4.20). Consequently, H-34 (δ_H = 7.01) was observed as a triplet due to the two equal *ortho* coupling constant values (J = 8 - 10 Hz). Meanwhile, the aromatic carbons of the benzyl moiety were each split into a doublet (Figure 4.21). As a result, the C-33 (X2) and C-34 (X2) signals were not twice as intense as the other carbon signals, as observed in the ^{13}C NMR spectra of the analogues bearing symmetrical phenyl or benzyl moieties.

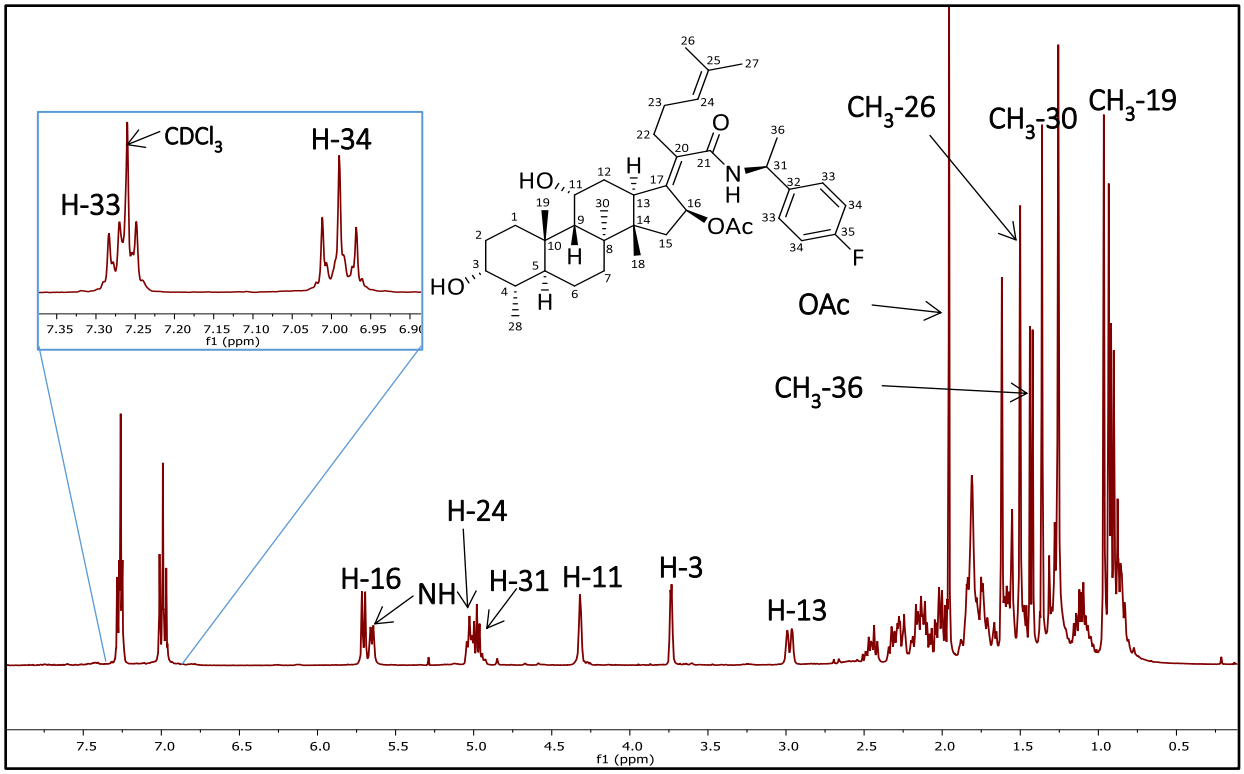

Figure 4.20: ^{1}H NMR ($CDCl_3$, 400 MHz) spectrum of **1.3**

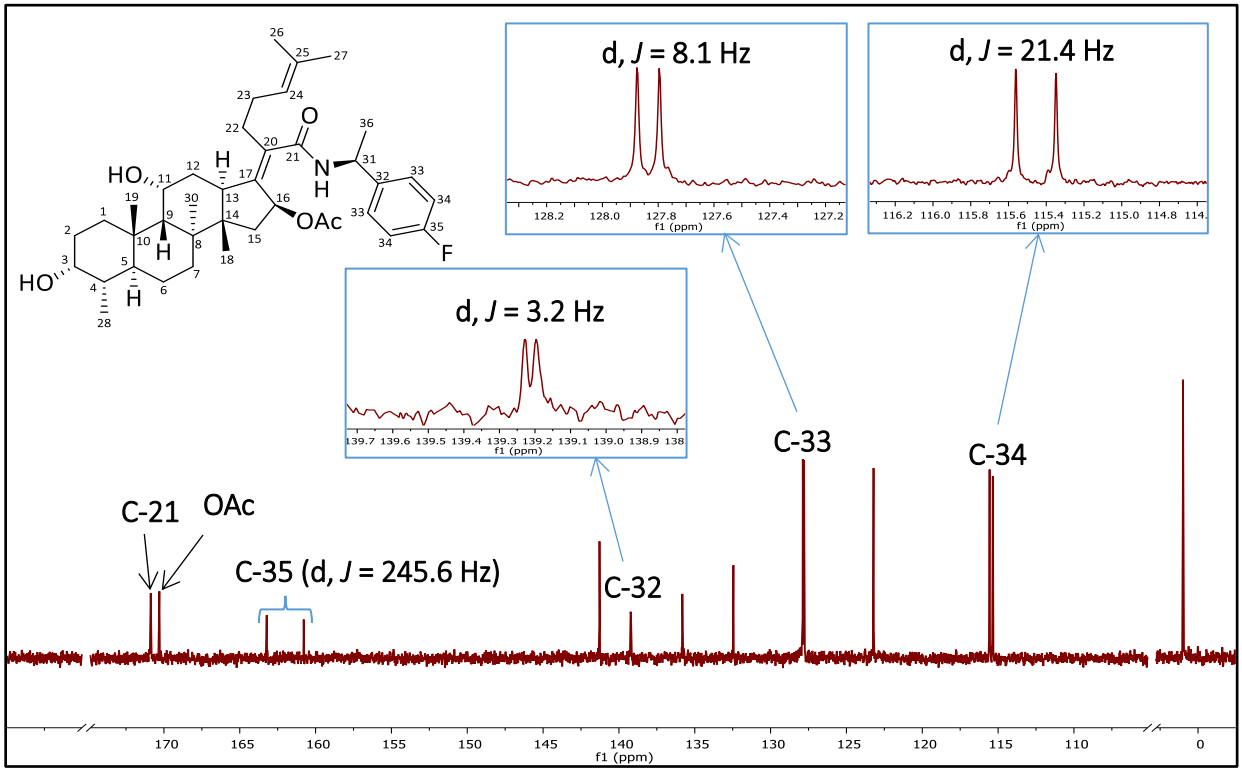

Figure 4.21: The olefinic region of the ^{13}C NMR ($CDCl_3$, 101 MHz) spectrum of **1.3**

4.3.2.2 Characterization of anilides

The ^{1}H and ^{13}C NMR spectroscopic data obtained for **1.23** were in agreement with **1.0**. The aromatic protons H-32 and H-33 occurred as doublets at δ_H 7.37 (d, J = 8.6 Hz, H-32) and δ_H 6.74 (d, J = 8.6 Hz, H-33), integrating for two protons each. The acetoxy methyl singlet resonated at δ_H 1.73 ppm (Figure 4.22). The amide carbonyl carbon was observed at δ_C 172.6 while the acetoxy carbonyl occurred at δ_C 172.3 in the ^{13}C NMR spectrum. Furthermore, **1.23** exhibited extra carbon signals in the olefinic region due to the presence of the symmetrical 4-hydroxyphenyl amide moiety (Figure 4.23). The signals of C-3, C-11 and C-16 were discernible at δ_C 72.4, 68.6 and 75.5, respectively. All other carbon signals occurred upfield in the range of δ_C 10.0 – 50.0 ppm, just like fusidic acid.

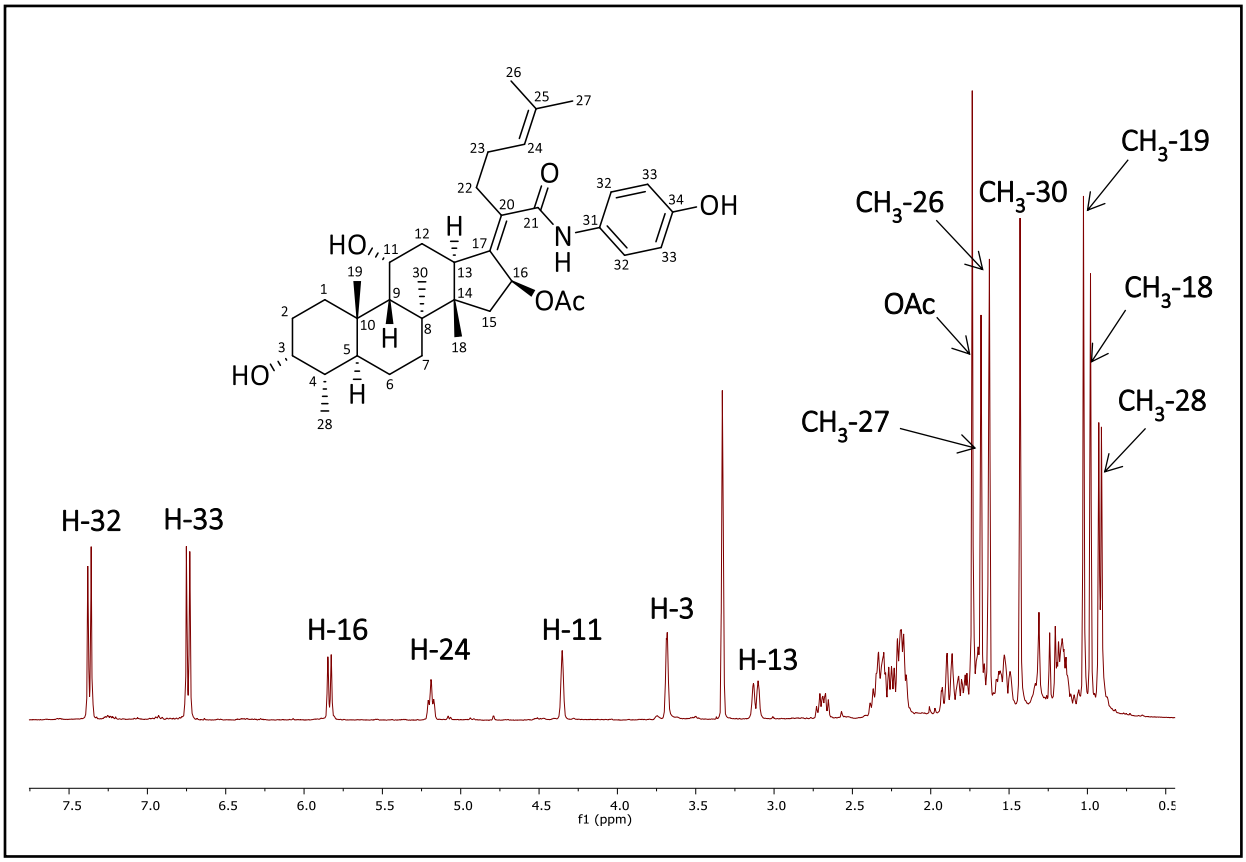

Figure 4.22: ^{1}H NMR (MeOH-d_4, 400 MHz) spectrum of **1.23**

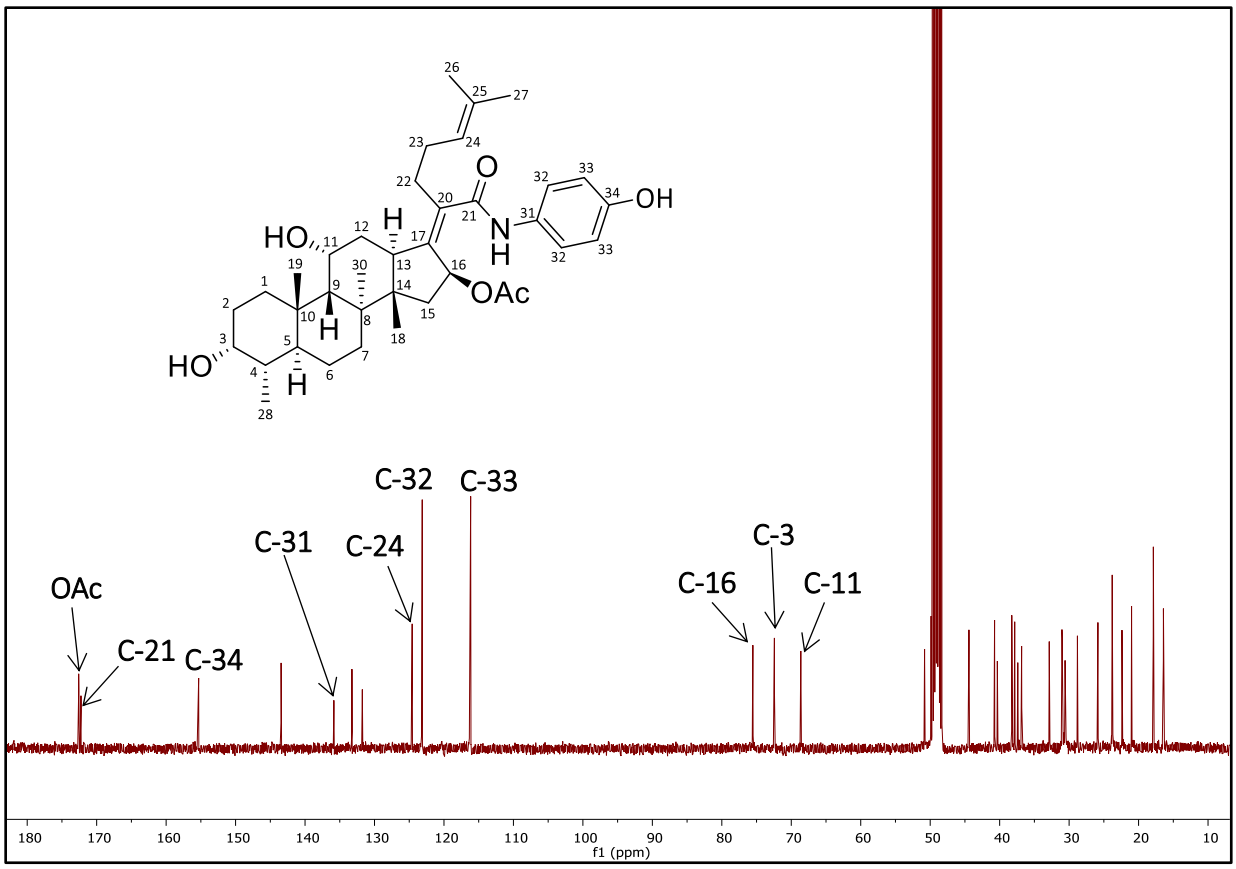

Figure 4.23: ^{13}C NMR (MeOH-d_4, 101 MHz) spectrum of **1.23**

Compound **1.24** exhibited three aromatic proton signals with the coupling pattern characteristic of a 1,3,4-trisubstituted phenyl ring in its ^{1}H NMR spectrum. The methine proton H-36 resonated at δ_H 7.29 (dd, *J* = 2.7, 8.6 Hz), the coupling constants supported a *meta* coupling to H-32 (δ_H 7.33, d, *J* = 2.6 Hz) and an *ortho* coupling to H-35 (δ_H 6.69, d, *J* = 8.5 Hz). Signals confirming the presence of the Mannich base side chain occurred at δ_H 3.86 (s, H_2-37), 2.75 (q, *J* = 7.1 Hz, 4H, 2×H_2-38), and 1.16 (t, *J* = 7.1 Hz, 6H, 2×H_3-39) which integrated for two, four, and six protons, respectively. All other proton signals were in agreement with fusidic acid (Figure 4.24). Figure 4.25 is the stacked ^{1}H NMR spectrum comparing **1.23** and **1.24**. Differences in the two spectra are observed in the aromatic protons signifying the change in splitting pattern of **1.24** compared to **1.23** as a result of substitution of the diethylaminomethyl side chain. Moreover, signals arising from the protons of the Mannich base side chain of **1.24** are discernible compared to **1.23**.

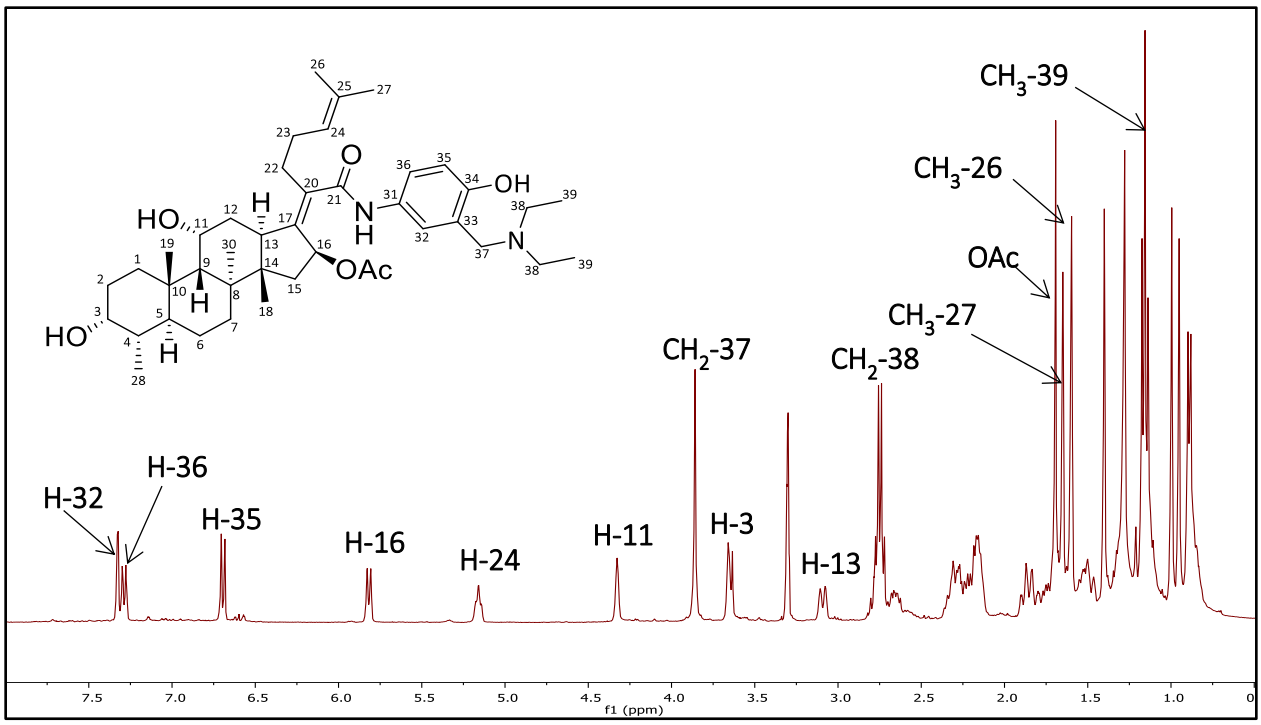

Figure 4.24: ^{1}H NMR (MeOH-d_4, 400 MHz) spectrum of **1.24**

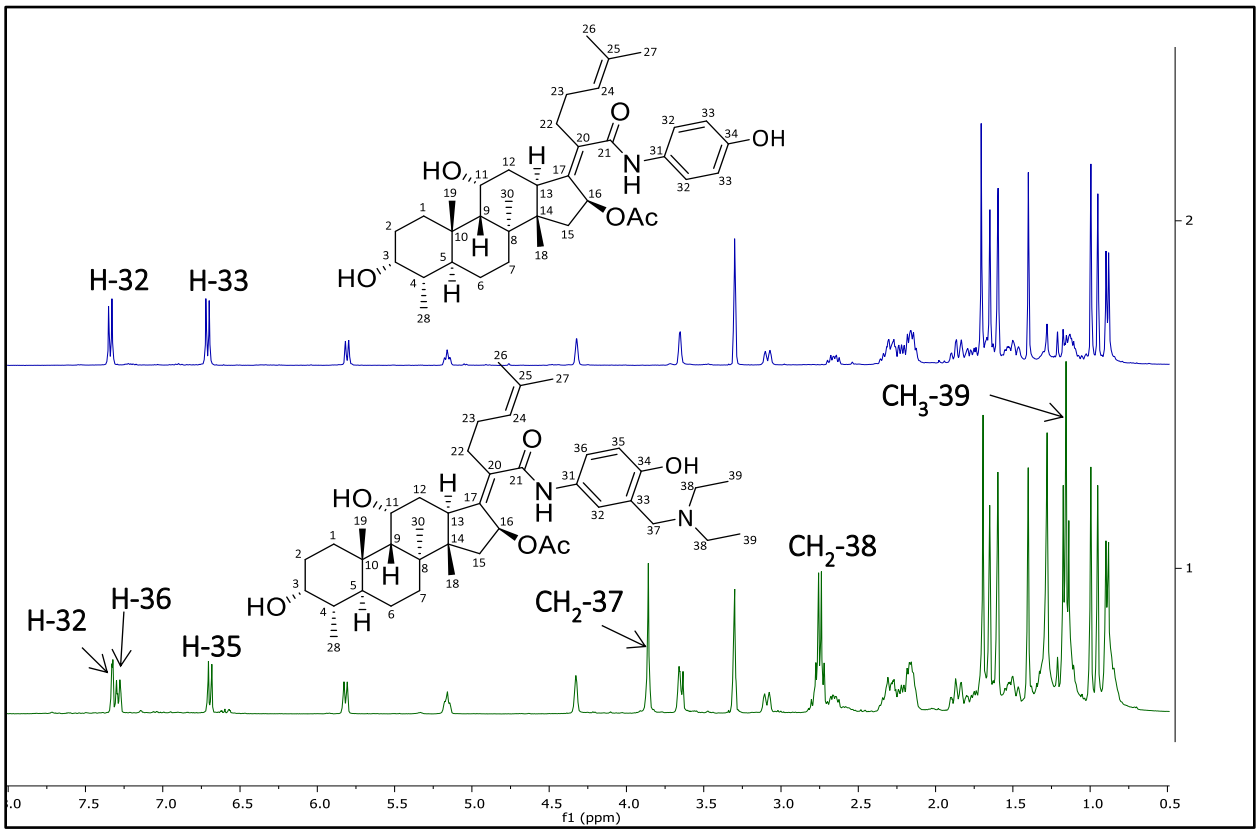

Figure 4.25: Stacked ^{1}H NMR (MeOH-d_4, 400 MHz) spectrum of **1.23** and **1.24**

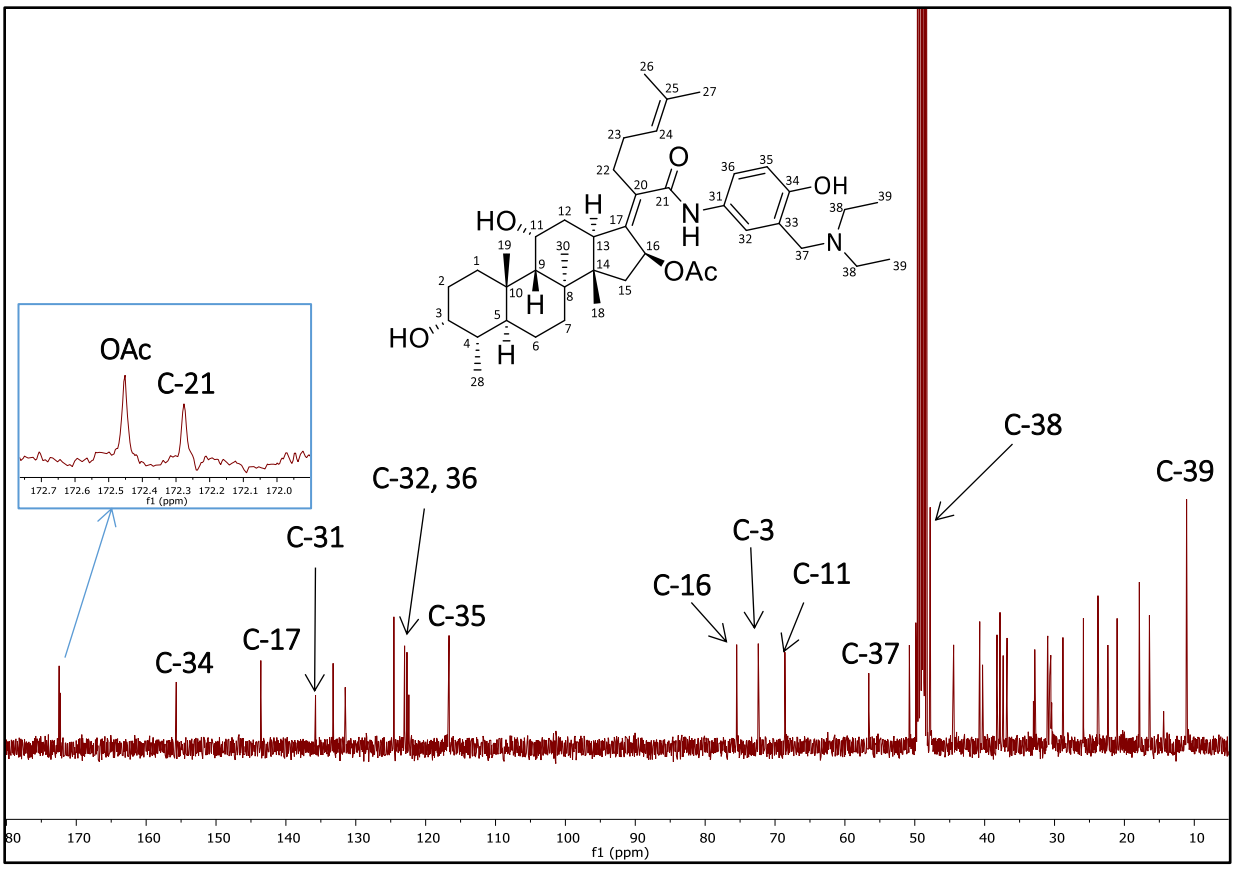

Figure 4.26: ^{13}C NMR (MeOH-d_4, 101 MHz) spectrum of **1.24**

The ^{13}C NMR spectrum of **1.24** exhibited 40 signals including 6 extra olefinic signals corresponding to the phenyl group. Signals due to the Mannich base side chain were observed at δ_C 56.6 (C-37), 47.8 (C-38) and 11.1 (C-39). The two carbonyl carbons occurred at δ_C 172.5 and 172.3, similar to **1.23** for the presence of the anilide moiety (Figure 4.26).

4.3.2.3 Characterization of N-benzyl amides

The *N*-benzyl amides exhibited comparable 1D NMR spectra. The presence of the benzylic protons was observed as two separate doublet signals, integrating for one proton each in the ^{1}H NMR spectrum, signifying that the methylene protons resonated as diastereotopic protons (H-31a and H-31b). The ^{1}H NMR spectrum of **1.28** is shown in Figure 4.26. All proton signals were congruent with fusidic acid (**1.0**). The benzylic methylene protons were observed at δ_H 4.15 (d, J = 14.3 Hz, H_2-31a) and δ_H 4.37 (d, J = 14.3 Hz, H_2-31b). The strong geminal (^2J) coupling between these

protons is accounted for by the large coupling constant (J = 14.3 Hz). The aromatic protons were observed at δ_H 7.11 (d, J = 8.5 Hz, 2H, 2×H-33) and 6.70 (d, J = 8.5, 2H, 2×H-34) (Figure 4.27).

The ^{13}C NMR spectrum (Figure 4.28) of **1.28** exhibited 36 signals, the signals at δ_C 116.4 (C-34) and 130.4 (C-33) integrating for two carbons each as a result of the symmetrical disubstituted benzyl moiety. The amide carbonyl carbon resonated at δ_C 174.0 while the acetoxy carbonyl was observed at δ_C 172.5 ppm. The four additional olefinic signals of the phenyl ring, assigned to C-32, C-33, C-34 and C-35, were observed at δ_C 135.7, 130.4 (X2), 116.4 (X2), and 158.0, respectively.

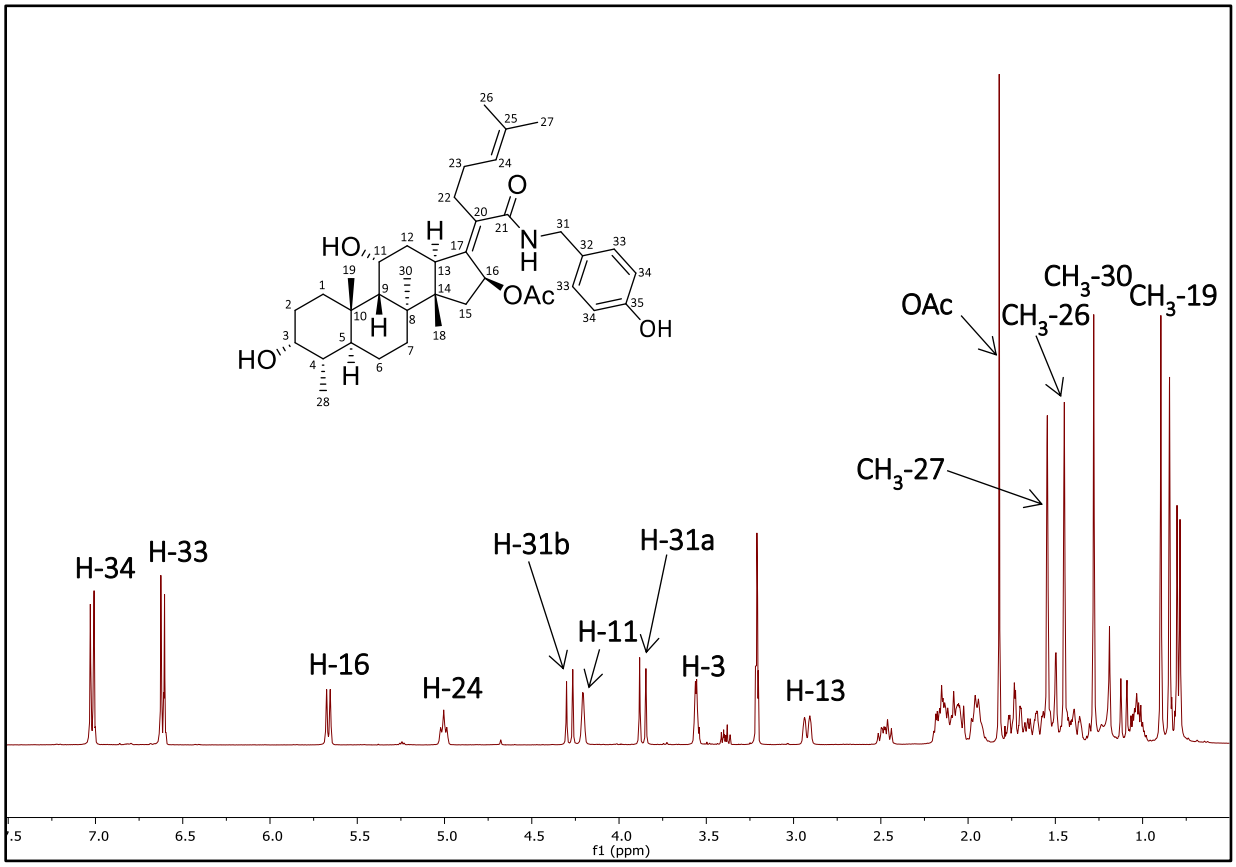

Figure 4.27: ^{1}H NMR (MeOH-d_4, 400 MHz) spectrum of **1.28**

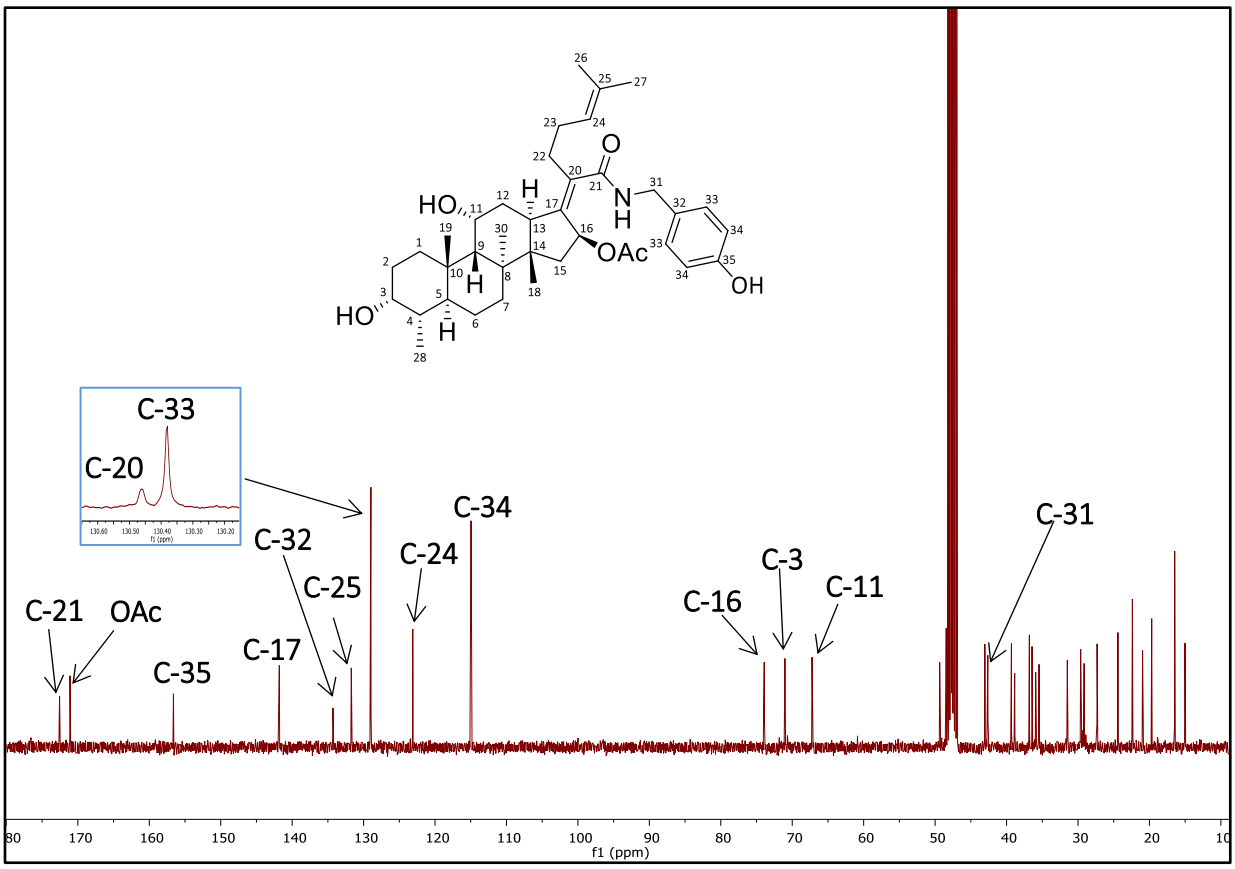

Figure 4.28: ^{13}C NMR (MeOH-d_4, 101 MHz) spectrum of **1.28**

4.4 Biological results and discussion

4.4.1 Antimycobacterial activity

In vitro antimycobacterial activity evaluation of all the synthesized analogues were carried out on the H_{37}Rv strain of *Mtb* by the TB Biology group of the UCT Drug Discovery and Development Centre, H3D, based at the Institute of Infectious Diseases and Molecular Medicine (IDM), University of Cape Town, South Africa. Two media were employed, namely 7H9 GLU ADC TW (Middlebrook 7H9 media enriched with albumin-dextrose-catalase (ADC) and supplemented with 0.4% Glucose and 0.05% Tween 80) and 7H9 GLU CAS TX (Middlebrook 7H9 media supplemented with 0.03% Casitone, 0.4% Glucose and 0.05% Tyloxpol). The former is a protein-based media containing the serum protein albumin, which is known to bind to drugs in the blood. However, the 7H9 GLU CAS TX is a non-protein-based media. The activity was evaluated at MIC_{90} (minimum concentration required to inhibit the growth of 90% of the bacterial population), using rifampicin

as the reference drug. The synthesized compounds were tested at a maximum concentration limit set at 125 µM.

Table 4.2: *In vitro* antimycobacterial ($H_{37}Rv$ strain) and cytotoxic (CHO cell line) activities of the fusidic acid amide analogues

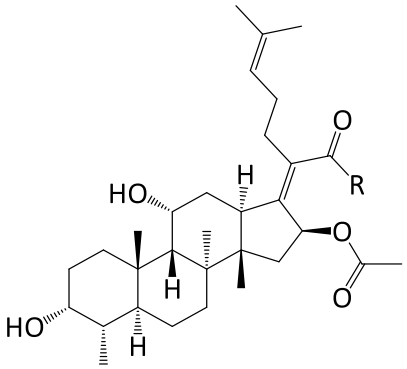

Compound	R	Antimycobacterial activity, $H_{37}Rv$, MIC_{90} (µM)		Cytotoxicity, IC_{50} (µM)
		7H9 GLU ADC TW	7H9 GLU CAS TX	CHO
1.1	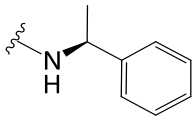	>125	8.90	45.95
1.2	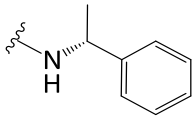	>125	11.00	47.61
1.3	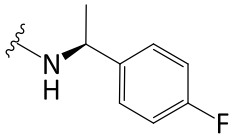	>125	7.59	47.40
1.4	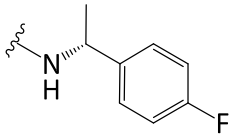	>125	>125	8.24
1.5	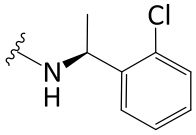	41.52	9.80	45.15

1.6	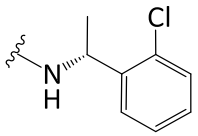	>125	10.10	18.16
1.7/	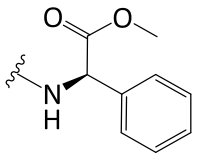	38.83	7.10	42.88
1.8	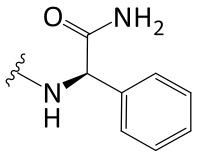	15.73	9.10	>50
1.9	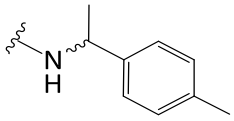	>125	2.91	47.90
1.10	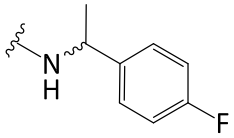	>125	19.82	45.30
1.11	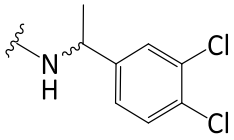	32.26	7.20	>50
1.12	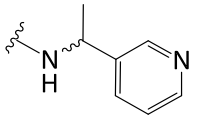	>125	17.87	>50
1.13	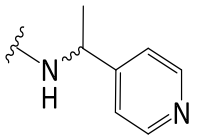	125	13.03	>50
1.14	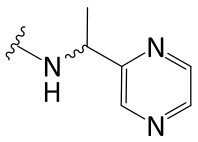	62.5	17.49	>50

1.15	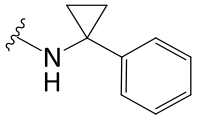	>125	13.90	36.84
1.16	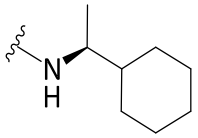	>125	4.50	44.69
1.17	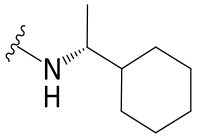	>125	7.45	>50
1.18	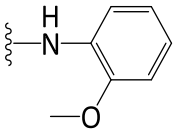	43.21	6.20	46.13
1.19	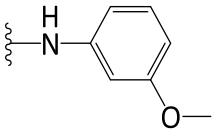	>125	>125	42.68
1.20	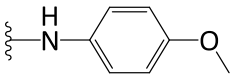	>125	>125	47.12
1.21	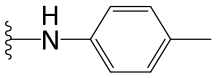	125	>125	>50
1.22	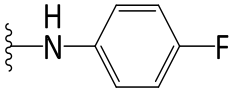	125	125	39.90
1.23	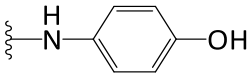	>125	6.90	45.39
1.24	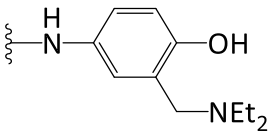	10.35	0.40	8.69

1.25	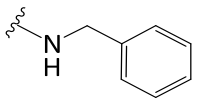	125	>125	44.10
1.26	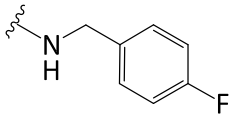	125	>125	40.20
1.27	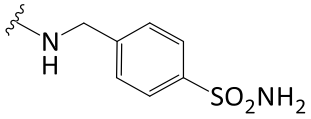	62.27	2.71	30.20
1.28	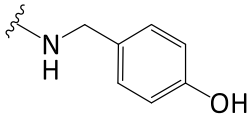	125	125	>50
1.29	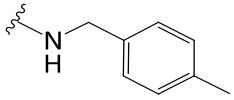	125	>125	>50
Rifampicin		0.009	0.02	
Emetine				0.02

To enable analysis of their SAR, all compounds with MIC_{90} ≤10 µM were regarded as active; those with MIC_{90} ranging from 10 – 20 µM had moderate activity; MIC_{90} = 20 – 125 µM denoted as poorly active; whereas compounds exhibiting MIC_{90} >125 µM were considered inactive. The SAR of the compounds are discussed within their chemical classes as ethanamides, anilides and benzyl amides.

In this regard, the fusidic acid ethanamide analogues were either poorly active or inactive in the protein-based 7H9/ADC media, except compound **1.8** which showed moderate activity (MIC_{90} = 15.73 µM). The poor activity could be attributed to binding to albumin since all the analogues (except **1.4**) showed improved potency in the non-protein-based media. In general, analogues with polar groups and/or substituents in close proximity to the amide bond showed inhibitory activity in the 7H9/ADC media, suggesting they were less bound to albumin. This is particularly exemplified

in the activities of **1.7**, **1.8**, **1.11** and **1.14**, which displayed MIC_{90} values of 38.83, 15.73, 32.26, and 62.5 µM, respectively (Table 4.2).

The enantiomerically pure fusidic acid ethanamide analogues exhibited comparable activity (MIC_{90} = 7 - 12 µM) in the 7H9/CAS media, except compound **1.4** which was inactive. Generally, the *S*-enantiomers were more potent than the *R*-enantiomers. The cyclohexyl congener **1.16** was the most potent analogue amongst the chiral fusidic acid ethanamides in the 7H9/CAS media, exhibiting about 2-fold better activity (MIC_{90} = 4.50 µM). Meanwhile, all diastereomeric ethanamide analogues exhibited moderate activity ((MIC_{90} = 13 - 20 µM), except compounds **1.9** (MIC_{90} = 2.91 µM) and **1.11** (MIC_{90} = 7.20 µM). The 4-pyridinyl analogue **1.13** was the most active (MIC_{90} = 13.03 µM) analogue amongst the nitrogen heterocyclic benzyl ethanamide fusidic acid analogues. The 3-pyridinyl and the 2,5-pyrazinyl congeners exhibited comparable activity (MIC_{90} ~17 µM).

Amongst the fusidic acid anilide analogues, it was observed that substitution at the *ortho* position favored activity in both the 7H9/ADC and 7H9/CAS media. This is exemplified by comparison of the activities of the three methoxy-substituted anilide regioisomers **1.18**, **1.19** and **1.20** (Table 4.2). Compound **1.18** with the methoxy group *ortho* to the amide bond displayed good activity (MIC_{90} = 6.20 µM) in the non-protein-based media but poor activity (MIC_{90} = 43.21 µM) in the protein-based media. However, the *meta*- and *para*-substituted congeners were not potent in both media. Similarly, compounds **1.21** and **1.22**, which bear lipophilic electron-releasing and electron-withdrawing groups, respectively, were equally inactive in both media. Meanwhile, it was observed that activity in the 7H9/CAS media was restored if the *para* position bears a hydrophilic electron-donating group capable of forming hydrogen bonds, as exemplified by **1.23** (MIC_{90} = 6.90 µM). Compound **1.24**, which bear the Mannich base side chain, was the most active of all the synthesized fusidic acid analogues. It exhibited good activity in both media (7H9/ADC: MIC_{90} = 10.35 µM; 7H9/CAS: MIC_{90} = 0.40 µM). Therefore, it can be hypothesized that the presence of the bulky diethylaminomethyl moiety, coupled with the basicity of the nitrogen atom, which is capable of forming intramolecular hydrogen bond to the *para*-hydroxyl group, enhances the antimycobacterial activity of **1.24**.

The fusidic acid benzyl amide analogues offered an opportunity to analyze the contribution of different Craig plot substituents to activity. It was observed that all analogues, including the unsubstituted benzyl amide **1.25**, were inactive in both 7H9/ADC and 7H9/CAS media, except compound **1.27** (7H9/ADC: MIC_{90} = 62.27 µM; 7H9/CAS: MIC_{90} = 2.71 µM), which bear a sulfonamide group at the *para* position. It can therefore be deduced that hydrophilic electron-withdrawing groups favor antimycobacterial activity. The data supports the hypothesis that bulky polar groups contribute to activity. Moreover, the good activity displayed by **1.27** is congruent with previously reported data on the importance of the sulfonamide group to the antimycobacterial activity of fusidic acid, as already mentioned in Section 4.1.3.1.

In summary, the ethanamide analogues of fusidic acid, generally, exhibited better activity than their anilide and benzyl amide congeners; however, the anilide analogue **1.24** exhibited the most potent antimycobacterial activity amongst the synthesized compounds. The enantiomerically pure ethanamide analogues showed better activity than the diastereomeric analogues, except **1.9**.

Safety profiling of the synthesized compounds to mammalian cells was evaluated as their cytotoxic activity against the Chinese Hamster Ovarian (CHO) cell line at H3D, Division of Clinical Pharmacology, University of Cape Town. The compounds were assayed using the 3-(4,5-dimethylthiazol-2-yl)-2,5-diphenyltetrazolium bromide (MTT) assay, which is a colorimetric assay that measures cell viability as a function of metabolism/reduction of MTT (yellow colour) to formazan (purple colour) by cytosolic NAD(P)H-dependent oxidoreductase enzymes. With an acceptable level of cytotoxicity cut-off set to IC_{50} >10 µM, all the synthesized compounds displayed low to no cytotoxicity, except compounds **1.3** (IC_{50} = 8.24 µM) and **1.24** (IC_{50} = 8.69 µM). Measurement of antimycobacterial activity as a MIC_{90} and cytotoxicity as IC_{50} could not allow for an assessment of the selectivity indices of the compounds.

4.4.2 Antiplasmodium and cytotoxic activities

The synthesized fusidic acid analogues were evaluated *in vitro* against asexual blood stage and gametocyte *P. falciparum* parasites. *In vitro* antiplasmodium activity was investigated against the asexual chloroquine-sensitive (NF54) and multi-drug resistant (K1) strains of *P. falciparum* and the early and late gametocyte marker cell line NF54-PfS16-GFP-Luc. The activity of the compounds against the asexual parasites was assessed using the modified [^{3}H]-hypoxanthine incorporation assay, except for the analogues, **1.6**, **1.7**, **1.14**, **1.21**, **1.22** and the benzyl amide derivatives, which were evaluated using the modified lactate dehydrogenase assay.[54] The former assay is based on the incorporation of radioactive [^{3}H]-hypoxanthine into parasite nucleic acids. The malaria parasite depends on hypoxanthine for nucleic acid synthesis and energy metabolism. Incorporation of radiolabeled hypoxanthine into parasite cultures ensures incorporation of the radiolabeled purine into the parasite's nucleic acids and, thus, enables the quantification of cell proliferation using a scintillation counter.[55] The [^{3}H]-hypoxanthine incorporation assay was conducted at the Swiss Tropical and Public Health Institute, University of Basel.

Lactate dehydrogenase (LDH) is an intracellular enzyme necessary for the interconversion of pyruvate and lactate with associated interconversion of NADH and NAD^+. Plasmodium lactate dehydrogenase (pLDH) can be distinguished from human LDH by its ability to use the NAD analog 3-acetyl pyridine adenine dinucleotide (APAD), in the conversion of lactate to pyruvate. Since pLDH can utilize APAD at ~200-fold more rapidly and effectively than human LDH isoforms, pLDH activity can easily be distinguished in blood samples of 0.2 – 10% parasitemia. Parasite proliferation was therefore measured by monitoring the conversion of APAD to APADH by pLDH.[54,56–58] For the purpose of discussion, test compounds are classified to have potent activity if they displayed low micromolar antiplasmodium activity (IC_{50} ≤1 µM). Compounds exhibiting IC_{50} values in the range of 1 - 5 µM were deemed moderately active while they are inactive if they exhibited IC_{50} value >5 µM.

Table 4.3: *In vitro* activity against blood stage (NF54 and K1 strains) and gametocyte (NF54 strain) P. falciparum parasites and cytotoxicity (CHO cell line) of the fusidic acid amide analogues

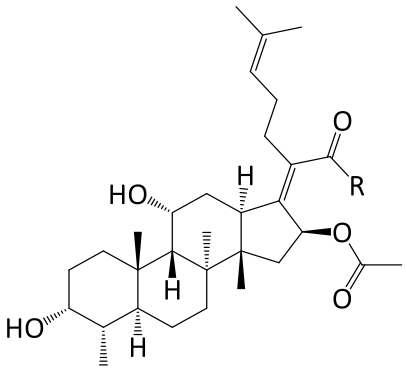

Compound	R	Asexual parasites, IC_{50} (µM)		Gametocyte parasites, % inhibition, 5 µM		Cytotoxicity IC_{50} (µM)	
		Pf(NF54)	*Pf*(K1)	Early stage	Late stage	CHO	SI
1.1	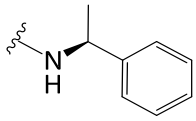	3.45	2.33	13	50	45.95	13.31
1.2	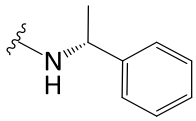	2.22	1.25	32	55	47.61	21.44
1.3	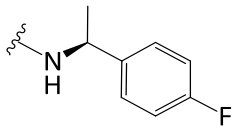	3.80	3.18	3	0	47.40	12.47
1.4	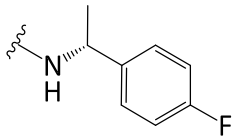	0.57	0.47	48	30	8.24	14.45
1.5	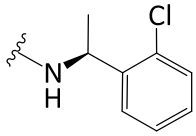	2.91	-	-	-	45.15	15.51

1.6	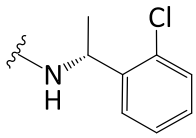	4.26	-	15	12	18.16	4.26
1.7	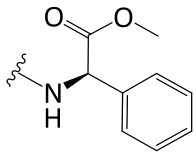	5.47	-	-	-	42.88	7.83
1.8	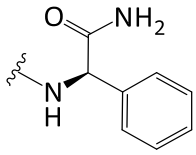	>10	>10	24	22	>50	-
1.9	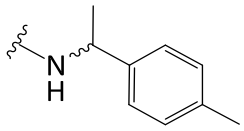	0.96	0.67	21	32	47.90	49.89
1.10	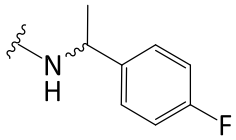	0.80	0.65	40	49	45.30	56.62
1.11	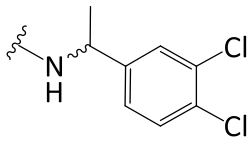	1.00	0.85	27	27	>50	>50
1.12	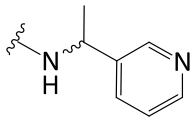	>10	>10	44	43	>50	-
1.13	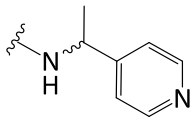	2.98	2.59	36	41	>50	>16.77
1.14	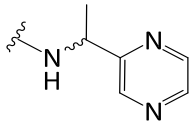	6.00	-	14	37	>50	>8.33

1.15	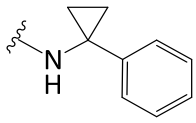	6.74	5.20	-	-	36.84	5.46
1.16	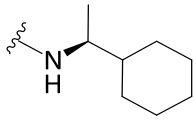	1.37	1.04	60	56	44.69	32.62
1.17	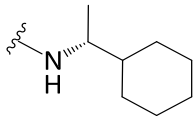	1.72	1.04	39	59	>50	>29.06
1.18	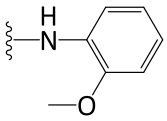	1.00	0.71	52	55	46.13	46.13
1.19	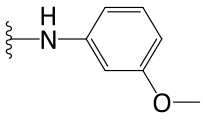	2.42	1.41	30	30	42.68	17.63
1.20	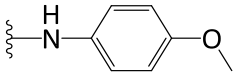	0.86	0.63	36	34	47.12	54.79
1.21	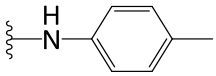	1.27	-	54	43	>50	>39.37
1.22	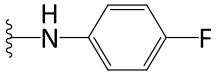	1.93	-	17	37	39.90	20.67
1.23	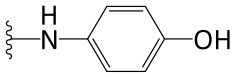	3.82	2.67	0	14	45.39	11.88
1.24	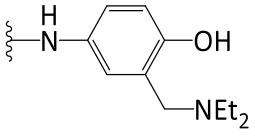	5.11	3.21	66	39	8.69	1.70
1.25	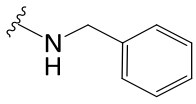	3.92	-	6	17	44.10	11.25

1.26	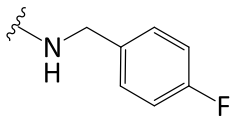	2.76	-	15	28	40.20	14.56
1.27	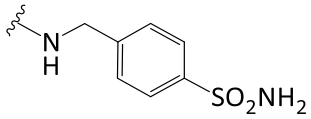	6.00	-	0	14	30.20	5.03
1.28	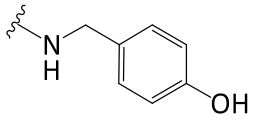	6.00	-	0	13	>50	8.33
1.29	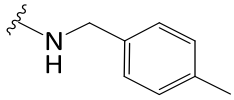	4.87	-	8	37	>50	10.26
Chloroquine		0.01	0.42				
Artesunate		4.42 nM	3.12 nM				
MMV390048				77	92		
Emetine						0.02	

In general, the synthesized fusidic acid analogues displayed better *in vitro* antiplasmodium potency against the multidrug-resistant K1 strain than the drug-sensitive NF54 strain, suggesting the absence of cross-resistance. The ethanamide analogues **1.4** (IC_{50} *Pf*NF54/K1 = 0.57/0.47 µM), **1.9** (IC_{50} *Pf*NF54/K1 = 0.96/0.67 µM), **1.10** (IC_{50} *Pf*NF54/K1 = 0.80/0.65 µM) and **1.11** (IC_{50} *Pf*NF54/K1 = 1.00/0.85 µM) displayed low micromolar activities against both asexual strains (Table 4.3). The comparable potencies of the 4-fluoro ethanamides, single diastereomer **1.4** and diastereomeric mixture **1.10**, coupled with the weak activity displayed by **1.3**, the opposite diastereomer of **1.4,** suggests that there is no antagonism from the opposite diastereomer. Analysis of the relative potencies of the enantiomerically pure ethanamides seem to suggest that the *R*-enantiomers are better inhibitors of parasite proliferation than their *S*-congeners, exemplified by compounds **1.2**, **1.4**, and **1.6**; however, **1.16** and **1.17** demonstrated comparable

activity (Table 4.3). Meanwhile, among the analogues with nitrogen-containing heterocyclic aromatic ring, the 3-pyridinyl and 2-pyrazinyl analogues, **1.12** and **1.14**, respectively, both lost activity while the 4-pyridinyl analogue, **1.13**, was moderately active (IC_{50} *Pf*NF54 = 2.98 µM). Similarly, the C-31-acetoxy and C-31 acetamido fusidic acid analogues, **1.7** (IC_{50} *Pf*NF54 = 5.47 µM) and **1.8** (IC_{50} *Pf*NF54 >10 µM), were both inactive, contrary to **1.1** or **1.2**, which exhibited moderate activity, suggesting that a bulky group at the C-31 position of the ethanamides compromises activity. The cyclohexyl ethanamides **1.16** (IC_{50} *Pf*NF54/K1 = 1.37/1.04 µM) and **1.17** (IC_{50} *Pf*NF54/K1 = 1.72/1.04 µM) were only slightly more potent than their phenyl counterparts, **1.1** (IC_{50} *Pf*NF54/K1 = 3.45/2.33 µM) and **1.2** (IC_{50} *Pf*NF54/K1 = 2.22/1.25 µM). In summary, among the ethanamide derivatives, antiplasmodium activity is not affected by diastereoisomerism, although *R*-enantiomers are more potent than their *S*-congeners. While nitrogen-containing heterocyclic phenyl rings led to loss of activity, saturation of the phenyl ring, as exemplified by **1.16** and **1.17**, is tolerated for activity. Finally, functionalization of the methyl group at C-31 (exemplified by **1.7** and **1.8**) or the presence of a bulky group, such as the cyclopropyl group in **1.15** (IC_{50} *Pf*NF54/K1 = 6.74/5.20 µM) at the C-31 position led to complete loss of activity.

The *ortho* and *para*-methoxy anilide analogues, **1.18** (IC_{50} *Pf*NF54/K1 = 1.00/0.71 µM) and **1.20** (IC_{50} *Pf*NF54/K1 = 0.86/0.63 µM), respectively, exhibited low micromolar potency against both asexual strains of *P. falciparum*. The *meta*-methoxy derivative, **1.19**, however, displayed moderate activity (IC_{50} *Pf*NF54/K1 = 2.42/1.41 µM), suggesting that *meta*-substitution leads to reduction in activity. Similarly, the 4-methyl (**1.21**), 4-fluoro (**1.22**) and 4-hydroxy (**1.23**) fusidic acid anilides were moderately active, the latter displaying about two-fold less potency (IC_{50} *Pf*NF54 = 3.82 µM) than **1.21** (IC_{50} *Pf*NF54 = 1.27 µM) and **1.22** (IC_{50} *Pf*NF54 = 1.93 µM). Compound **1.24**, which possessed the Mannich base side chain, was the least active (IC_{50} *Pf*NF54/K1 = 5.11/3.21 µM) analogue of the anilide derivatives. Compared to **1.23**, the reduction in antiplasmodium activity of **1.24** seems to suggest that the Mannich base side chain is not tolerated for antiplasmodium activity.

Meanwhile, the fusidic acid benzyl amides, **1.25**, **1.26** and **1.29**, displayed moderate activities with IC_{50} values of 3.92 µM, 2.76 µM, and 4.87 µM, respectively, against the NF54 strain. However,

compounds **1.27** and **1.28** were both inactive, suggesting that, on the basis of the contribution of Craig plot substituents to activity, hydrophilic groups, either electron-withdrawing or electron-donating, are not tolerated for *in vitro* asexual blood stage antiplasmodium activity. This is in marked contrast to the antimycobacterial activity.

Initial screening at 1 µM and 5 µM of the synthesized compounds against both early (EG) and late (LG) stage gametocytes was conducted using the luciferase reporter assay. Compounds **1.16** (% inhibition: EG = 60%, LG = 56%) and **1.18** (% inhibition: EG = 52%, LG = 55%) exhibited moderate activity against both gametocyte stages at 5 µM. The fusidic acid Mannich base anilide (**1.24**) displayed 66% inhibition at 5 µM against the early stage gametocyte but lost activity to the late gametocyte parasites. Similarly, compounds **1.1** and **1.2** were active only against the late gametocytes. They displayed moderate activity (% inhibition >50%). All other analogues were inactive at the test concentrations. (Table 4.3).

The safety profiles of the compounds were analyzed in terms of their selectivity indices with respect to the NF54 strain of *P. falciparum* (Table 4.3). The selectivity indices were calculated as a ratio of the IC_{50} (CHO) to IC_{50} (NF54). With SI ≥10 considered safe, most of the synthesized fusidic acid amides were generally non-cytotoxic, except compounds **1.3** (SI = 2.16), **1.6** (SI = 4.26), **1.7** (SI = 7.83), **1.14** (SI = 8.33), **1.15** (SI = 5.46), **1.24** (SI = 1.70), **1.27** (SI = 5.03), and **1.28** (SI = 8.33).

4.5 Conclusion and recommendations for future work

C-21 fusidic acid ethanamides, anilides and benzyl amides were synthesized as potential antimycobacterial and multi-stage antiplasmodium agents. Antimycobacterial activity was favored by the presence of bulky and/or polar substituents, notably, in close proximity to the amide bond. The most potent antimycobacterial analogue was found to be the fusidic acid Mannich base anilide, **1.24**. Future SAR aimed at exploring fusidic acid phenolic amides incorporating a Mannich base side chain and hydrophilic electron-withdrawing substituents is encouraged.

The fusidic acid ethanamides were, generally, the most potent of the analogues evaluated for multi-stage antiplasmodium activity with sub-micromolar IC_{50} values (0.5 – 0.9 µM) recorded for some analogues against the asexual parasites. Meanwhile, the compounds exhibited moderate to

no activity against *P. falciparum* gametocytes. It was observed that antiplasmodium activity was more favored by the ethanamide moiety and the presence of *para* substituted lipophilic groups. Thus, future SAR involving C-3 and C-16 fusidic acid ethanamides is highly encouraged.

The data generated and results reported confirms the initial hypothesis to identify new C-21 analogues of fusidic acid with superior antimycobacterial and multi-stage antiplasmodium activities through semi-synthesis.

4.6 Experimental

4.6.1 General Experimental Procedures

All chemicals and reagents were sourced from commercial vendors. Fusidic acid was purchased from AvaChem Scientific. All other reagents (starting materials) were purchased from Sigma-Aldrich, Combi-Blocks or Fluorochem. Solvents and reagents used to prepare the mobile phase for LCMS analyses were of HPLC-grade and were obtained Sigma-Aldrich (NH_4OAc as an additive), Merck (glacial acetic acid) and Microsep (acetonitrile and methanol). Bulk solvents used for extraction and purification purposes were obtained from Scienceworld Chemicals and were of CP or AR grade.

Reactions were monitored using aluminum silica pre-coated thin layer chromatography (TLC) plates (60 F_{254} from Merck or Al foils 60 Å medium pore diameter from Merck). Visualization of TLC spots were accomplished with the aid of either ultraviolent light (UV) at 245 nm or by using $Ce(SO_4)_2$ stain (15% aqueous sulfuric acid saturated with ceric sulfate).

Purification of synthesized compounds was achieved by preparative TLC (Silica gel GF254, 2000 µm on glass from Analtech). Melting points (uncorrected) were determined using a Stuart Automatic Melting Point Apparatus, SMP40 (Bibby Scientific).

Low Resolution-ESI-MS was acquired on an Agilent 1260 Infinity HPLC system (Agilent® 1260 Infinity Binary Pump, Agilent® 1260 Infinity Diode Array Detector (DAD), Agilent® 1290 Infinity Column Compartment, and Agilent® 1260 Infinity Standard Auto sampler) coupled to Agilent 6120 Quardrupole MS system and Peak Scientific® Genius 1050 Nitrogen Generator. Phenomenex

Kinetex® 2.6 µm EVO C18 100 Å (30 x 2.1 mm) reverse phase analytical column was used. The chromatographic method included a column temperature of 40 ^{o}C, an injection volume of 2 µL, flow rate of 0.7 mL/min and maximum column back pressure set at 600 bars. The mobile phase was made up of 10 mM NH_4OAc in water (A) and 10 mM NH_4OAc in methanol (B). The LC run is a 4.50 min duration beginning with 15% of B from 0 - 0.30 min, followed by a speedy increase in the gradient to 100% B over 0.90 min. The mobile phase composition at 100% of B is maintained to the 4.50 min.

Characterization of synthesized compounds was achieved by analyses of their MS and 1D NMR data. The NMR data was acquired on either a Bruker UltraShield-Plus (400 MHz and 101 MHz for ^{1}H and ^{13}C nuclei, respectively) spectrometer or on a BRUKER Ascend 600 cryoprobe prodigy (600 MHz and 151 MHz for ^{1}H and ^{13}C nuclei, respectively). The ^{1}H NMR data was acquired using standard proton pulse sequence while all ^{13}C NMR data were acquired using the full proton decoupled pulse program. All compounds were dissolved in deuterated solvents for analyses (referenced as follows: $CDCl_3$: δ_H 7.26, δ_C 77.0 ppm; MeOH-d_4: δ_H 3.30, δ_C 49.0 ppm; or DMSO-d_6: δ_H 2.50, δ_C 37.5 ppm). Chemical shifts (δ) are reported in part per million (ppm) to two decimal place for ^{1}H NMR and one decimal places for ^{13}C NMR relative to TMS at 0 ppm. Coupling constants (*J*) are reported in Hertz (Hz) to one decimal place. Proton (^{1}H) NMR splitting patterns are abbreviated as follows: s (singlet), broad singlet (br s), d (doublet), dd (doublet of doublets), t (triplet), q (quartet) and m (multiplet).

4.6.2 General Synthetic Procedure for compounds 1.1 - 1.22 and 1.25 - 1.29

To a mixture of fusidic acid (**1.0**) (1 eq.) and the respective amine (1.5 eq.) in DCM (1 mL) was added triethylamine (3 eq.) dropwise at 25 ^{o}C. T3P solution (3.0 eq., 50% w/v in EtOAc, d=0.534 g/mL) was added dropwise. The temperature of the reaction mixture was increased to 35 ^{o}C and left to stir until reaction was complete (5 – 24 h depending on amine). The progress of the reaction was followed by TLC and LCMS. On completion, the reaction mixture was diluted with DCM (20 mL) and the by-products were extracted with water (15 mL x2) in a separating funnel. The organic layer was dried with anhydrous sodium sulfate, filtered and concentrated *in vacuo* to obtain the crude product. Further purification was accomplished by normal phase preparative TLC using

DCM-EtOAc mixture or DCM-MeOH mixture as eluent depending on the amine. Bands were detected under UV-254 nm, scraped and extracted with EtOAc or acetone. After extraction of the compounds, the silica was filtered off and the filtrate was concentrated *in vacuo* to obtain the target compounds as amorphous solids.

N-((*S*)-1-(phenyl)ethyl)fusidic acid amide (1.1)

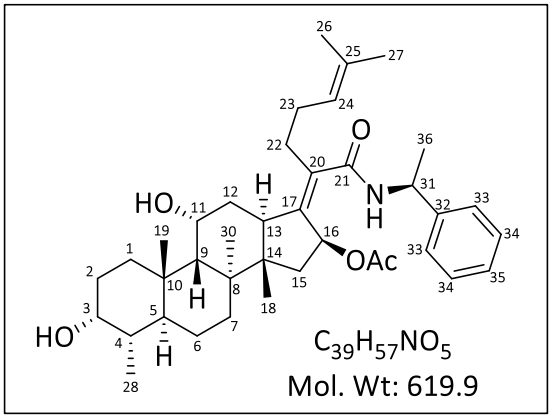

White powder (0.080 g obtained from 0.100 g of **1.0**, 65%); *R*f 0.6 (60% EtOAc:DCM); Mp 182-184 ^{o}C; ^{1}H NMR (400 MHz, $CDCl_3$) δ 7.30-7.16 (m, 5H, 2×H-33, 2×H-34 and H-35), 5.72 (d, *J* = 7.5 Hz, 1H, NH), 5.67 (d, *J* = 8.2 Hz, 1H, H-16), 5.01 (m, 1H, H-24), 5.00-4.93 (m, 1H, H-31), 4.28 (m, 1H, H-11), 3.69 (m, 1H, H-3), 2.94 (m, 1H, H-13), 2.48-2.37 (m, 1H, H-22), 2.35-2.29 (m, 1H, H-22), 2.27-2.24 (m, 1H, H-12), 2.17-1.97 (m, 5H, H-1, H-5, H-15 and 2×H-23), 1.90 (s, 3H, OAc), 1.85-1.61 (m, 4H, 2×H-2, H-7 and H-12), 1.58 (s, 3H, CH_3-27), 1.56-1.48 (m, 4H, H-1, H-4, H-6 and H-9), 1.47 (s, 3H, CH_3-26), 1.41 (d, *J* = 6.9 Hz, 3H, CH_3-36), 1.33 (s, 3H, CH_3-30), 1.30-1.24 (m, 1H, H-15), 1.13-0.99 (m, 2H, H-6 and H-7), 0.93 (s, 3H, CH_3-19), 0.90 (s, 3H, CH_3-18), 0.87 (d, *J* = 6.9 Hz, 3H, CH_3-28); ^{13}C NMR (101 MHz, $CDCl_3$) δ 170.9, 170.4, 143.3, 141.2, 135.9, 132.4, 128.7 (2C), 127.4, 126.2 (2C), 123.3, 74.1, 71.4, 68.3, 49.3, 49.1, 48.6, 43.3, 39.5, 39.4, 37.0, 36.3, 36.1, 35.7, 32.3, 30.2, 30.0, 29.6, 28.0, 25.6, 24.0, 22.8, 21.4, 21.1, 20.8, 17.8, 17.7 and 15.9; LC-MS (ESI): *m/z* 642 $[M+Na]^+$, 560 $[M-OAc]^+$; purity (LC-MS): 98% (t_R = 3.11 min.)

N-((*R*)-1-(phenyl)ethyl)fusidic acid amide (1.2)

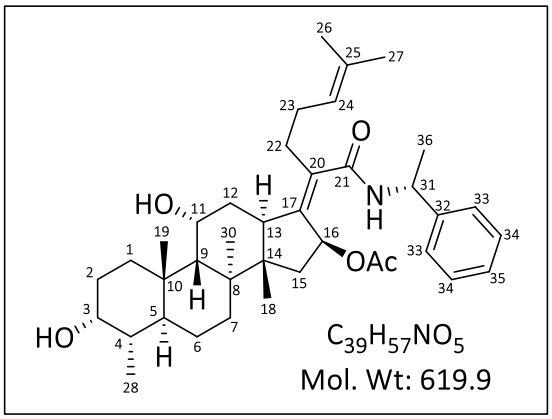

White powder (0.074 g obtained from 0.100 g of **1.0**, 60%); *R*f 0.5 (60% EtOAc:DCM); Mp 181-183 ^{o}C; ^{1}H NMR (400 MHz, $CDCl_3$) δ 7.38-7.18 (m, 5H, 2×H-33, 2×H-34 and H-35), 5.79 (d, *J* = 7.6 Hz, 1H, NH), 5.51 (d, *J* = 8.0 Hz, 1H, H-16), 5.09 (m, 1H, H-24), 5.03 (m, 1H, H-31), 4.31 (m, 1H, H-11), 3.72 (m, 1H, H-3), 2.97 (m, 1H, H-13), 2.56-2.43 (m, 1H, H-22), 2.38-2.31 (m, 1H, H-22), 2.30-2.22 (m, 1H, H-12), 2.18-2.00 (m, 5H, H-1, H-5, H-15 and 2×H-23), 1.78 (s, 3H, OAc), 1.85-1.61 (m, 4H, 2×H-2, H-7 and H-12), 1.66 (s, 3H, CH_3-27), 1.58 (s, 3H, CH_3-26), 1.56-1.48 (m, 4H, H-1, H-4, H-6 and H-9), 1.48 (d, *J* = 6.9 Hz, 3H, CH_3-36), 1.34 (s, 3H, CH_3-30), 1.30-1.24 (m, 1H, H-15), 1.15-1.00 (m, 2H, H-6 and H-7), 0.96 (s, 3H, CH_3-19), 0.92-0.88 (m, 6H, CH_3-18 and CH_3-28); ^{13}C NMR (101 MHz, $CDCl_3$) δ 170.4, 170.3, 142.8, 141.4, 135.8, 132.5, 128.8 (2C), 127.5, 126.4 (2C), 123.4, 74.5, 71.4, 68.3, 49.3, 49.1, 48.5, 43.2, 39.6, 37.0, 36.3, 36.1, 35.8, 32.3, 30.2, 30.0, 29.8, 28.1, 25.7, 24.0, 22.8, 21.8, 21.0, 20.8, 18.0, 17.8 and 15.9; LC-MS (ESI): *m/z* 642 $[M+Na]^+$, 560 $[M-OAc]^+$; purity (LC-MS): 98% (t_R = 3.07 min.)

N-((*S*)-1-(4-fluorophenyl)ethyl)fusidic acid amide (1.3)

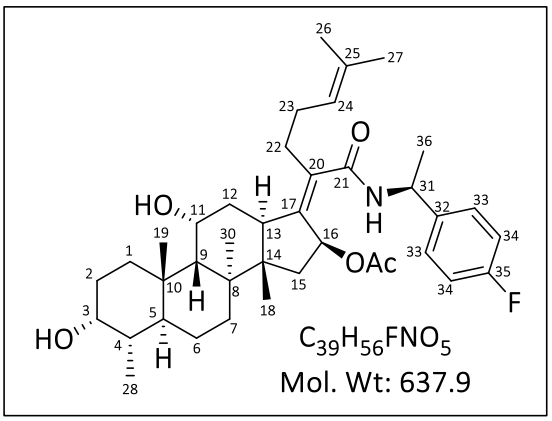

White powder (0.032 g obtained from 0.100 g of **1.0**, 25%); *R*f 0.6 (60% EtOAc:DCM); Mp 171-173 ^{o}C; ^{1}H NMR (400 MHz, $CDCl_3$) δ 7.30-7.23 (m, 2H, 2×H-33), 7.01 (t, *J* = 8.7 Hz, 2H, 2×H-34), 5.71 (d, *J* = 8.1 Hz, 1H, H-16), 5.65 (d, *J* = 7.5 Hz, 1H, NH), 5.02 (m, 1H, H-24), 5.00-4.94 (m, 1H, H-31), 4.32 (m, 1H, H-11), 3.74 (m, 1H, H-3), 2.98 (m, 1H, H-13), 2.53-2.40 (m, 1H, H-22), 2.36-2.29 (m, 1H, H-22), 2.30-2.23 (m, 1H, H-12), 2.21-1.96 (m, 5H, H-1, H-5, H-15 and 2×H-23), 1.96 (s, 3H, OAc), 1.89-1.64 (m, 4H, 2×H-2, H-7 and H-12), 1.62 (s, 3H, CH_3-27), 1.60-1.52 (m, 4H, H-1, H-4, H-6 and H-9), 1.50 (s, 3H, CH_3-26), 1.43 (d, *J* = 6.9 Hz, 3H, CH_3-36), 1.36 (s, 3H, CH_3-30), 1.30-1.24 (m, 1H, H-15), 1.15-1.00 (m, 2H, H-

6 and H-7), 0.96 (s, 3H, CH_3-19), 0.93 (s, 3H, CH_3-18), 0.91 (d, *J* = 6.8 Hz, 3H, CH_3-28); ^{13}C NMR (101 MHz, $CDCl_3$) δ 170.9, 170.3, 162.0 (d, *J* = 245.6 Hz, C-35), 141.3, 139.2 (d, *J* = 3.2 Hz, C-32), 135.8, 132.5, 127.8 (d, *J* = 8.0 Hz, 2×C-33), 123.2, 115.4 (d, *J* = 21.4 Hz, 2×C-34), 74.0, 71.4, 68.3, 49.3, 48.6, 48.4, 43.3, 39.5, 39.4, 37.1, 36.2 (2C), 35.7, 32.4, 30.3, 30.0, 29.6, 27.9, 25.6, 24.1, 22.7, 21.4, 21.1, 20.8, 17.9, 17.7 and 15.9; LC-MS (ESI): *m/z* 578 $[M\text{-}OAc]^+$; purity (LC-MS): 98% (t_R = 3.22 min.)

N-((*R*)-1-(4-fluorophenyl)ethyl)fusidic acid amide (1.4)

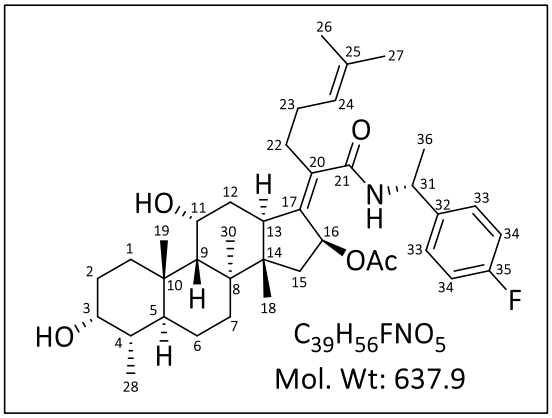

White powder (0.026 g obtained from 0.100 g of **1.0**, 20%); *R*f 0.5 (60% EtOAc:DCM); Mp 182-184 °C; ^{1}H NMR (400 MHz, $CDCl_3$) δ 7.29-7.23 (m, 2H, 2×H-33), 7.05-6.99 (t, *J* = 8.7 Hz, 2H, 2×H-34), 5.68 (d, *J* = 7.5 Hz, 1H, NH), 5.52 (d, *J* = 8.0 Hz, 1H, H-16), 5.08 (m, 1H, H-24), 5.00-4.94 (m, 1H, H-31), 4.31 (m, 1H, H-11), 3.73 (m, 1H, H-3), 2.97 (m, 1H, H-13), 2.53-2.43 (m, 1H, H-22), 2.38-2.29 (m, 1H, H-22), 2.30-2.23 (m, 1H, H-12), 2.21-2.03 (m, 5H, H-1, H-5, H-15 and 2×H-23), 1.80 (s, 3H, OAc), 1.89-1.61 (m, 4H, 2×H-2, H-7 and H-12), 1.66 (s, 3H, CH_3-27), 1.58 (s, 3H, CH_3-26), 1.56-1.48 (m, 4H, H-1, H-4, H-6 and H-9), 1.46 (d, *J* = 6.9 Hz, 3H, CH_3-36), 1.34 (s, 3H, CH_3-30), 1.30-1.24 (m, 1H, H-15), 1.15-1.00 (m, 2H, H-6 and H-7), 0.96 (s, 3H, CH_3-19), 0.93-0.88 (m, 6H, CH_3-18 and CH_3-28); ^{13}C NMR (101 MHz, $CDCl_3$) δ 170.4, 170.3, 162.0 (d, *J* = 245.6 Hz, C-35), 141.5, 138.6 (d, *J* = 3.2 Hz, C-32), 135.8, 132.5, 128.1 (d, *J* = 8.0 Hz, 2×C-33), 123.3, 115.5 (d, *J* = 21.3 Hz, 2×C-34), 74.0, 71.4, 68.3, 49.3, 48.6, 48.5, 43.2, 39.6, 39.3, 37.1, 36.2 (2C), 35.7, 32.5, 30.3, 30.0, 29.8, 28.1, 25.7, 24.1, 22.7, 21.4, 21.1, 20.8, 17.9, 17.7 and 15.9; LC-MS (ESI): *m/z* 578 $[M\text{-}OAc]^+$; purity (LC-MS): 98% (t_R = 3.21 min.)

N-((*S*)-1-(2-chlorophenyl)ethyl)fusidic acid amide (1.5)

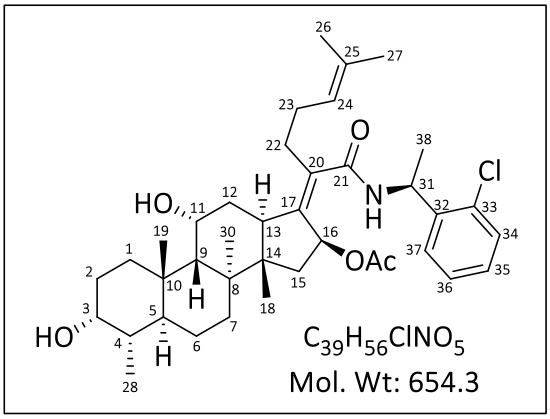

White powder (0.043 g obtained from 0.100 g of 1.0, 33%); *R*f 0.6 (60% EtOAc:DCM); Mp 237-239 °C; ^{1}H NMR (400 MHz, $CDCl_3$) δ 7.38-7.13 (m, 4H, H-34, H-35, H-36 and H-37), 5.81 (d, *J* = 7.0 Hz, 1H, NH), 5.75 (d, *J* = 8.2 Hz, 1H, H-16), 5.31-5.21 (m, 1H, H-31), 5.04 (m, 1H, H-24), 4.33 (m, 1H, H-11), 3.75 (m, 1H, H-3), 3.00 (m, 1H, H-13), 2.50-2.40 (m, 1H, H-22), 2.36-2.28 (m, 1H, H-22), 2.27-2.23 (m, 1H, H-12), 2.22-2.00 (m, 5H, H-1, H-5, H-15 and 2×H-23), 1.99 (s, 3H, OAc), 1.91-1.66 (m, 4H, 2×H-2, H-7 and H-12), 1.63 (s, 3H, CH_3-27), 1.64-1.55 (m, 4H, H-1, H-4, H-6 and H-9), 1.52 (s, 3H, CH_3-26), 1.46 (d, *J* = 6.9 Hz, 3H, CH_3-38), 1.38 (s, 3H, CH_3-30), 1.30-1.24 (m, 1H, H-15), 1.20-1.05 (m, 2H, H-6 and H-7), 0.97 (s, 3H, CH_3-19), 0.91-0.87 (m, 6H, CH_3-18 and CH_3-28); ^{13}C NMR (101 MHz, $CDCl_3$) δ 170.9, 170.1, 141.3, 140.6, 135.8, 132.8, 132.4, 130.2, 128.5, 127.3, 127.2, 123.3, 73.9, 71.4, 68.4, 49.3, 48.6, 47.4, 43.3, 39.5, 39.4, 37.1, 36.3, 36.2, 35.6, 32.6, 30.4, 30.0, 29.7, 27.9, 25.6, 24.2, 22.7, 21.1, 20.7, 20.5, 17.9, 17.7 and 15.9; LC-MS (ESI): *m/z* 594 [M-OAc]+; purity (LC-MS): 98% (t_R = 3.25 min.)

N-((*R*)-1-(2-chlorophenyl)ethyl)fusidic acid amide (1.6)

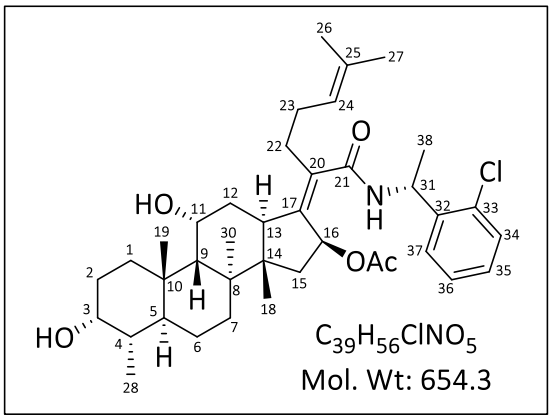

White powder (0.011 g obtained from 0.100 g of 1.0, 8%); *R*f 0.5 (60% EtOAc:DCM); Mp 178-180 °C; ^{1}H NMR (400 MHz, $CDCl_3$) δ 7.36 (dd, *J* = 1.7, 7.3 Hz, 1H, H-34), 7.28-7.17 (m, 3H, H-35, H-36 and H-37), 6.10 (d, *J* = 8.4 Hz, 1H, NH), 5.51 (d, *J* = 8.1 Hz, 1H, H-16), 5.48-5.38 (m, 1H, H-31), 5.10 (m, 1H, H-24), 4.33 (m, 1H, H-11), 3.74 (m, 1H, H-3), 2.99 (m, 1H, H-13), 2.55-2.46 (m, 1H, H-22), 2.40-2.32 (m, 1H, H-22), 2.31-2.24 (m, 1H, H-12), 2.21-2.00 (m, 5H, H-1, H-5, H-15 and 2×H-23), 1.90-1.70 (m, 4H, 2×H-2, H-7 and H-12), 1.68 (s, 3H, OAc), 1.67 (s, 3H, CH_3-27), 1.60-1.52 (m, 4H, H-1, H-4, H-6 and H-9),

1.59 (s, 3H, CH_3-26), 1.48 (d, *J* = 6.9 Hz, 3H, CH_3-38), 1.36 (s, 3H, CH3-30), 1.30-1.24 (m, 1H, H-15), 1.15-1.00 (m, 2H, H-6 and H-7), 0.96 (s, 3H, CH_3-19), 0.91-0.87 (m, 6H, CH3-18 and CH_3-28); ^{13}C NMR (101 MHz, $CDCl_3$) δ 170.2, 170.1, 141.5, 140.1, 135.7, 132.6, 132.4, 130.4, 128.6, 128.1, 127.3, 123.4, 74.4, 71.4, 68.4, 49.3, 48.5, 47.5, 43.1, 39.5, 39.3, 37.1, 36.2 (2C), 35.8, 32.4, 30.3, 30.0, 29.8, 28.2, 25.7, 24.1, 22.7, 21.4, 20.8 (2C), 18.0, 17.8 and 15.9; LC-MS (ESI): *m/z* 594 [M-OAc]+; purity (LC-MS): 98% (t_R = 3.26 min.)

N-((*R*)-2-(phenyl)methylacetyl)fusidic acid amide (1.7)

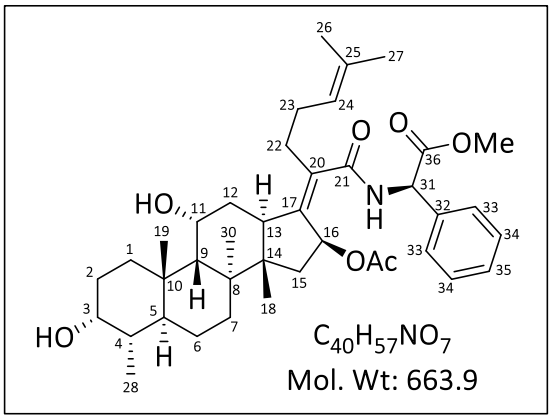

White powder (0.006 g obtained from 0.050 g of **1.0**, 9%); *R*f 0.6 (60% EtOAc:DCM); Mp 238-240 ^{o}C; ^{1}H NMR (400 MHz, $CDCl_3$) δ 7.40-7.27 (m, 5H, 2×H-33, 2×H-34 and H-35), 6.59 (d, *J* = 7.5 Hz, 1H, NH), 5.73 (d, *J* = 8.0 Hz, 1H, H-16), 5.50 (d, *J* =7.3 Hz, 1H, H-31), 5.06 (m, H-24), 4.33 (m, 1H, H-11), 3.75 (s, 3H, OMe), 3.71 (m, 1H, H-3), 3.02 (m, 1H, H-13), 2.54-2.44 (m, 1H, H-22), 2.39-2.30 (m, 1H, H-22), 2.29-2.23 (m, 1H, H-12), 2.21-2.00 (m, 5H, H-1, H-5, H-15 and 2×H-23), 1.84 (s, 3H, OAc), 1.85-1.65 (m, 4H, 2×H-2, H-7 and H-12), 1.64 (s, 3H, CH_3-27), 1.61-1.54 (m, 4H, H-1, H-4, H-6 and H-9), 1.53 (s, 3H, CH_3-26), 1.37 (s, 3H, CH_3-30), 1.35-1.24 (m, 1H, H-15), 1.18-0.99 (m, 2H, H-6 and H-7), 0.97 (s, 3H, CH_3-19), 0.93 (s, 3H, CH_3-18), 0.92 (d, *J* = 7.5 Hz, 3H, CH_3-28); ^{13}C NMR (101 MHz, $CDCl_3$) δ 171.0, 170.5, 170.1, 142.8, 136.8, 135.1, 132.5, 128.9 (2C), 128.4, 127.1 (2C), 123.2, 73.9, 71.4, 68.4, 56.2, 52.9, 49.3, 48.7, 43.4, 39.6, 39.3, 37.1, 36.3, 36.1, 35.7, 32.5, 30.3, 30.0, 29.5, 27.9, 25.6, 24.2, 22.6, 20.8, 20.7, 18.0, 17.7 and 15.9; LC-MS (ESI): *m/z* 604 $[M\text{-}OAc]^+$; purity (LC-MS): 98% (t_R = 3.21 min.)

N-((*R*)-2-(phenyl)acetamido)fusidic acid amide (1.8)

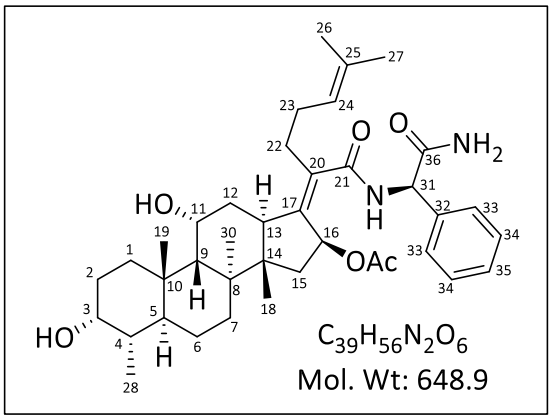

White powder (0.022 g obtained from 0.100 g of **1.0**, 17%); *R*f 0.4 (EtOAc); Mp 181-183 ^{o}C; ^{1}H NMR (400 MHz, $CDCl_3$) δ 7.42-7.28 (m, 5H, 2×H-33, 2×H-34 and H-35), 6.95 (d, *J* = 6.8 Hz, 1H, NH), 5.77 (d, *J* = 7.9 Hz, 1H, H-16), 5.39 (d, *J* =6.8 Hz, 1H, H-31), 5.05 (m, H-24), 4.32 (m, 1H, H-11), 3.74 (m, 1H, H-3), 3.02 (m, 1H, H-13), 2.53-2.41 (m, 1H, H-22), 2.39-2.30 (m, 1H, H-22), 2.32-2.22 (m, 1H, H-12), 2.20-1.99 (m, 5H, H-1, H-5, H-15 and 2×H-23), 1.79 (s, 3H, OAc), 1.88-1.63 (m, 4H, 2×H-2, H-7 and H-12), 1.64 (s, 3H, CH_3-27), 1.62-1.54 (m, 4H, H-1, H-4, H-6 and H-9), 1.51 (s, 3H, CH_3-26), 1.37 (s, 3H, CH_3-30), 1.35-1.24 (m, 1H, H-15), 1.16-1.01 (m, 2H, H-6 and H-7), 0.97 (s, 3H, CH_3-19), 0.93 (s, 3H, CH_3-18), 0.92 (d, *J* = 7.5 Hz, 3H, CH_3-28); ^{13}C NMR (101 MHz, $CDCl_3$) δ 171.7, 170.5, 170.2, 142.9, 138.1, 135.2, 132.5, 129.1 (2C), 128.4, 127.4 (2C), 123.2, 74.1, 71.4, 68.4, 56.8, 49.3, 48.7, 43.5, 39.6, 39.3, 37.1, 36.3, 36.2, 35.7, 32.5, 30.3, 30.0, 29.6, 27.9, 25.6, 24.1, 22.6, 20.9, 20.7, 18.1, 17.7 and 15.9; LC-MS (ESI): *m/z* 589 $[M\text{-}OAc]^+$; purity (LC-MS): 98% (t_R = 3.10 min.)

N-(1-(4-methylphenyl)ethyl)fusidic acid amide (1.9)

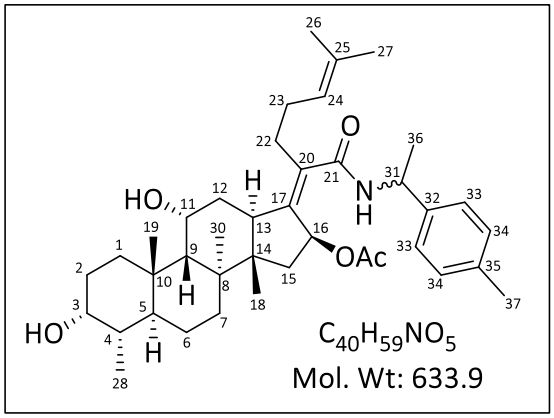

White powder (0.073 g obtained from 0.100 g of **1.0**, 58%); *R*f 0.5, 0.6 (60% EtOAc:DCM); a 2:1 mixture of diastereomers; **Major product**: ^{1}H NMR (400 MHz, $CDCl_3$) δ 7.16 (d, *J* = 8.0 Hz, 2H, 2×H-33), 7.13 (d, *J* = 8.0 Hz, 2H, 2×H-34), 5.75 (m, 1H, NH), 5.50 (d, *J* = 8.0 Hz, 1H, H-16), 5.08 (m, 1H, H-24), 4.97 (m, 1H, H-31), 4.30 (m, 1H, H-11), 3.70 (m, 1H, H-3), 2.95 (m, 1H, H-13), 2.56-2.46 (m, 1H, H-22), 2.42-2.34 (m, 1H, H-22), 2.32 (s, 3H, CH_3-37), 2.30-2.22 (m, 1H, H-12), 2.20-2.00 (m, 5H, H-1, H-5, H-15 and 2×H-23), 1.81 (s, 3H, OAc), 1.91-1.67 (m, 4H, 2×H-2, H-7 and H-12), 1.65 (s, 3H, CH_3-27), 1.62-1.45 (m, 4H, H-1, H-4, H-6 and H-9), 1.57 (s, 3H, CH_3-26), 1.45 (d, *J* = 6.8 Hz, 3H, CH_3-36), 1.33 (s, 3H, CH_3-30),

1.28-1.23 (m, 1H, H-15), 1.16-1.01 (m, 2H, H-6 and H-7), 0.95 (s, 3H, CH_3-19), 0.92-0.87 (m, 6H, CH_3-18 and CH_3-28); ^{13}C NMR (101 MHz, $CDCl_3$) δ 170.4, 170.3, 141.3, 139.7, 137.1, 135.9, 132.4, 129.4 (2C), 126.3 (2C), 123.4, 74.5, 71.4, 68.3, 49.4, 48.9, 48.5, 43.2, 39.6, 39.3, 37.0, 36.4, 36.0, 35.8, 32.2, 30.2, 30.0, 29.8, 28.1, 25.7, 23.8, 22.9, 21.7, 21.0 (2C), 20.9, 18.0, 17.8 and 15.9; **Minor product**: ^{1}H NMR (400 MHz, $CDCl_3$) δ 7.17 (d, *J* = 8.0 Hz, 2H, 2×H-33), 7.10 (d, *J* = 8.0 Hz, 2H, 2×H-34), 5.68 (m, 1H, NH), 5.50 (d, *J* = 8.0 Hz, 1H, H-16), 5.08 (m, 1H, H-24), 4.97 (m, 1H, H-31), 4.30 (m, 1H, H-11), 3.70 (m, 1H, H-3), 2.95 (m, 1H, H-13), 2.56-2.46 (m, 1H, H-22), 2.42-2.34 (m, 1H, H-22), 2.30 (s, 3H, CH_3-37), 2.30-2.22 (m, 1H, H-12), 2.20-2.00 (m, 5H, H-1, H-5, H-15 and 2×H-23), 1.92 (s, 3H, OAc), 1.91-1.67 (m, 4H, 2×H-2, H-7 and H-12), 1.61 (s, 3H, CH_3-27), 1.62-1.45 (m, 4H, H-1, H-4, H-6 and H-9), 1.50 (s, 3H, CH_3-26), 1.42 (d, *J* = 6.9 Hz, 3H, CH_3-36), 1.35 (s, 3H, CH_3-30), 1.28-1.23 (m, 1H, H-15), 1.16-1.01 (m, 2H, H-6 and H-7), 0.95 (s, 3H, CH_3-19), 0.92-0.87 (m, 6H, CH_3-18 and CH_3-28); ^{13}C NMR (101 MHz, $CDCl_3$) δ 170.9, 170.3, 141.1, 140.3, 137.0, 135.9, 132.3, 129.3 (2C), 126.1 (2C), 123.4, 74.1, 71.4, 68.3, 49.4, 48.8, 48.6, 43.3, 39.5, 39.3, 37.0, 36.4, 36.0, 35.7, 32.2, 30.2, 30.0, 29.7, 28.0, 25.6, 23.9, 22.9, 21.4, 21.1, 21.0, 20.8, 17.8, 17.7 and 15.9; LC-MS (ESI): *m/z* 574 $[M\text{-}OAc]^+$; purity (LC-MS): 98% (t_R = 3.30 min.)

N-(1-(4-fluorophenyl)ethyl)fusidic acid amide (1.10)

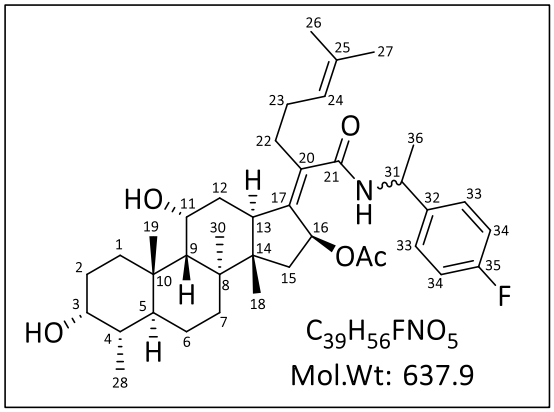

White powder (0.051 g obtained from 0.100 g of **1.0**, 40%); *R*f 0.5 (60% EtOAc:DCM); a 3:2 mixture of diastereomers; **Major product**: ^{1}H NMR (400 MHz, $CDCl_3$) δ 7.31-7.20 (m, 2H, 2×H-33), 7.07-6.94 (m, 2H, 2×H-34), 5.74 (d, *J* = 7.6 Hz, 1H, NH), 5.51 (d, *J* = 8.0 Hz, 1H, H-16), 5.08 (m, 1H, H-24), 5.05-4.93 (m, 1H, H-31), 4.31 (m, 1H, H-11), 3.72 (m, 1H, H-3), 2.97 (m, 1H, H-13), 2.55-2.44 (m, 1H, H-22), 2.40-2.31 (m, 1H, H-22), 2.29-2.20 (m, 1H, H-12), 2.18-2.00 (m, 5H, H-1, H-5, H-15 and 2×H-23), 1.89-1.67 (m, 4H, 2×H-2, H-7 and H-12), 1.79 (s, 3H, OAc), 1.66 (s, 3H, CH_3-27), 1.62-1.45 (m, 4H, H-1, H-4, H-6 and H-9), 1.57 (s, 3H, CH_3-26), 1.45 (d, *J* = 6.8 Hz, 3H, CH_3-36), 1.33 (s, 3H, CH_3-30), 1.28-1.23 (m, 1H, H-15), 1.16-1.01 (m, 2H, H-6 and H-7), 0.95 (s, 3H, CH_3-19), 0.92-0.87 (m, 6H, CH_3-18 and CH_3-

28); ^{13}C NMR (101 MHz, $CDCl_3$) δ 170.4, 170.3, 162.1 (d, *J* = 245.7 Hz, C-35), 141.5, 138.6 (d, *J* = 3.1 Hz, C-32), 135.7, 132.5, 128.1 (d, *J* = 8.1 Hz, 2×C-33), 123.3, 115.5 (d, *J* = 21.4 Hz, 2×C-34), 74.3, 71.4, 68.3, 49.3, 48.6, 48.4, 43.2, 39.5, 39.3, 37.0, 36.3 (2C), 35.7, 32.3, 30.2, 30.0, 29.7, 28.1, 25.7, 24.0, 22.8, 21.9, 21.0, 20.8, 18.0, 17.8 and 15.9; Minor product: ^{1}H NMR (400 MHz, $CDCl_3$) δ 7.31-7.20 (m, 2H, 2×H-33), 7.07-6.94 (m, 2H, 2×H-34), 5.71 (d, *J* = 7.6 Hz, 1H, NH), 5.70 (d, *J* = 8.0 Hz, 1H, H-16), 5.08 (m, 1H, H-24), 5.05-4.93 (m, 1H, H-31), 4.31 (m, 1H, H-11), 3.72 (m, 1H, H-3), 2.97 (m, 1H, H-13), 2.52-2.38 (m, 1H, H-22), 2.36-2.31 (m, 1H, H-22), 2.29-2.20 (m, 1H, H-12), 2.18-2.00 (m, 5H, H-1, H-5, H-15 and 2×H-23), 1.95 (s, 3H, OAc), 1.89-1.67 (m, 4H, 2×H-2, H-7 and H-12), 1.61 (s, 3H, CH_3-27), 1.62-1.45 (m, 4H, H-1, H-4, H-6 and H-9), 1.49 (s, 3H, CH_3-26), 1.42 (d, *J* = 6.8 Hz, 3H, CH_3-36), 1.35 (s, 3H, CH_3-30), 1.28-1.23 (m, 1H, H-15), 1.16-1.01 (m, 2H, H-6 and H-7), 0.95 (s, 3H, CH_3-19), 0.92-0.87 (m, 6H, CH_3-18 and CH_3-28); ^{13}C NMR (101 MHz, $CDCl_3$) δ 170.8, 170.3, 162.0 (d, *J* = 245.7 Hz, CF-35), 141.2, 139.2 (d, *J* = 3.2 Hz, C-32), 135.7, 132.4, 127.8 (d, *J* = 8.0 Hz, 2×C-33), 123.2, 115.4 (d, *J* = 21.4 Hz, 2×C-34), 74.0, 71.4, 68.3, 49.3, 48.6, 48.4, 43.3, 39.5, 39.4, 37.0, 36.0 (2C), 35.6, 31.9, 30.2, 30.0, 29.7, 27.9, 25.6, 24.0, 22.8, 21.4, 21.1, 20.8, 17.8, 17.7 and 15.9; LC-MS (ESI): *m/z* 578 $[M\text{-}OAc]^+$; purity (LC-MS): 98% (t_R = 3.25 min.)

N-(1-(3,4-dichlorophenyl)ethyl)fusidic acid amide (1.11)

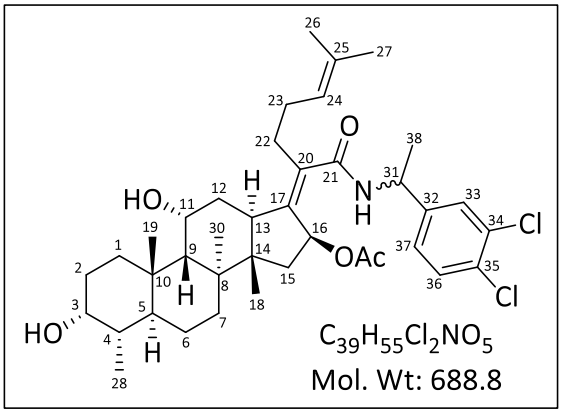

White powder (0.034 g obtained from 0.100 g of 1.0, 25%); *R*f 0.6 (60% EtOAc:DCM); a 1:1 mixture of diastereomers; ^{1}H NMR (400 MHz, $CDCl_3$) δ 7.41 (d, *J* = 8.5 Hz, 1H, H-36), 7.39 (d, *J* = 2.2 Hz, 1H, H-33), 7.37 (d, *J* = 8.2 Hz, 1H, H-36), 7.37 (d, *J* = 2.2 Hz, 1H, H-33), 7.16-7.11 (m, 2H, 2×H-37), 5.75-5.66 (m, 3H, 2×NH and H-16), 5.54 (d, *J* = 8.0 Hz, 1H, H-16), 5.09 (m, 1H, H-24), 5.03 (m, 1H, H-24), 5.00-4.94 (m, 1H, H-31), 4.94-4.87 (m, 1H, H-31), 4.32 (m, 2H, 2×H-11), 3.74 (m, 2H, 2×H-3), 2.98 (m, 2H, 2×H-13), 2.53-2.40 (m, 2H, 2×H-22), 2.36-2.29 (m, 2H, 2×H-22), 2.30-2.23 (m, 2H, 2×H-12), 2.21-1.96 (m, 10H, 2×H-1, 2×H-5, 2×H-15 and 4×H-23), 1.98 (s, 3H, OAc), 1.89-1.64 (m, 8H, 4×H-2, 2×H-7 and 2×H-12), 1.80 (s, 3H, OAc), 1.67 (s, 3H, CH_3-27), 1.63 (s, 3H, CH_3-27), 1.60-1.52 (m, 8H, 2×H-1, 2×H-

4, 2×H-6 and 2×H-9), 1.58 (s, 3H, CH_3-26), 1.51 (s, 3H, CH_3-26), 1.44 (d, *J* = 6.9 Hz, 3H, CH_3-38), 1.41 (d, *J* = 7.0 Hz, 3H, CH_3-38), 1.37 (s, 3H, CH_3-30), 1.34 (s, 3H, CH_3-30), 1.30-1.24 (m, 2H, 2×H-15), 1.15-1.00 (m, 4H, 2×H-6 and 2×H-7), 0.97 (s, 3H, CH_3-19), 0.96 (s, 3H, CH_3-19), 0.94 (s, 3H, CH_3-18), 0.95-0.86 (m, 9H, CH_3-18 and 2×CH_3-28); ^{13}C NMR (101 MHz, $CDCl_3$) δ 170.8, 170.4, 170.3, 170.2, 143.9, 143.2, 142.0, 141.6, 135.5 (2C), 132.7 (2C) 132.6 (2C), 131.5, 131.2, 130.8, 130.6, 128.5, 128.1, 126.0, 125.7, 123.2, 123.1, 74.3, 73.8, 71.4 (2C), 68.3 (2C), 49.3 (2C), 48.6 (2C) 48.2, 48.1, 43.4, 43.3, 39.6, 39.5, 39.4, 39.3, 37.1 (2C), 36.2 (3C), 36.1, 35.7, 35.6, 32.5 (2C), 30.3 (2C), 30.0 (2C), 29.7 (2C), 28.1, 27.9, 25.7, 25.6, 24.1 (2C), 22.7, 22.6, 21.7, 21.3, 21.1, 21.0, 20.7 (2C), 18.1, 17.8, 17.8, 17.7 and 15.9 (2C); LC-MS (ESI): *m/z* 628 $[M\text{-}OAc]^+$; purity (LC-MS): 98% (t_R = 3.31 min.)

N-(1-(3-pyridinyl)ethyl)fusidic acid amide (1.12)

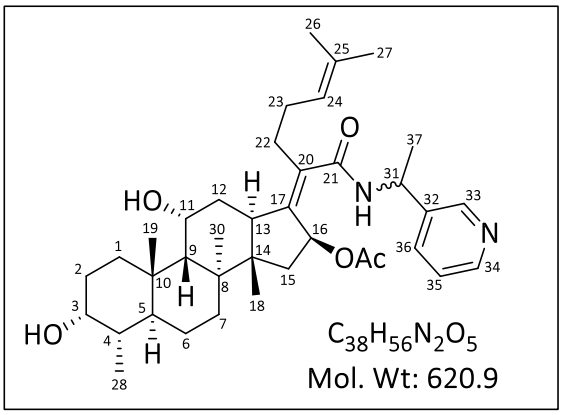

White powder (0.028 g obtained from 0.050 g of **1.0**, 48%); *R*f 0.3 (EtOAc); a 1:1 mixture of diastereomers; ^{1}H NMR (400 MHz, $CDCl_3$) δ 8.72-8.45 (m, 4H, 2×H-33 and 2×H-34), 7.75-7.67 (m, 2H, 2×H-35), 7.39-7.33 (m, 1H, H-36), 7.32-7.27 (m, 1H, H-36), 6.24 (d, *J* = 7.6 Hz, 1H, NH), 6.14 (d, *J* = 7.6 Hz, 1H, NH), 5.74 (d, *J* = 8.2 Hz, 1H, H-16), 5.53 (d, *J* = 8.2 Hz, 1H, H-16), 5.14-4.97 (m, 4H, 2×H-24 and 2×H-31), 4.31 (m, 2H, 2×H-11), 3.72 (m, 2H, 2×H-3), 2.95 (m, 2H, 2×H-13), 2.53-2.40 (m, 2H, 2×H-22), 2.39-2.30 (m, 2H, 2×H-22), 2.33-2.23 (m, 2H, 2×H-12), 2.23-1.96 (m, 10H, 2×H-1, 2×H-5, 2×H-15 and 4×H-23), 1.97 (s, 3H, OAc), 1.89-1.64 (m, 8H, 4×H-2, 2×H-7 and 2×H-12), 1.74 (s, 3H, OAc), 1.65 (s, 3H, CH_3-27), 1.60 (s, 3H, CH_3-27), 1.57 (s, 3H, CH_3-26), 1.59-1.53 (m, 8H, 2×H-1, 2×H-4, 2×H-6 and 2×H-9), 1.48 (s, 3H, CH_3-26), 1.53-1.49 (m, 6H, 2×CH_3-37), 1.34 (s, 3H, CH_3-30), 1.32 (s, 3H, CH_3-30), 1.30-1.24 (m, 2H, 2×H-15), 1.18-1.04 (m, 4H, 2×H-6 and 2×H-7), 0.96 (s, 6H, 2×CH_3-19), 0.95 (s, 3H, CH_3-18), 0.94-0.90 (m, 9H, CH_3-18 and 2×CH_3-28); ^{13}C NMR (101 MHz, $CDCl_3$) δ 170.9, 170.7, 170.5, 170.3, 147.7, 147.5, 147.2, 147.1, 141.9, 141.7, 135.7, 135.3 (2C), 135.0, 132.6, 132.5, 124.1, 123.8, 123.3 (2C), 123.2 (2C), 74.3, 73.9, 71.3 (2C), 68.3 (2C), 49.4, 49.3, 48.6,

48.5, 47.0, 46.9, 43.4, 43.3, 39.5 (2C), 39.4, 39.3, 37.0 (2C), 36.3 (2C), 36.1, 36.0, 35.7, 35.6, 32.3, 32.2, 30.2 (2C), 30.0 (2C), 29.7 (2C), 28.1, 28.0, 25.7, 25.6, 24.0, 23.9, 22.9 (2C), 21.7, 21.1 (2C), 20.9, 20.8 (2C), 17.9, 17.8 (2C), 17.7 and 15.9 (2C); LC-MS (ESI): *m/z* 644 $[M+H+Na]^+$, 561 $[M-OAc]^+$; purity (LC-MS): 98% (t_R = 3.06 min.)

N-(1-(4-pyridinyl)ethyl)fusidic acid amide (1.13)

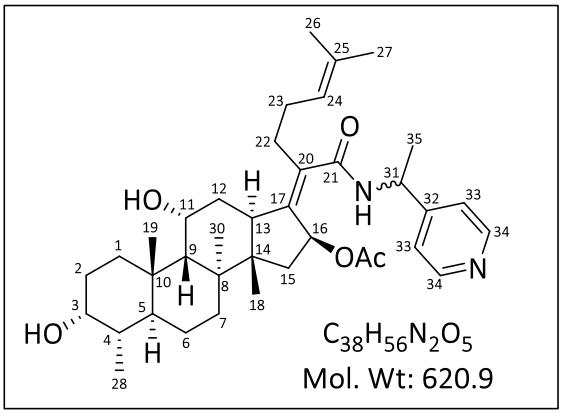

White powder (0.028 g obtained from 0.050 g of **1.0**, 48%); *R*f 0.5 (EtOAc); a 1:1 mixture of diastereomers; ^{1}H NMR (400 MHz, $CDCl_3$) δ 8.61-8.52 (m, 4H, 4×H-34), 7.37-7.30 (m, 4H, 4×H-33), 6.29-6.18 (m, 2H, 2×NH), 5.77 (d, *J* = 8.2 Hz, 1H, H-16), 5.58 (d, *J* = 8.0 Hz, 1H, H-16), 5.11-5.00 (m, 3H, 2×H-24 and H-31), 4.98-4.88 (m, 1H, H-31), 4.32 (m, 2H, 2×H-11), 3.73 (m, 2H, 2×H-3), 2.98 (m, 2H, 2×H-13), 2.50-2.38 (m, 2H, 2×H-22), 2.39-2.30 (m, 2H, 2×H-22), 2.33-2.23 (m, 2H, 2×H-12), 2.23-1.96 (m, 10H, 2×H-1, 2×H-5, 2×H-15 and 4×H-23), 1.98 (s, 3H, OAc), 1.88-1.68 (m, 8H, 4×H-2, 2×H-7 and 2×H-12), 1.73 (s, 3H, OAc), 1.66 (s, 3H, CH_3-27), 1.63 (s, 3H, CH_3-27), 1.58 (s, 3H, CH_3-26), 1.59-1.53 (m, 8H, 2×H-1, 2×H-4, 2×H-6 and 2×H-9), 1.51 (s, 3H, CH_3-26), 1.46 (d, *J* = 7.0 Hz, 3H, CH_3-35), 1.44 (d, *J* = 7.0 Hz, 3H, CH_3-35), 1.34 (s, 3H, CH_3-30), 1.33 (s, 3H, CH_3-30), 1.30-1.24 (m, 2H, 2×H-15), 1.16-1.02 (m, 4H, 2×H-6 and 2×H-7), 0.98 (s, 6H, 2×CH_3-19), 0.95 (s, 3H, CH_3-18), 0.94-0.87 (m, 9H, CH_3-18 and 2×CH_3-28); ^{13}C NMR (101 MHz, $CDCl_3$) δ 170.8, 170.8, 170.6, 170.5, 154.6, 154.0, 148.5 (2C), 142.0 (2C), 135.2, 135.1, 132.6 (2C), 132.5, 123.3 (2C), 123.2 (2C), 122.2 (2C), 121.8., 74.5, 73.8, 71.3 (2C), 68.3, 68.2, 49.4, 49.3, 48.6, 48.5, 47.0, 46.9, 43.4, 43.3, 39.5 (2C), 39.4, 39.3, 37.0 (2C), 36.3 (2C), 36.1, 36.0, 35.7, 35.6, 32.3, 32.2, 30.2 (2C), 30.0 (2C), 29.7 (2C), 28.1, 28.0, 25.7, 25.6, 24.0, 23.9, 22.9 (2C), 21.7, 21.1 (2C), 20.9, 20.8 (2C), 17.9, 17.8 (2C), 17.7 and 15.9 (2C); LC-MS (ESI): *m/z* 644 $[M+H+Na]^+$, 561 $[M-OAc]^+$; purity (LC-MS): 98% (t_R = 3.06 min.)

N-(1-(pyrazin-2-yl)ethyl)fusidic acid amide (1.14)

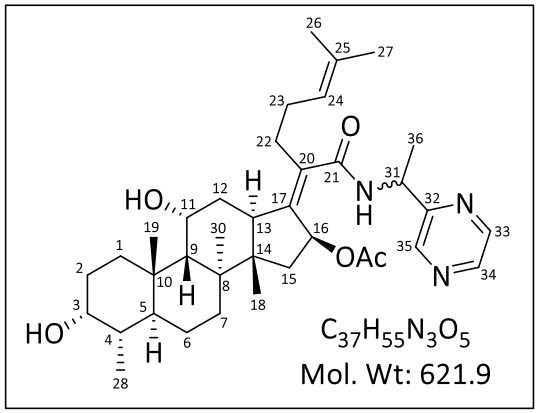

White powder (0.047 g obtained from 0.100 g of **1.0**, 40%); *R*f 0.3 (EtOAc); a 3:2 mixture of diastereomers; **Major product**: ^{1}H NMR (400 MHz, $CDCl_3$) δ 8.62-8.43 (m, 3H, H-33, H-34 and H-35), 6.80 (d, *J* = 8.2 Hz, 1H, NH), 5.47 (d, *J* = 8.2 Hz, 1H, H-16), 5.23 (m, 1H, H-31), 5.11 (m, 1H, H-24), 4.32 (m, 1H, H-11), 3.73 (m, 1H, H-3), 2.99 (m, 1H, H-13), 2.55-2.40 (m, 1H, H-22), 2.41-2.32 (m, 1H, H-22), 2.32-2.22 (m, 1H, H-12), 2.21-1.93 (m, 5H, H-1, H-5, H-15 and 2×H-23), 1.89-1.67 (m, 4H, 2×H-2, H-7 and H-12), 1.77 (s, 3H, OAc),1.59 (s, 3H, CH_3-27), 1.60-1.48 (m, 4H, H-1, H-4, H-6 and H-9), 1.50-1.42 (m, 6H, CH_3-26 and CH_3-36), 1.35 (s, 3H, CH_3-30), 1.21-1.15 (m, 1H, H-15), 1.15-1.00 (m, 2H, H-6 and H-7), 0.95 (s, 3H, CH_3-19), 0.95-0.87 (m, 6H, CH_3-18 and CH_3-28); ^{13}C NMR (101 MHz, $CDCl_3$) δ 170.3, 170.0, 156.1, 143.7, 143.3, 143.1, 141.7, 135.5, 132.4, 123.4, 74.0, 71.3, 68.3, 49.3, 48.5, 47.1, 43.2, 39.5, 39.2, 37.1, 36.3, 36.1, 35.7, 32.3, 30.3, 30.0, 29.5, 28.0, 25.7, 24.0, 22.8, 20.8 (2C), 20.7, 17.9, 17.8 and 15.9; **Minor product**: ^{1}H NMR (400 MHz, $CDCl_3$) δ 8.62-8.43 (m, 3H, H-33, H-34 and H-35), 6.56 (d, *J* = 7.6 Hz, 1H, NH), 5.74 (d, *J* = 8.2 Hz, 1H, H-16), 5.15 (m, 1H, H-31), 5.02 (m, 1H, H-24), 4.32 (m, 1H, H-11), 3.73 (m, 1H, H-3), 2.99 (m, 1H, H-13), 2.55-2.40 (m, 1H, H-22), 2.41-2.32 (m, 1H, H-22), 2.32-2.22 (m, 1H, H-12), 2.21-1.93 (m, 5H, H-1, H-5, H-15 and 2×H-23), 1.96 (s, 3H, OAc), 1.89-1.67 (m, 4H, 2×H-2, H-7 and H-12), 1.66 (s, 3H, CH_3-27), 1.60-1.48 (m, 4H, H-1, H-4, H-6 and H-9), 1.50-1.42 (m, 6H, CH_3-26 and CH_3-36), 1.37 (s, 3H, CH_3-30), 1.33-1.27 (m, 1H, H-15), 1.15-1.00 (m, 2H, H-6 and H-7), 0.96 (s, 3H, CH_3-19), 0.95-0.87 (m, 6H, CH_3-18 and CH_3-28); ^{13}C NMR (101 MHz, $CDCl_3$) δ 170.8, 170.7, 157.0, 143.9, 143.7, 143.3, 141.7, 135.5, 132.3, 123.3, 74.1, 71.3, 68.3, 49.3, 48.6, 47.7, 43.4, 39.5, 39.4, 37.1, 36.3, 36.1, 35.7, 32.4, 30.3, 30.0, 29.5, 27.9, 25.6, 24.0, 22.8, 21.5, 21.2, 20.8, 17.8, 17.7 and 15.9; LC-MS (ESI): *m/z* 644 $[M+Na]^+$, 562 $[M-OAc]^+$; purity (LC-MS): 98% (t_R = 3.10 min.)

N-(1-(phenyl)cyclopropyl)fusidic acid amide (1.15)

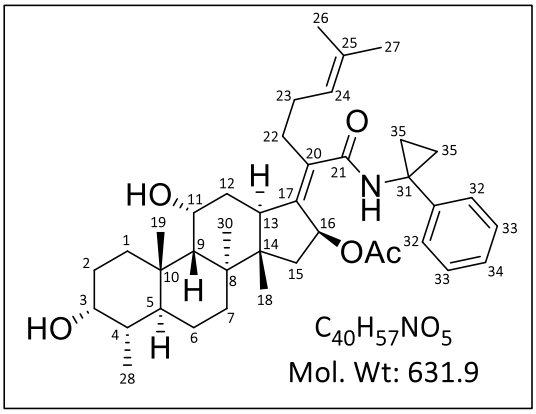

White powder (0.017 g obtained from 0.050 g of **1.0**, 28%); *R*f 0.6 (60% EtOAc:DCM); Mp 199-201 ^{o}C; ^{1}H NMR (400 MHz, $CDCl_3$) δ 7.36-7.31 (m, 2H, 2×H-33), 7.29-7.23 (m, 2H, 2×H-32), 7.21-7.15 (m, 1H, H-34), 6.13 (s, 1H, NH), 5.59 (d, *J* = 7.8 Hz, 1H, H-16), , 5.07 (m, 1H, H-24), 5.00-4.94 (m, 1H, H-31), 4.32 (m, 1H, H-11), 3.74 (m, 1H, H-3), 2.98 (m, 1H, H-13), 2.53-2.40 (m, 1H, H-22), 2.36-2.29 (m, 1H, H-22), 2.30-2.23 (m, 1H, H-12), 2.21-1.96 (m, 5H, H-1, H-5, H-15 and 2×H-23), 1.86-1.69 (m, 4H, 2×H-2, H-7 and H-12), 1.80 (s, 3H, OAc), 1.66 (s, 3H, CH_3-27), 1.62-1.47 (m, 4H, H-1, H-4, H-6 and H-9), 1.55 (s, 3H, CH_3-26), 1.36 (s, 3H, CH_3-30), 1.34-1.00 (m, 3H, H-6, H-7 and H-15), 0.97 (s, 3H, CH_3-19), 0.94-0.78 (m, 10H, CH_3-18, CH_3-28 and 4×H-35); ^{13}C NMR (101 MHz, $CDCl_3$) δ 171.1, 170.7, 142.4, 141.3, 136.3, 132.5, 128.4 (2C), 126.8 (2C), 126.7, 123.3, 74.3, 71.4, 68.4, 49.2, 48.5, 43.4, 39.5, 39.4, 37.2, 36.3, 36.1, 35.7, 35.3, 32.6, 30.4, 30.0, 29.9, 28.1, 25.7, 24.2, 22.6, 21.1, 20.7, 18.1, 17.8, 17.0, 16.2 and 15.9; LC-MS (ESI): *m/z* 572 $[M\text{-}OAc]^+$; purity (LC-MS): 98% (t_R = 3.07 min.)

N-((*S*)-1-(cyclohexyl)ethyl)fusidic acid amide (1.16)

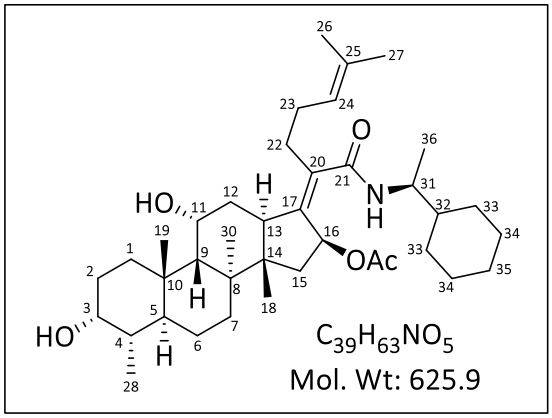

White powder (0.043 g obtained from 0.100 g of **1.0**, 35%); *R*f 0.6 (60% EtOAc:DCM); Mp 159-161 ^{o}C; ^{1}H NMR (400 MHz, $CDCl_3$) δ 5.58 (d, *J* = 8.1 Hz, 1H, H-16), 5.28 (d, *J* = 8.8 Hz, 1H, NH), 5.08 (m, 1H, H-24), 4.31 (m, 1H, H-11), 3.79-3.71 (m, 1H, H-31), 3.74 (m, 1H, H-3), 2.96 (m, 1H, H-13), 2.50-2.40 (m, 1H, H-22), 2.36-2.29 (m, 1H, H-22), 2.29-2.25 (m, 1H, H-12), 2.28-2.00 (m, 5H, H-1, H-5, H-15 and 2×H-23), 1.99 (s, 3H, OAc), 1.91-1.68 (m, 6H, 2×H-2, H-7, H-12, and 2×H-34), 1.66 (s, 3H, CH_3-27), 1.64-1.55 (m, 4H, H-4, H-6, H-9 and H-35), 1.58 (s, 3H, CH_3-26), 1.49 (m, 1H, H-1), 1.36 (s, 3H, CH_3-30), 1.35 (m, 1H, H-32), 1.30-1.24 (m, 1H, H-15), 1.23-1.05 (m, 6H, H-6, H-7, and 4×H-33), 1.05-0.93 (m, 3H,

2×H-34 and H-35), 1.00 (d, *J* = 6.7 Hz, 3H, CH_3-36), 0.95 (s, 3H, CH_3-19), 0.92 (s, 3H, CH_3-18), 0.89 (d, *J* = 6.7 Hz, 3H, CH_3-28); ^{13}C NMR (101 MHz, $CDCl_3$) δ 170.9, 170.5, 140.4, 136.4, 132.3, 123.3, 74.0, 71.4, 68.3, 49.5, 49.3, 48.5, 43.2, 42.9, 39.5, 39.4, 37.0, 36.3, 36.1, 35.6, 32.4, 30.3, 30.0, 29.7, 29.3, 28.6, 28.0, 26.4, 26.2 (2C), 25.7, 24.0, 22.8, 21.3, 20.8, 17.8, 17.8, 16.8 and 15.9; LC-MS (ESI): *m/z* 648 $[M+Na]^+$, 566 $[M-OAc]^+$; purity (LC-MS): 98% (t_R = 3.21 min.)

N-((*R*)-1-(cyclohexyl)ethyl)fusidic acid amide (1.17)

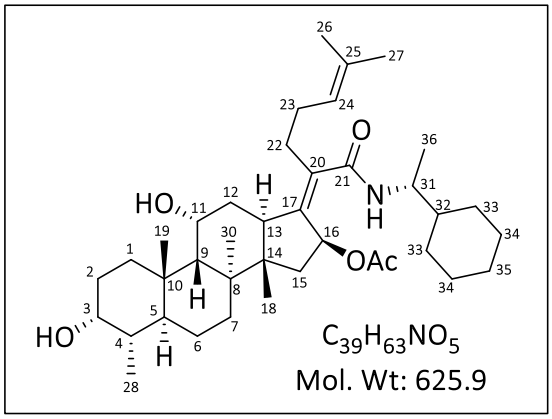

White powder (0.026 g obtained from 0.050 g of **1.0**, 43%); *R*f 0.5 (60% EtOAc:DCM); Mp 182-184 °C; ^{1}H NMR (400 MHz, $CDCl_3$) δ 5.58 (d, *J* = 8.1 Hz, 1H, H-16), 5.28 (d, *J* = 8.8 Hz, 1H, NH), 5.08 (m, 1H, H-24), 4.31 (m, 1H, H-11), 3.79-3.71 (m, 1H, H-31), 3.74 (m, 1H, H-3), 2.96 (m, 1H, H-13), 2.50-2.40 (m, 1H, H-22), 2.36-2.29 (m, 1H, H-22), 2.29-2.25 (m, 1H, H-12), 2.28-2.00 (m, 5H, H-1, H-5, H-15 and 2×H-23), 1.99 (s, 3H, OAc), 1.91-1.68 (m, 6H, 2×H-2, H-7, H-12, and 2×H-34), 1.66 (s, 3H, CH_3-27), 1.64-1.55 (m, 4H, H-4, H-6, H-9 and H-35), 1.58 (s, 3H, CH_3-26), 1.49 (m, 1H, H-1), 1.36 (s, 3H, CH_3-30), 1.35 (m, 1H, H-32), 1.30-1.24 (m, 1H, H-15), 1.24-1.08 (m, 6H, H-6, H-7, and 4×H-33), 1.05-0.93 (m, 3H, 2×H-34 and H-35), 1.00 (d, *J* = 6.7 Hz, 3H, CH_3-36), 0.95 (s, 3H, CH_3-19), 0.92 (s, 3H, CH_3-18), 0.89 (d, *J* = 6.7 Hz, 3H, CH_3-28); ^{13}C NMR (101 MHz, $CDCl_3$) δ 170.6, 170.5, 141.0, 136.5, 132.4, 123.4, 74.8, 71.4, 68.4, 49.5, 49.3, 48.6, 43.2, 42.7, 39.6, 39.4, 37.1, 36.2 (2C), 35.8, 32.4, 30.3, 30.1, 30.0, 29.6, 28.4, 28.1, 26.4, 26.3, 26.1, 25.7, 24.1, 22.7, 21.3, 20.8, 18.2, 17.8, 17.3 and 15.9; LC-MS (ESI): *m/z* 648 $[M+Na]^+$, 566 $[M-OAc]^+$; purity (LC-MS): 98% (t_R = 3.22 min.)

N-(2-methoxyphenyl)fusidic acid amide (1.18)

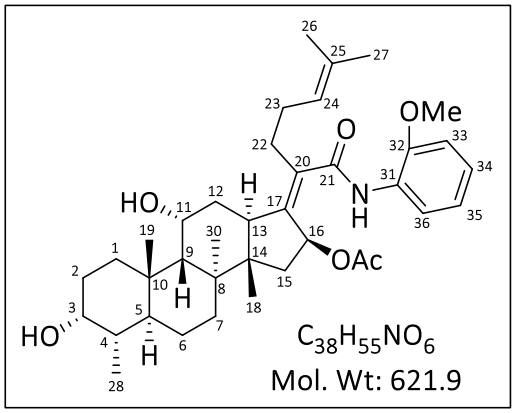

White powder (0.061 g obtained from 0.250 g of **1.0**, 20%); *R*f 0.6 (60% EtOAc:DCM); Mp 322-324 ^{o}C; ^{1}H NMR (400 MHz, $CDCl_3$) δ 8.40 (dd, *J* = 1.7, 7.9 Hz, 1H, H-36), 7.75 (s, 1H, NH), 7.01 (td, *J* = 1.7, 7.7 Hz, 1H, H-34), 6.92 (td, *J* = 1.4, 7.7 Hz, 1H, H-35), 6.85 (dd, *J* = 1.4, 8.0 Hz, 1H, H-33), 5.74 (d, *J* = 8.6 Hz, 1H, H-16), 5.11 (m, 1H, H-24), 4.36 (m, 1H, H-11), 3.88 (s, 3H, OMe), 3.75 (m, 1H, H-3), 3.06 (m, 1H, H-13), 2.63-2.51 (m, 1H, H-22), 2.45-2.39 (m, 1H, H-22), 2.36-2.28 (m, 1H, H-12), 2.26-2.05 (m, 5H, H-1, H-5, H-15 and 2×H-23), 1.93-1.71 (m, 4H, 2×H-2, H-7 and H-12), 1.68 (s, 3H, OAc), 1.65 (s, 3H, CH_3-27), 1.63-1.49 (m, 4H, H-1, H-4, H-6 and H-9), 1.59 (s, 3H, CH_3-26), 1.41 (s, 3H, CH_3-30), 1.28-1.22 (m, 1H, H-15), 1.17-1.06 (m, 2H, H-6 and H-7), 0.98 (s, 3H, CH_3-19), 0.94 (s, 3H, CH_3-18), 0.92 (d, *J* = 6.9 Hz, 3H, CH_3-28); ^{13}C NMR (101 MHz, $CDCl_3$) δ 170.5, 169.3, 147.8, 142.2, 135.5, 132.5, 127.7, 123.5, 123.3, 121.0, 119.3, 110.0, 73.8, 71.3, 68.4, 55.8, 49.4, 48.5, 43.1, 39.5, 39.4, 37.1, 36.3, 36.2, 35.7, 32.5, 30.3, 30.0, 29.4, 28.1, 25.6, 24.2, 22.8, 20.8, 20.5, 17.8, 17.7 and 15.9; LC-MS (ESI): *m/z* 644 $[M+Na]^+$ 562 $[M-OAc]^+$; purity (LC-MS): 98% (t_R = 3.24 min.)

N-(3-methoxyphenyl)fusidic acid amide (1.19)

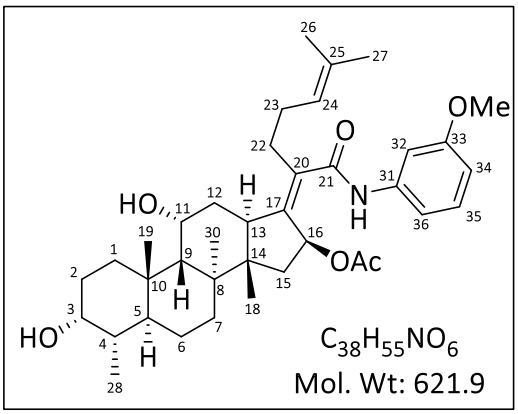

White powder (0.058 g obtained from 0.250 g of **1.0**, 19%); *R*f 0.6 (60% EtOAc:DCM); Mp 322-324 ^{o}C; ^{1}H NMR (400 MHz, $CDCl_3$) δ 7.27 (dd, *J* = 1.9, 2.4 Hz, 1H, H-32), 7.18 (t, *J* = 8.1 Hz, 1H, H-35), 7.12 (s, 1H, NH), 6.96 (dd, *J* = 1.9, 7.8 Hz, 1H, H-36), 6.64 (dd, *J* = 2.4, 8.2 Hz, 1H, H-34), 5.75 (d, *J* = 8.6 Hz, 1H, H-16), 5.11 (m, 1H, H-24), 4.36 (m, 1H, H-11), 3.79 (s, 3H, OMe), 3.75 (m, 1H, H-3), 3.05 (m, 1H, H-13), 2.63-2.51 (m, 1H, H-22), 2.47-2.37 (m, 1H, H-22), 2.34-2.26 (m, 1H, H-12), 2.26-2.05 (m, 5H, H-1, H-5, H-15 and 2×H-23), 1.91-1.71 (m, 4H, 2×H-2, H-7 and H-12), 1.76 (s, 3H, OAc), 1.67 (s, 3H, CH_3-27), 1.63-1.49 (m,

4H, H-1, H-4, H-6 and H-9), 1.60 (s, 3H, CH_3-26), 1.39 (s, 3H, CH_3-30), 1.28-1.22 (m, 1H, H-15), 1.17-1.06 (m, 2H, H-6 and H-7), 0.98 (s, 3H, CH_3-19), 0.95 (s, 3H, CH_3-18), 0.92 (d, *J* = 6.8 Hz, 3H, CH_3-28); ^{13}C NMR (101 MHz, $CDCl_3$) δ 170.6, 169.4, 160.1, 142.5, 139.1, 135.3, 132.7, 129.6, 123.2, 111.7, 110.1, 105.2, 73.8, 71.4, 68.3, 55.3, 49.4, 48.7, 43.1, 39.5, 39.3, 37.1, 36.3, 36.2, 35.7, 32.4, 30.3, 30.0, 29.4, 28.1, 25.7, 24.1, 22.8, 20.9, 20.8, 17.9, 17.8 and 15.9; LC-MS (ESI): *m/z* 644 $[M+Na]^+$ 562 $[M-OAc]^+$; purity (LC-MS): 98% (t_R = 3.22 min.)

N-(4-methoxyphenyl)fusidic acid amide (1.20)

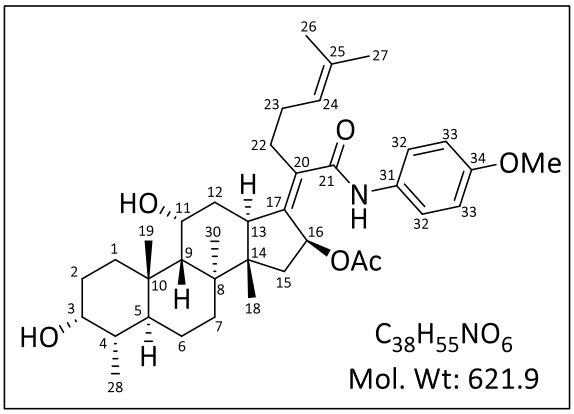

White powder (0.062 g obtained from 0.250 g of **1.0**, 21%); *R*f 0.5 (60% EtOAc:DCM); Mp 262-264 ^oC; ^{1}H NMR (400 MHz, $CDCl_3$) δ 7.40 (d, *J* = 8.9 Hz, 2×H, H-32), 7.08 (s, 1H, NH), 6.83 (d, *J* = 8.9 Hz, 2×H, H-33), 5.77 (d, *J* = 8.5 Hz, 1H, H-16), 5.12 (m, 1H, H-24), 4.35 (m, 1H, H-11), 3.77 (s, 3H, OMe), 3.74 (m, 1H, H-3), 3.03 (m, 1H, H-13), 2.62-2.51 (m, 1H, H-22), 2.50-2.37 (m, 1H, H-22), 2.34-2.26 (m, 1H, H-12), 2.26-2.07 (m, 5H, H-1, H-5, H-15 and 2×H-23), 1.91-1.71 (m, 4H, 2×H-2, H-7 and H-12), 1.76 (s, 3H, OAc), 1.67 (s, 3H, CH_3-27), 1.64-1.47 (m, 4H, H-1, H-4, H-6 and H-9), 1.60 (s, 3H, CH_3-26), 1.39 (s, 3H, CH_3-30), 1.28-1.22 (m, 1H, H-15), 1.17-1.06 (m, 2H, H-6 and H-7), 0.98 (s, 3H, CH_3-19), 0.94 (s, 3H, CH_3-18), 0.92 (d, *J* = 6.8 Hz, 3H, CH_3-28); ^{13}C NMR (101 MHz, $CDCl_3$) δ 170.7, 169.2, 156.3, 142.1, 135.5, 132.6, 131.0, 123.3, 121.3 (2C), 114.1 (2C), 73.8, 71.4, 68.3, 55.4, 49.4, 48.7, 43.1, 39.5, 39.3, 37.1, 36.3, 36.1, 35.7, 32.4, 30.3, 30.0, 29.4, 28.1, 25.7, 24.0, 22.8, 20.9, 20.8, 17.9, 17.8 and 15.9; LC-MS (ESI): *m/z* 644 $[M+Na]^+$ 562 $[M-OAc]^+$; purity (LC-MS): 98% (t_R = 3.22 min.)

N-(4-methylphenyl)fusidic acid amide (1.21)

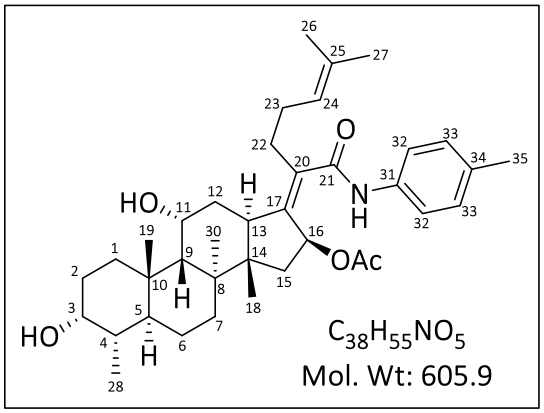

White powder (0.010 g obtained from 0.050 g of **1.0**, 16%); *R*f 0.6 (60% EtOAc:DCM); Mp 322-324 ^{o}C; ^{1}H NMR (400 MHz, MeOH-d_4) δ 7.43 (d, *J* = 8.4 Hz, 2H, 2×H-32), 7.09 (d, *J* = 8.2 Hz, 2H, 2×H-33), 5.80 (d, *J* = 8.6 Hz, 1H, H-16), 5.16 (m, 1H, H-24), 4.32 (m, 1H, H-11), 3.66 (m, 1H, H-3), 3.09 (m, 1H, H-13), 2.72-2.63 (m, 1H, H-22), 2.38-2.34 (m, 1H, H-22), 2.33-2.19 (m, 1H, H-12), 2.28 (s, 3H, CH_3-35), 2.19-2.09 (m, 5H, H-1, H-5, H-15 and 2×H-23), 1.91-1.70 (m, 4H, 2×H-2, H-7 and H-12), 1.67 (s, 3H, OAc), 1.64 (s, 3H, CH_3-27), 1.61-1.44 (m, 4H, H-1, H-4, H-6 and H-9), 1.59 (s, 3H, CH_3-26), 1.40 (s, 3H, CH_3-30), 1.22-1.16 (m, 1H, H-15), 1.17-1.07 (m, 2H, H-6 and H-7), 1.00 (s, 3H, CH_3-19), 0.95 (s, 3H, CH_3-18), 0.89 (d, *J* = 6.8 Hz, 3H, CH_3-28); ^{13}C NMR (101 MHz, MeOH-d_4) δ 172.6, 172.5, 143.7, 137.3, 135.8, 134.9, 133.3, 130.1 (2C), 124.5, 121.3 (2C), 75.5, 72.4, 68.6, 50.8, 49.9, 44.4, 40.7, 40.3, 38.3, 37.8, 37.4, 36.8, 32.9, 31.0 (2C), 30.6, 28.8, 25.9, 23.8 (2C), 22.4, 21.0, 20.9, 17.9 (2C) and 16.4; LC-MS (ESI): *m/z* 629 $[M+Na]^+$ 546 $[M-OAc]^+$; purity (LC-MS): 98% (t_R = 3.27 min.)

N-(4-fluorophenyl)fusidic acid amide (1.22)

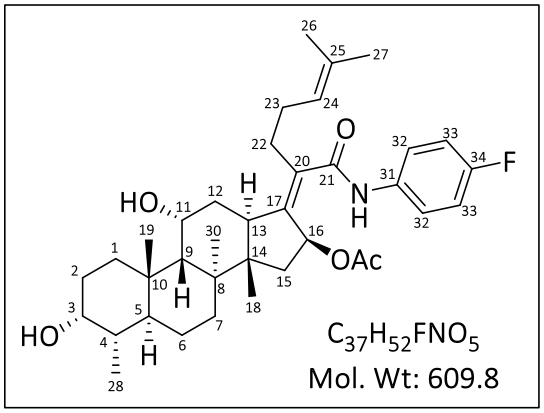

White powder (0.021 g obtained from 0.050 g of **1.0**, 35%); *R*f 0.5 (60% EtOAc:DCM); Mp 322-324 ^{o}C; ^{1}H NMR (400 MHz, $CDCl_3$) δ 7.47 (dd, *J* = 5.4, 8.6 Hz, 2H, 2×H-32), 7.13 (s, 1H, NH), 6.99 (t, *J* = 8.7 Hz, 2H, 2×H-33), 5.78 (d, *J* = 8.5 Hz, 1H, H-16), 5.12 (m, 1H, H-24), 4.36 (m, 1H, H-11), 3.76 (m, 1H, H-3), 3.06 (m, 1H, H-13), 2.64-2.53 (m, 1H, H-22), 2.49-2.38 (m, 1H, H-22), 2.35-2.27 (m, 1H, H-12), 2.26-2.01 (m, 5H, H-1, H-5, H-15 and 2×H-23), 1.91-1.71 (m, 4H, 2×H-2, H-7 and H-12), 1.74 (s, 3H, OAc), 1.67 (s, 3H, CH_3-27), 1.64-1.47 (m, 4H, H-1, H-4, H-6 and H-9), 1.60 (s, 3H, CH_3-26), 1.40 (s, 3H, CH_3-30), 1.28-1.22 (m, 1H, H-15), 1.17-1.06 (m, 2H, H-6 and H-7), 0.99 (s, 3H, CH_3-19), 0.95 (s, 3H, CH_3-18), 0.93 (d, *J* =

6.8 Hz, 3H, CH_3-28); ^{13}C NMR (101 MHz, $CDCl_3$) δ 170.6, 169.3, 159.1 (d, *J* = 244.4 Hz, C-34), 142.6, 135.2, 133.9, 132.8, 123.2, 121.2 (d, *J* = 7.7 Hz, 2×C-32), 115.6 (d, *J* = 22.4 Hz, 2×C-33), 73.8, 71.4, 68.3, 49.4, 48.7, 43.2, 39.5, 39.3, 37.1, 36.3, 36.2, 35.7, 32.4, 30.3, 30.0, 29.4, 28.1, 25.7, 24.1, 22.8, 20.8, 20.7, 17.9, 17.8 and 15.9; LC-MS (ESI): *m/z* 550 $[M\text{-}OAc]^+$; purity (LC-MS): 98% (t_R = 3.23 min.)

N-(benzyl)fusidic acid amide (1.25)

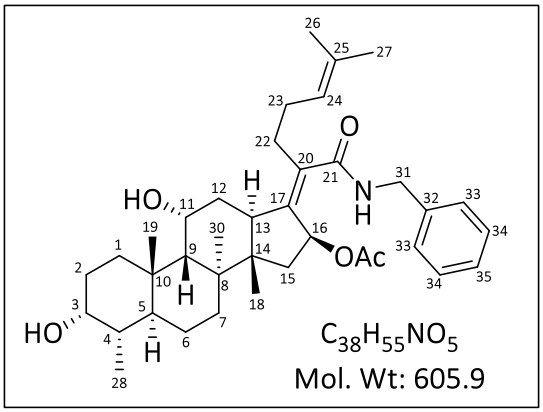

White powder (0.042 g obtained from 0.050 g of **1.0**, 70%); R*f* 0.6 (60% EtOAc:DCM); Mp 182-184 ^oC; ^1H NMR (400 MHz, $CDCl_3$) δ 7.35-7.27 (m, 5H, 2×H-33, 2×H-34 and H-35), 5.73 (d, *J* = 8.0 Hz, 1H, H-16), 5.39 (dd, *J* = 4.7, 5.6 Hz, 1H, NH), 5.07 (m, 1H, H-24), 4.59 (dd, *J* = 6.4, 14.4 Hz, 1H, H-31b), 4.32 (m, 1H, H-11), 4.11 (dd, *J* = 4.2, 14.4 Hz, 1H, H-31a), 3.73 (m, 1H, H-3), 2.97 (m, 1H, H-13), 2.56-2.46 (m, 1H, H-22), 2.43-2.31 (m, 1H, H-22), 2.29-2.21 (m, 1H, H-12), 2.18-1.99 (m, 5H, H-1, H-5, H-15 and 2×H-23), 1.98 (s, 3H, OAc), 1.89-1.67 (m, 4H, 2×H-2, H-7 and H-12), 1.63 (s, 3H, CH_3-27), 1.62-1.45 (m, 4H, H-1, H-4, H-6 and H-9), 1.55 (s, 3H, CH_3-26), 1.36 (s, 3H, CH_3-30), 1.30-1.25 (m, 1H, H-15), 1.17-1.03 (m, 2H, H-6 and H-7), 0.97 (s, 3H, CH_3-19), 0.94 (s, 3H, CH_3-18), 0.91 (d, *J* = 6.8 Hz, 3H, CH_3-28); ^{13}C NMR (101 MHz, $CDCl_3$) δ 171.1, 170.8, 141.8, 137.9, 135.6, 132.4, 128.8 (2C), 128.1 (2C), 127.6, 123.3, 73.7, 71.4, 68.3, 49.3, 48.7, 43.9, 43.2, 39.5, 39.3, 37.1, 36.2, 36.2, 35.7, 32.4, 30.3, 30.0, 29.4, 28.0, 25.6, 24.0, 22.7, 21.0, 20.8, 17.8, 17.8 and 15.9; LC-MS (ESI): *m/z* 628 $[M+Na]^+$, 546 $[M\text{-}OAc]^+$; purity (LC-MS): 98% (tr = 3.23 min.)

N-(4-fluorobenzyl)fusidic acid amide (1.26)

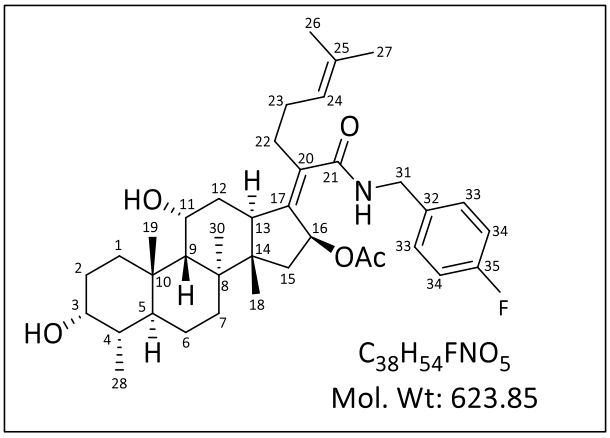

White powder (0.031 g obtained from 0.050 g of **1.0**, 50%); *R*f 0.5 (60% EtOAc:DCM); Mp 182-184 °C; ^{1}H NMR (400 MHz, $CDCl_3$) δ 7.25 (m, 2H, 2×H-33), 7.00 (t, *J* = 8.6 Hz, 2H, 2×H-34), 5.74 (d, *J* = 8.5 Hz, 1H, H-16), 5.39 (m, 1H, NH), 5.06 (m, 1H, H-24), 4.55 (dd, *J* = 6.5, 14.3 Hz, 1H, H-31b), 4.32 (m, 1H, H-11), 4.07 (dd, *J* = 4.2, 14.4 Hz, 1H, H-31a), 3.73 (m, 1H, H-3), 2.97 (m, 1H, H-13), 2.55-2.44 (m, 1H, H-22), 2.40-2.31 (m, 1H, H-22), 2.29-2.20 (m, 1H, H-12), 2.18-2.00 (m, 5H, H-1, H-5, H-15 and 2×H-23), 1.98 (s, 3H, OAc), 1.89-1.67 (m, 4H, 2×H-2, H-7 and H-12), 1.63 (s, 3H, CH_3-27), 1.62-1.45 (m, 4H, H-1, H-4, H-6 and H-9), 1.54 (s, 3H, CH_3-26), 1.35 (s, 3H, CH_3-30), 1.28-1.23 (m, 1H, H-15), 1.16-1.01 (m, 2H, H-6 and H-7), 0.97 (s, 3H, CH_3-19), 0.94 (s, 3H, CH_3-18), 0.91 (d, *J* = 6.8 Hz, 3H, CH_3-28); ^{13}C NMR (101 MHz, $CDCl_3$) δ 171.1, 170.7, 162.2 (d, *J* = 246.1 Hz, C-35), 141.9, 135.5, 133.8, 132.5, 129.8 (d, *J* = 8.1 Hz, 2×C-33), 123.3, 115.5 (d, *J* = 21.5, Hz, 2×C-34), 73.7, 71.4, 68.3, 49.3, 48.7, 43.3, 43.1, 39.5, 39.3, 37.1, 36.2 (2C), 35.6, 32.5, 30.3, 30.0, 29.4, 28.0, 25.6, 24.1, 22.7, 21.0, 20.7, 17.8 (2C) and 15.9; LC-MS (ESI): *m/z* 646 $[M+Na]^+$, 564 $[M-OAc]^+$; purity (LC-MS): 98% (t_R = 3.24 min.)

N-(4-sulfamoylbenzyl)fusidic acid amide (1.27)

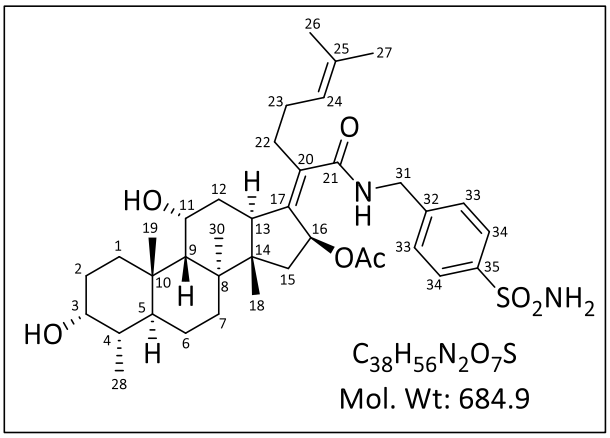

White powder (0.007 g obtained from 0.050 g of **1.0**, 10%); *R*f 0.5 (EtOAc); Mp 182-184 °C; ^{1}H NMR (400 MHz, MeOH-d_4) δ 7.83 (d, *J* = 8.3 Hz, 2H, 2×H-34), 7.46 (d, *J* = 8.3, 2H, 2×H-33), 5.79 (d, *J* = 8.4 Hz, 1H, H-16), 5.11 (m, 1H, H-24), 4.53 (d, *J* = 15.0 Hz, 1H, H-31b), 4.30 (m, 1H, H-11), 4.15 (d, *J* = 15.0 Hz, 1H, H-31a), 3.64 (m, 1H, H-3), 3.04 (m, 1H, H-13), 2.65-2.52 (m, 2H, 2×H-22), 2.30-2.19 (m, 1H, H-12), 2.19-2.01 (m, 5H, H-1, H-5, H-15 and 2×H-23), 1.91-1.69 (m, 4H, 2×H-

2, H-7 and H-12), 1.90 (s, 3H, OAc), 1.64 (s, 3H, CH_3-27), 1.63-1.43 (m, 4H, H-1, H-4, H-6 and H-9), 1.55 (s, 3H, CH_3-26), 1.38 (s, 3H, CH_3-30), 1.24-1.18 (m, 1H, H-15), 1.17-1.07 (m, 2H, H-6 and H-7), 0.99 (s, 3H, CH_3-19), 0.94 (s, 3H, CH_3-18), 0.89 (d, *J* = 6.7 Hz, 3H, CH_3-28); ^{13}C NMR (101 MHz, MeOH-d_4) δ 174.3, 172.5, 144.6, 144.0, 143.7, 135.5, 133.3, 129.4 (2C), 127.4 (2C), 124.4, 75.3, 72.4, 68.6, 50.8, 49.9, 44.6, 43.9, 40.7, 40.3, 38.2, 37.9, 37.3, 36.9, 32.9, 31.0 (2C), 30.6, 28.8, 25.8, 23.8, 23.7, 22.3, 21.1, 17.9 (2C) and 16.4; LC-MS (ESI): *m/z* 625 $[M\text{-}OAc]^+$; purity (LC-MS): 98% (t_R = 3.01 min.)

N-(4-hydroxybenzyl)fusidic acid amide (1.28)

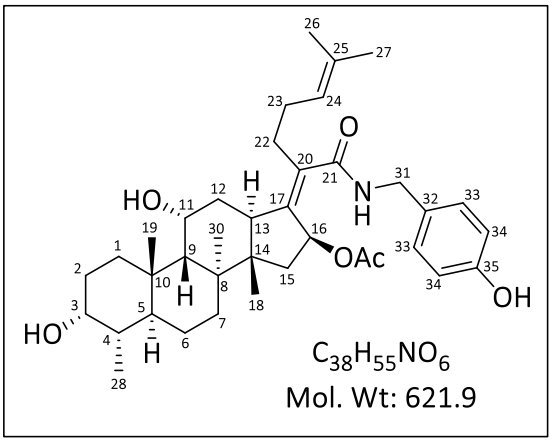

Brown powder (0.011 g obtained from 0.050 g of **1.0**, 17%); *R*f 0.3 (60% EtOAc:DCM); Mp 182-184 ^{o}C; ^{1}H NMR (400 MHz, MeOH-d_4) δ 7.11 (d, *J* = 8.5 Hz, 2H, 2×H-33), 6.70 (d, *J* = 8.5, 2H, 2×H-34), 5.76 (d, *J* = 8.4 Hz, 1H, H-16), 5.09 (m, 1H, H-24), 4.37 (d, *J* = 14.3 Hz, 1H, H-31b), 4.30 (m, 1H, H-11), 4.15 (d, *J* = 14.3 Hz, 1H, H-31a), 3.65 (m, 1H, H-3), 3.02 (m, 1H, H-13), 2.61-2.51 (m, 2H, 2×H-22), 2.28-2.19 (m, 1H, H-12), 2.19-2.00 (m, 5H, H-1, H-5, H-15 and 2×H-23), 1.91 (s, 3H, OAc), 1.89-1.70 (m, 4H, 2×H-2, H-7 and H-12), 1.64 (s, 3H, CH_3-27), 1.61-1.43 (m, 4H, H-1, H-4, H-6 and H-9), 1.54 (s, 3H, CH_3-26), 1.37 (s, 3H, CH_3-30), 1.24-1.16 (m, 1H, H-15), 1.17-1.07 (m, 2H, H-6 and H-7), 0.99 (s, 3H, CH_3-19), 0.94 (s, 3H, CH_3-18), 0.88 (d, *J* = 6.7 Hz, 3H, CH_3-28); ^{13}C NMR (101 MHz, MeOH-d_4) δ 174.0, 172.5, 158.0, 143.2, 135.7, 133.1, 130.5, 130.4 (2C), 124.5, 116.4 (2C), 75.3, 72.4, 68.6, 50.8, 49.9, 44.4, 44.0, 40.7, 40.3, 38.2, 37.8, 37.3, 36.9, 32.9, 31.0 (2C), 30.5, 28.7, 25.8, 23.9, 23.8, 22.4, 21.1, 17.9 (2C) and 16.4; LC-MS (ESI): *m/z* 644 $[M+Na]^+$, 562 $[M\text{-}OAc]^+$; purity (LC-MS): 98% (t_R = 3.09 min.)

N-(4-methylbenzyl)fusidic acid amide (1.29)

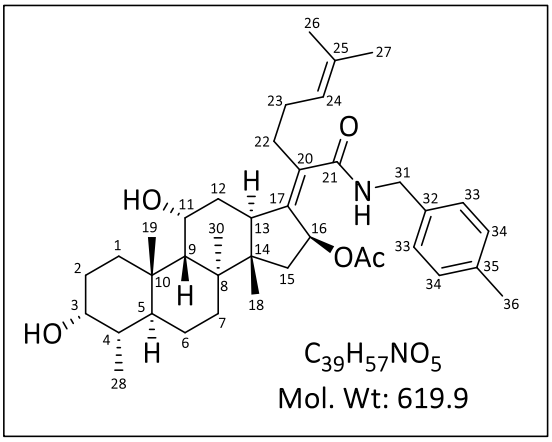

White powder (0.035 g obtained from 0.050 g of **1.0**, 56%); *R*f 0.6 (60% EtOAc:DCM); Mp 182-184 ^{o}C; ^{1}H NMR (400 MHz, $CDCl_3$) δ 7.16 (d, *J* = 8.1 Hz, 2H, 2×H-33), 7.12 (d, *J* = 8.0 Hz, 2H, 2×H-34), 5.72 (d, *J* = 8.4 Hz, 1H, H-16), 5.41 (m, 1H, NH), 5.07 (m, 1H, H-24), 4.53 (dd, *J* = 4.1, 14.2 Hz, 1H, H-31b), 4.32 (m, 1H, H-11), 4.07 (dd, *J* = 4.2, 14.2 Hz, 1H, H-31a), 3.73 (m, 1H, H-3), 2.96 (m, 1H, H-13), 2.56-2.46 (m, 1H, H-22), 2.42-2.34 (m, 1H, H-22), 2.32 (s, 3H, CH_3-36), 2.30-2.22 (m, 1H, H-12), 2.20-2.00 (m, 5H, H-1, H-5, H-15 and 2×H-23), 1.98 (s, 3H, OAc), 1.91-1.67 (m, 4H, 2×H-2, H-7 and H-12), 1.63 (s, 3H, CH_3-27), 1.62-1.45 (m, 4H, H-1, H-4, H-6 and H-9), 1.55 (s, 3H, CH_3-26), 1.35 (s, 3H, CH_3-30), 1.28-1.23 (m, 1H, H-15), 1.16-1.01 (m, 2H, H-6 and H-7), 0.96 (s, 3H, CH_3-19), 0.94 (s, 3H, CH_3-18), 0.91 (d, *J* = 6.8 Hz, 3H, CH_3-28); ^{13}C NMR (101 MHz, $CDCl_3$) δ 171.1, 170.7, 141.7, 137.3, 135.6, 134.7, 132.4, 129.4 (2C), 128.1 (2C), 123.3, 73.7, 71.4, 68.3, 49.3, 48.7, 43.7, 43.2, 39.5, 39.3, 37.1, 36.2 (2C), 35.7, 32.4, 30.3, 30.0, 29.4, 28.0, 25.6, 24.0, 22.7, 21.0 (2C), 20.8, 17.8 (2C) and 15.9; LC-MS (ESI): *m/z* 642 $[M+Na]^+$, 560 $[M-OAc]^+$; purity (LC-MS): 98% (t_R = 3.31 min.)

4.6.3 General synthetic procedure for the synthesis of compound 3.0

A mixture of 4-hydroxyaniline (1.0 eq.) and acetic anhydride (1.5 eq.) in THF was heated at 60 ^{o}C for 1 h. After completion of reaction (TLC and LCMS), solvent was removed under reduced pressure and residue was triturated with diethyl ether to obtain *N*-(4-hydroxyphenyl)acetamide (**3.0**).

N-(4-hydroxyphenyl)acetamide (3.0)

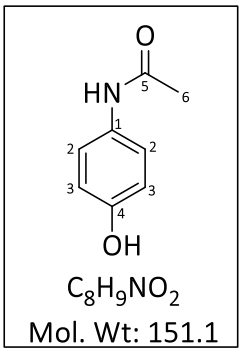

Light pink solid (1.3 g obtained from 1.0 g of **2.0**, 94%); *R*f 0.3 (7% MeOH-DCM); Mp 168-170 ^{o}C; ^{1}H NMR (600 MHz, MeOH-d_4) δ 7.35 (d, *J* = 8.8 Hz, 2H, 2×H-2), 6.72 (d, *J* = 8.8 Hz, 2H, 2×H-3), 2.06 (s, 3H, CH_3-6); ^{13}C NMR (151 MHz, MeOH-d_4) δ 171.2, 155.2, 131.5, 123.2 (2C), 116.0 (2C) and 23.3; LC-MS (ESI): *m/z* 152 $[M+H]^+$; purity (LC-MS): 98% (t_R = 0.19 min.)

4.6.4 General synthetic procedure for the synthesis of compound 4.0

Compound **3.0** (1 eq) was dissolved in EtOH (10 mL) and heated (80 ^{o}C) with diethylamine (1.5 eq) and formaldehyde (1.5 eq.) until completion (TLC, 2 h). The solvent was removed *in vacuo*. The residue was dissolved in DCM (20 mL) and acidified with 1M HCl (15 mL). The aqueous layer was separated through a separating funnel and basified with a saturated solution of NaOH to a pH of 8-10. This was followed by extraction of the target compound with DCM (2×20 mL). The combined organic phase was dried over anhydrous Na_2SO_4. After filtration, the solvent was removed under reduced pressure to obtain compound **4.0**.

N-(3-((*N*,*N*-diethylamino)methyl)-4-hydroxyphenyl)acetamide (4.0)

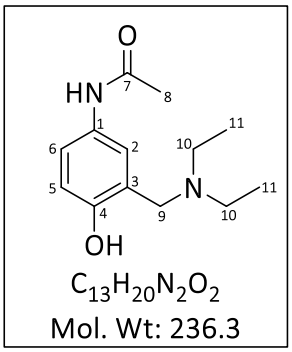

Yellow oil (0.500 g obtained from 0.500 g of **3.0**, 64%); *R*f 0.2 (7% MeOH-DCM); ^{1}H NMR (600 MHz, DMSO-d_6) δ 9.66 (br s, 1H, NH), 7.31 (d, *J* = 2.6 Hz, 1H, H-2), 7.26 (dd, *J* = 2.6, 8.6 Hz, 1H, H-6), 6.63 (d, *J* = 8.6 Hz, 1H, H-5), 3.70 (s, 2H, 2×H-9), 2.58 (q, *J* = 7.1 Hz, 4H, 4×H-10), 1.97 (s, 3H, CH_3-8), 1.03 (t, *J* = 7.1 Hz, 6H, 2×CH_3-11); ^{13}C NMR (151 MHz, DMSO-d_6) δ 167.6, 153.1, 130.8, 122.0, 120.4, 119.7, 115.1, 54.8, 45.9 (2C), 23.7 and 10.9 (2C); LC-MS (ESI): *m/z* 237 $[M+H]^+$; purity (LC-MS): 98% (t_R = 0.12 min.)

4.6.5 General synthetic procedure for the synthesis of compound 5.0

Compound **4.0** (2 mmol) was refluxed in 6N HCl (2 mL) at 100 ^{o}C for 2 h (TLC). Solvent was removed under reduced pressure. The residue was dissolved in EtOH (2×15 mL) and solvent was removed *in vacuo* to obtain product **5.0** (as HCl salt) as an oil.

4-Amino-2-((*N*,*N*-diethylamino)methyl)phenol (5.0)

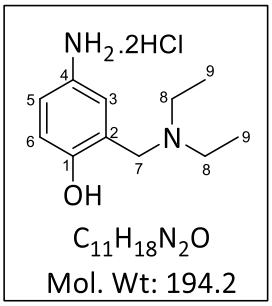

Brown viscous oil (0.360 g obtained from 0.500 g of **4.0**, 88%); *R*f 0.2 (20% MeOH-DCM); ^{1}H NMR (600 MHz, MeOH-d_4) δ 7.56 (d, *J* = 2.7 Hz, 1H, H-3), 7.40 (dd, *J* = 2.7, 8.7 Hz, 1H, H-5), 7.10 (d, *J* = 8.7 Hz, 1H, H-6), 4.37 (s, 2H, H-7), 3.06 (m, 4H, 4×H-8), 1.38 (t, *J* = 7.2 Hz, 6H, 2×CH_3-9); ^{13}C NMR (151 MHz, MeOH-d_4) δ 158.4, 128.5, 127.4, 123.5, 119.2, 117.8, 51.9, 48.9 (2C) and 9.2 (2C); LC-MS (ESI): *m/z* 195 $[M+H]^+$; purity (LC-MS): 98% (t_R = 0.12 min.)

4.6.6 General synthetic procedure for the synthesis of compound 6.0

To a mixture of fusidic acid **1.0** (1 eq) in DCM (5 mL) at 30 ^{o}C was added the base DIPEA (3 eq) dropwise. The reaction was allowed to stir for while (10 min.) after which HATU (2 eq.) was added. The reaction was allowed to proceed until completion (TLC, 2 h). The reaction was diluted with DCM (20 mL) and extracted with water (2x15 mL). The organic phase was dried over anhydrous Na_2SO_4, filtered and the solvent removed *in vacuo*. Further purification to obtain **6.0** was accomplished by flash chromatography using a mixture of DCM and EtOAc as mobile phase.

O-(3*H*-[1,2,3]triazolo[4,5-b]pyridin-3-yl)fusidic acid ester (6.0)

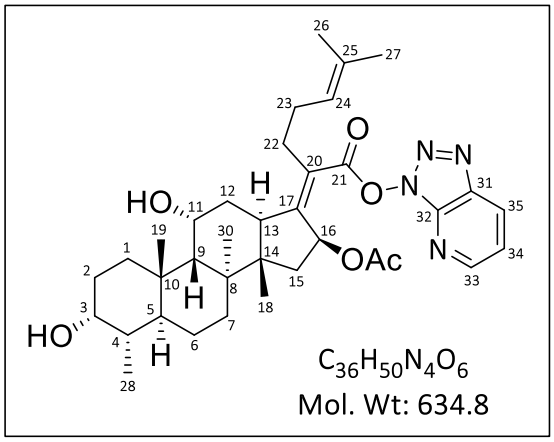

Yellow semi-solid (0.240 g obtained from 0.370 g of **1.0**, 53%); *R*f 0.6 (60% EtOAc:DCM); ^{1}H NMR (600 MHz, $CDCl_3$) δ 8.67 (dd, *J* = 1.4, 4.4 Hz, 1H, H-33), 8.39 (dd, *J* = 1.4, 8.3 Hz, 1H, H-35), 7.40 (dd, *J* = 4.4, 8.3, 1H, H-34), 5.93 (d, *J* = 8.4 Hz, 1H, H-16), 5.23 (m, 1H, H-24), 4.40 (m, 1H, H-11), 3.77 (m, 1H, H-3), 3.19 (m, 1H, H-13), 2.82-2.75 (m, 1H, H-22), 2.72-2.65 (m, 1H, H-22), 2.45-2.39 (m, 3H, H-12 and 2×H-23), 2.33-2.26 (m, 1H, H-15), 2.22-2.13 (m, 2H, H-1 and H-5), 2.12 (s, 3H, OAc), 1.99-1.92 (m, 1H, H-12), 1.92-1.72 (m, 3H, 2×H-2 and H-7), 1.71 (s, 3H, CH_3-27), 1.67 (s, 3H, CH_3-26), 1.66-1.52 (m, 4H, H-1, H-4, H-6 and H-9),1.41 (s, 3H, CH_3-30), 1.43-1.37 (m, 1H, H-15), 1.21-1.06 (m, 2H, H-6 and H-7), 1.01 (s, 3H, CH_3-19), 1.00 (s, 3H, CH_3-18), 0.91 (d, *J* = 6.8 Hz, 3H, CH_3-28); ^{13}C NMR (151 MHz, $CDCl_3$) δ 170.9, 164.9, 157.4, 151.5, 140.8, 135.0, 133.4, 129.2, 124.9, 122.5, 120.7, 74.3, 71.3, 68.2, 49.2, 49.0, 45.3, 39.5, 39.0, 37.1, 36.2 (2C), 35.6, 32.4, 30.3, 29.9, 29.0, 28.5, 25.7, 24.2, 22.8, 21.1, 20.7, 18.1, 17.8 and 15.9; LC-MS (ESI): *m/z* 635 $[M+H]^+$; purity (LC-MS): 98% (t_R = 3.23 min.)

4.6.7 General synthetic procedure for the synthesis of compounds 1.23 and 1.24

To a mixture of compound **6.0** and the corresponding amine (4-hydroxyaniline for **1.23** and **5.0** for **1.24**) in *n*-BuOH at 25 ^{o}C was added the base KH_2PO_4 (5 eq). The reaction was then heated gently to 100^{o}C until reaction was complete (TLC, LCMS; 16 h for **1.23** and 24 h for **1.24**). The solvent was removed completely by drying in the Genevac. Further purification to afford the target compounds was accomplished by preparative TLC using 10% MeOH:DCM as mobile phase.

N-(4-hydroxyphenyl)fusidic acid amide (1.23)

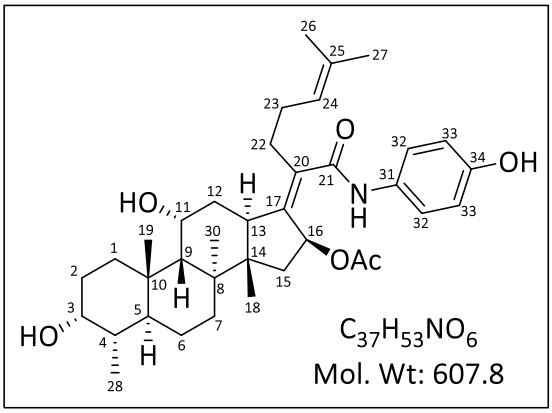

Brown powder (0.015 g obtained from 0.050 g of **6.0**, 32%); *R*f 0.3 (60% EtOAc:DCM); Mp 332-334 ^{o}C; ^{1}H NMR (400 MHz, MeOH-d_4) δ 7.37 (d, *J* = 8.6 Hz, 2H, 2×H-32), 6.74 (d, *J* = 8.6, 2H, 2×H-34), 5.84 (d, *J* = 8.5 Hz, 1H, H-16), 5.19 (m, 1H, H-24), 4.35 (m, 1H, H-11), 3.68 (m, 1H, H-3), 3.12 (m, 1H, H-13), 2.74-2.63 (m, 2H, 2×H-22), 2.39-2.29 (m, 1H, H-12), 2.29-2.15 (m, 5H, H-1, H-5, H-15 and 2×H-23), 1.94-1.65 (m, 4H, 2×H-2, H-7 and H-12), 1.73 (s, 3H, OAc), 1.68 (s, 3H, CH_3-27), 1.63 (s, 3H, CH_3-26), 1.60-1.45 (m, 4H, H-1, H-4, H-6 and H-9), 1.43 (s, 3H, CH_3-30), 1.24-1.18 (m, 1H, H-15), 1.20-1.11 (m, 2H, H-6 and H-7), 1.03 (s, 3H, CH_3-19), 0.98 (s, 3H, CH_3-18), 0.92 (d, *J* = 6.7 Hz, 3H, CH_3-28); ^{13}C NMR (101 MHz, MeOH-d_4) δ 172.6, 172.3, 155.3, 143.4, 135.8, 133.3, 131.8, 124.6, 123.1 (2C), 116.2 (2C), 75.5, 72.4, 68.6, 50.8, 49.9, 44.4, 40.7, 40.3, 38.3, 37.8, 37.4, 36.8, 32.9, 31.1, 31.0, 30.6, 28.8, 25.9, 23.9, 23.8, 22.4, 21.0, 17.9 (2C) and 16.4; LC-MS (ESI): *m/z* 631 $[M+Na]^+$, 548 $[M-OAc]^+$; purity (LC-MS): 98% (t_R = 2.92 min.)

N-(3-((*N*,*N*-diethylamino)methyl)-4-hydroxyphenyl)fusidic acid amide (1.24)

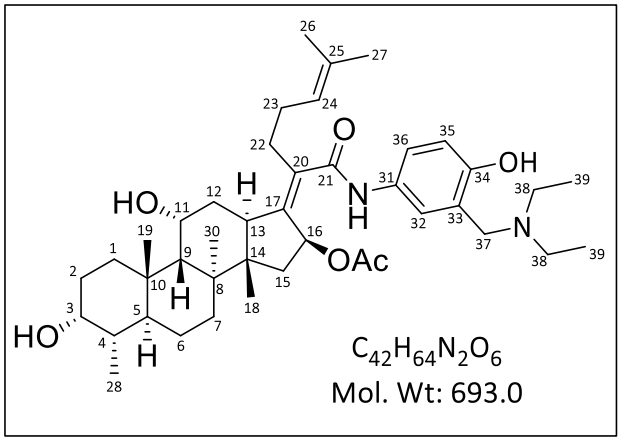

Brown powder (0.015 g obtained from 0.075 g of **6.0**, 21%); *R*f 0.5 (10% MeOH:DCM); Mp 332-334 ^{o}C; ^{1}H NMR (400 MHz, MeOH-d_4) δ 7.33 (d, *J* = 2.6 Hz, 1H, H-32), 7.29 (dd, *J* = 2.6, 8.6 Hz, 1H, H-36), 6.69 (d, *J* = 8.5, 1H, H-35), 5.82 (d, *J* = 8.5 Hz, 1H, H-16), 5.16 (m, 1H, H-24), 4.32 (m, 1H, H-11), 3.86 (s, 2H, 2×H-37), 3.65 (m, 1H, H-3), 3.09 (m, 1H, H-13), 2.75 (q, *J* = 7.1, 4H, 4×H-38), 2.71-2.60 (m, 2H, 2×H-22), 2.37-2.24 (m, 1H, H-12), 2.27-2.11 (m, 5H, H-1, H-5, H-15 and 2×H-23), 1.92-1.63 (m, 4H, 2×H-2, H-7 and H-12), 1.69 (s, 3H, OAc), 1.65 (s, 3H, CH_3-27), 1.60 (s, 3H, CH_3-26), 1.58-1.42 (m, 4H, H-1, H-4, H-6 and H-9), 1.40 (s, 3H, CH_3-30), 1.24-1.18 (m, 1H, H-15),

1.20-1.11 (m, 2H, H-6 and H-7), 1.16 (t, *J* = 7.1 Hz, 6H, 2×CH_3-39), 1.00 (s, 3H, CH_3-19), 0.95 (s, 3H, CH_3-18), 0.89 (d, *J* = 6.8 Hz, 3H, CH_3-28); ^{13}C NMR (101 MHz, MeOH-d_4) δ 172.5, 172.3, 155.7, 143.6, 135.8, 133.2, 131.5, 124.5, 123.0, 122.7, 122.4, 116.7, 75.5, 72.4, 68.6, 56.6, 50.8, 49.9, 47.8 (2C), 44.4, 40.7, 40.3, 38.2, 37.8, 37.4, 36.8, 32.8, 31.1, 31.0, 30.5, 28.8, 25.9, 23.9, 23.8, 22.4, 21.0, 17.9 (2C), 16.4 and 11.1 (2C); LC-MS (ESI): *m/z* 633 $[M\text{-}OAc]^+$; purity (LC-MS): 98% (t_R = 2.80 min.)

4.6.8 Antimycobacterial evaluation protocol

The minimum inhibitory concentration (MIC_{90}) that inhibits 90% of growth of the bacterial population was determined using the broth micro dilution method against the *Mtb* H_{37}Rv strain.[59] A 10 mL culture of the H_{37}Rv strain was grown to an optical density (OD_{600}) of 0.6 – 0.7. Test compounds were reconstituted in DMSO to a concentration 10 mM. Duplicate two-fold serial dilutions of the test compounds were prepared across 10 wells in a 96-well microtitre plate, in a volume of 50 µL, after which, 50 µL of the diluted *Mtb* culture (1:500) was added to each well in the plate (including the control wells). The final volume per well was 100 µL. The plate layout was a modification of the method previously described.[60] Controls used were a minimum growth control (Rifampicin at 2xMIC: 0.150 µM), a maximum growth control (DMSO), and a Rifampicin dose response (range 0.15 – 0.0002 µM). The microtitre plate was sealed in a secondary container and incubated at 37 ^oC with 5% CO_2 and humidification. Alamar Blue reagent was added to each well of the assay plate, 24 hours prior to the assay end data, after which the assay was re-incubated for 24 h. The assay was scored visually at day 7: the lowest concentration of material displaying no visible growth was scored as the MIC_{90}. Relative fluorescence (excitation 540 nm; emission 590 nm) was measured using a SpecraMax i3x Plate reader at day 7, while the data analyses was done using Softmax® Pro 6 software (Version 6.5.1).

<u>Media used</u>

7H9 GLU ADC TW: Middlebrook 7H9 media (Difco™) supplemented with 0.4% Glucose, Middlebrook albumin-dextrose-catalase (ADC) enrichment (Difco™) and 0.05% Tween 80.[61] The culture was diluted 1:500.

7H9 GLU CAS TX: Middlebrook 7H9 media (Difco™) supplemented with 0.03% Casitone, 0.4% Glucose and 0.05% Tyloxpol.[62] The culture was diluted 1:500.

Media recipe

Middlebrook 7H9 Broth 1 L – 7H9 GLU ADC TW

4.7 g powder

900 mL distilled water

2 g Glucose

100 mL Middlebrook ADC

0.05% Tween 80

Middlebrook 7H9 Broth 1 L – 7H9 GLU CAS TX

4.7 g powder

900 mL distilled water

4 g Glucose

0.3 g Casitone

0.81 g NaCl

0.05% Tyloxapol

The above components were dissolved in distilled water. The pH was adjusted to 6.6, if necessary, then filter sterilized (0.2 µM filter) and stored at 37 ^{o}C.

4.6.9 Antiplasmodium evaluation protocol

4.6.9.1 The modified [^{3}H]-hypoxanthine incorporation assay for asexual blood stage parasites

Compounds were screened against multidrug-resistant (K1) and chloroquine-sensitive (NF54) strains of *P. falciparum in vitro* using the modified [^{3}H]-hypoxanthine incorporation assay.[63] *P. falciparum* was cultivated in a variation of the medium previously described,[64,65] consisting of RPMI 1640 supplemented with 0.5% ALBUMAX® II, 25 mM Hepes, 25 mM $NaHCO_3$ (pH 7.3), 0.36 mM hypoxanthine and 100 µg/mL neomycin. Human erythrocytes served as host cells. Cultures were maintained at 37 ^oC in an atmosphere of 3% O_2, 4% CO_2 and 93% N_2 in humidified modular chambers. Compounds were dissolved by sonication in DMSO (10 mg/mL) and diluted in hypoxanthine-free culture medium. Infected erythrocytes (100 µL per well with 2.5% hematocrit and 0.3% parasitemia) were added to each drug titrated in 100 µL duplicates over a 64-fold range. After 48 h incubation, 0.5 µCi of [^{3}H]hypoxanthine in 50 µL medium was added and plates were incubated for an additional 24 h. Parasites were harvested onto glass-fiber filters and radioactivity was counted using a Betaplate liquid scintillation counter (Wallac, Zurich). The results were recorded as counts per minute (cpm) per well at each drug concentration and expressed as a percentage of the untreated controls. Fifty percent inhibitory concentrations (IC_{50}) were estimated by linear interpolation.[66]

4.6.9.2 The lactate dehydrogenase assay for asexual blood stage parasites

The test samples were tested in triplicate on two occasions against chloroquine-sensitive (CQS) strain of *P. falciparum* (NF54). Continuous *in vitro* cultures of asexual erythrocyte stages of *P. falciparum* were maintained using a modified method of Trager and Jensen.[67] Quantitative assessment of antiplasmodium activity *in vitro* was determined *via* the parasite lactate dehydrogenase assay using a modified method described by Makler and coworkers.[54]

The test samples were prepared to a 20 mg/mL stock solution in 100% DMSO. Stock solutions were stored at -20 ^oC. Further dilutions were prepared on the day of the experiment. Chloroquine (CQ) and artesunate were used as the reference drug in all experiments. A full dose-response was performed for all compounds to determine the concentration inhibiting 50% of parasite growth

(IC_{50} value). Test samples were serially diluted 2-fold in complete medium to give 10 concentrations. The same dilution technique was used for all samples. Control compounds were tested at a starting concentration of 1000 ng/ml. The highest concentration of solvent to which the parasites were exposed to had no measurable effect on the parasite viability. The IC_{50} values were obtained using a non-linear dose-response curve fitting analysis via Graph Pad Prism v.4.0 software.

4.6.9.3 The luciferase reporter assay for early and late gametocyte parasites

The luciferase reporter assay[68] was established to enable accurate, reliable and quantifiable investigations of the stage-specific action of gametocytocidal compounds for the early and late gametocyte marker cell line NF54-PfS16-GFP-Luc. Drug assays were set up on day 5 and 10 (representing >90% of either early stage II/III or mature stage IV/V gametocytes, respectively). In each instance, assays were set up using a 2 – 3% gametocytemia, 1.5% hematocrit culture and 48 h drug pressure in a gas chamber (90% N_2, 5% O_2, and 5% CO_2) at 37 ^oC. Luciferase activity was determined in 30 µL parasite lysates by adding 30 µL luciferin substrate (Promega Luciferase Assay System) at room temperature and detection of resultant bioluminescence at an integration constant of 10 s with the GloMax® Explorer Detection System with Instinct® Software. Methylene blue (5 µM) and internal project specific controls (MMV390048, 5 µM) are routinely included as controls. Dual point screens are routinely performed as technical triplicates for a single biological assay.

4.6.10 Cytotoxicity evaluation protocol

The *in vitro* cytotoxicity of the synthesized compounds was evaluated against the Chinese Hamster Ovarian (CHO) cancer cell line using the MTT [3-(4,5-dimethylthiazolyl-2)-2,5-diphenyltetrazolium bromide] assay, which is a colorimetric assay based on assessing the cell metabolic activity.[69]

The synthesized compounds were assayed in triplicate. Stock solutions of 2 mg/mL of test samples in DMSO were prepared with poorly soluble samples being tested as suspensions. The compounds were kept at -20 ^oC until required. In all experiments, emetine was used as a reference drug. Starting from an initial concentration of 100 µg/mL, ten-fold serial dilutions were made in

complete medium to give 6 concentrations to the lowest concentration of 0.001 µg/mL. The cell viability was not affected by the highest concentration of the solvent to which the cells were exposed. The full dose-response curves were plotted using a non-linear dose-response curve fitting analysis via GraphPad Prism V4 software. By this, the minimum concentration required for 50% inhibition (IC_{50}) values were determined for each compound.

4.7 References

(1) Zhao, M.; Gödecke, T.; Gunn, J.; Duan, J.-A.; Che, C.-T. Protostane and fusidane triterpenes: A Mini-Review. *Molecules* 2013, *18* (4), 4054–4080.

(2) Ibrahim, A.-R. S.; Ragab, A. E. Fusidic Acid ring B hydroxylation by *Cunninghamella elegans*. *Phytochem. Lett.* 2018, *25*, 86–89.

(3) Evans, L.; Hedger, J. N.; Brayford, D.; Stavri, M.; Smith, E.; O'Donnell, G.; Gray, A. I.; Griffith, G. W.; Gibbons, S. An antibacterial hydroxy fusidic acid analogue from *Acremonium crotocinigenum*. *Phytochemistry* 2006, *67* (19), 2110–2114.

(4) Godtfredsen, W. O.; Rastrup-Andersen, N.; Vangedal, S.; Ollis, W. D. Metabolites of *Fusidium coccineum*. *Tetrahedron* 1979, *35* (20), 2419–2431.

(5) Waksman, S. A.; Horning, E. S.; Spencer, E. L. The production of two antibacterial substances, fumigacin and clavacin. *Science (80-.).* 1942, *96* (2487), 202–203.

(6) Chain, E.; Florey, H. W.; Jennings, M. A.; Williams, T. I. Helvolic acid, an antibiotic produced by *Aspergillus fumigatus*, mut. helvola Yuill. *Br. J. Exp. Pathol.* 1943, *24*, 108–119.

(7) Jennings, M. A. Activity of helvolic acid against *Mycobacterium tuberculosis*. *Nature* 1945, *156*, 633.

(8) Zhao, J.; Mou, Y.; Shan, T.; Li, Y.; Zhou, L.; Wang, M.; Wang, J. Antimicrobial metabolites from the endophytic fungus *Pichia guilliermondii* isolated from *Paris polyphylla* var. Yunnanensis. *Molecules* 2010, *15* (11), 7961–7970.

(9) Feng, C.; MA, Y. Isolation and anti-phytopathogenic activity of secondary metabolites from *Alternaria* sp. FL25, an endophytic fungus in *Ficus carica**. *Chinese J. Appplied Environ. Biol.* 2010, *16* (1), 76–78.

(10) Li, X.-J.; Zhang, Q.; Zhang, A.-L.; Gao, J.-M. Metabolites from *Aspergillus fumigatus*, an endophytic fungus associated with *Melia azedarach* , and their antifungal, antifeedant, and toxic activities. *J. Agric. Food Chem.* 2012, *60* (13), 3424–3431.

(11) Kaise, H.; Ogawa, Y.; Sassa, T.; Munakata, K. Studies on the chlorosis-inducing substances produced by a fungus. *Agric. Biol. Chem.* 1972, *36* (1), 120–124.

(12) Kaise, H.; Munakata, K.; Sassa, T. Structures of viridominic acids A and B, new chlorosis-inducing metabolites of a fungus. *Tetrahedron Lett.* 1972, *13* (36), 3789–3792.

(13) Burton, H. S.; Abraham, E. P. Isolation of antibiotics from a species of *Cephalosporium*; cephalosporins P1, P2, P3, P4, and P5. *Biochem. J.* 1951, *50* (2), 168–174.

(14) Chou, T. S.; Eisenbraun, E. J.; Rapala, R. T. The chemistry of steroid acids from *Cephalosporium acremonium*. *Tetrahedron* 1969, *25* (16), 3341–3357.

(15) Ritchie, A. C.; Smith, N.; Florey, H. W. Some biological properties of cephalosporin P1. *Br. J. Pharmacol. Chemother.* 1951, *6* (3), 430–444.

(16) O'Neill, A. J.; Bostock, J. M.; Morais, M. A.; Chopra, I. Antimicrobial activity and mechanisms of resistance to cephalosporin P1, an antibiotic related to fusidic acid. *J. Antimicrob. Chemother.* 2002, *50* (6), 839–848.

(17) Godtfredsen, W. O.; Jahnsen, S.; Lorck, H.; Roholt, K.; Tybring, L. fusidic acid: A new antibiotic. *Nature* 1962, *193*, 987.

(18) Perry, M. J.; Hendricks-Gittins, A.; Stacey, L. M.; Adlard, M. W.; Noble, W. C. Fusidane antibiotics produced by dermatophytes. *J. Antibiot. (Tokyo).* 1983, *36* (12), 1659–1663.

(19) Cole, R. J.; Schweikert, M. A. *Handbook of Secondary Fungal Metabolites, Volume 1*;

Academic Press: New York, USA, 2003.

(20) Dobie, D.; Gray, J. Fusidic acid resistance in *Staphylococcus aureus*. *Arch. Dis. Child.* 2004, *89* (1), 74–77.

(21) Jones, R. N.; Mendes, R. E.; Sader, H. S.; Castanheira, M. *In vitro* antimicrobial findings for fusidic acid tested against contemporary (2008–2009) gram-positive organisms collected in the United States. *Clin. Infect. Dis.* 2011, *52* (suppl_7), S477–S486.

(22) Godtfredsen, W. O.; von Daehne, W.; Tybring, L.; Vangedal, S. Fusidic acid derivatives. I. Relationship between structure and antibacterial activity. *J. Med. Chem.* 1966, *9* (1), 15–22.

(23) von Daehne, W.; Godtfredsen, W. O.; Rasmussen, P. R. Structure-activity relationships in fusidic acid-type antibiotics. *Adv. Appl. Microbiol.* 1979, *25*, 95–146.

(24) Duvold, T.; Sørensen, M. D.; Björkling, F.; Henriksen, A. S.; Rastrup-Andersen, N. Synthesis and conformational analysis of fusidic acid side chain derivatives in relation to antibacterial activity. *J. Med. Chem.* 2001, *44* (19), 3125–3131.

(25) Duvold, T.; Jørgensen, A.; Andersen, N. R.; Henriksen, A. S.; Dahl Sørensen, M.; Björkling, F. 17S,20S-methanofusidic acid, a new potent semi-synthetic fusidane antibiotic. *Bioorg. Med. Chem. Lett.* 2002, *12* (24), 3569–3572.

(26) FUCITHALMIC® (fusidic acid) Product Monograph, version 1.0 (2014.02.03) http://methapharm.com/wp-content/uploads/2015/11/Fucithalmic-PM00025061.pdf (accessed Aug 13, 2018).

(27) Boolell, M.; Gepi-Attee, S.; Gingell, J. C.; Allen, M. J. Sildenafil, a novel effective oral therapy for male erectile dysfunction. *Br. J. Urol.* 1996, *78* (2), 257–261.

(28) Singhal, S.; Mehta, J.; Desikan, R.; Ayers, D.; Roberson, P.; Eddlemon, P.; Munshi, N.; Anaissie, E.; Wilson, C.; Dhodapkar, M.; et al. Antitumor activity of thalidomide in refractory multiple myeloma. *N. Engl. J. Med.* 1999, *341* (21), 1565–1571.

(29) Weiss, V. C.; West, D. P.; Mueller, C. E. Topical minoxidil in *Alopecia areata*. *J. Am. Acad. Dermatol.* 1981, *5* (2), 224–226.

(30) Matthews, H.; Usman-Idris, M.; Khan, F.; Read, M.; Nirmalan, N. Drug repositioning as a route to anti-malarial drug discovery: Preliminary investigation of the *in vitro* anti-malarial efficacy of emetine dihydrochloride hydrate. *Malar. J.* 2013, *12* (1), 359.

(31) Nzila, A.; Ma, Z.; Chibale, K. Drug repositioning in the treatment of malaria and TB. *Future Med. Chem.* 2011, *3* (11), 1413–1426.

(32) Cicek-Saydam, C.; Cavusoglu, C.; Burhanoglu, D.; Hilmioglu, S.; Ozkalay, N.; Bilgic, A. *In vitro* susceptibility of *Mycobacterium tuberculosis* to fusidic acid. *Clin. Microbiol. Infect.* 2001, *7* (12), 700–702.

(33) Van Caekenberghe, D. Comparative *in vitro* activities of ten fluoroquinolones and fusidic acid against *Mycobacterium* spp. *J. Antimicrob. Chemother.* 1990, *26* (3), 381–386.

(34) Witzig, R. S.; Franzblau, S. G. Susceptibility of *Mycobacterium kansasii* to ofloxacin, sparfloxacin, clarithromycin, azithromycin, and fusidic Acid. *Antimicrob. Agents Chemother.* 1993, *37* (9), 1997–1999.

(35) National Center for Biotechnology Information. PubChem BioAssay Database; AID=1332 https://pubchem.ncbi.nlm.nih.gov/bioassay/1332 (accessed Aug 8, 2018).

(36) Wasuna, A. PhD Thesis, University of Cape Town, 2017.

(37) Njoroge, M. PhD Thesis, University of Cape Town, 2014.

(38) Kaur, G. PhD Thesis, University of Cape Town, 2016.

(39) Turnidge, J. Fusidic acid pharmacology, pharmacokinetics and pharmacodynamics. *Int. J. Antimicrob. Agents* 1999, *12*, S23–S34.

(40) Omollo, C. PhD Thesis, University of Cape Town, 2017.

(41) Shanika, P. S. MSc Thesis, University of Cape Town, 2017.

(42) Strydom, N. PhD Thesis, 2016.

(43) Johnson, R. A.; McFadden, G. I.; Goodman, C. D. Characterization of two malaria parasite organelle translation elongation factor G proteins: The likely targets of the anti-malarial fusidic acid. *PLoS One* 2011, *6* (6), e20633.

(44) Kaur, G.; Singh, K.; Pavadai, E.; Njoroge, M.; Espinoza-Moraga, M.; De Kock, C.; Smith, P. J.; Wittlin, S.; Chibale, K. Synthesis of fusidic acid bioisosteres as antiplasmodial agents and molecular docking studies in the binding site of elongation factor-G. *Medchemcomm* 2015, *6* (11), 2023–2028.

(45) Espinoza-Moraga, M.; Singh, K.; Njoroge, M.; Kaur, G.; Okombo, J.; De Kock, C.; Smith, P. J.; Wittlin, S.; Chibale, K. Synthesis and biological characterisation of ester and amide derivatives of fusidic acid as antiplasmodial agents. *Bioorg. Med. Chem. Lett.* 2017, *27* (3), 658–661.

(46) Kaur, G.; Pavadai, E.; Wittlin, S.; Chibale, K. 3D-QSAR modeling and synthesis of new fusidic acid derivatives as antiplasmodial agents. *J. Chem. Inf. Model.* 2018, *58* (8), 1553–1560.

(47) Augustine, J. K.; Vairaperumal, V.; Narasimhan, S.; Alagarsamy, P.; Radhakrishnan, A. Propylphosphonic Anhydride (T3P®): An efficient reagent for the one-pot synthesis of 1,2,4-oxadiazoles, 1,3,4-oxadiazoles, and 1,3,4-thiadiazoles. *Tetrahedron* 2009, *65* (48), 9989–9996.

(48) Vishwanatha, T.; Panguluri, N.; Sureshbabu, V. Propanephosphonic acid anhydride (T3P®) - A benign reagent for diverse applications inclusive of large-scale synthesis. *Synthesis (Stuttg).* 2013, *45* (12), 1569–1601.

(49) Valeur, E.; Bradley, M. Amide bond formation: Beyond the myth of coupling reagents. *Chem. Soc. Rev.* 2009, *38* (2), 606–631.

(50) HATU https://en.wikipedia.org/wiki/HATU (accessed Aug 13, 2018).

(51) Kleinman, E. F. The bimolecular aliphatic Mannich and related reactions. In *Comprehensive Organic Synthesis*; Elsevier, 1991; pp 893–951.

(52) Betti reaction https://en.wikipedia.org/wiki/Betti_reaction (accessed Aug 13, 2018).

(53) Rastrup-Andersen, N.; Duvold, T. Reassignment of the 1H NMR spectrum of fusidic acid and total assignment of 1H and 13C NMR spectra of some selected fusidane derivatives. *Magn. Reson. Chem.* 2002, *40* (7), 471–473.

(54) Makler, M. T.; Ries, J. M.; Williams, J. A.; Bancroft, J. E.; Piper, R. C.; Gibbins, B. L.; Hinrichs, D. J. Parasite lactate dehydrogenase as an assay for *Plasmodium falciparum* drug sensitivity. *Am. J. Trop. Med. Hyg.* 1993, *48* (6), 739–741.

(55) Arnold, M. S. J.; Engel, J. A.; Chua, M. J.; Fisher, G. M.; Skinner-Adams, T. S.; Andrews, K. T. Adaptation of the [3H] hypoxanthine uptake assay for *in vitro*-cultured *Plasmodium knowlesi* malaria parasites. *Antimicrob. Agents Chemother.* 2016, *60* (7), 4361–4363.

(56) Vander Jagt, D. L.; Hunsaker, L. A.; Heidrich, J. E. Partial purification and characterization of lactate dehydrogenase from *Plasmodium falciparum*. *Mol. Biochem. Parasitol.* 1981, *4* (5–6), 255–264.

(57) Makler, M. T.; Hinrichs, D. J. Measurement of the lactate dehydrogenase activity of *Plasmodium falciparum* as an assessment of parasitemia. *Am. J. Trop. Med. Hyg.* 1993, *48* (2), 205–210.

(58) Makler, M. T.; Piper, R. C.; Milhous, W. K. Lactate dehydrogenase and the diagnosis of malaria. *Parasitol. Today* 1998, *14* (9), 376–377.

(59) Jorgensen, J. H.; Turnidge, J. D. Antibacterial Susceptibility Tests: Dilution and disk diffusion methods. In *Manual of clinical microbiology*; Murray, P. R., Baron, E. J., Jorgensen, J. H., Landry, M. L., Pfaller, M. A., Eds.; American Society for Microbiology: Washington, DC, 2007;

pp 1152–1172.

(60) Ollinger, J.; Bailey, M. A.; Moraski, G. C.; Casey, A.; Florio, S.; Alling, T.; Miller, M. J.; Parish, T. A dual read-out assay to evaluate the potency of compounds active against *Mycobacterium tuberculosis*. *PLoS One* 2013, *8* (4), e60531.

(61) Franzblau, S. G.; DeGroote, M. A.; Cho, S. H.; Andries, K.; Nuermberger, E.; Orme, I. M.; Mdluli, K.; Angulo-Barturen, I.; Dick, T.; Dartois, V.; et al. Comprehensive analysis of methods used for the evaluation of compounds against *Mycobacterium tuberculosis*. *Tuberculosis* 2012, *92* (6), 453–488.

(62) Tang, Y. J.; Shui, W.; Myers, S.; Feng, X.; Bertozzi, C.; Keasling, J. D. Central metabolism in *Mycobacterium smegmatis* during the transition from O2-Rich to O2-Poor conditions as studied by isotopomer-assisted metabolite analysis. *Biotechnol. Lett.* 2009, *31* (8), 1233–1240.

(63) Desjardins, R. E.; Canfield, C. J.; Haynes, J. D.; Chulay, J. D. Quantitative assessment of antimalarial activity *in vitro* by a semiautomated microdilution technique. *Antimicrob. Agents Chemother.* 1979, *16* (6), 710–718.

(64) Dorn, A.; Stoffel, R.; Matile, H.; Bubendorf, A.; Ridley, R. G. Malarial haemozoin/beta-haematin supports haem polymerization in the absence of protein. *Nature* 1995, *374* (6519), 269–271.

(65) Trager, W.; Jensen, J. B. Human malaria parasites in continuous culture. *Science* 1976, *193* (4254), 673–675.

(66) Huber, W.; Koella, J. C. A comparison of three methods of estimating EC50 in studies of drug resistance of malaria parasites. *Acta Trop.* 1993, *55* (4), 257–261.

(67) Trager, W.; Jensen, J. B. Human malaria parasites in continuous culture. 1976. *J. Parasitol.* 2005, *91* (3), 484–486.

(68) Reader, J.; Botha, M.; Theron, A.; Lauterbach, S. B.; Rossouw, C.; Engelbrecht, D.; Wepener, M.; Smit, A.; Leroy, D.; Mancama, D.; et al. Nowhere to hide: Interrogating different metabolic parameters of *Plasmodium falciparum* gametocytes in a transmission blocking drug discovery pipeline towards malaria elimination. *Malar. J.* 2015, *14*, 213.

(69) Mosmann, T. Rapid colorimetric assay for cellular growth and survival: Application to proliferation and cytotoxicity assays. *J. Immunol. Methods* 1983, *65* (1–2), 55–63.

Chapter Five: Synthesis and antiplasmodium and antimycobacterial evaluations of analogues of the privileged benzimidazole scaffold

5.1 General Introduction

5.1.1 Benzimidazole natural products

Benzimidazole is an aromatic bicycle containing an imidazole ring fused to a phenyl ring *via* its two adjacent carbon atoms.

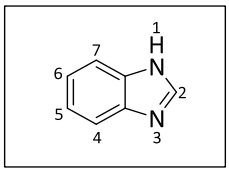

Figure 5.1: Chemical structure of benzimidazole

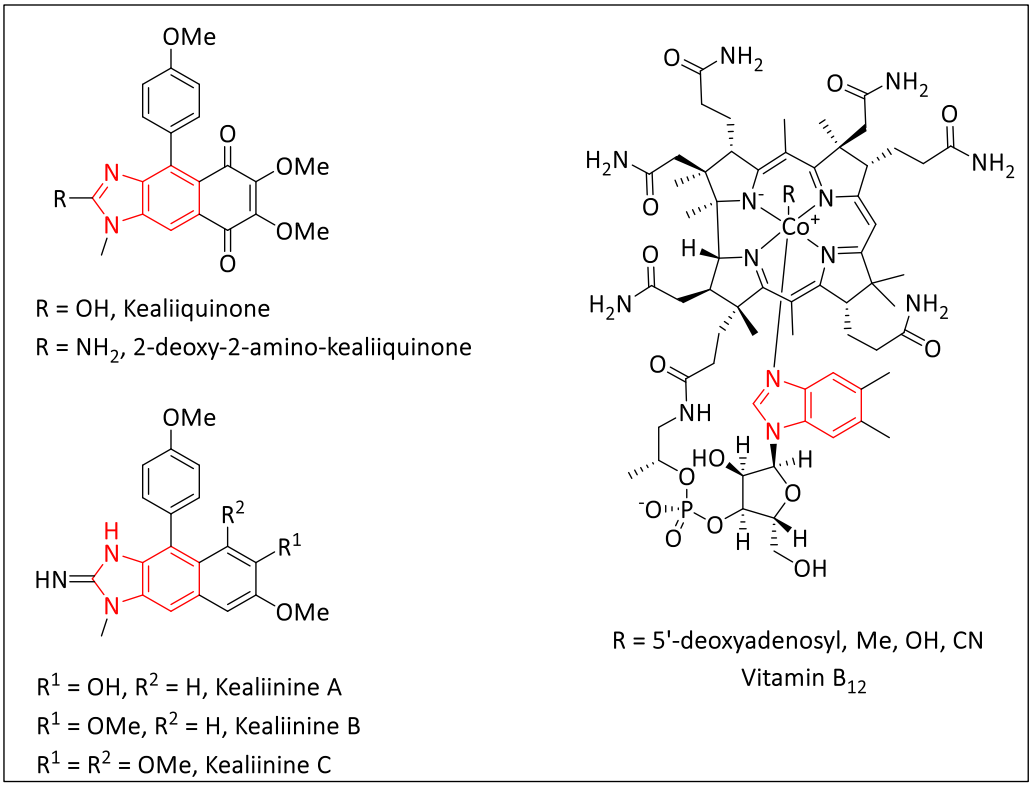

Figure 5.2: Chemical structures of benzimidazole-containing natural products

There are only a few reports of natural products containing the benzimidazole scaffold. Kealiiquinone is a benzimidazole containing natural product isolated from the Micronesian marine sponge *Leucetta* sp. (Figure 5.2).[1] Its congener, 2-deoxy-2-aminokealiiquinone, was isolated from another Micronesian sponge *Leucetta chagosensis*.[2] This marine sponge species also afforded three more benzimidazole metabolites, the kealiinines A-C.[3] The benzimidazole scaffold occurs in vitamin B_{12} (cobalamine) where it serves as a coordination site to the central cobalt cation (Figure 5.2).[4] The imidazole heteroaromatic moiety is however common in natural products. Examples of naturally occurring imidazole metabolites include oroidin, hymenidin, sceptrin, stylissazoles, dihydrosventrin, etc.

5.1.2 Properties of benzimidazole as a privileged scaffold

The benzimidazole scaffold is a substituted derivative of the imidazole heterocyclic compound. It therefore possesses some inherent physicochemical properties of the imidazole ring system which are modified as a result of the benzene ring. Benzimidazole has a lower basicity but an increased acidity compared to imidazole (pKa1: 5.53; pKa2: 12.8). The acid and base properties of benzimidazole confers on the scaffold the ability to form salts with strong acids or bases, which contributes to improved solubility in polar media.[5]

The presence of the benzene ring renders the benzimidazole scaffold more lipophilic (LogP: 1.50) compared to imidazole (LogP: -0.08). Further, the benzimidazole ring offers more opportunity to either increase lipophilicity by appropriate substitutions on the phenyl ring or decrease lipophilicity by incorporation of hydrophilic substituents or exchanging one or more CH of the phenyl ring with N. Thus, the benzimidazole molecular framework offers more room for diverse structural modifications well-suited to target diverse biological active sites.[5]

The benzimidazole scaffold possesses a H-bond donor site, a H-bond acceptor site and a lipophilic aromatic ring for hydrophobic and π-stacking interactions. Optimization of the structure for binding interactions can therefore be achieved by judicious substitution on the core benzimidazole scaffold. Effective binding of the benzimidazole scaffold to biological targets is supported by the fact that it is a structural isostere of naturally occurring scaffolds, especially the purine bases

adenine and guanine. The antagonistic effect of benzimidazole to the growth of some species of yeast and bacteria (e.g. *E. coli*) has long been reported.[6] However, it was also demonstrated that the aminopurines (adenine and guanine) are able to reverse the inhibitory effect of benzimidazole with guanine exhibiting a more potent antagonism than adenine.[6–10] Thus, although benzimidazole is not widespread in nature, it efficiently functions as a natural product mimetic to biological systems.[5]

The importance of benzimidazole as a privileged scaffold can also be viewed from the standpoint of its potential as a bioisostere of indole, which is common in natural products, being biosynthesized from the amino acid tryptophan. Due to structural similarities, the benzimidazole scaffold can also play similar roles in biological systems as do scaffolds like benzoxazole and benzofuran. It can also be employed as a substitute for other privileged scaffolds such as indoline, benzothiophene and indolozine in medicinal chemistry explorations.

5.1.3 Benzimidazoles: Chemistry and Biology

Historically, the first benzimidazole was prepared in 1872 by Hoebrecker, who obtained 2,5(or 2,6)-dimethylbenzimidazole by reducing 2-nitro-4-methylacetanilide.[11] Since then, a number of synthetic methods have been developed to obtain benzimidazole derivatives, depending on the substituents intended on the benzimidazole scaffold.[12]

A common starting reagent to benzimidazole is *o*-phenylenediamine, which is condensed with carbonyl groups present in carboxylic acid, acid anhydrides, esters, amides, acid chlorides, lactones, aldehydes and ketones (Figure 5.3). Other functional groups include nitriles, imino-ethers and imino-thioethers, amidines and guanidines. Moreover, synthetic methods to benzimidazole derivatives possessing C2-O or C2-N substitutions such as 2-hydroxybenzimidazole, 2-aminobenzimidazole, and 2-mercaptobenzimidazole have been reported in the literature. Meanwhile, 2-halo benzimidazole is also known.[12–14]

Benzimidazole derivatives have also been synthesized from other starting reagents including monoacyl- and diacyl-*o*-phenylenediamines, by reduction of acylated *o*-nitroanilines, *o*-aminoazo compounds, and Schiff bases. Derivatives with substituents on the phenyl ring have mostly been

synthesized from the corresponding substituted *o*-diaminobenzene or an appropriate precursor (Figure 5.3).[12]

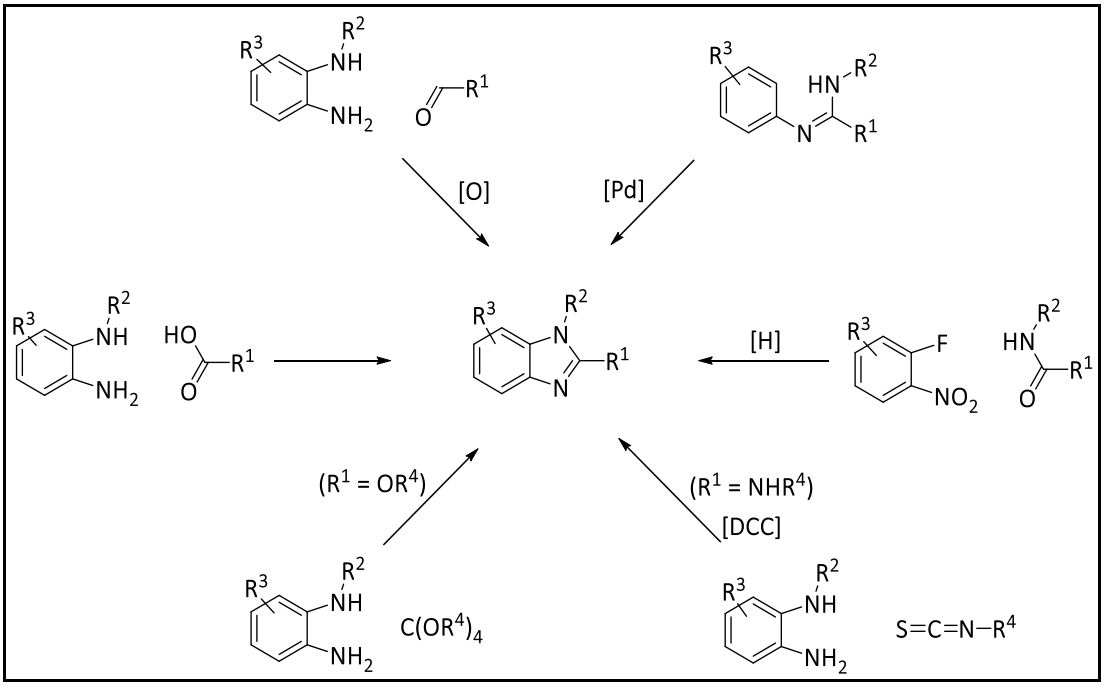

Figure 5.3: Syntheses of benzimidazole derivatives[5]

Reactions of benzimidazole derivatives may involve either the benzimidazole core scaffold or substituent groups on the scaffold. The nitrogen atoms of benzimidazole have been employed in alkylation, acylation and Mannich reactions. Grignard reagents react with the active hydrogen in the 1-position of benzimidazole to form benzimidazole-1-magnessium bromide, which readily affords 1-acylated benzimidazole derivatives upon reaction with carboxylic acid derivatives. The hydrogen in the 1-position of benzimidazoles is sufficiently acidic to be replaced by metals to give *N*-metal benzimidazoles. Other reactions reported for the benzimidazole scaffold include reduction, cleavage of the imidazole moiety, halogenation and nitration.[12]

The 2-position of benzimidazole is another important site of benzimidazole reactions. Reactions involving the 2-methylene group have been extensively documented.[12] Other 2-position reactions of benzimidazole have been reported for 2-benzimidazole carboxylic acids, 2-(α-haloalkyl) benzimidazoles, 2-hydroxybenzimidazoles, 2-mercaptobenzimidazole, 2-aminobenzimidazole,

and oxidation.[12] The benzimidazole scaffold therefore affords the organic chemist a wide range of opportunities for synthetic derivatizations.

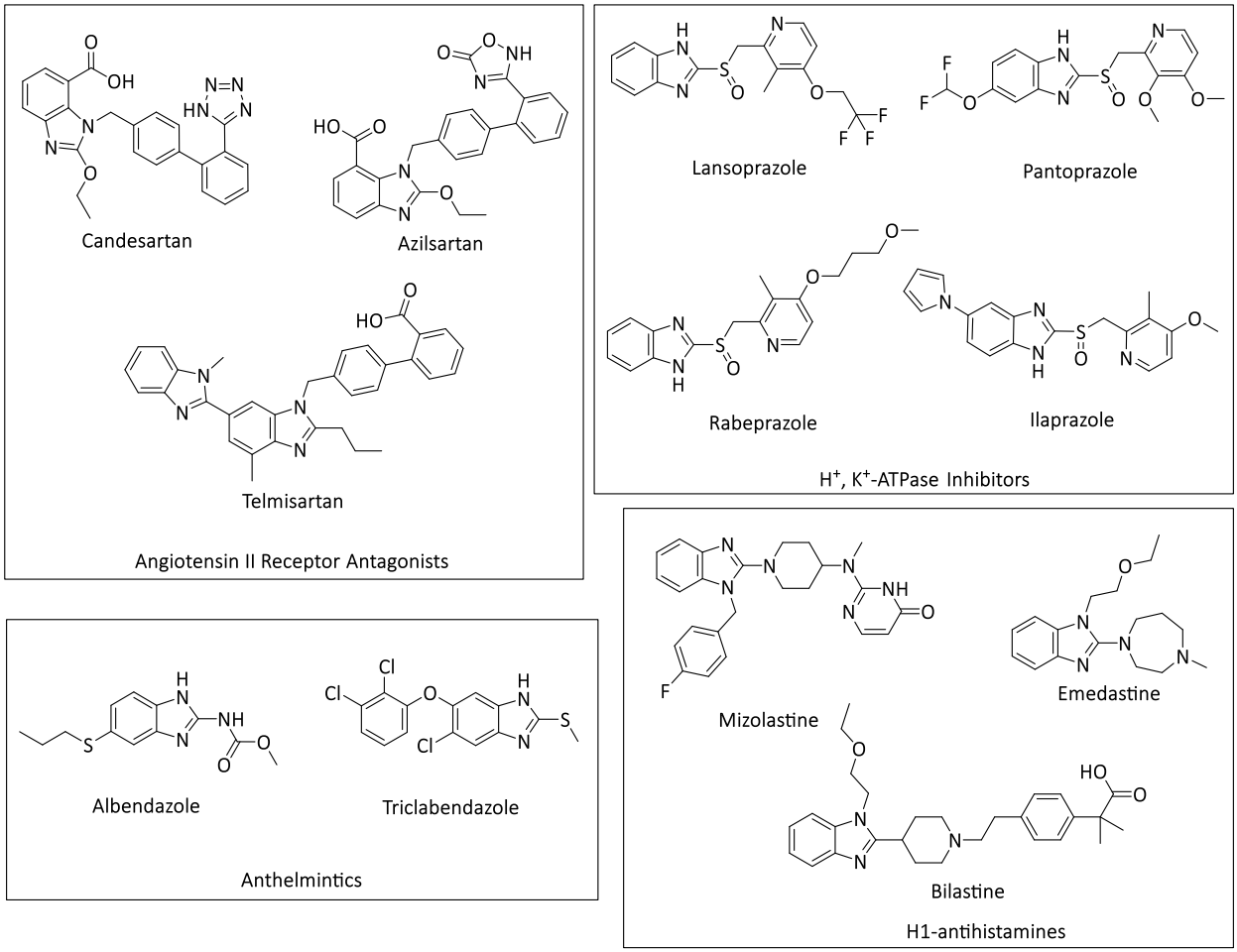

Figure 5.4: Chemical structures of some drugs containing the benzimidazole scaffold[5]

Complemented by its binding possibilities to a wide range of biological targets, the benzimidazole scaffold has been extensively explored in drug discovery (Figure 5.4 and Figure 5.5). Several reviews and research articles have been published on the diverse biological properties of benzimidazole derivatives. [15–17] These biological activities include antiparasitic, anticonvulsant, analgesic, antihistaminic, antiulcer, antihypertensive, antiviral, anticancer, antifungal, anti-inflammatory, anticoagulant and proton pump inhibition.[18–24] The Merck Index Online database (licensed to the Royal Society of Chemistry) records about 48 drug molecules based on the benzimidazole scaffold.[25] The medicinal chemistry explorations of the benzimidazole scaffold is an

active area of current research. This is evident in the over 200 publications so far reported in this year 2018 according to a PubMed search.[26]

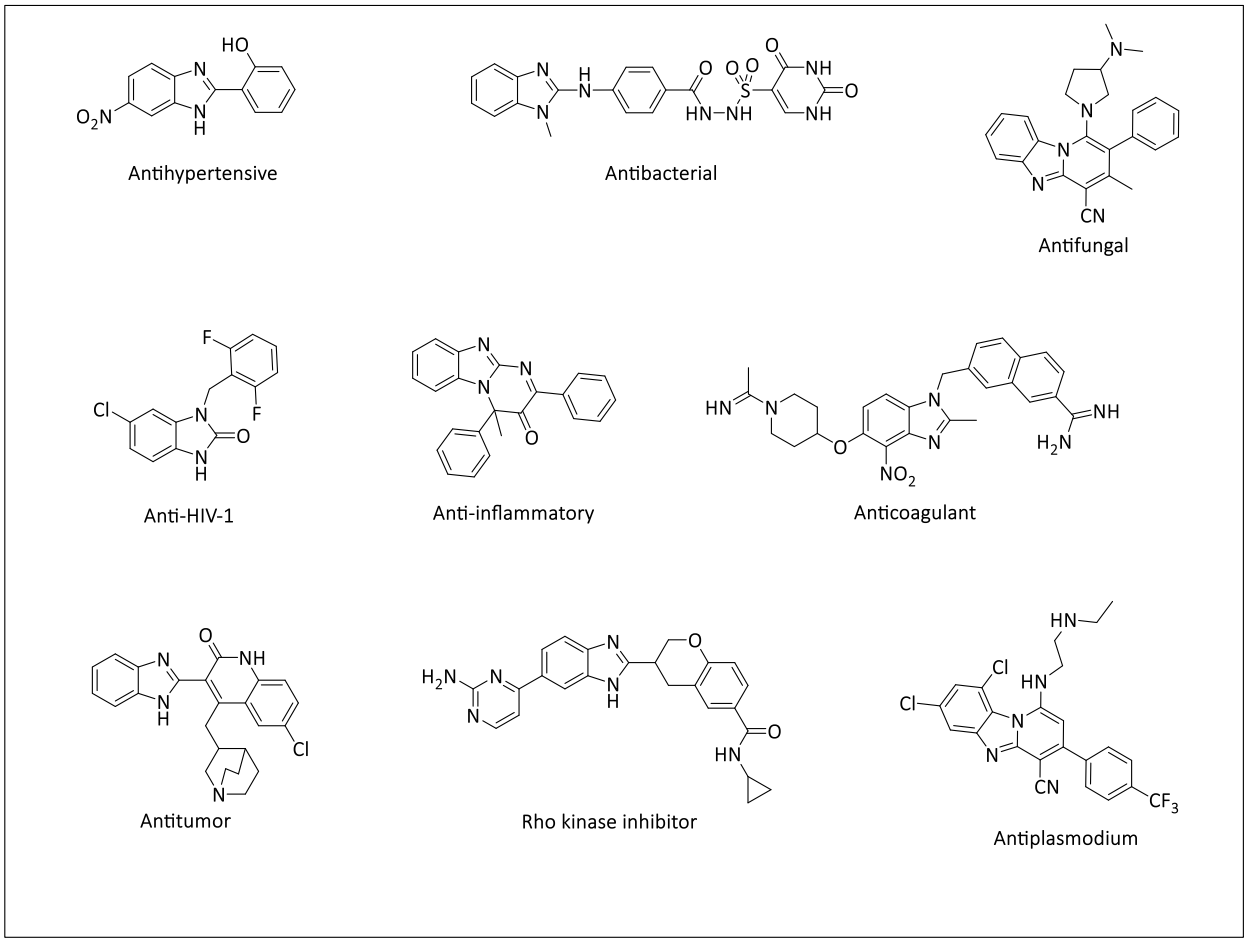

Figure 5.5: Some bioactive benzimidazole derivatives[16,27,28]

5.1.4 Mannich bases in medicinal chemistry and drug design

Mannich bases are a structurally heterogeneous class of chemical compounds that are generated from various substrates through the introduction of an aminomethylene moiety by means of the Mannich reaction. The Mannich reaction is a three-component condensation between, more generally, a substrate (X-H) containing at least one active hydrogen atom, an aldehyde component (R-CHO) and an amine reagent (NH_3, R-NH_2 or R^1R^2NH).[29] Variation in the structure of the substrate leads to structural diversity in the Mannich base formed (Figure 5.6). At least one Mannich base can be formed from a substrate depending on the number of active hydrogens present. Further,

the use of ammonia (in the form of an ammonium salt) or primary amine reagents can lead to bis- or tris-Mannich bases.[29] Structural diversity in the Mannich base compound is therefore not exhaustive and this provides a wide range of applications in synthetic explorations.

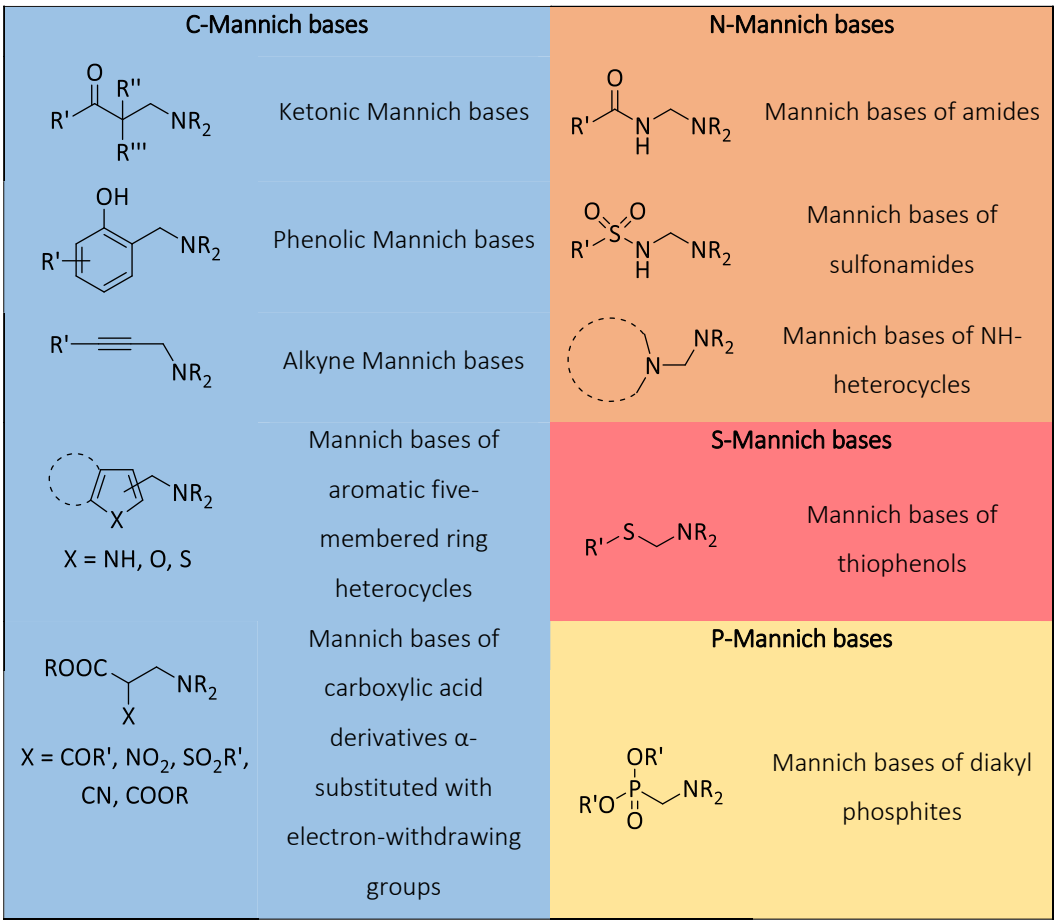

Figure 5.6: Examples of various types of Mannich bases[29]

These compounds have displayed diverse biological activities including antitumor, cytotoxicity, antibacterial, antifungal, antimalarial, antiviral, anticonvulsant, anti-inflammatory, analgesic and antioxidant. Other biological activities such as ability to regulate blood pressure or inhibit platelet aggregation, antiparasitic, anti-ulcer effects, and as agents for the treatment of mental disorders have been reported. Moreover, Mannich bases have been explored as inhibitors of enzymes and as ligands of receptors.[29–39] The biological usefulness of Mannich bases is evident in some current drugs on the market (Figure 5.7). Moreover, more biologically potent Mannich bases are continually being reported (at least 30 articles so far in 2018 according to PubMed database).[40]

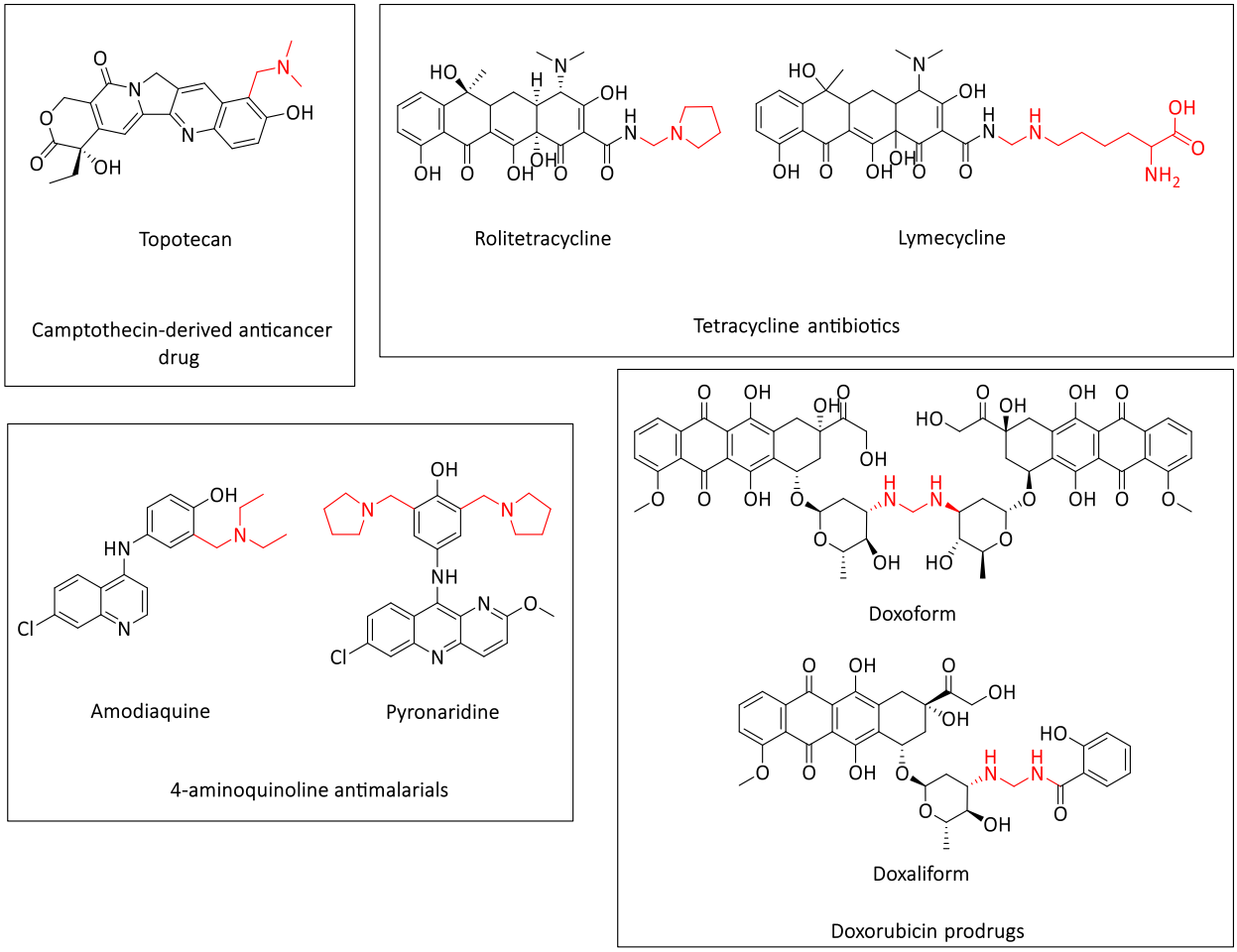

Figure 5.7: Examples of drugs with Mannich bases

Mannich bases have useful applications in medicinal chemistry. The Mannich side chain increases the hydrophilicity of a molecule attributable to the presence of the amino group. Moreover, quaternization of the amino group can enhance the solubility of a drug in water. This advantage of Mannich bases is exemplified in the tetracycline antibiotics rolitetracycline (reverin) and lymecycline (a congener which has further improved solubility due to the terminal polar groups) (Figure 5.7). The tetracyclines are a group of antibiotics first discovered from the soil sediment microbe *Streptomyces*. The first approved candidate was chlortetracycline (Aureomycin) in 1945.[41] According to a 1960 report, tetracycline administration was only possible by a permanent infusion of a large volume and therefore required a lot of time to administer the drug. The prodrug, pyrrolidino-methyl tetracycline (reverin), due to its enhanced solubility, arising from the Mannich side chain, offered the possibility of administration as a normal intravenous injection within 1

minute.[42] Further, the enhanced solubility enabled administration of the drug in small doses (250 mg/day) that did not affect enteric flora.[43]

Topotecan offers another example of the importance of the Mannich base side chain to aqueous solubility of bioactive compounds. This approach rescued the potent antitumor natural product camptothecin. The downsides of camptothecin, which hampered further development included toxicity (severe hemorrhagic cystitis) and poor aqueous solubility.[44,45] Topotecan hydrochloride is a semisynthetic derivative of camptothecin by incorporation of a dimethylamino methylene Mannich base side chain (Figure 5.7). It is this basic moiety of topotecan that confers water solubility at acid pH. The closed lactone ring of topotecan is important for its antitumor activity. The solubility of topotecan in acid medium is important because the lactone ring predominates at low pH. Topotecan acts by inhibiting the nuclear enzyme topoisomerase I, which is involved in DNA replication, by forming a covalent intermediate between topoisomerase I and DNA.[46,47]

Another application of Mannich bases in medicinal chemistry and drug design is their use as prodrugs to deliver bioactive compounds which hitherto may not make it as clinical drugs. As prodrugs, they release the active drug under controlled hydrolytic conditions *via* deaminomethylation or deamination.[48,49] This is exemplified in doxorubicin Mannich base prodrugs such as doxoform and doxaliform. Doxorubicin is a natural product obtained from a strain of *Streptomyces* which had been mutated using *N*-nitroso-*N*-methyl urethane.[50] It is used to treat cancer, including breast cancer, bladder cancer, Kaposi's sarcoma, lymphoma, and acute lymphocytic leukemia. It inhibits DNA replication through inhibition of topoisomerase II by intercalation of DNA.[51] Alkylation of DNA by doxorubicin *via* catalytic production of formaldehyde prompted the synthesis of doxoform, a bis-doxorubicin derivative, bearing formaldehyde moiety formed by an N-Mannich reaction.[52] Fenick and coworkers explained that doxorubicin catalyzes "*the production of superoxide and hydrogen peroxide through the redox machinery of the quinone functionality. These reactive oxygen species, through an iron-catalyzed Fenton reaction, oxidize cellular constituents to produce formaldehyde. The resulting formaldehyde reacts with the drug to produce doxoform or at least the respective mono-oxazolidines, 3′-N,4′-O-methylenedoxorubicin (the active metabolite). Doxoform (or the mono-oxazolidines) reacts with DNA to form virtual cross-*

links, which trigger apoptosis. Consequently, doxoform, which carry their own formaldehyde into the cells, are more effective against sensitive cells than their parent compounds". Doxoform was found to be 150-fold more toxic to MCF-7 sensitive and 10000-fold more toxic to MCF-7/ADR resistant breast cancer cells, respectively.[52]

Prolonged administration of doxorubicin leads to resistance by cancer cells. Further, doxoform has drawbacks of poor solubility, short lifetime and high toxicity.[52] Conjugation of doxorubicin with salicylamide led to the N-Mannich base doxaliform. Doxaliform is a water soluble prodrug of doxorubicin with a half-life of approximately one hour and is 4-fold and 10-fold more cytotoxic than doxorubicin against MCF-7 and MCF-7/ADR breast cancer cells, respectively.[53] Over 2000 analogs of doxorubicin are currently known.

Mannich bases derived from carbonyl substrates such as ketones and carboxylic acid derivatives or H-bond acceptors situated in close proximity to the Mannich side chain derived from ammonia or a primary amine can undergo reversible intramolecular hydrogen bonding. A similar phenomenon is true for substrates with H-bond donors located at a proximal distance to the Mannich base side chain to afford stable transient cyclic molecular conformations. Intramolecular hydrogen bonding (IMHB) introduces lipophilic character to a drug enabling a polar molecule to circumvent non-polar biological barriers, for example.[54] When present, IMHB greatly impacts the molecular properties, function, and interaction of the molecule with biological systems.[55–58]

Amodiaquine is the first Mannich base used to treat malaria. Although its mechanism of action is not well elucidated yet, it is believed to act *via* a similar mechanism as other 4-aminoquinolines through inhibition of hemozoin formation in the digestive vacuole of the *Plasmodium* parasite. Pyronaridine is a congener of amodiaquine successfully being used clinically as a drug.[59] WR-194,965 (Figure 5.8) is an aminomethylphenol discovered in the 1970s as part of a US Army Research Program in malaria. It exhibited high potency against both chloroquine-sensitive and chloroquine-resistant strains of *P. falciparum* with IC_{50} values in the sub-nanomolar range.[60] It exhibited *in vivo* blood schizontocidal activity against *P. berghei*.[61] The limited potency of WR-194,965, however, led to its termination in clinical development by the US Army. A new Mannich base, MK-4815, developed from WR-194,965 exhibited improved antimalarial potency with good

pharmacokinetic profile in the *P. berghei in vivo* mouse model. It displayed *in vitro* efficacy against six drug-resistant *P. falciparum* strains with IC_{50} values in the 14 - 110 nM range. *In vitro* studies showed that the compound selectively accumulated in infected red blood cells and was most effective against the metabolically active late trophozoite/early schizont stages.[62] JPC-2997 is related to WR-194,965 and MK-4815. It displayed high *in vitro* activity (IC_{50} = 7 - 34 nM) against the chloroquine-sensitive D6, the chloroquine-resistant W2, and the multidrug-resistant TM90-C2B *P. falciparum* strains.[60] JPC-2997 was twice as active as WR-194,965 *in vitro* against *P. falciparum* lines. With respect to the D6 strain of *P. falciparum*, JPC-2997 was found to be >2,500 times less cytotoxic to the human HepG2 and HEK293 cancer cell lines and BHK rodent cell line. Moreover, it displayed high *in vivo* potency and a long elimination half-life of 49.8 hours.[60]

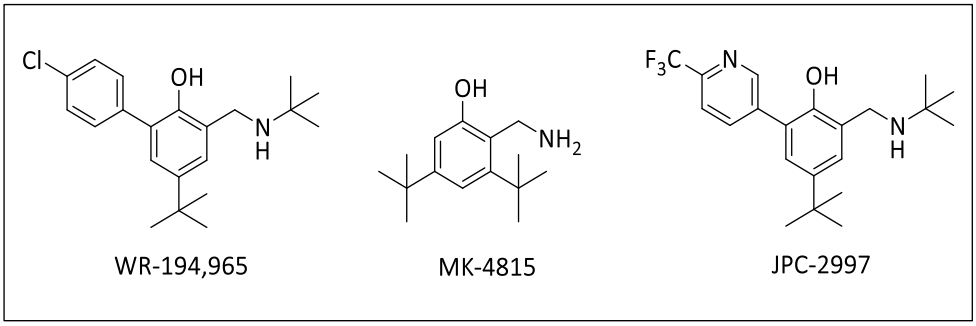

Figure 5.8: Chemical structures of WR-194,965, MK-4815 and JPC-2997

Amodiaquine is metabolized in the liver to its pharmacologically active metabolite, N-desethylamodiaquine, by the cytochrome p450 enzyme CYP2C8.[63] Like amodiaquine, the biological properties of some Mannich bases have been attributed to their active metabolites. For example, a high-throughput screening of 350000 compounds identified Mannich bases as a new class of thioredoxin reductase (TrxR) mechanism-based inhibitors. TrxR catalyzes the reduction of oxidized thioredoxin (Trx) by NADPH. It is involved in maintaining an adequate reducing environment and defense against oxidative stress in *P. falciparum*. Although TrxR is also present in humans, the protein sequences differ profoundly at the C-terminal redox center where human TrxR contains a cysteine-selenocysteine pair (Cys495′-Sec496′) while *P. falciparum* TrxR (PfTrxR) has two cysteine residues (Cys535′ and Cys540′) separated by four amino acids.[64] As a result, TrxR has been proposed as a possible target for antimalarial drug discovery. It was demonstrated that

α, β-unsaturated ketonic Mannich bases irreversibly inactivated TrxR by formation of an inactive macrocyclic species by bisalkylation, first of the C-terminal thiol of Cys540′ (the equivalent of SeCys in the human enzyme) and subsequently of Cys535′. It is essential that the ketonic Mannich base has two electrophilic sites (**I**, Figure 5.9) which includes the presence of an alpha proton to ensure bonding to both cysteine residues (Cys540′ and Cys535′). It was observed that the presence of only the alpha proton electrophilic site (**II**, Figure 5.9) allowed bonding to only one cysteine residue Cys540′. In both cases, the reactive metabolite (**III**, Figure 5.9) generated after deamination of the Mannich base was necessary for a Micheal addition to the dithiol 540′/535′ of PfTrxR.[64] In another related example, ketonic Mannich bases derived from acetophenones and α, β-unsaturated ketones (or those arising from deamination reactions) have been shown to exert their cytotoxic action through the alkylation of cellular thiols such as glutathione or cysteine.[65] Moreover, *ortho* phenolic Mannich bases (**IV**, Figure 5.9) readily undergo deamination reaction to form the quinone methine active metabolite (**V**, Figure 5.9) which is attributed to the potent cytotoxic activity of chalcones.[66]

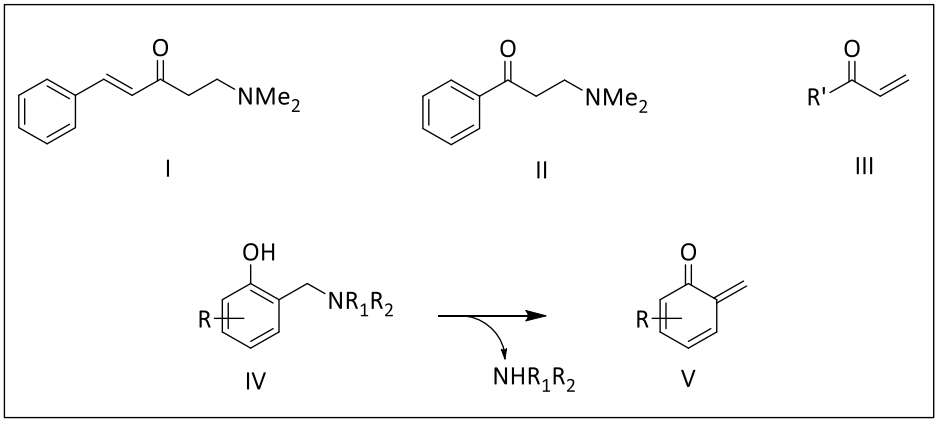

Figure 5.9: Chemical structures of compounds **I-V**

5.1.5 Hemoglobin degradation pathway and inhibitors of beta-hematin formation

The formation of hemozoin is a unique process adopted by *Plasmodium spp.* to detoxify free heme, which is a toxic by-product of the degradation of hemoglobin. Other hematophagous organisms such as *Rhodnius* and *Schistosoma* also make use of this process. Hemoglobin is ingested into the *Plasmodium* parasite's food vacuole by pinocytosis in small tubular vesicles, which arise from the

cystostome (Figure 5.10). In the acidic medium of the food vacuole, oxidation is followed by hydrolysis by aspartic proteases (plasmepsins I and II) to form denatured globin and heme (Fe^{2+}). Enzymatic hydrolysis by falcipain and falcilysin, followed by cytosolic exopeptidases, converts globin to peptides, and finally, amino acids, respectively (Figure 5.10).[67]

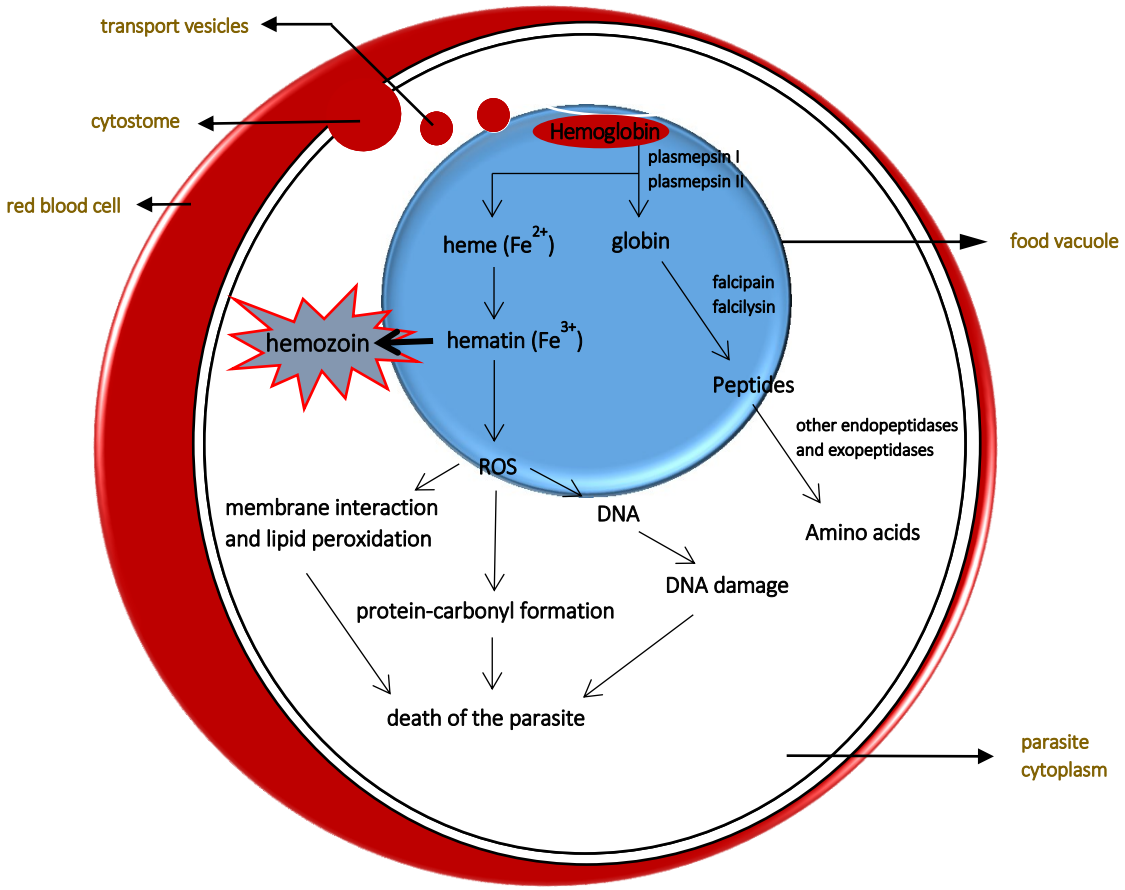

Figure 5.10: Degradation of hemoglobin in Plasmodium parasite[67,68]

Free heme (Fe^{2+}-protoporphyrin IX) is toxic to the parasite. It is inactivated in the food vacuole by peroxidases and superoxide dismutases.[69] In the presence of peroxide antimalarial drugs such as the artemisinins, free radical derivatives and other reactive derivatives of the drugs are generated.[70,71] These reactive species cannot be quenched and, thus, cause the death of the parasite.[68,72] Upon oxidation, however, heme (Fe^{2+}) is converted to the equally toxic hematin Fe^{3+} congener. The lipophilicity of hematin (Fe^{3+}) makes it easy to intercalate in the membrane of the

parasite, which may cause changes in membrane permeability and lipid organization and induce lipid peroxidation.[67] Hematin (Fe^{3+}) can induce oxidation of the components of the membrane, by forming reactive oxygen species (ROS), leading to cell lysis and eventually death of the parasite.[73] Heme detoxification is therefore an important process in the erythrocytic stage of the malaria parasite (Figure 5.11).

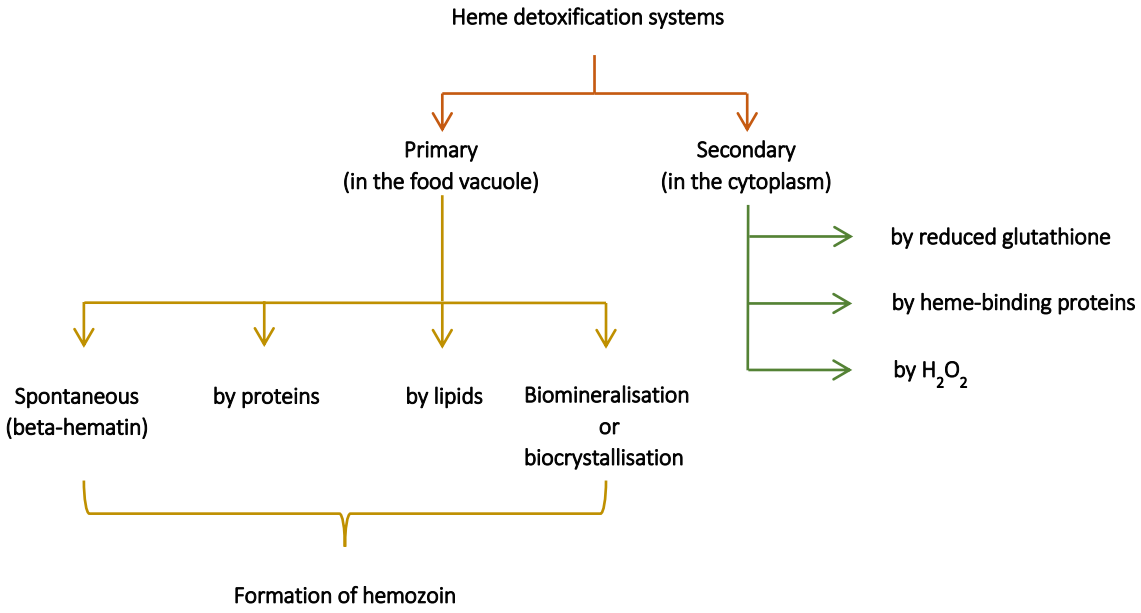

Figure 5.11: Mechanisms of heme detoxification in *Plasmodium* parasite[67]

Sequestration of heme into hemozoin is not an enzymatic process. It is a spontaneous process and occurs readily under appropriate physicochemical conditions.[74] In fact, beta-hematin can be spontaneously synthesized, *in vitro*, if monomeric hematin (Fe^{3+}) is allowed to incubate at physiological temperature (37 °C) at a pH of 4.8.[75] Under these conditions, synthetic beta-hematin can only be formed in the presence of some biological factors including the malaria parasite lysate, organic solvent extracts of the parasite lysate, histidine rich protein II or III, preformed hemozoin or beta-hematin and some unsaturated lipids.[75–78] Other methods of *in vitro* formation of beta-hematin have also been reported.[79–81] Structurally, a hemozoin crystal is composed of a series of hematin (Fe^{3+}-protoporphyrin IX) molecules linked into dimers through reciprocal iron-carboxylate bonds to the propionic side chains of each porphyrin, and that the dimers form chains linked by hydrogen bonds between the remaining propionate groups in the crystal.[82]

The major drug families, which inhibit beta-hematin formation include the quinolines, azoles, isonitriles, xanthones, methylene blue and its derivatives, and metalloporphyrins (Figure 5.12). The quinoline class of beta-hematin formation inhibitors include the antimalarials amodiaquine, chloroquine, tebuquine, pyronaridine, halofantrine, quinine, quinidine and bisquinoline. These compounds form complexes with hematin through π-π stacking interactions.[83–85] These interactions are believed to lead to oxidative stress, through the formation of reactive oxygen species (ROS), which may lead to peroxidation of parasite membrane lipids, damage of DNA, oxidation of protein and finally death of the parasite.[67] Structure-activity relationship (SAR) studies of the quinoline drugs have revealed the importance of the 7-chloro group to beta-hematin inhibition activity. It has been demonstrated that the 4-aminoquinoline nucleus of chloroquine and related antimalarials is responsible for complexing free heme, while the beta-hematin inhibition activity is attributable to the C-7 substituent.[86] Only few groups, such as the nitro and bromine substituents, are tolerated at the 7-position for beta-hematin activity. Optimum antimalarial activity is, however, achieved by the presence of the aminoalkyl side chain.[80,87] The length of the chain only has an effect on the activity of the drug against the chloroquine-sensitive and chloroquine-resistant strains of *P. falciparum*. Although the stereochemistry of the C-8 and C-9 is necessary for the antimalarial activities of the cinchona alkaloids, replacement of the quinuclidine group with a similarly basic piperidine has led to improvement in activity.[88]

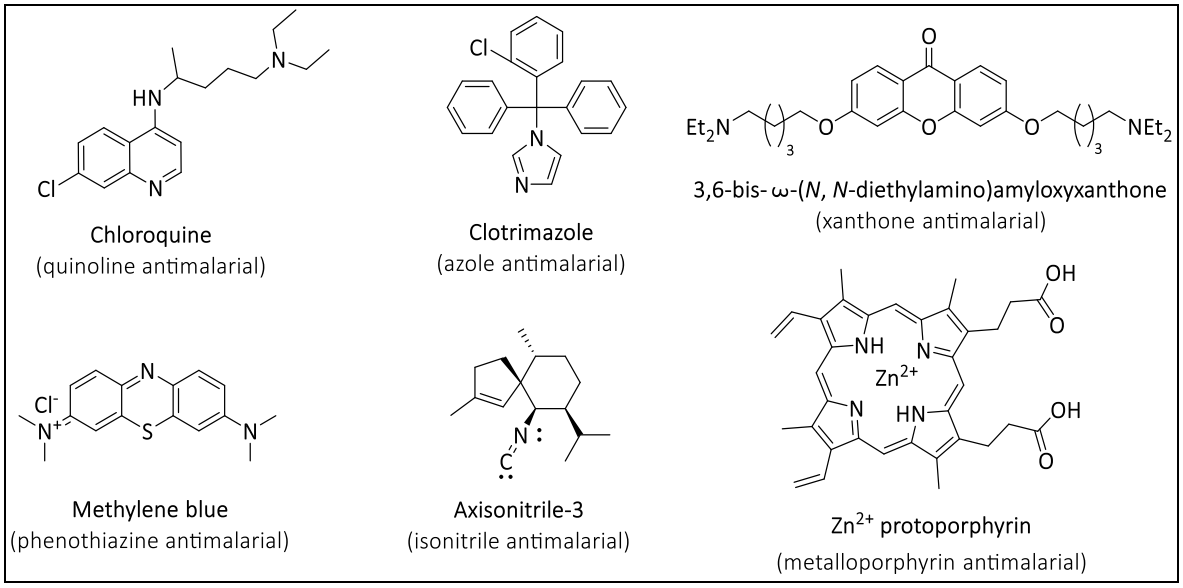

Figure 5.12: Examples of inhibitors of beta-hematin formation

Clotrimazole, a potent antimycotic drug, is an important member of the azole class of antimalarials. It inhibits *in vitro* parasite growth of different strains of chloroquine-sensitive and resistant of *P. falciparum* (IC_{50}, 0.2 – 1.1 μM).[89] Clotrimazole has a relative high affinity for heme, inhibits reduced glutathione-dependent heme catabolism, and enhances heme-induced hemolysis.[90] Other antifungal agents, such as ketoconazole and miconazole, have demonstrated antimalarial properties, however, they are less active compared to clotrimazole.[91] The azoles inhibit heme polymerization by displacing heme from histidine-rich peptide-heme complexes, which initiate heme polymerization.[91] A similar phenomenon has been observed in the reduced glutathione-heme complexes which dissipate the concentration of heme in the food vacuole through catabolism.[90] Two nitrogenous ligands derived from the imidazole moieties of two azole molecules are responsible for the stable azole-heme complexes. The importance of the imidazole scaffold to the activity of the azoles is supported by the reduction in activity (IC_{50} = 11 μM) of chlorophenyl-bis-phenyl methanol, one of *in vivo* metabolites of clotrimazole, which contains no imidazole group.[92]

The isonitrile class of hemozoin inhibitors were discovered from a series of terpenoid isonitrile natural products of marine origin.[93,94] The mechanisms responsible for their antimalarial properties include inhibiting the decomposition of H_2O_2, the peroxidative destruction of heme and the GSH-mediated breakdown of heme.[94] Wright and coworkers have demonstrated that the isonitriles, diisocyanoadociane and axisonitrile-3, form coordination complexes with Fe^{3+} of heme.[94] The phenothiazinium salt methylene blue [3, 7-bis (dimethylamino) phenothiazinium chloride] is the oldest known synthetic antimalarial drug. Methylene blue and its derivatives have exhibited antiplasmodium activity against various strains of *P. falciparum* (IC_{50}, 0.2 - 100 nM), primarily due to their inhibition of hemozoin formation.[95] While the antimalarial properties of these phenothiazines increased with an increase in the number of basic groups in the aminoalkyl side chain, as a result of increased drug accumulation in the parasite's food vacuole, their ability to inhibit polymerization of heme has been attributed to π-π stacking interactions between the aromatic moieties of the phenothiazine core scaffold and the porphyrin.[96]

It has been shown that trophozoites treated with the 2,3,4,5,6-pentahydroxyxanthone were arrested in their development and became degenerate in appearance within 24 hours of drug exposure, an observation which supports their mode of action as inhibitors of hemozoin formation.[97] The intermolecular interactions between xanthones and heme comprise of coordination between the Fe^{3+} and the carbonyl group of xanthone, hydrogen bonding between the xanthone hydroxyls and the propionate group of heme, and lastly, π-π stacking interactions between the aromatic moieties of both molecules.[98,99] The complexation of heme with xanthones was found to not only depend on pH and solvent, but also it acts in a unique way by forming a soluble complex with a heme dimer in aqueous solution.[98,99] Xanthones with high numbers of hydroxyl groups have exhibited better activity than those with lower numbers. More specifically, the most potent xanthone possesses hydroxyl groups at positions 3, 4, 5, and 6. The poor activity of the 1, 8 dihydroxy congener has been attributed to hydrogen bonding with the carbonyl oxygen, thereby leading to poor affinity for heme.[97,100] Further, incorporation of R-groups bearing basic nitrogen atoms have led to increased heme binding affinity. Two 3,6-bis-ω-diethylaminoalkoxyxanthone analogues, having side chains of 5 and 6 carbon atoms, exhibited IC_{50} values of 8.26 and 9.02 µM, respectively. The increase in heme binding affinity was attributed to the strong ionic interactions with the propionate side chains of heme and increased drug accumulation in the low pH medium of the parasite's food vacuole.[101]

Metalloporphyrins have exhibited moderate antiplasmodium activity (IC_{50}, 15.5 - 190 µM).[102] Their mode of action involves intercalation of heme molecules through metal-enhanced heteroporphyrin π–π assemblies. The poor stability of these assemblies leads to a build up of free heme which is toxic to the parasite.[102,103] The inhibitory activity of the metalloprotoporphyrins towards beta-hematin formation is highly dependent on the central metal ion, with the water exchange rate for the octahedral aqua complexes of the porphyrin's central metal ion playing a significant role.[103] Mg (II) PPIX, Zn (II) PPIX, and Sn (IV) PPIX are as much as six times more efficacious than the free ligand protoporphyrin IX in preventing hemozoin formation and four times as efficacious as chloroquine.[103] Other metals, such as Cr, Co, Mn, and Cu, have also been explored as metalloporphyrin antimalarial agents.

5.2 Research Program

5.2.1 Hypothesis

Benzimidazole analogues developed by incorporation of phenolic Mannich bases are potential novel antitubercular and antiplasmodium drug leads.

5.2.2 Main objective

To synthesize novel benzimidazole-phenolic Mannich base analogues for *in vitro* antimycobacterial and antiplasmodium activities evaluation.

5.2.3 Specific aims

- To synthesize benzimidazole-Mannich base analogues as potential antimycobacterial agents.
- To synthesize benzimidazole-Mannich base analogues as potential antiplasmodium agents.
- To evaluate the synthesized compounds for cytotoxic and beta-hematin inhibition activities.

5.3 Design, Synthesis and characterization of benzimidazole analogues

5.3.1 Design and Synthesis

In the current study, the antiplasmodium activity of phenolic Mannich bases developed from aminophenols was explored. This is supported by the fact that a cursory search through the literature revealed that Mannich bases relevant to antiplasmodium activity have been obtained from aminophenols, exemplified by the 4-aminoquinoline antimalarial drug amodiaquine.[29,30] Hence, five phenolic Mannich bases from readily available aminophenols were synthesized and evaluated for their antiplasmodium activity as analogues of benzimidazole. Mannich bases of two of the aminophenols, 3-aminophenol and 4-aminophenol, have shown potent antiplasmodium activity having been employed in isoquine (and *t*-butyl isoquine) and amodiaquine, respectively.

Further, another literature search revealed no reports of the antiplasmodium activity of 2-aminophenol, hence it was explored in the current work. The last two aminophenols investigated were the 3-methyl and 4-methyl substituted derivatives of 2-aminophenol.

Compounds for structure activity-relationship (SAR) studies were synthesized from 2-chloro-1*H*-benzimidazole and three 1-benzyl substituted 2-chlorobenzimidazole compounds. The choice of the benzyl moiety was inspired by previous SAR studies developed in our laboratory. In summary, four benzimidazole-based compounds were evaluated for their antiplasmodium activity by developing an SAR investigation which incorporated five phenolic Mannich bases.

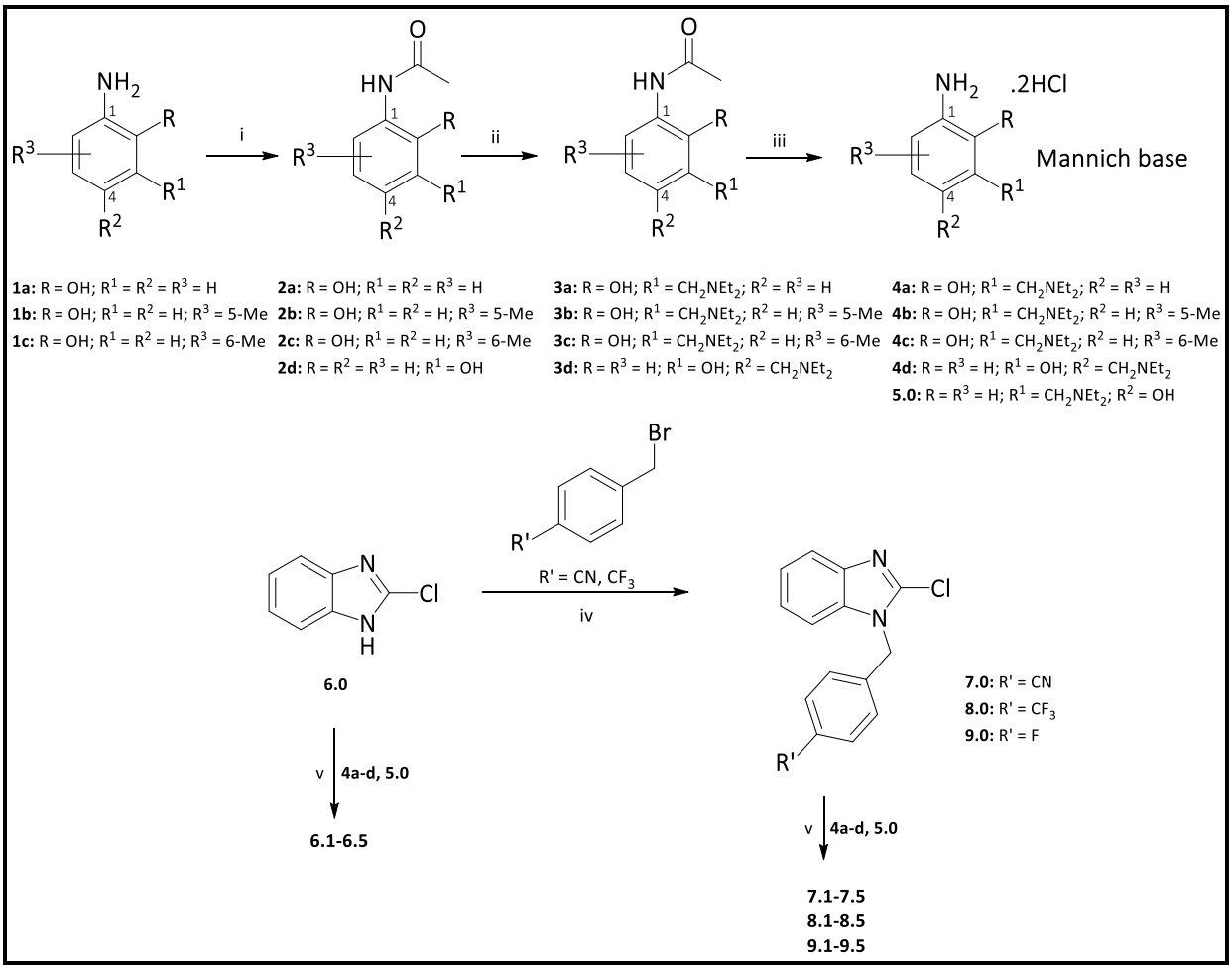

Scheme 5.1: Synthetic scheme to target compounds.

Reagents and conditions: (i) $(CH_3CO)_2O$, THF, 60 ^oC, 1 h; (ii) HCHO, $NHEt_2$, EtOH, 85 ^oC, 2 h; (iii) 6N HCl, 100 ^oC, 2 h; (iv) K_2CO_3, MeCN, 75 ^oC, 2 h; (v) KH_2PO_4, *n*-BuOH, 100 ^oC, 8 h

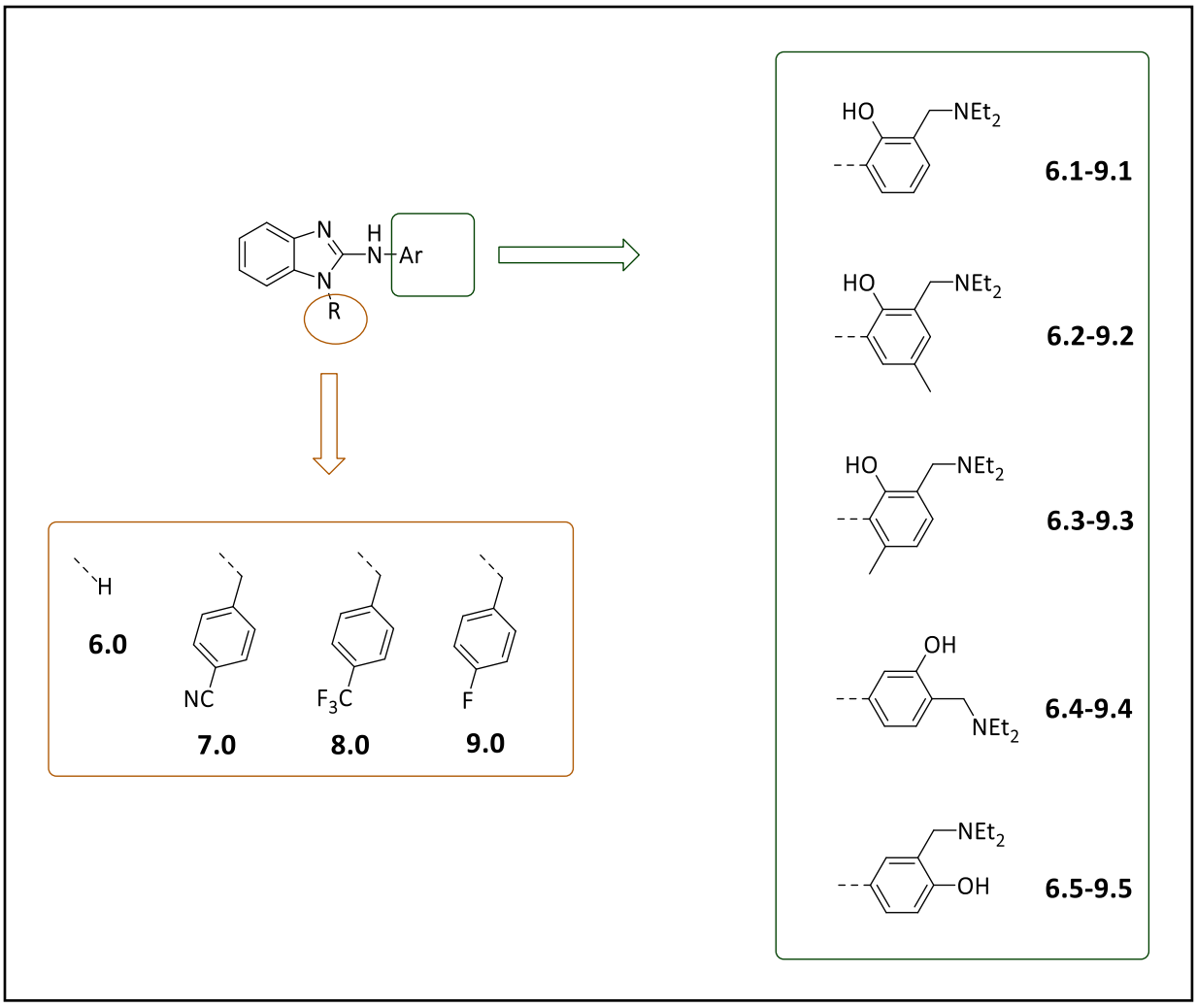

Figure 5.13: Summary of target compounds

The Mannich bases (**4a**-**4d**) were obtained in three steps (Scheme 5.1 (i) – (iii)). In the first step, the amino group was protected as the acetamide to reduce the possibility of regioisomers in the Mannich base products. The three 2-aminophenol congeners (**1a**-**1c**) were acetylated using acetic anhydride in THF at 60 ^{o}C to obtain the *N*-acetylated products **2a**-**2c**. The compounds (**2a**-**2c**) were then subjected to a Mannich reaction in the presence of formaldehyde and diethylamine in EtOH at 85 ^{o}C to afford **3a**-**3d**. The 3-hydroxyphenyl acetamide, **2d**, was obtained from a commercial source. Deacetylation of intermediates **3a**-**3d** in the presence of dilute HCl afforded the Mannich bases **4a**-**4d** as the HCl salts. The 4-aminophenol Mannich base **5.0** had already been synthesized and used in a previous reaction (Chapter four, Section 4.3.1) and so was used as such. All five Mannich bases were obtained as viscous oily matter in good yields (75 - 90%).

The two benzyl benzimidazole derivatives **7.0** and **8.0** were synthesized according to Scheme 5.1 (iv). The 2-chloro-1*H*-benzimidazole compound (**6.0**) was heated together with the *para*-substituted bromobenzyl reagent (4-CN and 4-CF_3) in acetonitrile in a nucleophilic substitution reaction to afford the 1-benzylated 2-chlorobenzimidazole intermediates **7.0** (4-CN) and **8.0** (4-CF_3) as white solids in quantitative yields (>98%). The reaction was conducted in the presence of K_2CO_3 as base to mop up the by-product HBr. Compound **9.0**, 1-(4-fluorobenzyl)-2-chlorobenzimidazole, was acquired from a commercial source.

The target compounds (**6.1**-**9.5**) were synthesized in another nucleophilic substitution reaction according to Scheme 5.1 (v). Each of the four benzimidazole compounds (**6.0**-**9.0**) was reacted separately with the Mannich bases **4a**-**4d** and **5.0**. The reaction conditions to obtain the target compounds, in a reproducible manner, involved KH_2PO_4 as base and *n*-BuOH as solvent, heated at the boiling point of *n*-BuOH (99 - 100^{o}C). The compounds were obtained in moderate to good yields (35 - 95%). Attempts to synthesize the compounds by using other routine polar laboratory solvents (EtOH, MeOH, dioxane, THF-DMF and DMF) and bases (NEt_3 and DIPEA) led to either no reaction at all or complex reaction mixtures, which made purification of the target compounds cumbersome. Twenty benzimidazole-phenolic Mannich base analogues (**6.1**-**9.5**) were synthesized in total.

The progress of all reactions was followed by normal phase silica TLC, together with acquisition of the mass on reversed phase C18 LCMS to track formation of the intended compound. The synthesized compounds were fully characterized by their TLC R*f* values in appropriate solvents, reversed phase C18 LC retention time, mass spectrometric and 1D NMR spectroscopic data. Where necessary, 2D NMR spectroscopic data was acquired to enable correct assignment of NMR signals.

5.3.2 Characterization of target benzimidazole analogues

All 1*H*-benzimidazole-Mannich base analogues (**6.1**–**6.5**) exhibited similar ^{1}H NMR spectrum as shown for **6.3** in Figure 5.14. The aromatic signals of the benzimidazole scaffold were observed in the olefinic region of the ^{1}H NMR spectrum resonating at δ_H 6.96 (dd, *J* = 3.2, 5.9 Hz, 2H) and 7.18

(dd, *J* = 3.1, 5.8 Hz, 2H) for H-5 and H-6, respectively. Meanwhile, the two olefinic protons of the Mannich base, H-10 and H-11, were observed at δ_H 6.71 (dd, *J* = 7.7 Hz, 1H) and 6.90 (d, *J* = 7.7 Hz, 1H). The methylene protons H_2-13 were assigned the chemical shift δ_H 3.84 (s, 2H) occurring downfield of the spectrum due to the deshielding effects of the phenyl ring and the diethylamino group. The signal at δ_H 2.24 (s, 3H) was assigned to the methyl group H_3-16. The two methyl protons of the diethylamino group resonated at δ_H 1.11 (t, *J* = 7.2 Hz, 6H, 2×H_3-15), being the most shielded of all the protons in **6.3**. Moreover, the signal at δ_H 2.69 (q, *J* = 7.2 Hz, 4H) were assigned to the two methylene groups represented by H_2-14. In a similar manner, based on the chemical environment, splitting pattern and the values of coupling constants, the ^{1}H NMR spectra of the other 1*H*-benzimidazole analogues (**6.1**, **6.2**, **6.4**, and **6.5**) were analyzed and characterized accordingly.

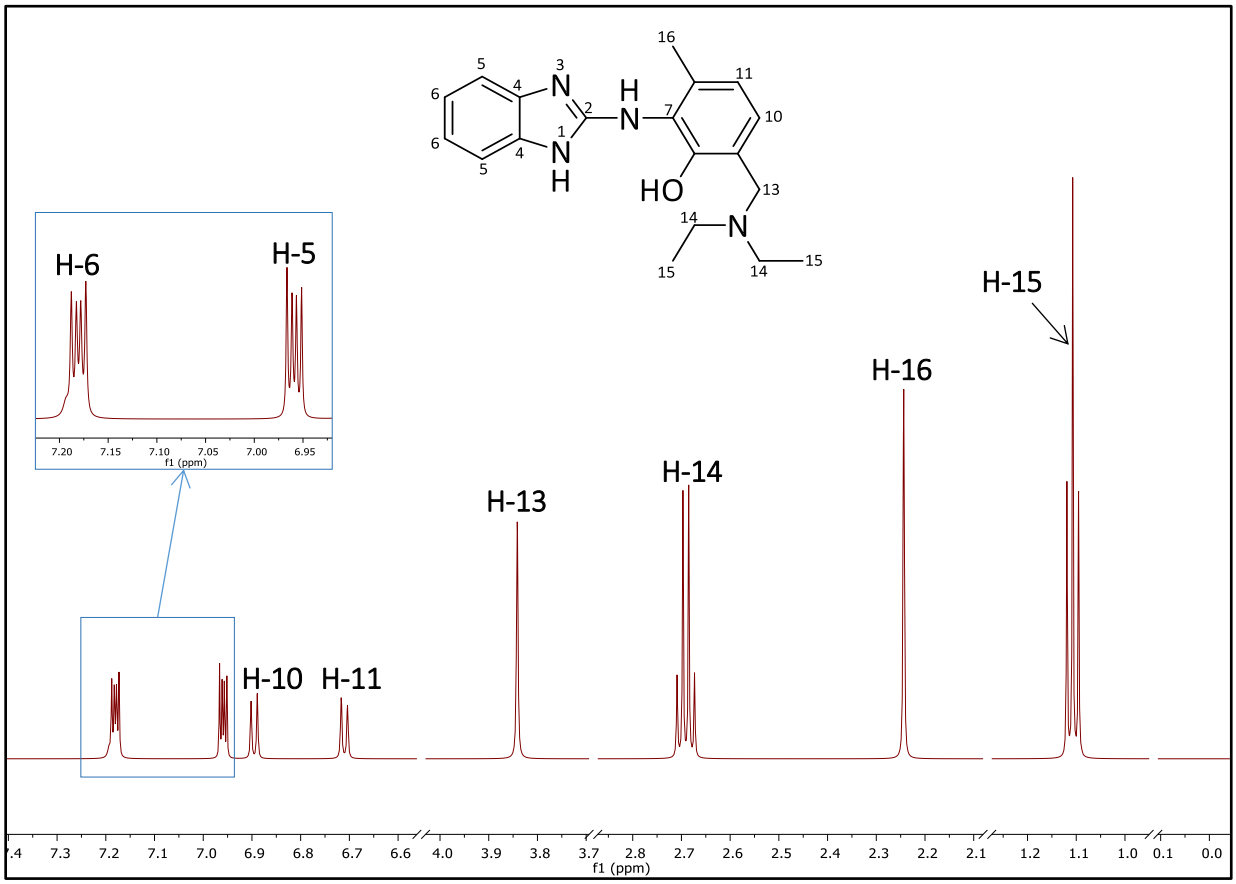

Figure 5.14: ^{1}H NMR (MeOH-d_4, 600 MHz) spectrum of **6.3**

The ^{1}H NMR spectra acquired for the 1-(4-cyanobenzyl) benzimidazole (**7.1**-**7.5**) and 1-((4-trifluoromethyl)benzyl) benzimidazole (**8.1**-**8.5**) target compounds are exemplified by the ^{1}H NMR spectrum of compound **8.3** (Figure 5.15). Olefinic signals attributable to the protons, H-12 and H-13, of the benzyl moiety were observed as doublets at δ_H 7.43 (d, *J* = 8.1 Hz, 2H) and 7.61 (d, *J* = 8.2 Hz, 2H) integrating for two protons each due to the symmetry of the benzyl group. The H-13 protons occurred downfield relative to H-12 as a result of the deshielding effect of the trifluoromethyl substituent at C-14. Meanwhile, the methylene protons (H_2-10) of the benzyl group resonated as a singlet signal at δ_H 5.49 (s, 2H).

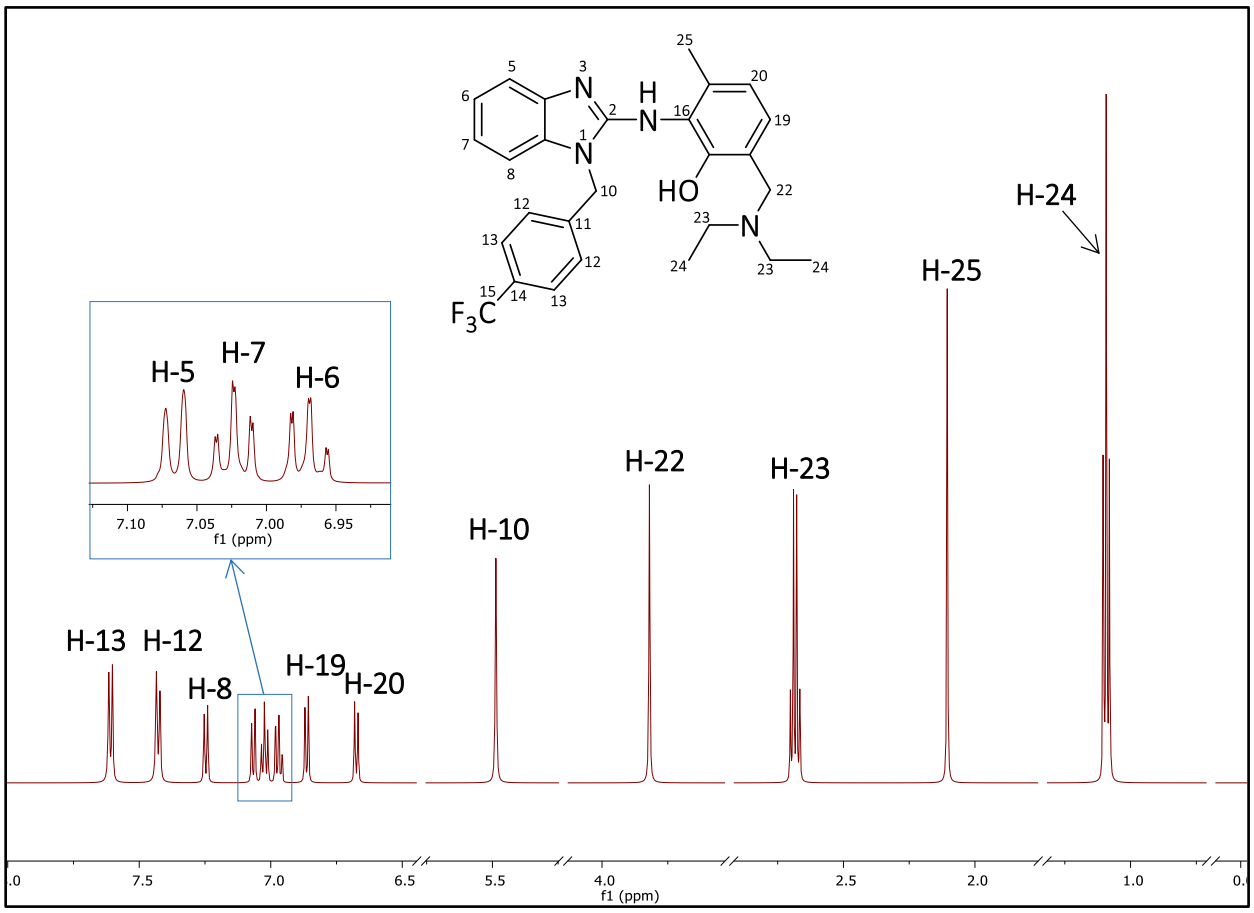

Figure 5.15: ^{1}H NMR (MeOH-d_4, 600 MHz) spectrum of **8.3**

Each olefinic proton of the benzimidazole scaffold of the benzylated benzimidazole analogues (**7.1**-**9.5**) exhibited a unique chemical shift. This is attributed to the fact that substitution of the benzyl group disrupted the tautomeric resonance of the imidazole substructure, which introduced

symmetry into the benzimidazole scaffold (Figure 5.15). The most deshielded of the protons, H-8, occurred at δ_H 7.25 (m, 1H) while H-5 resonated at δ_H 7.07 (m, 1H). Meanwhile, H-6 and H-7 each resonated at δ_H 6.97 (td, *J* = 7.5, 1.1 Hz, 1H) and 7.02 (td, *J* = 7.6, 1.2 Hz, 1H), respectively. Finally, the proton signals of the Mannich base were not significantly affected by substitution of the benzyl group on the benzimidazole scaffold, hence their chemical shifts are as they are in **6.3** (Figure 5.14).

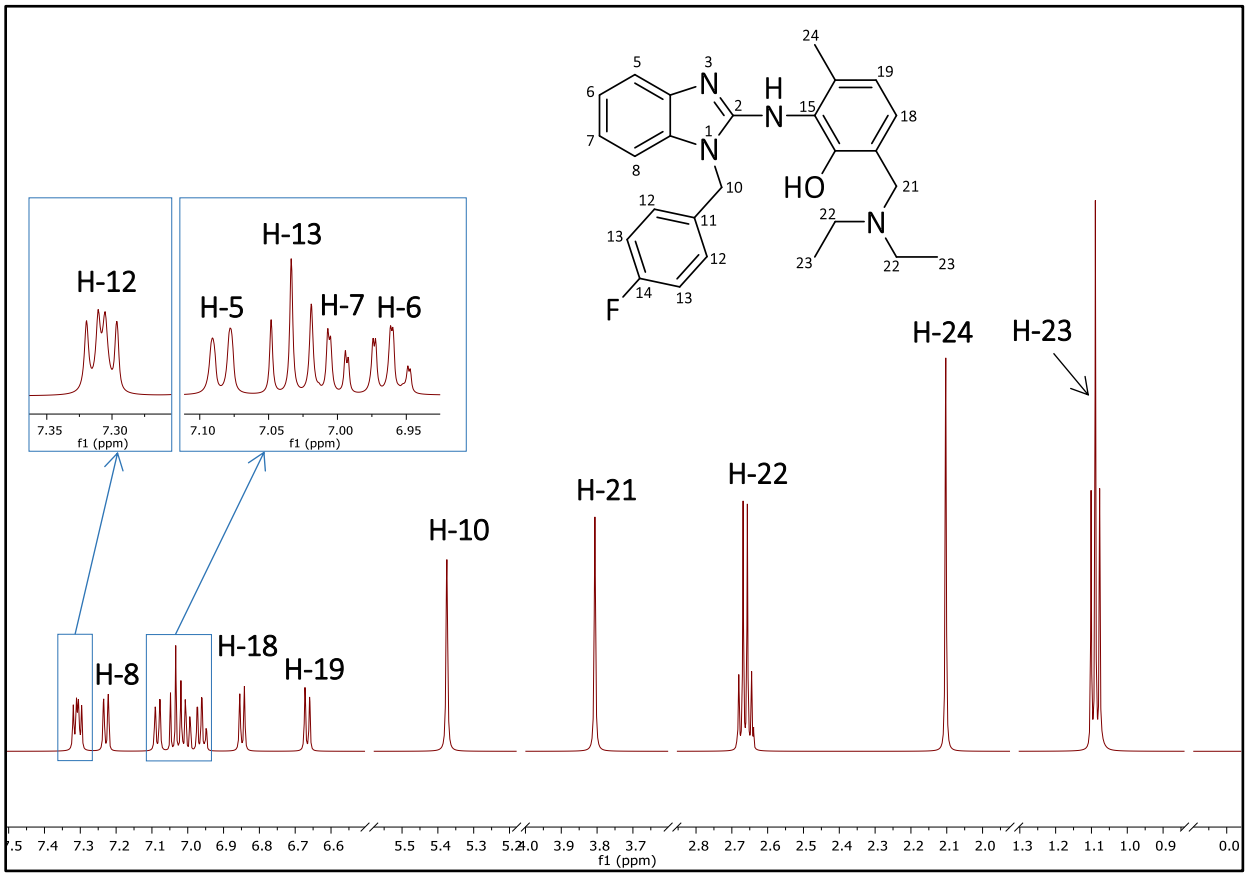

Figure 5.16: ^{1}H NMR (MeOH-d_4, 600 MHz) spectrum of **9.3**

The ^{1}H NMR spectra of the 1-(4-fluorobenzyl) benzimidazole analogues (**9.1**-**9.5**) were similar to the other benzylated derivatives (**7.1**-**8.5**). The chemical shifts and splitting pattern of the olefinic protons of the benzimidazole scaffold and the Mannich base protons were as previously observed. A key noticeable difference, however, was observed in the chemical shifts and splitting pattern of the olefinic protons of the benzyl group (Figure 5.16). Each of the protons H-12 and H-13 resonated as double doublets as a result of the extra coupling due to the fluorine atom. Hence,

the signals were assigned to the protons on the basis of the coupling constant observed. The H-13 methine protons were observed at δ_H 7.03 (t, *J* = 8.8 Hz, 2H) showing two strong *ortho* couplings to H-12 and the fluorine atom. The two methine protons H-12 occurred relatively downfield to H-13 at δ_H 7.31 (dd, *J* = 5.4, 8.6 Hz, 2H).

The ^{13}C NMR spectrum (Figure 5.17) of **9.3** also exhibited signals corroborating the effect of the fluorine atom. Each of the four carbon atoms of the benzyl moiety was split into a doublet due to coupling to the fluorine atom. C-14 exhibited the largest coupling constant (*J* = 244.4 Hz) while C-11, which is furthest away from the fluorine atom, exhibited the least coupling constant (*J* = 3.1 Hz).

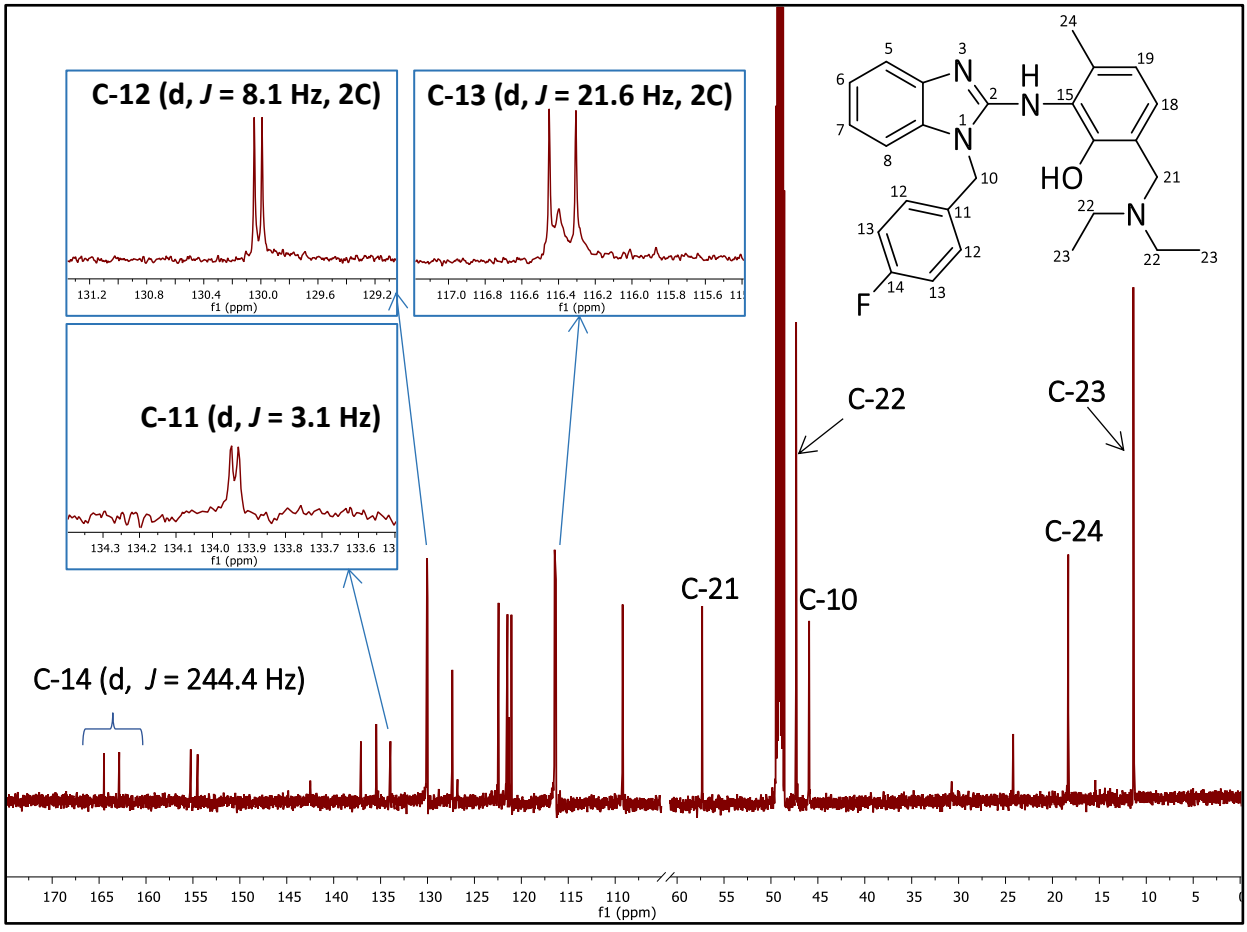

Figure 5.17: ^{13}C NMR (MeOH-d_4, 151 MHz) spectrum of **9.3**

5.4 Biological results and discussion

5.4.1 Antimycobacterial activity

Table 5.1: *In vitro* antimycobacterial ($H_{37}Rv$ strain) and cytotoxic (CHO cell line) activities of the benzimidazole analogues

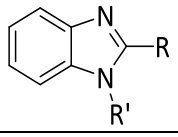

Compound	R	R'	*Mtb*($H_{37}Rv$), MIC_{90} (μM)		CHO IC_{50} (μM)
			7H9 GLU ADC TW	7H9 GLU CAS TX	
6.1	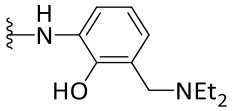	H	>125	17.13	>50
6.2	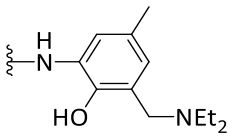	H	>125	8.97	>50
6.3	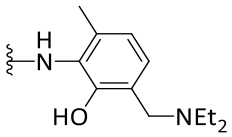	H	>125	16.00	>50
6.4	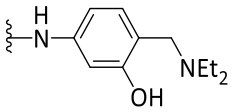	H	>125	>125	>50
6.5	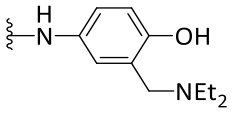	H	>125	>125	>50
7.1	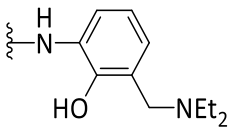	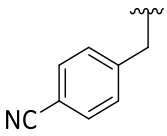	>125	30.52	>50
7.2	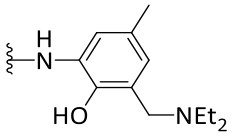	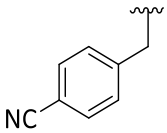	>125	9.55	14.19
7.3	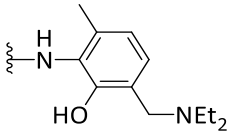	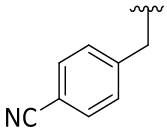	>125	15.67	>50

7.4	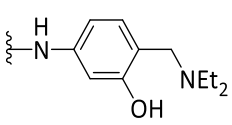	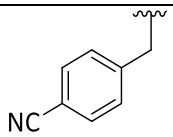	>125	17.49	39.04
7.5	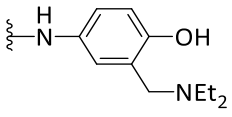	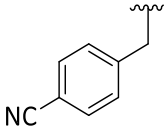	>125	34.84	>50
8.1	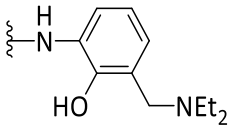	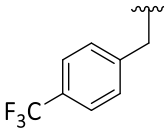	>125	3.80	>50
8.2	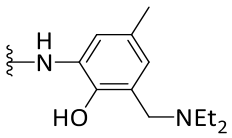	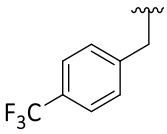	64.1	2.00	29.31
8.3	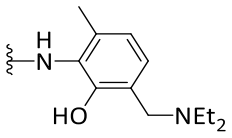	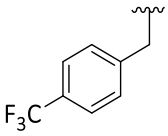	116	30.1	33.88
8.4	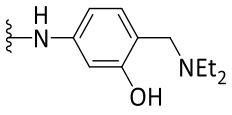	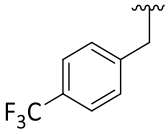	>125	6.49	41.50
8.5	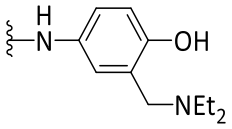	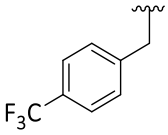	>125	7.81	17.50
9.1	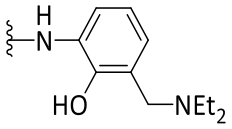	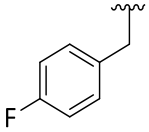	>125	6.46	>50
9.2	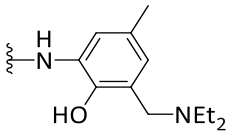	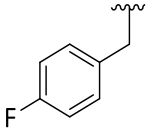	>125	7.09	18.70
9.3	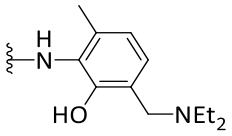	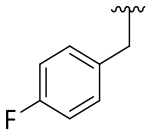	>125	5.90	>50
9.4	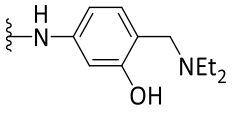	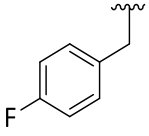	>125	7.21	45.79

9.5	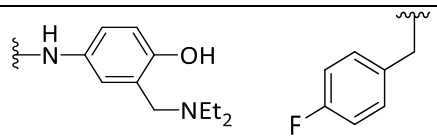	>125	21.41	11.99
Rifampicin		0.009	0.02	
Emetine				0.02

For the purpose of SAR analysis, all compounds with MIC_{90} ≤10 µM were regarded as active; those with MIC_{90} ranging from 10 – 20 µM had moderate activity; MIC_{90} = 20 – 125 µM denoted as poorly active; whereas compounds exhibiting MIC_{90} >125 µM were considered inactive. In this regard, the synthesized benzimidazole analogues were inactive in the 7H9/ADC media, except **8.2** (MIC_{90} = 64.10 µM) and **8.3** (MIC_{90} = 116 µM). However, they exhibited good to moderate activity in the 7H9/CAS media, except compounds **6.4** and **6.5** which were inactive. Among the 1*H*-benzimidazole analogues, it was observed that the hydroxyl group *ortho* to the nitrogen atom in the Mannich base moiety was essential for activity. Moreover, about a two-fold increase in activity was observed for compound **6.2** (MIC_{90} = 8.97 µM) when the methyl substituent was *para* to the hydroxyl group compared to **6.3** (MIC_{90} = 16.00 µM), which had the methyl substituent in a *meta* position.

Among the 1-(4-cyanobenzyl) benzimidazole analogues (**7.1**-**7.5**), compound **7.2** exhibited the best activity (MIC_{90} = 9.55 µM). Compounds **7.3** (MIC_{90} = 15.67 µM) and **7.4** (MIC_{90} = 17.49 µM) exhibited moderate activity while **7.1** and **7.5** were poorly active. Apart from **8.3**, which showed poor activity (MIC_{90} = 30.1 µM), the other 1-((4-trifluoromethyl)benzyl) benzimidazole analogues showed good potency (MIC_{90} <10 µM). Similarly, all the 1-(4-fluorobenzyl) benzimidazole analogues exhibited good activity, except **9.5** which displayed moderate activity (MIC_{90} = 21.41 µM).

In summary, the *N*-benzyl benzimidazole analogues exhibited better activity than the 1*H*-benzimidazole analogues. Generally, the analogues with Mannich base moieties bearing the hydroxyl group *ortho* to nitrogen atom exhibited better activity. Moreover, the activity was enhanced by substitution *para* to the hydroxyl group. With respect to substitution on the benzyl moiety, the fluoro and trifluoromethyl substituents led to an increase in activity compared to the

cyano group. Compound **8.2** exhibited the best activity (MIC_{90} = 2.00 µM) among the synthesized benzimidazole analogues.

5.4.2 Antiplasmodium activity and cytotoxicity

Table 5.2: *In vitro* activity against asexual (NF54 and K1 strains) and gametocyte (NF54 strain) *P. falciparum* parasites and cytotoxicity (CHO cell line) of the benzimidazole analogues

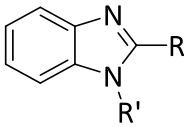

Compound	R	R'	Asexual parasites, IC_{50} (µM)		Gametocyte parasites, % inhibition, 1 µM		Cytotoxicity IC_{50} (µM)	
			Pf(NF54)	*Pf*(K1)	Early stage	Late stage	CHO	SI
6.1	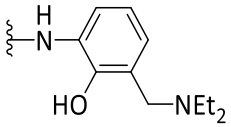	H	0.56	0.77	-	-	>50	>89.28
6.2	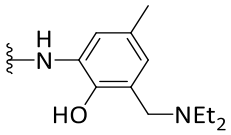	H	0.23	0.42	-	-	>50	>217.39
6.3	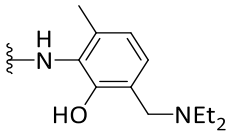	H	0.86	1.62	-	-	>50	>58.13
6.4	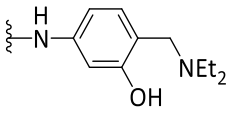	H	1.88	>10	-	-	>50	>26.59
6.5	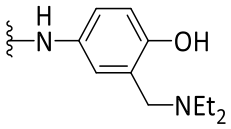	H	0.80	7.27	30	0	>50	>62.50
7.1	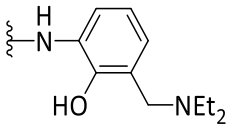	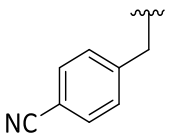	1.00	0.66	47	19	>50	>50
7.2	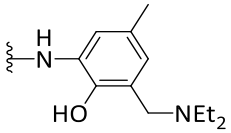	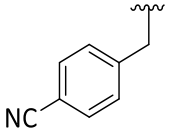	0.65	0.46	39	15	14.19	21.83

7.3	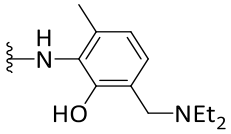	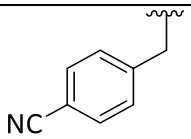	0.87	0.83	19	0	>50	>57.47
7.4	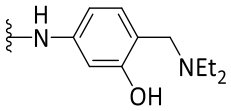	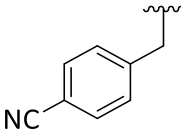	0.37	0.76	38	4	39.04	105.51
7.5	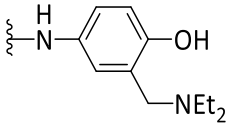	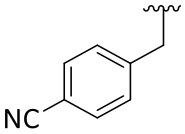	0.47	1.97	20	9	>50	>106.38
8.1	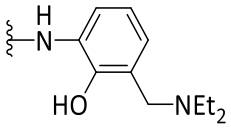	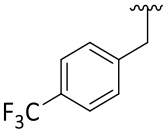	0.44	0.13	71	35	>50	>113.63
8.2	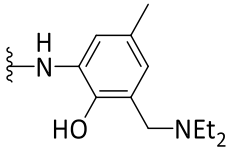	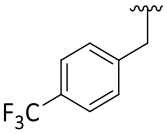	0.19	0.06	91	41	29.31	154.26
8.3	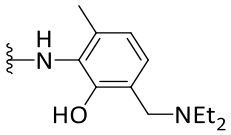	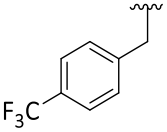	2.88	0.94	18	1	33.88	11.76
8.4	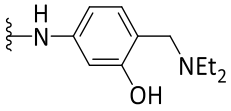	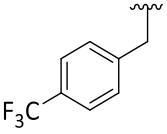	0.47	0.87	36	2	41.50	88.29
8.5	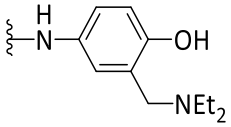	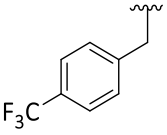	0.39	1.69	34	31	17.50	44.87
9.1	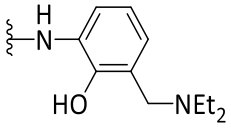	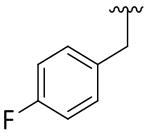	0.36	0.18	65	11	>50	>136.88

9.2	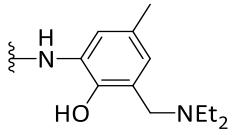	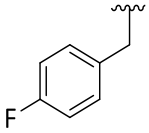	0.55	0.21	81	31	18.70	34.00
9.3	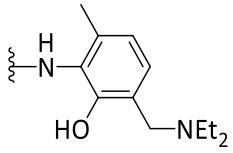	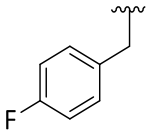	2.27	1.32	-	-	>50	>22.02
9.4	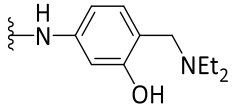	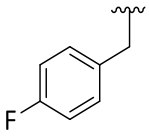	0.64	1.28	-	-	45.79	71.54
9.5	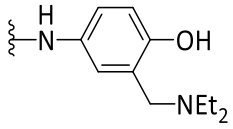	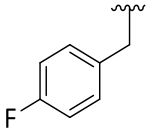	0.68	1.95	33	22	11.99	17.63
Chloroquine			0.01	0.42				
MMV390048					77	92		
Emetine							0.02	

The synthesized benzimidazole analogues were evaluated for their *in vitro* multi-stage antiplasmodium activity against asexual erythrocytic (NF54 and K1 strains) parasites and early and late stage gametocytes of *P. falciparum* (Table 5.2). The activity of the compounds against the asexual parasites was evaluated using the modified [^{3}H]-hypoxanthine incorporation assay while their potential to inhibit gametocyte growth was evaluated using the luciferase reporter assay.

In the synthesized 1*H*-benzimidazole series, compounds **6.1** and **6.2** displayed sub-micromolar potency against both chloroquine-sensitive NF54 and multidrug-resistant K1 strains of asexual parasites with IC_{50} *Pf*NF54/K1 = 0.56/0.77 µM and IC_{50} *Pf*NF54/K1 = 0.23/0.42 µM, respectively. Similarly, sub-miromolar activity was recorded by **6.3** and **6.5** against the NF54 parasites but the former displayed moderate activity (IC_{50} *Pf*K1 = 1.62 µM) against the K1 parasites while **6.5** lost activity. Compound **6.4** was the least potent of the 1*H*-benzimidazole analogues (IC_{50} *Pf*NF54/K1 = 1.88/>10 µM).

All analogues based on the *N*-benzyl benzimidazole scaffold displayed sub-micromolar activity against the chloroquine-sensitive strain of *P. falciparum*, except compounds **7.1** (IC_{50} *Pf*NF54 =

1.00 µM), **8.3** (IC_{50} *Pf*NF54 = 2.88 µM) and **9.3** (IC_{50} *Pf*NF54 = 2.27 µM). Generally, the compounds were more potent towards the multi-drug resistant strain (K1) than the sensitive NF54 strain. Within the benzyl benzimidazole series, the 1-((4-trifluoromethyl)benzyl) and 1-(4-fluorobenzyl) benzimidazole analogues displayed better activity than the 1-(4-cyanobenzyl) benzimidazole analogues. In regard to the SAR based on the Mannich base used, synthesized compounds based on the 3-((*N*,*N*-diethylamino)methyl)-2-hydroxy aniline and its 5-methyl derivative were better tolerated for activity. All *N*-benzyl analogues of the 3-((*N*,*N*-diethylamino)methyl)-4-hydroxy aniline Mannich base were the least active in each series (Table 5.2). In summary, compound **8.2** demonstrated the most potent activity against the asexual parasites (IC_{50} *Pf*NF54/K1 = 0.19/0.06 µM), with significant activity against the multidrug-resistant K1 strain. All the compounds were relatively non-cytotoxic (IC_{50} >10 µM) to the CHO cell line, recording acceptable selectivity indices, S1>10 (Table 5.2).

The benzimidazole analogues based on the *ortho*-hydroxy Mannich bases and its derivatives displayed good activity against both early and late stage *P. falciparum* gametocytes, evident in the %inhibition of parasite growth at 1 µM and 5 µM (Table 5.2). Generally, the 1-(4-fluorobenzyl) and 1-((4-trifluoromethyl)benzyl) benzimidazole analogues were more potent than their 1-(4-cyanobenzyl) congeners, which displayed moderate activity. Compound **8.2** was the most potent analogue inhibiting 91% of parasite growth at 1 µM.

5.4.3 Beta-hematin inhibition activity and turbidimetric (kinetic) solubility

Table 5.3: *In vitro* activity against asexual (NF54 strain), beta-hematin inhibition activity (BHIA) and solubility of the benzimidazole analogues

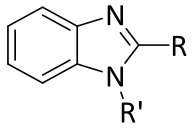

Compound	R	R'	*Pf*(NF54) IC_{50} (µM)	BHIA IC_{50} (µM)	Solubility, µM, pH 7.4
6.1	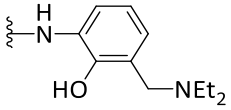	H	0.56	74.6	40
6.2	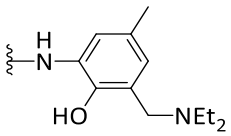	H	0.23	39.5	40
6.3	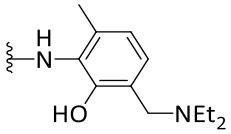	H	0.86	159.3	20
6.4	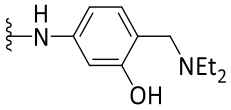	H	1.88	486.2	40
6.5	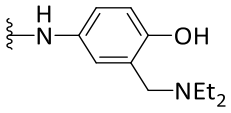	H	0.80	631.6	160
7.1	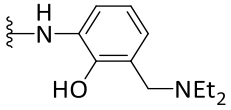	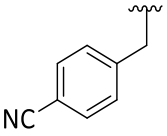	1.00	159.4	80
7.2	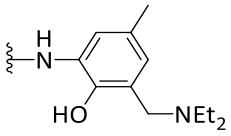	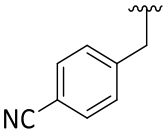	0.65	126.6	20
7.3	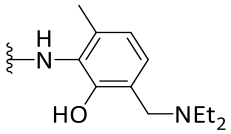	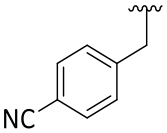	0.87	133.9	80

7.4	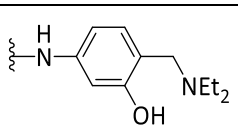	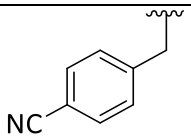	0.37	131.8	80
7.5	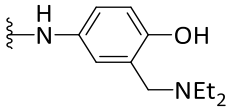	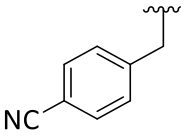	0.47	1079	160
8.1	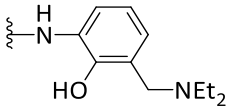	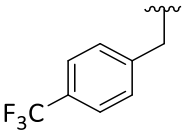	0.44	236.9	20
8.2	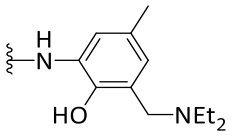	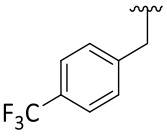	0.19	65.3	5
8.3	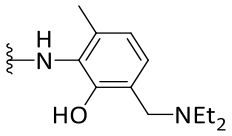	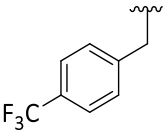	2.88	91.4	40
8.4	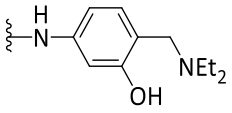	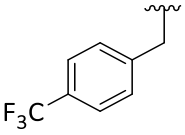	0.47	90.9	80
8.5	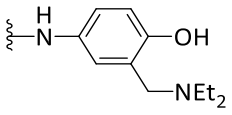	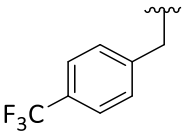	0.39	140.0	40
9.1	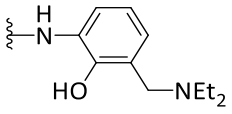	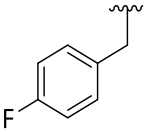	0.36	250.4	40
9.2	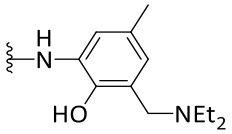	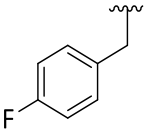	0.55	123.2	5
9.3	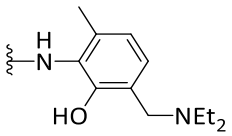	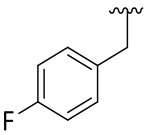	2.27	142.3	80
9.4	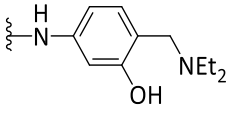	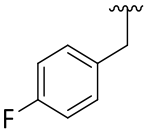	0.64	148.5	80

9.5	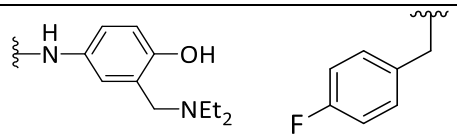	0.68	399.2	10
Chloroquine		0.01		
Amodiaquine			13.1	

The mechanistic potential of the synthesized analogues to inhibit hemozoin formation was evaluated *in vitro* by investigating their ability to inhibit beta-hematin formation. The Nonidet-P-40 (NP-40) detergent-mediated assay was employed and the assay was conducted in acetate buffer (pH 4.8) at 37 ^{o}C. With an acceptable cut-off of IC_{50} <100 µM for good inhibition, it was observed that only four analogues acted as active inhibitors of beta-hematin formation (Table 5.3). The most potent inhibitor was **6.2** (IC_{50} = 39.5 µM) while its 1-((4-trifluoromethyl)benzyl) benzimidazole derivative, **8.2**, was about two-fold less active with an IC_{50} value of 65.3 µM. Similarly, the 1-((4-trifluoromethyl)benzyl) benzimidazole derivatives, **8.3** and **8.4**, exhibited comparable activity with IC_{50} values of 91.4 µM and 90.9 µM, respectively.

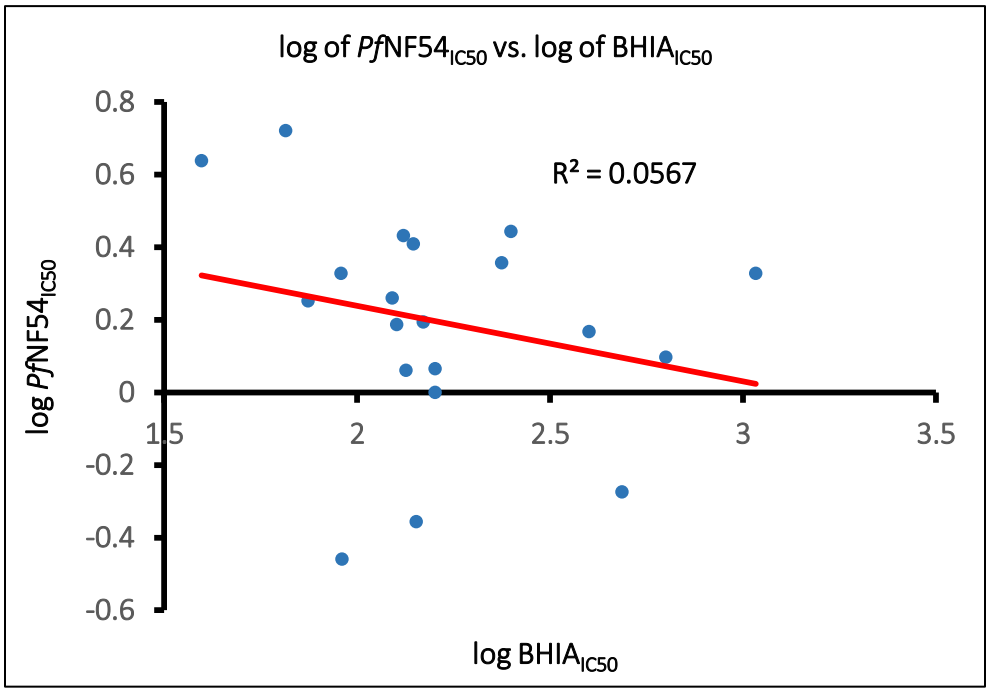

Figure 5.18: Linear correlation between erythrocytic whole cell activity (*Pf*NF54, IC_{50} values) and beta-hematin inhibition activity (BHIA) IC_{50} values

A linear correlation between whole cell activity (asexual blood stage NF54 parasites) and beta-hematin inhibition activity (BHIA) of the synthesized compounds (Figure 5.18) reveals no apparent correlation (R^2 = 0.0567). This data suggests that the compounds do not elicit their antiplasmodium potency via inhibition of hemozoin formation, and thus, they may act by a novel mode of action. This is supported by the observation that the compounds were generally more active against the multidrug-resistant K1 strain when compared to the sensitive NF54 strain. The good activities of the four compounds above could therefore be regarded as a surplus advantage specific to them.

The approximate aqueous solubility of the synthesized compounds was evaluated as the concentration value above which the compounds precipitate from an aqueous buffer (phosphate buffered saline (PBS), pH 7.4), at ambient temperature, and causes turbidity. The occurrence of turbidity was detected by measuring the UV-VIS absorbance of the suspension at 620 nm, since most compounds, including the synthesized compounds, do not absorb in this region. With soluble solutions of the compounds in DMSO serving as internal control, their aqueous solubility was predicted as the definite deviation (point of inflection) from the baseline (DMSO plot) of a graph of corrected absorbance at 620 nm and concentration of test compound (Figure 5.19).

The 1*H*-benzimidazole analogues showed moderate aqueous solubility (20 - 160 µM). Similarly, analogues of the benzyl benzimidazole series were moderately soluble, except compounds **8.2** (5 µM), **9.2** (5 µM), and **9.5** (10 µM), which were poorly soluble (Table 5.3). Generally, the 1-(4-cyanobenzyl) benzimidazole analogues were, as expected, more soluble than the lipophilic 1-(4-fluorobenzyl) and 1-((4-trifluoromethyl)benzyl) benzimidazole congeners of the same Mannich base moiety. Further, the 3-((*N*,*N*-diethylamino)methyl)-2-hydroxy-5-methyl aniline Mannich base moiety was not tolerated for aqueous solubility (Table 5.3, Figure 5.19), although it yielded the most potent analogues in three of the four benzimidazole series (**6.2**: IC_{50} *Pf*NF54/K1 = 0.23/0.42 µM; **7.2**: IC_{50} *Pf*NF54/K1 = 0.65/0.46 µM; **8.2**: IC_{50} *Pf*NF54/K1 = 0.19/0.06 µM; **9.2**: IC_{50} *Pf*NF54/K1 = 0.55/0.21 µM).

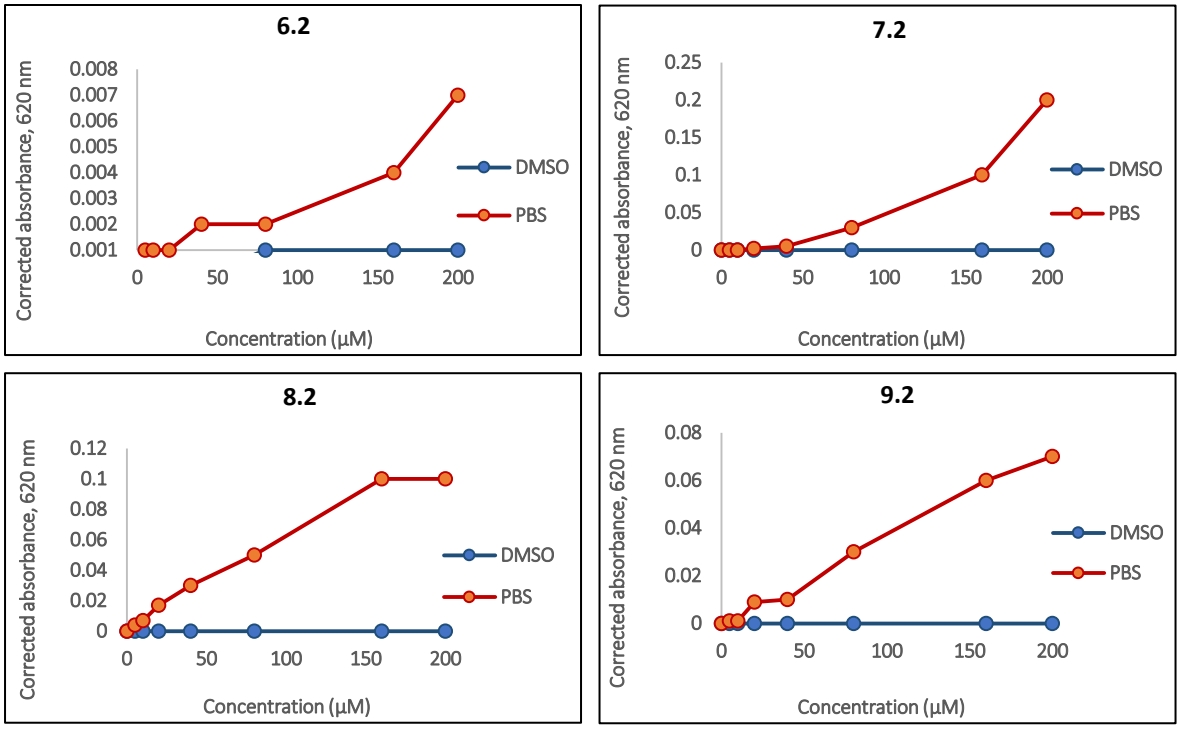

Figure 5.19: Representative graphical plots depicting the relative aqueous solubility of analogues based on the 3-((*N*,*N*-diethylamino)methyl)-2-hydroxy-5-methyl aniline Mannich base

5.4.4 'Solubility' structure-property relationship

In view of the aforementioned, the physicochemical properties that influence the solubility of the synthesized benzimidazole analogues were investigated. A drug's oral bioavailability is largely influenced by its aqueous solubility, permeability and metabolic stability. In drug discovery, solubility has a major impact on bioassays, formulation for *in vivo* dosing, and intestinal absorption.[104]

The solubility of a compound depends on its structure and solution conditions. The contributions from the structure of the compound arise from its physicochemical properties namely, the lipophilicity, hydrogen bonding, molecular volume, crystal energy and ionizability. Solution conditions include pH, co-solvents, additives, ionic strength, time and temperature. The dependence of solubility on the physicochemical properties of the compound is expressed in the equations **I**-**III** below.[104]

a. Lipophilicity and crystal energy (Yalkowsky general solubility equation[105]):

$$LogS_o = 0.5 - LogP - 0.01\,(MP - 25) \ldots\ldots\ldots\ldots (I)$$

where, S_o is the intrinsic solubility (solubility when all molecules are neutral), Log P represents lipophilicity, and MP refers to the melting point of the compound (a measure of crystal energy)

According to equation I, the solubility of a neutral/unionized compound generally decreases with increase in lipophilicity and crystal binding energy.

b. Hydrogen bonding, molecular volume and crystal energy (Abraham aqueous solubility equation[106]):

$$LogSw = 0.52 - R_2 + 0.77\pi_2^H + 2.2\alpha\Sigma_2^H + 4.2\beta\Sigma_2^H - 3.4\alpha\Sigma_2^H\beta\Sigma_2^H - 4V_x \ldots\ldots\ldots\ldots (II)$$

where the solubility of a compound is related to its polarity (π_2^H), hydrogen bond acidity ($\alpha\Sigma_2^H$), hydrogen bond basicity ($\beta\Sigma_2^H$), hydrogen bonding in the crystal ($\alpha\Sigma_2^H\beta\Sigma_2^H$), and molecular volume (V_x).

According to equation II, solubility generally increases as polarity and hydrogen bonding increases, and decreases with increase in molecular volume and crystal hydrogen bonding.

c. Ionizability (the 'modified' Henderson-Hasselbach equation[107]):

$$S_{acid} = S_o\,(1 + 10^{pH-pKa})$$

$$S_{base} = S_o\,(1 + 10^{pKa-pH}) \ldots\ldots\ldots\ldots (III)$$

Equation III relates the solubility of an ionizable compound to its intrinsic solubility (S_o), pKa and pH of the aqueous solution and expresses the logarithmic effect of the difference between the pH of the solution and the pKa of the compound. According the equation, ionization increases the solubility of the compound than its neutral form.[104]

Based on the equations above, the solubility of the benzimidazole compounds was expressed as a function of their LogP (or cLogP), melting point, polarity, hydrogen bond donors and acceptors, molecular volume and pKa.

Table 5.4: Physicochemical properties of the benzimidazole analogues

Compound	Calculated properties						Experimental properties		
	pKa (acid)	pKa (base)	V_x (mL)	LogP	HBD	HBA	t_R (min)	*R*f	LogS (µM)
6.1	5.56	11.42	249.16	2.90	3	5	0.36	0.30	1.60
6.2	5.51	11.43	265.53	3.32	3	5	0.60	0.30	1.60
6.3	5.59	11.43	265.43	3.32	3	5	0.34	0.20	1.30
6.4	6.76	11.53	249.16	2.86	3	5	0.33	0.20	1.60
6.5	7.42	11.36	249.16	2.93	3	5	0.38	0.20	2.20
7.1	5.37	11.41	360.06	4.44	2	6	2.46	0.70	1.90
7.2	5.32	11.43	375.02	4.82	2	6	2.54	0.70	1.30
7.3	5.41	11.43	375.02	4.82	2	6	2.45	0.50	1.60
7.4	6.69	11.53	360.06	4.42	2	6	2.41	0.30	1.90
7.5	7.36	11.36	360.06	4.49	2	6	2.38	0.40	2.20
8.1	5.38	11.41	377.26	5.41	2	5	2.65	0.70	1.30
8.2	5.33	11.43	392.43	5.76	2	5	2.68	0.70	0.69
8.3	5.41	11.43	392.43	5.76	2	5	2.64	0.50	1.60
8.4	6.69	11.53	377.26	5.35	2	5	2.61	0.30	1.90
8.5	7.36	11.36	377.26	5.39	2	5	2.59	0.40	1.60
9.1	5.39	11.41	350.14	4.75	2	5	2.55	0.70	1.60
9.2	5.34	11.43	365.31	5.12	2	5	2.61	0.70	0.69
9.3	5.42	11.43	365.31	5.12	2	5	2.51	0.50	1.90
9.4	6.69	11.53	350.14	4.71	2	5	2.52	0.30	1.90
9.5	7.36	11.36	350.14	4.77	2	5	2.41	0.40	1.00

Table 5.4 lists the calculated and experimentally determined physicochemical properties of the synthesized compounds. The calculated LogP, numbers of hydrogen bond donors (HBD) and hydrogen bond acceptors (HBA) were predicted using Optibrium™ StarDrop™ Version 6.4, while

the molecular volume (V_x) and pKa values were calculated using ACD/Labs Release 2017.2.1 and Chemdraw Professional 16, respectively. The polarity of the compounds was described by their HPLC retention time (t_R) and TLC retardation factor (*R*f) acquired under similar experimental conditions. However, the melting point parameter could not be described because the compounds were isolated as either viscous oils or semi-solids, which is congruent with some reported derivatives of benzimidazoles. For example, 1-methylbenzimidazole has a melting point of 59 - 62 ^{o}C.[12,108] The compounds are therefore predicted to have low crystal binding energy, and hence, according to equation I, must contribute to increased intrinsic solubility.

A critical examination of Table 5.4 revealed that the four physicochemical properties pKa (of the Mannich base side chain), V_x, HBD and HBA did not either change from one benzimidazole series to another or from one analogue to another within the same series. For example, the pKa (base, that is, of the Mannich base) varied marginally within the range of 11.41 - 11.53 across all four benzimidazole series while pKa (acid, that is, of the phenolic hydroxyl group) varied within a wider range, 5.32 - 7.42. Further, it is observed that within the same benzimidazole series, analogues based on the three unsubstituted Mannich bases (that is, **6.1**, **6.4** and **6.5**; **7.1**, **7.4** and **7.5**; **8.1**, **8.4** and **8.5**; **9.1**, **9.4** and **9.5**) shared a similar molecular volume, as was the case for the analogues derived from the methyl substituted Mannich base. A similar trend was observed for numbers of HBD and HBA present in the synthesized analogues. In contrast, however, the pKa (acid), cLogP, t_R and *R*f varied among analogues of the same series and from one series to another. It was therefore hypothesized that these physicochemical properties could significantly contribute to the observed solubility of the synthesized benzimidazole compounds.

Linear correlation graphs (Figure 5.20 A-D) of the experimental aqueous solubility (LogS) of the benzimidazole compounds as a function of the aforementioned physicochemical parameters were therefore generated using Microsoft® Office Excel 2013. Generally, the plots revealed normal correlations between each of the four physicochemical properties and LogS of analogues within the same series.

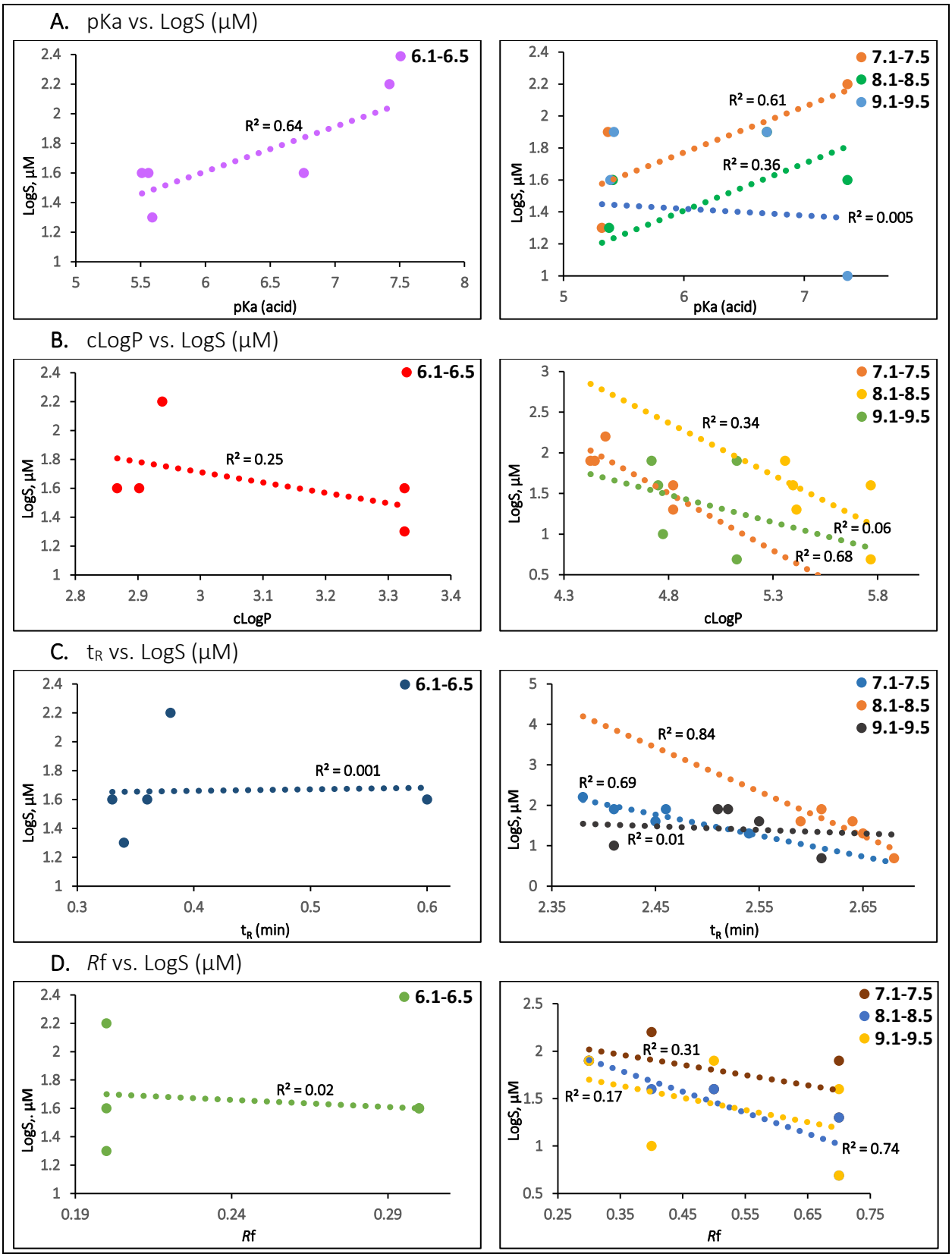

Figure 5.20: Plot of pKa, cLogP, t_R, and *Rf* against LogS of the benzimidazole analogues

The solubility of the 1*H*-benzimidazole series (**6.1**-**6.5**) seems to be influenced by the pKa (acid) and LogP, while almost zero correlation was observed between LogS and the polarity (t_R and *R*f) of the analogues. Meanwhile, the 1-(4-cyanobenzyl) and 1-((4-trifluoromethyl)benzyl) benzimidazole series, **7.1**-**7.5** and **8.1**-**8.5**, respectively, exhibited good correlation between LogS and the four physicochemical parameters. In contrast, however, the 1-(4-fluorobenzyl) benzimidazole series (**9.1**-**9.5**) showed poor correlation.

Analyses of the physicochemical property of analogues within each series revealed that analogues based on the 3-((*N*,*N*-diethylamino)methyl)-2-hydroxy-5-methyl aniline Mannich base (**6.2**, **7.2**, **8.2**, and **9.2**) exhibited the lowest pKa (acid) and polarity (t_R and *R*f). As expected, these analogues had slightly elevated cLogP values due to the presence of the lipophilic methyl group. The high acidity of these analogues could be attributed to the complimentary effect of electron-donation from the *ortho*-NH group and the electron-release from the *para*-methyl group. This hypothesis is corroborated by the comparatively higher pKa and polarity, irrespective of higher cLogP, of analogues based on the 3-(*N*,*N*-diethylaminomethyl)-2-hydroxy-6-methyl aniline Mannich base (**6.3**, **7.3**, **8.3** and **9.3**) than the unsubstituted 3-(*N*,*N*-diethylaminomethyl)-2-hydroxy aniline Mannich base analogues (**6.1**, **7.1, 8.1** and **9.1**) (Table 5.4).

Finally, Figure 5.21 is a heat map of $LogS_o$, LogP and LogD of the most potent antiplasmodium and antimycobacterial benzimidazole analogue, **8.2**. Briefly, the intrinsic solubility (S_o) could be increased by incorporating polar atoms or groups on the aromatic rings and increasing the polarity of the Mannich side chain by synthesizing the desalkyl or dealkylated analogues, while maintaining the 5-methyl group (Figure 5.21A). The lipophilicity (LogP) can be reduced largely by increasing the polarity of the hydroxyl group. This will require the replacement of the 5-methyl group with appropriate substituents that will increase the polarity and decrease the acidity of the hydroxyl group. The LogD, which is the partition coefficient of an ionizable molecule between a buffered aqueous solution and octanol, is largely affected by the hydroxyl group while it is unaffected by the basic Mannich base side chain. Polar or solubilizing groups on the aromatic rings will increase this parameter. These analyses and conclusions highlight some of the medicinal chemistry methodologies to improving the aqueous solubility of drug agents, namely introduction of polar

and ionizable groups, reduction of lipophilicity (LogP or LogD), addition of hydrogen-bonding moieties, and reduction of aromaticity. Other approaches, such as salt formation, disruption of molecular planarity and symmetry, lowering of molecular weight, design of chiral non-flat compounds, as well as construction of prodrugs are also well known.[109–111] Although one or more of the aforementioned modifications could result in increased aqueous solubility, essentially, the activity of **8.2** must be enhanced and not compromised.

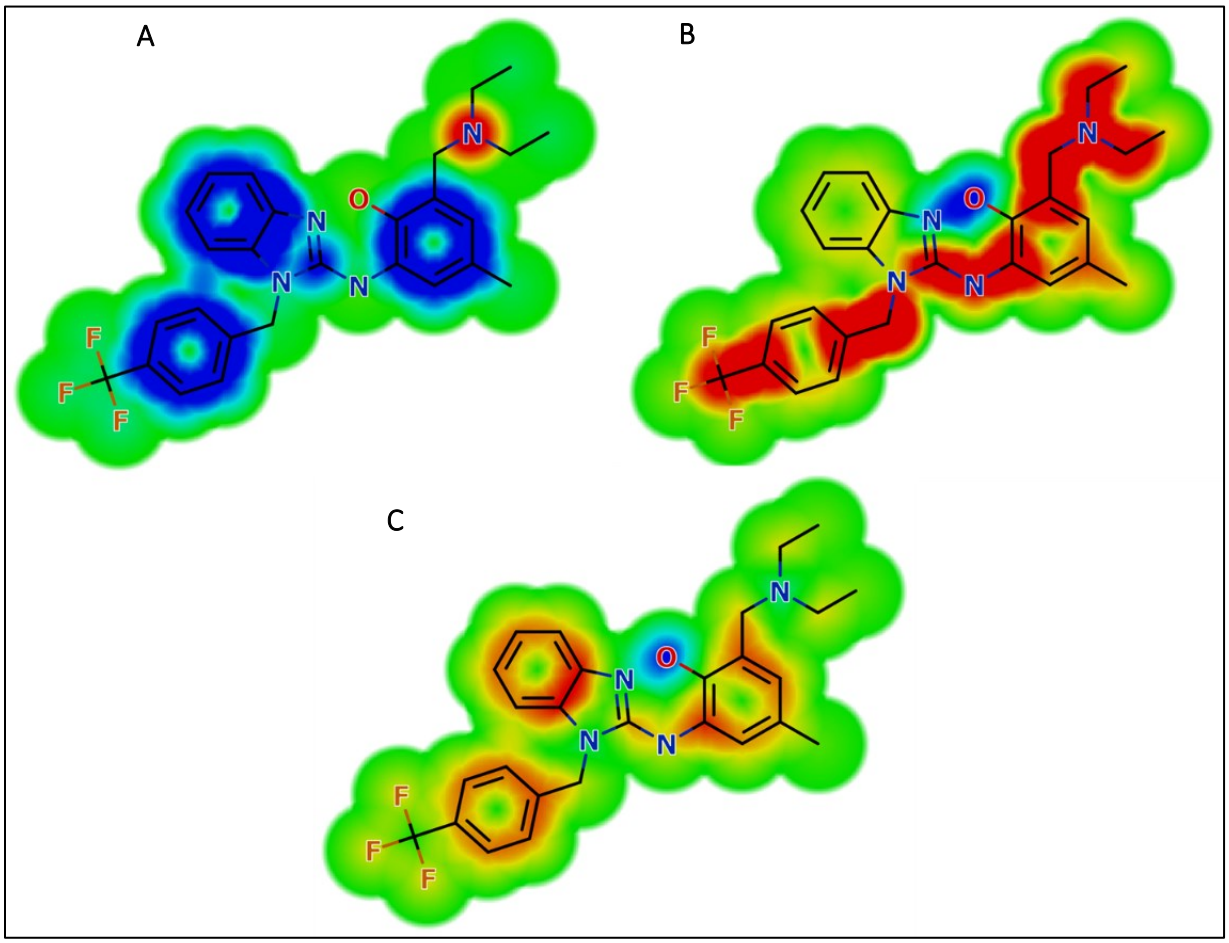

Figure 5.21: Heat map of compound **8.2**. (A). $LogS_o$; (B). LogP; (C). LogD

Colour code: **red** increases, **blue** decreases and **green** has no overall influence on the physicochemical property. Images were generated using Optibrium™ Stardrop™ Version 6.4.

5.4.5 Antimalarial 'drug-likeness' of compound 8.2

The Lipinski's rule of five (RO5) has become an important guideline in modern day drug discovery campaigns, as it postulates acceptable cut-offs for the physicochemical properties necessary for good adsorption and permeability of an orally administered drug. According to this rule, the molecular weight must be ≤500 Da, cLogP ≤5, HBD ≤5, and HBA ≤10.[112] Meanwhile, Veber's rules on a drug's oral bioavailability takes into consideration the compound's molecular flexibility (<10 rotatable bonds), total number of both HBD and HBA (HBD + HBA ≤12) and topological polar surface area (tPSA ≤140 $Å^2$).[113] Such rules/guidelines have become important as they predict a compound's drug-likeness to ensure acceptable pharmacokinetic properties (adsorption, distribution, metabolism, excretion and toxicity: ADMET) prior to development. Table 5.5 lists the aforementioned physicochemical parameters of compound **8.2** in comparison to well established antimalarial drugs on the market or in advanced stages of drug development.

In this regard, compound **8.2** conformed to both Lipinski and Veber rules for oral absorption and bioavailability. The antimalarial drugs were also in conformity to the rules, except four, riboflavin, azithromycin, doxycycline and thiostrepton, which is expected as natural products are exceptions to these rules (Table 5.5). To investigate the chemical space, in terms of polarity occupied by **8.2** to ascertain its closeness to the different antimalarial drug chemotypes, a plot of tPSA against total number of HBD and HBA [HBD + HBA] was generated using Microsoft® Office Excel 2013 (Figure 5.22). The compounds under study showed a strong linear correlation between tPSA and the total number of HBD and HBA (R^2 >0.9) (Figure 5.22A). Moreover, with the exception of the four 'outlier' compounds, all the compounds including **8.2** clustered in a common chemical space, in good conformity to Veber's rules for an orally bioavailable drug (tPSA <140 $Å^2$, HBD + HBA <12) (Figure 5.22B). Significantly, however, **8.2** shared a similar chemical space with the 4-aminoquinoline drug naphthoquine. A comparison of key physicochemical properties of the two compounds is presented in Figure 5.23.

Table 5.5: Compound **8.2/GAD025** and some antimalarial drugs and their Lipinski's drug-likeness

Drug class	Compound	Lipinski's RO5				tPSA, (Å²)
		MW ≤500	logP ≤5	HBD ≤5	HBA ≤10	
Endoperoxides (EP)	artemisinin	282.3	2.9	0	5	53.9
	Artermether	298.4	2.9	0	5	46.1
	Artemisone	401.5	1.4	0	7	74.3
	Dihydroartemisinin	284.3	2.1	1	5	57.1
	Artesunate	384.4	2.5	1	8	100.5
	OZ439	469.6	2.9	0	6	49.3
	OZ277	392.5	1.9	2	6	82.8
4-aminoquinolines (4-AQ)	Amodiaquine	355.9	4.2	2	4	49.3
	AQ-13	291.8	3.7	1	3	82.8
	Chloroquine	319.9	4.6	1	3	49.3
	Hydroxychloroquine	335.9	3.6	2	4	82.8
	Naphthoquine	410.0	5.0	3	4	49.3
	Piperaquine	535.5	4.5	0	6	82.8
	Pyronaridine	518.1	3.9	2	7	49.3
	tert-butyl isoquine	355.9	4.1	3	4	82.8
8-aminoquinolines (8-AQ)	Bulaquine	369.5	3.1	2	6	72.4
	NPC-1161B	434.4	4.5	2	5	69.4
	Primaquine	259.3	1.6	2	4	60.1
	Diethyl primaquine	315.5	3.8	1	4	37.3
	Tafenoquine	463.5	4.0	2	6	78.6
Amino alcohols (AA)	Mefloquine	378.3	3.5	2	3	45.1
	Halofantrine	500.4	7.6	1	2	23.4
	Lumefantrine	528.9	8.0	1	2	23.4
Antifoliates (AF)	Pyrimethamine	248.7	2.5	2	4	77.8
	Cycloquanil	251.7	0.7	2	5	80.0
	Proguanil	253.7	2.5	5	5	83.7
	Trimethoprim	290.3	1.5	2	7	105.5
Amino biaryls (AB)	MMV048	393.4	2.5	1	5	85.9
	UCT943	427.4	2.9	2	6	84.1
Sulfonamides (SFN)	Sulfadoxine	310.3	0.8	2	8	116.4
	Sulfamethoxazole	253.3	0.8	2	6	98.2
Others (OTH)	Atovaquone	366.8	5.3	1	3	54.3
	DHEA	288.4	3.2	1	2	37.3
	Cycloheximide	281.3	0.5	2	5	83.4
	Azithromycin	749.0	2.9	5	14	180.1
	Doxycyclin	444.4	-0.2	6	10	181.6
	Riboflavin	376.4	-0.7	5	10	161.6
	Thiostrepton	1665	0.7	17	37	562.7
	8.2	482.5	5.7	2	5	53.3

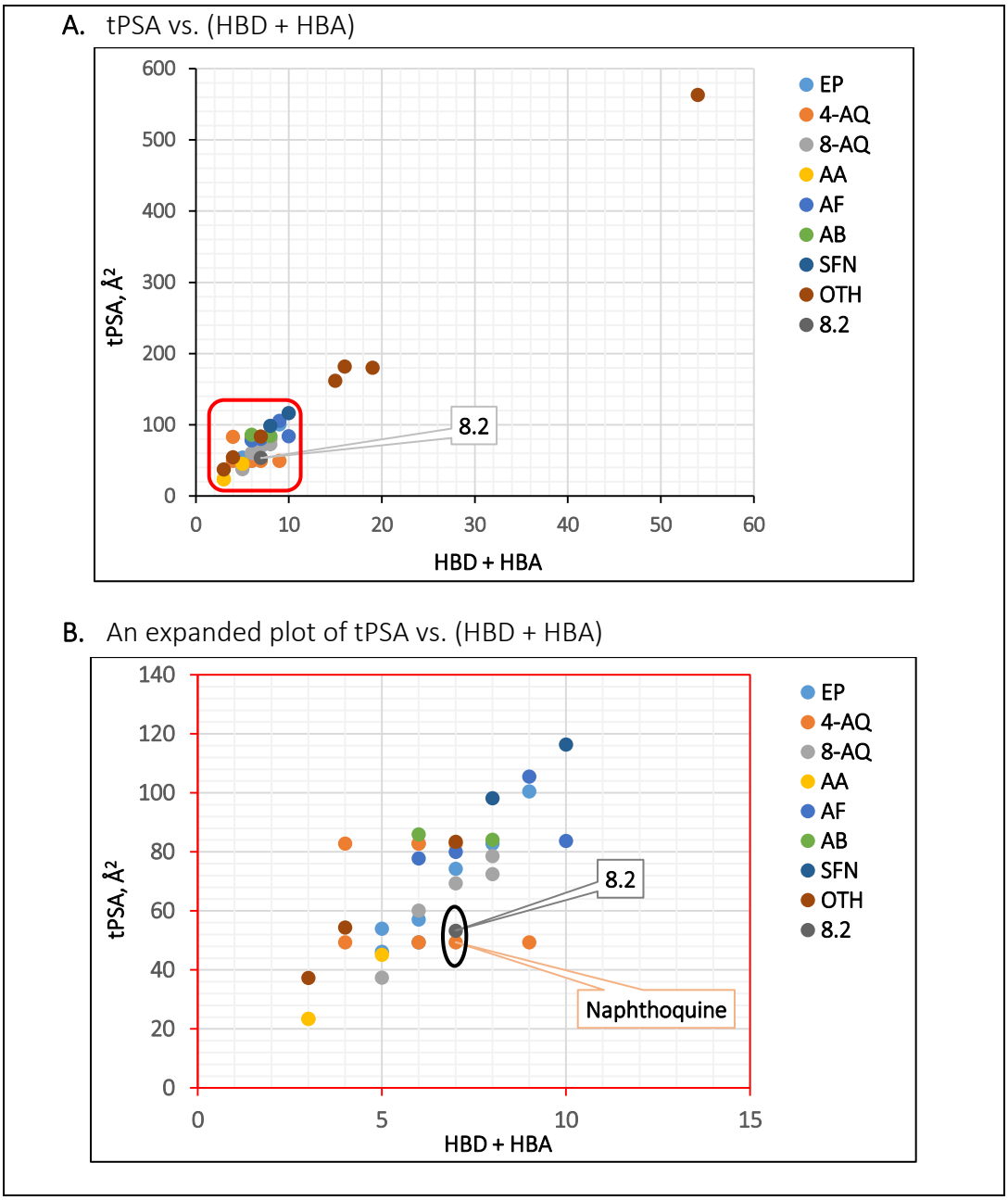

Figure 5.22: Plot of tPSA vs. [HBD + HBA]. Plots highlights the chemical space of **8.2** with respect to established antimalarial agents

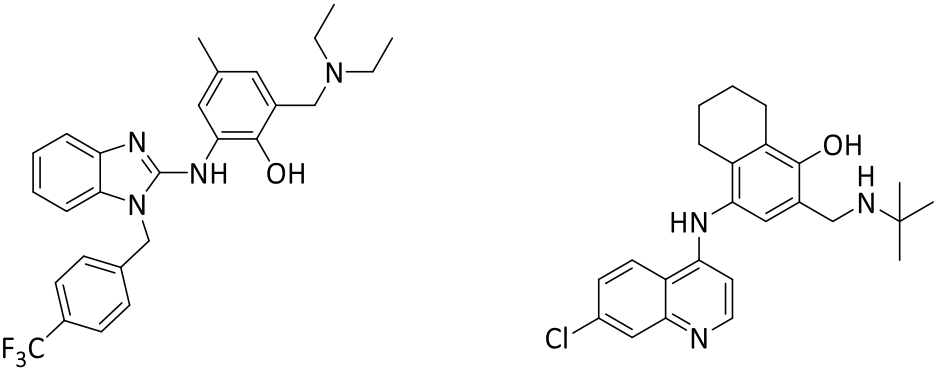

8.2	**Naphthoquine**
MW: 483.5	MW: 410.0
cLogP: 5.7	cLogP: 5.0
HBD: 2	HBD: 3
HBA: 5	HBA: 4
tPSA: 53.3	tPSA: 49.4
LogS @ pH 7.4: 1.0	LogS @ pH 7.4: 0.6
LogD: 3.8	LogD: 3.1

Figure 5.23: Chemical structures of 8.2 and naphthoquine

5.5 Conclusion and recommendations for future work

Analogues based on the benzimidazole privileged scaffold with incorporated phenolic Mannich bases were successfully synthesized as potential and novel antimycobacterial and multi-stage (asexual blood and gametocyte stages) antiplasmodium agents. Evaluation of the aforementioned biological activities of the synthesized compounds revealed good *in vitro* potency towards *Mtb* in the 7H9/CAS media and sub-micromolar activity against the asexual blood stage *P. falciparum* parasites. Most of the compounds exhibited better potency against the multidrug-resistant K1 strain than the chloroquine-sensitive NF54 strain of *P. falciparum*. One of the analogues, compound 8.2, emerged the most active compound in all the assays investigated albeit it displayed poor aqueous solubility.

It is recommended that future work aimed at expanding the antimycobacterial and antiplasmodium SAR be explored. The SAR explorations must incorporate strategies to improve the aqueous solubility while improving antimycobacterial and antiplasmodium potency.

Acquisition of the IC_{50} values of the analogues towards the early and late stage gametocyte parasites of *P. falciparum* is highly encouraged. The data could suggest the potential activity of the benzimidazole analogues as dual-inhibiting antimalarials. Finally metabolite identification studies on **8.2** should be performed *in vitro* in microsomal preparations as well as *in vivo* in mice so as to identify sites of metabolism and associated metabolites. This will be critical for lead optimization studies towards an *in vivo* proof-of-concept in the relevant mouse model.

5.6 Experimental

5.6.1 General Experimental Procedures

The general experimental procedures, with respect to solvents, instruments and materials for chromatographic and spectroscopic analyses of all reactions and the synthesized compounds, have been previously described in Chapter four, Section 4.6.1. The starting reagents, 2-chloro benzimidazole, 1-(4-fluorobenzyl)-2-chlorobenzimidazole and the aminophenols, were purchased from Sigma Aldrich.

5.6.2 General Synthetic Procedure for compounds 2a – 2c

A mixture of the corresponding hydroxyaniline (1.0 eq.) and acetic anhydride (1.5 eq.) in THF was heated at 60 ^{o}C for 1 h. After completion of reaction (TLC and LCMS), solvent was removed under reduced pressure and residue was triturated with diethyl ether to obtained *N*-(hydroxyphenyl) acetamides (**2a – 2c**).

N-(2-hydroxyphenyl)acetamide (2a)

White solid (1.3 g obtained from 1.0 g of **1a**, 94%); *R*f 0.5 (7% MeOH-DCM); Mp 198-200 ^{o}C; ^{1}H NMR (600 MHz, MeOH-d_4) δ 7.56 (dd, *J* = 1.6, 7.9 Hz, 1H, H-6), 6.98 (td, *J* = 7.5, 1.6 Hz, 1H, H-4), 6.85 (dd, *J* = 1.4, 8.0 Hz, 1H, H-3), 6.79 (td, *J* = 7.6, 1.4 Hz, 1H, H-5), 2.16 (s, 3H, CH_3-8); ^{13}C NMR (151 MHz, MeOH-d_4) δ 172.2, 149.7, 127.1, 126.8, 124.0, 120.6, 117.3 and 23.4; LC-MS (ESI): *m/z* 152 $[M+H]^+$; purity (LC-MS): 98% (t_R = 0.23 min.)

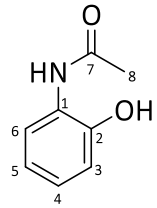

$C_8H_9NO_2$
Mol. Wt: 151.17

N-(2-hydroxy-5-methylphenyl)acetamide (2b)

White solid (1.2 g obtained from 1.0 g of **1b**, 95%); *R*f 0.5 (7% MeOH-DCM); Mp 197-199 ^{o}C; ^{1}H NMR (600 MHz, MeOH-d_4) δ 7.35 (d, *J* = 2.0 Hz, 1H, H-6), 6.80 (dd, *J* = 2.2, 8.1 Hz, 1H, H-4), 6.73 (d, *J* = 8.1 Hz, 1H, H-3), 2.22 (s, 3H, CH_3-9), 2.15 (s, 3H, CH_3-8); ^{13}C NMR (151 MHz, MeOH-d_4) δ 172.2, 147.4, 130.1, 127.3, 126.8, 124.3, 117.3, 23.4, and 20.7; LC-MS (ESI): *m/z* 166 $[M+H]^+$; purity (LC-MS): 98% (t_R = 0.64 min.)

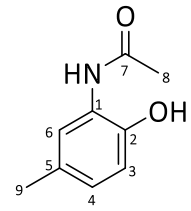

$C_9H_{11}NO_2$
Mol. Wt: 165.2

N-(2-hydroxy-6-methylphenyl)acetamide (2c)

Yellow solid (1.2 g obtained from 1.0 g of **1c**, 95%); *R*f 0.4 (7% MeOH-DCM); Mp 164-166 ^{o}C; ^{1}H NMR (600 MHz, MeOH-d_4) δ 7.00 (t, *J* = 7.8 Hz, 1H, H-4), 6.71 (m, 2H, H-3 and H-5), 2.18 (s, 3H, CH_3-9), 2.16 (s, 3H, CH_3-8); ^{13}C NMR (151 MHz, MeOH-d_4) δ 172.9, 153.9, 137.6, 128.8, 124.4, 122.3, 115.0, 22.6 and 18.2; LC-MS (ESI): *m/z* 166 $[M+H]^+$; purity (LC-MS): 98% (t_R = 0.26 min.)

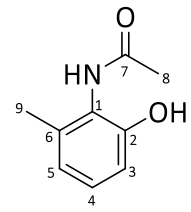

$C_9H_{11}NO_2$
Mol. Wt: 165.2

5.6.3 General Synthetic Procedure for compounds 3a – 3d

The *N*-(hydroxyphenyl) acetamides (**2a – 2d**) (1 eq.) were dissolved in EtOH (10 mL) and heated (80 ^{o}C) with diethylamine (1.5 eq) and formaldehyde (1.5 eq.) until completion (TLC, 2 h). The solvent was removed *in vacuo*. The residue was dissolved in DCM (20 mL) and acidified with 1M HCl (15 mL). The aqueous layer was separated through a separating funnel and basified with a saturated solution of NaOH to a pH of 8-10. This was followed by extraction of the target compound with DCM (2×20 mL). The combined organic phase was dried over anhydrous Na_2SO_4. After filtration, the solvent was removed under reduced pressure to obtain compounds **3a – 3d**.

N-(3-((*N*,*N*-diethylamino)methyl)-2-hydroxyphenyl)acetamide (3a)

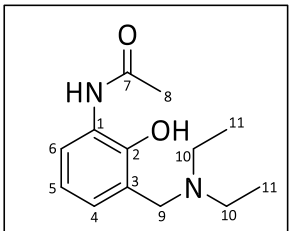

$C_{13}H_{20}N_2O_2$
Mol. Wt: 236.3

Yellow oil (0.616 g obtained from 0.500 g of **2a**, 79%); *R*f 0.3 (7% MeOH-DCM); ^{1}H NMR (400 MHz, MeOH-d_4) δ 7.82 (dd, *J* = 1.7, 8.1 Hz, 1H, H-6), 6.81 (d, *J* = 8.1 Hz, 1H, H-4), 6.71 (t, *J* = 7.9 Hz, 1H, H-5), 3.51 (s, 2H, 2×H-9), 2.55 (q, *J* = 7.1 Hz, 4H, 4×H-10), 2.18 (s, 3H, CH_3-8), 1.08 (t, *J* = 7.1 Hz, 6H, 2×CH_3-11); ^{13}C NMR (101 MHz, MeOH-d_4) δ 171.6, 150.7, 128.4, 127.2, 126.9, 123.0, 122.7, 57.9, 47.3 (2C), 23.8 and 11.4 (2C); LC-MS (ESI): *m/z* 237 $[M+H]^+$; purity (LC-MS): 98% (t_R = 0.13 min.)

N-(3-((*N*,*N*-diethylamino)methyl)-2-hydroxy-5-methylphenyl)acetamide (3b)

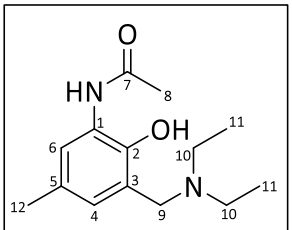

$C_{14}H_{22}N_2O_2$
Mol. Wt: 250.3

Yellow oil (0.510 g obtained from 0.500 g of **2b**, 67%); *R*f 0.3 (7% MeOH-DCM); ^{1}H NMR (600 MHz, MeOH-d_4) δ 7.61 (d, *J* = 2.0 Hz, 1H, H-6), 6.61 (d, *J* = 2.0 Hz, 1H, H-4), 3.76 (s, 2H, 2×H-9), 2.64 (q, *J* = 7.2 Hz, 4H, 4×H-10), 2.20 (s, 3H, CH_3-12), 2.14 (s, 3H, CH_3-8), 1.11 (t, *J* = 7.2 Hz, 6H, 2×CH_3-11); ^{13}C NMR (151 MHz, MeOH-d_4) δ 171.6, 148.0, 128.5, 126.7, 125.9, 122.9, 122.8, 57.6, 47.4 (2C), 23.8, 20.9 and 11.5 (2C); LC-MS (ESI): *m/z* 251 $[M+H]^+$; purity (LC-MS): 98% (t_R = 0.15 min.)

N-(3-((*N*,*N*-diethylamino)methyl)-2-hydroxy-6-methylphenyl)acetamide (3c)

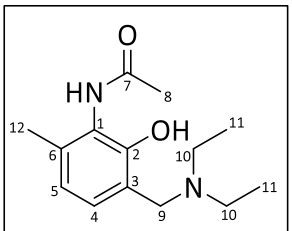

$C_{14}H_{22}N_2O_2$
Mol. Wt: 250.3

Yellow oil (0.500 g obtained from 0.500 g of **2c**, 66%); *R*f 0.2 (7% MeOH-DCM); ^{1}H NMR (600 MHz, MeOH-d_4) δ 6.84 (d, *J* = 7.6 Hz, 1H, H-4), 6.62 (d, *J* = 7.6 Hz, 1H, H-5), 3.77 (s, 2H, 2×H-9), 2.63 (q, *J* = 7.1 Hz, 4H, 4×H-10), 2.15 (s, 3H, CH_3-12), 2.14 (s, 3H, CH_3-8), 1.10 (t, *J* = 7.1 Hz, 6H, 2×CH_3-11); ^{13}C NMR (151 MHz, MeOH-d_4) δ 172.6, 155.2, 137.0, 128.1, 124.2, 121.5, 120.9, 57.4, 47.4 (2C), 22.6, 18.2 and 11.5 (2C); LC-MS (ESI): *m/z* 251 $[M+H]^+$; purity (LC-MS): 98% (t_R = 0.18 min.)

N-(4-((*N*,*N*-diethylamino)methyl)-3-hydroxyphenyl)acetamide (3d)

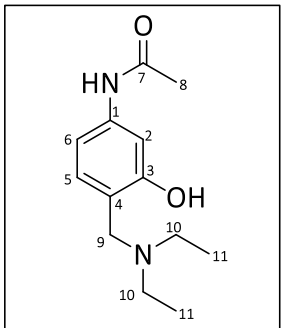

$C_{13}H_{20}N_2O_2$
Mol. Wt: 236.3

Yellow oil (0.473 g obtained from 0.500 g of **2d**, 61%); *R*f 0.2 (7% MeOH-DCM); ^{1}H NMR (600 MHz, MeOH-d_4) δ 6.98 (d, *J* = 1.5 Hz, 1H, H-2), 6.92-6.90 (m, 2H, H-5 and H-6), 3.73 (s, 2H, 2×H-9), 2.61 (q, *J* = 7.1 Hz, 4H, 4×H-10), 2.07 (s, 3H, CH_3-8), 1.09 (t, *J* = 7.1 Hz, 6H, 2×CH_3-11); ^{13}C NMR (151 MHz, MeOH-d_4) δ 171.5, 159.7, 140.2, 129.7, 119.5, 111.9, 108.9, 57.1, 47.4 (2C), 23.8 and 11.5 (2C); LC-MS (ESI): *m/z* 237 $[M+H]^+$; purity (LC-MS): 98% (t_R = 0.13 min.)

5.6.4 General Synthetic Procedure for compounds 4a – 4d

Compounds **3a – 3d** (2 mmol) were refluxed in 6N HCl (2 mL) at 100 ^{o}C for 2 h (TLC). Solvent was removed under reduced pressure. The residue was dissolved in EtOH (2×15 mL) and solvent was removed *in vacuo* to obtain the corresponding *N*-deactylated Mannich base products **4a – 4d** (as HCl salt).

6-Amino-2-((*N*,*N*-diethylamino)methyl)phenol (4a)

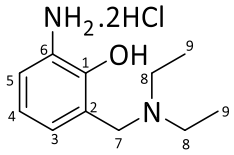

$C_{11}H_{18}N_2O$
Mol. Wt: 194.3

Brown viscous oil (0.362 g obtained from 0.500 g of **3a**, 88%); *R*f 0.6 (20% MeOH-DCM); ^{1}H NMR (600 MHz, MeOH-d_4) δ 7.61 (dd, *J* = 1.6, 7.7 Hz, 1H, H-5), 7.52 (dd, *J* = 1.6, 7.9 Hz, 1H, H-3), 7.17 (t, *J* = 7.8 Hz, 1H, H-4), 4.49 (s, 2H, 2×H-7), 3.25 (m, 4H, 4×H-8), 1.38 (t, *J* = 7.3 Hz, 6H, 2×CH_3-9); ^{13}C NMR (151 MHz, MeOH-d_4) δ 151.2, 134.7, 127.3, 123.2, 123.0, 122.2, 52.0, 48.5 (2C) and 9.1 (2C); LC-MS (ESI): *m/z* 195 $[M+H]^+$; purity (LC-MS): 98% (t_R = 0.13 min.)

6-Amino-2-((*N*,*N*-diethylamino)methyl)-4-methylphenol (4b)

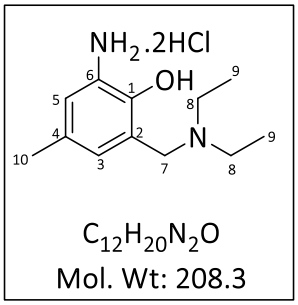

Brown viscous oil (0.430 g obtained from 0.500 g of **3b**, 86%); *R*f 0.6 (20% MeOH-DCM); ^{1}H NMR (600 MHz, MeOH-d_4) δ 7.44 (d, *J* = 1.9 Hz, 1H, H-5), 7.33 (d, *J* = 1.8 Hz, 1H, H-3), 4.43 (s, 2H, 2×H-7), 3.24 (m, 4H, 4×H-8), 2.35 (s, 3H, CH_3-10), 1.37 (t, *J* = 7.2 Hz, 6H, 2×CH_3-9); ^{13}C NMR (151 MHz, MeOH-d_4) δ 148.6, 134.9, 133.6, 127.6, 122.7, 122.1, 52.1, 48.5 (2C), 20.4 and 9.2 (2C); LC-MS (ESI): *m/z* 209 $[M+H]^+$; purity (LC-MS): 98% (t_R = 0.14 min.)

6-Amino-2-((*N*,*N*-diethylamino)methyl)-5-methylphenol (4c)

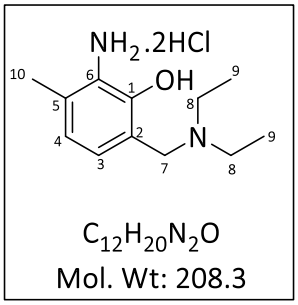

Brown viscous oil (0.400 g obtained from 0.500 g of **3c**, 80%); *R*f 0.6 (20% MeOH-DCM); ^{1}H NMR (600 MHz, MeOH-d_4) δ 7.56 (d, *J* = 7.9 Hz, 1H, H-3), 7.07 (d, *J* = 7.9 Hz, 1H, H-4), 4.44 (s, 2H, 2×H-7), 3.24 (m, 4H, 4×H-8), 2.44 (s, 3H, CH_3-10), 1.37 (t, *J* = 7.3 Hz, 6H, 2×CH_3-9); ^{13}C NMR (151 MHz, MeOH-d_4) δ 150.8, 137.0, 133.8, 125.4, 122.4, 119.6, 52.1, 48.3 (2C), 17.6 and 9.1 (2C); LC-MS (ESI): *m/z* 209 $[M+H]^+$; purity (LC-MS): 98% (t_R = 0.15 min.)

5-Amino-2-((*N*,*N*-diethylamino)methyl)phenol (4d)

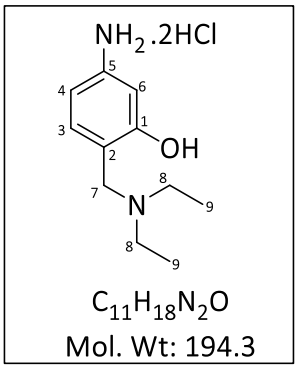

Brown viscous oil (0.330 g obtained from 0.450 g of **3d**, 75%); *R*f 0.2 (20% MeOH-DCM); ^{1}H NMR (600 MHz, MeOH-d_4) δ 7.61 (d, *J* = 8.1 Hz, 1H, H-3), 7.10 (d, *J* = 2.1 Hz, 1H, H-6), 7.00 (dd, *J* = 2.1, 8.1 Hz, 1H, H-4), 4.36 (s, 2H, 2×H-7), 3.23 (m, 4H, 4×H-8), 1.37 (t, *J* = 7.2 Hz, 6H, 2×CH_3-9); ^{13}C NMR (151 MHz, MeOH-d_4) δ 159.1, 135.4, 134.6, 118.9, 115.5, 111.6, 51.8, 48.8 (2C), 9.2 (2C); LC-MS (ESI): *m/z* 195 $[M+H]^+$; purity (LC-MS): 98% (t_R = 0.12 min.)

5.6.5 General Synthetic Procedure for compounds 7.0 and 8.0

A mixture of benzimidazole (**6.0**) (1 eq.) and the corresponding benzyl bromide (1.1 eq.) in acetonitrile were refluxed at 75 ^{o}C in the presence of K_2CO_3 (1.1 eq.) as base. Upon completion (TLC, 2 h), the reaction mixture was allowed to cool, diluted with DCM, filtered and the filtrate removed *in vacuo* to obtain a white amorphous solid residue. The residue was triturated with diethyl ether to remove unreacted benzyl bromide. The benzylated benzimidazole intermediates (**7.0** and **8.0**) were used for the next reaction without any further purification.

2-Chloro-1-(4-cyanobenzyl)benzo[*d*]imidazole (7.0)

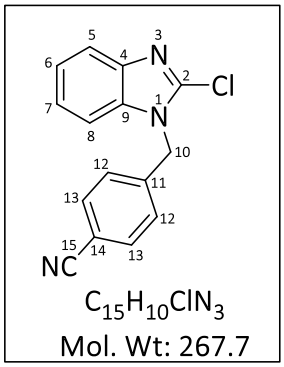

$C_{15}H_{10}ClN_3$
Mol. Wt: 267.7

White solid (0.174 g obtained from 0.100 g of **6.0**, 99%); *R*f 0.7 (5% MeOH-DCM); Mp 149-151 ^{o}C; ^{1}H NMR (600 MHz, MeOH-d_4) δ 7.70 (d, *J* = 8.3 Hz, 2H, 2×H-13), 7.65-7.61 (m, 1H, H-8), 7.45-7.42 (m, 1H, H-5), 7.34 (d, *J* = 8.3 Hz, 2H, 2×H-12), 7.33-7.29 (m, 2H, H-6 and H-7), 5.62 (s, 2H, 2×H-10); ^{13}C NMR (151 MHz, MeOH-d_4) δ 142.4, 142.3, 142.0, 136.3, 133.9 (2C), 128.8 (2C), 125.1, 124.6, 119.7, 119.3, 113.1, 111.5 and 48.2; LC-MS (ESI): *m/z* 268 $[M+H]^+$; purity (LC-MS): 98% (t_R = 2.62 min.)

2-Chloro-1-((4-trifluoromethyl)benzyl)benzo[*d*]imidazole (8.0)

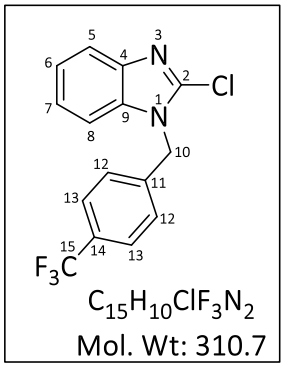

$C_{15}H_{10}ClF_3N_2$
Mol. Wt: 310.7

White solid (0.200 g obtained from 0.100 g of **6.0**, 98%); *R*f 0.7 (5% MeOH-DCM); Mp 96-98 ^{o}C; ^{1}H NMR (600 MHz, MeOH-d_4) δ 7.64-7.59 (m, 3H, H-8 and 2×H-13), 7.43-7.40 (m, 1H, H-5), 7.34 (d, *J* = 8.3 Hz, 2H, 2×H-12), 7.31-7.29 (m, 2H, H-6 and H-7), 5.59 (s, 2H, 2×H-10); ^{13}C NMR (151 MHz, MeOH-d_4) δ 142.3, 142.0, 141.3, 136.3, 131.3 (q, *J* = 32.4 Hz, C-14), 128.5 (2C), 126.9 (q, *J* = 3.8 Hz, 2×C-13), 125.4 (q, *J* = 270.0 Hz, C-15), 125.1, 124.5, 119.7, 111.5 and 48.2; LC-MS (ESI): *m/z* 311 $[M+H]^+$; purity (LC-MS): 98% (t_R = 2.85 min.)

5.6.6 General Synthetic Procedure for compounds 6.1 – 9.5

A mixture of the corresponding benzimidazole (**6.0** – **9.0**) (1.0 eq.) in *n*-BuOH and the respective phenolic Mannich base (**4a** – **4d** and **5.0**) (1.1 eq.) in *n*-BuOH was heated at 100 ^{o}C in the presence of excess KH_2PO_4 as base. Upon completion (TLC, 8 h), the reaction mixture was allowed to cool, diluted with water and the solvent was removed under reduced pressure. The residue was dissolved in a mixture of DCM: MeOH 1:1 v/v and completely dried in the Genevac to remove all traces of *n*-BuOH. The target compounds (**6.1** – **9.5**) were obtained after column chromatography or preparative TLC on silica gel using mixtures of DCM and MeOH as mobile phase.

2-(3-((*N*,*N*-diethylamino)methyl)-2-hydroxyanilino)-1*H*-benzo[*d*]imidazole (6.1)

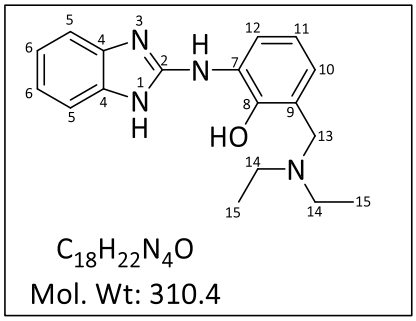

Brown semi-solid (0.081 g obtained from 0.100 g of **6.0**, 40%); *R*f 0.3 (10% MeOH-DCM); ^{1}H NMR (600 MHz, MeOH-d_4) δ 7.86 (dd, *J* = 1.5, 7.9 Hz, 1H, H-12), 7.28 (dd, *J* = 3.3, 6.6 Hz, 2H, 2×H-6), 7.03 (dd, *J* = 3.3, 6.6 Hz, 2H, 2×H-5), 6.77 (t, *J* = 7.7 Hz, 1H, H-11), 6.71 (dd, *J* = 1.5, 7.7 Hz, 1H, H-10), 3.84 (s, 2H, 2×H-13), 2.68 (q, *J* = 7.1 Hz, 4H, 4×H-14), 1.13 (t, *J* = 7.1 Hz, 6H, 2×CH_3-15); ^{13}C NMR (151 MHz, MeOH-d_4) δ 153.0, 149.3, 129.2 (2C), 123.1 (2C), 122.8, 122.5 , 121.8 (2C), 119.5 (2C), 118.7, 57.7, 47.5 (2C) and 11.5 (2C); LC-MS (ESI): *m/z* 311 $[M+H]^+$; purity (LC-MS): 98% (t_R = 0.36 min.)

2-(3-((*N*,*N*-diethylamino)methyl)-2-hydroxy-5-methylanilino)-1*H*-benzo[*d*]imidazole (6.2)

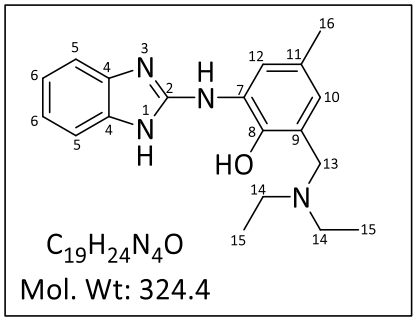

Yellow semi-solid (0.110 g obtained from 0.100 g of **6.0**, 52%); *R*f 0.3 (10% MeOH-DCM); ^{1}H NMR (600 MHz, MeOH-d_4) δ 7.69 (d, *J* = 1.9 Hz, 1H, H-12), 7.29 (dd, *J* = 3.1, 5.8 Hz, 2H, 2×H-6), 7.03 (dd, *J* = 3.1, 5.8 Hz, 2H, 2×H-5), 6.52 (d, *J* = 1.9 Hz, 1H, H-10), 3.77 (s, 2H, 2×H-13), 2.65 (q, *J* = 7.1 Hz, 4H, 4×H-14), 2.27 (s, 3H, CH_3-16), 1.12 (t, *J* = 7.1 Hz, 6H, 2×CH_3-15); ^{13}C NMR (151 MHz, MeOH-d_4) δ 153.0, 146.6, 129.1 (2C), 128.8, 123.6 (2C), 122.6, 121.8 (3C), 119.2 (2C), 57.7, 47.5 (2C), 21.0 and11.6 (2C); LC-MS (ESI): *m/z* 325 $[M+H]^+$; purity (LC-MS): 98% (t_R = 0.60 min.)

2-(3-((*N*,*N*-diethylamino)methyl)-2-hydroxy-6-methylanilino)-1*H*-benzo[*d*]imidazole (6.3)

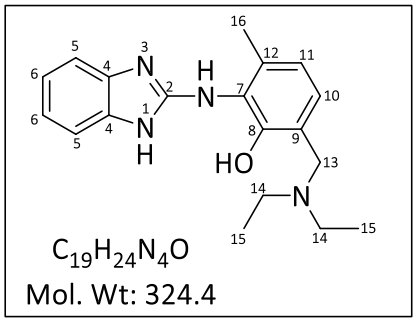

Brown viscous oil (0.106 g obtained from 0.100 g of **6.0**, 50%); *R*f 0.2 (15% MeOH-DCM); ^{1}H NMR (600 MHz, MeOH-d_4) δ 7.18 (dd, *J* = 3.1, 5.8 Hz, 2H, 2×H-6), 6.96 (dd, *J* = 3.1, 5.8 Hz, 2H, 2×H-5), 6.90 (d, *J* = 7.7 Hz, 1H, H-10), 6.71 (d, *J* = 7.7 Hz, 1H, H-11), 3.84 (s, 2H, 2×H-13), 2.69 (q, *J* = 7.1 Hz, 4H, 4×H-14), 2.24 (s, 3H, CH_3-16), 1.11 (t, *J* = 7.1 Hz, 6H, 2×CH_3-15); ^{13}C NMR (151 MHz, MeOH-d_4) δ 155.7, 155.6, 138.5, 137.2, 127.8 (2C), 126.1, 121.6 (2C), 121.5, 121.4 (2C), 113.0, 57.2, 47.4 (2C), 18.2 and 11.3 (2C); LC-MS (ESI): *m/z* 325 $[M+H]^+$; purity (LC-MS): 98% (t_R = 0.34 min.)

2-(4-((*N*,*N*-diethylamino)methyl)-3-hydroxyanilino)-1*H*-benzo[*d*]imidazole (6.4)

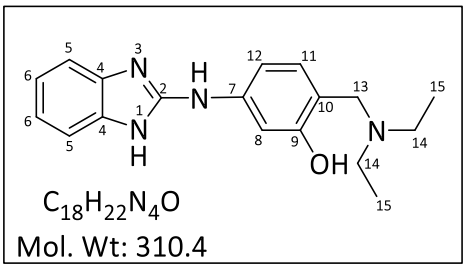

Brown viscous oil (0.071 g obtained from 0.100 g of **6.0**, 35%); *R*f 0.2 (15% MeOH-DCM); ^{1}H NMR (600 MHz, MeOH-d_4) δ 7.59 (br s, 2H, 2×H-6), 7.46 (d, *J* = 8.1 Hz, 1H, H-11), 7.16 (dd, *J* = 3.1, 5.9 Hz, 2H, 2×H-5), 6.91 (d, *J* = 2.1 Hz, 1H, H-8), 6.88 (dd, *J* = 2.2, 8.1 Hz, 1H, H-12), 4.31 (s, 2H, 2×H-13), 3.26 (q, *J* = 7.2 Hz, 4H, 4×H-14), 1.40 (t, *J* = 7.2 Hz, 6H, 2×CH_3-15); ^{13}C NMR (151 MHz, MeOH-d_4) δ 159.2, 152.5, 142.2, 135.1 (2C), 123.4 (2C), 113.9 (2C), 112.3 (2C), 108.1 (2C), 52.5, 48.7 (2C) and 9.3 (2C); LC-MS (ESI): *m/z* 311 $[M+H]^+$; purity (LC-MS): 98% (t_R = 0.33 min.)

2-(3-((*N*,*N*-diethylamino)methyl)-4-hydroxyanilino)-1*H*-benzo[*d*]imidazole (6.5)

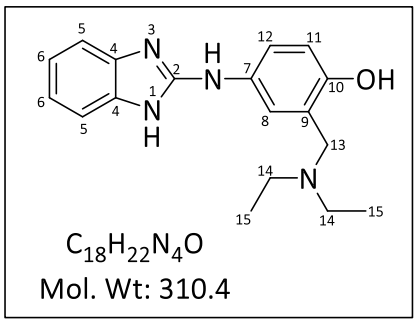

Brown viscous oil (0.082 g obtained from 0.100 g of **6.0**, 41%); *R*f 0.2 (15% MeOH-DCM); ^{1}H NMR (400 MHz, DMSO-d_6) δ 7.69 (d, *J* = 2.7 Hz, 1H, H-8), 7.46 (dd, *J* = 3.2, 5.9 Hz, 2H, 2×H-6), 7.35 (dd, *J* = 2.7, 8.7 Hz, 1H, H-12), 7.21 (dd, *J* = 3.2, 5.9 Hz, 2H, 2×H-5), 7.13 (d, *J* = 8.6 Hz, 1H, H-11), 4.25 (s, 2H, 2×H-13), 3.14 (q, *J* = 7.1 Hz, 4H, 4×H-14), 1.31 (t, *J* = 7.1 Hz, 6H, 2×CH_3-15); ^{13}C NMR (101 MHz, DMSO-d_6) δ 154.5, 148.3, 130.8 (2C), 127.9, 126.8, 125.6, 122.7 (2C), 117.1, 116.8,

111.8 (2C), 49.5, 46.0 (2C) and 8.3 (2C); LC-MS (ESI): *m/z* 311 $[M+H]^+$; purity (LC-MS): 98% (t_R = 0.38 min.)

1-(4-cyanobenzyl)-2-(3-((*N*,*N*-diethylamino)methyl)-2-hydroxyanilino)benzo[*d*]imidazole (7.1)

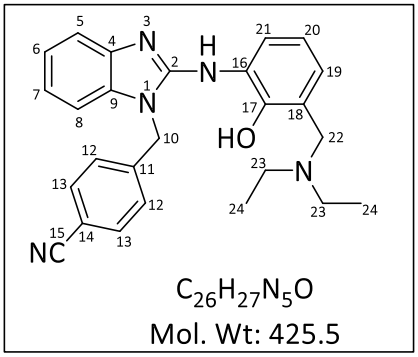

Brown semi-solid (0.119 g obtained from 0.100 g of **7.0**, 75%); *R*f 0.7 (10% MeOH-DCM); ^{1}H NMR (400 MHz, MeOH-d_4) δ 7.74 (dd, *J* = 2.9, 6.5 Hz, 1H, H-21), 7.65 (d, *J* = 8.3 Hz, 2H, 2×H-13), 7.44-7.40 (m, 1H, H-8), 7.36 (d, *J* = 8.3 Hz, 2H, 2×H-12), 7.19-7.15 (m, 1H, H-5), 7.11 (td, *J* = 7.7, 1.3 Hz, 1H, H-7), 7.05 (td, *J* = 7.7, 1.3 Hz, 1H, H-6), 6.76-6.69 (m, 2H, H-19 and H-20), 5.47 (s, 2H, 2×H-10), 3.82 (s, 2H, 2×H-22), 2.67 (q, *J* = 7.2 Hz, 4H, 4×H-23), 1.10 (t, *J* = 7.1 Hz, 6H, 2×CH_3-24); ^{13}C NMR (101 MHz, MeOH-d_4) δ 152.4, 150.5, 143.3, 142.6, 135.0, 133.8 (2C), 129.3, 128.9 (2C), 123.9, 123.0, 122.6, 122.0, 120.2, 119.4, 119.2, 117.5, 112.7, 109.3, 57.6, 47.4 (2C), 46.4 and 11.3 (2C); LC-MS (ESI): *m/z* 426 $[M+H]^+$; purity (LC-MS): 98% (t_R = 2.46 min.)

1-(4-cyanobenzyl)-2-(3-((*N*,*N*-diethylamino)methyl)-2-hydroxy-5-methylanilino)benzo[*d*]imidazole (7.2)

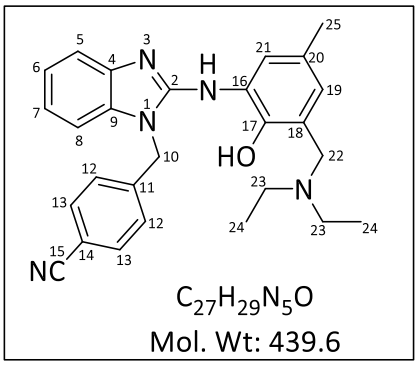

Yellow semi-solid (0.145 g obtained from 0.100 g of **7.0**, 88%); *R*f 0.7 (10% MeOH-DCM); ^{1}H NMR (400 MHz, MeOH-d_4) δ 7.64 (d, *J* = 8.0 Hz, 2H, 2×H-13), 7.55 (d, *J* = 1.9, Hz, 1H, H-21), 7.45-7.40 (m, 1H, H-8), 7.35 (d, *J* = 7.8 Hz, 2H, 2×H-12), 7.19-7.14 (m, 1H, H-5), 7.11 (td, *J* = 7.6, 1.3 Hz, 1H, H-7),7.05 (td, *J* = 8.1, 1.3 Hz, 1H, H-6), 6.54 (d, *J* = 1.9, Hz, 1H, H-19), 5.46 (s, 2H, 2×H-10), 3.76 (s, 2H, 2×H-22), 2.67 (q, *J* = 7.4 Hz, 4H, 4×H-23), 2.23 (s, 3H, CH_3-25), 1.09 (t, *J* = 7.1 Hz, 6H, 2×CH_3-24); ^{13}C NMR (101 MHz, MeOH-d_4) δ 152.4, 147.7, 143.3, 142.6, 135.0, 133.8 (2C), 128.9, 128.8 (2C), 128.7, 124.4, 123.0, 122.5, 122.0, 120.8, 119.4, 117.4, 112.7, 109.3, 57.5, 47.5 (2C), 46.4, 21.0 and 11.4 (2C); LC-MS (ESI): *m/z* 440 $[M+H]^+$; purity (LC-MS): 98% (t_R = 2.54 min.)

1-(4-cyanobenzyl)-2-(3-((*N*,*N*-diethylamino)methyl)-2-hydroxy-6-methylanilino)benzo[*d*]imidazole (7.3)

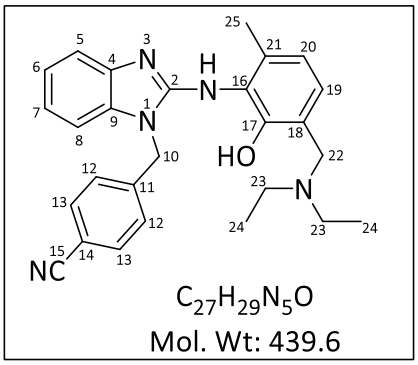

Brown semi-solid (0.098 g obtained from 0.100 g of **7.0**, 60%); *R*f 0.5 (10% MeOH-DCM); ^{1}H NMR (600 MHz, MeOH-d_4) δ 7.67 (d, *J* = 8.1 Hz, 2H, 2×H-13), 7.42 (d, *J* = 8.1 Hz, 2H, 2×H-12), 7.26-7.23 (m, 1H, H-8), 7.07-7.03 (m, 2H, H-5 and H-7), 6.97 (td, *J* = 7.5, 1.1 Hz, 1H, H-6), 6.85 (d, *J* = 7.7 Hz, 1H, H-19), 6.67 (d, *J* = 7.7 Hz, 1H, H-20), 5.49 (s, 2H, 2×H-10), 3.80 (s, 2H, 2×H-22), 2.66 (q, *J* = 7.1 Hz, 4H, 4×H-23), 2.11 (s, 3H, CH_3-25), 1.08 (t, *J* = 7.1 Hz, 6H, 2×CH_3-24); ^{13}C NMR (151 MHz, MeOH-d_4) δ 155.3, 154.6, 143.8, 142.5, 137.2, 135.4, 133.6 (2C), 128.9 (2C), 127.5, 126.8, 122.7, 121.5, 121.3, 121.2, 119.5, 116.5, 112.4, 109.0, 57.3, 47.3 (2C), 46.2, 18.3 and 11.4 (2C); LC-MS (ESI): *m/z* 440 $[M+H]^+$; purity (LC-MS): 98% (t_R = 2.45 min.)

1-(4-cyanobenzyl)-2-(4-((*N*,*N*-diethylamino)methyl)-3-hydroxyanilino)benzo[*d*]imidazole (7.4)

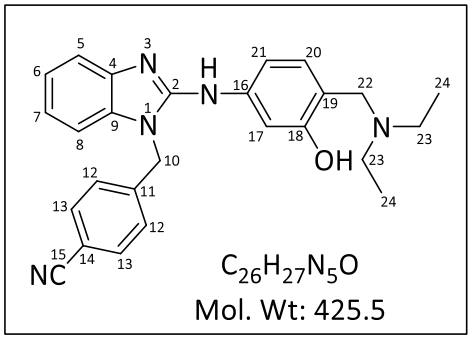

Brown semi-solid (0.087 g obtained from 0.100 g of **7.0**, 55%); *R*f 0.3 (10% MeOH-DCM); ^{1}H NMR (600 MHz, MeOH-d_4) δ 7.63 (d, *J* = 8.2 Hz, 2H, 2×H-13), 7.43-7.39 (m, 1H, H-8), 7.26 (d, *J* = 7.8 Hz, 2H, 2×H-12), 7.14-7.07 (m, 2H, H-5 and H-7), 7.05-7.01 (m, 1H, H-6), 6.94-6.84 (m, 3H, H-17, H-20 and H-21), 5.49 (s, 2H, 2×H-10), 3.73 (s, 2H, 2×H-22), 2.63 (q, *J* = 7.1 Hz, 4H, 4×H-23), 1.10 (t, *J* = 7.1 Hz, 6H, 2×CH_3-24); ^{13}C NMR (151 MHz, MeOH-d_4) δ 160.0, 152.4, 143.7, 142.3, 134.9, 133.7 (2C), 131.6, 130.1, 128.5 (2C), 123.1, 122.0, 119.4, 117.9, 117.5, 112.4, 111.3, 109.6, 108.1, 57.1, 47.3 (2C), 46.3 and 11.6 (2C); LC-MS (ESI): *m/z* 426 $[M+H]^+$; purity (LC-MS): 98% (t_R = 2.41 min.)

1-(4-cyanobenzyl)-2-(3-((*N*,*N*-diethylamino)methyl)-4-hydroxyanilino)benzo[*d*]imidazole (7.5)

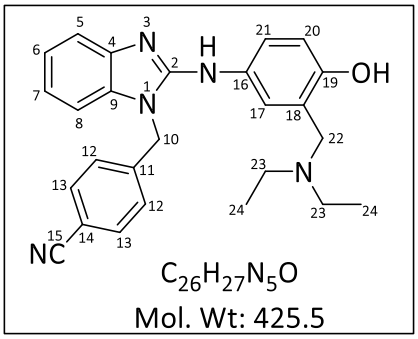

Pink semi-solid (0.150 g obtained from 0.100 g of **7.0**, 94%); *R*f 0.4 (10% MeOH-DCM); ^{1}H NMR (600 MHz, MeOH-d_4) δ 7.70 (d, *J* = 8.1 Hz, 2H, 2×H-13), 7.63 (d, *J* = 2.6 Hz, 1H, H-17), 7.42-7.39 (m, 1H, H-8), 7.39-7.35 (m, 3H, 2×H-12 and H-21), 7.20-7.16 (m, 2H, H-5 and H-7), 7.11 (td, *J* = 7.6, 1.0 Hz, 1H, H-6), 6.97 (d, *J* = 8.6 Hz, 1H, H-20), 5.60 (s, 2H, 2×H-10), 4.32 (s, 2H, 2×H-22), 2.66 (q, *J* = 7.2 Hz, 4H, 4×H-23), 1.39 (t, *J* = 7.2 Hz, 6H, 2×CH_3-24); ^{13}C NMR (151 MHz, MeOH-d_4) δ 155.0, 152.5, 142.8, 138.9, 134.2, 133.8 (2C), 132.2, 128.6 (2C), 127.6, 127.0, 123.9, 122.9, 119.4, 118.2, 117.4, 115.9, 112.7, 110.1, 52.5, 48.5 (2C), 46.4 and 9.1 (2C); LC-MS (ESI): *m/z* 426 $[M+H]^+$; purity (LC-MS): 98% (t_R = 2.38 min.)

1-((4-trifluoromethyl)benzyl)-2-(3-((*N*,*N*-diethylamino)methyl)-2-hydroxyanilino)benzo[*d*]imidazole (8.1)

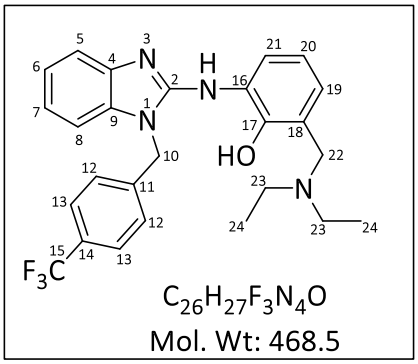

Brown semi-solid (0.105 g obtained from 0.100 g of **8.0**, 70%); *R*f 0.7 (10% MeOH-DCM); ^{1}H NMR (400 MHz, MeOH-d_4) δ 7.77 (dd, *J* = 2.2, 7.2 Hz, 1H, H-21), 7.59 (d, *J* = 8.0 Hz, 2H, 2×H-13), 7.44-7.40 (m, 1H, H-8), 7.38 (d, *J* = 8.0 Hz, 2H, 2×H-12), 7.19-7.15 (m, 1H, H-5), 7.11 (td, *J* = 7.6, 1.3 Hz, 1H, H-7), 7.05 (td, *J* = 7.5, 1.1 Hz, 1H, H-6), 6.77-6.67 (m, 2H, H-19 and H-20), 5.46 (s, 2H, 2×H-10), 3.81 (s, 2H, 2×H-22), 2.64 (q, *J* = 7.2 Hz, 4H, 4×H-23), 1.09 (t, *J* = 7.1 Hz, 6H, 2×CH_3-24); ^{13}C NMR (101 MHz, MeOH-d_4) δ 152.4, 150.4, 142.6, 142.0, 135.1, 131.1 (q, *J* = 32.4 Hz, C-14), 129.3, 128.6 (2C), 126.8 (q, *J* = 3.7 Hz, 2×C-13), 125.5 (q, *J* = 270.0 Hz, C-15), 123.8, 122.9, 122.5, 121.9, 120.0, 119.3, 117.4, 109.4, 57.6, 47.4 (2C), 46.3 and 11.3 (2C); LC-MS (ESI): *m/z* 469 $[M+H]^+$; purity (LC-MS): 98% (t_R = 2.65 min.)

1-((4-trifluoromethyl)benzyl)-2-(3-((*N*,*N*-diethylamino)methyl)-2-hydroxy-5-methylanilino)benzo[*d*]imidazole (8.2)

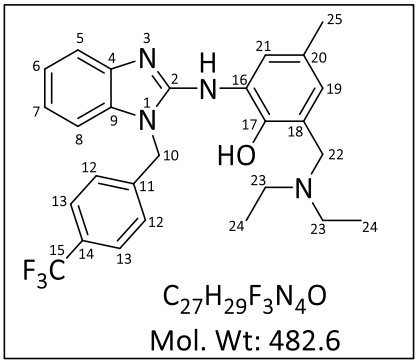

Yellow semi-solid (0.115 g obtained from 0.100 g of **8.0**, 74%); *R*f 0.7 (10% MeOH-DCM); ^{1}H NMR (400 MHz, MeOH-d_4) δ 7.61-7.56 (m, 3H, 2×H-13 and H-21), 7.46-7.41 (m, 1H, H-8), 7.37 (d, *J* = 7.8 Hz, 2H, 2×H-12), 7.20-7.16 (m, 1H, H-5), 7.11 (td, *J* = 7.6, 1.3 Hz, 1H, H-7), 7.05 (td, *J* = 7.6, 1.2 Hz, 1H, H-6), 6.53 (d, *J* = 1.9, Hz, 1H, H-19), 5.44 (s, 2H, 2×H-10), 3.75 (s, 2H, 2×H-22), 2.63 (q, *J* = 7.1 Hz, 4H, 4×H-23), 2.23 (s, 3H, CH_3-25), 1.07 (t, *J* = 7.1 Hz, 6H, 2×CH_3-24); ^{13}C NMR (101 MHz, MeOH-d_4) δ 152.4, 147.5, 142.6, 142.0, 135.1, 131.1 (q, *J* = 32.2 Hz, C-14), 128.9, 128.8, 128.6 (2C), 126.8 (q, *J* = 3.8 Hz, 2×C-13), 125.5 (q, *J* = 270.0 Hz, C-15), 124.3, 122.9, 122.5, 121.9, 120.6, 117.4, 109.3, 57.5, 47.5 (2C), 46.3, 21.0 and 11.4 (2C); LC-MS (ESI): *m/z* 483 $[M+H]^+$; purity (LC-MS): 98% (t_R = 2.68 min.)

1-((4-trifluoromethyl)benzyl)-2-(3-((*N*,*N*-diethylamino)methyl)-2-hydroxy-6-methylanilino)benzo[*d*]imidazole (8.3)

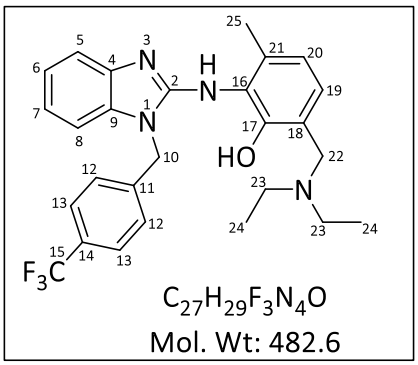

Brown semi-solid (0.096 g obtained from 0.100 g of **8.0**, 62%); *R*f 0.5 (10% MeOH-DCM); ^{1}H NMR (600 MHz, MeOH-d_4) δ 7.61 (d, *J* = 8.2 Hz, 2H, 2×H-13), 7.43 (d, *J* = 8.1 Hz, 2H, 2×H-12), 7.26-7.23 (m, 1H, H-8), 7.08-7.05 (m, 1H, H-5), 7.02 (td, *J* = 7.6, 1.2, Hz, 1H, H-7), 6.97 (td, *J* = 7.5, 1.1 Hz, 1H, H-6), 6.86 (d, *J* = 7.7 Hz, 1H, H-19), 6.67 (d, *J* = 7.7 Hz, 1H, H-20), 5.49 (s, 2H, 2×H-10), 3.82 (s, 2H, 2×H-22), 2.68 (q, *J* = 7.1 Hz, 4H, 4×H-23), 2.11 (s, 3H, CH_3-25), 1.09 (t, *J* = 7.1 Hz, 6H, 2×CH_3-24); ^{13}C NMR (151 MHz, MeOH-d_4) δ 155.2, 154.5, 142.5, 142.4, 137.3, 135.4, 130.7 (q, *J* = 32.2 Hz, C-14), 128.6 (2C), 127.6, 126.6 (q, *J* = 4.1 Hz, 2×C-13), 125.5 (q, *J* = 270.0 Hz, C-15), 124.7, 122.6, 121.5, 121.2, 121.1, 116.4, 109.1, 57.1, 47.4 (2C), 46.2, 18.3 and 11.2 (2C); LC-MS (ESI): *m/z* 483 $[M+H]^+$; purity (LC-MS): 98% (t_R = 2.64 min.)

1-((4-trifluoromethyl)benzyl)-2-(4-((*N*,*N*-diethylamino)methyl)-3-hydroxyanilino)benzo[*d*]imidazole (8.4)

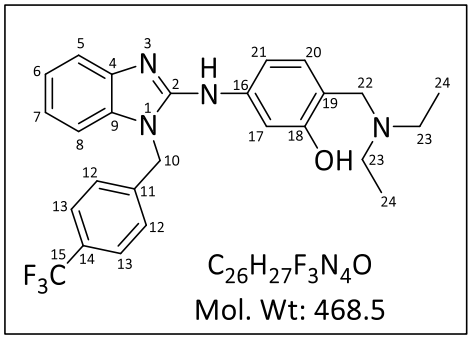

Brown semi-solid (0.075 g obtained from 0.100 g of **8.0**, 50%); *R*f 0.3 (10% MeOH-DCM); ^{1}H NMR (600 MHz, MeOH-d_4) δ 7.59 (d, *J* = 8.1 Hz, 2H, 2×H-13), 7.45-7.42 (m, 1H, H-8), 7.29 (d, *J* = 8.3 Hz, 2H, 2×H-12), 7.17-7.09 (m, 4H, H-5, H-7, H-17 and H-20), 7.07 (td, *J* = 7.7, 1.1 Hz, 1H, H-6), 6.93 (dd, *J* = 2.2, 8.2 Hz, 1H, H-21), 5.53 (s, 2H, 2×H-10), 4.04 (s, 2H, 2×H-22), 2.97 (q, *J* = 7.2 Hz, 4H, 4×H-23), 1.25 (t, *J* = 7.2 Hz, 6H, 2×CH_3-24); ^{13}C NMR (151 MHz, MeOH-d_4) δ 159.1, 151.9, 144.3, 142.4, 134.9, 132.3, 131.7, 130.9 (q, *J* = 32.7 Hz, C-14), 128.2, 128.1 (2C), 126.7 (q, *J* = 3.8 Hz, 2×C-13), 125.5 (q, *J* = 270.0 Hz, C-15), 123.2, 122.3, 117.6, 111.4, 109.9, 107.1, 54.5, 48.0 (2C), 46.3 and 10.1 (2C); LC-MS (ESI): *m/z* 469 $[M+H]^+$; purity (LC-MS): 96% (t_R = 2.61 min.)

1-((4-trifluoromethyl)benzyl)-2-(3-((*N*,*N*-diethylamino)methyl)-4-hydroxyanilino)benzo[*d*]imidazole (8.5)

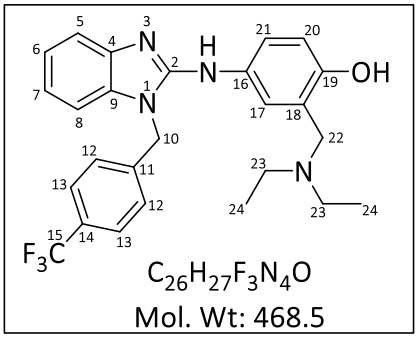

Pink semi-solid (0.127 g obtained from 0.100 g of **8.0**, 84%); *R*f 0.4 (10% MeOH-DCM); ^{1}H NMR (600 MHz, MeOH-d_4) δ 7.67 (d, *J* = 8.2 Hz, 2H, 2×H-13), 7.63 (d, *J* = 2.6 Hz, 1H, H-17), 7.46-7.42 (m, 3H, H-8 and 2×H-12), 7.40 (dd, *J* = 2.7, 8.7 Hz, 1H, H-21), 7.28-7.25 (m, 1H, H-5), 7.23 (td, *J* = 7.6, 1.2 Hz, 1H, H-7), 7.18 (td, *J* = 7.6, 1.1 Hz, 1H, H-6), 7.02 (d, *J* = 8.6 Hz, 1H, H-20), 5.63 (s, 2H, 2×H-10), 4.33 (s, 2H, 2×H-22), 3.26 (q, *J* = 7.3 Hz, 4H, 4×H-23), 1.39 (t, *J* = 7.3 Hz, 6H, 2×CH_3-24); ^{13}C NMR (151 MHz, MeOH-d_4) δ 155.9, 152.0, 141.1, 136.3, 133.6, 131.2 (q, *J* = 32.5 Hz, C-14), 131.0, 128.4 (2C), 126.9 (q, *J* = 3.9 Hz, 2×C-13), 125.5 (q, *J* = 270.0 Hz, C-15), 126.4, 124.6, 124.5, 123.7, 118.6, 117.6, 115.2, 110.6, 52.4, 48.6 (2C), 46.6 and 9.1 (2C); LC-MS (ESI): *m/z* 469 $[M+H]^+$; purity (LC-MS): 98% (t_R = 2.59 min.)

1-(4-fluorobenzyl)-2-(3-((*N*,*N*-diethylamino)methyl)-2-hydroxyanilino)benzo[*d*]imidazole (9.1)

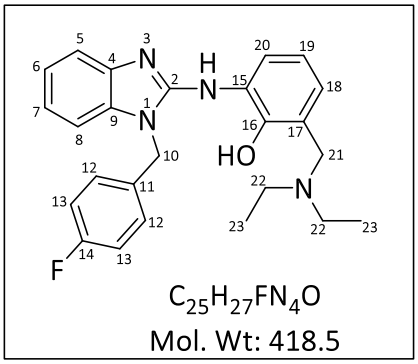

Brown semi-solid (0.112 g obtained from 0.100 g of **9.0**, 70%); *R*f 0.7 (10% MeOH-DCM); ^{1}H NMR (400 MHz, MeOH-d_4) δ 7.77 (dd, *J* = 2.2, 7.3 Hz, 1H, H-20), 7.44-7.40 (m, 1H, H-8), 7.27 (dd, *J* = 5.2, 8.6 Hz, 2H, 2×H-12), 7.25-7.21 (m, 1H, H-5), 7.13-7.06 (m, 2H, H-6 and H-7), 7.03 (t, *J* = 8.7 Hz, 2H, 2×H-13), 6.77-6.69 (m, 2H, H-18 and H-19), 5.36 (s, 2H, 2×H-10), 3.84 (s, 2H, 2×H-21), 2.69 (q, *J* = 7.2 Hz, 4H, 4×H-22), 1.12 (t, *J* = 7.2 Hz, 6H, 2×CH_3-23); ^{13}C NMR (101 MHz, MeOH-d_4) δ 163.8 (d, *J* = 245.0 Hz, C-14), 152.2, 150.1, 142.6, 135.1, 133.4 (d, *J* = 3.2 Hz, C-11), 130.0 (q, *J* = 8.2 Hz, 2×C-12), 129.4, 123.6, 122.8, 122.5, 121.9, 119.5, 119.3, 117.4, 116.7 (d, *J* = 22.0 Hz, 2×C-13), 109.4, 57.6, 47.5 (2C), 46.1 and 11.3 (2C); LC-MS (ESI): *m/z* 419 $[M+H]^+$; purity (LC-MS): 98% (t_R = 2.55 min.)

1-(4-fluorobenzyl)-2-(3-((*N*,*N*-diethylamino)methyl)-2-hydroxy-5-methylanilino)benzo[*d*]imidazole (9.2)

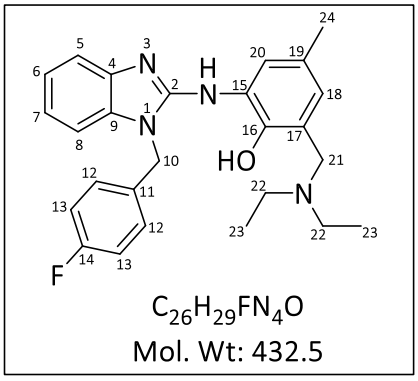

Yellow semi-solid (0.140 g obtained from 0.100 g of **9.0**, 84%); *R*f 0.7 (10% MeOH-DCM); ^{1}H NMR (400 MHz, MeOH-d_4) δ 7.61 (d, *J* = 2.0 Hz, 1H, H-20), 7.45-7.41 (m, 1H, H-8), 7.24 (dd, *J* = 5.3, 8.6 Hz, 2H, 2×H-12), 7.22-7.19 (m, 1H, H-5), 7.14-7.06 (m, 2H, H-6 and H-7), 7.03 (t, *J* = 8.7 Hz, 2H, 2×H-13), 6.53 (d, *J* = 2.0 Hz, 1H, H-18), 5.32 (s, 2H, 2×H-10), 3.77 (s, 2H, 2×H-21), 2.65 (q, *J* = 7.2 Hz, 4H, 4×H-22), 2.24 (s, 3H, CH_3-24), 1.09 (t, *J* = 7.2 Hz, 6H, 2×CH_3-23); ^{13}C NMR (101 MHz, MeOH-d_4) δ 163.8 (d, *J* = 245.1 Hz, C-14), 152.2, 147.2, 142.5, 135.1, 133.4 (d, *J* = 3.2 Hz, C-11), 130.0 (q, *J* = 8.3 Hz, 2×C-12), 129.0, 128.9, 124.2, 122.8, 122.4, 121.9, 120.2, 117.4, 116.7 (q, *J* = 21.9 Hz, 2×C-13), 109.4, 57.5, 47.5 (2C), 46.1, 21.0 and 11.4 (2C); LC-MS (ESI): *m/z* 433 $[M+H]^+$; purity (LC-MS): 98% (t_R = 2.61 min.)

1-(4-fluorobenzyl)-2-(3-((*N*,*N*-diethylamino)methyl)-2-hydroxy-6-methylanilino)benzo[*d*]imidazole (9.3)

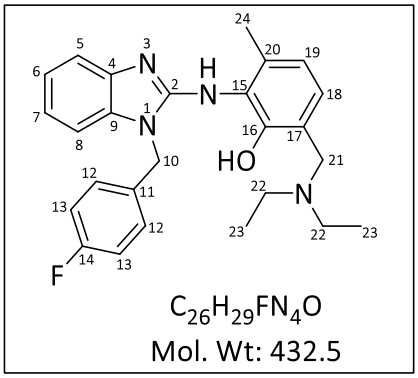

Brown semi-solid (0.112 g obtained from 0.100 g of **9.0**, 68%); *R*f 0.5 (10% MeOH-DCM); ^{1}H NMR (600 MHz, MeOH-d_4) δ 7.31 (dd, *J* = 5.3, 8.6 Hz, 2H, 2×H-12), 7.24-7.21 (m, 1H, H-8), 7.10-7.07 (m, 1H, H-5), 7.03 (t, *J* = 8.7 Hz, 2H, 2×H-13), 7.00 (td, *J* = 7.5, 1.3 Hz, 1H, H-7), 6.96 (td, *J* = 7.5, 1.1 Hz, 1H, H-6), 6.85 (d, *J* = 7.7 Hz, 1H, H-18), 6.67 (d, *J* = 7.7 Hz, 1H, H-19), 5.37 (s, 2H, 2×H-10), 3.81 (s, 2H, 2×H-21), 2.66 (q, *J* = 7.2 Hz, 4H, 4×H-22), 2.10 (s, 3H, CH_3-24), 1.09 (t, *J* = 7.1 Hz, 6H, 2×CH_3-23); ^{13}C NMR (151 MHz, MeOH-d_4) δ 163.7 (d, *J* = 244.4 Hz, C-14), 155.2, 154.5, 142.4, 137.1, 135.5, 133.9 (d, *J* = 3.1 Hz, C-11), 130.0 (d, *J* = 8.1 Hz, 2×C-12), 127.4, 126.7, 122.4, 121.5, 121.3, 121.1, 116.5 (d, *J* = 21.6 Hz, 2×C-13), 116.4, 109.2, 57.3, 47.3 (2C), 45.9, 18.3 and 11.4 (2C); LC-MS (ESI): *m/z* 433 $[M+H]^+$; purity (LC-MS): 98% (t_R = 2.51 min.)

1-(4-fluorobenzyl)-2-(4-((*N*,*N*-diethylamino)methyl)-3-hydroxyanilino)benzo[*d*]imidazole (9.4)

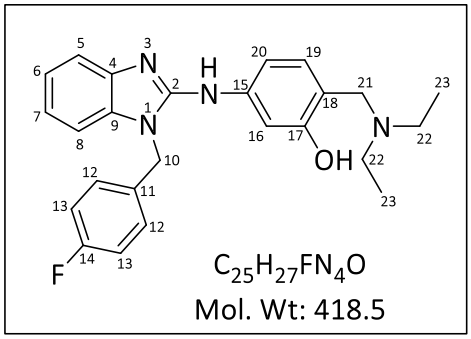

Brown semi-solid (0.102 g obtained from 0.100 g of **9.0**, 63%); *R*f 0.3 (10% MeOH-DCM); ^{1}H NMR (600 MHz, MeOH-d_4) δ 7.41-7.38 (m, 1H, H-8), 7.16 (dd, *J* = 5.3, 8.5 Hz, 2H, 2×H-12), 7.13-7.10 (m, 1H, H-5), 7.08 (td, *J* = 7.7, 1.1 Hz, 1H, H-7), 7.03 (td, *J* = 7.7, 1.1 Hz, 1H, H-6), 7.00 (t, *J* = 8.7 Hz, 2H, 2×H-13), 6.95-6.84 (m, 3H, H-16, H-19 and H-20), 5.37 (s, 2H, 2×H-10), 3.74 (s, 2H, 2×H-21), 2.63 (q, *J* = 7.2 Hz, 4H, 4×H-22), 2.10 (s, 3H, CH_3-24), 1.10 (t, *J* = 7.1 Hz, 6H, 2×CH_3-23); ^{13}C NMR (151 MHz, MeOH-d_4) δ 163.6 (d, *J* = 244.4 Hz, C-14), 160.0, 152.3, 142.5, 134.9, 133.8 (d, *J* = 3.3 Hz, C-11), 131.6, 130.1, 129.7 (d, *J* = 8.2 Hz, 2×C-12), 122.9, 121.9, 117.8, 117.3, 116.5 (d, *J* = 21.8 Hz, 2×C-13), 111.2, 109.8, 108.1, 57.1, 47.3 (2C), 46.0 and 11.6 (2C); LC-MS (ESI): *m/z* 419 $[M+H]^+$; purity (LC-MS): 98% (t_R = 2.52 min.)

1-(4-fluorobenzyl)-2-(3-((*N*,*N*-diethylamino)methyl)-4-hydroxyanilino)benzo[*d*]imidazole (9.5)

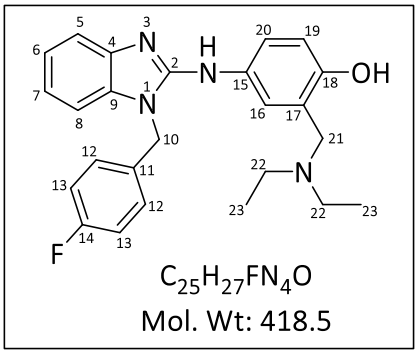

Pink semi-solid (0.146 g obtained from 0.100 g of **9.0**, 91%); *R*f 0.4 (10% MeOH-DCM); ^{1}H NMR (600 MHz, MeOH-d_4) δ 7.64 (d, *J* = 2.6 Hz, 1H, H-16), 7.46-7.44 (m, 1H, H-8), 7.43 (dd, *J* = 2.6, 8.6 Hz, 1H, H-20), 7.36 (dd, *J* = 5.2, 8.5 Hz, 2H, 2×H-12), 7.35-7.32 (m, 1H, H-5), 7.26 (td, *J* = 7.7, 1.4 Hz, 1H, H-7), 7.23 (td, *J* = 7.6, 1.3 Hz, 1H, H-6), 7.11 (t, *J* = 8.7 Hz, 2H, 2×H-13), 7.07 (d, *J* = 8.6 Hz, 1H, H-19), 5.55 (s, 2H, 2×H-10), 4.34 (s, 2H, 2×H-21), 3.27 (q, *J* = 7.2 Hz, 4H, 4×H-22), 1.40 (t, *J* = 7.2 Hz, 6H, 2×CH_3-23); ^{13}C NMR (151 MHz, MeOH-d_4) δ 163.9 (d, *J* = 245.5 Hz, C-14), 156.8, 151.2, 133.6, 132.9, 132.0 (d, *J* = 3.3 Hz, C-11), 130.1 (d, *J* = 8.3 Hz, 2×C-12), 129.9, 129.8, 129.0, 124.9, 124.3, 118.9, 117.9, 116.9 (d, *J* = 22.0 Hz, 2×C-13), 114.3, 111.3, 52.2, 48.6 (2C), 46.6 and 9.1 (2C); LC-MS (ESI): *m/z* 419 $[M+H]^+$; purity (LC-MS): 98% (t_R = 2.41 min.)

5.6.7 Antimycobacterial evaluation protocol

The *in vitro* antimycobacterial evaluation protocol has already been described in Section 4.6.8

5.6.8 Antiplasmodium evaluation protocol

The *in vitro* antiplasmodium evaluation protocol has already been described in Sections 4.6.9.1 and 4.6.9.3.

5.6.9 Cytotoxicity evaluation protocol

The *in vitro* cytotoxic activity protocol has already been described in Section 4.6.10

5.6.10 Beta-hematin inhibition assay

The inhibition of beta-hematin formation assay was conducted to investigate the possible mechanism of antiplasmodium activity of the synthesized benzimidazole analogues as inhibitors

of heme polymerization. This non-cell assay evaluates the ability of the test compounds to prevent the synthetic dimerization of hematin (beta-hematin) in lipid medium.

Hundred microliters of a solution containing water/305.5 µM NP-40/DMSO at a v/v ratio of 70%/20%/10%, respectively, was added to every well in columns 2 - 12 of a 96-well plate. To column 1 was added 140 µL of water and 40 µL of 305.5 µM NP-40. Twenty microliters of the test compounds (20 mM), that is, the synthesized compounds and control, was added to column 1 in duplicate. One hundred microliters of the test solution was diluted to column 11, with column 12 left as a blank (0 µM of compound). A 178.8 µL aliquot of hematin (hemin) stock was suspended in 20 mL of a 1 M acetate buffer, pH 4.8 and 100 µL of this hematin suspension added into each well. Plates were then incubated for ~5 hours at 37 ^{o}C after which 32 µL of pyridine solution (20% water, 20% acetone, 10% 2M HEPES buffer (pH 7.4), 50% pyridine) was added followed by addition of 60 µL of acetone to all wells. Plates were again read at 405 nm on a Thermo Scientific Multiscan Go Microplate Spectrophotometer. The IC_{50} values were determined using GraphPad Prism 6.

5.6.11 Turbidimetric (kinetic) solubility assay

The aqueous solubility of the synthesized compounds were assessed using the thermodynamic 'kinetic' solubility assay in a 96-well microtiter plate. Stock solutions (10 mM) of the compounds were prepared in DMSO. The pre-dilution plate was prepared by making serial dilutions of the stock solution in DMSO, in triplicate, to obtain concentrations ranging from 0.25 to 8.0 mM. From the pre-dilution plate, the assay plate was prepared by pipetting 4 µL of solution and making secondary dilutions in DMSO and 0.01M pH 7.4 PBS, also in triplicate, to obtain the final volume in each assay plate well to be 200 µL. Thus, the concentrations of the wells in the assay plate range from 0 to 200 µM. The plates were then covered and left to incubate at ambient temperature (37 ^{o}C) for 2 h. Absorbance measurements were taken at 620 nm on a Thermo Scientific Multiscan Go Microplate spectrophotometer. A plot of corrected absorbance against concentration was generated using Microsoft® Office Excel 2013 and used to identify the limit of solubility of each compound.

5.7 References

(1) Akee, R. K.; Carroll, T. R.; Yoshida, W. Y.; Scheuer, P. J.; Stout, T. J.; Clardy, J. Two imidazole alkaloids from a sponge. *J. Org. Chem.* 1990, *55* (6), 1944–1946.

(2) Fu, X.; Barnes, J. R.; Do, T.; Schmitz, F. J. New imidazole alkaloids from the sponge *Leucetta chagosensis*. *J. Nat. Prod.* 1997, *60* (5), 497–498.

(3) Hassan, W.; Edrada, R.; Ebel, R.; Wray, V.; Berg, A.; van Soest, R.; Wiryowidagdo, S.; Proksch, P. New imidazole alkaloids from the Indonesian sponge *Leucetta chagosensis*. *J. Nat. Prod.* 2004, *67* (5), 817–822.

(4) Bonnett, R. The chemistry of the vitamin B 12 group. *Chem. Rev.* 1963, *63* (6), 573–605.

(5) *Privileged Scaffolds in Medicinal Chemistry*; Bräse, S., Ed.; Drug Discovery; Royal Society of Chemistry: Cambridge, 2015.

(6) Woolley, D. W. Some biological effects produced by benzimidazole and their reversal by purines. *J. Biol. Chem* 1944, *152*, 225.

(7) Edwards, P. C.; Starling, D.; Mattocks, A. M.; Skipper, H. E. The folic acid activity and antagonism of two structurally related derivatives of benzimidazole. *Science (80-.).* 1948, *107* (2770), 119–120.

(8) Klotz, I. M.; Mellody, M. The reversal of benzimidazole inhibition of growth by nucleic acid. *J. Bacteriol.* 1948, *56* (2), 253–255.

(9) Pelletier, S. V. *Chemistry of the Alkaloids*; Van Nostrand Reinhold Company: New York, 1970.

(10) Acheson, R. M. *Introduction to the Chemistry of Heterocyclic Compounds*; Wiley: New York, 1976.

(11) Hobrecker, F. *Ber* 1872, *5*, 920–926.

(12) Wright, J. B. The chemistry of the benzimidazoles. *Chem. Rev.* 1951, *48* (3), 397–541.

(13) Alaqeel, S. I. Synthetic approaches to benzimidazoles from O-phenylenediamine: A literature review. *J. Saudi Chem. Soc.* 2017, *21* (2), 229–237.

(14) Preston, P. N. Benzimidazoles; 2008; pp 1–285.

(15) Narasimhan, B.; Sharma, D.; Kumar, P. Benzimidazole: A medicinally important heterocyclic moiety. *Med. Chem. Res.* 2012, *21* (3), 269–283.

(16) Bansal, Y.; Silakari, O. The therapeutic journey of benzimidazoles: A review. *Bioorg. Med.*

Chem. 2012, *20* (21), 6208–6236.

(17) Salahuddin; Shaharyar, M.; Mazumder, A. Benzimidazoles: A biologically active compounds. *Arab. J. Chem.* 2017, *10*, S157–S173.

(18) McKellar, Q. A.; Scott, E. W. The benzimidazole anthelmintic agents - a review. *J. Vet. Pharmacol. Ther.* 1990, *13* (3), 223–247.

(19) Spasov, A. A.; Yozhitsa, I. N.; Bugaeva, L. I.; V.A., A. Benzimidazole derivatives: Spectrum of pharmacological activity and toxicological properties (a review). *Pharm. Chem. J.* 1999, *33* (5), 232–243.

(20) Patil, A.; Ganguly, S.; Surana, S. A systematic review of benzimidazole derivatives as an antiulcer agent. *Rasayan J. Chem* 2008, *1*, 447–460.

(21) Rossignol, J. F.; Maisonneuve, H. Benzimidazoles in the treatment of Trichuriasis: A review. *Ann. Trop. Med. Parasitol.* 1984, *78* (2), 135–144.

(22) Dubey, A. K.; Sanyal, P. K. Benzimidazoles in a wormy world. *Online Vet. J.* 2010, *5*, 63.

(23) Barot, K. P.; Nikolova, S.; Ivanov, I.; Ghate, M. D. Novel research strategies of benzimidazole derivatives: A review. *Mini Rev. Med. Chem.* 2013, *13* (10), 1421–1447.

(24) Boiani, M.; González, M. Imidazole and benzimidazole derivatives as chemotherapeutic agents. *Mini Rev. Med. Chem.* 2005, *5* (4), 409–424.

(25) Merck Index Online https://www.rsc.org/Merck-Index/searchresults?searchterm=benzimidazole (accessed Aug 27, 2018).

(26) Benzimidazole https://www.ncbi.nlm.nih.gov/pubmed/?term=benzimidazole (accessed Aug 27, 2018).

(27) Singh, K.; Okombo, J.; Brunschwig, C.; Ndubi, F.; Barnard, L.; Wilkinson, C.; Njogu, P. M.; Njoroge, M.; Laing, L.; Machado, M.; et al. Antimalarial pyrido[1,2- a]benzimidazoles: Lead optimization, parasite life cycle stage profile, nechanistic evaluation, killing kinetics, and i*n vivo* oral efficacy in a mouse model. *J. Med. Chem.* 2017, *60* (4), 1432–1448.

(28) Sessions, E. H.; Yin, Y.; Bannister, T. D.; Weiser, A.; Griffin, E.; Pocas, J.; Cameron, M. D.; Ruiz, C.; Lin, L.; Schürer, S. C.; et al. Benzimidazole- and benzoxazole-based inhibitors of Rho kinase. *Bioorg. Med. Chem. Lett.* 2008, *18* (24), 6390–6393.

(29) Roman, G. Mannich bases in medicinal chemistry and drug design. *Eur. J. Med. Chem.* 2015,

89, 743–816.

(30) Biersack, B.; Ahmed, K.; Padhye, S.; Schobert, R. Recent developments concerning the application of the Mannich reaction for drug design. *Expert Opin. Drug Discov.* 2018, *13* (1), 39–49.

(31) Martín-Escolano, R.; Moreno-Viguri, E.; Santivañez-Veliz, M.; Martin-Montes, A.; Medina-Carmona, E.; Paucar, R.; Marín, C.; Azqueta, A.; Cirauqui, N.; Pey, A. L.; et al. Second generation of Mannich base-type derivatives with *in vivo* activity against *Trypanosoma cruzi*. *J. Med. Chem.* 2018, *61* (13), 5643–5663.

(32) Bala, S.; Sharma, N.; Kajal, A.; Kamboj, S.; Saini, V. Mannich bases: An important pharmacophore in present scenario. *Int. J. Med. Chem.* 2014, *2014*, 1–15.

(33) Li, Y.; Qiang, X.; Luo, L.; Yang, X.; Xiao, G.; Liu, Q.; Ai, J.; Tan, Z.; Deng, Y. Aurone Mannich base derivatives as promising multifunctional agents with acetylcholinesterase inhibition, anti-β-amyloid aggragation and neuroprotective properties for the treatment of Alzheimer's disease. *Eur. J. Med. Chem.* 2017, *126*, 762–775.

(34) Mahal, K.; Ahmad, A.; Schmitt, F.; Lockhauserbäumer, J.; Starz, K.; Pradhan, R.; Padhye, S.; Sarkar, F. H.; Koko, W. S.; Schobert, R.; et al. Improved anticancer and antiparasitic activity of new lawsone Mannich bases. *Eur. J. Med. Chem.* 2017, *126*, 421–431.

(35) Ahmad, A.; Mahal, K.; Padhye, S.; Sarkar, F. H.; Schobert, R.; Biersack, B. New ferrocene modified lawsone mannich bases with anti-proliferative activity against tumor cells. *J. Saudi Chem. Soc.* 2017, *21* (1), 105–110.

(36) Aeluri, R.; Alla, M.; Polepalli, S.; Jain, N. Synthesis and antiproliferative activity of imidazo[1,2-a]pyrimidine Mannich bases. *Eur. J. Med. Chem.* 2015, *100*, 18–23.

(37) Moreno-Viguri, E.; Jiménez-Montes, C.; Martín-Escolano, R.; Santivañez-Veliz, M.; Martin-Montes, A.; Azqueta, A.; Jimenez-Lopez, M.; Zamora Ledesma, S.; Cirauqui, N.; López de Ceráin, A.; et al. *In vitro* and *in vivo* anti-*Trypanosoma cruzi* activity of wew arylamine Mannich base-type derivatives. *J. Med. Chem.* 2016, *59* (24), 10929–10945.

(38) Hackler, L.; Ózsvári, B.; Gyuris, M.; Sipos, P.; Fábián, G.; Molnár, E.; Marton, A.; Faragó, N.; Mihály, J.; Nagy, L. I.; et al. The curcumin analog C-150, influencing NF-KB, UPR and Akt/Notch pathways has potent anticancer activity *in vitro* and *in vivo*. *PLoS One* 2016, *11*

(3), e0149832.

(39) Nyantakyi, S. A.; Li, M.; Gopal, P.; Zimmerman, M.; Dartois, V.; Gengenbacher, M.; Dick, T.; Go, M.-L. Indolyl azaspiroketal Mannich bases are potent antimycobacterial agents with selective membrane permeabilizing effects and *in vivo* activity. *J. Med. Chem.* 2018, *61* (13), 5733–5750.

(40) Mannich base https://www.ncbi.nlm.nih.gov/pubmed (accessed Aug 29, 2018).

(41) Jukes, T. H. Some historical notes on chlortetracycline. *Rev. Infect. Dis. 7* (5), 702–707.

(42) Rathscheck, H. J. Reverin in a tropical hospital. *Singapore Med. J.* 1960, *1* (3), 119–121.

(43) Eidus, L.; Maniar, A. C.; Greenberg, L. Comparative *in vivo* experiments on the tetracycline analogues. *Canad. Med. Ass. J.* 1962, *86*, 366–369.

(44) Xie, Z.-F.; Ootsu, K.; Akimoto, H. Convergent approach to water soluble camptothecin derivatives. *Bioorg. Med. Chem. Lett.* 1995, *5* (19), 2189–2194.

(45) Eckardt, J.; Eckhardt, G.; Villalona-Calero, M.; Drengler, R.; D, V. H. New anticancer agents in clinical development. *Oncology* 1995, *9*, 1191–1199.

(46) Underberg, W. J.; Goossen, R. M.; Smith, B. R.; Beijnen, J. H. Equilibrium kinetics of the new experimental anti-tumour compound SK&F 104864-A in aqueous solution. *J. Pharm. Biomed. Anal.* 1990, *8* (8–12), 681–683.

(47) Carmichael, J.; Ozols, R. Topotecan, an active new antineoplastic agent: Review and Current Status. *Expert Opin. Investig. Drugs* 1997, *6* (5), 593–608.

(48) Simplício, A. L.; Clancy, J. M.; Gilmer, J. F. β-aminoketones as prodrugs with pH-controlled activation. *Int. J. Pharm.* 2007, *336* (2), 208–214.

(49) Huttunen, K. M.; Rautio, J. Prodrugs - an efficient way to breach delivery and targeting barriers. *Curr. Top. Med. Chem.* 2011, *11* (18), 2265–2287.

(50) Arcamone, F.; Cassinelli, G.; Fantini, G.; Grein, A.; Orezzi, P.; Pol, C.; Spalla, C. Adriamycin, 14-hydroxydaunomycin, a new antitumor antibiotic from *S. Peucetius* var. Caesius. *Biotechnol. Bioeng.* 1969, *11* (6), 1101–1110.

(51) Tacar, O.; Sriamornsak, P.; Dass, C. R. Doxorubicin: An update on anticancer molecular action, toxicity and novel drug delivery systems. *J. Pharm. Pharmacol.* 2013, *65* (2), 157–170.

(52) Fenick, D. J.; Taatjes, D. J.; Koch, T. H. Doxoform and Daunoform: Anthracycline–formaldehyde conjugates toxic to resistant tumor cells. *J. Med. Chem.* 1997, *40* (16), 2452–2461.

(53) Cogan, P.; Fowler, C.; Post, G.; Koch, T. Doxsaliform: A novel N-Mannich base prodrug of a doxorubicin formaldehyde conjugate. *Lett. Drug Des. Discov.* 2004, *1* (3), 247–255.

(54) Kuhn, B.; Mohr, P.; Stahl, M. Intramolecular hydrogen bonding in medicinal chemistry. *J. Med. Chem.* 2010, *53* (6), 2601–2611.

(55) Hickey, J. L.; Zaretsky, S.; St. Denis, M. A.; Kumar Chakka, S.; Morshed, M. M.; Scully, C. C. G.; Roughton, A. L.; Yudin, A. K. Passive membrane permeability of macrocycles can be controlled by exocyclic amide bonds. *J. Med. Chem.* 2016, *59* (11), 5368–5376.

(56) Sakamoto, T.; Koga, Y.; Hikota, M.; Matsuki, K.; Murakami, M.; Kikkawa, K.; Fujishige, K.; Kotera, J.; Omori, K.; Morimoto, H.; et al. Design and synthesis of novel 5-(3,4,5-trimethoxybenzoyl)-4-aminopyrimidine derivatives as potent and selective phosphodiesterase 5 inhibitors: Scaffold hopping using a pseudo-ring by intramolecular hydrogen bond formation. *Bioorg. Med. Chem. Lett.* 2014, *24* (22), 5175–5180.

(57) Alex, A.; Millan, D. S.; Perez, M.; Wakenhut, F.; Whitlock, G. A. Intramolecular hydrogen bonding to improve membrane permeability and absorption in beyond rule of five chemical space. *Medchemcomm* 2011, *2* (7), 669.

(58) Giordanetto, F.; Tyrchan, C.; Ulander, J. Intramolecular hydrogen bond expectations in medicinal chemistry. *ACS Med. Chem. Lett.* 2017, *8* (2), 139–142.

(59) Chang, C.; Lin-Hua, T.; Jantanavivat, C. Studies on a new antimalarial compound: Pyronaridine. *Trans. R. Soc. Trop. Med. Hyg. 86* (1), 7–10.

(60) Birrell, G. W.; Chavchich, M.; Ager, A. L.; Shieh, H.-M.; Heffernan, G. D.; Zhao, W.; Krasucki, P. E.; Saionz, K. W.; Terpinski, J.; Schiehser, G. A.; et al. JPC-2997, a new aminomethylphenol with high *in vitro* and *in vivo* antimalarial activities against blood stages of *Plasmodium*. *Antimicrob. Agents Chemother.* 2015, *59* (1), 170–177.

(61) Peters, W.; Robinson, B. L. The chemotherapy of rodent malaria, XXXVII. *Ann. Trop. Med. Parasitol.* 1984, *78* (6), 561–565.

(62) Powles, M. A.; Allocco, J.; Yeung, L.; Nare, B.; Liberator, P.; Schmatz, D. MK-4815, a potential

new oral agent for treatment of malaria. *Antimicrob. Agents Chemother.* 2012, *56* (5), 2414–2419.

(63) Gil, J. P.; Gil Berglund, E. CYP2C8 and antimalaria drug efficacy. *Pharmacogenomics* 2007, *8* (2), 187–198.

(64) Davioud-Charvet, E.; McLeish, M. J.; Veine, D. M.; Giegel, D.; Arscott, L. D.; Andricopulo, A. D.; Becker, K.; Müller, S.; Schirmer, R. H.; Williams, C. H.; et al. Mechanism-based inactivation of thioredoxin reductase from *Plasmodium falciparum* by Mannich bases. Implication for Cytotoxicity†. *Biochemistry* 2003, *42* (45), 13319–13330.

(65) Pati, H.; Das, U.; Sharma, R.; Dimmock, J. Cytotoxic thiol alkylators. *Mini-Reviews Med. Chem.* 2007, *7* (2), 131–139.

(66) Dimmock, J. R.; Kandepu, N. M.; Hetherington, M.; Quail, J. W.; Pugazhenthi, U.; Sudom, A. M.; Chamankhah, M.; Rose, P.; Pass, E.; Allen, T. M.; et al. Cytotoxic activities of Mannich bases of chalcones and related compounds. *J. Med. Chem.* 1998, *41* (7), 1014–1026.

(67) Kumar, S.; Guha, M.; Choubey, V.; Maity, P.; Bandyopadhyay, U. Antimalarial drugs inhibiting hemozoin (β-hematin) formation: A mechanistic update. *Life Sci.* 2007, *80* (9), 813–828.

(68) Ridley, R. G. Haemoglobin Degradation and haem polymerization as antimalarial drug targets. *J. Pharm. Pharmacol.* 1997, *49* (S2), 43–48.

(69) Olliaro, P. L.; Goldberg, D. E. The *Plasmodium* digestive vacuole: Metabolic headquarters and choice drug target. *Parasitol. Today* 1995, *11* (8), 294–297.

(70) Haynes, R. K.; Vonwiller, S. C. The behaviour of Qinghaosu (Artemisinin) in the presence of heme iron(II) and (III). *Tetrahedron Lett.* 1996, *37* (2), 253–256.

(71) Posner, G. H. Antimalarial endoperoxides that are potent and easily synthesized. *J. Pharm. Pharmacol.* 1997, *49* (S2), 55–57.

(72) Meshnick, S. R.; Taylor, T. E.; Kamchonwongpaisan, S. Artemisinin and the antimalarial endoperoxides: From herbal remedy to targeted chemotherapy. *Microbiol. Rev.* 1996, *60* (2), 301–315.

(73) Schmitt, T. H.; Frezzatti, W. A.; Schreier, S. Hemin-induced lipid membrane disorder and increased permeability: A molecular model for the mechanism of cell lysis. *Arch. Biochem.*

Biophys. 1993, *307* (1), 96–103.

(74) Slater, A. F. G.; Cerami, A. Inhibition by chloroquine of a novel haem polymerase enzyme activity in malaria trophozoites. *Nature* 1992, *355* (6356), 167–169.

(75) Dorn, A.; Vippagunta, S. R.; Matile, H.; Jaquet, C.; Vennerstrom, J. L.; Ridley, R. G. An assessment of drug-haematin binding as a mechanism for inhibition of haematin polymerisation by quinoline antimalarials. *Biochem. Pharmacol.* 1998, *55* (6), 727–736.

(76) Dorn, A.; Stoffel, R.; Matile, H.; Bubendorf, A.; Ridley, R. G. Malarial haemozoin/β-haematin supports haem polymerization in the absence of protein. *Nature* 1995, *374* (6519), 269–271.

(77) Sullivan, D. J.; Gluzman, I. Y.; Goldberg, D. E. Plasmodium hemozoin formation mediated by histidine-rich proteins. *Science* 1996, *271* (5246), 219–222.

(78) Fitch, C. D.; Cai, G.; Chen, Y.-F.; Shoemaker, J. D. Involvement of lipids in ferriprotoporphyrin IX polymerization in malaria. *Biochim. Biophys. Acta - Mol. Basis Dis.* 1999, *1454* (1), 31–37.

(79) Bohle, D. S.; Helms, J. B. Synthesis of β-hematin by dehydrohalogenation of hemin. *Biochem. Biophys. Res. Commun.* 1993, *193* (2), 504–508.

(80) Egan, T. Structure-function relationships in chloroquine and related 4-aminoquinoline antimalarials. *Mini-Reviews Med. Chem.* 2001, *1* (1), 113–123.

(81) Parapini, S.; Basilico, N.; Mondani, M.; Olliaro, P.; Taramelli, D.; Monti, D. Evidence that haem iron in the malaria parasite is not needed for the antimalarial effects of artemisinin. *FEBS Lett.* 2004, *575* (1–3), 91–94.

(82) Pagola, S.; Stephens, P. W.; Bohle, D. S.; Kosar, A. D.; Madsen, S. K. The structure of malaria pigment β-haematin. *Nature* 2000, *404* (6775), 307–310.

(83) Egan, T. J.; Mavuso, W. W.; Ross, D. C.; Marques, H. M. Thermodynamic factors controlling the interaction of quinoline antimalarial drugs with ferriprotoporphyrin IX. *J. Inorg. Biochem.* 1997, *68* (2), 137–145.

(84) Leed, A.; DuBay, K.; Ursos, L. M. B.; Sears, D.; de Dios, A. C.; Roepe, P. D. Solution structures of antimalarial drug–heme complexes. *Biochemistry* 2002, *41* (32), 10245–10255.

(85) Loria, P.; Miller, S.; Foley, M.; Tilley, L. Inhibition of the peroxidative degradation of haem as the basis of action of chloroquine and other quinoline antimalarials. *Biochem. J.* 1999,

339 (Pt 2, 363–370.

(86) Egan, T. Haemozoin formation as a target for the rational design of new antimalarials. *Drug Des. Rev. - Online* 2004, *1* (1), 93–110.

(87) Egan, T. J.; Hunter, R.; Kaschula, C. H.; Marques, H. M.; Misplon, A.; Walden, J. Structure-function relationships in aminoquinolines: Effect of amino and chloro groups on quinoline-hematin complex formation, inhibition of beta-hematin formation, and antiplasmodial activity. *J. Med. Chem.* 2000, *43* (2), 283–291.

(88) Slater, A. F. Chloroquine: Mechanism of drug action and resistance in *Plasmodium falciparum*. *Pharmacol. Ther. 57* (2–3), 203–235.

(89) Tiffert, T.; Ginsburg, H.; Krugliak, M.; Elford, B. C.; Lew, V. L. Potent antimalarial activity of clotrimazole in *in vitro* cultures of *Plasmodium falciparum*. *Proc. Natl. Acad. Sci. U. S. A.* 2000, *97* (1), 331–336.

(90) Huy, N. T.; Kamei, K.; Yamamoto, T.; Kondo, Y.; Kanaori, K.; Takano, R.; Tajima, K.; Hara, S. Clotrimazole binds to heme and enhances heme-dependent hemolysis. *J. Biol. Chem.* 2002, *277* (6), 4152–4158.

(91) Huy, N. T.; Kamei, K.; Kondo, Y.; Serada, S.; Eanaori, K.; Takano, R.; Tajima, K.; Hara, S. Effect of antifungal azoles on the heme detoxification system of malarial parasite. *J. Biochem.* 2002, *131* (3), 437–444.

(92) Saliba, K. J.; Kirk, K. Clotrimazole inhibits the growth of *Plasmodium falciparum in vitro*. *Trans. R. Soc. Trop. Med. Hyg.* 1998, *92* (6), 666–667.

(93) Angerhofer, C. K.; Pezzuto, J. M.; König, G. M.; Wright, A. D.; Sticher, O. Antimalarial activity of sesquiterpenes from the marine sponge *Acanthella klethra*. *J. Nat. Prod.* 1992, *55* (12), 1787–1789.

(94) Wright, A. D.; Wang, H.; Gurrath, M.; König, G. M.; Kocak, G.; Neumann, G.; Loria, P.; Foley, M.; Tilley, L. Inhibition of heme detoxification processes underlies the antimalarial activity of terpene isonitrile compounds from marine sponges. *J. Med. Chem.* 2001, *44* (6), 873–885.

(95) Atamna, H.; Krugliak, M.; Shalmiev, G.; Deharo, E.; Pescarmona, G.; Ginsburg, H. Mode of antimalarial effect of methylene blue and some of its analogues on *Plasmodium falciparum*

in culture and their inhibition of *P. Vinckei* Petteri and *P. Yoelii* Nigeriensis *in vivo*. *Biochem. Pharmacol.* 1996, *51* (5), 693–700.

(96) Kalkanidis, M.; Klonis, N.; Tilley, L.; Deady, L. W. Novel phenothiazine antimalarials: Synthesis, antimalarial activity, and inhibition of the formation of β-haematin. *Biochem. Pharmacol.* 2002, *63* (5), 833–842.

(97) Riscoe, M.; Winter, R. W.; Ignatushchenko, M. V. Xanthones as antimalarial agents: Stage specificity. *Am. J. Trop. Med. Hyg.* 2000, *62* (1), 77–81.

(98) Xu Kelly, J. A Spectroscopic investigation of the binding interactions between 4,5-dihydroxyxanthone and heme. *J. Inorg. Biochem.* 2001, *86* (2–3), 617–625.

(99) Ignatushchenko, M. V.; Winter, R. W.; Bächinger, H. P.; Hinrichs, D. J.; Riscoe, M. K. Xanthones as antimalarial agents; studies of a possible mode of action. *FEBS Lett.* 1997, *409* (1), 67–73.

(100) Fotie, J.; Nkengfack, A. E.; Rukunga, G.; Tolo, F.; Peter, M. G.; Heydenreich, M.; Fomum, Z. T. *In vivo* antimalarial activity of some oxygenated xanthones. *Ann. Trop. Med. Parasitol.* 2003, *97* (7), 683–688.

(101) Kelly, J. X.; Winter, R.; Peyton, D. H.; Hinrichs, D. J.; Riscoe, M. Optimization of xanthones for antimalarial activity: The 3,6-Bis-ω-diethylaminoalkoxyxanthone series. *Antimicrob. Agents Chemother.* 2002, *46* (1), 144–150.

(102) Begum, K.; Kim, H.-S.; Kumar, V.; Stojiljkovic, I.; Wataya, Y. *In vitro* antimalarial activity of metalloporphyrins against *Plasmodium falciparum*. *Parasitol. Res.* 2003, *90* (3), 221–224.

(103) Cole, K. A.; Ziegler, J.; Evans, C. A.; Wright, D. W. Metalloporphyrins inhibit β-hematin (hemozoin) formation. *J. Inorg. Biochem.* 2000, *78* (2), 109–115.

(104) Kerns, E. H.; Di, L.; Carter, G. T. *In vitro* solubility assays in drug Discovery. *Curr. Drug Metab.* 2008, *9* (9), 879–885.

(105) Jain, N.; Yalkowsky, S. H. Estimation of the aqueous solubility I: Application to organic nonelectrolytes. *J. Pharm. Sci.* 2001, *90* (2), 234–252.

(106) Abraham, M. H.; Le, J. The correlation and prediction of the solubility of compounds in water using an amended solvation energy relationship. *J. Pharm. Sci.* 1999, *88* (9), 868–880.

(107) Sanghvi, T.; Jain, N.; Yang, G.; Yalkowsky, S. Estimation of aqueous solubility by the general

solubility equation (GSE) The Easy Way. *QSAR Comb. Sci.* 2003, *22* (2), 258–262.

(108) 1-methylbenzimidazole http://www.chemspider.com/Chemical-Structure.86565.html (accessed Oct 31, 2018).

(109) Savjani, K. T.; Gajjar, A. K.; Savjani, J. K. Drug solubility: Importance and enhancement techniques. *ISRN Pharm.* 2012, *2012*, 195727.

(110) Williams, H. D.; Trevaskis, N. L.; Charman, S. A.; Shanker, R. M.; Charman, W. N.; Pouton, C. W.; Porter, C. J. H. Strategies to address low drug solubility in discovery and development. *Pharmacol. Rev.* 2013, *65* (1), 315–499.

(111) Jain, S.; Patel, N.; Lin, S. Solubility and dissolution enhancement strategies: Current understanding and recent trends. *Drug Dev. Ind. Pharm.* 2015, *41* (6), 875–887.

(112) Lipinski, C. A.; Lombardo, F.; Dominy, B. W.; Feeney, P. J. Experimental and computational approaches to estimate solubility and permeability in drug discovery and development settings. *Adv. Drug Deliv. Rev.* 2001, *46* (1–3), 3–26.

(113) Veber, D. F.; Johnson, S. R.; Cheng, H.-Y.; Smith, B. R.; Ward, K. W.; Kopple, K. D. Molecular properties that influence the oral bioavailability of drug candidates. *J. Med. Chem.* 2002, *45* (12), 2615–2623.

Chapter Six: Conclusion

6.1 Summary

Oberlies and Kroll (2004) wrote: "The events surrounding the discovery and development of these drugs (*Camptothecin and Taxol*) provide numerous examples of the power of natural products to uncover new therapeutic agents and define novel drug targets. Moreover, central to all of these lessons are the drive and persistence of two complementary researchers whose dedication to science transcended the obstacles encountered during the 30-plus year journey of these molecules from bench to bedside. Individually, both of these discoveries are seminal accomplishments, and taken together, this work represents a truly historic achievement in natural products research".[1] With few exceptions where a natural product (NP) ended up in the clinic in its original isolated form (for example, fusidic acid), most drugs inspired by natural products share a common testimony with camptothecin and taxol. The drug discovery journey is indeed a long, tedious, and cost-intensive venture. Many 'potent' NPs (extracts, fractions or pure compounds) have only ended up in the cupboards of academic research groups or safe repositories of pharmaceutical companies who once embarked on NP-led drug discovery but for reasons earlier highlighted in Chapter One of this thesis have abandoned such projects.

In the current work reported in this thesis, eleven new NPs were isolated and fully characterized from three marine organisms, comprising a newly identified red seaweed (*Laurencia alfredensis*) and two sponges (*Halichondria sp.* and *Hymeniacidon sp.*). The new compound **7** (alfredensinol C) isolated from the seaweed exhibited selective anti-proliferative activity against the MDA-MB-231 breast cancer cell line (IC_{50} = 8.8 µM) compared to the HeLa cervical carcinoma (IC_{50} = 133.8 µM). It would be useful to investigate the cytotoxicity of this compound against a normal human cell line to investigate its selectivity profile. However, the new compounds isolated from *Halichondria sp.* lacked antiplasmodium activity against the chloroquine-sensitive NF54 strain of *Plasmodium falciparum*. It will be worth investigating the biological activity of these compounds in other assays, for example, in those reported for congeners in the literature, such as antifouling, antibacterial and nematicidal activities to increase the scope of structure-activity relationships (SAR) of the naturally occuring betaine molecules.[2–8]

The fusidane triterpenoid fusidic acid has been used as an antibiotic drug since 1962. It is one of the successful stories of a NP in the clinic as a drug in its original isolated form. With a novel antibacterial mechanism of action, a drug-repositioning approach was embarked on towards identifying anti-tubercular and anti-malarial drug lead (s) based on fusidic acid. While our research group has previously explored and reported antimycobacterial and antiplasmodium derivatives through semi-synthesis of fusidic acid,[9–11] the current work progressed on the available data to further expand the SAR in the two biological assays. The data generated and the results reported in this thesis will further inspire and direct future lead optimization efforts on fusidic acid. The (*R*)-4-fluoro ethanamide analogue (**1.4**) was found to display comparable asexual erythrocytic blood stage antiplasmodium potency to the previous frontrunner compound with IC_{50} values of 0.57 and 0.47 µM against the NF54 and K1 strains of *P. falciparum*, respectively. Meanwhile, the Mannich base 3-((*N*,*N*-diethylamino)methyl)-4-hydroxy Mannich base anilide congener (**1.24**) recorded the most potent antimycobacterial activity with MIC_{90} values of 0.40 µM and 10.35 µM in the 7H9/CAS and 7H9/ADC media, respectively, which is comparable to fusidic acid but far more potent than the frontrunner compounds in the current research. Future work aimed at further exploring the antiplasmodium and antimycobacterial SAR inspired by the two compounds, **1.4** and **1.24**, is highly recommended.

Further medicinal chemistry work, as reported in this thesis, led to the identification of a potent novel antiplasmodium and antimycobacterial agent based on the privileged benzimidazole scaffold, which is a structural isostere of the purine bases, adenine and guanine, and a potential bioisostere of indole, a very common scaffold in most natural products. Amongst the twenty synthesized analogues, comprising four benzimidazole scaffolds and five Mannich bases, compound **8.2** exhibited sub-micromolar antiplasmodium activity against the asexual blood stage drug sensitive NF54 strain (IC_{50} = 0.19 µM) and multidrug resistant K1 strain (IC_{50} = 0.06 µM) of *P. falciparum*, and early stage (II/III) gametocidal activity (inhibiting 91% of parasite growth at 1 µM). The compound occupies a similar chemical space to the antimalarial drug naphthoquine albeit it exhibited poor aqueous solubility at pH 7.4. Further, **8.2** was active against the $H_{37}Rv$ strain of *Mycobacterium tuberculosis* with a MIC_{90} = 2.31 µM in the 7H9/CAS media. It will be expedient to undertake follow up investigations, comprising of exploring additional benzimidazole-Mannich

base analogues as well as profiling for microsomal metabolic stability and *in vivo* efficacy of the benzimidazole frontrunner compound (**8.2**).

According to Borris (1996), "Natural products research is a part, and in truth a small part, of the discovery process. The screening of natural products is one of the earliest steps in drug discovery, namely 'lead' identification. A lead compound, as the term is currently used, is a compound with many of the characteristics of a desired new drug which will be used as a model for chemical modification. It must be potent, but it does not need to possess the potency at the nanomolar or picomolar levels expected of a product candidate. It must be specific for the desired target, but it does not need to possess the exquisite biochemical specificity required for a new drug. Finally, it must be available in sufficient quantities to support the early stages of development, such as biological characterization and toxicity studies, while a total synthesis of the product candidate is being completed. It is much easier to find a lead compound than to find a product candidate. The transition from looking for drugs to looking for leads has been made possible by the tremendous advances that have occurred in organic and medicinal chemistry in the last few decades. We now expect that our chemists will be able to improve the potency and/or specificity of a good lead compound, perhaps by several orders of magnitude. It is thus the task of the medicinal chemist to take a lead compound and turn it into a drug".[12]

The work presented in this thesis well represents both the early discovery stages of natural products-based drug discovery and the lead identification stages from a medicinal chemistry perspective. As rightly indicated by Borris (1996),[12] collaboration between the chemistry fields of natural products and medicinal chemistry is useful to move a lead NP compound to the bedside as a drug. In such a venture, the role of medicinal chemistry is inevitable. While the current work demonstrates the usefulness of such collaboration, drug discovery is an unending journey; for even when a drug finally makes it to patients, it is expedient to discover second, third, fourth, etc. generations so as to keep the disease in check, due in part to drug resistance.

6.2 References

(1) Oberlies, N. H.; Kroll, D. J. Camptothecin and Taxol: Historic Achievements in Natural Products Research ⊥. *J. Nat. Prod.* **2004**, *67* (2), 129–135.

(2) Ackermann, D.; List, P. H. On the Composition of Zooanemonine and Herbipoline. *Hoppe Seyler's Z. Physiol. Chem.* 1960, *318(3/6)*, 281.

(3) Hattori, T.; Matsuo, S.; Adachi, K.; Shizuri, Y. Isolation of Antifouling Substances from the Palauan Sponge Protophlitaspongia Aga. *Fish. Sci.* 2001, *67* (4), 690–693.

(4) Sauleau, P.; Moriou, C.; Al Mourabit, A. Metabolomics Approach to Chemical Diversity of the Mediterranean Marine Sponge Agelas Oroides. *Nat. Prod. Res.* 2017, *31* (14), 1625–1632.

(5) Cafieri, F.; Fattorusso, E.; Taglialatela-Scafati, O. Novel Betaines from the Marine Sponge Agelas Dispar. *J. Nat. Prod.* 1998, *61* (9), 1171–1173.

(6) Weinheimer, A. J.; Metzner, E. K.; Mole, M. L. A New Marine Betaine, Norzooanemonin, in the Gorgonian Pseudopterogorgia Americana. *Tetrahedron* 1973, *29* (20), 3135–3136.

(7) Gupta, K. C.; Miller, R. L.; Williams, J. R.; Blount, J. F. Norzooanemonin in the Hydroid Tubularia Larynx I. *Experientia* 1977, *33* (12), 1556.

(8) Capon, R. J.; Vuong, D.; McNally, M.; Peterle, T.; Trotter, N.; Lacey, E.; Gill, J. H. (+)-Echinobetaine B: Isolation, Structure Elucidation, Synthesis and Preliminary SAR Studies on a New Nematocidal Betaine from a Southern Australian Marine Sponge, Echinodictyum Sp. *Org. Biomol. Chem.* 2005, *3* (1), 118–122.

(9) Kaur, G.; Singh, K.; Pavadai, E.; Njoroge, M.; Espinoza-Moraga, M.; De Kock, C.; Smith, P. J.; Wittlin, S.; Chibale, K. Synthesis of Fusidic Acid Bioisosteres as Antiplasmodial Agents and Molecular Docking Studies in the Binding Site of Elongation Factor-G. *Medchemcomm* 2015, *6* (11), 2023–2028.

(10) Espinoza-Moraga, M.; Singh, K.; Njoroge, M.; Kaur, G.; Okombo, J.; De Kock, C.; Smith, P. J.; Wittlin, S.; Chibale, K. Synthesis and Biological Characterisation of Ester and Amide Derivatives of Fusidic Acid as Antiplasmodial Agents. *Bioorg. Med. Chem. Lett.* 2017, *27* (3), 658–661.

(11) Kaur, G.; Pavadai, E.; Wittlin, S.; Chibale, K. 3D-QSAR Modeling and Synthesis of New Fusidic

Acid Derivatives as Antiplasmodial Agents. *J. Chem. Inf. Model.* 2018, *58* (8), 1553–1560.

(12) Borris, R. P. Natural Products Research: Perspectives from a Major Pharmaceutical Company. *J. Ethnopharmacol.* 1996, *51* (1–3), 29–38.